

PUBLICATION NO. 43 1/2011

NORDIC CONCRETE RESEARCH

**EDITED BY
THE NORDIC CONCRETE FEDERATION**

**CONCRETE ASSOCIATIONS OF: DENMARK
FINLAND
ICELAND
NORWAY
SWEDEN**

**PUBLISHER: NORSK BETONGFORENING
POSTBOKS 2312, SOLLI
N - 0201 OSLO
NORWAY**

PROCEEDING

XXI NORDIC CONCRETE RESEARCH SYMPOSIA

HÄMEENLINNA, FINLAND, 2011

VODSKOV, MAY 2011

Preface

This publication is a compilation of papers presented in the XXI Nordic Concrete Research Symposium arranged in Spa Hotel Rantasipi Aulanko, Hämeenlinna, Finland. The Symposium took place 30th May to 1st June 2011. It was arranged by Concrete Association of Finland in cooperation with the Research Committee of Nordic Concrete Federation.

Nordic Concrete Research Symposium is organised after every three year. The event circulates between the member countries of the Nordic Concrete Federation, i.e. Finland, Denmark, Norway, Iceland and Sweden, in this order.

The aim of the symposium is to present most recent research projects and their results in the field of concrete technology, construction and maintenance of concrete structures. Another important intention is to collect people working with concrete and concrete research together to promote co-operation between researchers, research organisations as well as practising engineers in the Nordic regime. The symposium also presents and documents the versatile concrete research conducted in Nordic research laboratories, universities and companies.

In this years Symposium, altogether 115 papers were presented along with 15 different themes. Major part, altogether 97 papers, come from Nordic countries. Altogether 29 papers come from Sweden, 18 from Norway, 17 from Denmark and 2 from Iceland. Researchers from Finland as the hosting country sent 32 papers. Altogether 18 papers come from other countries, most distant from Japan, USA and Canada.

Having this occasion I would like to express my warm thanks to all the authors, speakers and chairpersons for their valuable contribution as well as to the symposium participants who together make the symposium fruitful. Warm thanks also to Dr Dirch H. Bager, the editor of this publication.

Helsinki, May 2011

Jussi Mattila

Managing Director, Concrete Association of Finland
Chairman of the Nordic Concrete Research Committee

Scientific Committee

Dr. Dirch H. Bager, DHB-Consult (DK)

Mr. Claus Pade, Danish Technological Institute, Concrete Centre (DK)

Dr. Jussi Mattila, Concrete Association of Finland (FI)

Lic.Sc.Tech. Klaus Juvas, Consolis Technology Oy Ab (FI)

Dr. Børge J. Wigum, Mannvit (IS)

Dr. Jón E. Wallevik, Innovation Center Iceland (IS)

Dr. Terje F. Rønning, Norcem R&D Department (NO)

Mr. Hans Stemland, SINTEF (NO)

Tekn.Dr. Docent Mikael Hallgren, Tyréns AB (SE)

Tekn.Dr. Peter Utgenannt, CBI Swedish Cement and Concrete Research (SE)

Organizing Committee

Dr. Jussi Mattila, Concrete Association of Finland (FI)

Lic.Sc.Tech. Klaus Juvas, Consolis Technology Oy Ab (FI)

Ms. MarjaLeena Pekuri, Concrete Association of Finland (FI)

CONTENTS

OPENING SESSION

Jouni Punkki, Aleksi Lounamaa & Seppo Junnila
Role of building materials on the CO₂-emissions of buildings..... 3

Tor Arne Hammer
COIN - Concrete Innovation Centre, Midterm status 7

SUSTAINABILITY - Session A1

Henrik Stang, Mette Geiker & Michael D. Lepech.
Framework for Sustainable Repair and Rehabilitation of Civil Infrastructure... 13

Margareta Wahlström & Jutta Laine-Ylijoki.
Sustainable Construction Materials and Products in Renovation..... 17

Kaspars Kravalis & Jānis Ošlejs.
Compatibility of concrete flooring systems with LEED and BREEAM sustainable construction guidelines..... 21

Anna Kronlöf, Liisa Salparanta & Tapio Vehmas.
Discoloration of White Concrete Containing Photoactive TiO₂ 25

Arto Puurula, Ola Enochsson, Gabriel Sas, Björn Täljsten & Lennart Elfgren
Load carrying capacity of a RC Bridge in Örnsköldsvik, Sweden 29

MODELLING AND TESTING - Session A2

Carmen Andrade & Esperanza Menendez
Chloride Diffusion Study made from the Pre-Testing of Oresund Bridge Mix Proportions 35

Hendrik Schlune, Sven Thelandersson, Mario Plos, Thomas Svensson & Kent Gylltoft.
A New Safety Format for Nonlinear Analysis..... 41

Martin Kaasgaard & Claus Pade
Experiences with the use of a semi industrial size concrete mixing plant for research and documentation within concrete properties..... 45

Liisa Salparanta
From research to practice in Finland 51

Rasmus Rempling
Modelling of Concrete Subjected to Cyclic Loading..... 55

<i>Posters:</i>	
Lamis Ahmed & Anders Ansell Experimental and Numerical Investigation of Stress Wave Propagation in Shotcrete	59
Håkan Hansson & Richard Malm Initial study of oblique hard target projectile impact of normal and high strength concrete targets	63
SCC - Session A3	
Hannele Kuosa High water-cement ratio SCC robustness with novel cellulose based admixture	69
Ya Peng & Stefan Jacobsen SCC Stability affected by fillers and VMA	73
Hedda Vikan & Klaartje De Weerd Rheological Properties of Self-Consolidating Concrete Stabilized with Fillers or Admixtures	77
Dag Vollset & Øystein Mortensvik Rheological properties for self compacting concrete (SCC)	81
Jan Skoček Prediction of flow induced inhomogeneities in self compacting concrete	87
Lars N. Thrane, Jørgen Schou, Thomas Juul Andersen & Claus Pade Flow Properties of SCC for the Casting of Complex Shaped Pavilion	91
Stefan Jacobsen. SCC flow visualization in formfilling with black and grey concrete	95
Peter Simonsson & Mats Emborg Modelling of Concrete Subjected to Cyclic Loading	99
CARBONATION, CHLORIDES AND CORROSION - Session A4	
Filip Nilenius, Fredrik Larsson, Karin Lundgren & Kenneth Runesson. A multi-scale method for modelling of moisture and chloride ion transport in concrete	107
Ueli Angst, Øystein Vennesland, Claus K. Larsen & Bernhard Elsener Results from the Norwegian COIN project on chloride induced reinforcement corrosion in concrete	111
Nelson Silva, Tang Luping, Jan Erik Lindqvist & Dimitrios Boubitsas Critical Conditions for Depassivation of Steel in Concrete: Interface Chloride Profiles	115

Ylva Edwards Degradation and corroding problems for concrete in biological treatment plants make surface protection necessary	119
Karla Hornbostel, Claus K. Larsen & Mette Geiker The Electrical Resistivity of Concrete as Service Life Parameter	123
<i>Posters</i>	
Rui M. Ferreira & Pedro M. Costa The effect of metakaolin on chloride penetration into concrete	127
Michael Vogel & Harald S. Müller Modelling combined deterioration mechanisms related to chloride and carbonation induced corrosion	131
In-Seok Yoon Chloride Binding Behaviours by AFm and C-S-H in Artificial Pore Solution of Concrete	135
FROST ACTION - Session A5	
Anna Knutsson, Tang Luping & Anders Lindvall Freeze/Thaw Durability of Concrete with Fly Ash	141
Christian Gottlieb, Idar Olsen, Jesper Frej Henningsen, Thomas Rohde, Kurt Kielsgaard Hansen & Bent Grelk Valuation of the 12 year old Concrete in the Ulkebugt Bridge, Sisimiut, Greenland	145
Dag Vollset & Øystein Mortensvik Air void structure of produced frost resistant concrete – an on site study	149
Johanna Tikkanen & Hanna-Reea Välimäki Freeze-thaw resistance of inert mineral powder concretes	153
Martin Rosenqvist Moisture Transport in Concrete Structures in Swedish Hydro Power Plants	159
<i>Posters</i>	
Stefan Jacobsen Ice abrasion by hydraulic pore pressure at rough concrete surface-ice indentation	163
Ali Akbar Ramezaniapour, Mohsen Jafari Nadushan & Mansur Peydayesh De-icing Salt Scaling Resistance of Concrete Containing New Composite Cement	167
STRUCTURAL BEHAVIOUR - Session A7	
David Fall, Karin Lundgren & Kent Gylltoft Reinforcement in tailor-made concrete structures	175

Kamyab Zandi Hanjari, Karin Lundgren, Mario Plos & Kent Gylltoft Corroded reinforced concrete structures: Effects of high corrosion and corroded stirrups	179
Mikael Hallgren Punching Shear on Steel Edge Columns	183
Oskar Larsson Extreme Values of Climatic Thermal Stresses in Concrete Box Cross-sections .	187
Richard Malm & Anders Ansell Verifying the Behaviour of a Concrete Buttress Dam Subjected to Temperature Variations	191
Olli Kerokoski, Tommi Rantala & Antti Nurmikolu Loading Tests of Concrete Monoblock Railway Sleepers	195
<i>Poster</i>	
Shuaib H. Ahmad, S.F.A.Rafeeqi & Shamsoon Faree Shear Strength of High Strength- High Performance Reinforced Concrete Beams	199
MODELLING AND TESTING - Session A8	
Mia Schou Lund, Lotte Braad Sander, Bent Grellk & Kurt Kielsgaard Hansen Chloride Ingress into Concrete under Water Pressure	207
Terje Kanstad, Gunrid Kjellmark, Anja B. E. Klausen & Øyvind Bjøntegård Updated Temperature-Stress-Testing-Machine (TSTM): Introductory test results and determination of material properties development	211
Lasse Frølich Kristensen Development of New Method for Determination of Concrete Setting Time	215
Brad J. Pease, Mette Geiker, Henrik Stang & Jason Weiss Experimental Methods for Consideration of Concrete Cracking in Service Life Design	219
Anders Ansell Numerical Study of Shotcrete as Rock Support on Irregular Tunnel Surfaces ..	225
Anna Kronlöf Fine Particles - a Fracture Mechanical Approach	229
FIELD TESTING OF DURABILITY - Session A9	
R. Doug Hooton, Amir Ramezaniapour & Reza M. Ahani Issues Related to the Use of Portland-Limestone Cements in Sulphate Exposure	235

Erika Holt, Markku Leivo Concrete Durability Based on Coupled Laboratory Deterioration by Frost, Carbonation and Chloride	239
Fahim Al-Neshawy, Esko Sistonen & Jukka Piironen Effect of NaCl and different CO₂ concentrations on the mineral compositions of a hardened cement paste	243
Hannele Kuosa Concrete durability field testing in Finland	247
Karl Peterson & Lawrence Sutter Impact of Hydrated Cement Paste Content and Entrained Air-Void System Parameters on the Durability of Concrete	251
Erkki Vesikari Modelling of Carbonation and Chloride Penetration Interacted by Frost Damage in Concrete	255
Jukka Piironen, Esko Sistonen, Olli-Pekka Kari, Jari Puttonen & Fahim Al-Neshawy The Effect of Cracking on Chloride Migration in Concrete	259
BINDERS AND ADMIXTURES - Session B1	
Leif Fjällberg & Björn Lagerblad A new type of accelerator for Portland cement	265
Tapio Vehmas & Anna Kronlöf A study of early-age Ordinary Portland Cement Hydration according to Autocatalytic Reaction Model	269
Kien Dinh Hoang, Mette Rica Geiker, Harald Justnes & Roar Myrdal Effect of chemical admixtures on the early strength development of fly ash blended cement at low temperature	273
Andrzej Cwirzen & Karin Habermehl-Cwirzen Reactive magnesium oxide as alternative secondary binder for Portland cement	277
Tapio Vehmas & Markku Leivo A Novel Cellulose Based Stabilizing Admixture for Self Compacting Concrete	281
AGGREGATES AND ADDITIVES - Session B2	
Sara Laustsen Engineered Air-entrainment of Concrete	289
Olli Skyttä Accuracy of sand flow cone in characterizing fine aggregates	293

Klaartje de Weerd, Harald Justnes & Knut O. Kjellsen Synergetic effect between fly ash and limestone powder in Portland composite cements	297
Taisto Haavasoja Feasibility of Optical Moisture Measurement in Concrete Aggregates	301
Björn Lagerblad, Mikael Westerholm & Hans-Erik Gram How to evaluate crushed rocks for concrete production	305
Hannu Pyy & Erika Holt Finland's Emerging Alkali-Aggregate Reaction Problem?	311
<i>Posters</i>	
N. Salehi, R. Khosravian An investigative study on the effects of silica flour, zeolite and silica fume on the water absorption of Roller compacted concrete	315
Makoto Kagaya, Noritoshi Saito & Yoshitsugu Shirokado Evaluation of Curing Effect of Blast-Furnace Slag Concrete by Using Odor Sensor	327
Navid Salehi, AmirHossein Khodaeeyan & MohammadReza Vafaie An Investigative Study on the Effects of Natural Pozzolan and Limestone Powder on the Mechanical Properties of Roller Compacted Concrete	331
MIX DESIGN AND RHEOLOGY - Session B3	
Claus Pade, Martin Kaasgaard Production of concrete for the Fehmarn Belt Fixed Link exposure site	339
Marianne Tange Hasholt, Claus Pade Concrete with superabsorbent polymers (SAP) - experience from the Fehmarn field exposure station in Rødbyhavn	343
Tom C. Lundin, Kristian R. Gunnelius & Jarl B. Rosenholm X-ray characterisation of early-age cement structuration for phase kinetics ..	347
Kristian R. Gunnelius, Tom C. Lundin & Jarl B. Rosenholm Rheological and Structural Characterization of Early-age Cement Pastes	353
Rolands Cepuritis, Stefan Jacobsen, Bård Pedersen, Hedda Vikan, Espen Rudberg, Klaartje DeWeerd, Ya Peng & Børge Wigum. Rheology of matrix with different crushed mineral fillers and admixtures	359
<i>Poster</i>	
Ganesh Babu, Durga Prasad. R & Chandra Sekhar. B An appraisal of the strength to water cement ratio relations	363

EXECUTION OF CONCRETE STRUCTURES AND SURFACES - Session B4	
Thomas Juul Andersen & Tine Aarre Tailormade Concrete Structures with the use of Digital Fabrication and Self Compacting Concrete	369
Johannes Rauf Greisen, Lars Nyholm Thrane, Claus Pade & Christoffer Dupont Double curved concrete surfaces with precisely embedded optical fibres displaying live images.	373
Olli-Pekka Tynkkynen The Effect of Damage and Repair to carrying Capacity of a Bridge	377
Mette Glavind Danish Expert Centre for constructions to the infrastructure	381
Eeva Kaataja, Juha Rämö New Innovations in Finnish Prestressed Concrete Production.....	385
<i>Poster</i>	
Ganesh Babu. K, Chandra Sekhar B & Durga Prasad R Effect of temperatures on the accelerated curing of concrete	389
USE OF FIBRES - Session B5	
Terje Kanstad & Sindre Sandbakk Ductile High Tensile Strength Concrete	395
Sindre Sandbakk & Terje Kanstad Panel- and Beam testing of Fibre Reinforced Concrete.....	399
Andrejs Krasnikovs, Olga Kononova, Videvuds Lapsa & Andrejs Pupurs High-Performance Steel Fibreconcrete Strength	403
Andrejs Krasnikovs, Amjad Khabbaz, Angelina Galushchak & Arturs Machanovskis Fibre Reinforced Concrete (FRC) (with Glass, Steel and Carbon Fibres) Strength	407
Karin Habermehl-Cwirzen, Vesa Penttala & Andrzej Cwirzen Development of Cardboard Fibre Engineered Cementitious Composite (CFECC).....	411
<i>Posters</i>	
René Čechmánek, Pavel Šteffan & Jiří Junek Formulations of Electrically Conductive Cement-based Composites	415
Magureanu Cornelia, Heghes Bogdan Deformability of high strength concrete.....	419

NUCLEAR AND FIRE SAFETY - Session B6

Johan Silfwerbrand

**Concrete and Fire – Swedish Recommendations for Preventing Spalling
in Civil Engineering Structures** 425

Arezou Babaahmadi, Tang Luping, Zareen Abbas & Gunnar Gustafson

Ageing of Cementitious Materials for Storage of Nuclear Waste..... 429

Mikael Persson

Climatic Condition inside Nuclear Reactor Containments..... 433*Poster*

Jan Cervenka

Nonlinear Analysis of Pre-stressed Concrete Nuclear Containments 437**MAINTENANCE AND RENOVATION - Session B7**

Torsten Lunabba & Hemming Paroll

Moisture Control in Concrete Bridges 443

Mika Mäkitalo, Fahim Al-Neshawy & Tomi Laurila

**Wireless Monitoring Sensor System for Tracking the Hydrothermal
Behaviour and Deterioration of Building Structures**..... 447

Jukka Lahdensivu

**Repair Possibilities of Concrete Facades made Insufficient
Frost Resistant Concrete** 453

Eythor Thorhallsson, Arngrimur Konradsson & Stefan Kubens

Concrete Cylinders Confined with Basalt Fibre Reinforced Polymer 457

Arto Köliö & Jukka Lahdensivu

**The Calculated Repair Need of Finnish Concrete Facade and
Balcony Structures** 463*Poster*

Jaakko Säntti & Jarno Komulainen

Petroleum hydrocarbons in concrete and their effect on indoor air quality..... 467**SHRINKAGE AND CRACKING - Session B8**

Jonas Carlswärd

Shrinkage cracking of thin concrete overlays 473

Peter Fjellström, Henrik Bäckström & Jan-Erik Jonasson

Crack-Free Concrete – An Understanding of Creep 477

Gunrid Kjellmark & Terje Kanstad

**Autogenous deformation of concrete: Introductory tests with 7 new
temperature controlled dilation rigs** 481

Björn Lagerblad	
Properties of shotcrete-shrinkage problems	485
Lars Elof Bryne & Anders Ansell	
Restrained Shrinkage Tests of Fibre Concrete for Shotcrete Applications in Hard Rock Tunnels.....	489
STRUCTURAL BEHAVIOUR - Session B9	
Robert Hällmark, Peter Collin & Martin Nilsson	
A study of concrete shear keys in prefabricated bridges with dry deck joints ...	495
Peter Lundqvist & Nils Rydén	
Short- and Long-Term Measurements of Resonance Frequencies on Prestressed Concrete Beams.....	501
Andrea Folli	
Highly Active Photocatalytic Innovative Concretes.....	505
Linn Grepstad Nes & Jan Arve Øverli	
Investigation of material parameters and structural performance of hybrid concrete beams.....	509
Ulf Jönsson & Christian Munch-Petersen	
Concrete Strategy for the Fehmarnbelt Fixed Link Project – Concrete Strategy for 120 years lifetime of the Concrete structures.....	513
Katarina Malaga, Örjan Petersson, Kristian Tammo, Thomas Blanksvard & Mathias Flansbjer	
Textile reinforced concrete sandwich panels.....	517
Mari Bøhnsdalen Eide, Hedda Vikan, Kristin Kaspersen & Helene Schulerud	
Classification System for Formed Concrete Surfaces	521
CONCRETE TEACHING - Concrete Café	
Per Goltermann	
Renewing the teaching by using the students contributions.....	527
CLOSING SESSION	
Johan Larsson & Mats Emborg	
A study of the future for concrete bridge construction in Sweden	533

OPENING SESSION

Role of building materials on the CO₂-emissions of buildings



Jouni Punkki
Dr. Tech.
Consolis Technology
Äyritie 12b,
FIN-01510 Vantaa
jouni.punkki@consolis.com



Aleksi Lounamaa
M.Sc. (Tech)
NCC Property Development
Oy
Mannerheimintie 105,
FIN-00281, Helsinki
aleksi.lounamaa@ncc.fi



Seppo Junnila
Professor., Dr. Tech.
Aalto University/
Real Estate Business
seppo.junnila@aalto.fi

ABSTRACT

In the study the CO₂-emissions of two real buildings (apartment and office building) were calculated during the whole service life of the buildings. The construction phase, use phase, maintenance and the demolition phase were separated. The construction phase was further divided into construction materials and site operations. From the construction materials special attention was focused on the pre-cast concrete elements

In near future, significant changes are expected to take place in the heating energy consumption of buildings as well as on the CO₂-emissions profiles of the energy. In the study these future changes in energy consumption and in CO₂-profile were evaluated. In addition to changes in energy, future development in the production of building materials was estimated. The results show that the share of the use phase will significantly decrease due to the changes in energy consumption and in the CO₂-profiles of energy. However, the use phase still remains the biggest source of CO₂-emissions of the building.

Key words: sustainable construction, CO₂-emissions, pre-cast concrete, energy.

1. INTRODUCTION

1.1 General

Traditionally the use phase has been dominating the CO₂-emissions as well as the energy consumption during the life cycle of buildings. The share of the construction phase has been normally reported to be 10...20% from the total CO₂-emissions or energy consumption. However, it is obvious that the share of construction phase will continuously increase in near future because the radical savings in energy consumption in new buildings. In addition, the energy production is gradually changing from non-renewable sources to renewable sources and this development will decrease the CO₂-emissions of the energy. The effects of these future

changes have been just speculated, but only very few comprehensive calculations has been presented. Therefore, two Master's theses were made in Aalto University, Finland. The objectives of the studies were to create a transparent calculation model for the CO₂-emissions and energy consumption. One thesis was concentrating in the effects of pre-cast concrete elements and another thesis focused on the effects of on-site activities. This article summarises the results of the thesis concentrating in the pre-cast concrete elements.

2. STRUCTURE OF LCA MODEL

Own spread sheet models for apartment and office buildings were created. The user has a possibility select the accurate values for the amounts of different building components, energy consumption (heating, cooling, heating of water and lighting) and CO₂-emissions of the energy sources. In addition the properties of pre-cast concrete elements can be selected in details:

- Mix design (cement content, cement type, aggregate content, secondary cementitious material type and content, admixtures, water)
- Insulation material
- Reinforcement (reinforcement steel, prestressing steel, stainless steel, other steel parts)
- Process water usage
- Energy consumption (electricity, heating energy, other energy)
- Transportation (distance, load, return-load)

The calculation model contains the reference values for all the above-mentioned parameters. The values have been collected from different sources, and it is clear that the values cannot be universally valid for different production facilities. However, the user can freely use own actual values whenever available.

3. RESULTS AND DISCUSSIONS

In the study, the life cycle of building was divided into four main phases; Construction, Use, Maintenance and. Demolition. The construction phase contained both the building materials and the on-site operations. An apartment and an office building were calculated, the both buildings were located in Southern Finland and the service life of the buildings was assumed to be 50 years. The office building has a gross area of 9710 m^2 and the apartment building 2488 m^2 . The energy consumptions of the buildings were selected to follow the normal requirement level in 2009. The different energy consumptions have been given in Table 1.

Table 1 – Energy consumptions of apartment and office building used in the calculations.

Energy	Energy consumption [kWh/m ² * a]	
	Apartment building	Office building
Space heating	145	91.3
Water heating	30	2.1
Cooling	0	6.3
Electricity	66	93.9

2.1 Environmental loads of the buildings

During the life cycle the office building caused CO₂-emissions of 3 456 kg/gram² and the energy consumption was 42 535 MJ/gram². The use phase caused app. 84% from the total CO₂-emissions and app. 82% from the total energy consumption. The share of construction phase was 12.1% from the CO₂-emissions and 13.6% from the total energy use. The rest of the life cycle phases, maintenance and demolition, were estimated to cause some 4% of the CO₂-emissions and some 4% of the total energy.

The values of the apartment buildings were rather similar compared to those of the office building. The total CO₂-emissions were 4 064 kg/gram² and the total energy consumption was 50 836 MJ/gram². The use phase caused 87.6% from the total CO₂-emissions and app. 90% from the total energy consumption. The share of construction phase was 9.4% (CO₂) and 7.8% (energy). The rest of the life cycle phases, maintenance and demolition, were estimated to cause some 3% of the CO₂-emissions and some 2% of the total energy.

2.2 Sensitivity evaluation

The sensitivity evaluations were made for the office building and separate analyses were made for the whole building and for the manufacturing of the pre-cast elements. The building level analyses contained the sensitivity of the length of the life cycle, electricity use, heating energy consumption and the environmental loads of cement and steel. Figure 2 shows the sensitivity of the changes in the environmental loads of cement and steel as well as in the heating energy and electricity consumption on the CO₂-emissions of the building.

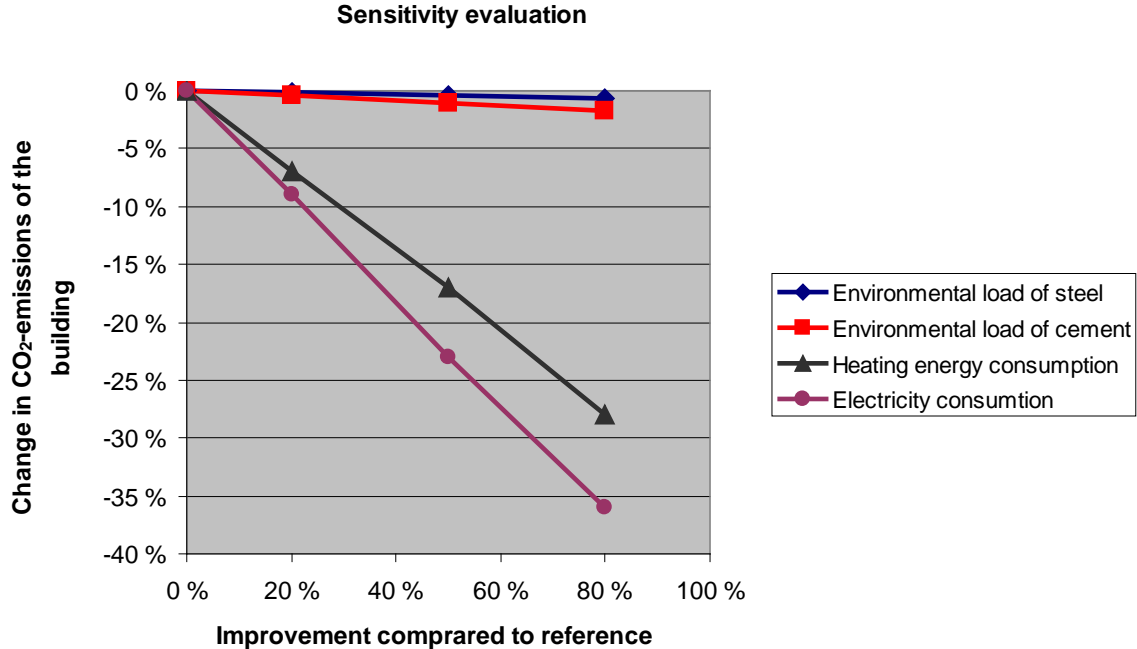


Figure 1 – Sensitivity evaluation of CO₂-emissions of the office building.

As can be assumed the energy consumption in the use phase is playing such a dominating role in the base case 2009 scenario that even radical changes in the environment loads of cement or steel (or in cement /steel consumption) cannot change the CO₂-emissions of the building.

2.3 Scenario 2020

One of the main objectives of the study was to analyse how the future changes in the energy consumption as well as energy quality (carbon content) will change the CO₂-emissions of the buildings. This was done in the Scenario 2020 and it was made only for the office building. The following assumptions were made:

- Heating energy consumption will be on Passive house level: 25 kWh/m², electricity consumption on level of 73 kWh/m²
- No changes in use of cooling energy consumption or water heating
- CO₂-emissions of heating energy will be 1/3 compared to the present
- CO₂-emissions of electricity will be 50% compared to the present

The changes may appear rather demanding. However, the new EU targets will require even lower energy consumption for new buildings in 2021 (close to zero-energy level). In addition to the changes in the energy consumption, 10% improvement was assumed to take place in pre-cast concrete manufacturing (amount of cement and steel, heating energy and electricity consumption). The CO₂-emissions of the cement was assumed to decrease by 100 kg/tn-cement from the present level. There will be similar development with other building materials, but in some cases (e.g. insulation materials) the increased use of materials will compensate the development in the manufacturing.

Based on the presented scenario the CO₂-emissions of the office building will decrease radically in near future (see Fig 2). And due to the significant reduction in the use phase, the share of the construction phase will increase (from 12.1% to 29.7%). However, the use phase still remains the biggest source of CO₂-emissions of the building.

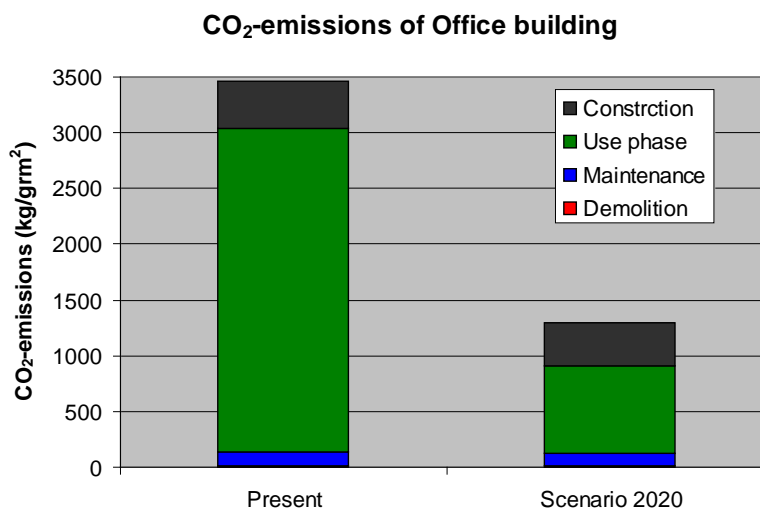


Figure 2 – CO₂-emission of an office building. Present level and Scenario 2020 presented.

REFERENCES

1. Lounamaa, A., “CO₂-emissions during the life cycle of Apartments and Office Buildings – Effects of precast concrete elements”, Master’s thesis. Aalto University. Faculty of Engineering and Architecture. Department of Structural Engineering and Building Technology. 2010. 80 p.

COIN - Concrete Innovation Centre, Midterm status



Tor Arne Hammer
 Dr.philos., Centre Manager
 COIN - Concrete Innovation Centre
 SINTEF Building and Infrastructure
 N-7465 Trondheim
 E-mail: tor.hammer@sintef.no

ABSTRACT

COIN - Concrete Innovation Centre (www.coinweb.no) - is one of presently 14 Centres for Research based Innovation (CRI), which is an initiative by the Research Council of Norway. The main objective for the CRIs is to enhance the capability of the business sector to innovate by focusing on long-term research based on forging close alliances between research-intensive enterprises and prominent research groups. COIN started in 2007 and is planned to run until 2014 with grants from the Research Council of Norway (RCN). During the fall 2010 RCN performed a “mid-term evaluation” of all 14 CRIs. The conclusion is that RCN will enter into new contract with 9 of the CRIs without requesting further actions, one of them being COIN. It means that COIN can anticipate NOK 38 mill from RCN in the coming 4 years.

Keywords: Concrete, research, innovation, attractiveness

1 INTRODUCTION

The vision of COIN is creation of more attractive concrete buildings and constructions. Attractiveness implies aesthetics, functionality, sustainability, energy efficiency, indoor climate, industrialized construction, improved work environment, and cost efficiency during the whole service life. The primary goal is to fulfil this vision by bringing the development a major leap forward by more fundamental understanding of the mechanisms in order to develop advanced materials, efficient construction techniques and new design concepts combined with more environmentally friendly material production.

COIN started in 2007 and is planned to run until 2014 with grants from the Research Council of Norway (RCN). During the fall 2010 RCN performed a “mid-term evaluation” of all 14 CRIs. The conclusion is that RCN will enter into new contract with 9 of the CRIs without requesting further actions, one of them being COIN. It means that COIN can anticipate NOK 38 mill from RCN in the coming 4 years. The intention is that COIN continues as a research centre beyond 2014 also, and a strategy for financing is now being discussed.

An evaluation report from two panels of international experts in research organisation and in concrete research, respectively, was an important basis for the decision. Their report is generally encouraging, and regarding PhD-students they say: *“The panel had a chance to meet the vast majority of these students during the evaluation visit and was impressed with their evident quality and commitment to their research”*. Their main conclusion is stated in the panel report:

“COIN is an efficiently managed and productive SFI, producing research results of scientific value and of use to partners in their development of processes and products. Projects are well planned and reviewed through clearly defined procedures but generally involve little risk”. They listed 7 recommendations for the next period of COIN.

2 ORGANISATION

The Consortium has a Board of Directors, and 3 Technical Advisory Committees (TACs) a manager and a management group. The Centre manager reports to the Board. The Board has nine members; seven from corporate partners, one from NTNU and one from SINTEF. The Board chair is from a corporate partner. All partners are represented in the TACs, acting as technical expertise groups as well as having the responsibility to establish innovation objectives and criteria, prioritizing and reporting. The TACs also break down the overall objectives into manageable and adequate action plans and tasks. There are presently eight projects, each having a Project Manager (from SINTEF, NTNU or corporate partners) and project groups with participants from all partners in principle, reporting to TAC.

The initial project structure (from 2007), was reorganised during 2009. This was considered to be necessary, even if COIN had a good start in 2007 with high activity, a great engagement, good cooperation between the Partners and with the projects apparently well anchored in the innovation strategies of the Partners. The industry Partners, the Research Council as well as the researchers seemed satisfied with the work in the first two years. However, as time went by it turned out that the many wishes from the partners resulted in too many, and partly fragmented activities. Therefore, we realized that the work should be more concentrated in order to fulfil the objectives and success criteria of COIN. This was supported by the Research Council, the industry partners and SINTEF/NTNU. The process of reorganisation started in November 2008 aiming to have a reorganised project structure and implemented a clearer process for selection of new projects by the start of 2010. The technical activities are now reorganized, and more concentrated, in 3 focus areas (FA), with belonging projects (presently 2-3 projects per FA):

Focus area F1) Environmental friendly concrete structures

Focus area F2) Economically competitive construction

Focus area F3) Technical performance

2.1 Innovation and relation to Centre user partners

The key issues were made specific by the Consortium Partners in a 2-days workshop at the start of COIN, and anchored in the Partners' innovation and research strategies. This was confirmed by the Partners' Directors or other representatives from their Management Group, in RCN's Site Visit in 2008, and later by the Partners' TAC-members in connection with preparing the research plan for the coming 4 years. The partners must show that any new project ideas are anchored in a set of selection criteria made by the Board.

The main measures to establishing links and integration between the partners, and to ensure competence transfer between the partners, are to have joint activities from project initiation and planning to report and to involve many persons from each industry partner. More specifically, it is by:

- All partners represented in Technical Advisory Committee, TAC
- Close cooperation with NTNU Faculty of Engineering Science and Technology. Professors at the Department of Structural are disciplinary responsible for the presently eight COIN projects. Adjunct professors at NTNU are strongly involved in COIN. PhD-students and MSc-students are partly involved in both NTNU and partner projects.
- The partners cooperate through the work in the projects, i.e. technical work and joint projects meetings - more than 60 persons from the industrial partners are on the list of personnel involved in COIN work and in TAC.
- Annual COIN in-house seminars to present findings from the research work.
- Five partners have personnel taking part in the Master of Science education at NTNU.
- There is a common WEB-based archive with administrative and technical information accessible for all workers in COIN.
- All reports are sent to partners for commenting/ verification.

3 A GLANCE ON MAIN RESULTS

The COIN researches, the presently 13 PhDs included, have been very productive, and produced more than 100 publications in approx. 3 years (30 state-of-the-art-reports included) . See www.coinweb.no for more information. Some main research achievements are shown below. More specific results are presented elsewhere in the proceedings.

It has been proven chemical synergy between fly ash and limestone that gives higher strength than fly ash alone as cement replacement for more sustainable concrete. This opened for production of all round cements with considerably reduced clinker content and thus correspondingly reduced CO₂ emission from the production. Ordinary clay and marl can be used as a cement replacement when calcined at medium temperature. This can solve the resource problem when the demand for supplementary cementing materials will increase as the trend of making blended cements are put into global practice. Preliminary results show that 50 % cement replacement by calcined marl gives equal 28 day strength!

Field data from North Sea structures over several decades have been used to develop reliable input parameters to modelling of chloride ingress into concrete; particularly relating to the time dependency of chloride diffusion coefficients in concretes at different ages and exposures. New knowledge has been established on disturbing electrode potentials during electrochemical measurement in concrete. These potentials can lead to misinterpretation of data from electrochemical measurement techniques, e.g. when chloride levels in concrete are measured by chloride sensitive electrodes embedded in the concrete. These achievements enable better design and modelling of service life of concrete structures. If the life time of all Norwegian concrete bridges could be prolonged by one year it would mean an annual saving of approx. 100 million NOK.

The work on fibre reinforcement has resulted in reliable test methods, which is a pre-requisite for design, specification and control, as well as for further research to achieve optimal mix design and fibre design. Also, the framework and expert group for preparing a guideline to design fibre reinforced concrete has been established. The guideline is ready spring 2011.

Developing classification methods and system for concrete surfaces is started, as there is to date no suitable and available tool to describe wanted appearance of a concrete surface. The system

defines different quality classes in terms of measurable parameters such as pore size distribution, number of pores and grey tone variations.

Crushed/ manufactured aggregates will increasingly meet the needs of the construction industry with natural sand/gravel resources being rapidly depleted all over Europe. The research area has a very cross-sectored character, and it is a major achievement so far in the project to have a multidiscipline research team operational, comprising experts from aggregate processing, processing equipment, engineering geology and concrete technology. Use of manufactured sand in concrete also has some obvious economical benefits: Fine fractions from the production process are often considered as residue. Instead it can be converted into high quality concrete sand. The potential increase in annual sales value is estimated to NOK 12-15 mill. Also, it is a major benefit for the society to be able to use aggregates locally to reduce transportation costs as well as CO₂ emission. If the average transportation distance of aggregates in Norway is reduced by 5 km, the annual reduction in transportation costs is roughly NOK 30-40 mill.

In the field of alkali aggregate reactions (AAR) there is a PhD with the objective to document and evaluate the influence of various curing and storage conditions on moisture content, extent of alkali leaching and expansion of concrete samples during accelerated laboratory testing, and how these accelerated methods relates to field observations. The work is in close cooperation with RILEM TC 219-ACS and leading international researchers. One finding resulted in withdrawal of one of the existing European draft methods for AAR testing that was replaced with an alternative testing procedure. In addition, the testing procedure of another draft test method was totally changed based on our results.

The research to develop a new high strength light weight aggregate for concretes with target density of 1000 kg/m³, based on expanded blue clay has made extensive progress: An initial study on fibre reinforcing the lightweight aggregate in the production showed very promising results in terms of considerably increased strength (without any significant density change). Along with a very effective coating (contributes to both higher strength and water tightness) system newly tested, the chance of having "superlight high strength aggregate" in near future is rather high.

Ice abrasion on concrete structures has been actualized by the oil industry moving north. New concretes have been tested in the ice abrasion machine in our laboratory, and life time models developed from that. The results has given Aker Solution the possibility of offering concrete structure without the cost demanding steel lining in pack ice areas.

4 PROJECT DATA AND FINANCING

COIN has an annual budget of NOK 25 mill, and is financed by the Research Council of Norway (approx. 40 %), industrial partners (approx 45 % of which ¼ is cash) and by SINTEF and NTNU (in all approx 15 %). Many partners spend more in-kind than planned, resulting in a total contribution per year exceeding NOK 30 mill in some years. The present industrial partners are:

Aker Solutions, Norcem, Norwegian Public Roads Administration, Rescon Mapei, Weber Saint Gobain, Skanska, Spenncon, Unicon and Veidekke.

Session A1 – SUSTAINABILITY

Framework for Sustainable Repair and Rehabilitation of Civil Infrastructure



Henrik Stang, Ph.D.
Tech. Univ. of Denmark, Dept. of
Civil Engineering (DTU Byg),
Brovej, DK-2800 Kgs. Lyngby,
Denmark hs@byg.dtu.dk



Michael D. Lepech, Ph.D.
Stanford University, Dept. of Civil
Engineering (DTU Byg), Kgs. Lyngby,
Denmark mge@byg.dtu.dk



Mette Geiker, Ph.D.
Tech. Univ. of Denmark, Dept. of
Civil Engineering (DTU Byg),
Kgs. Lyngby, Denmark
mge@byg.dtu.dk
Norwegian Univ. of Sci. and Tech.
(NTNU), Trondheim, Norway

ABSTRACT

The paper presents a probabilistic-based framework for the design of civil infrastructure repair to achieve targeted improvements in quantitative sustainability indicators. The framework consists of two types of models: (i) service life prediction models combining one or several deterioration mechanisms with a suite of limit states and (ii) life cycle assessment (LCA) models for measuring the impact of a given construction work; here repair understood in general terms as repair, rehabilitation, or strengthening.

Keywords: Repair, Rehabilitation, Structures, Sustainability, Service life modelling. Life Cycle Assessment.

1. INTRODUCTION

The design and construction of civil infrastructure that is more environmentally, socially, and economically responsible over its full life cycle from extraction of raw construction materials to end of life management is increasingly desirable worldwide. Altogether these three design goals of improved environmental, social, and economic performance are commonly known as the “triple bottom line” of sustainability [1]. The civil infrastructure constitute a critical set of systems that support our quality of life and enable global development and progress while consuming vast amounts of material resources and energy, thus it is essential that it is designed according to these broad, long term design goals for the benefit of our planet and the current and future generations of humans, animals, and plants that will call it home.

While the goals are well intended, the creation and execution of civil infrastructure designs that are socially, environmentally, and economically sustainable is not functionally possible for current infrastructure designers. Furthermore, a very important part of the sustainability of the total life of a given structure is governed by its maintenance and repair time line and the environmental impacts of such activities. The present paper describes an attempt to develop a quantitative, probabilistic framework that allows for environmental assessment of this part of the life of a given structure. The work described herein is a part of a larger project “Sustainable Renovation of Civil Structures”, sponsored by Nordic Innovation Centre (NICE). In this project the overarching scientific and technical objective is to develop an innovative decision support

system for optimized sustainable renovation and maintenance of large civil structures such as bridges and dams.

2. FRAMEWORK AND METHODS

The proposed framework adopts a probabilistic approach to the design and evaluation of a sustainable repair strategy for the civil infrastructure. The framework involves quantification of the cumulative impact of a repair timeline up to the time of functional obsolescence, t_{fo} , see Figures 1 and 2. Cumulative impact could be expressed as midpoint environmental indicators such as global warming potential (kg CO₂ equivalents), polluted water produced (L), solid waste generated (kg), or total primary energy consumed (MJ). As also shown in Figure 1., the time at which any repair is made (t_{rj}) is probabilistically characterized based on reaching a service life limit state corresponding to a reduction in materials quality or structural performance beyond that which is accepted by the owner or the appropriate structural design code. The probabilistic time between repairs ($t_{rj+1} - t_{rj}$) is based on the chosen repair strategy, the quality of the repair work, the variable nature of exposure and load conditions, the limit state, etc.

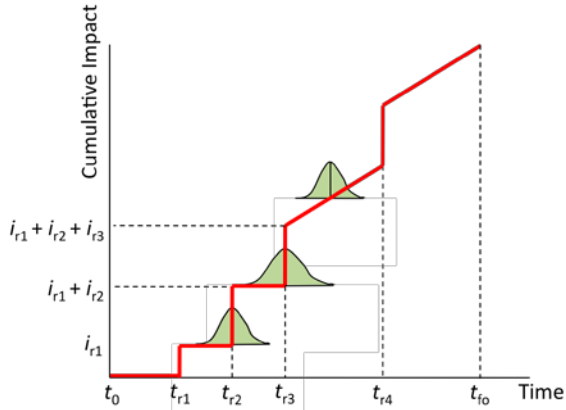


Figure 1. Cumulative impact versus time to repair in a typical scenario. The time to the j 'th repair, t_{rj} , is probabilistically characterized based on reaching the end of a repair service life limit state.

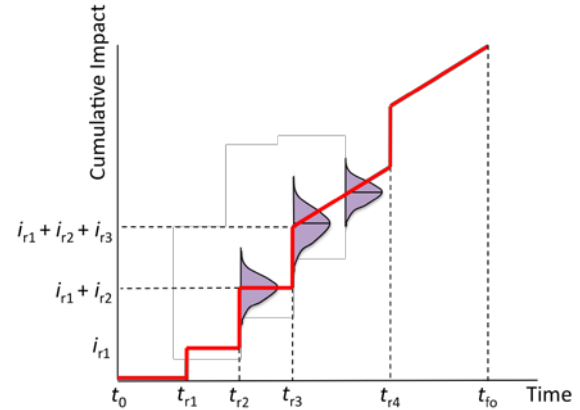


Figure 2. Cumulative impact versus time to repair in a typical scenario. The impact associated with a given repair, i_{rj} , can vary due to uncertainty in repair and rehabilitation construction processed actually used.

The cumulative impact of the repair timeline is defined as:

$$I = \sum_j i_{rj}(t) \quad (1)$$

where I is the cumulative impact and $i_{rj}(t)$ is the impact due to the j^{th} repair event as measured using ISO 14040 series life cycle assessment methods [2,3]. In addition to the probabilistic determination of the time of repairs, the amount of impact associated with each repair is also probabilistic in nature as indicated in Figure 2. Combining the probabilistic models for both repair timeline (t_{rj}) and amount of impact (i_{rj}), a probabilistic envelope can be constructed for the entire infrastructure service life from the time of initial construction (t_0) up to the time of functional obsolescence (t_{fo}). Based on the boundaries of this larger envelope (shown in Figure 3 using red dashes), an aggregated probabilistic assessment for cumulative impact at any time, t , for the rehabilitated or repaired structure can be constructed. Investigation of alternative repair methods and materials and be investigated within this framework with reductions in environmental impact midpoint indicators in mind, and an alternative repair scenario can be

designed to improve upon the *status quo*. The timeline of such alternative repair scenario is shown in Figure 4 and compared to status quo. In Figure 4, the failure probability of not meeting reduction targets (P_f) is also shown as a function of time.

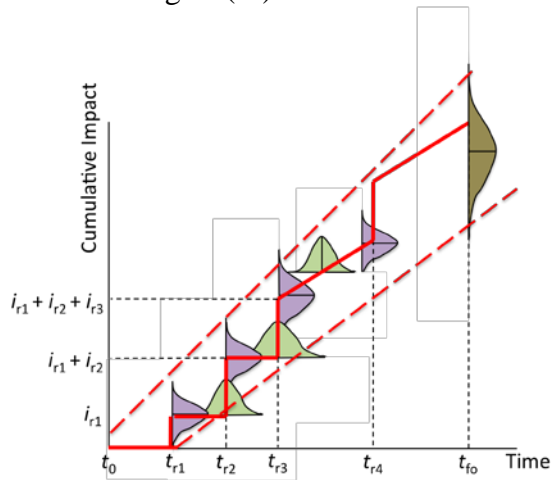


Figure 3. Combining the probabilistic models for both repair timeline (t_{ij} , Figure. 1.) and amount of impact (i_{ij} , Figure 2.) a probabilistic envelope can be constructed for the entire infrastructure service life.

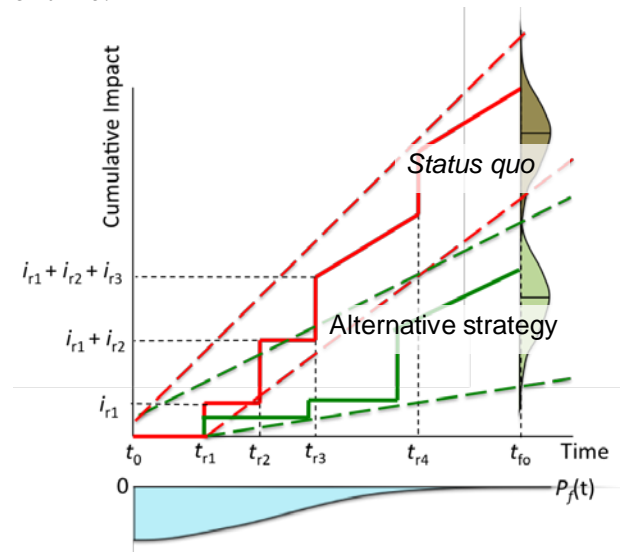


Figure 4. Level of impact reduction using an alternative repair timeline versus the status quo repair timeline can be estimated at any time in the future and associated with a given level of confidence for actually realizing that reduction.

3. MODELS

The framework described above relies on two types of models: First, quantitative, probabilistic service life models. In the current work two limit states are used to determine the time of repair, a materials-based limit state and a structure-based limit state. The materials-based limit state is initiation of corrosion due to chloride ingress (i.e. depassivation of reinforcing steel). The second, more comprehensive, limit state is unacceptable loss of structural performance due to chloride induced reinforcement corrosion. Secondly the framework requires a quantitative life cycle assessment model. Life cycle assessments are governed by ISO 14040 series standards. In this project, in which environmental midpoint indicators will be used to determine the comparative sustainability of alternative repair timelines, these indicators include metrics such as global warming potential (CO₂ equivalents), acidification potential (H⁺ mol equivalents), and similar indicators

4. FRAMEWORK DEMONSTRATION

To demonstrate the potential of the suggested probabilistic design framework for the sustainable repair of civil infrastructure case studies have been selected. One case which adopts the materials-based limit state of corrosion initiation, consists of two trial repair activities (mechanical repair and surface treatment using elastic mortar) performed on the OFU Gimsøystraumen Bridge during 1993 [8]. Early results showing estimated probability distribution of cumulative impact of mechanical repair activities obtained through Monte Carlo simulation are shown in Figure 5 as part of the total repair time line for the bridge.

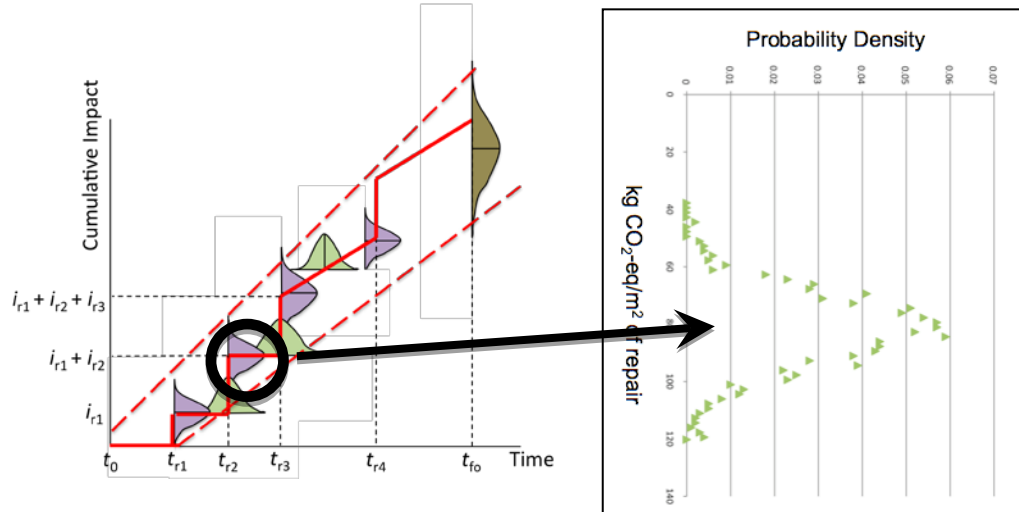


Figure 5 – An example of the probability distribution of cumulative impact in a given scenario, in this case kg CO₂ – equivalent per m² of bridge girder surface repair estimated through Monte Carlo simulation.

4. SUMMARY AND CONCLUSION

A probabilistic, quantitative framework for evaluation of the sustainability of repair and maintenance strategies has been developed and presented. The framework is currently being assessed and demonstrated through case studies including the OFU-Gimsøystraumen Bridge Repair Project. Support from *Nordic Innovation Center* (NICE) project 08190 SR, Sustainable rehabilitation of Civil and Building Structures is greatly acknowledged.

REFERENCES

1. Elkington, J. (1994) "Towards the sustainable corporation: Win-win-win business strategies for sustainable development." *California Management Review* **36**(2): 90-100
2. International Organization for Standards (2006) 14040: Environmental management - Life cycle assessment – Principles and framework. Geneva, Switzerland.
3. International Organization for Standards (2006) 14044: Environmental management - Life cycle assessment - Requirements and guidelines. Geneva, Switzerland.
4. Bare, J., Norris, G., Pennington, D., McKone, T. (2003) "The Tool for the Reduction and Assessment of Chemical and Other Environmental Impacts" *Journal of Industrial Ecology* 6(3-4):49-78
5. Goedkoop, M., Heijungs, R., Huijbregts, M., De Schryver, A., Struijs, J., van Zelm, R. (2009) "A life cycle impact assessment method which comprises harmonized category indicators at the midpoint and endpoint level – Report I: Characterization" Dutch Ministry of Housing, Spatial Planning, and Environment (VROM). Pp. 126
6. Wenzel, H., Hauschild, M., Alting, L. (1997) "Environmental Assessment of Products, Vol. 1: Methodology, tools and case studies in product development", Chapman and Hall, London.
7. Hauschild, M., Wenzel, H. (1998) "Environmental Assessment of Products, Vol. 2: Scientific background", Chapman and Hall, London.
8. Blankvoll, A. (1998) "OFU Gimsøystraumen bru, Hovedresultater og oversikt over sluttokumentasjon: Publication 89", Vegdirektoratet, Veglaboratoriet, Oslo, July 1998

Sustainable Construction Materials and Products in Renovation

Margareta Wahlström, Senior Research Scientist, margareta.wahlstrom@vtt.fi

Jutta Laine-Ylijoki, Senior Research Scientist, jutta.laine-yljoki@vtt.fi

VTT

P.O. Box 1000

FI 02044 VTT

Finland

ABSTRACT

This paper describes the current status of tools under development for the evaluation of the environmental sustainability of construction products and materials. The focus is on the release to soil and water in outdoor constructions. In the future also the recyclability of construction products is of high interest in the development of sustainable construction material.

Key words: sustainability, construction, recycling, reuse, environmental, ecodesign

1. INTRODUCTION

The emphasis in the building sector is moving from new buildings towards maintenance and renovation. Today 40 % of construction activities in Finland, respective 60 % in Sweden, are related to renovation. This trend will probably further increase by the energy conservation activities that will be required to achieve the 20-20-20 goals outlined by the EC resulting in a need of renovation of a huge amount of buildings. Environmental aspects related to construction products concern the entirely lifecycle, i.e. from manufacturing to construction with a safe use and sustainable handling and recycling of waste arising from renovation, maintenance and final demolition.

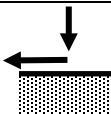
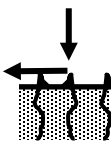
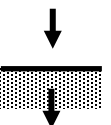
The background to this paper is the results of a Nordic project “Handbook: Environmental assessment of construction products” (2006-2008)” financed by the Nordic Innovation Centre (NICE). In the handbook specific features to be considered in the assessment of release of dangerous substances are discussed. A new Eracobuild-project “Sustainability of construction products and materials in renovation” (2010-2012) has recently started and will focus on assessment and decision making tools for the evaluation of environmental sustainability of construction products and materials in renovation.

This paper is especially focussing on tools for assessment of release to soil and water.

2. TOOLS FOR MEASUREMENT OF RELEASE TO SOIL/WATER

Three basic release scenarios are relevant for construction products, based on the water contact mode and the hydraulic properties of the construction products. These scenarios developed in the NICE project are illustrated in Table 1. Note that all three scenarios are relevant for products used above ground, under ground, or submerged into water. Both the construction product and the specific use of that product will influence which category of scenario is relevant in a given case.

Table 1 Description of the three basic leaching scenarios and examples of typical product types.

Scenario	Specification	Product example ¹⁾
I	 <p>Non-permeable product. Water is flowing over the surface of the product</p>	<p>Products used above ground this is surface runoff: paint coated sheet metal, surface coating, glazed tiles, glass surfaces etc.</p> <p>Products used underground, or submerged in water: foundations made from steel piles. A cover of polythene, epoxy, or zinc is commonly used as corrosion protection.</p>
II	 <p>Low permeable product. Water is transported into the matrix by capillary forces; contribution from core to surface²⁾</p>	<p>Typical monolithic products used above ground, underground, or submerged in water: tiles (non-glazed), bricks, (reinforced) concrete, treated wood, mortar, coatings, road materials, construction debris and pipes.</p> <p>Sheet-like products such as roofing felt (tar paper) may belong here or under scenario I depending on the product's characteristics.</p>
III	 <p>Permeable product. Water may infiltrate into the matrix driven by gravity</p>	<p>Products used above ground, underground or submerged in water: unbound aggregate, drainage aggregates, porous granular material, construction debris</p>

1) Note: It is possible that some generic type of products (e.g. coatings) include different specific products that due to their characteristics might fall under different scenarios. The selection of the scenario depends on their physical properties.

2) A special case is permeable compacted granular material used in constructions where it is partially sealed by impermeable layers, for example a paved construction. The physical properties of the pavement structure influence the way and the extent to which the construction material becomes exposed to water. Different zones of water contact develop dominated by gravity flow, capillary flow and diffusion, respectively.

For concrete materials especially the scenario 1 is of concern. In this scenario (and also in scenario 2) the release is determined by a tank leaching procedure, where a test specimen is immersed in water and the water is renewed according a specific timetable. The eluates from water renewal are collected and analysed. For crushed reclaimed concrete (scenario 3) the release is determined by a percolation procedure, where a column is filled the test material and water is pumped at the bottom of the column and eluates are collected from the top.

The test conditions to be considered in release studies were evaluated in the NICE-project. An important outcome of the NICE project was to give guidance covering all steps from sampling, method selection, preparations for testing and to guidance for the evaluation of results. The key aspect under assessment of release is to take into account the conditions in the intended use.

3. ASSESSMENT OF IMPACT TO SOIL AND WATER

In order to determine the environmental impact of construction products, the intended use of the product has to be clarified. The steps to be considered in an impact study on the ambient environment are illustrated in Figure 1. In laboratory test methods, the release of substances from a construction product should preferably be determined under conditions reflecting a relevant use scenario of the product.

A full characterisation of leaching properties of the construction product addresses both the total potential release and also the release pattern (behaviour) as a function of time. Total potential release means here total “release burden” from construction products in a specific construction and within a chosen timeframe (e.g. total flux from a lighting column under its lifetime). The evaluation of the release behaviour needs also to take into account the effects of changes in material properties (e.g. material ageing) as well as external factors such as site specific conditions in intended use and other sources of dangerous substances.

Environmental assessment of a construction product in this context includes an assessment of the emissions/release of dangerous substances from the product during the intended use and transport to a local or near-field receptor or a far-field receptor. Local or near-field receptor refers to soil or groundwater etc. relatively close to the construction product may be even right at the edge of the construction product. A far-field receptor on the other hand is a point that is located at a larger distance from the construction product. However, it will be at this reference point that the release of substances is compared with e.g. regulatory limit values.

A wide environmental assessment study focuses not only on the release of hazardous substances but also other aspects such as the consumption of raw materials and energy, emission of greenhouse gasses, and production and recycling of waste. Thus every step of Figure 1 will be taken into account, and the assessment is carried out from a lifecycle perspective. This is the proposed scope of a revised and modernised community regulation on constructions products - Constructions Products Regulation (CPR). Results from ER3 testing and assessment of today may in the future be a part of input data needed for lifecycle considerations (LCC) of construction products or a risk assessment .

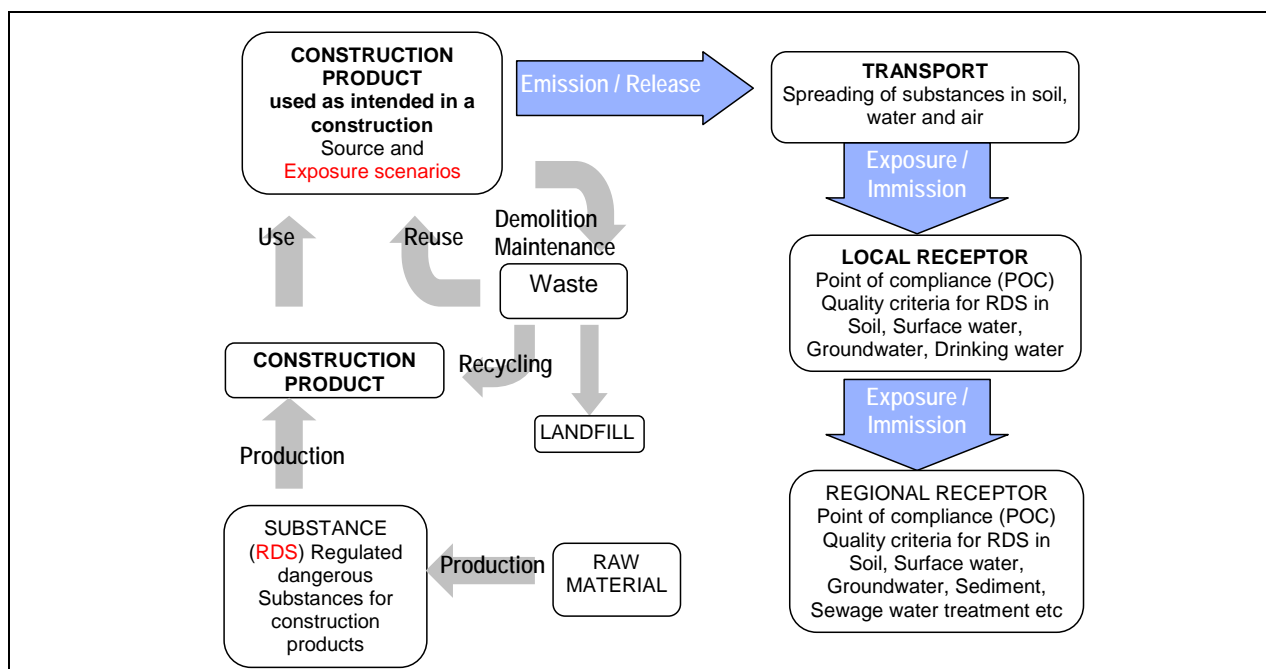


Figure 1 – Impact to be included in a complete life-cycle consideration of construction products starting from production and ending with disposal.

4. FUTURE WORK

The basis for the evaluation of sustainable construction products is to identify the priority substances in construction products/materials that are or will in the future be restricted or be of concern because of the new legislation or environmental safety targets set at the EU level. One of the key issues in the future will be to develop guidance values for interpretation of test results and to have knowledge on which specific Nordic features (e.g. soil type, background levels, intended use) could give rationale for a lower or higher emission criteria.

Release of substances from construction products need in the future to be part of LCA in order to prove the low risks of construction products. Here it is important that Nordic conditions are highlighted in scenario developments and calculations.

Furthermore, it is also important in development of construction products to take into account the recyclability of construction products arising from renovation. Especially the selective demolition will be crucial to ensure that the high quality of waste streams arising in the renovation work and minimises the amount of waste to be disposed. Both the technology for material recovery and the development of recycling concept (new technologies for recovered materials) will need even further attention.

REFERENCE

1. Wahlström, M., Laine-Ylijoki, J., Kaartinen, T., Rautiainen, L., Hjelmar, O., Oberender, A., Bendz, D., Wik, O., Gustafsson, H., Engelsen, C.J. & Birgisdottir, H. 2010. Handbook: Environmental assessment of construction products – an introduction to test methods and other procedures related to CE -marking. Nordtest Technical report 618, Nordic Innovation Centre. Oslo. Norway

Compatibility of concrete flooring systems with LEED and BREEAM sustainable construction guidelines



Kaspars Kravalis
M.Sc., R&D Director
Primekss
3 Smerla street, Riga, Latvia
kaspars.kravalis@primekss.com



Jānis Ošlejs
CEO
Primekss
3 Smerla street, Riga,
Latvia
janis.oslejs@primekss.com

ABSTRACT

This paper compares compatibility of different industrial concrete flooring systems with requirements laid out in LEED and BREEAM and points towards flooring systems that are better from the perspective of the international environmental certification standards. Such guidance might be important for some environmentally conscious customers and contractors choosing the right type of floor for their buildings.

Key words: Concrete flooring systems, CO₂ emissions, LEED, BREEAM, PrimeComposite

1. INTRODUCTION

Construction industry today must answer to the societal demands for sustainable practices. It is well known that concrete industry is a major source of CO₂ emissions. With the advent of global warming, building practices that avoid excessive generation of CO₂ gases, both during construction and usage phase, are gaining ground globally. Steps need to be taken to reduce these emissions in every branch of concrete production and usage.

LEED and BREEAM are industry leading environmental certification systems. Both systems, besides CO₂ emissions, evaluate various other aspects of sustainable construction. Leadership in Energy & Environmental Design (LEED) is an internationally recognized green building certification system, providing third-party verification that a building or community was designed and built using strategies intended to improve performance in metrics such as energy savings, water efficiency, CO₂ emissions reduction, improved indoor environmental quality, and stewardship of resources and sensitivity to their impacts. It is developed by the U.S. Green Building Council, LEED is intended to provide building owners and operators a concise framework for identifying and implementing practical and measurable green building design, construction, operations and maintenance solutions. BRE Environmental Assessment Method (BREEAM) is a voluntary measurement rating for green buildings that was established in the UK by the Building Research Establishment (BRE).

Both systems are awarding points for CO₂ emissions saving when speaking about concrete in new projects. Concrete is the most voluminous manufactured product in the world with the annual consumption approaching 20 000 million tons. The carbon emissions associated with concrete use are mostly attributable to cement production [1]. Manufacturing process releases 1 ton of CO₂ per ton of clinker.

Sustainability of cement can be reached using minimizing the consumption of concrete through innovative architecture, using less cement in concrete mix designs and less clinker in cements.

2. METHODS

Concrete as a material has two drawbacks. It is weak in elongation and it shrinks during hardening, which results in cracks and curling. Concrete industry solves these circumstances by adding steel. The first idea was to use steel bars, which later was superseded by idea to use steel fibers.

A typical design for industrial slab-on-ground for, say, heavily – loaded warehouse could be 200 mm if reinforced using steel bars, 170 mm, if reinforced using steel fibers, and 100 mm if produced using PrimeComposite. As can be seen from this example, PrimeComposite saves very significant amounts of cement.

Primekss has succeeded to create concrete (PrimeComposite) that is tough, durable and more like steel. Our pioneering application of very large amounts of fibers in a special concrete matrix enhanced by proprietary chemicals, builds up concrete that is highly ductile yet with eliminated shrinkage. PrimeComposite is so strong it does not need traditional steel reinforcement bars.

PrimeComposite is especially suitable for industrial floors. It is also used in foundation rafts, pavements, suspended slabs on piles, suspended elevated slabs and even multistory steel fiber reinforced concrete (SFRC) buildings. The complete elimination of traditional rebars and meshes together with the elimination of the time and planning for their installation.

However, the environmental benefit from using PrimeComposite is derived from the fact that the ground-bearing elements produced using PrimeComposite can be made substantially more slender due its improved strength. The slenderness allows for reduction of the concrete consumption and thus savings of CO₂ are achieved.

The methods how CO₂ emissions through PrimeComposite are reduced - less cement per m³ keeping same concrete compressive strength and less concrete per m² due to fact it is more durable and stronger. It is possible to use less cement because of concrete matrix is build with more and larger aggregates, it is more even and with high dosage rates of steel fibers. Thank to better fatigue endurance, improved shrinkage and crack control, increased tensile, compression, shear and flexural strength, improved ductile behavior after matrix failure, it is possible significantly reduce floor's slab thickness and it saves CO₂.

Being friendly to nature, good value to customer and strong, built to last, is the Nordic approach - our EKO-EKO Economy+Ecology philosophy. LEED and BREEAM envisage awards of certification points for reduction of concrete usage and thus CO₂.

LEED states that 4 points are available through Innovation Credits if the reduction in cement usage through better design reaches 40 per cent [2]. BREEAM recommends earn some of 15 credits what comes from CO₂ emissions saving [3].

PrimeComposite design is innovative and allows for reduction of more than 40 per cent, as typically it is possible to construct a floor 100 mm thick, where a traditional design would envisage 170 mm.

Such LEED points are unavailable when choosing other concrete flooring systems. Our care for environment does not stop there. We use steel fibers that are 80% produced from recycled steel, use no VOCs. Such practices also contribute towards strategy of working in environmentally friendly way.

This is typical PrimeComposite load bearing capacity:

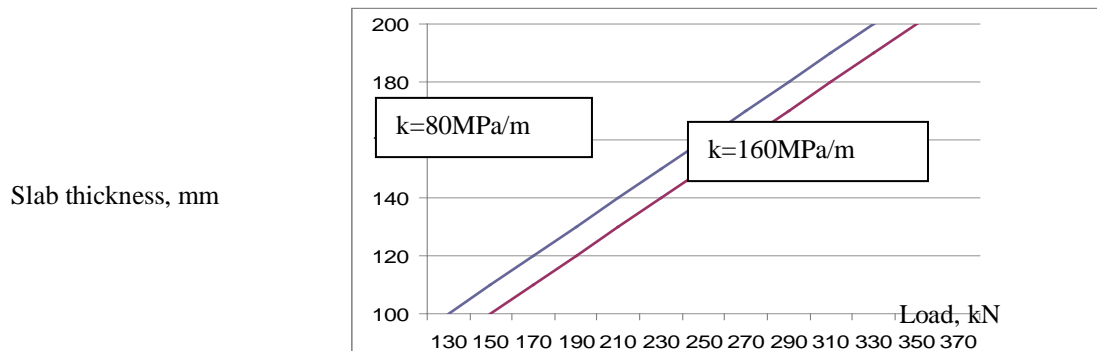


Figure 1 – PrimeComposite load bearing capacity

Following chart shows how many CO₂ emission tons it is possible to save using PrimeComposite for standard 10 000m² logistic center concrete floor building.

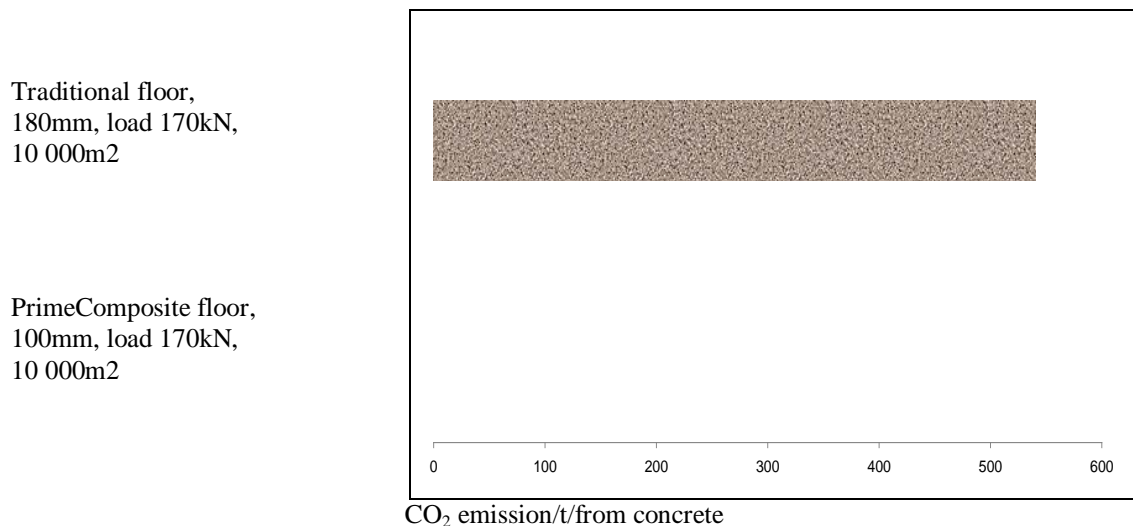


Figure 2 - CO₂ emission tons compare traditional and PrimeComposite

56-day or even 90-day strength requirement instead of traditional 28-day is one more possible tool for significant reducing of cement content. Many of concrete are consumed by structural elements that are rarely subjected to serious loads in the first months after installation.

3. CONCLUSIONS

LEED and BREEAM are the leading certification authorities promoting sustainable Construction practices with the aim of reducing man-made CO₂ emissions.

PrimeComposite, due its superior strength, is installed at lower thicknesses, which allows for reduction in cement consumption and thus CO₂ emissions.

REFERENCES

1. Kumar Mehta, P., Meryman, H., "Tools for Reducing Carbon Emissions Due to Cement Consumption," *Structure Magazine*, January 2009, pp 11-15.
2. Portland Cement Association, 'Building Green with Concrete', see at http://www.cement.org/buildings/green_leed.asp [cited 2011-03-07]
3. BREEAM Global, 'BREEAM Scheme Document SD5068, Issue 1.1', 2010, 310 pp.

Discoloration of White Concrete Containing Photoactive TiO₂



Anna Kronlöf
Dr. (Tech.), Senior Research
Scientist
VTT Technical Research
Centre of Finland
anna.kronlof@vtt.fi



Liisa Salparanta
M.Sc. (Tech.), Research
Scientist
VTT Technical Research
Centre of Finland
liisa.salparanta@vtt.fi



Tapio Vehmas
M.Sc. (Tech.), Research
Scientist
VTT Technical Research
Centre of Finland
tapio.vehmas@vtt.fi

ABSTRACT

Photoactive titania is able to activate chemical reactions in the presence of UV radiation by producing a free electron and an electron hole. These can activate e.g. decomposition of organic compounds and oxidation. This phenomena has inspired the development of new products that possess so called photoactive functional surface properties. Being a fine powder, titania needs to be bound with some kind of adhesive material. Organic binders have the disadvantage of becoming potentially decomposed in the course of the photoactive reactions, whereas inorganic binders remain intact. Cement (OPC) as the most widely used binder would be one obvious choice. White mortar samples containing titania (TiO₂) were found to turn yellow during the exposure to UV-light both in outdoor and laboratory conditions. The discoloration could harm the visual appearance of high quality concrete surfaces if not taken into consideration while selecting the titania type. Key words: Photoactivity, UV exposure, titania, concrete, discoloration

Keywords: Titania, photoactivity, functional surface, discoloration

1. INTRODUCTION AND OBJECTIVES

Photoactive titania is able to activate chemical reactions in the presence of UV radiation by producing a free electron and an electron hole. Those can activate e.g. decomposition of organic compounds and oxidation of NO_x. This phenomenon has inspired development of new products that possess so called photoactive functional surface properties. Being a fine powder, titania needs to be bound with some kind of adhesive material to the product. Organic binders have the disadvantage of becoming potentially decomposed in the course of the photoactive reactions whereas inorganic binders remain intact. Cement (OPC) as the most widely used binder would be one obvious choice. White mortar samples containing titania (TiO₂) were found to turn yellow under the exposure of UV-light both in outdoor and laboratory conditions. The discoloration could harm the visual appearance of high quality concrete surfaces if not taken into consideration while selecting the titania type. The objectives of the present study were to investigate white mortar surface discoloration in outdoor conditions, to verify the discoloration lab conditions and to identify the conditions and components required to produce the discoloration.

2. MATERIALS AND EXPERIMENTAL SET UP

Tables 1 and 2 give information on the titanias and mortar mixes used. According to the XRD analysis both titanias were well crystallized anatase. The peaks of titania B were clearly wider, indicating smaller crystallite size. DTG measurement revealed about 3 times larger weight loss of titania B within both of the temperature ranges, 25 – 173 °C (8.45 w %) and 173 – 700°C (3.87 w %), compared to titania A (2.39 and 1.16 wt %). The first weight loss was attributed to free moisture and the second one bound water or hydroxides (Mettler TGA 851e). In the filtered specimens the reference material to white cement was pure precipitated calcium carbonate (PCC, product name "Calofort U") produced by Specialty Minerals. Iron oxide was Fe₂O₃, a fine powder produced by Merk Chemicals by the product code 3924. All colorimetric measurements were with a Minolta spectrophotometer CM -525i.

Table 1. Titanium dioxides used in the tests. The batches as well as their chemical composition were delivered by Sachtleben Pigments.

Property	Titania A	Titania B
Crystal Form	Anatase	Anatase + Ti hydroxide
Crystal size [nm]	10 – 30	6
Specific surface area [m ² /g]	70 – 120	250 – 350
Particle size (d50) [µm]	1 – 3	1 – 2
pH-value (approx.)	4 – 7	5 – 7
TiO ₂ content (approx.) [%]	99	> 85
S content [%]	< 0.4	< 0.3
Fe [mg/kg]	< 70	< 70
Na [mg/kg]	< 250	< 1000

Table 2. Mortars.

Component	Content
White OPC (Aalborg White)	600 - 700 kg/m ³
Water	240 – 280 kg/m ³
Aggregate (White limestone R22 0-2 mm by Finnsementti)	1300 – 1500 kg/m ³
Superplasticizer (Glenium 51 by BASF, 17.5 %)	6 kg/m ³
Titania 0-12 w% (of cement) *)	0 - 84 kg/m ³

**) Part of the water, superplasticizer and TiO₂ were mixed to produce a "milky" suspension prior to adding to the mix*

2.1 UV exposure of mortars

The mortar specimens were cured in the dark at T 20 ± 2 °C, RH 40 % until the age of 14 months. In the outdoor conditions the specimens were at a 45 degrees inclination, tested surface on top, facing south, close to a motorway in Espoo (Helsinki area), Finland. The outdoor storage started in August 2006 and ended in February in 2009. In lab conditions the mortar specimens were subjected to cyclic treatment consisting of UV radiation, rain and darkness. The filter combination was selected to simulate the UV radiation of a cloudy summer afternoon in the Helsinki area. The duration of 5.5 cycles corresponded to the UV and rain of one summer month.

2.2 Preparation and UV exposure of filtered specimens

The filtered specimens were prepared by filtering the tested material combinations on a glass fiber from a dilute water suspensions. No aggregate was used in the filtered specimens. This technique allowed the preparation of samples also without OPC. The thickness of the cake was approximately 3 mm. In the first stage UV exposure the filtered specimens were placed between two acryl plates (thickness 3 mm) into a UV chamber that enabled uniform radiation. Each sample was followed by one reference sample covered by aluminum foil in order to block the UV-light (Figure 1). The chamber test was cyclic, with each cycle consisting of 8 h of UV radiation in a dry atmosphere followed by 4 h of condensation in vapor. After the first stage, the specimens were exposed to the second stage UV radiation in outdoor conditions in a horizontal position on the roof of VTT research facility for 66 days starting in June 2009.

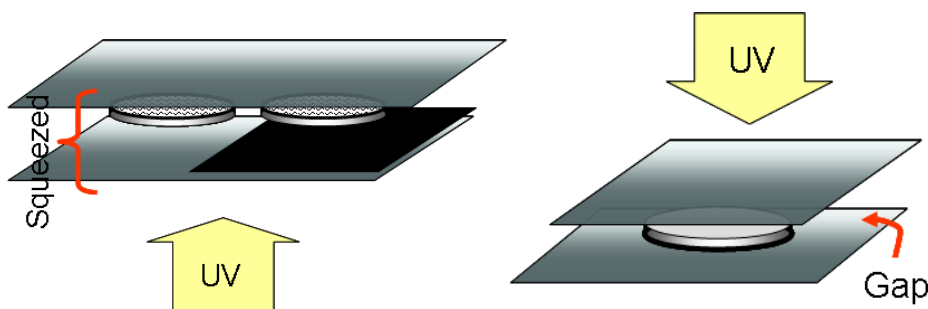


Figure 1. Schematic presentation of the 1st stage UV exposure of the filtered specimens on the left and second stage on the right. In the first stage the total duration of cyclic test was 800 hours: 533 h in UV and 267 in dark. The acryl plates and sample holder were squeezed together, which limited the access of H₂O, CO₂ as well as other environmental gasses to the specimens. In the 2nd stage the samples on VTT roof top in the Helsinki area for 66 days in summer 2009.

3. RESULTS

During the first seven month period which fell to the dark seasons the color of all mortars changed. The specimens darkened slightly (dL) and their increased chromaticity was mainly caused by the yellow component. Over the whole measuring period the marked color change of the titania A containing samples could be divided into stepwise increase of the yellow shade during the strong UV exposure of the summer period (Figure 2) and continuous but diminishing darkening regardless of UV-exposure. The darkening in the traffic area is mainly caused by the accumulation of soot particles. Over the same period the darkening of titania B containing samples was rather diminishing than increasing and chromaticity due to yellowing stayed at a constant level. The results in lab conditions showed that the yellowing was caused by titania (Figure 3). The results of the filtered specimens can be given here only as a condensed conclusions (below), but will be published elsewhere.

4. CONCLUSIONS

- White cement mortars made with photoactive titania A showed a clear yellow discoloration tendency in outdoor and lab conditions when exposed UV radiation.

- In outdoor conditions the yellow shade of the mortars made with titania A increased in a stepwise manner, with summer season being more effective than winter.
- The mortars made with titania B clearly showed less yellowing tendency, being very close to that of the references.
- The discoloration was related to the presence of cement because calcite titania A suspension filtered on a glass fiber filter did not turn yellow in similar conditions.
- Without titania, white cement faded when exposed to UV radiation.
- The superplasticizer tested (Glenium 51) did not cause discoloration. It rather faded than turned increasingly yellow in UV-exposure.
- The presence of iron oxide diminished the effect of UV radiation.

This research was done as a part in of two projects: SIPI (Internal surfaces of mineral based functional materials), collaboration with VTT, Aalto, and Åbo Akademi, funded by VTT, TEKES, Nordkalk Oy Ab, Cementsa Ab and Tikkurila Oyj and NANOCRETE funded by Cementsa Ab and Sachtleben Pigments.

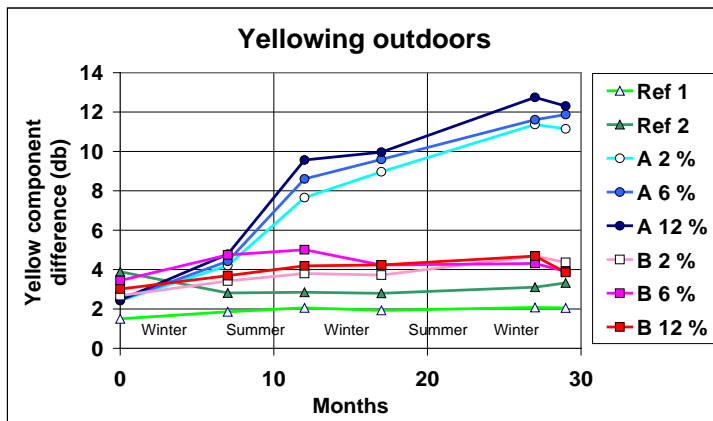


Figure 2. The yellow component difference db of mortar surfaces compared to absolute white in outdoor conditions starting in August 2006 and ending in February 2009.

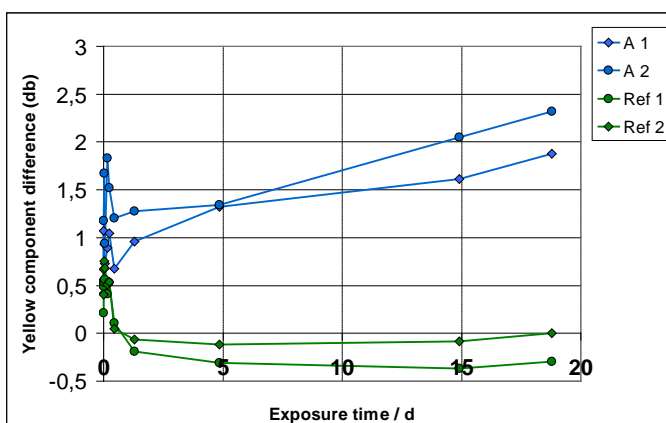


Figure 3. The yellow component difference db of mortar surfaces compared to absolute white in laboratory UV climate chamber experiments. Climate chamber environment was according ISO4892-2. Ref 2 and sample A 2 contained 2% (by weight of cement) zinc stearate.

Load carrying capacity of a RC Bridge in Örnsköldsvik, Sweden



Arto Puurula, Tekn. Lic. LTU and
Principal Lecturer in Structural
Engineering, Savonia University of
Applied Sciences, Opistotie 2, Box 88,
FIN-70101 Kuopio, Finland
Email: Arto.Puurula@savonia.fi
Ola Enochsson, Tekn. Lic., LTU
Gabriel Sas, MSc., LTU



Björn Täljsten, Tekn Dr., Prof.
Lennart Elfgren, Tekn. Dr., Emeritus
Prof.
Div. of Structural Engineering,
Luleå University of Technology,
SE-971 87 Luleå, Sweden
Email: Name.Name@ltu.se

ABSTRACT

A reinforced concrete railway trough bridge has been strengthened and loaded to failure. The aim was to test and calibrate methods developed in the European Research Project “Sustainable Bridges” regarding: (a) condition appraisal and inspection, (b) load carrying capacity, (c) monitoring and (d) strengthening.

A failure in combined shear, bending and torsion was reached for an applied mid span load of 11,7 MN. 3D-non linear FEM calculations with discrete reinforcement have been used to simulate the loading process. The developed calculation methods give accurate predictions of the response of the bridge during the increasing loading.

Key words: Bridge, Shear, Strengthening, Ultimate load carrying capacity, Failure



Figure 1 - View of tested bridge in Örnsköldsvik in northern Sweden.

1. INTRODUCTION

Field tests have been carried out on an existing reinforced concrete railway bridge in a European Research Project “Sustainable Bridges”. The aim of the project was to develop improved procedures and methods for inspection, assessment, monitoring and strengthening of railway bridges. A consortium, consisting of 32 partners drawn from railway bridge owners, consultants, contractors, research institutes and universities carried out the Project during 2003 – 2008, see SB [1] and www.sustainablebridges.net.

The bridge presented in this paper was loaded to failure to demonstrate and test methods developed in the project. The bridge was a reinforced concrete railway trough bridge in the form of a frame with two spans 12+12 m, see Figure 1. It was located in Örnsköldsvik in northern Sweden. It was built in 1955 and was taken out of service in 2005 due to the building of a new high-speed railway, the Botnia Line. The bridge was planned to be demolished in 2006 and this gave the opportunity to test it to failure before that.

2. MATERIAL PROPERTIES AND MONITORING

In order to prevent an unwanted flexural failure, the bridge slab was strengthened with bars of Carbon Fibre Reinforced Polymers (CFRP) Sto FRP Bar M10C with a length of 10 m, see Figure 2. In Table 1 a summary of material properties is presented.



Figure 2 – Grooves were sawn in the bottom of the slab (15×15 mm) and then filled with an epoxy and 9 + 9 = 18 rectangular bars of CFRP (10×10 mm) in order to enhance the flexural resistance of the slab. The bars had a modulus of Elasticity $E_f = 250$ GPa and a rupture strain $\varepsilon_r = 11\%$. The bars were mounted as Near Surface Mounted Reinforcement (NSMR) in sawn out grooves spaced at 100 mm distances at the soffit of the decking slab.

Table 1 - Summary of material properties.

Stage	Type of value	Concrete				Steel		
		f_c [MPa]	E_c [GPa]	f_t [MPa]	G_F [Nm/m ²]	$f_{sy} = R_{eh}$ [MPa]	$f_{su} = R_m$ [MPa]	E_s [GPa]
Initial properties <small>(These values are assumed or taken from original drawings)</small>	Characteristic	31	32	1.8	-	Ø16: 410 Ø 25: 390	Ø 16: 500 Ø 25: 500	Ø 16: 200 Ø 25: 200
		Mean properties based on tests <small>(Standard deviations are given in parenthesis)</small>	Mean	68.5 (8)	25.4 (1.7)	2.2 (0.5)	154 (82)	Ø 16: 441 (12) Ø 25: 411 (8.2)



Figure 3 – A shear-bending failure was initiated by loss of bond between the epoxy resin used to embed the carbon fibre reinforcement, NSMR in the grooves, and concrete followed by rupture of a stirrup after yielding (photo to the right). The shear-bending crack went through the entire bridge and the corresponding stirrup ruptured also on the other side of the bridge; see Figures 4 and 7, where the failure process started.

3. ASSESSMENT WITH A NON LINEAR 3D-MODEL

The Övik Bridge was modeled with a non linear 3d model presented in Figures 4-7 using Abaqus based Brigade software.

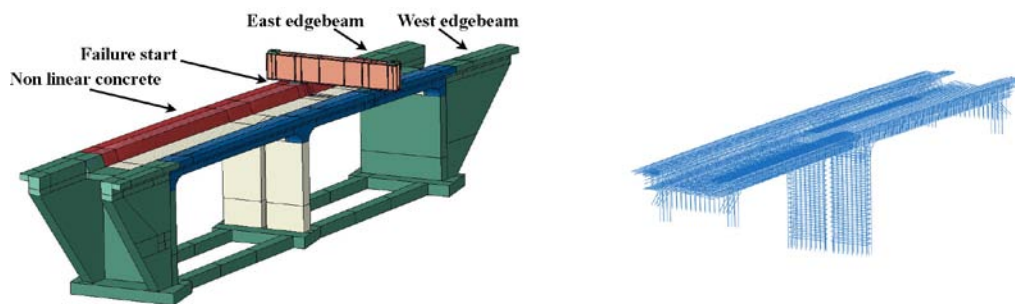


Figure 4 – Failure started in the East edgebeam. Concrete in the green parts of the bridge is elastic, concrete in other parts of the bridge is non linear. Non linear calculation means calculation in the cracked stage with non linear discrete reinforcement (picture to the right) added in the model.

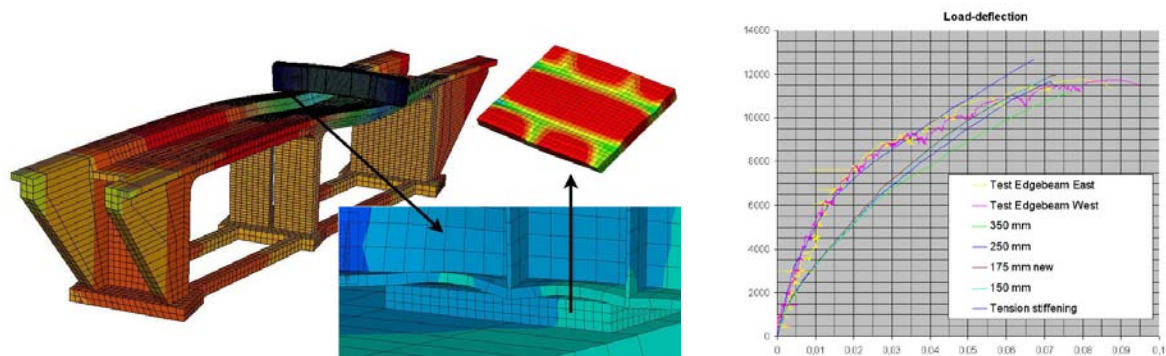


Figure 5 – Left: Displacements. Also the contact between steel beam and the bridge is illustrated. Right: Load-deformation diagram. An element size of 175 or less doesn't affect the result. Including the tension stiffening in the reinforcement material definition gave a stiff enough response close to the load-deflection curve from the test situation.

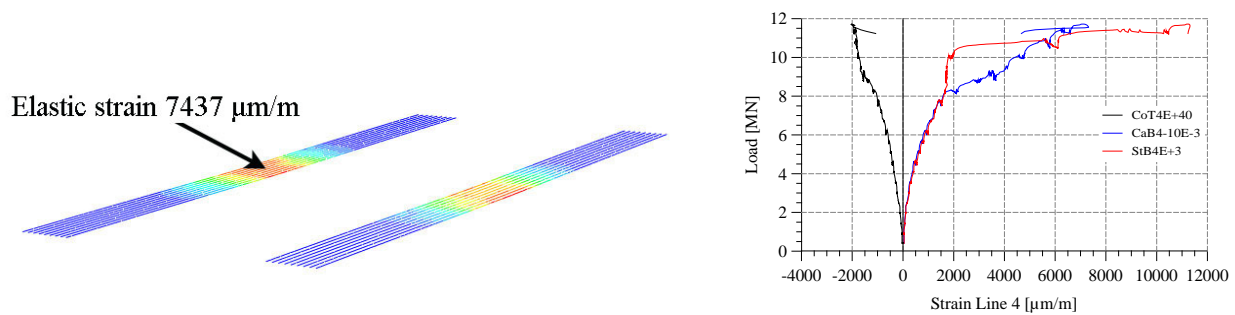


Figure 6 – Left: Elastic strains in the carbon fibre reinforcement, NSMR. Right: Strains in concrete, carbon fibre bars and reinforcement in the mid span of the east beam. The calculated strain, $7437\mu\text{m/m}$, correspond well to the measured strains, the blue curve, CaB 4 + $10E-3$.

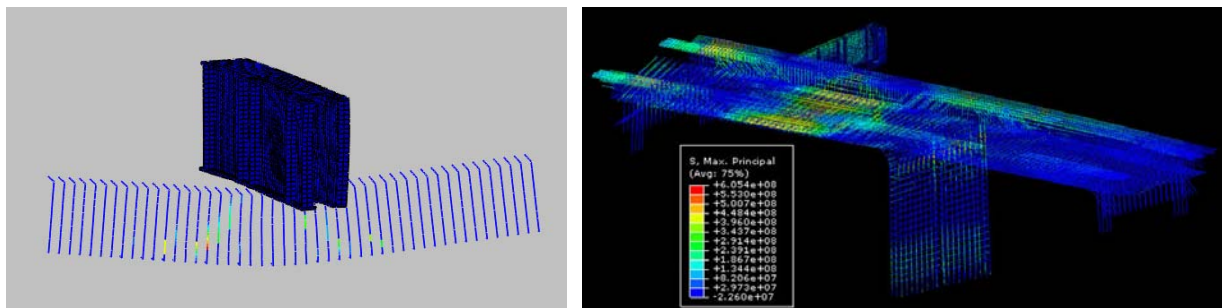


Figure 7 – Left: Plastic strains in the stirrups in the East edgebeam. The location of the maximum strain coincides with the ruptured stirrup. Right: The principal stresses of the reinforcement at test failure load.

4. SUMMARY AND CONCLUSIONS

In this paper focus has been on the assessment of the load carrying capacity. In the final test, a failure in combined shear, bending and torsion was reached for an applied mid span load of 11,7 MN. The failure was initiated by loss of bond between epoxy resin and concrete followed by rupture of a stirrup. The behaviour of the bridge during increasing load can be closely predicted with the calibrated 3D non linear finite element method model up to load when the bond failure occurred. It is easy to see the response of the bridge when a one to one model with discrete reinforcement is used. The method developed described in this paper can be used to get close estimations of the load carrying capacity of concrete bridges e.g. for trainloads.

REFERENCES

1. SB (2007): *Sustainable Bridges – Assessment for Future Traffic Demands and Longer Lives*, A European Integrated Research Project during 2003-2008 within FP6, No TIP3-CT-2003-001653, see www.sustainablebridges.net. Four guidelines have been prepared. Background documents with state-of-art reports, analytical and numerical analyses and test results are also provided. [cited 2011-01-30].

Session A2 – MODELLING AND TESTING

Chloride Diffusion Study made from the Pre-Testing of Oresund Bridge Mix Proportions



Carmen Andrade
Centre for Safety and
Durability of Structures and
Materials.
CSIC-UPM. Madrid. Spain
andrade@ietcc.csic.es



Esperanza Menendez
Institute of Construction
Sciences- “Eduardo Torroja”-
CSIC-Madrid- Spain
emm@ietcc.csic.es

ABSTRACT

Oresund Bridge was built before the year 2000 and the concrete spans were fabricated in the south of Spain. In present paper are given results of chloride penetration measured through the APM 302 and ASTM 1202 tests in the mix proportions prepared for the concrete elements. From several of the spans not finally transported to the site, two pieces were cut and transported to a beach in Huelva in the Atlantic south cost of Spain. The results indicate that the profiles in the pretesting are very different from those found in the spans after 7 years exposure. The Surface concentration in the tests was much higher than in the real exposure. Some comments are made on the use of the results for modelling the chloride penetration in real conditions.

Key words: chlorides, modelling, oresund, aging.

1. INTRODUCTION

In marine environments, chloride can penetrate concrete cover and provoke reinforcement corrosion. Testing resistance of concrete to chloride ingress and modelling of its evolution are fundamental tools for the prediction of service life [1-4]. In the case of Øresund bridge no modeling was prescribed in the design phase for chloride ingress risk. It was preferred instead a performance approach. This approach consisted in specifying tests and threshold values to be fulfilled by the concrete mixes in a program of pre-testing. The nominal service life was of 100 years. In present paper are presented some of the results of chloride ingress obtained in some of the mixes tried in the pre-testing program as the experiments regarding chloride resistance were carried out at the Institute of Construction Science “Eduardo Torroja”, IETcc, in Madrid. The results have been treated to know the some aspects related to the possibility of using the values for predicting future performance of the concrete and in particular in present paper, the relation between free and combined chlorides are analyzed.

2. EXPERIMENTAL

Øresund link between Denmark and Sweden was agreed in 1991 and the Øresund Bridge was inaugurated in July 2000. It is composed of a high bridge and two approach bridges (Figure 1). The high bridge has the longest cable-stayed main span in the world for both road and rail traffic. The bridge two-level superstructure is fabricated from steel and concrete. The steel girder supports the upper deck, which accommodates the motorway, and the lower deck where

the railway is located. The tracks are placed in a concrete trough along the approach bridges, which changes to a steel deck on the high bridge. For this bridge, Grupo Dragados, S.A, of Spain supplied the spans [5] for the two approach bridges to the central cable-stayed bridge (figure 2), in 42 spans 140 m long plus seven spans 120 m long, making a total of 6.7 kilometers. The spans were manufactured at the facilities of Dragados Off-Shore, S.A., in Cadiz bay (Spain) and transported to the place by shipping (figure 2).

Two pieces of these spans taken from some not translated to the bridge place were placed in a beach near Huelva harbor in the south of Spain. Huelva is near Cadiz and this beach is a site experimental station of the IETcc where other concretes and specimens are exposed to the tide of the sea for long term observation. Figure 3 shows a general view of the beach with other concrete blocks and the Øresund spans pieces (small and large). Periodic inspections are carried out in which cores are drilled and the reinforcement corrosion is measured.



Figure 1 General view of Øresund Bridge



Figure 2 Transport of spans from Cadiz- Spain



Figure 3.- Left: Site experimental station of IETcc in a beach in Huelva-Spain. Center Right: An aspect of the small pilot Øresund block during the measurement of reinforcement corrosion.

2.1. Materials

Table 1 shows the concrete composition:

Microsilica ("slurry")	29 kg/m ³	under 5% of the weight of the cement
Water	139 kg/m ³	with the maximum chloride content limited to 600 mg/l,
Plasticising agent	0.76 kg/m ³	
Air-entraining agent	0.45 kg/m ³	
Sand 0-2 mm	624 kg/m ³	The aggregate used was granite originating from the province of Madrid, from the Pola quarries for the 2-6, 6-12 and 12-25 mm sizes and from the Jaramasa quarry for the 0-2 mm sand
Aggregate 2-6 mm	137 kg/m ³	
Aggregate 6-12 mm	438 kg/m ³	
Aggregate 12-32 mm	564 kg/m ³	
Cement	380 Kg/m ³	Portland type CEM I 42.5 or CEM I 52.5 cement

The requirement for compressive strength in 15x30 cm cylindrical specimen had to be over 50 MPa, and an entrained air content of over 3%. The nominal cover depth was of 75 mm in the external faces in above the splash zones. Other smaller cover depths were also specified (30 and 50 mm). In present paper are given results of some of the mixes tested during the pretesting and some of the mortar and concretes to be qualified for repairing. The samples were specimens and cores drilled from spans. In present work the results of Diffusion tests after curing and at 7 years of exposure to the action of natural sea water in a beach are reported for the sake of comparison.

Two tests were prescribed: ASTM C 1202-94 standard and the Danish standard APM 302. The threshold value of the diffusion coefficient calculated from the chloride profile was of $2 \times 10^{-12} \text{ m}^2/\text{s}$ and the Coulombs should be smaller than 1000. The value of the D_e is calculated from the initial resistivity obtained from the current circulating in the ASTM C1202 test applying [6] the formula: $D_e = \frac{23 \cdot 10^{-5}}{\rho}$ and the D_a values from the APM 302 ones. In the case of the spans in the beach the resistivity has been obtained by means of the disc method incorporated in the GECOR 08 corrosion rate meter.

For the calculation of the bound and free chloride ratio only lineal binding has been considered. Although non lineal binding is the expected real behavior, in present paper due the uncertainties of the relatively few experiments only the equation suggested by Atkinson and Nickerson [4] has been used.

3. RESULTS

In figure 4 are given some of the profiles obtained in the specimens/cores with the APM 302 test and those of the cores drilled in the spans placed in the beach.

It can be commented that the resistivity values measured in the laboratory specimens are in general in the order but in the lower range than those measured in the spans alter 7 years.

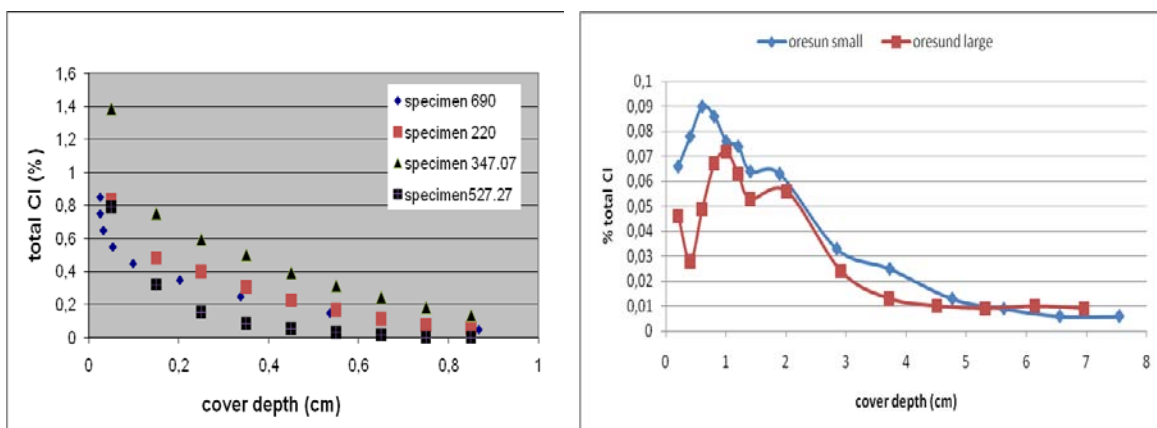


Figure 4 Left: Examples of Chloride profiles obtained in the specimens for the pretesting. Right Left small-span and large-span profiles after 7 years of exposure

4. DISCUSSION

The results in the spans submitted to the real action of the sea show that the penetration has been of several cm, as is appreciated in figure 4 but very low values of surface concentration and Da values are recorded. In the case of the specimens/cores tested in the laboratory during the pretesting, the Da values measured are also low although a bit higher, but almost all of them fulfilled the threshold value given in the specification of being smaller than 2E-13 m²/s. Oppositely to the real exposure the Cs is very high in the laboratory tests and then any prediction from these high values would have aimed into erroneous calculations. In the reality the performance has been much better than in the pretesting and then, the disagreement is from the safe side.

On the opposite, the values of resistivity obtained in the laboratory and in the spans in the beach present a much better accordance and seem to show an aging as they are higher in the spans than

in the short term test. Aging factors [7] have been calculated from: $\rho(t) = \rho_0 \cdot \left(\frac{t_i}{t_0} \right)^q$. The aging

factor q calculated from the resistivity is not exactly the same than that calculated from the change in Da value as justified in [7]. The values obtained ranged from 0.1 to 0.39.

4.1. Prediction of life

For the sake of making some predictions, either the error function equation, the time lag equations have been used, neglecting an aging action because it is on the safe side.

Table 2 Some examples of calculation of time to corrosion neglecting any aging effect or binding (formula 7). Cover depth considered was 75 mm.

	Cs	Cx	Da m ² /s)	Time life (years)
Error function Equation	0.07	0.03	0.629E-12	206
Time lag Equation			0.629E-12	142
Time lag Equation			0,397E-12	224.6

In table 2 are given the results. They indicate that the life of 100 years may be feasible for the covers of 75 mm providing no cracks are present. It is necessary to end accepting that this exercise is very simplified and approximated but it indicates that the concrete specified and fabricated seem to be a good mix for the life requested.

5. CONCLUSIONS

Although numerous simplifications have been assumed for the exercise here presented, the results analyzed enable the following main conclusions:

1. The pilot spans held for 7 years in a beach in the south of Spain show very low Apparent Diffusion coefficients Da, and very low chloride concentrations in the profiles.
2. The APM 302 test used in the pretesting on the opposite gave much higher chloride profile concentrations.
3. The ASTM C1202 test was giving values of resistivity that are lower but in the same order of magnitude than those measured on the pilot spans and therefore seem more reliable to predict service life of reinforcements.

ACKNOWLEDGEMENTS

The authors are grateful to Dragados Group for the funding of the pretesting and for providing the span pieces for long term observation.

REFERENCES

1. O. V. Gjorv, O. Vennesland. Diffusion of chloride ions from sea water into concrete. *Cement and Concrete Research* vol 9 (1979)229-238.
2. Page, C.L. Short, N.R. and Tarras, A., "Diffusion of chloride ions in hardened cement pastes". *Cement and Concrete Research*, 11, (3) (1981) 395-406.
3. Mangat, P.S., Molloy, B.T.(1994): Predicting of long term chloride concentration in concrete. *Materials and Structures*, Vol. 27, pp. 338-346.
4. A. Atkinson; A. K. Nickerson,: "The diffusion of ions through water-saturated cement". *Journal of Materials Science*, 19, (1984) 3068-3078.
5. G. Serrano, J. Obregón, J. Rodríguez, P. Trigo, F. Hué y L. Peset, Manufacture of spans for the Öresund bridge between Denmark and Sweden. *Hormigón y Acero*, nº 230, 4º Trimestre, 2003
6. Andrade, C., 'Calculation of chloride diffusion coefficients in concrete from ionic migration measurements' *Cement and Concrete Research*, 23 (3) (1993) 724-742.
7. C. Andrade, M. Castellote, R. d'Andrea.- measurement of aging effect on chloride diffusion coefficients in cementitious matrices. *Journal of Nuclear Materials*. January (2011)

A New Safety Format for Nonlinear Analysis



Hendrik Schlune
Ph.D. student
Concrete Structures
Chalmers Uni. of Technology
SE – 412 96 Gothenburg
Sweden
hendrik.schlune@chalmers.se



Sven Thelandersson
Professor
Structural Engineering
Lund University
SE – 221 00 Lund
Sweden
sven.thelandersson@kstr.lth.se



Mario Plos
Associate Professor
Concrete Structures
Chalmers Uni. of Technology
SE – 412 96 Gothenburg,
Sweden
mario.plos@chalmers.se



Thomas Svensson
Researcher
Building Tech. & Mechanics
SP, Technical Research
Institute of Sweden,
Sweden
thomas.svensson@sp.se



Kent Gylltoft
Professor
Concrete Structures
Chalmers Uni. of Technology
SE – 412 96 Gothenburg,
Sweden
kent.gylltoft@chalmers.se

ABSTRACT

With the increasing use of nonlinear analysis of concrete structures, questions concerning an appropriate safety format have been raised. When the safety format for nonlinear analysis according to EN 1992-2 was developed a model uncertainty which corresponds to simple beam and frame analysis was accounted for. However, when the safety format is applied on more difficult to model failure modes, which result in a higher model uncertainty, the safety format leads to design resistances below the target reliability. A new safety format for nonlinear analysis was proposed which leads to better agreement with the target reliability.

Key words: nonlinear analysis, model uncertainty, safety format, reliability

1. INTRODUCTION

Concrete structures are most often analysed based on a two-step procedure. The first step consists of a structural analysis to compute sectional forces. This is usually done using mean material parameters with the intention to obtain a realistic stiffness distribution. The second step consists of the analysis of all critical components of the structure. To obtain structures with the intended reliability level, the component analysis is done using design material parameters, conservative models or both.

Today the two step procedure is more and more often substituted by a nonlinear finite element (FE) analysis. The nonlinear FE analysis gives directly the maximum resistance of the structure and the employed material laws guarantee automatically the equilibrium in all components. This means that the nonlinear FE analysis fulfils the purpose of both steps in the two step procedure.

This has raised the question about the choice of a safety format with appropriate input parameters for the nonlinear analysis, CEB Bulletin 229 [1] and CEB Bulletin 239 [2]. Mean material parameters allow to realistically model the structural response but can not be used to assure the intended reliability level. On the other hand, design material parameters can be used to assure the intended reliability level but lead to an unrealistically modelled response.

To overcome the incompatibility of realistic modelling and assuring safety, a new safety format has been introduced in EN 1992-2 [3]. The safety format allows to use realistic material parameters in the nonlinear analysis and assures the safety by using an additional safety factor, $\gamma_{d'}$. At the time when the safety format was introduced, nonlinear analyses were mainly used to analyse beams, columns and frames subjected to normal forces and bending moments. For these types of analyses the failure mechanisms is well understood and quite easy do describe numerically. This results in a small model uncertainty.

Today, nonlinear analysis is increasingly used to analyse more advanced structures with more difficult to model failure modes. A review of round robin exercises and modelling competitions showed that the model uncertainty varies considerably depending on the type of failure, [4]. For difficult to model failure modes a higher model uncertainty must be accounted for. This is not done in the safety format according to EN 1992-2 [3] which uses the same safety factors for all types of nonlinear analysis. This observation led to the development of a new safety format for nonlinear analysis which is summarised in the following and described in more detail in [4].

2. A NEW SAFETY FORMAT FOR NONLINEAR ANALYSIS

To allow for realistic modelling of the structural response, mean material parameters and nominal geometrical parameters are to be used in the nonlinear analysis to calculate the resistance, $R_m = R(f_{ym}, f_{cm, is}, f_{ctm, is}, \alpha_{nom})$, where f_{ym} is the mean yield strength of the reinforcement steel, $f_{cm, is}$ is the mean in situ concrete compressive strength, $f_{ctm, is}$ is the mean in situ tensile strength and α_{nom} represents the nominal geometrical parameters. The design resistance, R_d is obtained by division of the resistance, R_m , by a resistance safety factor, γ_R :

$$R_d = \frac{R_m}{\gamma_R} = \frac{R(f_{ym}, f_{cm, is}, f_{ctm, is}, \alpha_{nom})}{\gamma_R} \quad (1)$$

The resistance safety factor is calculated according to

$$\gamma_R = \exp\left(\alpha_R \beta \sqrt{V_G^2 + V_M^2 + V_F^2}\right) \quad (2)$$

where $\alpha_R = 0.8$ is the weight factor for the resistance according to EN 1990 [5], $\beta = 3.8$ is the target reliability index for a reference period of 50 years according to [5], and V_G, V_M and

V_F are the coefficients of variation to account for the geometrical-, model -, and material strength uncertainty.

2.1 Geometrical uncertainty

A coefficient of variation of $V_G = 5\%$ was recommended for reinforced concrete structures to account for the geometrical uncertainties, [4].

2.2 Model uncertainty

Due to the large variability of the model uncertainty, Schlune et al. [4] recommended to use a problem specific coefficient of variation which depends mainly on the failure mode and the chosen modelling approach. If no modelling guidelines are followed, the model uncertainty will often be the dominant source of the resistance uncertainty. This results in a high safety factor and less economic designs. Therefore, modelling guidelines should be developed to decrease the model uncertainty and hence lead to more economic designs. Without modelling guidelines and any information about the model uncertainty, the values given in [6] can be used as a first approximation to quantify, V_M .

2.3 Material uncertainty

To quantify the coefficient of variation to account for the material uncertainty Schlune et al. [4] proposed to use a sensitivity study. For the sensitivity study additional nonlinear analysis are needed, one with reduced steel strength to calculate the resistance $R_{\Delta f_y}$, one with reduced concrete tensile strength to calculate $R_{\Delta f_{ct}}$ and one with reduced concrete compressive strength to calculate the $R_{\Delta f_c}$. The coefficient of variation to account for the material uncertainty, V_F , can then be approximated to

$$V_F \approx \frac{1}{R_m} \sqrt{\left(\frac{R_m - R_{\Delta f_c}}{\Delta f_c}\right)^2 \sigma_{f_c}^2 + \left(\frac{R_m - R_{\Delta f_{ct}}}{\Delta f_{ct}}\right)^2 \sigma_{f_{ct}}^2 + \left(\frac{R_m - R_{\Delta f_y}}{\Delta f_y}\right)^2 \sigma_{f_y}^2} \quad (3)$$

where Δf_y , Δf_c and Δf_{ct} are the step sizes to decrease the yield strength of the reinforcement steel, the concrete compressive strength and the concrete tensile strength respectively, and σ_{f_y} , σ_{f_c} , and $\sigma_{f_{ct}}$ are the standard deviations of the associated material parameters.

3. TESTING OF THE NEW SAFETY FORMAT

To test the new safety format it was applied on numerous structures to calculate the design resistance. The same was done with the safety format for nonlinear analysis according to EN 1992-2 [3]. In a next step fully-probabilistic analysis were used to determine the probability that the resistance was below the design resistance, $P(R < R_d)$. The safety formats were tested on beams sections in bending [4], short columns [7], beam sections in shear loading, [7] and beams loaded in a combination of shear force and bending moments, [6]. The new safety format led for all structures to a good agreement with the target reliability. The safety format

according to EN 1992-2 led to good agreement with the target reliability when it was applied on beams in bending and on short columns when a small model uncertainty was assumed. However, it led to design resistances that were far below the target reliability when it was applied on structures for which a higher model uncertainty was assumed, i.e. for beams loaded in shear and beams loaded by a combination of bending moments and shear forces.

4. CONCLUSIONS

The safety format for nonlinear analysis according to EN 1992-2 leads to reliability below the target reliability when it is applied on structural models and failure modes with a high model uncertainty. The new safety format leads to better agreement with the target reliability but needs a quantification of the model uncertainty.

To decrease the model uncertainty, which allows for using smaller safety factor and hence to more economic concrete structures, modelling guidelines must be developed.

5. ACKNOWLEDGEMENTS

The authors would like to thank the Swedish Research Council, Formas and the Swedish Transport Administration, Trafikverket, for their financial support.

REFERENCES

1. CEB. "New Developments in Non-linear Analysis Methods." Comite Euro-International du Beton, Bulletin d'information No 229, Lausanne, 1995.
2. CEB. "Non-linear Analysis: Discussion Papers from the Working Party in Commission 1; Safety Evaluation and Monitoring: Discussion Papers from Task Group 1.4." Comite Euro-international du Beton, Bulletin d'information No 239, Lausanne, 1997.
3. CEN. "EN 1992-2, Eurocode 2: Design of concrete structures - Part 2: Concrete bridges. Design and detailing rules " CEN European Committee for Standardization, Brussels, 2005.
4. Schlune, H., Plos, M., and Gylltoft, K. "Safety Formats for Nonlinear Analysis of Concrete Structures." submitted to Structural Safety, June 2010.
5. CEN. "EN 1990, Eurocode - Basis of structural design." CEN, European Committee for Standardization, European Standard EN 1990, Brussels, Belgium, 2002.
6. Schlune, H., Plos, M., and Gylltoft, K. "Testing of Safety Formats for Nonlinear Analysis on Concrete Beams Subjected to Shear Forces and Bending Moments." submitted to Engineering Structures, January 2011
7. Schlune, H., Plos, M., and Gylltoft, K. Comparative Study of Safety Formats for Nonlinear Finite Element Analysis of Concrete Structures in 11th International Conference on Applications of Statistics and Probability in Civil Engineering. Zurich, Switzerland, 2011.

Experiences with the use of a semi industrial size concrete mixing plant for research and documentation within concrete properties



Martin Kaasgaard
M.Sc., Consultant
Concrete Centre, Danish
Technological Institute
Gregersensvej,
DK-2630 Taastrup
E-mail:
mkaa@teknologisk.dk



Claus Pade
M.Sc., Senior Consultant
Concrete Centre, Danish
Technological Institute
Gregersensvej, DK-2630
Taastrup
E-mail: cpa@teknologisk.dk

ABSTRACT

In 2007 a semi industrial size concrete mixing plant with a capacity of 250 liter concrete was installed at the Danish Technological Institute. The purpose of the mixing plant is to facilitate research and documentation on industrial scale and thereby increase the potential value/impact of the results. Through the implementation of a customized batching procedure, concrete can be mixed with high batching accuracy.

This paper describes the mixing plant and how the high batching accuracy is achieved. Furthermore examples of applications of the mixing plant are presented.

Key words: mixing plant, batching accuracy, aggregate moisture, concrete properties.

1. INTRODUCTION

One of the problems often faced when doing laboratory scale research within the field of concrete is the conversion to industrial scale. This problem relates to both the relative large difference in batch size and the fact that laboratory mixers often are not as effective as industrial mixers. As a consequence, mixing procedures on laboratory and industrial scale are typically not the same. This can lead to differences in for example concrete homogeneity and air void distribution, which will affect the hardened concrete properties. Hence results based on laboratory mixing of concrete may not immediately be applicable on the industrial/practical scale. The purpose of the concrete mixing plant installed at the Danish Technological Institute (DTI) is to facilitate research and documentation on industrial scale and thereby eliminate questions concerning the validity/applicability of the results.

Another difference between laboratory and industrial scale concrete mixing is that aggregate materials are often dried when doing laboratory mixing, while industrial mixing is done using moist aggregate materials. The latter presents the challenge of determining aggregate moisture, which needs to be done relative accurately depending on the requirements to water/cement ratio precision. Aggregate moisture is often determined using a microwave based sensor placed in the flowing aggregate material. However this method requires determination of a reliable reference curve for each aggregate material and it is dependent on a relatively continuous flow of material over time (fine aggregate material will tend to pack around the sensor). For research and documentation purposes, with focus on achieving exactly the desired water/cement ratio, the aggregate moisture determination needs to be more precise. As a consequence, a customized

batching procedure has been developed at DTI, with focus on achieving accurate determination of aggregate moisture. Through application of this batching procedure, concrete can be mixed with a batching variation of less than 0.5 % for all constituents.

So far the mixing plant has been applied in a range of different projects, including documentation of different types of co-combustion fly ash [1], documentation of new concrete additives, investigation of the effect of water/VMA on SCC rheology [2], investigation of the effect of steel fibres on SCC rheology and production of a large number of concrete blocks as a part of the pre-testing program for the FehmarnBelt Fixed Link. In this paper some selected results from the use of the mixing plant will be presented.

2. EQUIPMENT AND BATCHING PROCEDURE

The concrete mixing plant at DTI consists of a counter-current mixer with a capacity of 250 liter concrete, four powder silos and five aggregate silos (see figure 1). Powder is weighed into a pre-silo and aggregate is weighed onto a conveyor belt.



Figure 1 – The mixing plant at DTI left and the counter-current mixer right.

In order to achieve accurate determination of aggregate moisture, the following customized batching procedure is used, when mixing concrete on the mixing plant:

1. Aggregates are weighed onto the conveyor belt according to initial guess on moisture content, and 3 representative samples are taken of each aggregate for determination of moisture content using microwave ovens (takes around 30 minutes).
2. Aggregates are transferred to the mixer.
3. Powder is weighed into pre-silo.
4. Additives are weighed.
5. After moisture content determination the necessary amount of water is calculated and weighed into pre-silo.
6. The mixer is started and materials are added according to the desired mixing procedure.

3. CASES

3.1 Production of concrete blocks for FehmarnBelt Fixed Link pre-testing

As a part of the FehmarnBelt Fixed Link pre-testing program, DTI has produced a number of small (0.2x1x1 m) and large (0.2x1x2 m) concrete blocks based on possible mix designs for the construction. The large concrete blocks have been placed at a field exposure site in Rødbyhavn harbour and the condition of the concrete will be monitored periodically until the end of construction.

The requirements to batching accuracy were relatively high, with a maximum allowable batching deviation of 1 % for all constituents. The motivation behind this requirement was to be able to compare the different binder systems tested at well-documented water/cement ratio. The requirements to batching accuracy were met by the mixing plant at DTI in combination with the customized batching procedure. As can be seen from table 1, the 1 % maximum batching deviation was achieved for all constituents.

Table 1 – Batching deviations for all constituents used.

Constituent	Deviation [%]			
	Min	Max	Average	Standard
Cement	0.00	0.56	0.18	0.15
Fly ash	0.00	0.42	0.08	0.13
Microsilica	0.00	0.22	0.04	0.06
Slag	0.00	0.28	0.01	0.04
0/2 mm aggregate	0.00	0.99	0.28	0.27
4/8 mm aggregate	0.00	0.32	0.09	0.07
8/16 mm aggregate	0.00	0.37	0.08	0.07
16/22 mm aggregate	0.00	0.35	0.09	0.10
Air entraining agent	0.00	0.98	0.32	0.30
Superplasticizer	0.00	0.87	0.39	0.26
Water	0.01	0.72	0.29	0.18
w/c	0.00	0.86	0.26	0.21

3.2 Documentation of co-combustion fly ash

During the last 7-8 years, DTI has carried out testing of different types of co-combustion fly ash for the Danish power plant operators. The testing program consists of chemical/physical characterization of the fly ash and documentation of properties of fly ash concrete (both aggressive and passive environmental class as defined by DS 2426). The fly ash concrete is mixed on the DTI mixing plant, followed by measurement of fresh concrete properties (e.g. slump, air content, density and heat development) and hardened concrete properties (strength development and air void analysis).

The latest co-combustion fly ash tested originated from co-combustion of waste and coal. Measured properties of the concretes are presented in table 2. In general, the co-combustion ash performs similar to the pure coal ash reference when used in concrete. However, the passive class concrete containing co-combustion ash has a 10 % higher strength compared to the pure coal ash. This difference is not reflected in the aggressive class concrete. When comparing the measured slumps, it appears that the passive class concrete containing co-combustion ash has a considerably lower slump. This could be due to the co-combustion ash concrete having a slightly lower water/cement ratio, which would result in both a lower slump and a higher strength. The concretes were mixed before implementation of the described customized

batching procedure, where aggregate moisture was determined from one sample taken from the bottom of the silo before mixing. This means that the moisture content could have been lower than determined (most likely the fine aggregate moisture), resulting in a lower water content in the concrete and hence a lower water/cement ratio.

Table 2 – Measured properties of different fly ash concretes.

Concrete type	Slump [mm]	Air content [%]	Strength, 28 days [MPa]
A – coal ash	140	8.0	39.4
A – coal/waste ash	150	6.5	38.5
P – coal ash	150	5.5	31.0
P – coal/waste ash	110	5.5	34.0

3.3 Investigation of the influence of water on SCC rheology

In order to investigate the influence of less/extra water (for example due to incorrect aggregate moisture content determination) on SCC rheology, a 3-powder (cement, fly ash and microsilica) SCC with w/c 0.40 was mixed, first with the correct amount of water (reference) and then with respectively plus and minus 5 liter of water pr. m³ of concrete. The rheological properties were measured using the 4C-Rheometer [3], and cylinders were cast for determination of compressive strength at 28 days and chloride migration coefficient (D_{nssm}) according to NT Build 492. The results are presented in tables 3 and 4.

Table 3 – Measured rheological properties of SCC with different water content.

Concrete type	Slump flow [mm]			Viscosity [Pa·s]		
	5 min	30 min	60 min	5 min	30 min	60 min
Reference	500	580	580	41	23	48
÷5 l/m ³ water	470	530	530	47	45	59
+5 l/m ³ water	530	620	600	27	23	39

Table 4 – Measured properties of SCC with different water content.

Concrete type	w/c	Air content [%]	Strength [MPa]*	D_{nssm} [m ² /s]
Reference	0.401	3.2	60.7	7.4×10^{-12}
÷5 l/m ³ water	0.388	4.8	63.5	6.3×10^{-12}
+5 l/m ³ water	0.412	3.5	56.0	8.0×10^{-12}

*Normalized to 4 % air content by assuming 1 % air reduces strength by 4 %.

It clearly appears, that a 5 l/m³ difference in water content, which corresponds to 0.8 %-point inaccuracy of the fine aggregate moisture content, influences both the fresh and hardened concrete properties. This emphasizes the importance of both batching accuracy and correct aggregate moisture determination when mixing concrete.

4. CONCLUDING REMARKS

Through application of the mixing plant at DTI, concrete can be mixed with a batching variation below 0.5 % and well documented water/cement ratio. The importance of well-documented water/cement ratio has been demonstrated, as both fresh and hardened concrete properties are influenced by small variations in water/cement ratio. Research, but in reality also regular testing and documentation, requires that the composition of the concrete does not vary too much from the theoretical mix design. Hence the mixing plant at DTI is a valuable tool for research and documentation within concrete properties.

REFERENCES

1. Pade, C., Kaasgaard, M., "The use of fly ash from co-combustion in the production of concrete", *Conference Proceedings of EuroCoalAsh 2010*, pp. 213-218.
2. Thrane, L. N., Pade, C. & Kaasgaard, M., "Use of stabilizer/VMA to adjustment of the flow properties of SCC at the job site", *Nordic Concrete Research* no. 40, 2009, pp. 1-10.
3. Thrane, L. N., Pade, C. & Nielsen, C. V., "Determination of Rheology of Self-Consolidating Concrete Using the 4C-Rheometer and How to Make Use of the Results", *Journal of ASTM International* vol. 7, 2010.

From research to practice in Finland



Liisa Salparanta
Research Scientist
VTT Technical Research Centre of Finland
Kemistintie 3, Espoo
P.O. Box 1000
FI-02044 VTT, Finland
liisa.salparanta@vtt.fi

ABSTRACT

Continuity and *Cooperation* are the key words of concrete technological studies that have been carried out for over 40 years in a consortium between VTT (Technical Research Centre of Finland) and several public building owners.

The Finnish Transport Agency (formerly the Road Administration and Finnish Railroad Administration), the Radiation and Nuclear Safety Authority and some city authorities have formed a consortium combining their funds and investing in concerted research. This is how they get more with the same money as they would if they acted alone. Research is focused on solving practical problems, developing processes and methods, preparing directions, setting requirements, etc.

Key words: concrete, bridges, studies

1. INTRODUCTION

The common interest of all partners is concrete structures. Nearly all parties are interested in concrete bridges, while the nuclear safety authorities are mainly interested in pre or post tensioned structures and structures in marine environments. The partners agree which topics they wish to be studied and to what extent.

This paper reviews some of the types of work that have been done over the years, shedding light on Finland's expertise on practical partnerships. Topics include examples such as corrosion, internal curing, form-liners, and structural instrumentation. The paper also examines how the practical partnership with owners has led to deeper research and development topics funded by the national government, such as long-term field performance monitoring, modifying service life tools, and interacted chloride durability research. A description about international links to the projects is included, as well as future cooperation potential.

1. WHAT HAS BEEN DONE

Numerous topics have been studied during the years. Examples of practical studies the results of which have been directly applied in practice are:

- Relative humidity and temperature measurements using cast-in sensors
- Long term durability studies
- Requirements for fresh and hardened self compacting concrete, directions for concreting and quality control of self compacting concrete
- Design and execution directions of cathodic protection
- Quality requirements and verification methods of concrete substrate to be repaired
- The quality requirements of formliners
- Mould technics for underwater concreting.

Long-term theoretical studies including service life investigations based on information compiled from real bridges have yielded simulation methods for the ageing of concrete structures, as well as models to calculate deterioration, service life, and design service life, and a calculation method for lifecycle analyses. On the bases of this work so called P factor method was developed. For more than 20 years Finnish Transport Agency has used this method by which the compliance of concrete can be verified without tests on hardened concrete. On the basis of mix design, curing and air content measured on site P factor is calculated as shown in equation 1.

$$P = \frac{46 * k_{jh} * k_{sid}}{10 * (WAS)^{1,2} \sqrt{a} - 1} \quad (1)$$

where

k_{jh} is curing factor calculated from curing time

k_{sid} is binder factor calculated from effective binder content and binder composition

WAS is reduced void-binder ratio calculated from effective water and binder contents and air content

a is air content (%).

Directions for using P factor are described in the publication /1/. The publication is available on the www-pages of the Finnish Transport Agency. An excel file for calculating P factor is also given on the Finnish Transport Agency 's www-pages /2/.

2. WHAT IS GOING ON?

Service life investigations continue by studying the effect of the CO₂ and Cl⁻-permeability of repair materials on service life. The aim is to create a model and set parameters to determine the thickness of repair material layer with known permeability properties to reach a desired service life.

Last year also the studying of the applicability of infrared heating method equipment using liquefied petroleum gas for the heating and drying of a concrete bridge deck before the assembling of water proofing under cold and wet conditions was started.

The correlation of different freeze-thaw and frost-salt test methods will be determined. The aim is to enable replacement of expensive tests by cheaper ones.

3. GETTING INTERNATIONAL

There has a long-term field study of concrete durability been going on for four years. In this research the co-operation has widened to be international. There are partners from Norway, Canada, Portugal and USA involved in the project in which the effect of interacted deterioration parameters on service life of concrete structures in cold environments are studied. The novelty of this research is to combine different damage models to one service-life calculation model and apply this model in wide geographical area. The objective of the project is to make service life calculation models accounting for interaction when several types of deterioration are acting simultaneously. There is more information about this research in the papers by Erika Holt & Markku Leivo (Concrete durability based on coupled laboratory deterioration by frost, carbonation and chloride), Hannele Kuosa (Concrete durability and testing in Finland) and Erkki Vesikari (Modelling of carbonation and chloride penetration interacted by frost damage in concrete).

4. REPORTS

All the directions and instructions prepared within the co-operation and also many of the reports are available on the Finnish Transport Agency's www-pages. The studies that are partly funded by private companies are normally not public and therefore not available in the internet.

5. FINALLY

The co-operation goes on year after year. New needs for research appear and new studies are planned continuously. As the co-operation between orderers and researchers is intensive, all parties are well aware of each others needs and potentials and the studies are planned and accomplished in such a way that all parties get the best benefit out them.

The experiences of all parties involved have been positive. The orderers get more with their money than they would if they acted alone. The research results are well spread through all participants. The continuity of the co-operation combined with interesting topics are an ideal combination from the researchers point of view. In addition to this is very rewarding to see that the results are applied with success. You get a feeling that your work is useful.

REFERENCES

1. Siltabetonien P-lukumenettely. Tiehallinto. TIEH 2200054-v-08. Helsinki 2008. 17 p. + Attachments 3 p. http://alk.tiehallinto.fi/sillat/julkaisut/siltabetonien_p-lukumenettely_10062008.pdf (In Finnish)
2. <http://alk.tiehallinto.fi/sillat/rakenta1.htm> (In Finnish)

Modelling of Concrete Subjected to Cyclic Loading



Rasmus Rempling
Ass. Professor
Department of Civil and Environmental Engineering
Structural Engineering, Concrete Structures
Chalmers University of Technology
Gothenburg, Sweden
rasmus.rempling@chalmers.se

ABSTRACT

The infrastructure of today depends heavily on concrete structures. Most of these structures are subjected to repeated loads, known as fatigue or cyclic loads: the loads weaken the structure. The aim of this project is to add to the knowledge of the deterioration phenomenon and to develop models that can describe the response of concrete subjected to cyclic loading. To deepen the understanding of concrete subjected to cyclic loading, the phenomenon was investigated on the meso-scale level and macro-scale level. It was found that the interfacial transition zones are crucial in amount and strength and the results of the analyses show an overall agreement with experimental observations.

Key words: concrete, plasticity, damage, cyclic loading, energy dissipation

1. INTRODUCTION

Cyclic loading is one of the deterioration processes of great importance for concrete structures such as piles, sleepers, machinery foundations, parts of bridges, etc. The deterioration of concrete structures entails heavy costs for the society. These costs can be cut down by an increased understanding of the cyclic-loading phenomenon and by the development of constitutive models with an increased accuracy. Due to the non-linear stress-strain response that concrete exhibits, cyclic loading can be divided into two main characteristic responses: pre-peak cyclic loading and post-peak cyclic loading. Pre-peak cyclic loading is cyclic loading before maximum load is reached, while post-peak cyclic loading is cyclic loading after maximum load and localization of deformation. These phenomena are equally important as parts of cyclic loaded structures may be in pre-peak state, while other parts are in post-peak state. The work presented here deals with concrete subjected to cyclic loading in compression and tension with focus on improving the analysis methods for such cases and increasing the understanding of the deterioration processes related to repeated loading. Plasticity, damage mechanics, and the combination of both, are often used to describe the non-linear response of concrete, e.g. of models [1]-[3]. Moreover, the concept of bounding surface, introduced by [4], has been proved to be useful to describe the hysteresis loops that concrete exhibits when subjected to cyclic loading: [5]-[6]. Research that identifies the characteristic hysteresis loops has been conducted by [7]-[8]. The combination of plasticity and damage mechanics used in this investigation was previously investigated by e.g. [9]-[12] and [13], and shows good results for complex crack patterns.

2. PROPOSED MODELS

2.1 Meso model

In a meso-scale study concrete is characterised by aggregates, mortar paste and interfacial zones that surround the aggregates. The aggregates are interpreted as stiff inclusions and are modelled as a linear elastic material, while the mortar and the interfacial zones are modelled by an interfacial model. The interfacial model is based on a combination of damage mechanics and the theory of plasticity. The system of coordinates for the interface used in this study is defined by one normal and two tangential directions, i.e. the strain is defined as $\boldsymbol{\varepsilon} = (\varepsilon_n, \varepsilon_s, \varepsilon_t)$. The stress-strain relationship for this combination was as

$$\boldsymbol{\sigma} = (\mathbf{1} - \omega)\mathbf{D}_e(\boldsymbol{\varepsilon} - \boldsymbol{\varepsilon}_p) \quad (1)$$

where $\boldsymbol{\sigma}$ is the stress tensor, ω is the damage parameter, $\boldsymbol{\varepsilon}_p$ is the plastic strain tensor and \mathbf{D}_e is the elastic stiffness tensor defined to fit the system of coordinates according to

$$\mathbf{D}_e = \begin{bmatrix} E & \mathbf{0} & \mathbf{0} \\ \mathbf{0} & \gamma E & \mathbf{0} \\ \mathbf{0} & \mathbf{0} & \gamma E \end{bmatrix} \quad (2)$$

where E and γ are material parameters. The interfacial model is characterised by a parameter, μ , which determines the ratio of plastic strain and total inelastic strain for tension, as well as compression; $\mu = 0$ corresponds to a pure damage mechanics response, while on the other hand, $\mu = 1$ corresponds to a pure plastic one.

2.1 Macro models

Two macro models were formulated and implemented in this project. The first model was formulated as a serial combination of damage mechanics and the theory of plasticity. The first approach to a macro model of concrete subjected to cyclic loading in this project aims to describe cyclic loading of concrete in tension by means of the bounding surface concept. To introduce the concept of a bounding surface is, in fact, to define a hardening law based on surfaces that bound different states of stress. The plastic part of the model is described by two such surfaces: one elastic bounding surface that limits the elastic domain (i.e. inside this domain the response is linear elastic). On the edge of the elastic domain, the material starts to yield. Thus, the elastic bounding surface is the same as a yield surface. As soon as yielding starts, the stress point is repelled by the second bounding surface which bounds all admissible states of stress. The repelled stress state finds a new position of the elastic domain, and plastic strain develops. This continues until the outer bounding surface is reached; thus, the actual stress point is positioned on both surfaces. From this position, all strains that develop are plastic ones. At this point damage is initiated. The damage is determined by an isotropic damage variable which is driven by the developed plastic strain when the two bounding surfaces are in contact. The damage variable decreases the outer bounding surface such that the admissible stress domain is reduced with increased damage. If the deformation is reversed at this stage, the state of stress leaves the surfaces; the response consequently becomes elastic until the border of the elastic domain is reached at a different position. Again, when the state of stress is at the elastic bounding surface, yielding is initiated and the stress point is repelled by the outer bounding surface. As an illustration, the process described above can be pictured as a point of stress inside two rings that define the bounding surfaces. The inner ring can move inside the outer ring in the direction

of the movement. The outer ring repels the movement of the inner ring which yields plastic strains. The second approach to a macro-model was, instead of a serial combination of damage mechanics and the theory of plasticity, a parallel combination. The fundamental part of the formulation of the parallel combination is the variable, α_e , which controls the contribution of each part to the stiffness according to

$$\sigma = (1 - \alpha_e)(1 - \omega)D_e \varepsilon + \alpha_e D_e (\varepsilon - \varepsilon_p) \quad (3)$$

The total nominal stress is thus achieved by adding the nominal stress of the sub-parts which are evaluated separately. The basic idea was that the damage part should give the overall response, while the plastic part gives the cyclic response. The formulation reveals a need for a softening of both parts, as no damage is added to the plastic part. The plastic part of the formulation is based on two yield surfaces defined by stress invariants: one outer and one inner yield surface. The outer one is based on the Ottosen yield surface; the inner one is of the von Mises type. In the hydrostatic stress space, this results in a curved outer yield surface while the inner yield surface is a line parallel to the hydrostatic axis. However, in the deviatoric stress space, both yield surfaces are circular. The fact that the inner yield surface is circular in the deviatoric section causes a numerical problem, as the surface must be concave to yield a solution. To solve this, the inner yield surface is not active until the stress state is inside the space enclosed by the inner yield surface. This is achieved by computing the value of the distortional energy. When the distortional energy is negative, the inner yield surface can be activated and remains so as long as the distortional energy is negative. The result shows that this corresponds to the part of the unloading with low stress and stiffness.

3. CONCLUSION

In the project the following conclusions are drawn:

The bounding surface model describes the cyclic response well, except for the stiffness reduction due to increased numbers of cycles and consequent damage. The deficiency in describing the stiffness reduction was traced back to the chosen localisation model.

The meso-scale approach with the new interface model results in realistic failure patterns in the form of shear bands. The amount of localized permanent displacement has a strong influence on the material response for repeated loading. With localised permanent displacement, the stress-strain curves are characterised by hysteresis loops and damage evolves during repeated loading. At meso-scale, five parameters were investigated and their influence on the cyclic response is summarised here.

- A decrease in the volume fraction of aggregates increases the ultimate strength of concrete, since a smaller proportion of aggregates corresponds to a reduction of interfacial transition zones which weaken the material. The decrease also reduces the size of the hysteresis loops, due to fewer interfacial transition zones. Localised permanent displacements are the main reason for describing hysteresis loops.
- The size range of aggregates does not strongly influence the response of concrete subjected to monotonic and cyclic loading.
- Less permanent displacement in the interfacial transition zones results in a reduction of the size of the hysteresis loops.
- A decrease of the number of permanent displacements in the mortar phase results in a reduction of the size of the loops in the post-peak regime, which is where localised permanent displacements occur in the mortar phase.

- The strength of the mortar and the interfacial transition zones have a strong influence on both the monotonic and cyclic responses. An increase of the strength of the interfacial zones leads to an increase of the compressive strength, since the permanent displacements in the interfacial zones are reduced.
- Furthermore, the size of the hysteresis loops is described.

The proposed material parameter, α_e , influences the size of the hysteresis loops in a direct fashion, making the model easy to calibrate.

The distortional energy is related to the plastic deformation at unloading. During plastic unloading the distortional energy is negative, which makes it useful as a parameter for controlling this state.

REFERENCES

1. Papa, E., Taliercio, A., “Anisotropic damage model for the multiaxial static and fatigue behaviour of plain concrete”, *Engineering Fracture Mechanics*, Vol. 55, 1996, pp. 163–179.
2. Ragueneau, F., Norderie, C.L., Mazars, J., “Damage model for concrete like materials coupling cracking and friction, contribution towards structural damping: uniaxial applications”, *Mechanics of Cohesive-Frictional Materials*, Vol. 5, 2000, pp. 607–625.
3. Desmorat, R., Ragueneau, F., & Pham, H., “Continuum damage mechanics for hysteresis and fatigue of quasi-brittle materials and structures”, *International Journal for Analytical and Numerical Methods in Geomechanics*, Vol. 31, 2007, pp. 307–329.
4. Dafalias, Y., “Bounding surface plasticity. i: Mathematical foundation and hypoplasticity”, *Journal of Engineering Mechanics*, Vol. 112, No. 9, 1986, pp. 966–987.
5. Voyiadjis, G. Z., Abulebdeh, T. M., “Damage model for concrete using bounding surface concept”, *Journal of Engineering Mechanics-ASCE*, Vol. 119, No. 9., 1993, pp. 1865–1885.
6. Voyiadjis, G.Z., Abulebdeh, T.M., “Plasticity model for concrete using the bounding surface concept”, *International Journal of Plasticity*, Vol. 10, No. 1., 1994, pp. 1–21.
7. Reinhardt, H. W., Cornelissen, H. A. W., Hordijk, D. A., “Tensile tests and failure analysis of concrete”, *Journal of Structural Engineering*, Vol. 112, No. 11., 1986, pp. 2462–2477.
8. Gopalaratnam, V., Shah, S., “Softening response of plain concrete in direct tension”, *Journal of the American Concrete Institute*, Vol. 82, No. 3, 1985, pp. 310–323.
9. Jason, L., Pijaudier-Cabot, G., Huerta, A., Crouch, R., Ghavamian, S., “An elastic plastic damage formulation for the behavior of concrete” ,in V.Li, C.Leung, K.Willam, S. Billington, eds., *Fracture mechanics of concrete structures*, 2004, pp. 549–556.
10. Bazant, Z., Oh, B., “Crack band theory for fracture of concrete”, *Materiaux et Constructions*, Vol. 16, No. 93, 1983, pp. 155–177.
11. Dafalias, Y., Popov, E., “Model of nonlinearly hardening materials for complex loading”, *Acta Mechanica*, Vol. 21, No. 3, 1975, pp. 173–192.
12. Spooner, D., Pomeroy, C., & Dougill, J., “Damage and energy-dissipation in cement pastes in compression”, *Magazine of Concrete Research*, Vol. 28, No. 94, 1976, pp. 21–29.
13. Bazant, Z., & Shieh, C., “Hysteretic fracturing endochronic theory for concrete”, *Journal of the Engineering Mechanics Division-Asce*, Vol. 106, No. 5, 1980, pp. 929–950.

Experimental and Numerical Investigation of Stress Wave Propagation in Shotcrete



Lamis Ahmed
Ph.D. Student
KTH Royal Institute of Technology
Division of Concrete Structures
SE-100 44 Stockholm, Sweden
lamis.ahmed@byv.kth.se



Anders Ansell
Ph.D., Associate Professor
KTH Royal Institute of Technology
Division of Concrete Structures
SE-100 44 Stockholm, Sweden
anders.ansell@byv.kth.se

ABSTRACT

During blasting in tunnels and mines, the shotcrete support is affected by propagating stress waves that may lead to structural failure. Shotcrete is studied through nondestructive laboratory experiments with P-wave propagation along a concrete beam, with properties similar to rock. Cement based grout with properties that resembles shotcrete is applied on one end of the beam with a hammer impacting the other. The shape of the stress waves traveling towards the shotcrete is registered using accelerometers positioned along the beam. With a three-dimensional FE model the propagation of the stress waves is captured and this will facilitate further modelling with more complex geometries.

Key words: Shotcrete, Vibrations, Blasting, Testing, Finite element model.

1. INTRODUCTION

Detonation of explosives during excavations of tunnels and underground spaces give rise to stress waves that transport energy through the rock and these may, depending on the magnitude of the waves, cause severe damage to permanent installations and support systems within the rock, such as shotcrete (sprayed concrete). Today there are no reliable and established guidelines for when blasting can be allowed close to shotcrete support systems. This work was initiated to provide a basic knowledge to serve as recommendations for practical use in civil engineering underground work, tunnelling and mining. First, a laboratory scale model was used to experimentally simulate the behaviour of rock and shotcrete exposed to stress waves. By using a striker bar (hammer) that impacts a test beam instead of explosives, the vibration of the shotcrete can be monitored using accelerometers. These results could then be used to estimate the impacting force, or velocity, needed to damage the adhesive bond between shotcrete and rock. The scale model experiment was then modelled using a FE (finite element) program from which the results will be evaluated and refined through comparisons between calculated and measured data.

2. EXPERIMENTAL WORK

Stress wave propagation through good quality granite, from an explosive charge towards a shotcreted rock surface, has been simulated in the laboratory. Only longitudinal P-waves were considered and the rock mass could therefore be represented by a beam, due to practical reasons made of concrete with similar material properties as rock. Stress waves, similar to those observed in situ, were induced in the beam through impact of a striker bar made of steel. The set up for this hammering test method is shown in Figure 1, with the concrete beam hanging in cables attached to a steel frame. The impacting hammer was mounted on a swing arm, hitting the beam end perpendicularly. To ensure that the hammer impact was applied uniformly, a 2 mm thick fiber board was attached to the end of the beam. The length of the hammer arm L , the swing angle θ and the gravity constant $g = 9.81 \text{ m/s}^2$ gives the velocity of the striker bar as:

$$v_h = \sqrt{2 g L (1 - \cos \theta)} \quad (1)$$

The shotcrete was represented by cement grout, with composition similar to shotcrete, which was cast at the opposite end of the concrete beam. A series of tests with 50 and 100 mm thick, up to 18 hours old shotcrete has been carried out where the shotcrete has been subjected to different intensity of hammer blows.

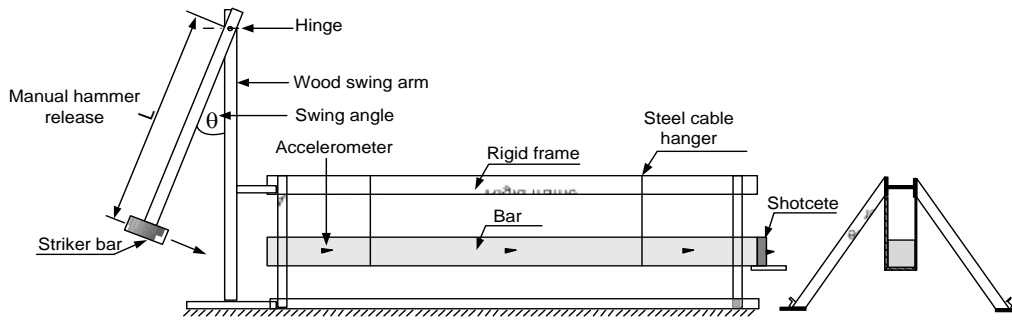


Figure 1 – Schematic of set up for hammering test.

The concrete beam was cast with dimensions as in Figure 2. The density (ρ) and compressive strength (f_c) were 2337 kg/m^3 and 81 MPa , respectively. By assuming that the stress wave propagates solely in the longitudinal direction (P-wave), the propagation velocity (c) follows

$$c = \sqrt{E / \rho} \quad (2)$$

which is valid for elastic materials with Young's modulus (E), see e.g. [1,2]. The wave propagation velocity in the tested beam is thus about 4030 m/s . It should be noted that these properties are close to those of typical Swedish rock (granite) which often has ρ and c around 2400 kg/m^3 and 4000 m/s , respectively [3]. As shown in Figure 2, three accelerometers were positioned along the bar, with a fourth glued onto the shotcreted end. To prevent out-of-band signals 'aliasing', the transducer signals were filtered using a low-pass (Bessel) filter with 1200 Hz sample rate, available in the data acquisition system. Also, in order not to exceed the accelerometer capacity, the length of the swing arm was limited to 1.5 m and the tests carried out within swing angles of 5° – 25° .

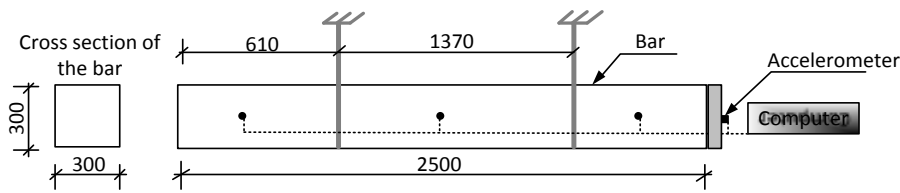


Figure 2 – Details of the test specimen.

3. FINITE ELEMENT ANALYSIS

The engineering simulation software Abaqus [4] was used to create a three-dimensional FE model analyzed with the Abaqus/Explicit solver. A model of the tested beam is shown in Figure 3, with solid elements and features according to Table 2. The interaction between the striker bar, the concrete beam and the shotcrete layer were constrained using displacement boundary conditions, thus restricting the model to primarily describe particle displacements in the wave propagation direction. Between the concrete beam and the striker bar free translation was only allowed in the axial direction. Tie constraints between the concrete beam and shotcrete were used. The incident disturbing stress wave, caused by the striker bar, was applied as a surface to surface contact using the kinematic contact method with definition of the initial velocity in the axial direction for the striker, with the velocity assumed to follow Equation (1). The acceleration–frequency spectra of the FE model for various points are compared to the acceleration spectra of the measured data to determine the element size and time steps used in the explicit analysis.

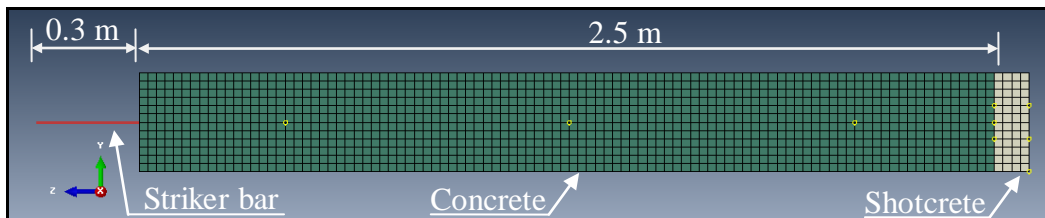


Figure 3 – Finite element model of the experiment beam.

Table 2 – Properties for the Abaqus/Explicit model with shotcrete, beam and striker bar.

Specific properties	Part		
	Shotcrete	Concrete beam	Striker bar
Cross section, m ²	0.3 × 0.3	0.3 × 0.3	0.1 × 0.1
Thickness, m	0.05 and 0.1	2.5	0.3
Elements type	C3D8R*	C3D8R*	B31**

*C3D8R Explicit, 8-node linear, reduced integration, hourglass control.

**B31 Explicit, 2-node linear beam in space.

4. RESULTS

Measurement results are compared to numerical results in Figure 4. The velocity of the striker bar versus the acceleration is shown in Figure 4a. The stresses of young shotcrete (18 hours) at the concrete beam-shotcrete interface, as obtained in the numerical analyses, are shown in Figure 4b. Note that only two of the tests resulted in shotcrete failure.

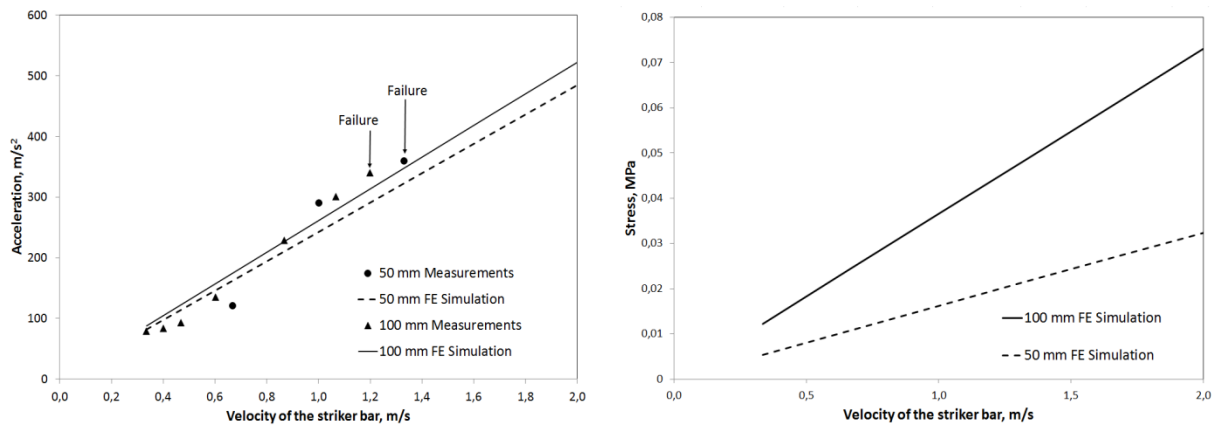


Figure 4 – Examples of accelerations of the shotcreted surface, from measurements and FE simulations (a). Velocity of the striker bar versus the stresses at the beam-shotcrete interface (b). Shotcrete age is 18 hours.

5. CONCLUSIONS

The comparison between the results of accelerations from FE simulation and measurements shows good agreement with respect to maximum acceleration on the surface of the shotcrete, for the velocity range of 0.5–1.5 m/s. It should be noted that there is a small difference in the maximum acceleration between 50 and 100 mm shotcrete thicknesses, as shown in Figure 4a. The comparison in Figure 4b of the stresses at the beam-shotcrete interface, with respect to the first arriving stress maxima, shows that with increasing velocity the stresses for 100 mm thick shotcrete becomes much higher than for 50 mm shotcrete.

6. ONGOING RESEARCH

The ongoing research aims at an extension of the FE model in Abaqus/Explicit to also describe 3D geometries and displacements of realistic tunnel sections. To describe the stress wave propagation a rather large volume of rock will have to be modelled, depending on the distance between the shotcrete and the detonation of the explosives. The further work will focus on newly sprayed and hardening shotcrete and the simulation of the wave propagation along tunnel walls following blasting at a tunnel front. The goal is to identify safe distances between shotcrete and the point of blasting, also accounting for shotcrete age, tunnel geometry and rock mass properties.

REFERENCES

1. Meyers, M.A., “Dynamic behavior of materials”, John Wiley & Sons, New York, 1994.
2. Dowding, C.H. 1996. Construction Vibrations. Upper Saddle River: Prentice-Hall.
3. Ansell, A., “In situ testing of young shotcrete subjected to vibrations from blasting,” *Tunnelling and Underground Space Technology*, Vol. 19, No. 6, November 2004, pp. 587–596.
4. Simulia. http://www.simulia.com/products/abaqus_explicit.html, 2011.

Initial study of oblique hard target projectile impact of normal and high strength concrete targets



Håkan Hansson
M.Sc., Ph.D. student
KTH Royal Institute of
Technology
Division of Concrete
Structures
SE-100 44 Stockholm
hakan.hansson@byv.kth.se



Richard Malm
Ph.D., Researcher
KTH Royal Institute of
Technology
Division of Concrete
Structures
SE-100 44 Stockholm
richard.malm@byv.kth.se

ABSTRACT

The ability to predict penetration resistance in concrete is necessary to evaluate the vulnerability of protective designs for impacts by penetrating weapons, or deformable projectiles. The paper presents experimental work regarding oblique projectile impact of both normal strength and high performance concrete targets with modern type of hard target penetrators. Furthermore, finite element (FE) analyses of non-normal projectile impacts of the normal strength concrete targets are presented, and its limitations discussed.

Key words: Concrete penetration, non-normal impact, high performance concrete, HPC.

1. INTRODUCTION

Several empirical and numerical tools have been developed for this purpose. However, the penetration performance for projectile impact at a non-normal angle is not thoroughly investigated. Penetration experiments of a hard target penetrator impacting unreinforced normal strength concrete and high performance concrete targets, at both normal and non-normal impact conditions, were therefore performed.

2. EXPERIMENTAL DATA

The average cylinder strengths after 28 days for the used normal strength concrete (NSC) and High Performance Concrete (HPC) were approximately 45 and 129 MPa [1], respectively. A model scale hard target penetrator designed at FOI, with a diameter of 50 mm and a length of 450 mm, weighting approximate 4.50 kg, was used for all the experiments. The studied penetrator has a nose section with an ogive radius of 400 mm. Penetration tests were performed both with normal impact (i.e. zero degree obliquity) and 59.5° inclined targets, the later results in a 30.5° obliquity for the projectiles. The impact conditions for penetrators and experimental results are given in Table 1. Furthermore, the rotation of the penetrators during penetration of the targets for tests no. 04-25 and 04-26 were approximate 9° and 10°, respectively. The front faces of targets numbers 04-25 and 04-27 are shown in Figure 1.

Table 1 - Experimental penetration results [1].

Test identity	04-6	04-25	04-26	04-3	04-8	04-27	04-13
Concrete type	NSC	NSC	NSC	NSC	HPC	HPC	HPC
Target diameter (m)	1.20	1.50	1.50	1.20	1.20	1.50	1.20
Target length (m)	0.60	0.54	0.54	0.90	0.51	0.45	0.90
Impact angle (°)	90.0	59.5	59.5	90.0	90.0	59.5	90.0
Impact velocity (m/s)	425	424	422	409	421	421	422
Pitch angle (°)	1.1	1.1	1.2	0.7	1.6	1.0	1.3
Yaw angle (°)	0.2	0.0	0.2	0.8	0.3	0.8	0.1
Penetration (m)	---	---	0.50	0.64	---	0.25	0.41
Exit velocity (m/s)	139	16	---	---	136	---	---
FE analysis no.	FE1	FE2	FE2	FE3	---	--	---



Figure 1 - Front faces of NSC target no. 04-25 (left) and HPC target no. 04-27 (right) after projectile impacts.

3. FINITE ELEMENT ANALYSES

FE analyses of the experiments with normal strength concrete targets were performed with Autodyn 3D. The FE models used a 3D Lagrangian solid element formulation with a single integration point, in combination with the RHT material model for the concrete [2]. A uni-axial compressive strength of 48 MPa was used for the concrete, representing the 90 day compressive strength for the concrete (Hansson, 2005). A tensile strength of 4.0 MPa was assumed for the concrete. The simulations were performed with nominal impact angles (i.e. 90.0° and 60.0°), and 420 m/s as impact velocity. Furthermore, the yaw and pitch for the penetrator were zero degree in the FE-analyses, and the mass of the penetrator was 4.53 kg. A friction coefficient of 0.05 was used for the interaction between the penetrator and the target. The element length was approximately 5 mm in the central part of the targets, and one symmetry plane was used for the models to reduce the number of elements. The number of elements was approximately 1.10×10^6 and 1.65×10^6 for the simulations of normal and inclined impact, respectively. The heavily distorted concrete elements within the target were removed from the mesh during the analysis at a geometric strain equal to 2.0. The simulation methodology is further described in [3]. Table 2 show the simulation results, and Figure 2 shows the cross-sections of models FE1 and FE2 after perforation of the targets.

Table 2 - Simulation results for penetration in NSC [3].

FE analysis Model identity	Penetration depth (m)	Exit velocity (m/s)	Experimental result, see also Table 1.
FE1	---	143	Exit velocity 139 m/s
FE2	---	117	Exit velocity 16 m/s and penetration depth 0.50 m, respectively
FE3	0.53	---	Penetration depth 0.64 m

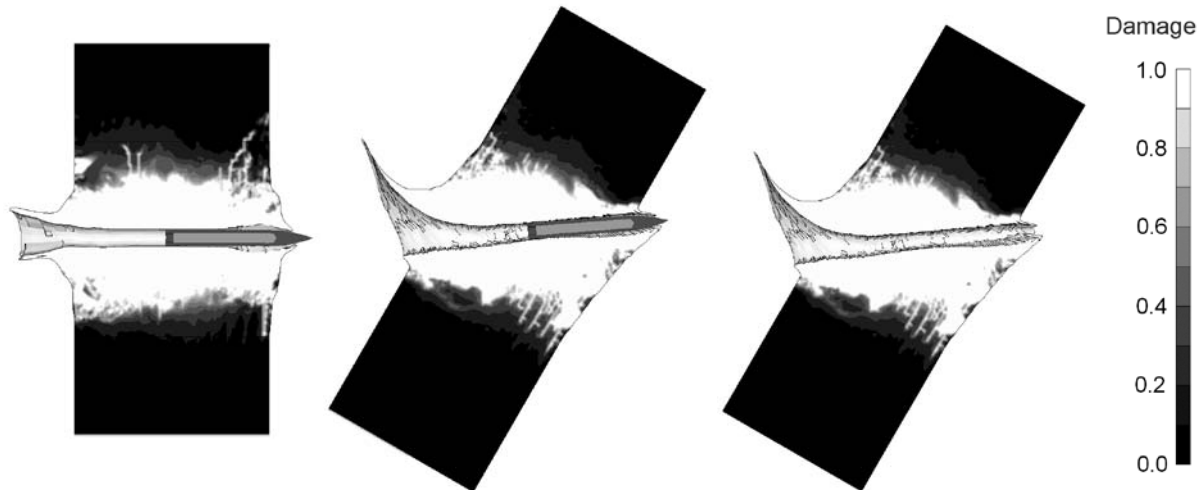


Figure 2 - Damage plot of normal strength concrete targets impacted at 0° and 30° obliquity [3], respectively. Model with oblique impact shown with and without the penetrator.

4. DISCUSSION AND SUMMARY

The HPC targets showed an increased penetration resistance compared to the NSC targets for the case with normal impact conditions. In addition to this, the tests with HPC targets and 30.5° obliquity of the projectiles showed a major improvement of the protection level for the HPC targets compared to the NSC targets. Further, the tests with oblique impact of the HPC targets showed a major decrease in penetration performance of the penetrators, compared to the penetration performance at normal impact conditions for HPC targets. The influence of reinforcement in HPC targets is unknown. The reinforcement may even stabilize the penetrator during an oblique penetration of a HPC target, and thereby reduce the protection level of the target.

The use of 3D FE analyses allowed for problem geometries with varying impact angles for the projectiles, and the performed simulations considers both normal and oblique impact conditions of the projectiles. The numerical results showed fair agreement when compared with the experimental results for this type of penetrator impacting the NSC at zero degree obliquity. However, the penetrators were not likely to be subjected to any significant deceleration force during the crater-formation at the front face of the targets during the experiments. The energy needed for the crater-formation is likely to be only a small fraction of the energy required to deform the concrete during the penetration of the targets. This is a phenomena not well described by the performed FE analyses. Furthermore, the use of this numerical methodology seems to have a severe limitation when oblique projectile impact was considered. As a result, the simulation of the oblique projectile impact is less accurate than the simulations with normal

impact conditions.

The deviation angle for the penetrator in the simulation of the inclined NSC target was approximate 4° , compared to a deviation of approximate 9° and 10° for tests no. 04-25 and 04-26, respectively. According to this, the deviation for the penetrator in the simulation was less than half the deviation obtained in the experiments. A major limitation for the FE analyses of oblique impacts was the numerical erosion used for distorted solid elements. The rotation of the missile during impact of a target is likely to cause more severe distortion of elements on one side of the penetrator's nose. Based on this, the lateral forces acting on the penetrator are likely to be underestimated and due to this underestimate the rotation of the penetrator. Simulations were not performed for the HPC targets, since the used methodology needs to be improved for studies of oblique impacts.

5. FUTURE RESEARCH

The use of the smooth particle hydrodynamic (SPH) formulation, or another particle formulation, for the target eliminates the need to remove distorted elements in the simulation models. However, this methodology is likely to increase the CPU time for the simulations considerably. Using a particle formulation only for the region with large deformation, i.e. in the centre of the model, would reduce the simulation time, although an undesired interface within the model is introduced. Modified erosion methodologies are available within the EPIC code [4] and the IMPETUS Afea solver, where distorted 3D elements are converted to particles. The advantage with this methodology is that the element formulation can be used for the main part of the model, and the use of the particle formulation is limited to a small part of the model with large deformations. Furthermore, the use of this methodology for future research is likely to improve the modelling of the interface between penetrator and target, especially for simulations of oblique penetrator impacts, without considerably increase of required the simulation time. FE analyses of penetration experiments with HPC targets, including oblique impact conditions, may be possible to perform with this methodology.

ACKNOWLEDGEMENTS

The hard target penetrator experiments and simulations were performed at FOI, at the research division Defence & Security, Systems and Technology, and were sponsored by the Swedish Armed Forces.

REFERENCES

1. Hansson, H., "Penetration in concrete for projectiles with $L/D \approx 9$ ", FOI-R--1659--SE, FOI, Tumba, 2005, 124 pp.
2. Riedel, W., "Beton unter dynamischen lasten, Meso- und makromechanische modelle und ihre parameter", EMI-Bericht 6/00, Fraunhofer EMI, Freiburg, 2000, 210 pp.
3. Hansson, H., "Experimental and numerical study of projectile penetration in concrete", Proceedings, 6th Asia-Pacific Conference on Shock and Impact Loads on Structures, Perth, Australia, December 2005, pp. 243-250.
4. Johnson, G.R., Stryk, R.A., "Conversion of 3D distorted elements into meshless particles during dynamic deformation", *International Journal of Impact Engineering* no. 9, Vol. 28, 2003, pp. 947-966.

Session A3 – SCC

High water-cement ratio SCC robustness with novel cellulose based admixture



Hannele Kuosa
M.Sc. (Tech.), Research Scientist
VTT Technical Research Centre of Finland
P.O. BOX 1000
FI-02044 VTT, Finland
E-mail: hannele.kuosa@vtt.fi

ABSTRACT

Novel cellulose based admixture (NCBA) grades were used to enhance medium strength SCC (w/c 0.60) robustness. Comparison was made with the use of limestone powder and a commercial stabilizer. Robustness was evaluated by measuring the effect of water content variation on slump-flow, viscosity by t_{500} -time, sieve segregation and water bleeding. Hardened concrete segregation and strength was also evaluated. Robustness assessment was based on selected limiting values for both workability and stability properties. Novel cellulose based admixture was an effective way in SCC robustness enhancement. Robustness evaluation was possible by common SCC testing.

Key words: Self compacting concrete (SCC), robustness, stability, novel cellulose based admixture

1 INTRODUCTION

There are several well known advantages in the use of self compacting concrete (SCC), but it may be difficult to produce robust SCC with a relatively high water-cement ratio (w/c), e.g. with w/c 0.50 – 0.60. The use of extra fine powder material is not always desired and availability of good filler may also be a problem. It would also be an advantage to be able to spare natural filler material resources when producing medium strength concrete.

In this study two grades of a novel cellulose based admixture (NCBA) were used. The effect of NCBA on the robustness of a SCC with w/c 0.60 was studied. Measurement of compressive strength was included. Comparison was made with a SCC with limestone powder (LP) and a SCC with commercial viscosity modifying stabilizer (S). This study is related to rheological studies with cement pastes, mortars and concretes presented here elsewhere [Vehmas 2011] and studies on the effect of NCBA on microstructure and hydration. Applicability of NCBA for other cement based products such as injection grouts and foam concrete are also underway and have already confirmed the effects of NCBA on cement based materials rheological properties and robustness.

The action of NCBA in SCC is based on the fact that it forms a stable gel-like structure with water. Only a low dry material content is needed for the reaction (dry material < 1 % in water). This gel has a high yield stress but low viscosity with a thixotropic nature.

2 EXPERIMENTS

2.1 Methods

The main idea was to first make basic SCC-mixes (4 basic mixes with w/c 0.60) with as optimal properties as possible by using two DCBA grades, limestone (GL) and a commercial stabilizer (S). The basic SCC slump-flow was 660 – 690 mm and t_{500} -time was 2.0 – 3.2 seconds. After that all the mixes were reproduced, but now with 5 % lower and 5 % higher total effective water content (± 10.5 litres/m³), i.e. with w/c 0.57 and w/c 0.63. The robustness of all the mixes was evaluated by the same measurable ways. Robustness checking is commonly recognized as an important step in the SCC mixture design process.

2.2 Materials and mixing

Cement CEM II/A-M(S-LL) 42.5 N (Yleisementti from Finnsementti Oy) was used in all the mixes. Natural Finnish aggregates and filler were used. Ground limestone SB63 (from Nordkalk OyAb) was used in powder type for the SCC mixes (GL). The superplasticizer was Glenium 51 from BASF. In one mix (S) commercial melamine sulphonate based stabilizer was used (dry material content 3 %). The novel cellulose based admixture grades, designated here as NCBA-1 and NCBA-2, were from UPM-Kymmene Corporation. Mixing was performed with a normal laboratory concrete mixer. NCBA and S were added last, with 3 min mixing time after adding.

2.3 Mixes

Mix designs for the basic SCC-mixes with w/c 0.60 are presented in Table 1. Each mix was repeated two times but then with the total effective water content either 5 % lower or higher (w/c was 0.57 or 0.63, see Table 2).

Table 1. *Mix designs for the basic SCC-mixes.*

	Basic SCC			
	NCBA-1	NCBA-2	S	GL
Cement [kg/m ³]	350	350	350	350
Aggregates [kg/m ³]	1785	1785	1785	1474
Ground Limestone (GL) [kg/m ³]	0	0	0	311
Effective water [kg/m ³]	210	210	210	210
Water/Cement ratio (w/c)	0.60	0.60	0.60	0.60
Plasticizer Glenium 51 (17.5 % [% of cement])	1.60	1.60	1.60	1.40
Dry NCBA [% of cement]	0.080	0.220	0	0
Stabilizer, S [% of cement]	0	0	1.00	0

2.4 Fresh and hardened concrete testing

Fresh concrete testing was performed soon after mixing. Workability testing was done first, including slump-flow [EN 12350-8] and t_{500} time measurement. After that was sieve segregation testing [EN 12350-11] and measurement of water bleeding. For bleeding a container with a volume of 2 litres was used and these container-specimens were split vertically after hardening to detect concrete homogeneity and possible aggregate settlement. 150 mm cubes were made

from the basic SCC mix (w/c 0.60) for the measurement of compressive strength at 1 d, 7 d and 28 d.

2.5 Results

Fresh and hardened concrete measurement results are presented in Table 2 and Figure 1.

Table 2. Fresh and hardened concrete measurement results.

w/c	SCC	t_{500} -time [s]	Slump-flow [mm]	Bleeding (2 h) [vol.-%] ¹⁾	Sieve segregation [w.-%]	Compressive strength [MPa]		
						1 d	7 d	28 d
0,57	NCBA-1 -5% water	8,0	540	0,2	0,6	-	-	-
0,60	NCBA-1	2,4	690	0,3	3,2	5,5	33,0	39,8
0,63	NCBA-1 +5% water	1,1	730	1,5	8,3	-	-	-
0,57	NCBA-2 -5% water	16,0	500	0,2	0,4	-	-	-
0,60	NCBA-2	3,2	660	1,3	3,2	5,5	30,6	36,1
0,63	NCBA-2 +5% water	2,5	675	1,8	7,2	-	-	-
0,57	S -5% water	3,0	610	0,8	2,4	-	-	-
0,60	S	2,9	690	2,7	10,4	5,3	31,9	37,5
0,63	S +5% water	2,5	630	2,8	16,7	-	-	-
0,57	GL -5% water	2,4	570	0,1	3,7	-	-	-
0,60	GL	2,0	670	0,1	5,4	11,1	37,3	43,4
0,63	GL +5% water	1,1	780	0,2	8,8	-	-	-

1) Vol. = 2 litres, h = ca. 160 mm, A = ca. 140 cm²

Based on visual examination, there was no significant settlement of aggregates in any SCC.

3 ROBUSTNESS EVALUATION AND CONCLUSIONS

Robustness can be evaluated based on the testing results by finding out the range for permissible water content variation, and thus also for the corresponding w/c range. Based on the selected limiting values, several values for robustness could be calculated. The lower limiting value for w/c can be based on slump-flow or t_{500} -time and the higher value on sieve segregation or water bleeding. Two examples on robustness evaluation are presented in Figure 2. In Table 3 there are three robustness values based on limiting values: slump-flow 550 mm, t_{500} -time 7 s, sieve segregation 10 % and water bleeding 1.5 %. In some cases minor extrapolation was necessary for robustness evaluation and in some cases the lowest/highest value for w/c could not be measured as testing results were far ahead of the limiting value. In Table 3 there is also the minimum determined robustness value (minimum $\Delta(w/c)$), i.e. the lowest w/c range meeting all the limiting values.

The novel cellulose based admixture, and in this case especially NCBA-1, was effective in enhancing high w/c (0.60) SCC robustness. It was competent even compared with the powder type GL-SCC and e.g. robustness based on slump-flow and sieve segregation was even better with NCBA-1 than with a high content of limestone powder. For the basic NCBA-1, the t_{500} -time was about the same as for GL-SCC, but it decreased more than for GL-SCC with 5 % less water. Overall, the presented way for robustness evaluation was versatile and made it possible to select the most relevant limiting values for the actual case.

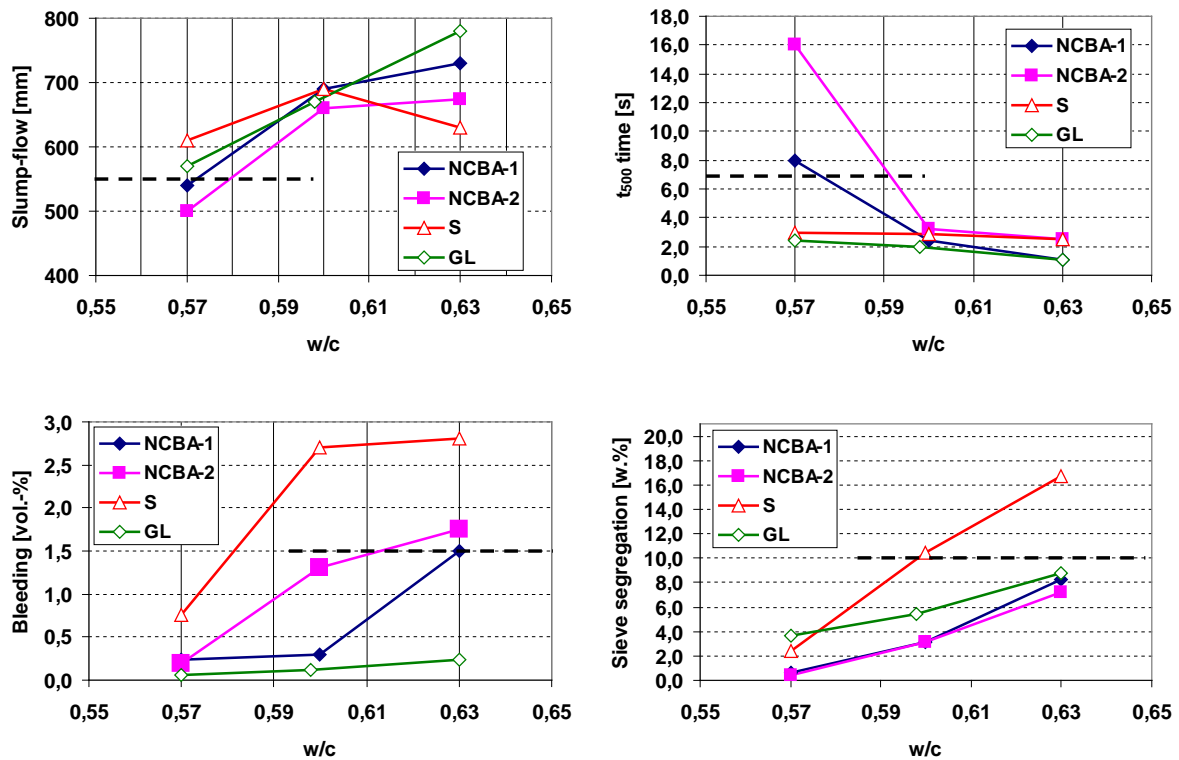


Figure 1. Fresh SCC measurement results as function of w/c.

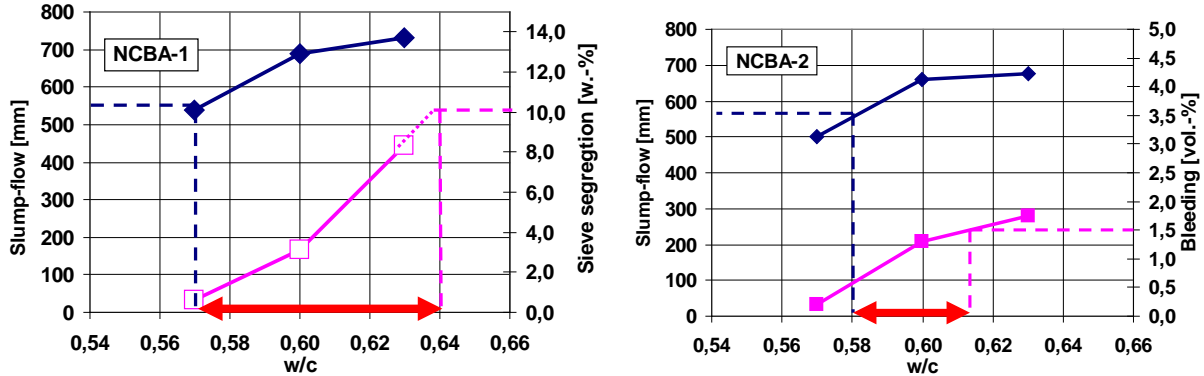


Figure 2. Example of robustness evaluation. Allowable w/c-range for slump-flow >550 mm and sieve segregation <10 %.

Table 3. Determined limiting w/c values for robustness representing slump-flow >550 mm, t₅₀₀-time >7 s, sieve segregation <10 % and water bleeding <1.5 %.

SCC	Limiting w/c-values for robustness evaluation						Minimum Robustness [Δ(w/c)]
	Slump-flow and Bleeding		Slump-flow and Sieve-segregation		t ₅₀₀ -time and Sieve segregation		
NCBA-1	0,575	0,630	0,568	0,638	0,576	0,636	0,055
NCBA-2	0,580	0,615	0,577	0,647	0,592	0,648	0,035
S	0,553	0,583	0,548	0,596	0,570 ²⁾	0,597	0,030
GL	0,566	0,630 ¹⁾	0,562	0,636	0,570 ²⁾	0,636	0,074

1) The real value is much higher, but could not be estimated

2) The real value is much lower, but could not be estimated

SCC Stability affected by fillers and VMA



Ya Peng
MSc, PhD student
COIN Dept of Structural Eng.
NTNU
N-7491Trondheim
ya.peng@ntnu.no



Stefan Jacobsen
Professor.
COIN Dept of Structural Eng.
NTNU
N-7491Trondheim
stefan.jacobsen@ntnu.no

ABSTRACT

Chemical admixtures are added to concrete in order to achieve self-compacting properties. The improved fluidity sometimes causes stability problems. The phenomena of segregation and bleeding occur due to density difference between particles and fluids. The Kozeny-Carman equation (KCE) quantifies the effects of w/c (or solid fraction), density difference solid-fluid, specific surface and fluid viscosity on bleeding. Some calculation examples are shown indicating that increased fluid viscosity can be more efficient to improve stability than use of powder. The stability of particles towards sinking as described by Stokes law for a yield stress fluid indicates that yield stress is more important than plastic viscosity for stability of particles. Effects of VMA on both fluid viscosity and rheology of matrix should be measured, particularly at higher solid fractions $\Phi > \approx 0.40$ beyond where relative viscosity increases steeply with increased Φ . The effects of powder- and VMA-stabilisation on bleeding and segregation/sedimentation will be studied in an experimental program in progress.

Key words: SCC, stability, filler, admixtures,

1. INTRODUCTION - STABILITY

Due to the density differences of the constituents of SCC, which span from fluid density $\rho_f = 1000 \text{ kg/m}^3$ for water to solid density $\rho_s = 3150 \text{ kg/m}^3$ for portland cement, the liquid-like fresh material can have stability problems with liquid flowing up and particles sinking.

1.1 Bleeding – Kozeny Carmans equation

Bleeding and settlement of fresh cement paste without admixtures was measured and calculated in [1] with Kozeny-Carmans equation (KCE) applied to the experimental results. KCE is derived entirely based on viscous flow of a Newtonian fluid through a bed of particles and was written on the form:

$$[Q(1-\varepsilon)]^{1/3} = \left[\frac{C}{k_c \sigma^2} \right]^{1/3} \varepsilon \Leftrightarrow Q = \frac{\varepsilon^3}{1-\varepsilon} \frac{C}{k_c \sigma^2} \quad (1)$$

Where Q: bleeding rate, -flow

ε : pore volume fraction = $\rho_c / [\rho_c + (\rho_w / (w/c))]$ (solid fraction $\Phi = 1 - \varepsilon$)
 $C = (\rho_s - \rho_f)g / \eta$: ρ_s, ρ_f : densities of solid and fluid, g : gravity and
 η : viscosity of water or fluid between particles
 k_c : Carman constant
 σ : specific surface

By writing the KCE on this form the driving force for bleeding, the hydraulic pressure, is embedded so that the permeability coefficient is omitted. The bleeding curves (Q vs Φ , Q vs w/c , Q vs ε) quantify the stability of a given mix. Figures 1 and 2 show calculated bleeding rate as function of solid fraction for reduced density difference (from 2150 to 1200 kg/m³), increased specific surface (from 9450 to 15750 cm²/cm³) and increased liquid viscosity (from 0.001 to 0.005 Pa·s). Looking at the plots it is useful to remember that 1 mm/h bleeding equals a flow $Q = 0.001\text{m}/3600\text{ s} \approx 2.8 \cdot 10^{-6}$ m/s and that the curves are only valid before settlement begins.

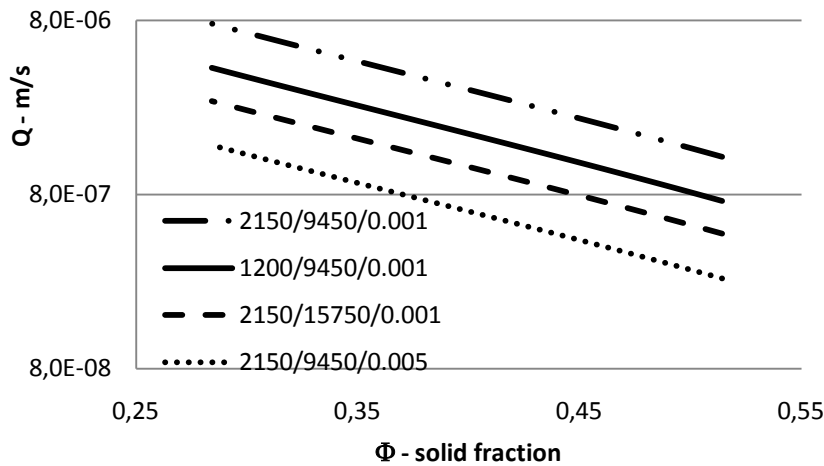


Figure 1 – Φ vs bleeding according to KCE: effect of density, specific surface and fluid viscosity

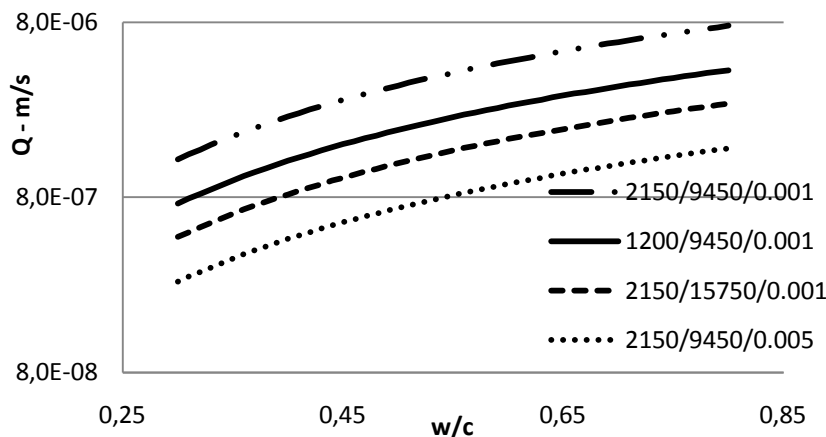


Figure 2 – w/c vs bleeding (KCE): parameter variation as in fig.1

Figures 1 and 2 show that the effect on bleeding of reducing the powder density from 3150 to 2200 kg/m³ (which is a large change, hardly possible to obtain with any known matrix material) is smaller than the effect of increasing the specific surface from 9450 to 15750 cm²/cm³ (which at the actual constant powder density corresponds to an increase from 300 to 500 m²/kg – note the use of volumetric specific surface). This effect of increasing the fineness should be quite possible to obtain in practice by increasing the cement fineness or replacing parts of the cement by other materials such as fine fillers and/or pozzolana, and remembering to proportion so that the effect is calculated on a volumetric basis (which has to be done in order to be able to predict

the results with eq.(1)). The lowest curve shows the effect of increasing the liquid viscosity 5 times; from 0.001 Pa.s (pure water) to 0.005 Pa.s (perhaps by VMA). Apparently this is more effective than using the actual filler example. Figure 2 only yields for a pure cement paste. For matrix, Φ must always be used, and not w/c, w/b or w/p, when comparing different powders.

1.2 Particles sinking in yield stress fluid – plastic viscosity (Stokes law)

The stability of a particle immersed in a yield stress fluid was reviewed by Roussel [2]. Assuming that the particle sinks according to Stokes law as the yield stress is passed, Stokes law was combined with Bingham fluid behaviour. Making appropriate assumptions about the shear rate around the particle [2], the moving speed V_s (m/s) of particles with equal diameter d immersed in a Bingham fluid is given by eq (2). This equation is useful for plotting and evaluating the effect on moving speed on density differences and rheology.

$$V_s = \frac{d}{\mu_p} \left(\frac{d}{18} (\rho_s - \rho_f) g - \tau_0 \right) \quad (2)$$

Where: V_s : moving speed of particle (m/s)
 τ_0 = yield stress [Pa]
 μ_p = plastic viscosity [Pa.s]

1.3 Particle stability – yield stress

For a particle at rest $V_s =$ zero and the stability criterion in eq.(2) can be written as eq.(3). For a yield stress fluid this is then an expression for the critical diameter, d_c , which is the maximum diameter of a spherical particle not sinking in a Bingham fluid:

$$d_c = \frac{K\tau_0}{|\rho_s - \rho_f|g} \quad (3)$$

Where: K : constant with theoretical value = 18

Theoretically it is easy to show from eq. (2) and (3) that yield stress is the rheological parameter of a Bingham fluid that governs stability. Eq. (2) will give very high sinking velocities at zero yield stress even for very small diameters whereas eq.(3) will keep much bigger particles at rest at realistic yield stress values.

2. MEASURING STABILITY

From existing results some experiences can be summarized. Bonen et al. [3] concluded that stability is controlled by the viscosity and yield stress of the mixture, the binder density, aggregate size and density, as well as the content of fines. This implies that the stability can be enhanced by increasing both yield stress, viscosity and solid volume fraction, Φ_{matrix} , and also by decreasing the maximum size and density of aggregate, especially for self-compacting concrete with low yield stress. A short, preliminary, summary of findings can be given as: 1) Lower w/c-, w/b-ratio and/or superplasticizer-dosage (SP/c-ratio) increase stability and therefore robustness of cementitious materials; 2) Greater fines content increases stability; Carsward, et al. [4]. Bonen and Shah [5] reported that silica fume is an example of a viscosity modifier, slag and limestone are examples of density modifier; Khayat et al. [6] reported that SCC can exhibit greater resistance to surface settlement when the content of total fines in the mixture (smaller than 80 μm in his case) increases for mixture with similar aggregate packing densities, this was especially the case for SCC with medium to low content of binder; 3) Many researchers claimed that viscosity modifying admixture (VMA) can be used to reduce the variability of the mixtures,

thus increasing the stability and robustness. 4) Large aggregate size and high density decrease stability and vice-versa. However, within common ranges of SCC admixture and densities of aggregate, Bonen and Shah argued that the most important factor that governs the rate of sedimentation is the aggregate size; 5) VMA improves stability significantly. Mehta and Monteiro [7] reported that the molecular structure of VMA facilitates the removal of large amount of water by physical adsorption. This explanation indicates that the effect on rheology could be both to increase viscosity and yield stress. The name “viscosity modifier” implies an effect on viscosity, whereas the adsorption mechanism could immobilize free water, perhaps also affecting yield stress. The maximum packing fraction (Φ/Φ_{\max}), also called the crowding factor, expresses the spacing of the particles and relates to stability [2]. Also the effect of fluid viscosity on matrix viscosity should be evaluated. Justnes and Vikan [8] observed a very steep increase of viscosity for paste as $\Phi > \approx 0.40$ in line with the Krieger-Dougherty equation. This might seriously limit the possibility to use VMA to reduce bleeding, either due to too high liquid viscosity or because the high Φ will stabilize the mix, making VMA unnecessary.

3. FURTHER RESEARCH

In this PhD-project an experimental program on the stability of matrix with various fillers and VMAs is about to begin. This will bring new understanding of the relations between stability and both material parameters (Φ , specific surface, density, liquid viscosity, SP, VMA, Φ/Φ_{\max} , viscosity of fluid without/with VMA) and rheological parameters of matrix (yield stress – both statically and dynamically, plastic viscosity, relation Φ – relative viscosity etc). Different industrial fillers, SP and VMA will be investigated. Quantitative analysis of relations between stability and chemical and physical characteristics of constituents will be made. Mechanisms such as viscous flow, yield stress build-up and particle crowding will be studied. Presently various methods for observing stability are investigated including bleeding- (gravimetrically, visually with web cam etc) and segregation measurements (ultrasonic pulse velocity, density differences etc) as well as particle packing characterisation and liquid fraction separation (centrifuge). Experimentally and practically there is a need for measurement methods for settlement, bleeding and static yield stress to evaluate the effect of different material parameters on stability. Presently we are following some of the above mentioned approaches.

REFERENCES

1. Powers, T.(1968) The Properties of Fresh Concrete, Wiley & Sons, London, 664 p.
2. Roussel N.(2006) A theoretical frame to study stability of fresh concrete, M&S 39;1 pp.81-91
3. Bonen D et al.(2007) Robustness of SCC – Chapter 1 of “Self Consolidating Concrete”, A White Paper by Researchers at the Center of Advanced Cement Based Materials (ACBM)
4. Carlsward, J., Emborg, M. et al (2003) Effects of constituents on the workability and rheology of self-compacting concrete,”Proc 3rd Intern. RILEM Symp on SCC. 143-153
5. Bonen, D. and Shah, S.P.(2004) The effects of formulation on the properties of SCC, Concrete Science and Engineering, Int. RILEM Symp. Eds. K. Kovler, J. Marchand, S. Mindess, and J. Weiss, RILEM Publ, NW Univ USA pp.43-56
6. Khayat, K.H., Hu, C. and Monty, H.,(1999) Stability of SCC, advantages and potential appl.,” in RILEM Int. Confer. On SCC, Stockholm
7. Mehta, PK, and Monteiro, PJM.(1993) Concrete - Structure, Properties, and Materials, Second Edition, Prentice Hall, New Jersey.
8. Justnes H. Vikan H.(2005) Influence of w/c on viscosity of cement paste, NCR proc(33)159-161

Rheological Properties of Self-Consolidating Concrete Stabilized With Fillers or Admixtures



Hedda Vikan
PhD, Researcher
SINTEF Building and
Infrastructure
Forskingsveien 3B
N-0314 Oslo
Hedda.vikan@sintef.no



Klaartje De Weerd
PhD student
SINTEF Building and
Infrastructure
Richard Birkelandsvei 3
N-7034 Trondheim
Klaartje.De.Weerd@sintef.no

ABSTRACT

The mix design of self-consolidating concrete (SCC) is crucial in order to obtain a robust SCC that is fluid enough to completely fill the form and simultaneously stable against segregation of aggregates and bleeding. This study investigates the effect of chemical stabilizers or additional filler on the castability and rheological properties of concrete and its matrix. Viscosity and thus thixotropy is of special interest since these parameters are believed to influence stability, form-filling ability, the migration and evacuation of entrapped air bubbles and thus the final surface quality of hardened concrete elements.

Key words: SCC, stability, rheology.

1. INTRODUCTION

1.1 Importance of robustness and stability of SCC

Self-consolidating concrete (SCC) has been described as one of the most innovative developments in the field of concrete technology [1]. Improved placing of the concrete and better work environment are two of the most important benefits of using SCC compared with traditional vibrated concrete. Unfortunately, SCC cast in-situ in Norway has stagnated at a low market share. The main reasons are probably the low robustness against fluctuations in the concrete production, and subsequently the higher demand for quality control [2].

Robustness can be defined as the ability of fresh concrete to maintain its properties within narrow limits when the proportions of constituent materials change significantly [1]. The stability of fresh SCC defines the ability of a concrete mixture to retain its homogeneity through the fresh phase, both at rest and subjected to loads due to transport, form-filling and compaction [3]. Dynamic stability refers to the characteristic of the concrete mixture to resist segregation during production, transport and casting. Static stability refers to the ability of the concrete mixture to resist bleeding, segregation and settlement once all placement and casting operations have been completed [4].

1.2 Principal objectives and scope

The importance of mix design is crucial in order to obtain self-consolidating concrete (SCC) that is fluid enough to completely fill the form and simultaneously stable against segregation of

aggregates and bleeding. Stability of SCC can be achieved in at least two ways: By aid of fines, or by aid of chemical stabilizers [5-7].

This study has a practical approach based on scenarios that could occur on an actual building site, i.e. addition of fines or chemical stabilizers to ensure consistent stability and castability of fresh concrete. Rheological properties of concretes and matrices stabilized by either of these methods are studied, bearing in mind that concretes stabilized with fines generally have a higher matrix content than concretes stabilized with chemical admixtures. Special attention is given to the viscosity and the thixotropy since these parameters are believed to influence the stability, the form-filling ability, the migration and evacuation of entrapped air bubbles and thus the final surface quality of the hardened concrete elements.

2. EXPERIMENTAL

2.1 Materials

EN 197-1-CEM II/A-V 42.5 R Portland fly ash cement was used for all experiments. The cement had a Blaine fineness of 450 m²/kg and density of 3010 kg/m³

Gneiss/Granite aggregates of fractions 0/8mm and 8/16 mm were used for all concretes. Filler (< 0.125 µm) sieved from the 0/8 mm sand was used to prepare concrete equivalent matrix.

Three powdered materials have been used as stabilizers:

- Limestone powder of density 2700 kg/m³ and Blaine 360 m²/kg
- Filler sieved from non-washed, crushed 0/8mm sand. Density: 2730 kg/m³.
- Filler produced from the same material as crushed 0/8 mm sand. The 0/8 mm sand was sieved to obtain the 0/2 mm fraction, washed and sieved once more to obtain the filler. Density: 2730 kg/m³.

Two chemical stabilizers have been used: S1 is based on a polymer with high molecular weight. The normal dosage is 0.3-1.2% of cement weight. The selected dosage was 0.4%. S2 is based on cellulose derivate. The normal dosage is 1-2% of cement weight. The selected dosage was 1%.

Two types of acrylic superplasticizer were used. SP2 has lower molecular weight, longer side chains and higher charge density than SP1. These properties result in higher degree of sterical hindrance and rapid slump loss.

A Gluconat based set retarder was added to all concretes at a dosage of 0.4% in order to eliminate the effect of hydration on the rheological measurements.

2.2 Recipies

The basis of the test matrix was a low-grade concrete (M60 according to NS-EN 206-1) with an aimed slump flow of 675 ± 15 mm. The reference concrete was designed in order to be on the verge of separation (i.e. instability).

The mineral fillers were added in two dosages, namely 40 kg/m³ (filler-cement ratio 0.12) and 80 kg/m³ (filler-cement ratio 0.24) while adjusting the superplasticizer dosage in order to keep the slump flow within a slump flow range of 675 ± 15 mm. The chemical stabilizers were added according to recommended dosage given by the producer while adjusting the superplasticizer dosage. The concrete recipes are given in Table 1.

Table 1 - Concrete mix design

	Reference	40 kg/m ³ Filler	80 kg/m ³ Filler
w/c	0.58	0.58	0.58
w/p	0.46	0.44	0.40
f/c (%)	-	12	24
Matrix (l/m ³)	325	338	352
Paste (l/m ³)	300	314	328
Cement (kg/m ³)	326	326	326
0/8 mm (kg/m ³)	1089.6	1067.1	1043.8
8/16 mm (kg/m ³)	725.0	711.4	695.9

A forced pan mixer with a volume of 50 litres from Eirich was used to prepare the concretes. The volume of the concrete batches was 40 litres.

Slump flow and T₅₀₀ were measured according to EN 1235080: 2010 10 minutes after water addition. Simultaneously, the torque was measured as a function of the rotational speed by aid of a ConTec Rheometer-4SCC.

Concrete equivalent matrices were made with cement ratio 0.45 for all mixes. All pastes were added 0.4% gluconate per cement weight. Total paste volume was 200 ml. Concrete equivalent superplasticizer dosages were used for the main test series. In order to eliminate the effect of variable superplasticizer dosage, additional test series were made for which it was kept constant. The matrices were blended in a high shear mixer from Braun (MR5550CA).

Rheological parameters of the matrix such as Bingham parameters of the flow curve, thixotropy, and static yield stress were recorded by a parallel plate (1 mm gap, upper and lower plate serrated) rheometer MCR 300 from Physica. The rheometer temperature was set to 20°C.

3 CONCLUSION

The aim of this investigation was to compare two ways to stabilize concrete: by adding additional filler or chemical stabilizers. It was shown that the effect of the stabilizers depended on the plasticizer type and the dosage: Increased dispersion is linked to decreased structural buildup.

Of the two chemical stabilizers, the polymer type had stronger thixotropic effect than the cellulose type. However, for both superplasticizers, addition of filler gave a stronger viscosity increase than the chemical stabilizers.

Matrix viscosity increased with increasing volume fraction of solids in line with the Krieger-Dougherty equation [8].

Viscosity and thixotropy increase of the matrix dispersed with SP2 related to the filler fineness; limestone producing the highest values and filler from crushed 08 mm producing the lowest.

It should also be noted that the viscosity parameters measured for concrete and concrete equivalent matrix, namely H , T_{500} and plastic viscosity were interrelated. The yield stress parameters, on the other hand, only seem to correlate vaguely. This might be due to the fact that the yield stress parameters varied in a narrow range as all concrete were designed to obtain a slump flow within ± 15 mm.

Further research will be conducted on the effect of the combination of both additional filler and chemical stabilizers on the stability of both matrix and concrete. The final aim of the project is to develop robust recipes for SCC with materials available in Norway, and additionally to link the rheological properties with quality of the finished concrete surface.

3 ACKNOWLEDGEMENTS

The authors acknowledge the COcrete INnovation centre, COIN (<http://www.coinweb.no>) for facilitating this project.

REFERENCES

1. De Schutter, G.M., et al., Self-compacting concrete. 2008, Scotland, UK: Whittles Publishing.
2. Vikan, H. Means of improving concrete construction productivity - State of the art. in COIN Project report. 2008.
3. Daczko, J.A. Stability of self-consolidating concrete, assumed or ensured? in The First North American Conference on the Design and Use of Self-Consolidating Concrete. 2002.
4. Smeplass, S. Chapter 3 - Fresh concrete workability. in TKT 4125 Concrete Technology 1. 2009.
5. Takada, K., G.I. Pelova, and J.C. Walraven. Self-compacting concrete produced by japanese method with dutch materials. in 12th European Ready Mixed Concrete Congress. 1998. Lisbon: p. 775-785.
6. Kim, J.K., et al. Experimental research on the material properties of super flowing concrete. in International RILEM Conference on Production and Workability Methods of Concrete. 1996. Paisley: p. 271-284.
7. Corradi, M., R. Khurana, and R. Magarotto. User friendly self-compacting concrete in precast production. in The Third International RILEM Symposium on Self-Compacting Concrete. 2003. Reykjavik: p. 457.
8. Krieger, I.M. and T.J. Dougherty, A mechanism for non-newtonian flow in suspensions of rigid spheres. *Transactions of the Society of Rheology*, 1959. 3: p. 137-152.

Rheological properties for self compacting concrete (SCC)



Dag Vollset
Concrete engineer
Product manager
admixtures
Rescon Mapei AS
Vallsetvegen 6



Øystein Mortensvik
M. Sc.
R&D admixtures
Rescon Mapei AS
Vallsetvegen 6
N – 2120 Sagstua

ABSTRACT

In this project, traditional methods for describing self compacting concrete - slump flow, slump flow with J-ring, T_{500} and T_{end} – were compared with rheological properties; yield stress and plastic viscosity. Different mix designs with both natural and 100 % crushed aggregates were compared in the laboratory and on site. These mixes gave knowledge to define an “acceptance window” for the rheological properties to determine whether the batched concrete could be delivered to the construction site. Mixes that were outside the window could be brought into the window by adding different materials; admixtures, binders, et cetera.

The mixes in the laboratory were studied with Viscometer 5 and Rheometer 4SCC, while mixes on site were measured with ViscoProbe 1 and Rheometer 4SCC.

Key words: crushed aggregate, SCC, admixture, yield stress, plastic viscosity.

1. INTRODUCTION

In the beginning of 2010, Rescon Mapei invested in rheological instruments, Viscometer 5 and Rheometer 4 SCC, both from Con-Tech, Iceland. A project in cooperation with Velde Betong was initiated. Velde is located on the west coast of Norway, close to Stavanger, where they produce their own aggregate. Aggregates are crushed and sieved in four steps and cubically shaped. The result is 8 different fractions of 100 % crushed materials ranging from 0-0.063 and up to 16-22. In one of their 2 m³ mixers Velde has installed a Visco Probe 1 from Convi, Denmark.

Traditional method for measuring self compacting concrete is the *slump flow* (EFNARC, European SCC Guidelines May 2005). By using Abram’s cone, concrete is filled into the cone, lifted straight up. The diameter is measured in X and Y axis, and the average of the two is the result, given in millimeters. *Slump flow with J-ring*. This test is designed to disclose any blocking of aggregates around reinforcement bars. The slump flow is measured in the same way as the “normal” slump flow. The height difference of concrete on the inside and on the outside of the ring is measured. T_{500} , the time it takes for the concrete to flow from the slump cone is lifted until a diameter of 500 mm. In addition T_{end} was measured: the time it takes from the slump cone is lifted until the concrete has stopped flowing. Rheology is considered by some to be a better way of describing self compacting concrete. Yield stress (*Pascal*) is the amount of force needed to make the concrete start moving. Plastic viscosity (*Pascal * second*) is the resistance to increase the rate of flow of the concrete.

The materials used in this project were as following:

Table 1 – overview materials

Cement	Silica fume	Crushed aggregate	Natural aggregate	Admixtures
CEM II B/S 52.5 N	Densified silica fume	0 / 0.063	Limestone filler	Superplasticizer 1
		0.063 / 0.25	0 / 8	Superplasticizer 2
		0.25 / 2	8 / 16	Superplasticizer 3
		2 / 5.6		Superplasticizer 4
		5.6 / 8		Stabilizer 1
		8 / 11.2		Air entraining agent 1
		11.2 / 16		

All necessary materials were sent to the laboratory at Rescon Mapei for preliminary testing.

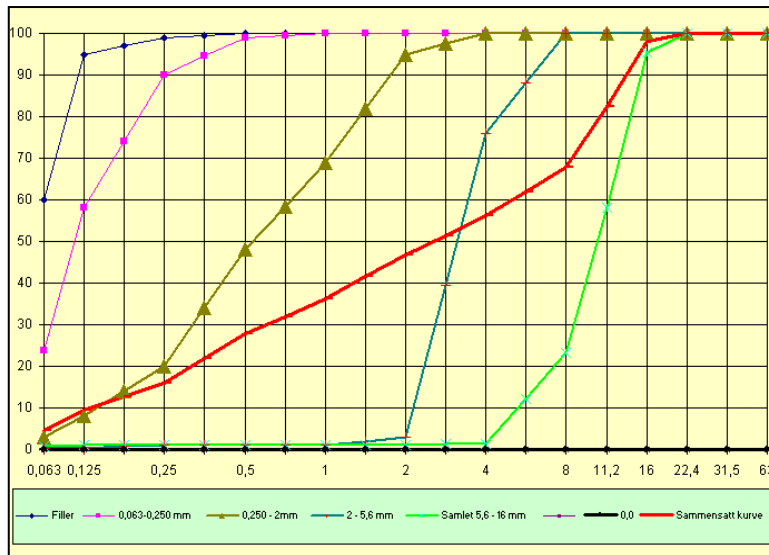


Figure 1 - Sieve analysis of crushed aggregate

The mix design was changed during the project. The 7 fractions of crushed aggregate gave the opportunity to design any mix; high/low matrix ranging from 340 to 375 liters of matrix volume, Füller curve, linear sieve curve, etc.

Amount of cement was kept constant at 325 kg/m^3 , and the w/c-ratio at 0.59.

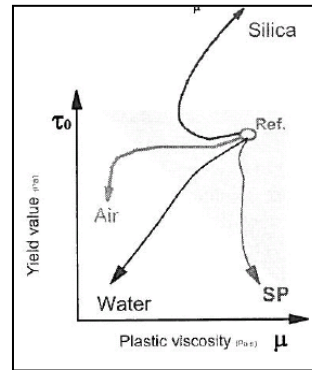
A self compacting concrete classified as K2, T2 (according to Norsk Betongforenings publikasjon nr. 29) was the target for the SCC. K2 means a slump flow between 580 and 700 mm, T2 means a T_{500} of more than 2 seconds.

For a concrete to have a slump flow larger than 550 mm, the yield stress had to be lower than 50 Pa. As for the plastic viscosity there seemed to be few limitations.

The different effects of added materials were, from a rheological point of view, considered from O. Wallevik's studies in 1983, see figure 2.

The different effects of added materials were, from a traditional point of view, considered based on 40 years of experience in mix design and concrete behavior.

Figure 2 - Rheological effect of materials.



2. RESULTS

Natural aggregate vs. crushed aggregate

A direct comparison between natural aggregate and crushed aggregate was performed. The sieve analysis was composed to be exactly the same, the matrix volume was the same, the amount of superplasticizer 3 was the same and the water/cement-ratio was the same.

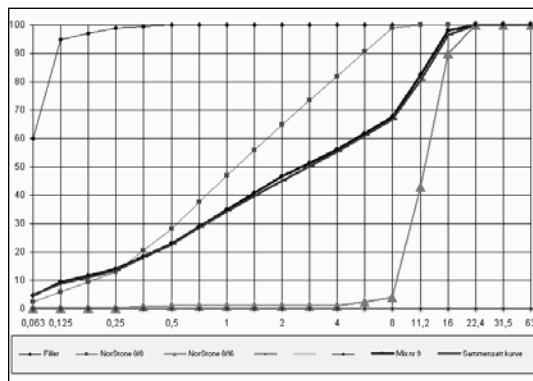


Figure 3 - Sieve analysis for natural aggregate.

Table 2 – results mix 9 and mix 13

Mix number	Mix 9 (Crushed)	Mix 13 (Natural)
Fineness Modulus	4.11	4,19
Matrix volume (l/m ³)	362	363
Slump flow (mm)	620	615
T ₅₀₀ (s) / T _{end} (s)	2.1 / 16	1.5 / 12
Yield stress (Pa)	43	44
Plastic viscosity (Pa*s)	35	25
Comp. strength (N/mm ²)	56.2	56.3

The normal measurements did not reveal any significant difference between the two mixes. As for the rheological measurements the yield stress was the same, but the plastic viscosity was rather different. The plastic viscosity for the concrete mix with natural aggregate had a plastic viscosity of 25 (Pa*s), whereas the crushed aggregate had 35 (Pa*s).

When the two concretes were to be described in words the mix with natural aggregates was described as a concrete with nice flow and workability. The mix with crushed aggregates was considered to have a slow flow and being too sticky. In other words, not a concrete that casting crew would be happy to receive.

There was no difference between natural aggregate and crushed aggregate in terms of compressive strength. The strength was measured after 1, 2, 7 and 28 days and the differences were less than 0.5 N/mm².

Exchanging fillers in natural aggregate

As the 0/8 fraction of the natural aggregate had a low amount of filler, limestone was introduced to increase the matrix volume without increasing the amount of cement. The mix 13 contained

crushed filler, and in mix 16 this was exchanged with limestone filler. Mix 16 had a better flow, almost at the brink of separation. As a result of this difference, the fillers were sent to the analytical laboratory in Mapei, Italy.

There was a big difference in particle size distribution, particle shape and specific surface.

Table 3 – Results of mix 13 and 16

Mix number	Mix 13 (limestone)	Mix 16 (crushed filler)
Fineness Modulus	4.19	4.10
Matrix volume (l/m ³)	363	360
Slump flow (mm)	615	670
T ₅₀₀ (s) / T _{end} (s)	1.5 / 12	1.3 / 17
Yield stress (Pa)	44	30
Plastic viscosity (Pa*s)	25	25
Comp. strength (N/mm ²)	56.3	53.5

Use of different super plasticizers

Table 4 – Information of admixture

Admixture nr:	Nr of polymers	Dry matter:	Effects:
Superplasticizer 1	One	30.0 %	Splitting, medium loss of consistency
Superplasticizer 2	One	19.5 %	No loss of consistency for 90 minutes
Superplasticizer 3	Two	18.5 %	Splitting, slow loss of consistency
Superplasticizer 4	Two	24.0 %	Splitting, stabilizing, slow loss of consistency

The different superplasticizers were studied in the same mix design, and repeated three times to investigate the repeatability.

SP 1 consists of one polymer and SP 2 consist of another polymer. These two polymers were mixed together in SP 3. The rheological properties of SP 3 are quite different from SP 1 and 2. SP 4 is based on the same polymers as SP 3, but also contain stabilizer 1.

One interesting question often raised is “does crushed materials require a different type of superplasticizer?”.

Table 5 – results of different admixture

Admixture nr:	Slump flow	T ₅₀₀ / T _{end}	Yield stress	Plastic viscosity
Superplasticizer 1	690	1,5 / 18	36,8	30,7
Superplasticizer 2	650	2,0 / 14	41,3	30,3
Superplasticizer 3	710	1,5 / 12	43,8	26,7
Superplasticizer 4	680	1,5 / 17	37,0	32,0

3. CONCLUSION

It is possible to make highly flowable self compacting concrete with crushed materials. The particle shape, size distribution and water demand of the crushed aggregate are of great importance.

Rheological measurements seem to be able to describe SCC better than normal measurements, and are operator independent.

The need for specially designed superplasticizers for crushed aggregate seems to be unnecessary. Different superplasticizers are able to change the yield stress and the plastic viscosity, but only at an insignificant level compared to other adjustments of the mix design. Slump retention might be a very important property that is decisive in choosing the proper SP.

4. ACKNOWLEDGEMENT

The project benefited greatly from the assistance of Velde Betong, Norway, Rheological laboratory, Mapei S.p.A, Italy, Analytical laboratory, Mapei S.p.A, Italy and Concrete laboratory, Mapei S.p.A, Italy.

REFERENCES

- 1 Norsk betongforening, *Publikasjon nr. 29 "Spesifikasjon og produksjonsveiledning for selvkomprimerende betong"*, 2007
- 2 Wallevik Olafur H., "*Introduction to Rheology of fresh concrete*", Course compendium, 2009.
- 3 Wallevik, Jón E., "*Fresh concrete, mortar and cement paste with various types of lignosulfonates*", doctoral thesis, 2003, ISBN 82-471-5566-4

Prediction of flow induced inhomogeneities in self compacting concrete



Jan Skoček, Ph.D.
Tech. Univ. of Denmark, Dept. of Civil
Engineering (DTU Byg), Brovej, DK-
2800 Kgs. Lyngby, Denmark
jas@byg.dtu.dk



Oldřich Švec
Tech. Univ. of Denmark, Dept. of
Civil Engineering (DTU Byg),
Brovej, DK-2800 Kgs. Lyngby,
Denmark olsv@byg.dtu.dk



Mette Geiker, Ph.D.
Tech. Univ. of Denmark, Dept. of Civil
Eng. (DTU Byg), Denmark
mge@byg.dtu.dk
Norwegian Univ. of Sci. and Tech.
(NTNU), Trondheim, Norway
mette.geiker@ntnu.no



Nicolas Roussel
Laboratoire Central des Ponts et
Chaussées
Université Paris Est
Paris, France
Nicolas.Roussel@lcpc.fr

ABSTRACT

A model for simulation of flow of suspension of a non-Newtonian fluid and particles of arbitrary shape is briefly introduced and demonstrated on examples of flow of self compacting concrete. The model is based on the lattice Boltzmann method for flow, the immersed boundary method with direct forcing representing the fluid - particle interactions, newly developed algorithm solving the dynamics and interactions of particles and a free surface algorithm based on the mass tracing algorithm. These techniques separating the complex problem into several levels result in a robust and accurate model that allows direct fully coupled simulations of typical laboratory experiments.

Keywords: Self compacting concrete, Casting, Rheology, Flow prediction, Segregation

1. INTRODUCTION

Self Compacting Concrete (SCC) does not require vibrations and will, if stable, result in an improved homogeneity of the hardened material. However, heterogeneities induced during the casting of the SCC may lead to variations of local properties and hence to a potential decrease of the load carrying capacity and durability of structures. Heterogeneities in SCC are primarily caused by static and dynamic segregation of coarse aggregates. Thus, to predict castings with SCC numerical model(s) capable of simulating flow patterns at the structural scale and at the same time the impact of the varying volume fraction of aggregates and other phenomena at the scale of aggregates on the flow are necessary. At the structural scale, a finite volume based single-flow model with a proper particle tracking technique can be used. In this contribution, a micro-mechanical fully coupled model for flow of particulate suspensions based on the Lattice Boltzmann Method (LBM) [1] providing the link between local flow patterns and arrangement of phases with effective properties on the macro-scale is presented. The basic ingredients of the model are briefly overviewed and discussed and then the capabilities of the model are demonstrated on case studies relevant for practical casting of SCC and fibre-reinforced SCC.

2. MODELLING STRATEGY

The complex problem of the flow of suspension of rigid bodies in a non-Newtonian fluid is separated into three levels allowing robust and efficient simulations. The levels, with reference

to Fig.1, and their assumptions are: a) Level of particles with exact (analytical) geometry used for dynamics (position and velocities $\mathbf{u}(t)$, $\boldsymbol{\omega}(t)$) and interactions (collisions and force $\mathbf{i}(t)$) of particles; b) Level of fluid-particles interaction with particles discretized by Lagrangian nodes $\mathbf{x}^L(t)$ solved by the Immersed Boundary Method (IBM) with direct forcing $\mathbf{f}(\mathbf{x}^E, t)$ and c) Level of fluid where the LBM is used for flow of a non-Newtonian fluid with external force $\mathbf{f}(\mathbf{x}^E, t)$.

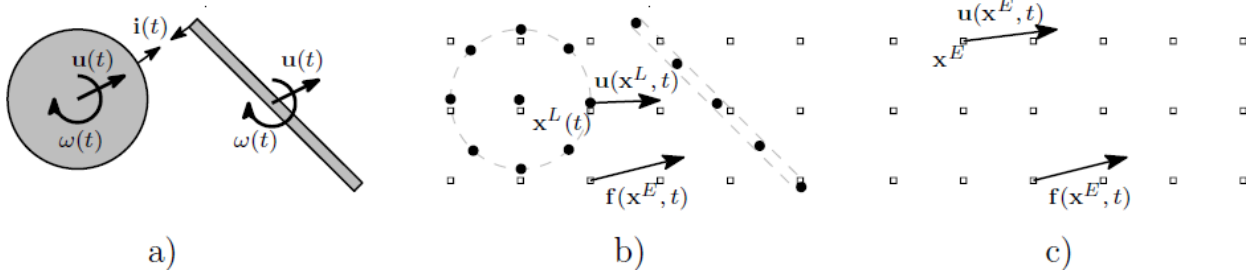


Figure 1 – a) level of particles, b) level of fluid-particles interaction and c) level of fluid.

2.1 Level of fluid: fluid dynamics solver

In contrast to the traditional CFD methods where the problem is formulated in spatially and time dependent velocity and pressure fields (macroscopic quantities, top-bottom approach) the LBM, with its roots in the kinetic theory of gases, treats fluid as individual particles discretized by a set of discrete particle distribution functions and provides rules for their mutual collisions and propagation. The macroscopic quantities can be then computed as moments of the distribution functions (bottom-up approach). Typically, the computational domain is discretized by a set of cells of a uniform size. Continuous fields of macroscopic variables are then approximated by sets of average values of the variables in the cells. Similarly, time is discretized into uniform time steps. In a given time step, velocity and pressure of the fluid in a cell described by the particle distribution functions depend on a local collision of particles and streaming of particle distribution functions from neighbouring cells from the previous time step. The local nature of the method, together with the simple algebra involved, leads to a favourably low computational costs and simple implementation.

2.2 Level of fluid: free surface algorithm

A free surface has been implemented in the form of a Mass Tracking Algorithm (MTA) [2]. Although the method theoretically conserves the mass exactly, small discrepancies due to the discretization were observed. The difference is negligible in one time step but systematic which leads to its accumulation during the computation making the error important. Therefore, a simple correction based on comparison of actual total mass with its initial value and distribution of the missing mass uniformly to all interface cells is adopted.

2.3 Level of fluid-particles interaction: immersed boundary method

The IBM with direct forcing [3] represents the particles in the fluid in a form of a force field. It is assumed that the velocity of the particle and fluid should be equal at Lagrangian points due to the no-slip boundary condition. Non-equal velocities are transformed into force field acting both on the particle and on the fluid assuming Newton's second law of motion. Since, generally, Lagrangian nodes do not coincide with Eulerian nodes, the velocity of the fluid in Lagrangian nodes is obtained by a volume averaging of the velocity field obtained from the LBM solution. The IBM, contrary to most methods assuming bounce-back walls at the fluid level, provides smooth and stable change in positions and forces acting on particles and makes e.g. coupling with the free surface algorithm easier. However, the most important feature of the IBM lies in its

ability to accurately simulate small objects of only a few lattice units or even sub-grid objects, see [4]. This results in a significant reduction of the computational time needed.

2.4 Level of particles: adaptive sub-stepping algorithm

The dynamics of immersed particles is driven by the Newton's second law of motion discretized with the explicit forward Euler method. However, when the force acting on the particle varies significantly during one lattice time step (e.g. light particles, fibres), the method might become unstable. A variable sub-stepping algorithm has been proposed in [5] to address the problem. In the algorithm the duration of an adaptive sub-step is computed analytically by restricting change in the forces exerted on the. This ensures stability of the simulation for highly variable forces.

2.5 Level of particles: interaction of particles

Force and direct interactions of particles are solved at the level of particles. The direct interactions (collisions) are simulated using the approach of force impulses. The normal impulse is assumed inelastic while the tangential impulse obeys Coulomb friction. The variable sub-step algorithm ensures stable simulation for arbitrary force interaction between two moving particles. In this contribution a lubrication force correcting term from [6] is used.

4. APPLICATIONS

4.1 Effect of particles on effective rheological properties

The effect of two types of rigid particles – spheres and fibres – on effective rheological properties was investigated. Suspensions of a Bingham fluid and a varying volume fractions of particles were sheared in the Couette geometry with different shear rates. The effective rheological properties were computed from volumetrically averaged strain rate eliminating the wall effect and stress exerted on the plates. Fig. 2 shows the results and their comparison to theoretical solutions. Details can be found in [4,5,8].

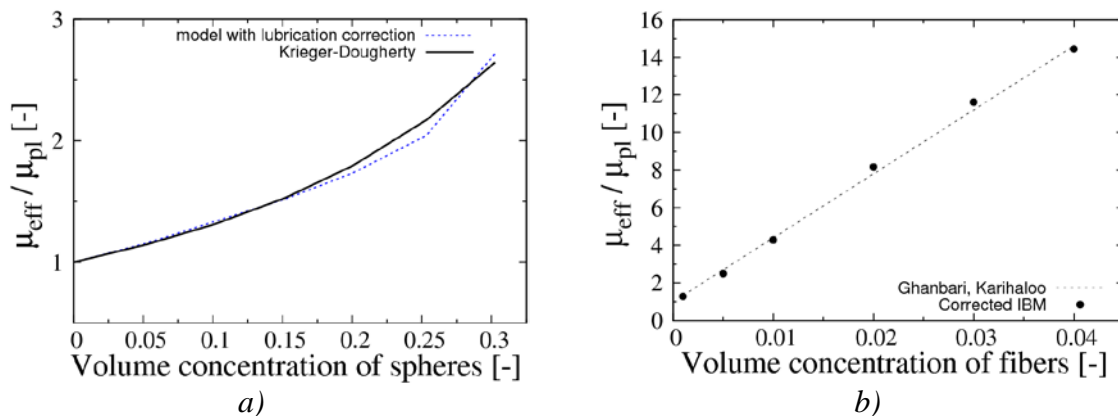


Figure 2 – Effect of volume fraction of spherical aggregates (a) and fibres (b) on effective plastic viscosity compared to theoretical predictions.

4.2 Dynamic segregation in a complex flow

A flow of suspension of rigid spheres and a Bingham fluid poured slowly into a rectangular domain was simulated. Fig. 3a) shows the configuration of the experiment, see [7] for all details. The final shape of the suspension and the final distribution of the particles and its comparison to experimental findings are shown in Fig. 3b). Note that more than 3300 particles were simulated using an ordinary PC.

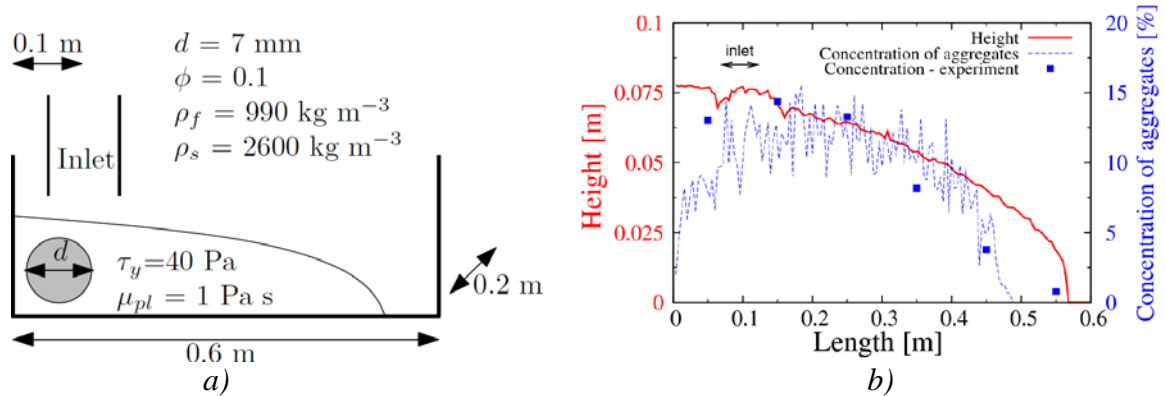


Figure 3 – Configuration of the experiment (a) and final shape and distribution of aggregates in comparison with experimental findings (b).

4. SUMMARY AND CONCLUSIONS

The developed model for flow of suspensions of non-Newtonian fluid and rigid particles was introduced and demonstrated. The model is robust and efficient – particles of an arbitrary shape in an arbitrary fluid and with arbitrary interaction rules can be simulated at typical experimental scales. It was further shown that the model captures correctly the main mechanisms – effect of particles on rheological properties and dynamic segregation of particles – needed to simulate realistically flow of SCC in real structures.

ACKNOWLEDGEMENTS

The work was funded by the Danish Agency for Science Technology and Innovation (project 09-065049/FTP: Prediction of flow induced inhomogeneities in self compacting concrete). Authors would like to acknowledge contributions of J. Spangenberg (DTU MEK), H. Stang (DTU Byg), J. Hattel (DTU MEK) and P. Szabo (DTU KT).

REFERENCES

1. C. K. Aidun, J. R. Clausen (2010). “Lattice-Boltzmann Method for Complex Flows”, Annual Review of Fluid Mechanics 42(1):439–472.
2. C. Körner, M. Thies, T. Hofmann, N. Thürey, N., U. Rude (2005), “Lattice Boltzmann Model for Free Surface Flow for Modeling Foaming”, Journal of Statistical Physics
3. Z. Feng, E. Michaelides (2005), “Proteus: a direct forcing method in the simulations of particulate flows”, Journal of Computational Physics 202(1):20–51
4. O. Švec, J. Skoček, H. Stang, J.F. Olesen, P.N. Poulsen (2011), “Flow simulation of fiber reinforced self compacting concrete using Lattice Boltzmann method”, Proceedings of 13th International Congress on the Chemistry of Cement, Madrid 2011
5. J. Skoček, O. Švec, J. Spangenberg, H. Stang, M.R. Geiker, N. Roussel, J. Hattel (2011), “Modeling of flow of particles in a non-Newtonian fluid using lattice Boltzmann method”, Proceedings of 13th International Congress on the Chemistry of Cement, Madrid 2011
6. N.Q. Nguyen, A. Ladd (2002). “Lubrication corrections for lattice-Boltzmann simulations of particle suspensions”, Physical Review E 66(4):1–12
7. J. Spangenberg, N. Roussel, J.H. Hattel, M.R. Geiker (2011), “Dynamic segregation during self-compacting concrete (scc) casting: Theoretical frame and experimental results on model fluids”, in preparation
8. O. Švec, J. Skoček, H. Stang, J.F. Olesen, P.N. Poulsen (2011), “Fully coupled Lattice Boltzmann simulation of fiber reinforced self compacting concrete flow,” Proceedings of Computer Methods in Mechanics 2011, Warsaw, Poland

Flow Properties of SCC for the Casting of Complex Shaped Pavilion



Lars N. Thrane
Consultant, Civ. Eng., Ph.d.
Danish Technological Institute
Gregersensvej,
DK – 2630 Taastrup
lnth@dti.dk



Jørgen Schou
Product Engineer
Unicon A/S
Sandagervej 15
DK - 7400 Herning
joergen.schou@unicon.dk



Thomas Juul Andersen
Consultant, Cand. Arch.
Danish Technological Institute
Gregersensvej,
DK – 2630 Taastrup
tja@teknologisk.dk



Claus Pade
Senior Consultant, M.Sc.
Danish Technological Institute
Gregersensvej,
DK – 2630 Taastrup
cpa@dti.dk

ABSTRACT

SCC was used to cast a complex shaped concrete pavilion, which was the final demonstration project in a Danish research project called “Unique Concrete Structures” ending in 2010. The casting was split in two parts. The first casting comprised the three supporting columns and the second one the capitals, rib structure and top plate. At the job site, the flow properties were measured with the 4C-Rheometer and approved before the castings were initiated. The project showed that relatively simple considerations of the challenges involved in the casting helped to ensure a positive outcome.

Key words: SCC, rheology, casting, complex shape.

1. INTRODUCTION

Many architects see concrete as fundamental construction material but also as a material, which offers unique opportunities in terms of shaping; and with SCC it is possible to cast even more complex shaped structures. The flow properties should be specified taking into account the form geometry, reinforcement configuration and casting technique. If the concrete is too fluid the risk of segregation increases and if it is too stiff there is a risk of improper form filling and poor encapsulation of the reinforcement [1],[2]. This paper describes the simple considerations made when selecting the target range for the flow properties of the two castings involved in the construction of a complex shaped concrete pavilion. The Pavilion was designed at the School of Architecture in Aarhus making use of topology optimization simulations [3]. The structure consists of three singular shaped columns, capitals, a rib structure, and a top plate with a thickness of 70 mm. All in all a complex shaped structure with a size of 12 x 6 x 4 m. The formwork parts were produced by milling polystyrene blocks using the industrial robot at the Danish Technological Institute. A total of 32 difference parts were produced. It was decided only to use a top shuttering over the capitals as it would be far too complicated to prepare a top shuttering covering the whole of the top plate. Instead, it was decided to let the top shuttering

cover the capitals until a slope of 5 % was reached, and design a SCC which could withstand this slope.

2. FLOW PROPERTIES – TARGET RANGE

Various diagrams and guidelines have been proposed to help target the flow properties of SCC. In this case, the rheology diagram proposed in Guidelines on Execution of SCC was applied [4]. The target ranges selected for the two castings are shown in Figure 1 and further described in the sections below.

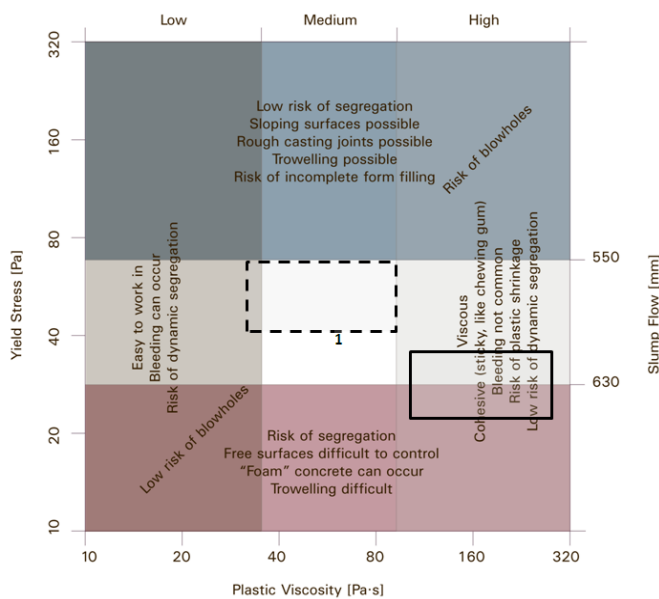


Figure 1 –The target range suggested for the two castings. The solid box represents the columns. The dotted box represents the capitals, rib structure and top plate.

2.1 First casting – the columns

The first casting comprised the three supporting columns. The space was confined by the drainpipe and reinforcement, and it was only possible to place the inlet at the top so the concrete would have to drop approximately 3.0 m. The challenge was to obtain a cohesive SCC that would tolerate the drop without segregating while not compromising its form filling ability. In the narrow parts of the form the concrete would have to pass congested regions with spacing down to 20 mm. To ensure complete form filling, it was decided to select a target fluidity in terms of slump flow as 630 mm \pm 25 mm. To obtain good cohesiveness during the drop a high plastic viscosity was chosen. To avoid blocking, the maximum aggregate size was set to 8 mm. Results from vertical castings have shown that SCC being cast from the top is actually less prone to dynamic segregation than SCC being pressed up from the bottom, however, the risk of entrapped air at the surfaces are higher. Therefore, a relatively low casting rate was specified to allow the air voids to escape in order to avoid blow holes at the surfaces.

2.2 Second casting – capitals, rib structure and top plate

The second casting comprised the capitals, rib structure and the top plate. Again, the challenge

was to find a compromise. On the one hand, the concrete should be fluid enough to fill the formwork and encapsulate the reinforcement, in particular flowing under the top shuttering over the capitals. On the other hand, the concrete should be stiff enough to retain a slope of approximately 5 %. Therefore, a small trial casting was carried out in the lab. Part of the formwork representing the top plate next to the top shuttering was produced. The slump flow of the trial concrete was 550 mm and it was possible to obtain the slope. It was concluded that it would also be possible to obtain the slope at higher slump flows, however, care would have to be taken by the personnel on site to e.g. avoid casting too fast. Therefore, based on these considerations it was decided to set the target range to 570 mm \pm 20 mm. The plastic viscosity was set to medium range to make the manual operations easier to perform without the concrete being too “sticky”.

2.2 Concrete composition

Table 1 – Concrete composition [kg/m³]. Top: For the columns. Bottom: for the top plate.

White cement	White pigment (slurry 50%)	Water	sand 0/4 mm	Aggregate 4/8	Plasticiser.	Superplast.	AEA	Air content [%]
449	18	147	797	904	2.2	6.4	0.81	6.0
449	18	170	740	904	2.2	5.0	0.81	6.0

3. RESULTS

For the first casting (columns) the inlet shifted between the three columns four times. The three columns were cast in 40 minutes corresponding to a low casting rate of approximately 5.0 m per hour. The flow properties were measured with the 4C-Rheometer and were within the target range. No problems were observed during casting and very few blowholes were observed after demoulding.

Table 2 – Flow properties at the job site. Measured using the 4C-Rheometer [2].

		Mix 1 Columns		Mix 2 Top plate	
		Before casting	After casting	Before casting	After casting
Yield stress	[Pa]	28	25	34	39
Plastic viscosity	[Pas]	120	164	67	93
Slump flow	[mm]	637	650	614	595
t ₅₀₀	[sec]	5.2	7.8	3.8	5.4

For the second casting the slump flow was a little too high, however, it was accepted taking into account the slump flow loss over time. Approximately 5 m³ of concrete were cast at a slow rate and the casting lasted approximately 1.5 hours. The contractor waited to the right time before manually finishing the top surface to obtain the required slope. The plastic viscosity was within the target range.



Figure 2 – Pictures of the final structure.

4. CONCLUSION

White SCC has been used for casting of a unique shaped concrete pavilion. The pavilion was designed using topology optimising tools. Based on simple considerations target ranges for the concrete flow properties were defined. The target ranges were then used as input to the mix design process, and at the job site the flow properties were measured and approved using the 4C-Rheometer. In general, the results were positive with respect to form filling, segregation resistance and surface finish.

5. ACKNOWLEDGEMENT

The authors would like to thank all the involved partners in the Danish research project “Unique Concrete Structures” and in particular the Danish National Foundation for Advanced Technology for their funding of the project.

REFERENCES

1. Roussel, N., “Rheology of fresh concrete: from measurements to predictions of casting processes”, *Materials and Structures*, Vol. 40, Issue. 10, pp. 1001-1012, 2007.
2. Thrane, L.N., Pade, C., Nielsen, C.V., “Determination of rheology of self-consolidating concrete using the 4C-Rheometer and how to make use of the results” *Journal of ASTM International*, Vol. 7, No. 1, 2010.
3. Dombrowsky, P., Søndergaard, A., “Three-dimensional topology optimisation in architectural and structural design of concrete structures”, *Proceedings of the International association for shell and spatial structures (IASS) symposium*, Valencia, 2009.
4. Thrane, L.N., Nielsen, C.V., Pade, C., “Guidelines for execution of SCC”, Danish Technological Institute, Taastrup, 2007, pp. 42.

SCC flow visualization in formfilling with black and grey concrete



Stefan Jacobsen, Professor.
COIN Dept of Structural Eng.
NTNU
N-7491Trondheim
stefan.jacobsen@ntnu.no



Rolands Cepuritis, MSc student
COIN Dept of Structural Eng.
NTNU
N-7491Trondheim
rolands.cepuritis@hcb.lv



Ya Peng, MSc, PhD student
COIN Dept of Structural Eng.
NTNU
N-7491Trondheim
ya.peng@ntnu.no

ABSTRACT

Studies of flow conditions during SCC formwork filling were made in a new flow box method with black SCC flowing after grey SCC. Flow conditions are visualized after hardening and sawing as a “frozen” image of the border between grey and black concrete. 3 different self compacting mixes were investigated with D_{max} 8mm and 40 vol-% matrix with $w/b = 0.50$, 0.65 and 0.65 with Viscosity Modifying Admixture (VMA). The 3 mixes were made in both gray and black with similar rheological properties. The results show maximum flow rate in the centre of the box near the top and lowest flow rate near the formwork. However, different flow profiles occur, depending on concrete, formwork and flow rate: plug flow between reinforcement and formwork, sheared flow with a wave form, apparently due to flow interaction with regularly spaced vertical reinforcement bars, as well as shear flow seemingly unaffected by the reinforcement bars.

Key words: SCC, formwork filling, flow visualization, pigments, rheology

1. INTRODUCTION AND SCOPE

The flow conditions in SCC form filling (at surfaces, over crosssection, around reinforcement) are little known. In a previous study the flow conditions were visualized as different SCCs were flowing in different pipes [1]. Observing the boundary between flowing gray and black concrete after hardening showed boundary flow (slip, no-slip etc) and variation of rate of flow over the cross section (flow profiles, plugs etc) in pipes. The review [1] showed few/no other reliable methods available. Recently [2] an effort to study particle segregation and flow using MRI was made, unfortunately applying model materials and not concrete. In this study black SCC flowing after grey SCC is used to visualize the flow conditions in form filling. Gray SCC is flowing in front of black pigmented SCC. The black SCC has as equal composition and rheology to the grey one as possible. The flow conditions are visualized on sawn surfaces after hardening.

2. EXPERIMENTS AND MATERIALS

2.1 Flow box for visualization of SCC flow in formwork with reinforcement

The test set-up consists of flow boxes (1.2 m long by 0.1 m wide by 0.13m high) made either of rough wood formwork or a smooth plywood formwork material (Wisa form). The reinforcement is $\text{\O}6\text{mm}$ 150x150mm welded mesh cut into 1.2 m long horizontal bars with 8 vertical bars (lengths equal to the 130 mm box height) at 150mm distance along the horizontal bar. The horizontal reinforcement-”ladders” are placed on each side with 22mm concrete cover depth over the horizontal bar and 16mm cover over the vertical bars. The ladder is fixed vertically on the bottom formwork plate in 8 holes. Upstream there is a shutter made of a thin steel plate and a vertical $\text{\O}100\text{mm}$ 1.5 m high PVC feeding pipe connected to the bottom of a ≈ 50 litre cylindrical feeding container. A video camera with timer was used to measure inflow rate towards a scale in the feeding container. Downstream there is an electronic balance logging the outflow from a 100 by 100mm square opening over a 20mm horizontal threshold, also with a steel plate shutter. There are shutters to allow accurate control of inflow, outflow and easy change of inflowing concrete. The box is first filled completely with grey SCC and both inflow and outflow recorded. Then, the out- and inflow shutters are closed, the vertical pipe and filling reservoir are rapidly emptied and refilled with black concrete readily produced and tested in the nearby concrete mixing lab. Then, the black SCC is swiftly let flowing into the formwork box after the grey by first opening the upstream shutter and then the downstream shutter. The black SCC is then flowing after the grey until approximately half the flow box volume is filled with black concrete, pushing out an equal amount of grey SCC downstream. Then the downstream- and the upstream shutters are closed and the flow box carefully left to harden for a few days before sawing. Recording of inflow by video and of outflow by balance gave the variation of flow (dv/dz) during the two-step filling process. The form filling operations should last as few minutes as possible to reduce different ageing between grey and black concrete. Longitudinal saw cuts (z -direction = flow direction) in the hardened specimens were made both horizontally (x -direction) and vertically (y -direction) to observe the variation in dv/dx and dv/dy . Each resulting 1.2x0.1x0.13 m concrete specimen was thus cut in four 1.2m long prisms showing frozen images of the interface between grey and black SCC.

2.2 Grey and black SCC for visualization of flow conditions.

3 SCC mixes were designed and efforts made to obtain equal rheological properties between the 3 pairs of grey and black “twin” mixes. Matrices were made with $w/b = 0.50, 0.65$ and 0.65VMA . The filler replacement levels $V_{\text{filler}}/V_{\text{powder}} = 0.20, 0.38$ and 0.31 respectively. The $w/b = 0.65\text{VMA}$ mix with $V_{\text{filler}}/V_{\text{powder}} = 0.31$ was made with 2.5 % VMA of powder mass. All mixes were made with standard Norwegian fly ash cement with 2950 kg/m^3 average particle density and constant SP dosage = 0.4 % of cement (Rescon SP 130 co-polymer). The solid volume fractions of the three matrices were $\Phi = 0.459, 0.459$ and 0.429 , or voids ratio = $V_{\text{water}}/V_{\text{powder}} = 1.18, 1.18$ and 1.33 , respectively. The filler was crushed igneous quartz diorite rock from Tau with particle density 2780 kg/m^3 . The black pigment (Ferroxon) replaced the filler volumetrically (3 %). Mortars or mini SCC were made with a washed granitic aggregate (0-8mm) from Årdal (NSBR) with less than 3 % material $< 0.125 \text{ mm}$ and 400 litres/m^3 matrix. Rheological measurements were made on mortar (slump flow, T500, density, air and BML coaxial viscometre) and on matrix (Physica MCR300 Rheometer with parallel plate).

3. RESULTS

3.1 Matrix and concrete rheology

The rheological measurement showed that the 3 % pigment replacement required to obtain a very clear border between black and grey concrete affects rheology. Air is entrained and even when adding an air damping admixture both Bingham yield stress and plastic viscosity increased in the matrix due to ferroxon, in line with earlier findings [1]. Therefore the SP dosage in the SC mortar mixes for the flow box experiments were increased to 1.2 – 1.6 % of cement in the black concrete, while being 0.8 – 1.1 % in the grey concrete. The air damper admixture Rescon RM was used at a dosage of 2.5 kg/m^3 in the black mortar. Thus the main effect of the black pigment on rheology of the final mortar mixes for flow box studies was to increase the yield stress seen as an upwards parallel displacement of most of the BML flow curves. There was no clear effect of pigment on T500, slumpflow nor plastic viscosity. Of the 12 concrete batches made (3 mixes x 2 colors x 2 types of formwork), 9 had slump flow > 600 mm and all > 500 mm. T_{500} was < 2 seconds for 10 of the 12 batches.

3.2 Flow box and visualization

The flow in the longitudinal (z-) direction of the formwork was mainly non-steady state with (dv/dz) both positive and negative depending on which part of the gravitational flow experiment that is considered. Figure 1 shows an example of the variation of flow rate

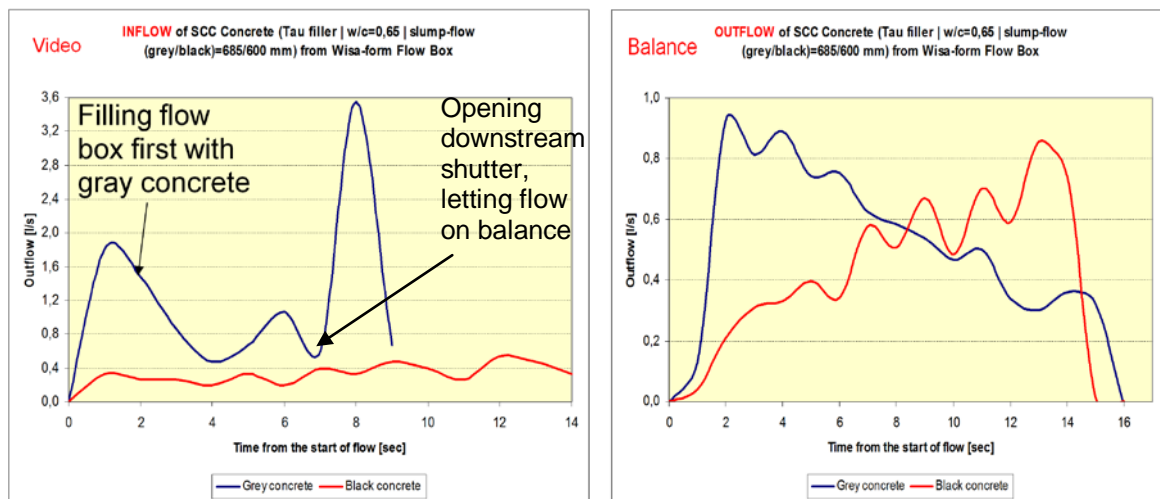


Figure 1 - Inflow (avg grey 1.24, black 0.35 lit/s) - Outflow (avg grey 0.55, black 0.45 lit/s), $w/c = 0.65$ mix flowing in plywood formwork with reinforcement, $1 \text{ lit/s} \approx 0.08 \text{ m/s}$

The flow was always faster through boxes made of smooth (wisa) form than through rough wood boxes as expected. The black $w/c = 0.50$ concrete, which had lowest consistency of all mixes in terms of slump flow and BML-measurements, did not flow through the rough wood box at all even though it flowed through the smooth wisa form box.

After hardening, observations were first made of black colour towards the formwork surface (boundary flow). Then the tip of the flow profile on the sawn surface (maximum flow rate) was observed. For this purpose the specimens were first sawn longitudinally (z) and vertically (y) at the centre so that the complete flow variation with height could be seen (dv/dy) . The results are quite encouraging. The average flow rates through the flow boxes were relatively low; in the order of 0.1 m/s, and the saw cuts showed clear images of the local flow conditions. Generally the flow rate was at a maximum close to the centre and minimum at the formwork. The vertical

gradient of flow rate (dv/dy) showed a turning point $1/4^{\text{th}}$ - $1/5^{\text{th}}$ of the height from the top. That is, the inflowing black concrete did not flow entirely on top of the gray concrete. The reason is that the flow boxes were made with lids. Pilot studies showed that the concrete flow rised too fast vertically compared to the forward flow in open-topped boxes. Apparantly there is a scale problem since the sideway flow is to slow compared to the inflow rate. The experiment is suppose to represent a wall formwork with concrete flowing sideways on top of the rising wall. In order to be able to study flow conditions at the chosen scale, lids were therefore used since the main point was to observe flow towards formwork and around reinforcement parallel to the formwork. Detailed analysis of boundary and maximum flow rate, comparison with flow rates and rheology will be made in a full paper. In the following a few examples of resulting flow conditions for different concrete mixes, formwork material, reinforcement and flow rates are shown. The horizontal velocity gradient (dv/dx) sometimes crosses the reinforcement undisturbed near the formwork. In other cases a plug flow between the form work and the reinforcement could clearly be seen, i.e. sometimes no shear flow in the cover zone. The latter can be seen in figure 2 below.

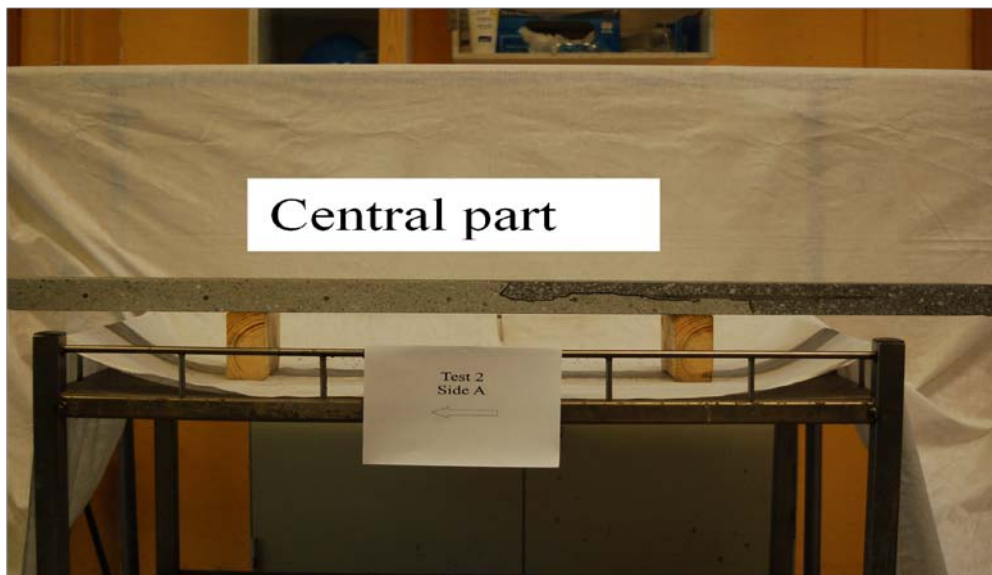


Figure 2 – Plug flow between vertical formwork and reinforcement seen from above ($=dv/dx$)
 $w/b=0.65$, $w/V_p=1.18$, $V_f/V_p=0.38$, wisa form, $v_{average}\approx 0.1$ m/s

In between the sheared flow and the plug flow there were also cases where a flow interference with the vertical reinforcement bars at 150 mm distance could be seen causing a wave form of the flow gradient towards the formwork surface. Further analysis and writing of a complete journal paper on the results are in progress.

4. ACKNOWLEDGEMENT

Thanks to lab engineers O.Loraas, S.Seehuus and G.Loraas and to support of COIN TG 2.1/2.3.

REFERENCES

1. Jacobsen S Haugan L Hammer TA Kalogiannidis E (2009) Cem. Con Res (39) 997-1006
2. Hafid H., Ovarlez G., Roussel N et al (2010) Estimating measurement artifacts in concrete Rheometres from MRI on model materials, Proc SCC2010, RILEM, Springer, pp.127-137

Increasing the use and performance of SCC in bridges



Peter Simonsson
M.Sc., Ph.D. Student
Luleå University of Technology
Dept. of Structural Engineering
SE - 97187 Sweden
Peter.Simonsson@ltu.se



Mats Emborg
Professor
Luleå University of Technology
Dept. of Structural Engineering
SE - 97187 Sweden
Mats.Emborg@ltu.se

ABSTRACT

Although Self Compacting Concrete (SCC) has many advantages over vibrated concrete, such as significantly improved pouring effectiveness and being associated with a better working environment, its rate of adoption in cast in-situ construction is still low. As well as higher costs that are not always offset by its potential economic benefits, several technical issues hinder the introduction of SCC to a wider market. This research aims to establish recommendations for robust mixes of target values of flowability for concrete to be used in specific parts of structural elements. We demonstrate that it is possible to develop robust SCC mixes that are tailored to the requirements of certain parts of structural elements.

Key words: Industrialization; Productivity; SCC; Flowability; Robustness; Aggregate moisture; Viscosity Modifying Agent.

1. INTRODUCTION AND OBJECTIVE

SCC with all of its inherent advantages is an important part of the development of an industrialized process for on-site concrete construction. If SCC is utilized properly, and if castings are planned correctly, the use of SCC can reduce the number of workers needed during castings. SCC is also physically easier to use than traditional vibrated concrete (TVC) since it is less complicated to handle on-site. Studies have shown that the working environment can be improved by up to three times when TVC is replaced with SCC [1]. It has been reported [2] that SCC may enhance the quality of the end product since any variations in the quality of the work on the finished structure due to compaction are eliminated.

In Sweden, there is often only one type of SCC offered for civil engineering applications. To increase the use of SCC and realize its potential benefits, the contractor needs to become more engaged in the whole process specifying their own criteria for the product, taking into consideration pouring methods, section geometry, weather conditions etc.

The overall objective of this research is to increase the use of SCC which is achieved when the concrete used is that best suited the project of interest. A robust adaptable product is therefore fundamental for the utilization of SCC for industrialization purposes. VMA is introduced in order to create a robust SCC using less powder material.

2. THEORY

According to recent international findings, SCC is on the cutting edge of scientific and technological developments [3] [4] and it is essential to introduce the technique in a broader manner to cast in-situ concrete construction. There are several possible definitions of SCC and they all revolve around a common factor: “the ability to flow under its own weight without

blocking between reinforcement bars and without segregation” see e.g. [5]. The performance of the product can be characterized using three main parameters: filling ability, passing ability and segregation proneness [6]. For these parameters, it could be possible to establish acceptance criteria that are dependent on the geometry of the structure to be cast, form type, reinforcement, and the method and/or local tradition applied to the pouring of the concrete.

In our suggestion of adapted SCC, two sets of slump flow and T50 data are shown in Figure 1: SCC-a is adapted for vertical parts of a bridge e.g. front wall and column, where a more flowable concrete that exhibits low risk of blocking, good quality surfaces and low input of resources is required. SCC-b is designed for horizontal elements e.g. bridge deck and foundations, where a stiffer concrete is better for a controlled casting front etc.

Viscosity Modifying Agents (VMAs) is used to stabilize the properties of the fresh concrete by modifying the rheological properties of the cement paste [7] [8] [9] [10] [11]. The intention of introducing VMA is to reduce the powder content and to make the concrete less sensitive to changes in the component materials. In addition, as noted by [12] VMA can be used to produce a robust [13] and more cost-effective SCC.

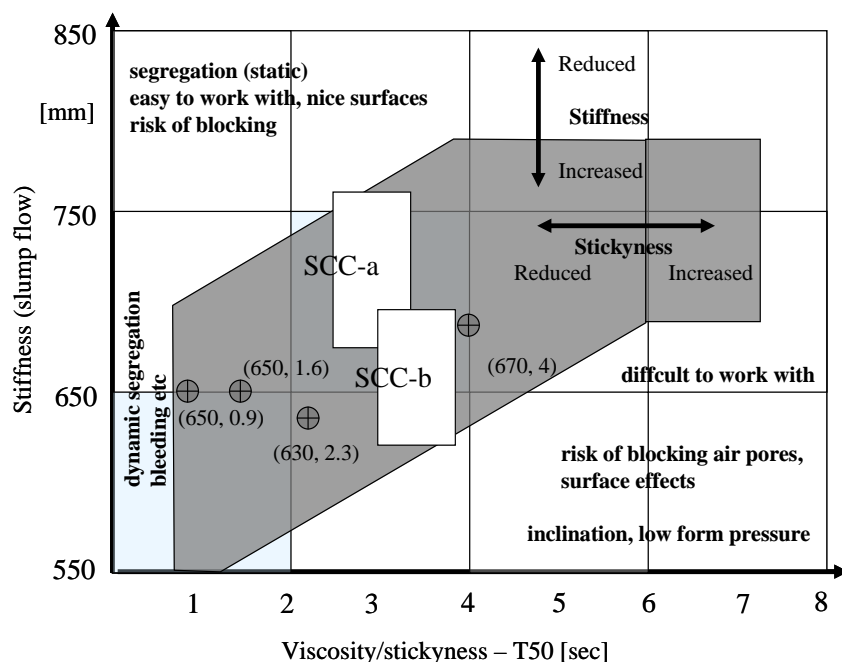


Fig. 1. Workability diagram (slump flow vs. T50). Concrete targeted for use in civil engineering structures. Suggestion for two types of adapted concrete, SCC-a and SCC-b (target values 720 mm +/-40 mm, 3 s +/-0.5 s and 650 mm +/-40 mm, 3.5 s +/-0.5 s respectively. Effects of excessively high/low values are also shown as well as an example of performance of some Swedish commercial SCC (modified from [14]).

3. RESEARCH

Several full scale castings both with TVC and SCC were studied prior to laboratory testing. Eight different sets of SCC have been tested in the research laboratory and at local laboratories at RMC plant, varying in amount of cement, filler, aggregate, VMA and superplastiziser. These have been divided between SCC-a and SCC-b in Figure 1. The mixing procedure remained the same for all the series and the properties of the fresh concrete were documented by means of visual inspection, workability and rheology tests.

Figure 2 shows results when testing one mix, which is a concrete with a target slump flow of 650mm +/- 40mm and T50 of 3.5s +/- 0.5s. Some difficulties arose in achieving insensitivity to

water content variations, especially for high filler content and dry concrete (see the figure). Filler reduction had a detrimental effect on the concrete flow with excessive sensitivity to sand moisture variations. Adding a viscosity modifying agent to the mix evidently increased the robustness, yielding values more or less within the limits. In fact, it seems possible to exclude the filler by adding an appropriate volume of VMA.

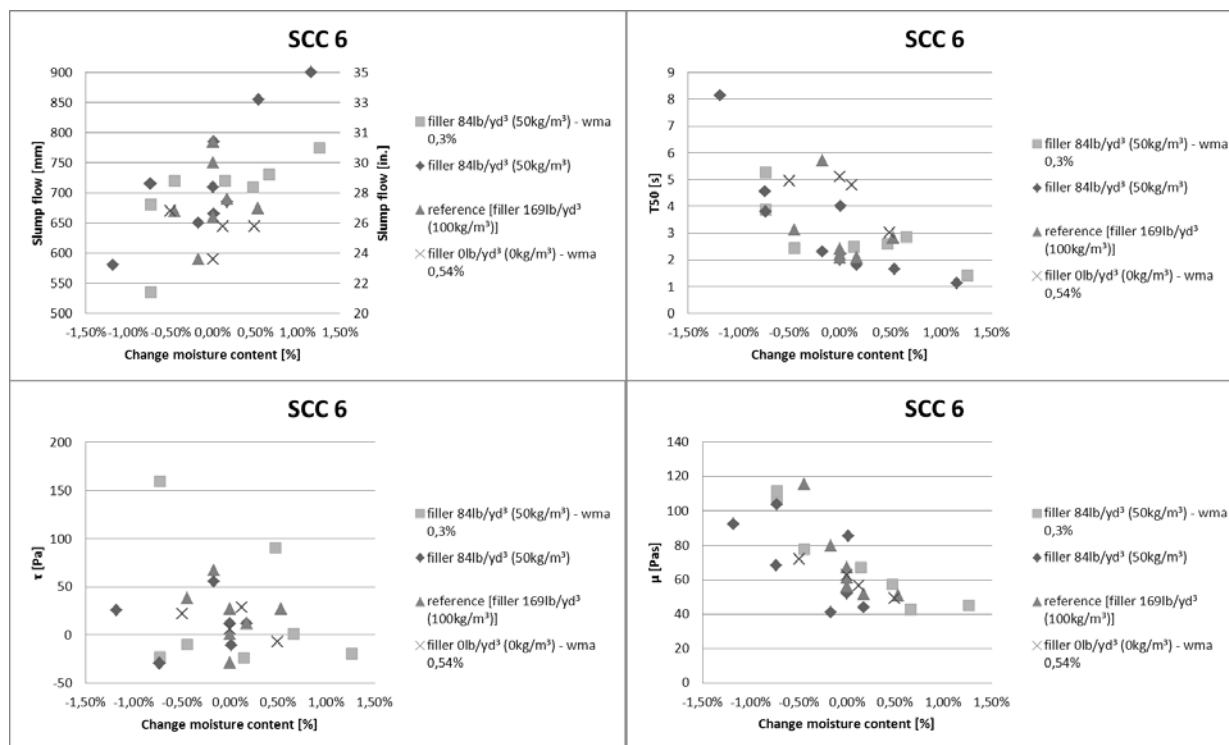


Fig. 2. Influences in Test Series 3 on workability (slump flow, T50 flow time) and rheology (shear stress, τ in ConTec 3 viscometer tests) of sand moisture variations and reduction of filler content. Concrete SCC6, $w/c=0.40$, reference limestone filler content: 100kg/m³.

4. CONCLUSIONS

Based on the results from the laboratory studies the following observations can be made:

- It is possible, without requiring complex measurements to be taken, to adapt the parameters of the fresh concrete to meet target values and related accepted variations in those values for use in specific structural parts of constructions such as bridges.
- Reference concrete mixes using local aggregate, use of additives, manufacturing tradition and various criteria from both contractors and clients all seem to be rather insensitive to the variation in aggregate which can be explained by a rather high volume of fines (cement paste and filler < 0.125mm).
- Reduction of filler content sometimes results in degradation of the quality of fresh concrete, e. g. when levels of filler content, are reduced too much.
- Various mix design philosophies to obtain same concrete have an obvious influence on the robustness when sand moisture is varied.
- It is possible to establish mixes for civil engineering purposes without any limestone filler, or similar additive, by the use of a viscosity modifying agent (VMA).

The remarks above are supported by visual observations made of full scale casting of bridges and other types of civil engineering structures.

5. FINAL COMMENTS

The utilization of SCC in on-site production can be increased considerably through better marketing of the concrete, and by making contractors aware of its benefits such as productivity increases, lower costs and faster construction of projects. It is important to consider SCC as a method rather than “just” a building material.

However, there is no room for mistakes when using SCC in full scale. An unsuccessful project will create far more scepticism than a successful project would create confidence.

This research demonstrates that a robust SCC, that is not too expensive, can be achieved by reducing the filler content and using VMA instead, without impairing the quality of the product. The concrete mixes studied were, in general, robust enough such that their original mixture only needed slight modification. For example, it would be possible to substitute some of the filler (at least 50% of the original amount) for VMA without compromising the quality of the concrete and hence the quality of any structures built using it.

REFERENCES

1. Rwamamara R and Simonsson P., 2011, “Self compacting concrete uses for construction work environment sustainability”. *Journal of Civil Engineering and Management*. Accepted for publication
2. De Schutter, G., Barthos, P.J.M., Domone, P. and Gibbs, J. (2008). *Self-Compacting Concrete*. CRC Press, Taylor & Francis Group, Boca Roton, USA. ISBN 978-1-4200-6833-7
3. Cussigh, F. (2007). SCC in practice: opportunities and bottlenecks. 5th international RILEM symposium on SCC, 3-5 Sept., Ghent, Belgium, pp 21-27.
4. Shah, S.P.; Ferron, R.P.; Ferrara, L.; Tregger, N.; and Kwon, S., 2007, “Research on SCC: some emerging themes,” 5th international RILEM symposium on SCC 3-5 Sept 2007, Ghent. PP 3-14.
5. Swedish Concrete Association., 2002, “Self-compacting concrete – recommendations for use,” *Concrete report no 10 (2002)*, 84 pp.
6. Testing SCC., 2004, “Technical report of the Growth project: Testing SCC Measurement of properties of fresh self-compacting concrete, 2001 – 2004,” Coordinator ACM Centre, Univ. of Paisley, UK CONTRACT N° G6RD-CT-2001-00580, 66 pp.
7. Nanthagopalan P, Santhanam M, 2010, “A new empirical test method for the optimisation of viscosity modifying agent dosage in self-compacting concrete”. *Materials and Structures*, No 43 pp 203-212
8. ERMCO., 2005, “The European Guidelines for Self Compacting Concrete, specification, production and use,” BIBM, CEMBUREA, EFCA, ERNARC, 68 pp.
9. Khayat K, 1998, “Viscosity-Enhancing Admixtures for Cement-Based Materials – An Overview”, *Cement and Concrete Composites*, Elsevier Science Ltd, No 20, pp 171- 188.
10. Khayat K; Hwang S-D; Belaid K, 2010, “Performance of Cast-in-Place Self-Consolidating Concrete Made with Various Types of Viscosity-Enhancing Admixtures”, *Technical Paper, ACI Materials Journal*, July-August, pp 403 - 412.
11. Billberg, P., and Westerholm, M., 2008, “Robustness of fresh VMA-modified SCC to varying aggregate moisture,” *Nordic Concrete Research No 38, 2/2008*, The Nordic Concrete Federation, pp 113- 131.
12. Lachemi M, Hossain KMA, Lambros V, Bouzoubaa N, 2003, “Development of cost effective self-consolidating concrete incorporating fly ash, slag, cement or viscosity-modifying admixtures”, *ACI Materials Journal*, 100(5), pp 419 – 425.

13. Taguchi, Genichi., 2000, “Robust engineering, Subir Chowdhury”, Shin Taguchi ISBN 0-07-134782-8.
14. Emborg, M., 2008, “How to increase the market of SCC – experiences from Nordic Countries”, Proceeding of the 3rd ASTM conference on Self-Consolidating Concrete, Chicago.

Session A4 – CARBONATION, CHLORIDES AND CORROSION

A MULTI-SCALE METHOD FOR MODELING OF MOISTURE AND CHLORIDE ION TRANSPORT IN CONCRETE



Filip Nilenius*
M.Sc., PhD-student
Chalmers University of
Technology
412 96 Göteborg
filip.nilenius@chalmers.se



Fredrik Larsson**
M.Sc., PhD, Docent
Chalmers University of
Technology
412 96 Göteborg
fredrik.larsson@chalmers.se



Karin Lundgren*
M.Sc., PhD, Docent
Chalmers University of
Technology
S - 412 96 Göteborg
karin.lundgren@chalmers.se



Kenneth Runesson**
M.Sc., PhD, Professor
Chalmers University of
Technology
S - 412 96 Göteborg
kenneth.runesson@chalmers.se

* Department of Building and Environmental Engineering

** Department of Applied Mechanics

ABSTRACT

Modelling and simulation of moisture and chloride ion transport in concrete is carried out using a multi-scale approach due to the strongly heterogeneous structure of concrete. The macro-scale problem is solved using the finite element method (FEM) where the material response in each Gauss-point is obtained by setting up a new finite element problem on a representative volume element (RVE). The RVE, in turn, consists of the meso-scale constituents of concrete and the solution to the RVE problem is homogenized and sent back to the macro-scale domain. Hence, the RVE problem serves in this fashion as a constitutive model for the macro-scale problem.

Key words: Multi-scale, mass transport, transient, moisture, chloride ions.

1. INTRODUCTION

Chloride ion ingress in concrete is of great concern for concrete structures as the ions can initiate corrosion of embedded reinforcement bars. Therefore, it is of interest to accurately model this transport phenomenon to better predict the initiation period, cf. [1], of reinforcement corrosion.

In this model, the meso-scale constituents of concrete are the cement paste, gravel and the Interfacial Transition Zone (ITZ). The porosity of the cement paste and ITZ allows for transport of the chloride ions. Furthermore, the transport of chloride ions within the cement paste is nonlinearly coupled to the transport of moisture as consequence of the constitutive relation chosen in model. Due to the inherent coupling, and the strongly heterogeneous meso-scale

structure of concrete, it is of interest to find a suitable homogenization tool in order to simulate mass transfer on the macro-scale level.

Modelling of this problem has been done in [2] on one-scale using analytical homogenization. With this contribution, the aim is to model the same problem using a two scale approach with numerical homogenization. In this manner, the influence of the meso-scale structure can be analyzed by altering the meso-scale setup. Control parameters for the meso-scale are mainly the gravel content, size and distribution.

2. PROBLEM FORMULATION

The macro-scale Ω , in this context, consists of concrete considered a homogenous material, while the meso-scale Ω_{\square} consists of the cement paste, gravel and the ITZ between the cement paste and gravel, all having unique material properties. The multi-scale modelling framework applied to this transport problem was developed in [3].

The transient transport problem is modelled on the meso-scale using the general mass conservation law stating that

$$\partial_t \Phi_v + \mathbf{q}_v \cdot \nabla = 0 \text{ in } \Omega_{\square} \quad (1)$$

$$\partial_t \Phi_c + \mathbf{q}_c \cdot \nabla = 0 \text{ in } \Omega_{\square} \quad (2)$$

where Φ_v is the moisture content, Φ_c is the chloride content, $\mathbf{q}_v(\nabla v, \nabla C; v, C)$ is the flux of moisture and $\mathbf{q}_c(\nabla v, \nabla C; v, C)$ is the flux of chloride ions. It thus follows from the formulation that the vapour content, $v(\mathbf{x}, t)$, and the chloride concentration, $C(\mathbf{x}, t)$, are the two unknown scalar fields which will be solved for.

The explicit choice of constitutive relations, used on the meso-scale, for the flux vectors is taken from [4] as

$$\mathbf{q}_v = \varepsilon_c D_c \nabla C + D_v \nabla v \quad (3)$$

$$\mathbf{q}_c = D_c \nabla C + \varepsilon_v D_v \nabla v \quad (4)$$

where $D_v(v)$ and $D_c(v, C)$ are diffusion coefficients for the pure cement paste and ε_v and ε_c are coupling parameters. Hence, the choice of constitutive relations cross-couples eqs. (1) and (2). Constitutive relations for the moisture content, $\Phi_v(v)$, and chloride content, $\Phi_c(C)$, have been taken from [5,6].

3. NUMERICAL EXAMPLES

3.1 Single scale – Comparison of different meso-scale setups

In Figure 1, numerical results are presented for different setups of meso-structures. The left domain shows a meso-structure including pure cement paste; the middle one includes gravel and the ITZ, while the fare right meso-structure contains cement paste and gravel only. The initial

values and boundary conditions were the same for all domains. It is notable how the meso-structure influences the diffusion process, and how the ITZ can increase the rate of diffusion. By only including gravel the diffusion rate will be decreased in comparison with pure cement paste. But if the ITZ is included, the net effect of gravel is an increase in diffusion rate. It follows that having a physically realistic setup of the meso-structure is crucial in order to execute proper diffusion simulations.

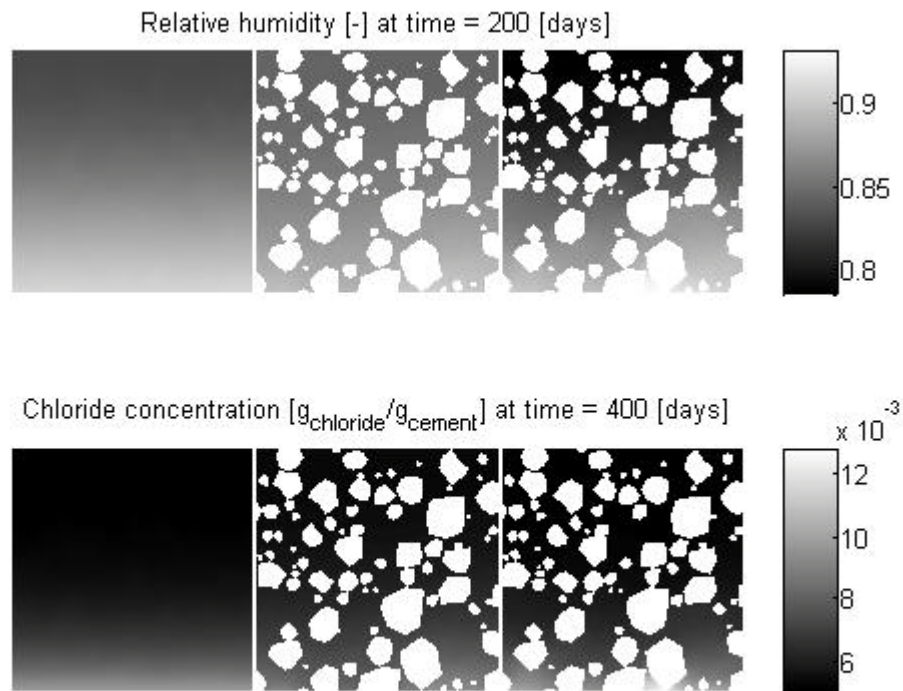


Figure 1 – Numerical results for relative humidity and chloride concentration. Convective boundary conditions are applied to the lower horizontal boundary. All other boundaries are insulated. Left: meso-structure including pure cement paste t , middle: includes also gravel and the ITZ, right: cement paste and gravel only.

3.2 Two scale simulation – FE²

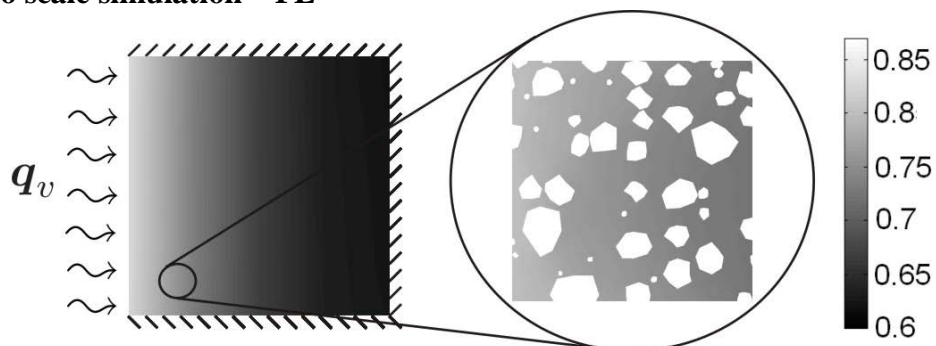


Figure 2 – Snapshot of relative humidity for a certain time step. The macro-scale domain has dimensions of $0.5 \times 0.5 \text{ [m}^2\text{]}$ whereas the RVE has dimensions of $10 \times 10 \text{ [cm}^2\text{]}$. The white objects in the RVE are representations of gravel.

4. SUMMARY

By employing a multi-scale method for modeling transport phenomena in concrete, the strongly heterogeneous structure of the material can be accounted for. This method enables modeling of concrete as a homogenous material by actually consider it as a composition of three materials, namely the cement paste, gravel and ITZ. The aim here, using this model, is to better predict the over-all transport properties of concrete.

REFERENCES

1. K. Tutti, "Corrosion of Steel in Concrete", *Swedish Cement and Concrete Research Institute*, Report: Fo. 4, 1982.
2. A. Suwito, X.-C. Cai and Y. Xi, "Parallel Finite Element Method for Coupled Chloride and Moisture Difusion in Concrete", *International Journal for Numerical Analysis and Modeling*, 2006, Vol. 3, pp. 481-503.
3. F. Larsson, K. Runesson and F. Su, "Variationally Consistent Computational Homogenization of Transient Heat Flow", *International Journal for Numerical Methods in Engineering*, 2010, Vol. 81, pp. 1659-1686.
4. A. Ababneh, F. Benboudjema and Y. Xi, "Chloride Penetration in Nonsaturated Concrete", *Journal of Materials in Civil Engineering*, 2003, Vol. 15, pp. 183-191.
5. Z.P. Bazant and L.J. Najjar, "Nonlinear Water Diffusion in Nonsaturated Concrete", *Materials and Structures*, 1991, Vol. 5, pp. 3-20.
6. L. Tang and L.O. Nilsson, "Chloride Binding Capacity and Binding Isotherms of OPC Pastes and Mortars", *Cement and Concrete Research*, 1993, Vol. 23, pp. 247-253.

Results from the Norwegian COIN project on chloride induced reinforcement corrosion in concrete



Ueli Angst, PhD student
COIN – Concrete Innovation Centre
NTNU Norwegian University of Science and Technology, Department of
Structural Engineering, N-7491 Trondheim, Norway.
ueli.angst@ntnu.no

Øystein Vennesland, Professor
COIN – Concrete Innovation Centre
NTNU Norwegian University of Science and Technology, Department of
Structural Engineering, N-7491 Trondheim, Norway.
oystein.vennesland@ntnu.no

Claus K. Larsen, Dr
COIN – Concrete Innovation Centre
Norwegian Public Roads Administration, N-0033 Oslo, Norway.
claus.larsen@vegvesen.no

Bernhard Elsener, Professor Dr
ETH Zurich, Institute for Building Materials (IfB), Switzerland.
elsener@ethz.ch

ABSTRACT

Within the framework of the Norwegian COIN research project (Concrete Innovation, initiated in 2007), the topic of chloride induced reinforcement corrosion was studied. The present paper summarises some of the most important findings. Firstly, the concept of the critical chloride content was reviewed and implications for test methods and service life models discussed. Secondly, chloride induced reinforcement corrosion was experimentally studied. In a third part, probabilistic considerations on the effect of specimen size of laboratory setups and implications for the application of measured chloride threshold values in service life models were discussed.

Key words: critical chloride content; chloride threshold value; pitting corrosion.

1. INTRODUCTION

Penetration of chloride from seawater or de-icing salts into concrete presents a risk for reinforcement corrosion which is in many countries regarded as the most important degradation mechanism for reinforced concrete infrastructure. Within the framework of the Norwegian COIN research project (Concrete Innovation Centre, see acknowledgements), chloride induced reinforcement corrosion was studied. The investigations formed part of the PhD project of the first author. The topic of chloride induced reinforcement corrosion was approached from various angles, namely by reviewing the concept of critical chloride content, by experimental

investigations, and by theoretical considerations regarding the size effect and probabilistic service life modelling. The most important findings are briefly summarised in the following sections; for more detailed information, the reader is referred to the given references.

2. LITERATURE REVIEW OF CRITICAL CHLORIDE CONTENT

The critical chloride content or chloride threshold value (both expressions here having the same meaning), abbreviated as C_{crit} , is usually defined as the chloride content at which corrosion starts. The issue of critical chloride content was reviewed with particular focus on test setups used in the literature to experimentally determine C_{crit} [1]. It was found that critical chloride contents reported by different authors scatter considerably. This was explained by the wide variety of used experimental setups. In fact, certain features inherent to the experimental procedure appear to have a stronger influence on the outcome, viz. the measured C_{crit} , than the parameters under study (e.g. water/cement ratio, binder type). In particular application of an electric field to accelerate chloride ingress or potentiostatic control of the rebar were identified to significantly affect the level of C_{crit} .

Furthermore, it was concluded that the state of the art does not allow improving the current engineering practice of condition assessment; neither does it offer a base for selecting reliable input parameters to be used in service life predictions (service life modelling). The latter is mainly due to lack of chloride threshold values for non-traditional binders such as cement types containing pozzolanic or other mineral additions, the use of which has nowadays become common. In addition, the literature data does not offer knowledge of the statistic distribution of the parameter C_{crit} (type of distribution, mean value, variance). In order to perform probabilistic service life modelling, however, this data is required. It was concluded that there is a strong need for a realistic and generally accepted test method for C_{crit} .

3. EXPERIMENTAL STUDY OF CHLORIDE INDUCED CORROSION

3.1 Materials and methods

Based on the literature review [1], an experimental setup was selected in order to study chloride induced reinforcement corrosion. The detailed experimental programme is described in Refs. [2,3]. In summary, concrete specimens were cast with embedded reinforcement steel (ribbed, in as-received condition), cured for 42 d and subsequently subjected to 1-dimensional chloride ingress induced by wetting/drying cycles. Each specimen was also equipped with an embedded reference electrode (MnO_2), a counter electrode (stainless steel bar) and an additional ordinary reinforcement steel bar as well as with six combined resistivity/chloride sensors. The latter allow non-destructive and thus continuous measurement of the concrete resistivity in the cover zone and the free chloride ion activity in the pore solution at depth 10 mm [4,5]. During exposure to chloride for more than one year, also the potential and linear polarisation resistance of the rebar under study were automatically monitored. After corrosion initiation, the process of early stage pitting corrosion was studied during a couple of weeks (by means of electrochemical measurements) before the samples were split for visual investigation and analysis of acid-soluble chlorides.

3.2 Main results

The following main observations were made:

Effect of steel/concrete interface

It was in this study observed that chloride induced corrosion initiated always on the rebar underside (with respect to casting), regardless of the direction of chloride ingress [2,3]. This was particularly surprising for the cases where, owing to the configuration of exposure to chloride, the chloride content in the concrete was higher on the front side of the steel. It was suggested that this behaviour is due to different characteristics of the steel/concrete interface on upper and lower rebar sides. It has been reported in the literature, that during casting, a bleed-water zone forms below the reinforcement owing to plastic settlement and collection of bleed-water [6,7]. In the present study, by examination of polished sections cut perpendicularly to the rebar in backscattered electron imaging mode, the presence of such a bleed-water zone was confirmed; gaps of widths of up to 200 μm were observed on the rebar undersides, but not on the upper sides. It might also be interesting to note that these findings were made for concretes with relatively high workability (slump ca. 200 mm) and both without and with fly ash (20%).

Another observation regarding interfacial defects was that although large entrapped air voids (several mm in diameter) were directly present at the steel/concrete interface, corrosion never initiated at these sites. It was suggested that as long as macro-pores are not water-filled, they are harmless from a corrosion viewpoint. Only for concrete submerged for a considerable time, these pores will fill up with solution and present local weaknesses and likely initiation sites for corrosion.

Depassivation behaviour of unpolarised steel in concrete

Thanks to the high time-resolution of the data logging equipment, numerous depassivation/repassivation events were recorded during exposure of the specimens to chloride. In some cases, after depassivation and repassivation, the steel remained passive for several months or even more than 1 year, although chloride exposure continuously raised the chloride content at the steel surface. For the cases where stable corrosion initiated, it was found that transition from the passive to the active state can occur over a long period of time rather than a well-defined instant (as is assumed in Tuutti's schematic model of service life [8]). Moreover, in many cases, after the first signs of depassivation, a considerable increase in chloride content was required to prevent repassivation and to enable stable pit growth. It was in Ref. [2] discussed that if in a laboratory setup the chloride content is measured at the very first depassivation event, it will be too conservative for engineering purposes in practice.

4. PROBABILISTIC CONSIDERATIONS ON EFFECT OF SPECIMEN SIZE

The effect of specimen size, viz. exposed steel surface area, was on a theoretical level discussed by the present authors in Ref. [9]. The considerations were based on the observation described in the literature that the susceptibility to chloride induced corrosion of a metal increases with increasing exposed metal surface area (see references cited in Ref. [9]). The reason for this is believed to be the fact that the probability for the presence of likely corrosion initiation sites increases with increasing metal area.

A probabilistic model was thus used to predict the critical chloride content for reinforcement corrosion in concrete as a function of rebar length (i.e. specimen size). Generally, the larger the specimen, the lower becomes the critical chloride content, and, in addition, the lower becomes

the scatter of measured critical chloride contents. It was thus concluded that the usually rather small specimen size is likely to be one of the reasons for the large scatter of chloride threshold values reported in the literature. In addition, the size effect was also suggested to be a reason for the high chloride threshold levels often observed in laboratory setups.

Furthermore, the question was raised whether specimen sizes in common experimental setups, e.g. those reviewed in Ref. [1], are sufficient to yield chloride threshold values relevant for practice. This led to suggestions on how to transfer the parameter C_{crit} , measured on relatively small laboratory specimens, to structural members of practical dimensions. In this context, it was also discussed how the size effect might be taken into account for probabilistic service life modelling.

ACKNOWLEDGEMENT

The paper is based on the work performed in COIN – Concrete Innovation Centre (www.coinweb.no) – which is a Centre for Research based Innovation, initiated by the Research Council of Norway (RCN) in 2006. COIN has an annual budget of NOK 25 mill, and is financed by RCN (approx. 40 %), industrial partners (approx 45 % of which ¼ is cash) and by SINTEF and NTNU (in all approx 15 %). The Centre is directed by SINTEF, with NTNU as a research partners and with the present industrial partners: Aker Solutions, Norcem, Norwegian Public Roads Administration, Rescon Mapei, Skanska, Spenncon, Unicon, Veidekke and Weber Saint Gobain.

REFERENCES

1. U. Angst, B. Elsener, C.K. Larsen, and Ø. Vennesland. Critical chloride content in reinforced concrete – A review, *Cement and Concrete Research* 39 (2009), 1122-1138.
2. U. Angst, B. Elsener, C.K. Larsen, and Ø. Vennesland. Chloride induced reinforcement corrosion: electrochemical monitoring of initiation stage and chloride threshold values, *Corrosion Science* (in press)
3. U. Angst, C.K. Larsen, Ø. Vennesland, and B. Elsener. Influence of casting direction on chloride-induced rebar corrosion. Presented at CONSEC'10 6th Int. Conf. on Concrete under Severe Conditions, Environment and Loading, Volume 1, Mérida, México, 2010.
4. U. Angst, B. Elsener, C.K. Larsen, and Ø. Vennesland. Potentiometric determination of the chloride ion activity in cement based materials, *Journal of Applied Electrochemistry* 40 (2010), 561-573.
5. B. Elsener, L. Zimmermann, and H. Böhni. Non destructive determination of the free chloride content in cement based materials, *Materials and Corrosion* 54 (2003), 440-446.
6. T.A. Soylev, and R. Francois. Corrosion of reinforcement in relation to presence of defects at the interface between steel and concrete, *Journal of Materials in Civil Engineering* 17 (2005), 447-455.
7. A.T. Horne, I.G. Richardson, and R.M.D. Brydson. Quantitative analysis of the microstructure of interfaces in steel reinforced concrete, *Cement and Concrete Research* 37 (2007), 1613-1623.
8. K. Tuutti. *Corrosion of steel in concrete*. Swedish Cement and Concrete Research Institute (1982).
9. U. Angst, A. Rønnequist, B. Elsener, C.K. Larsen, and Ø. Vennesland. Probabilistic considerations on the effect of specimen size on the critical chloride content in reinforced concrete, *Corrosion Science* 53 (2011), 177-187.

Critical Conditions for Depassivation of Steel in Concrete: Interface Chloride Profiles



Nelson Silva
PhD Student
Division of Building
Technology
Chalmers University of
Technology
SE-412 96 Gothenburg,
Sweden
nelson.silva@chalmers.se



Tang Luping
Professor
Division of Building
Technology
Chalmers University of
Technology
SE-412 96 Gothenburg,
Sweden
tang.luping@chalmers.se



Jan Erik Lindqvist
Senior Researcher
Materials Group
CBI Swedish Cement and
Concrete Research Institute
Box 857, SE-501 15 Borås,
Sweden
janerik.lidqvist@cbi.se



Dimitrios Boubitsas
Assistant Consultant / PhD
student
Materials Group
CBI Swedish Cement and
Concrete Research Institute
Box 857, SE-501 15 Borås,
Sweden
dimitrios.boubitsas@cbi.se

ABSTRACT

This paper describes an ongoing research project that aims to improve the knowledge and understanding of the critical conditions for depassivation of steel by studying the micro/meso-scale chloride profiles along the steel-concrete interface and correlating these with aspects of its microstructure and composition.

Key words: LA-ICP-MS, Micro-scale, Chloride Profiles, Reinforced Concrete, Corrosion.

1. INTRODUCTION

The chloride threshold value (C_{th}) is one of the most important parameters for the assessment of the service life of reinforced concrete structures. So far, however, there is no standard test method for the determination of C_{th} . Although there are some standard chloride analysis methods, the available procedures cannot representatively sample the concrete at the interface with the steel. This has been recognized as the main parameter influencing C_{th} and yet, chloride, calcium hydroxide (CH) and porosity profiles across this interface have been reported.

The physical barrier and pH buffering capacity of a denser CH layer surrounding the steel has been postulated as the main inhibitive factor for the initiation of chloride induced corrosion [1]. Experimental evidence that this CH layer leads to higher chloride contents required to initiate corrosion has been presented [2] and quantitative analysis has shown 18% more CH close to the steel as compared to that in the bulk cement paste [3]. However in [4], the preferential formation of CH at the interface was not observed and it was concluded that the pH buffering capacity should be extended to other solid hydroxyl phases.

Another important interface-related parameter that strongly influences the C_{th} is porosity and the presence of air-voids resulting in a non-uniform CH densification of the interface. In vertically cast rebars, an increase by up to 30% in the porosity level close to the steel when compared to the bulk concrete was measured [3]. In [5] an increase in the air void content at the interface resulted in a sharp decrease in the C_{th} and an empirical relationship was suggested.

Finally, the higher chloride bands, observed by means of SEM-EDS and reported in [6] and [7], suggest that the accumulation of chlorides at the interface may lead to higher chloride content values than those measured in the bulk concrete. Moreover, Yu [8] observed a non-uniform chloride content distribution along the interface and measured higher chloride contents at corrosion active sites when compared to passive locations along the bar.

Because the composition and microstructure of the interface plays a significant role, the distribution of chlorides along the steel-concrete interface should also be taken in consideration when determining the C_{th} , i.e., to account for the possibility of the measured chloride level, at a macro-scale, to be different from that responsible for the initiation of corrosion at one specific spot at the interface.

2. EXPERIMENTAL

The specimens used in this work are part of a larger project aiming the development of a test method for the determination of the C_{th} where T-shaped corrosion cells were developed based on the procedure described in [9]. Smooth steel bars were cast at four different cover depths (10, 15, 20 and 25 mm) and the specimens were exposed to salt solutions of 3% and 10% NaCl. Details regarding mixture proportions and corrosion monitoring techniques can be found in [10]. When depassivation was first detected, the section of the cell containing the corroding bar was cut-out and opened by cutting two grooves along the steel bar in order to allow removal of the steel bar with minimum interference in the interface. The aim was to obtain samples that represent a very early stage of corrosion. This made it possible to study the relations in the initial stage of corrosion. The total length of the interface subjected to chloride exposure was 100 mm. Of this, approximately 40 mm were studied, corresponding to the segment where corrosion was observed.

In order to study the chloride distributions along the concrete-steel interface, laser ablation inductively coupled plasma mass spectrometry (LA-ICP-MS) technique was employed. The method was calibrated using concrete powder pellets as a reference material. The chloride content in the pellets was determined by potentiometric titration. Iron and calcium distributions were also analysed and the latter was used as an internal standard to improve the robustness of the calibration. Further details can be found in [11]. In order to verify the non-uniform distribution of chlorides along the interface and the accuracy of the LA-ICP-MS measurements, some of the specimens was sectioned and analyzed by means of EDS and potentiometric titration.

In the next stage of the project after quantitative analysis, the specimens will be impregnated with epoxy resin without chlorides and containing fluorescent dye. Visual inspection with focus on void analysis (size and distribution) and multi-element surface cartography around the pitting positions will be carried at different depths by step-wise polishing the samples. For some specimens, the corrosion products ought to be characterized by XRD.

3. SUMMARY OF RESULTS

Figure 1 shows an example of a steel-concrete interface where LA-ICP-MS technique was successfully applied for chloride profiling. Reproducibility of the analysis was investigated through the ablation of 2 parallel scan lines. Although point-to-point vertical reproducibility is affected by variations in the microstructure and in the surface geometry due to pitting and diffusion of corrosion products, a good agreement was found and the differences in analytical results shown in scan line *a* and *b* match the differences in microstructure shown in the micrograph, indicating that observed trends are reproducible.

EDS analysis confirmed the trends in the chloride distributions obtained by LA-ICP-MS. Around the corrosion active sites, higher chloride levels were measured, a phenomena that cannot be revealed by macro-scale sampling. In general, the total chloride content measured by potentiometric titration appeared lower than the values measured around the pitting positions. However, when considering only passive regions, the results a macro level measurement and the meso level (LA-ICP-MS) measurement are fairly comparable [11].

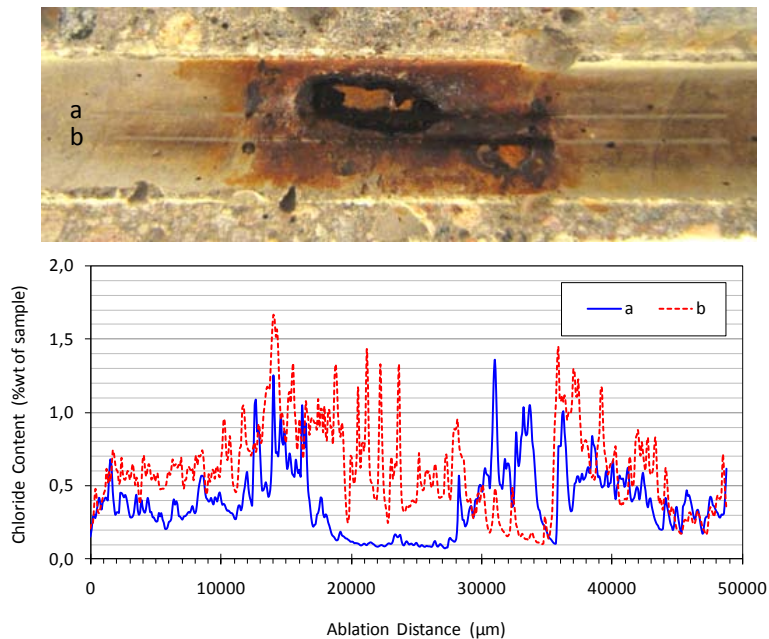


Figure 1 – LA-ICP-MS scan lines and chloride distributions along the interface.

During this study, corrosion was observed mainly in the bottom half of the specimens due to surface defects. In depth step grinding and BSE multi-element mapping revealed the accumulation of chlorides in iron rich areas and depletion of calcium and several corrosion products, such as goethite, lepidocrocite and akaganeite were identified. For further details and discussion of the results presented in this paper, please refer to [11].

4. CONCLUSIONS

A new technique (LA-ICP-MS) for determination of chloride profiles along the steel-concrete interface was adopted. Within a resolution range smaller than 300 μm , linear calibration curves with correlation coefficients between 0.95-0.99 were obtained.

Non-uniform chloride distribution along the interface was observed and higher chloride contents at corrosion sites were found. The results were confirmed by EDS analysis. Through the combination of these two methods the relation between chloride distribution and interface structure can be analysed from meso to micro-scale. These chloride levels differ from those obtained by potentiometric titration of the bulk concrete, thus reinforcing the necessity for the evaluation of the conditions at the interface and their influence in the C_{th} measured at macro-scale.

Surface defects play a significant role in the corrosion initiation with major impact on the C_{th} . Therefore a more systematic approach to directly relate air void size and distribution with the pitting positions and the distribution of chlorides around these is required.

ACKNOWLEDGEMENTS

The support of the Swedish Research Council (FORMAS project No. 243-2007-1512) is acknowledged.

REFERENCES

1. Page, C.L., "Mechanism of corrosion protection in reinforced concrete marine structures", *Nature* 258 (1975) 514-515.
2. Glass, G.K. and Buenfeld, N.R., "The inhibitive effects of electrochemical treatment applied to steel in concrete", *Corrosion Science* 42 (2000) 923-927.
3. Horne, A.T., Richardson, I.G. and Brydson, R.M.D., "Quantitative analysis of the microstructure of interfaces in steel reinforced concrete", *Cement and Concrete Research* 37 (2007) 1613-1623.
4. Glass, G.K., Yang, R., Dickhaus, T. and Buenfeld, N.R., "Backscattered electron image of the steel-concrete interface", *Corrosion Science* 43 (2001) 605-610.
5. Ann, K.Y., and Song, H-W., "Chloride threshold level for corrosion of steel in concrete", *Corrosion Science* 49 (2007) 4113-4133.
6. Yu, H., Shi, X., Hartt, W.H. and Lu, B., "Laboratory investigation of reinforcement corrosion initiation and chloride threshold content for self-compacting concrete", *Cement and Concrete Research* 40 (2010) 1507-1516.
7. Poupard, O., Aït-Mokhtar, A. And Dumargue, P., "Corrosion by chlorides in reinforced concrete: determination of chloride concentration threshold by impedance spectroscopy", *Cement and Concrete Research* 34 (2004) 991-1000.
8. Glasser, F.P. and Sagoe-Crentsil, K.K., "Steel in concrete: Part II. Electron microscopy analysis", *Magazine of Concrete Research* 41 (1989) 213-220.
9. Nygaard, P.V. and Geiker, M.R., "A method for measuring the chloride threshold level required to initiate reinforcement corrosion in concrete", *Materials and Structures* 38 (2005) 489-494.
10. Boubitsas, D. and Tang, L., "An approach for measurement of chloride threshold values", in *Advances in Concrete Structural Durability, Proceeding of the 2nd International Conference on Durability of Concrete Structures ICDCS2010*, pp. 275-284.
11. Silva, N., Tang, L., Lindqvist, J.E. and Boubitsas, D., "Chloride contents at the concrete-steel interface", in *Advances in Concrete Structural Durability, Proceeding of the 2nd International Conference on Durability of Concrete Structures ICDCS2010*, pp. 275-284.

Degradation and corroding problems for concrete in biological treatment plants make surface protection necessary



Ylva Edwards
Techn. Dr.
Swedish Cement and Concrete Research Institute, CBI
Drottning Kristinas väg 26
SE – 100 44 Stockholm
ylva.edwards@cbi.se

ABSTRACT

This paper describes selected parts of a joint project regarding degradation and corrosion problems for concrete used at biological treatment plants in Sweden. Results from an initial study show that concrete used in such plants cannot resist attack by leachate from food waste, and therefore needs surface protection. In a second part of the project, requirements specification was developed in order to ensure the function of such surface protection products and systems, as well as the concrete, in different parts of a biological treatment plant. A test program is proposed, focusing on chemical resistance and wear resistance. A test solution corresponding to leachate from food waste is specified.

Key words: Composting, digestion, corrosion, food waste, concrete, sealing coat, leachate, polyurea, epoxy, MMA, mastic asphalt.

1. INTRODUCTION

A study on the degradation and corrosion of concrete in biogas and composting plants was conducted in 2009/2010, and reported [1]. Results clearly show that concrete used in such plants cannot resist attack by leachate from food waste. Leachate test samples from a number of treatment plants were analyzed in the laboratory and found to be acidic, containing several aggressive chemical components with devastating impact on concrete. Furthermore, the temperature during food waste treatment will increase to around 70 °C in the process. Mechanical abrasion from gathering vehicles in receiving halls also has to be considered.

In Sweden, there are today some 20 biogas plants, and about one hundred composting plants for waste from parks, gardens, and/or food waste. More are planned and many have to be repaired and rebuilt. Also in the rest of Europe, more such plants are being built. However, there are no specific standards for the concrete to be used or for protection coatings in such environments.

1.1 Concrete degradation

Concrete is a strong, durable and comparably cheap building material. Within certain areas of use, it may, however, need protection. Reasons for this could be limited resistance to chemicals, or its porosity/permeability. Pre-treatment of the concrete surface is very important prior to applying any surface coating. Depending on concrete surface quality, different types of cleaning

or adjustment may be necessary, such as grinding, milling, blasting crack sealing etc. Laitance and curing compounds must always be removed from fresh concrete surfaces.

There are a variety of grades and fields of application for concrete. In recent decades, the development of new additives and materials made possible entirely new types of concrete. Self-compacting concrete (SCC) is such an example, using flow improvers/super plasticizers as a very important component. In spite of great improvements of concrete quality, the penetration of certain chemicals cannot entirely be avoided, as all concrete has a tendency to crack, and it is not possible to produce a completely crack-free concrete surface.

Concerning exposure classification and risk of corrosion, eighteen different classes within six different types of exposure are defined in EN 206-1 [2]:

1. No risk of corrosion or attack (X0)
2. Corrosion induced by carbonation (XC1, XC2, XC3 and XC4)
3. Corrosion induced by chlorides other than from sea water (XD1, XD2 and XD3)
4. Corrosion induced by chlorides from seawater (XS1, XS2 and XS3)
5. Freeze/thaw attack with or without de-icing agents (XF1, XF2, XF3 and XF4)
6. Chemical attack (XA1, XA2 and XA3)

In the case of exposure 6, chemical attack in soil and ground water at temperatures between 5 and 25 °C is referred to. XA3 is described as highly aggressive chemical environment according to some specified conditions, and the most onerous value for a single chemical component determines the class. Fields of application for concrete in aggressive chemical environment are bridges, garages and parking decks, animal stables and biological treatment plants.

In the initial study of the project, chlorides, organic as well as inorganic acids, ammonia, and ammonium ions were identified. They are all aggressive to concrete.

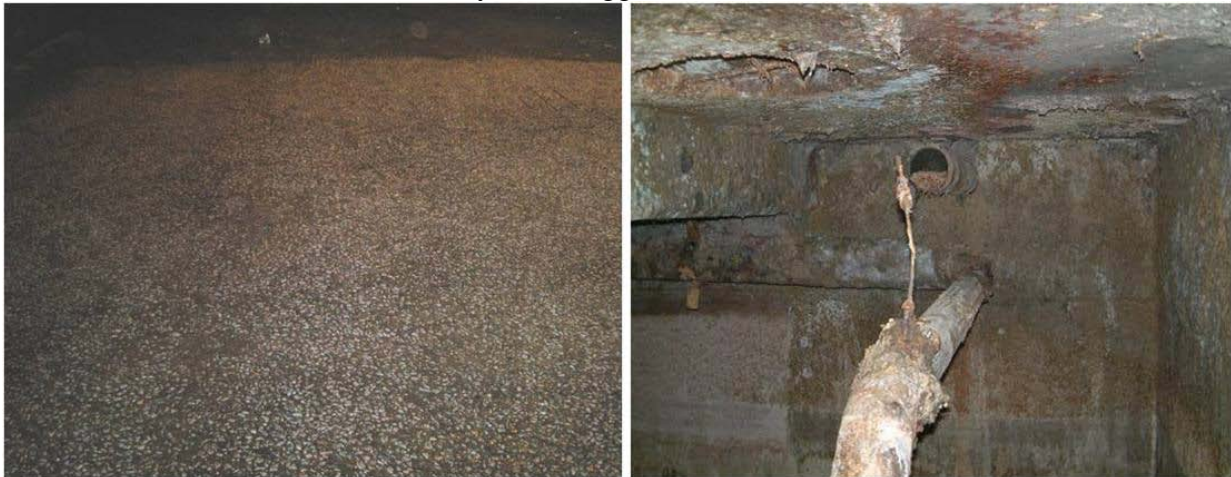


Figure 1 – Damage in reception hall for food waste and in reception tank at biogas plant.

2. METHODOLOGY

Several producers, experts and contractors were contacted in the project concerning possible products and technologies for the protection of concrete in biological treatment plants. Literature was reviewed as well as specifications and testing methods for similar fields of application. In particular, chemical resistance and wear resistance were focused on. Test liquid, corresponding to leachate, and test procedures were proposed. Furthermore, a number of systems were

recommended by producers in the project, and product data sheets were required for these systems. Possible technologies are based on material such as epoxy, polyurethane, polyurea, acrylates (MMA) and bitumen based materials. Three systems, already used in Swedish biological treatment plants, were compared regarding reported characteristics, performance and testing by the producer. Finally, test program and specification were proposed.

3. SPECIFICATIONS AND REQUIREMENTS FOR PRODUCTS AND SYSTEMS USED FOR THE PROTECTION OF CONCRETE STRUCTURES

There is a set of European standards for products and systems used for the protection and repair of concrete structures (EN 1504, Part 1-10). EN 1504-9 deals with general principles and EN 1504-2 with surface protection systems including a lot of standards for the characterization of different types of systems [3, 4]. For chemical resistance, EN 13529 is referred to and for wear resistance the Taber Abraser [5]. In addition to EN 1504, there are several specifications dealing with special fields of application such as road and railway concrete bridges.

3.1 Specifications for Swedish bridges

Mainly two types of waterproofing are used and specified for Swedish road bridges, namely polymer modified flexible sheets and polymer modified mastic asphalt. The products are both specified in VVTBT according to requirements based on EN 14695 (for sheets) and EN 12970 (for mastic asphalt), respectively [6, 7, 8]. Liquid applied technologies with thermo sets are normally not used on road bridges in Sweden, mainly because there is no relevant specification for such technologies. Liquid applied systems may, however, be used on railway bridges.

Both CEN (Comité Européen de Normalization) and EOTA (European Organization for Technical Approvals) are working with harmonized specifications and test methods within the field of waterproofing for concrete bridge decks. If there is no EN standard for a certain product, an ETA (European Technical Approval) can be developed. ETAG 033 is such a general guideline for liquid applied systems on concrete bridges [9]. Normally, the system is not to be exposed to direct traffic or ballast. The guideline is referred to for liquid applied systems on railway bridges in Sweden.

4. CHEMICAL RESISTANCE AND WEAR

There is a need for developing performance related criteria for the evaluation of protection systems on concrete, as well as guidelines for the selection of products and systems under different types of exposure. Based on existing methods according to EN 1504-2 and EN 13529, this was done for biological treatment plants within the project. Suggested test liquid, corresponding to leachate from food waste, is:

Acetic acid 2 %

pH \leq 4

Phosphates 0,2 %

Ammonia/ammonium ions 0,2 %

Hardness 20

According to requirements specification in EN 1504-2, the resistance to wear is tested using the Taber Abrasion test or testing according to EN 13813 (for flooring) [10]. Testing of wear is discussed in the report, and testing according to EN ISO 5470-1 (ASTM 4060 Taber test) including choice of test parameters, depending on type of application, is suggested [11, 12]. For high resistance to wear, testing is performed with wheel H 22 or methodology according to EN-13892.

5. COMMENTS AND CONCLUSIONS

It is concluded in the report that there are technologies, materials and systems available that will probably perform well as surface protection on concrete in biological treatment plants. However, relevant specifications are lacking and different test methods therefore are being used by producers, making it difficult to compare systems for the same type of application.

Chemical resistance to leachate is very important, and so is wear resistance (for the protection of floors in receiving halls). Future laboratory work is suggested in the report, including evaluation of suggested methods for chemical resistance and wear. Test sites and follow-up activities are suggested as well. The full report is published on www.wasterefinery.se.

6. REFERENCES

1. Boubitsas D., Hellström H., Henriksson G., Åkesson U., "Kartläggning av vittrings- och korrosionsskador på biologiska behandlingsanläggningar", Waste Refinery rapport, 2010.
2. EN 1206-1 "Concrete – Part 1: Specification, performance, production and conformity", 2000.
3. EN 1504-9 "Products and systems for the protection and repair of concrete structures - Definitions, requirements, quality control and evaluation of conformity - Part 9: General principles for the use of products and systems", 2008.
4. EN 1504-2 "Products and systems for the protection and repair of concrete structures - Definitions, requirements, quality control and evaluation of conformity - Part 2: Surface protection system", 2004
5. EN 13529 "Products and systems for the protection and repair of concrete structures – Test methods – Resistance to severe chemical attack", 2003.
6. VVTBT "Tätskikt på broar 09", Vägverket, Publikation 2009:112.
7. EN 14695 "Flexible sheets for waterproofing - Reinforced bitumen sheets for waterproofing of concrete bridge decks and other trafficked areas of concrete - Definitions and characteristics", 2010.
8. EN 12970 "Mastic asphalt for waterproofing – Definitions, requirements and test methods", 2001
9. ETAG 033" Liquid Applied Bridge Deck Waterproofing Kits", 2010.
10. EN 13813 "Screed material and floor screeds. Screed material. Properties and requirements", 2002.
11. EN ISO 5470-1 "Rubber- or plastics-coated fabrics – Determination of abrasion resistance – Part 1: Taber abrader (ISO 5470-1:1999)", 1999.
12. ASTM D4060-90 "Test Method for Abrasion Resistance of Organic Coatings by Taber Abraser".
13. EN 13892-5 "Methods of test for screed materials. Determination of wear resistance to rolling wheel of screed material for wearing layer", 2003.

The Electrical Resistivity of Concrete as Service Life Parameter



Karla Hornbostel, Dip.Ing.
PhD Student
Norwegian University of Science and Technology (NTNU)
Department of Structural Engineering
Richard Birkelandsvei 1a, 7491 Trondheim, Norway
Karla.Hornbostel@ntnu.no



Claus K. Larsen, Dr.Ing.
Norweg. Public Roads Admin.
Tunnel- and concrete division
Oslo, Norway
Claus.Larsen@vegvesen.no
Norwegian Univ. of Sci. and Tech.
Dept. of Structural Eng. (NTNU),
Trondheim, Norway



Mette Geiker, PhD
Tech. Univ. of Denmark,
Dept. of Civil Eng. (DTU Byg),
Lyngby, Denmark
mge@byg.dtu.dk
Norwegian Univ. of Sci. and Tech.
Dept. of Structural Eng. (NTNU),
Trondheim, Norway
mette.geiker@ntnu.no

ABSTRACT

A PhD project was started in December 2009 at NTNU Trondheim as part of COIN. The project aims at improving the basis for assessment of the service life of reinforced concrete structures in chloride containing environment, especially after initiation of reinforcement corrosion. Prediction models including the propagation phase of reinforcement corrosion are presently under intense discussion. As electrical resistivity of concrete is seen as one of the main parameter controlling the corrosion process, it is the aim of the PhD project to determine the applicability of resistivity as a measure for the corrosion rate.

Key words: concrete resistivity, reinforcement corrosion, propagation period, corrosion rate

1 INTRODUCTION

Reinforced concrete surrounds us in our everyday life; it is important for social and industrial buildings and indispensable for infrastructure like bridges and tunnels. In general, concrete is considered as a durable construction material with a lifespan over many decades. Nevertheless, some of our reinforced concrete structures are either reaching the end of their calculated service lifetime or showing distinct signs of damage. To assure sufficient structural safety for these structures, it is fundamental to gain knowledge about their deterioration processes.

Reinforcement corrosion initiated by chloride ions is one of the main causes for repair and maintenance of concrete structures in Norway, especially bridges. Many bridges suffer from chloride ingress, depassivation of steel reinforcement and on-going corrosion while still in service. Therefore it is a strong need for easy and reliable prediction and assessment of corrosion rate.

There is today a growing tendency for increased use of blended cements with high dosages of fly ash and slag. These cements results in concretes with very high electrical resistivity over time, which we consider beneficial for low corrosion rates, i.e. long service life. However, there

is a lack of verification and specific knowledge about the correlation between corrosion rate and resistivity for these types of concrete.

2 BACKGROUND

Initially introduced by Tuutti [1], the reinforcement corrosion process may be divided into two main periods. The initiation period, describing the penetration of damaging matters as chloride ions through the concrete cover to the embedded steel and consequently causes the so called depassivation of the reinforcement and, the propagation period, where the actual deterioration processes takes place.

Current service life models are concentrating on the initiation period and mostly predicting the end of service life as the point of depassivation (e.g. *fib Model Code for Service Life*). However, there are obvious reasons to consider a possible extension of the life span of concrete structures beyond the onset of corrosion. The time between depassivation of the reinforcement and the first occurrence of visual degradation signs like, cracks or spalling can be several years or even decades [2]. Assuming that the cross sectional reduction of the steel does not cause any major reduction in the load carrying capacity, this would lengthen the calculated service life considerably and thus lead to a prolonged utilization of existing structures. However, reliable prognoses for the development of corrosion are necessary to achieve sufficient safety standards. The concrete resistivity could in this respect be a useful parameter to assess corrosion rate.

The electrical resistivity of a material describes its ability to withstand the flow of current. It is estimated from the electrical resistance (quotient of potential and current) multiplied by a geometrical factor, referred to as k .

For concrete, the electrical resistivity describes the resistance to flow of ions through the pore structure which can be connected to corrosion of steel embedded in concrete. Bertolini and co-workers [3] explained reinforcement corrosion caused by the presence of chloride ions as an electrochemical cycle including anodic and cathodic reactions (“processes”) on the steel surface as well as transport processes through the steel and concrete (see *Figure 1*).

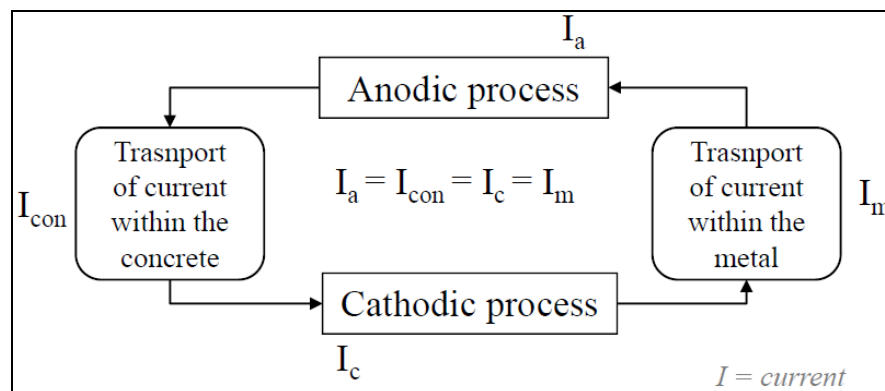


Figure 1 - Electrochemical process of corrosion after [3]

Each process can be described in form of a process current (I_a , I_{con} , I_c , I_m). All part-currents have to equal each other. The overall macro cell rate (corrosion rate I_{corr}) is limited to the slowest of the four processes. The resistivity of steel is with respect to the resistance of the other mechanisms so low that the transport of current within the metal unlikely will be rate limiting.

However, depending upon a range of factors amongst the electrical resistance of concrete the cathodic, anodic or electrolyte resistance can dominate the overall reaction rate.

Numerous investigations undertaken during the last 30 years e.g. [4-8] showed that linear relationships between corrosion rate and concrete resistivity exist in the log-log scale, as can for example be seen in *Figure 2*. However, the relationship appeared to be dependent both on concrete and exposure properties [9] and seems also to vary between different experimental setups.

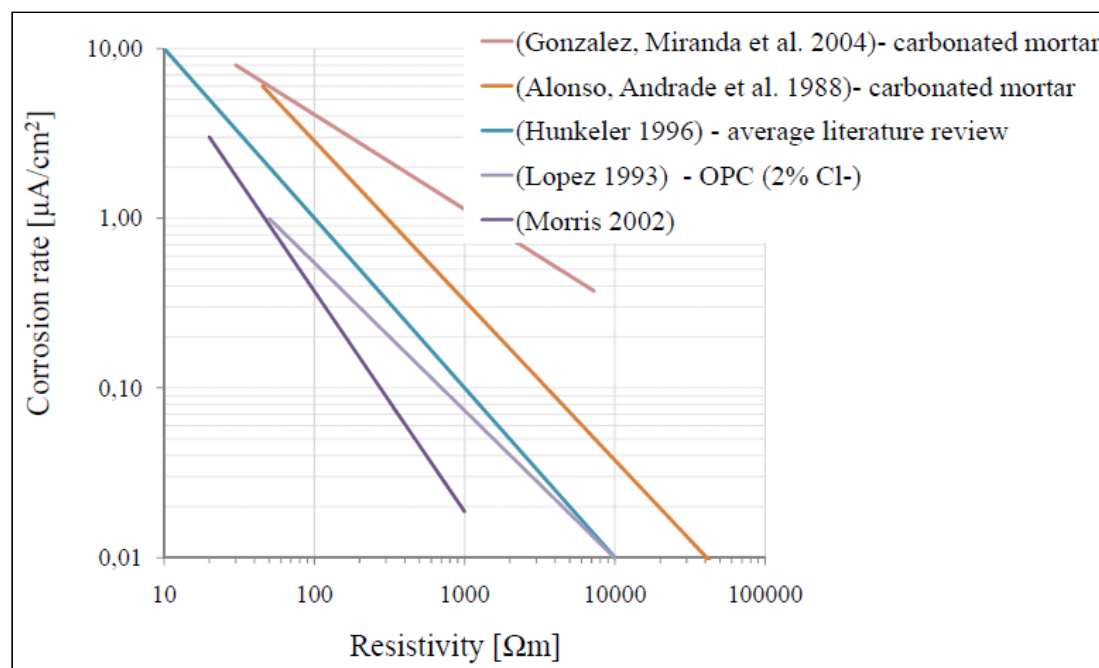


Figure 2 – Selected observations of corrosion rate vs. concrete resistivity

Many investigations led to the conclusion that the dependency of corrosion rate on concrete resistivity is caused by a resistance control of the corrosion process (see *Figure 1* - I_{con}). But the observations could also indicate that both the cathodic reaction and the anodic process show a dependency on concrete resistivity, as both mechanisms involve transport of matters through the concrete. However, at present it is not clear if this would lead to a similar strong relation between corrosion rate and resistivity.

3 OBJECTIVES AND SCOPE

As previously mentioned there is a strong need for a better understanding of the fundamentals of the relation between corrosion rate and resistivity in concrete. Hence, the main objective of the presented PhD project is to identify and describe this relationship and thus enhance service life prediction models.

According to this main objective, a detailed literature review will be provided to identify the lack of knowledge in the current discussion on the propagation period of reinforcement corrosion in concrete structures and to propose hypotheses for the relationship between corrosion rate and concrete resistivity. The suggested hypotheses will be studied with the help of, as far as possible, realistic investigations with experimental parameters limited to conditions (material and exposure) found for Norwegian concrete structures.

The experimental results should help in the proposal of guidelines for in-situ measurements of electrical resistivity (and possible supplementary parameters) and to assess criteria for evaluating corrosion propagation.

4 EXPECTED RESULTS

It is the aim of the PhD project to give a suitable explanation of the often detected linear relation between corrosion rate and concrete resistance. The PhD project and its results could thus be a further step on our way to reliable service life prediction models and assessment methods after corrosion onset.

5 ACKNOWLEDGEMENT

The paper is based on the work performed in COIN - Concrete Innovation Centre (www.coinweb.no) - which is a Centre for Research based Innovation, initiated by the Research Council of Norway (RCN) in 2006. COIN has an annual budget of NOK 25 mill, and is financed by RCN (approx. 40 %), industrial partners (approx 45 % of which ¼ is cash) and by SINTEF and NTNU (in all approx 15 %). The Centre is directed by SINTEF, with NTNU as a research partner and with the present industrial partners: Aker Solutions, Norcem, Norwegian Public Roads Administration, Rescon Mapei, Skanska, Spenncon, Unicon, Veidekke and Weber Saint Gobain.

REFERENCES

1. Tuutti, K., *Corrosion of steel in concrete*. 1982, Swedish Cement and Concrete Research Institute: Stockholm.
2. Raupach, M., *Models for the propagation phase of reinforcement corrosion - an overview*. Materials and Corrosion-Werkstoffe Und Korrosion, 2006. **57**(8): p. 605-613.
3. Bertolini, L., et al., *Corrosion of steel in concrete*. 2004, Weinheim: WILEY VCH.
4. Alonso, C., C. Andrade, and J.A. Gonzalez, *Relation between Resistivity and Corrosion Rate of Reinforcements in Carbonated Mortar Made with Several Cement Types*. Cement and Concrete Research, 1988. **8**(5): p. 687-698.
5. Gonzalez, J.A., J.M. Miranda, and S. Feliu, *Considerations on reproducibility of potential and corrosion rate measurements in reinforced concrete*. Corrosion Science, 2004. **46**(10): p. 2467-2485.
6. Hunkeler, F., *The resistivity of pore water solution - A decisive parameter of rebar corrosion and repair methods*. Construction and Building Materials, 1996. **10**(5): p. 381-389.
7. López, W. and J.A. González, *Influence of the Degree of Pore Saturation on the Resistivity of Concrete and the Corrosion Rate of Steel Reinforcement*. Cement and Concrete Research, 1993. **23**: p. 368-376.
8. Morris, W., et al., *Corrosion of reinforcing steel evaluated by means of concrete resistivity measurements*. Corrosion Science, 2002. **44**(1): p. 81-99.
9. Bertolini, L. and R.B. Polder, *TNO report - Concrete resistivity and reinforcement corrosion rate as a function of temperature and humidity of the environment*. 1997: TNO Building and Construction Research.

The effect of metakaolin on chloride penetration into concrete



Rui M. Ferreira
M.Sc., Ph.D.
University of Minho, C-TAC
Campus de Azurém
4800-058 Guimarães, Portugal
rmf@civil.uminho.pt



Pedro M. Costa
M.Sc.
University of Minho, C-TAC
Campus de Azurém
4800-058 Guimarães, Portugal
pedrocosta.bo@hotmail.com

ABSTRACT

Extensive research and practical experience have shown that partial replacement of cement by metakaolin improves concrete durability as a result of the refinement of the pore structure. While literature confirms much research on the performance of concrete with metakaolin, it is scarce concerning the performance with regards to chloride penetration.

For the study, reference mixes were made with CEM I 42,5R cement. Two contents levels were defined: 330 kg/m³ and 440 kg/m³ based on mix designs currently used in the ready-mix industry for C20/25 and C30/37 concretes. Cement was partially replaced with metakaolin with levels varying from 10-20%. All mixes were tested for compressive strength, electrical resistivity and chloride diffusion characteristics (migration and immersion testing).

The results demonstrate the improved resistance to chloride penetration of concretes with metakaolin additions. In addition, a beneficial effect on strength and durability properties of metakaolin also observed. Service life design calculations of reinforced concrete structures in marine environment based on the result obtained show a significant increase in the time to fulfill the serviceability limit state of corrosion initiation.

Key words: Durability, metakaolin, chloride penetration, electrical resistivity, service life

1. INTRODUCTION

Metakaolin (MK) is produced from calcining kaolin clay at a specific temperature range (600-800 °C) to make it reactive, with the general form Al₂O₃-SiO₂. Literature confirms that partial replacement of cement by MK improves concrete strength and durability as a result of the refinement of the pore structure. Besides the performance benefits of using MK in concrete, there are also ecological benefits, which make MK concrete a more sustainable alternative to OPC concrete. The production of MK does not release CO₂ as does that of OPC as a result of the decarbonation of limestone, and, lower temperatures are required to produce MK, hence lower energy required. While much research on the mechanical and durability performance of concrete with MK has been performed, it is scarce with regards to chloride penetration. Kim [1] shows the identical performance of MK with silica fume (SF) measuring the total charge passed (ASTM C 1202). Studies by Boddy [2] show that circa 8% MK in concrete can reduce diffusion coefficients by 50%, whereas 12% MK can reduce apparent diffusion coefficient (D_A) by 30%. Zeljkovic [3] also studied the total charge passed and D_A with similar results. Nokken [4] work shows similar tendencies, with 8% MK having identical performance as that of 4% SF.

2. MATERIALS, CONCRETE MIXTURES AND TEST PROCEDURES

In this study, the pozzolanic effect of MK additions in OPC concrete was studied. Two cement contents levels were chosen based on mix designs currently used in the ready-mix industry for C20/25 and C30/37 concretes: 330 kg/m³ and 440 kg/m³, respectively. Cement was replaced with MK with levels varying from 10-20%. All concretes were tested for compressive strength, electrical resistivity, non-steady state chloride migration and chloride immersion.

A CEM I 42,5R (Secil) cement was used in the production of concrete specimens, in accordance to the NP EN 197-1. A commercially available metakaolin (Optipozz) used was - Class N according to the ASTM C 618. In Table 1 the chemical and physical characteristics of the cements and metakaolin used are presented.

Table 1 – Properties of cements and metakaolin

Parameters (%)	SiO ₂	Al ₂ O ₃	K ₂ O	Na ₂ O	Fe ₂ O ₃	CaO	SO ₃	MgO	Cl	Sg*	Ss*
CEM I 42,5R	19.55	4.24	-	-	3.34	62.61	3.26	2.51	0.03	3.12	4071
Metakaolin	51.50	44.51	0.21	0.11	0.45	0.02	-	0.12	-	2.20	

* Sg – specific gravity; Ss – specific surface (cm²/g)

Two coarse aggregates and a river sand were used. The coarse aggregates with size 5-15 mm and 15-30 mm have specific gravity of 2.65 g/cm³ water absorption of 1.50 %. The river sand had specific gravities of 2.63 g/cm³ and absorption of 1.04 %. Mix design was based on maintaining a constant water/binder (w/b) ratio. A 0.45 w/b ratio for mixes with 440 kg/m³ of binder, and a 0.60 w/b ratio for mixes with 330 kg/m³ of binder. Each series was comprised of a reference mixture with no MK, and mixes with 10%, 15% and 20% of cement replacement with MK. Details of the concrete mixtures are presented in Table 2. Concrete workability was kept within the S2 class of the NP EN 206-1.

Table 2 – Concrete compositions for reference mixtures

Series	w/b	Water (l/m ³)	Binder (kg/m ³)		Aggregate (kg/m ³)			Slump (mm)
			Cement	MK	Course 1	Course 2	Sand	
330-0 (REF)	0.60	198	300	0	405	835	710	80
440-0 (REF)	0.45	200	440	0	420	820	600	90

All concrete mixes were produced in a vertical axis mixer with a 120 litre capacity. Cubic specimens of 100 mm and 150 mm in dimension and cylinders of 100 mm in diameter and 200 mm in height were cast in steel moulds and compacted using a vibrating table. 24 hours after casting the specimens were removed from the moulds and permanently cured in water tanks at 20 ± 3 °C until testing. Testing was performed at 7, 14, 28, 90 and 180 days.

The compressive strength of the concrete was evaluated on 150 mm cubes according to the NP EN 12390-3. The electrical resistivity (ER) of the concrete was determined using a four-probe resistivity-meter (RM MK II - alternating trapezoidal current wave - 13 Hz) on 150 mm cubic concrete specimens, according to LMC testing procedure for ER of concrete [5]. The non-steady state chloride migration coefficient was determined on cylindrical specimens of 100 mm diameter and 50 mm height according to the LNEC E463 [6]. The chloride immersion test was

performed on 100 mm cubic specimens according to the LNEC E390 [7].

3. RESULTS AND DISCUSSION

An analysis of the result in Table 3 reveals the well-known beneficial effect of metakaolin on compressive strength, *i.e.*, refinement of the pore structure due to pozzolanic reaction. All levels of replacement showed improvement (already at 28 days). Significant improvement is observed for 15% replacement for the 440 kg/m³ mixes ($\pm 20\%$).

Table 3 – Compressive strength and electrical resistivity results

Series	Average compressive strength (MPa)					Average electrical resistivity (Ωm)			
	7 days	14 days	28 days	90 days	180 days	7 days	28 days	90 days	180 days
330-0 (REF)	18.87	22.17	23.87	28.07	29.07	30.03	39.53	49.48	50.80
330-10	17.00	22.20	26.60	31.10	31.83	25.58	73.13	74.05	74.89
330-15	14.93	20.97	25.03	31.53	33.10	21.67	65.36	65.68	66.37
330-20	12.37	18.77	23.40	29.63	33.60	20.30	62.46	63.18	65.93
440-0 (REF)	30.53	33.73	40.62	44.03	44.77	38.27	54.84	71.58	72.53
440-10	30.23	35.87	40.90	44.80	45.40	32.58	95.51	95.93	96.68
440-15	32.67	40.43	47.97	53.67	54.57	39.34	124.75	127.10	127.98
440-20	24.73	32.07	39.73	46.77	47.63	30.16	85.99	107.61	112.53

The electrical resistivity (ER) results in Table 4 show an improvement in the performance of concrete with MK additions at early ages. At 28 days, 25-75% increase in ER is observed in concrete with MK. From this date onward no significant increase is observed except for a slight increase in the values of the reference concrete.

Table 4 – Results of the non-steady state migration and immersion test

Series	Migration coefficient ($\text{e}^{-12} \text{m}^2/\text{s}$)				D_A ($\text{e}^{-12} \text{m}^2/\text{s}$) / c_s (%/mass binder) *		
	7 days	28 days	90 days	180 days	D_A	c_s	Depth (mm) of 0.08% cl
330-0 (REF)	53.99	31.28	30.66	29.41	12.00	5.24	> 40
330-10	47.77	15.84	13.43	13.38	3.52	7.98	[15-20]
330-15	59.13	17.05	14.31	14.22	3.95	8.73	[20-25]
330-20	51.06	23.10	15.15	14.86	2.78	6.99	[20-25]
440-0 (REF)	25.11	15.49	13.18	13.15	4.82	5.34	[20-25]
440-10	26.69	8.52	8.32	8.14	3.62	4.65	[15-20]
440-15	24.15	7.03	6.64	5.77	2.32	6.59	[10-15]
440-20	27.35	10.49	7.34	6.26	1.35	11.86	[10-15]

* D_A – Average apparent diffusion coefficient; c_s – Average surface chloride concentration

From table 4 it can be observed that the chloride migration coefficient at 28 days, for mixes with MK, is already 50% lower than the reference mixes. At 180 days the tendency maintains. The apparent diffusion coefficient calculated by curve fitting of the chloride profiles is roughly 75% lower for the 330 kg/m³ binder mixes, and between 20-70% lower for the 440 kg/m³ binder

mixes. For all concretes with MK, the depth of the critical chloride concentration is always lower than that of the reference mixes.

The average chloride profiles measured from the specimens subject to the immersion test are presented in Figures 1 and 2. The results of the curve fitting of Fick's 2nd Law of diffusion to the chloride profiles (D_A and c_S) are presented in Table 4.

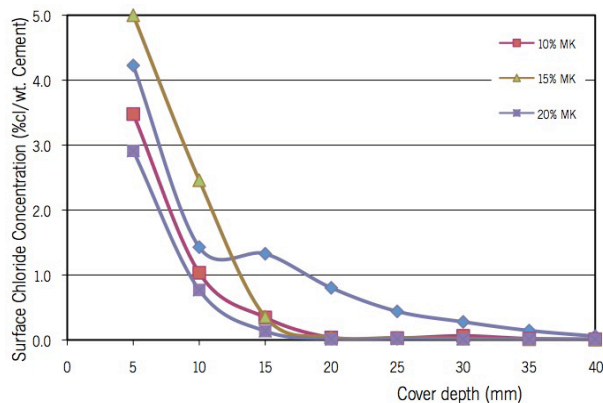


Figure 1 – Chloride profiles for 330 kg/m³ binder mixes

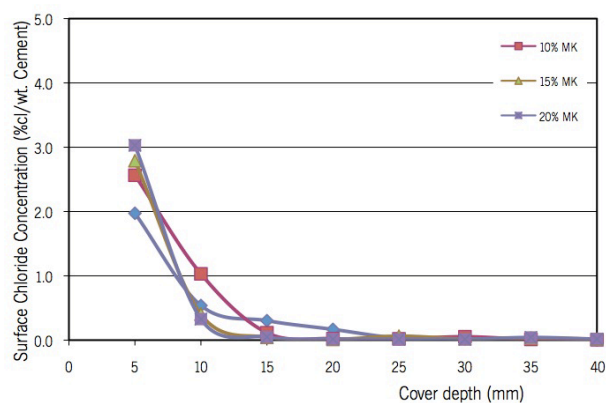


Figure 2 – Chloride profiles for 440 kg/m³ binder mixes

4. CONCLUSIONS

The present study was only based on a limited number of test methods, which may not reflect the complete performance of concrete against chloride penetration. However, based on the results obtained, MK additions improve the performance OPC concrete (when < 20%) with regards to chloride penetration. Concretes with MK have lower apparent diffusion coefficients from immersion testing, lower diffusion migration coefficients and higher electrical resistivity, especially from 28 days onwards, independent of the % of MK substitution. Concrete will have a longer service life in marine environment due to the beneficial effect of MK.

REFERENCES

1. Kim, H.S., Lee, S.H., Moon, H.Y., "Strength properties and durability aspects of HSC using Korean metakaolin," *Construction & Building Materials*, Vol 21, 2007, pp. 1229-1237
2. Boddy, A.; Hooton, R.D.; and Gruber, K.A., "Long-term testing of the chloride-penetration resistance of concrete containing high-reactivity metakaolin," *Cement & Concrete Research*, Vol. 31, 2001, pp. 759-765
3. Zeljkovic, M., "Metakaolin effects on concrete durability". Master Thesis. University of Toronto. 2009. 163 pp.
4. Nokken, M.R., Boddy, A., Hooton, R.D., Thomas, M.D., "Time-Dependant Diffusion in Concrete" *Cement and Concrete Research*, Vol. 36, No. 1, 2006, pp. 200-207
5. PE-002, "Concrete. Electrical resistivity - Measuring the electrical resistivity of a concrete element," (in portuguese) *Construction Materials Laboratory*, University of Minho, 2005, 9 pp.
6. LNEC E 463 "Concrete. Determining the chloride diffusion coefficient by migration in non steady state," (in portuguese) LNEC, 2005, 8 pp.
7. LNEC E 390, "Concrete. Determining the resistance to chloride penetration. Imersion test," (in portuguese) LNEC, 1993, 2 pp.

Modelling combined deterioration mechanisms related to chloride and carbonation induced corrosion



Michael Vogel
Dipl.-Ing.
Institute of Concrete Structures
and Building Materials,
Karlsruhe Institute of
Technology (KIT)
D-76131 Karlsruhe, Germany
michael.vogel@kit.edu



Harald S. Müller
Prof. Dr.-Ing.
Institute of Concrete Structures
and Building Materials,
Karlsruhe Institute of
Technology (KIT)
D-76131 Karlsruhe, Germany
sekretariat-bt@imb.kit.edu

ABSTRACT

For an effective life cycle management it is important to predict the changing material behaviour with time and thus the durability of civil concrete structures, which underlie different and complex deterioration mechanisms. The knowledge about mechanisms of individual exposures is well developed in contrast to the understanding of the effects of combined deterioration mechanisms. Therefore, a new approach towards an advanced system and risk management was developed according to combined deterioration mechanism related to chloride and carbonation induced corrosion. The new approach involves time variant deterioration models concerning the durability of concrete structures as well as singular structural risks for the lifetime prognosis.

Key words: combined deterioration mechanisms, chloride, carbonation, singular risks, service life prediction.

1. INTRODUCTION

Concrete deterioration mechanisms have significant effects on the durability and the service life of civil concrete structures like e. g. concrete bridges. In contrast to the knowledge about single exposures such as chloride or carbonation attack the knowledge about the impact of combined durability actions on concrete structures is very limited. In practice, however, the exposures always occur in a combined manner. Especially combined actions and singular risks (e. g. corrosion of tendons) are responsible for tremendous deteriorations, which reduce the service life of concrete structures significantly. This paper shows a new approach to model combined deterioration mechanisms in a realistic way. The focus is on the relevant deterioration mechanisms concerning the durability aspects of concrete according to chloride and carbonation induced corrosion.

2. MODELLING OF INTERACTIONS

In order to exemplarily demonstrate the procedure of the new concept for modelling the interactions of combined actions a reliability analysis has been carried out. The identified deterioration processes can be described realistically by means of the deterioration time models e. g. introduced by the fib model code for service life design [1]. The individual steps of the procedure of a probability design study can be taken from the literature [2, 3]. The following

deterioration mechanisms and singular risks were chosen: carbonation and chloride induced corrosion, alkali-silica reaction (ASR) and an insufficient grouting of the tendon ducts which leads to corrosion of tendons. Figure 1 shows the fault tree of a bridge element superstructure modelled for the mentioned deterioration mechanisms. The superstructure of the bridge represents a series system. The interaction factor η_{carbo} is at first not considered and therefore $\eta_{\text{carbo}} = 1.0$.

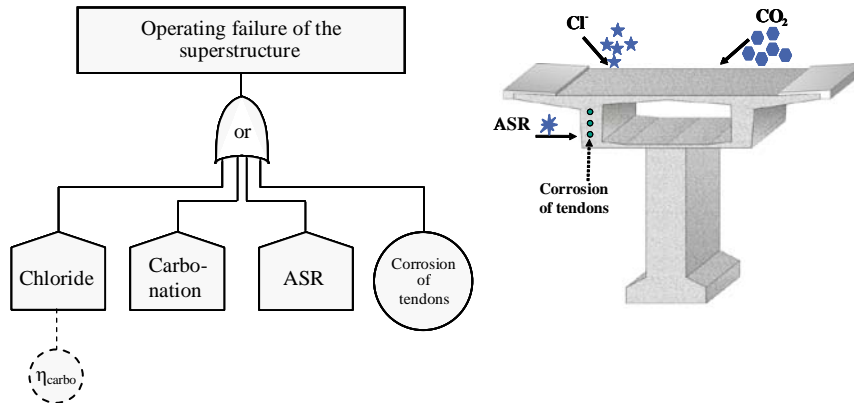


Figure 1 – Fault tree of the series system modelled for a bridge superstructure.

On the basis of [1] the limit state related probabilities (expressed as reliability indices β) were calculated. Appropriate values for the model parameters were selected from the literature [3, 4, 5]. For the deterioration caused by alkali-silica reaction and the corrosion of tendons failure probabilities were taken from an example in the literature [6]. The related value for an alkali-silica reaction (ASR) is $p_{f,ASR} = 0,5 \%$, and for the corrosion of tendons the failure probability was assumed to be $p_{f,corr} = 2,0 \%$. The prediction of the system failure probability of the bridge superstructure was performed for a service life of 100 years. The determination of the time dependent reliability β_{sys} was calculated using the software STRUREL [7]. Here, only the upper bounds of the series system “superstructure of the bridge” were calculated, see Figure 2 and eq. (1).

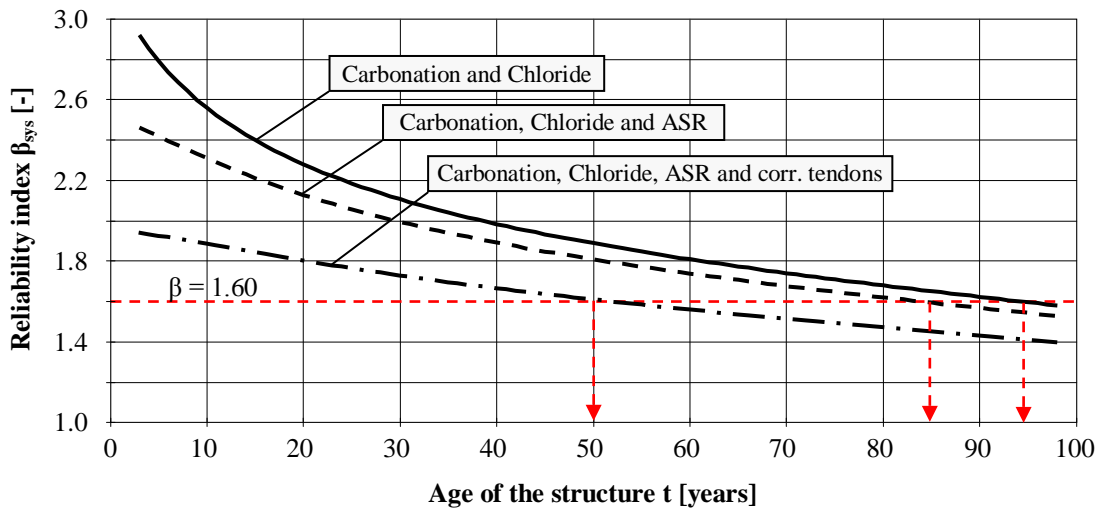


Figure 2 – Reliability index β_{sys} vs. time t of the superstructure of the bridge.

$$\max[p_{fi}] \leq p_{f,series} \leq 1 - \prod_{i=1}^n (1 - p_{fi}) \quad (1)$$

The lower bound (left) in eq. (1) indicates the reliability index in case of full correlated failure modes and the upper bound (right) in case of uncorrelated failure modes. The correlation term used in this sense has only a mathematical reason. Material technological correlations or interactions are not considered.

The results displayed in Figure 2 show that the reliability of the system superstructure of the bridge decreases when the number of the deterioration mechanisms increases. For example the limit state (here $\beta = 1.6$) is reached after 95 years if only the deterioration mechanisms carbonation and chloride induced corrosion take place. In the case that all exposures take place (carbonation, chloride, ASR and corrosion of tendons) the limit state is reached already after 50 years.

In order to implement the material technological interactions the factor η_{carbo} is introduced, see Figure 1. By using the interaction factor η_{carbo} it is possible to take into account an interaction of carbonation and chloride ingress. There are different possible effects which might be caused by this interaction. On the one hand due to the carbonation the concrete might have an increased density and lower porosity which in turn might therefore impede the further ingress of substances from the environment. On the other hand the binding capacity of the concrete is lowered due to the carbonation process. The total chloride concentration might be higher than in non-carbonated concrete since the bound chlorides are released. To indicate the influence of carbonation on the chloride ingress the chloride ingress process is modified by introducing the factor η_{carbo} . The effect simulated can be described by the assumption that the chloride migration coefficient is either increased or decreased. The chronology in which the different actions occur plays an important role within this context, which is not further discussed here.

In the following example the interaction is limited to the influence of carbonation on the chloride ingress. Other effects can be neglected. Therefore, the corrosion of the tendons does not have an impact on the chloride ingress nor does the carbonation. The ASR can be considered to be independent from the other accompanying factors. In Table 1 the varying ranges of the reliability index β_η and the failure probability p_f according to the varying factor η_{carbo} are given.

Table 1 – Parameter study on reliability β_η and probability p_f depending on the factor η_{carbo}

η_{carbo} [-]	Upper bound		
	β_η [-]	p_f [%]	
0.5	1.8	3.6	
1.0	1.6	5.5	
1.5	1.4	7.7	
2.0	1.3	10.0	

For this study the factor η_{carbo} was varied from 0.5 to 2.0. The parameter study was performed at a lifetime of 50 years. The influence of an increasing (> 1.0) or decreasing (< 1.0) factor η_{carbo} on the development of the reliability is shown in Table 1. The average chloride diffusion

coefficient is increased with a factor η_{carbo} higher than 1.0 which leads to less reliability. Correspondingly the reliability increases with a decreasing chloride diffusion coefficient as a result of a factor η_{carbo} lower than 1.0. The results in Table 1 shows that within the range of the factor η_{carbo} the reliability of the series system varied from $\beta = 1.3$ ($p_f = 10\%$) to 1.8 ($p_f = 3.6\%$). If the factor η_{carbo} is 0.5 the allowed safety level, related to the reliability index $\beta = 1.6$ ($\eta_{\text{carbo}} = 1.0$), is reached after 115 years. Otherwise if the factor η_{carbo} is 2.0 the allowed safety level is reached after 15 years. The variation of the factor η_{carbo} and therefore the extent of the interaction of chloride ingress and carbonation has a pronounced impact on the reliability of the series system superstructure of the bridge.

3. CONCLUSION AND OUTLOOK

A new approach for the quantification of the durability of concrete structures by modeling combined deterioration mechanisms was presented. The calculated example proves the feasibility of the new concept. By this introduced method a first step is made towards an interaction model that is suitable, flexible and gives the possibility to be extended. The level of detail can be increased if necessary. Furthermore, the service life prediction can be extended by singular failure risks caused by structural safety problems.

Although the feasibility of the developed concept has been verified by a computer based example, it becomes clear, that there is a high need for extended research. Next to the general methods as well the material technological aspects of interactions have to be subject of further research. A quantitative specification of the characteristic values for the factor η_{carbo} can be derived from testing based research of the material characteristics.

REFERENCES

1. fib Model Code for Service Life Design. In: fib bulletin 34; International Federation for Structural Concrete; ISBN 2-88394-074-6; Lausanne, 2006
2. Müller, H. S., Vogel, M.: Lebenszyklusmanagement im Betonbau. In: beton, Heft 5 (2008), S. 206-214
3. Durable and Reliable Tunnel Structures (DARTS) – The Reports (CD Rom) CUR Gouda, May 2004
4. The European Union Brite Eu Ram II I: Modelling of Degradation. DuraCrete: Probabilistic Performance based Durability Design of Concrete Structures, Contract BRPR-CT95-0132, Project BE95-1347, Document BE95-1347/R4-5, December 1998
5. The European Union – Brite EuRam III: Statistical Quantification of the Variables in the Limit State Functions, DuraCrete: Probabilistic Performance based Durability Design of Concrete Structures, Contract BRPR-CT95-0132, Project BE95-1347, Document BE95-1347/R9, January 2000
6. Zhu, W.: An Investigation into Reliability based Methods to include Risk of Failure in Life Cycle Cost Analysis of Reinforced Concrete Bridge Rehabilitation (Master Thesis). School of Civil, Environmental and Chemical Engineering, Science, Engineering and Technology Portfolio, RMIT University, July 2008
7. RCP GmbH: STRUREL, A Structural Reliability Analysis Program System, (STATREL Manual 1999; COMREL & SYSREL Manual, 2003). RCP Consulting GmbH München

Chloride Binding Behaviours by AFm and C-S-H in Artificial Pore Solution of Concrete



In-Seok Yoon
 Prof., Ph.D.
 Dept. of Construction Info. Eng.
 Induk University
 Choansan14, Nowongu, Seoul,
 Korea
 isyoon@induk.ac.kr

ABSTRACT

Chloride binding capacity in cementitious materials is a crucial factor for service life prediction of marine concrete. Many researchers have dealt with experimental works and got experimental constants within the scope of Freundlich / Langmuir binding isotherm. However, the constants depend on mixing proportion properties of the cementitious materials and the degree of hydration. Thus, it is necessary to explore reasonable approach to integrate chloride binding behavior of cementitious materials and that is a good motivation of this study.

Firstly chloride binding isotherm of major cement hydrates is examined and then chloride binding isotherm is estimated from the chloride binding of these hydrates. The result shows that monosulfates and C-S-H phase have significant binding capacity and this is main mechanism of the binding capacity. The chloride binding by monosulfate hydrates is attributed to produce Friedel's salt. C-S-H hydrates also can lead to physic-chemical binding. Based on the experiment results, to develop integrated system for prediction of chloride binding behaviors is final goals.

Key words: Chloride binding capacity, Service life prediction, Cement hydrates, Isotherm

1. INTRODUCTION

1.1 General

Chloride penetration is one of the main causes of the reinforcement corrosion in concrete. Among the governing factors of chloride penetration in concrete, chloride binding reduces the amount of movable chloride and then reduce the critical chloride content for reinforcement corrosion. The studies reporting chloride binding isotherm have involved the experimental measurement of the total chloride content and water soluble chloride content. However, there is no agreement on its value because the studies have tried to define chloride binding isotherm within the scope of their experimental concrete mix proportion at arbitrary time although chloride binding is influenced by many factors such as mixing proportion properties of concrete, type / amount of binder (cement and admixture), degree of hydration, and so on.

Chloride ions are existed in concrete as two forms: water soluble chloride ions (free chloride) in the aqua phase of cement paste, and bound chloride ions in the solid phase. Bound chlorides can be divided as; Friedel's salt by C_3A / C_4AF , bound chloride by C-S-H physically and chemically. Affecting factor of the bound chlorides is schematically shown in Figure 1. The mechanism of

bound chloride is very complicated; Friedel's salt due to C_3A or C_4AF , Kuzel's salt, and bound chlorides by C-S-H.

The purpose of this study is to investigate and to quantify chloride binding capacity by means of reaction experiment. The contributions of C-S-H and AFm to produce bound chlorides are examined, based on main mechanism of chloride binding in cementitious materials.

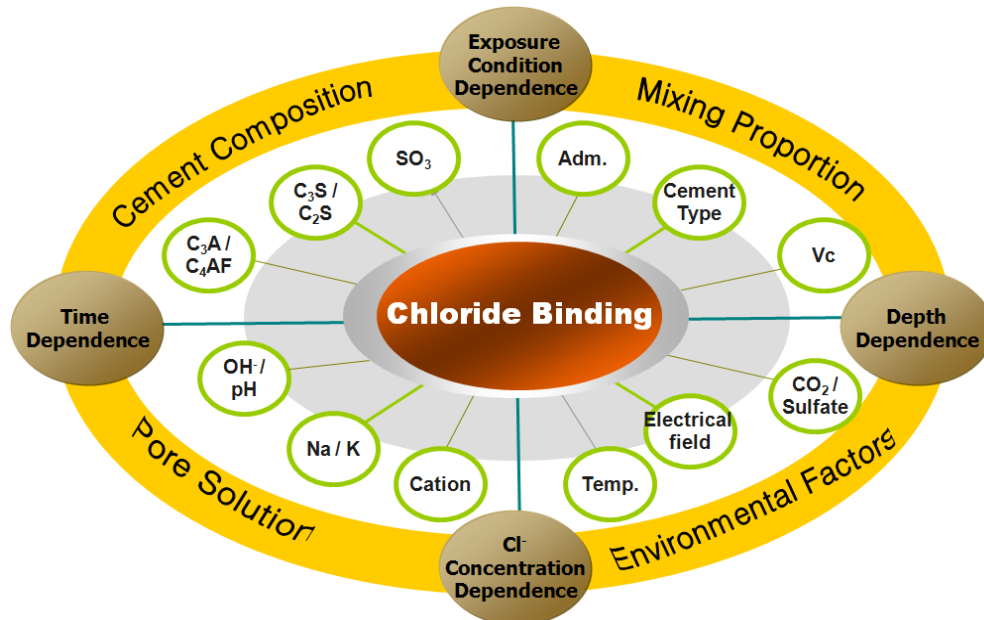


Figure 1 – Affecting factors of chloride binding

2. EXPERIMENTAL DESIGN

2.1 Materials

AFm was synthesized as follows : C_3A , gypsum and water were mixed at molar ratios of 1:1:5 respectively, then seal-cured at 20°C, then at 40 °C and again at 20°C. The curing time was 3 days. C-S-H with 1.50 of Ca/Si ratio was synthesized by mizing C_3S with water at a water to solid ratio of 1:10 at 20°C, and cured for 2 months under sealed condition.

2.2 Chloride Binding Experiment

Synthesized AFm, C-S-H were added to chloride solution with various concentrations. The apparatus was sealed with rubber cap in order to prevent decreasing of pH due to carbonation. The adsorption-reaction experiment was carried out for 10 days at 20 °C.

For the duration of the experiment, synthesized products were reacted with chloride solution and this leads to chloride binding. Before measurement of chloride concentration, the solution was stirred for enough time.

Ion chromatography method was used to measure the amount of chloride solution. The difference between initial chloride concentration before and after reaction experiments was regarded as the amount of adsorbed chemically or physically chloride in solid phase because of AFm or C-S-H.

3. RESULTS AND DESCUSSION

Figure 2 shows the amount of bound chloride adsorbed by AFm. The amount of bound chloride adsorbed by AFm increases, with the increase of chloride concentration in liquid phase. In order to express the relationship between chloride content in aqua phase and bound chloride content adsorbed by AFm, it is thought that Langmuir isotherm is more suitable than Freundlich isotherm. The bound chloride content at chloride concentration of 1 mol is only 0.44 mol per 1 mol of AFm. This value is significantly lower than 2 mol of stoichiometrical value.

Figure 3 represents the chloride binding capacity of C-S-H. C-S-H has a large surface area this leads physical adsorption of chloride by Van der Waals' force. Like AFm, the amount of bound chloride increases with the increase of chloride concentration in aqua phase. The binding isotherm shows a perfect fit for the regression curve of Langmuir isotherm. 1 g of C-S-H can bind chloride with 0.45 mMol at the chloride concentration of 1 Mol/L. Thus, the contribution of C-S-H is significant for chloride binding capacity of concrete. Physical and chemical properties of C-S-H depend on Ca/Si ratio. It is necessary to examine the Ca/Si ratio of C-S-H on chloride binding.

Finally, behavior of chloride binding can be expressed by Eq. (1) and Eq. (2). Eq. (1) is a contribution of AFm, while Eq. (2) is a contribution of C-S-H. Common trend of two binding isotherms, Langmuir & Freundlich, is decreasing with increase of chloride concentration in aqua phase. By chloride concentration with 1.0 mol/L in aqua phase, the value of Langmuir isotherm is higher than that of Freundlich isotherm.

$$[\text{Cl}^- (\text{s})](\text{AFm}) = \frac{1.081 [\text{Cl}^- (\text{aq})]}{1 + 1.456 [\text{Cl}^- (\text{aq})]} \quad (1)$$

$$[\text{Cl}^- (\text{s})](\text{CSH}) = \frac{1.079 [\text{Cl}^- (\text{aq})]}{1 + 1.395 [\text{Cl}^- (\text{aq})]} \quad (2)$$

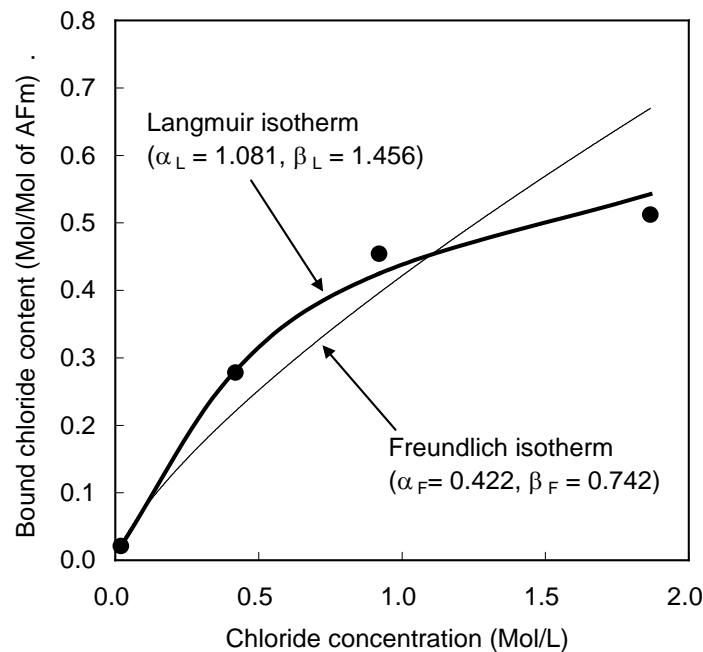


Figure 2 – Chloride binding behavior by AFm

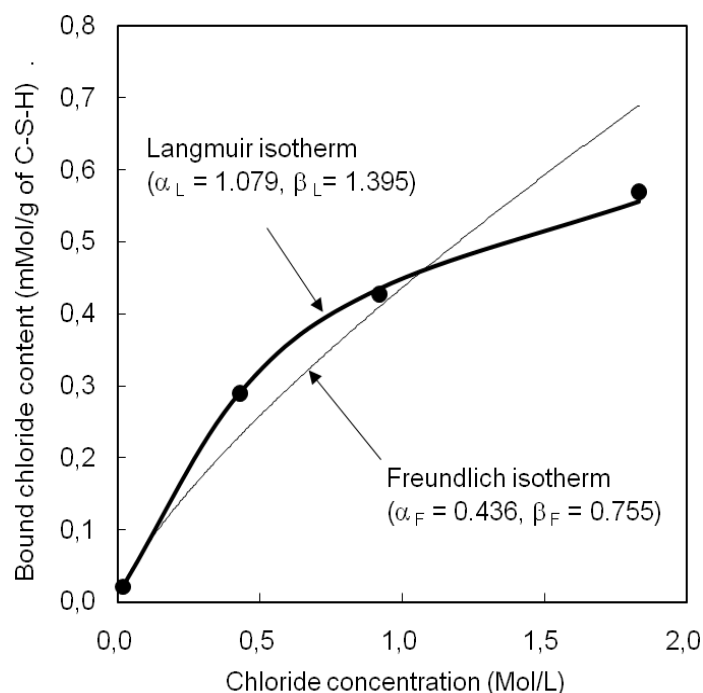


Figure 3 – Chloride binding behavior by C-S-H

However, the trend is reverse after the concentration. Bound chloride content is significantly decreased with increase of chloride concentration in aqua phase and Langmuir binding isotherm has good agreement with the trend consequently.

This study is the first step of experiment for investigation to quantify the amount of bound chloride in cementitious materials. Based on the result of this study, new model to predict chloride binding will be suggested. AFm and C-S-H are generated by hydration of cementitious materials, such as Portland cement, fly ash, granulated blast furnace slag, and developed with elapsed time. Developments of AFm and C-S-H will be coupled with the chloride binding isotherm of this study, as shown in Figure 4.

ACKNOWLEDGEMENT

The author acknowledges the financial support of NRF, National Research Foundation, 2010-0005732, Korea.

REFERENCES

1. Hirao, H., Yamada, K., Tarahashi, and H. Zibara H., "Chloride Binding of Cement Estimated by Binding Isotherms of Hydrates," *Journal of Advanced Concrete Technology*. Vol. 3, No.1, 2005, pp.77-84.
2. Suzuki, K., Nishikawa, T., and Ito N., "Formation and Carbonation of C-S-H in Water," *Cement and Concrete Research*. No.15, 1985, pp.212-224.
3. Saeki, T., and Sasaki, K., "Hydration Model for Cementitious Materials Containing Mineral Admixtures," *2nd International RILEM Workshop on Concrete Durability and Service Life Planning – ConcreteLife'09*, Haifa, Israel, September, 2009, pp.466-473.
4. Zibara, H., "Binding of External Chlorides by Cement Paste," PhD Thesis, University of Toronto, 2001

Session A5 – FROST ACTION

Freeze/Thaw Durability of Concrete with Fly Ash

Anna Knutsson
M.Eng.
Chalmers Univ. of Techn.
Div. of Building Technology
S-412 96, Gothenburg
annaknutsson83@yahoo.se



Tang Luping*
Ph.D., Prof
Chalmers Univ. of Techn.
Div. of Building Technology
S-412 96, Gothenburg
tang.luping@chalmers.se

* Corresponding author

Anders Lindvall
PhD
Thomas Concrete Group AB
C. lab
Ringögatan 14
S-417 07 Gothenburg
anders.lindvall@tcg.nu

ABSTRACT

This paper presents results from a study of frost resistance of air entrained concrete with additions of fly ash. In this study, concrete with different additions of fly ash were cured at different ages and elevated temperature prior to the standard frost scaling test. The equivalent water-binder ratio was fixed at 0.45, with efficiency factors of either 0.4 or 1.0. The results show that properly air entrained concrete with fly ash achieved a frost resistance similar or even better than that of Portland cement concrete. Curing for longer ages or at elevated temperature did not improve the freeze/thaw durability.

Key words: Concrete, durability, fly ash, freeze/thaw, scaling.

1. INTRODUCTION

Fly ash, which is a by-product from combustion of pulverized coal, can partly replace the cement in concrete. With the new concrete standard SS-EN 206-1 (2001), additions of fly ash in concrete have been allowed in Sweden. The performance of concrete with additions of fly ash is in many situations improved compared to that of concrete mixed with Portland cement only, i.e. increase in the long time strength and reduction of the permeability. However, concerns have been raised regarding the freeze/thaw durability of concrete with fly ash.

Results from the literature have generally shown that the freeze/thaw durability of air entrained concrete with fly ash is similar, or slightly worse, compared Portland cement concretes [1-7]. This observation is explained by the fact that the hydration of fly ash concrete is slower than that of Portland cement concrete [3, 6, 7] and that there are problems with the compatibility between the fly ash and the air entraining agent that is used to create air pores in the concrete [8,9].

2. TESTING PROGRAM

2.1 Material and specimens

In this study, concretes with different amounts of fly ash (0%, 6% and 20% of cement by weight) have been studied regarding the freeze/thaw durability. The equivalent water-binder ratio, $(w/c)_{eq}$, was fixed at 0.45, with efficiency factors, k of either 0.4 or 1.0. Descriptions of the concrete mixes are shown in Table 1. The entrained air was controlled in the range of $(4.5\pm 0.5)\%$ by concrete volume. As a main binder Cementa Degerhamn Anläggningcement (CEM I 42.5 N MH/SR/LA) was used in all mixes. The fly ash used was Warnow Füller (Rostock), which complies with SS-EN 450-1 (2007)

Table 1 Proportions of each concrete mix.

Mix No.	1-4	5	6	7	8
% fly ash (of cement content, b.w.)	20	20	0	0	6
k -factor	0.4	1.0	-	-	0.4
w/c	0.49	0.54	0.45	0.45	0.46
$(w/c)_{eq}$	0.45	0.45	0.45	0.45	0.45
AEA [% of cement b.w.]	0.4	0.4	0.1	0.1	0.1

2.2 Tests

The resistance regarding scaling under freeze/thaw, was tested according to SS-13 72 44 (2005), procedure IA. However, due to the lower strength gain at early ages of concretes with fly ash, concrete with 20% fly ash were cured at elevated temperature or during prolonged curing time prior to the test. The curing regime for concrete from each mix is shown in Table 2. The structure of the air void system in the hardened concrete was determined by analysis according to SS-EN 480-11 (2005).

Table 2 Curing regime for each mix tested for scaling at freezing, no. of days

Mix	% fly ash	k	Curing regime	In mould	Water cured, 20 °C	Water cured, 55 °C	Climate chamber	Exposed to water	Total
1	20	0.4	55 °C, 28 d	1	6	21	7	3	38
2	20	0.4	55 °C, 42 d	1	6	35	7	3	52
3	20	0.4	20 °C, 56 d	1	54	-	6.5	2.5	64
			20 °C, 90 d	1	89	-	7	3	100
4	20	0.4	Standard	1	19	-	7	3	30
			20 °C, 56 d	1	62	-	7	3	73
5	20	1.0	20 °C, 90 d	1	90	-	7	3	101
			55 °C, 28 d	1	6	21	7	3	38
6	0	-	Standard	1	20	-	7	3	31
7	0	-	Standard	1	19	-	7	3	30
8	6	0.4	Standard	1	19	-	7	3	30

3. RESULTS

3.1 Scaling under freeze/thaw

The results from the scaling under freeze/thaw are shown in Figure 1. The concretes from all mixes performed very well, according to the criteria in SS-13 72 44 (2005). A very good durability is achieved if the scaling after 56 freeze/thaw cycles is less than 0.10 kg/m^2 .

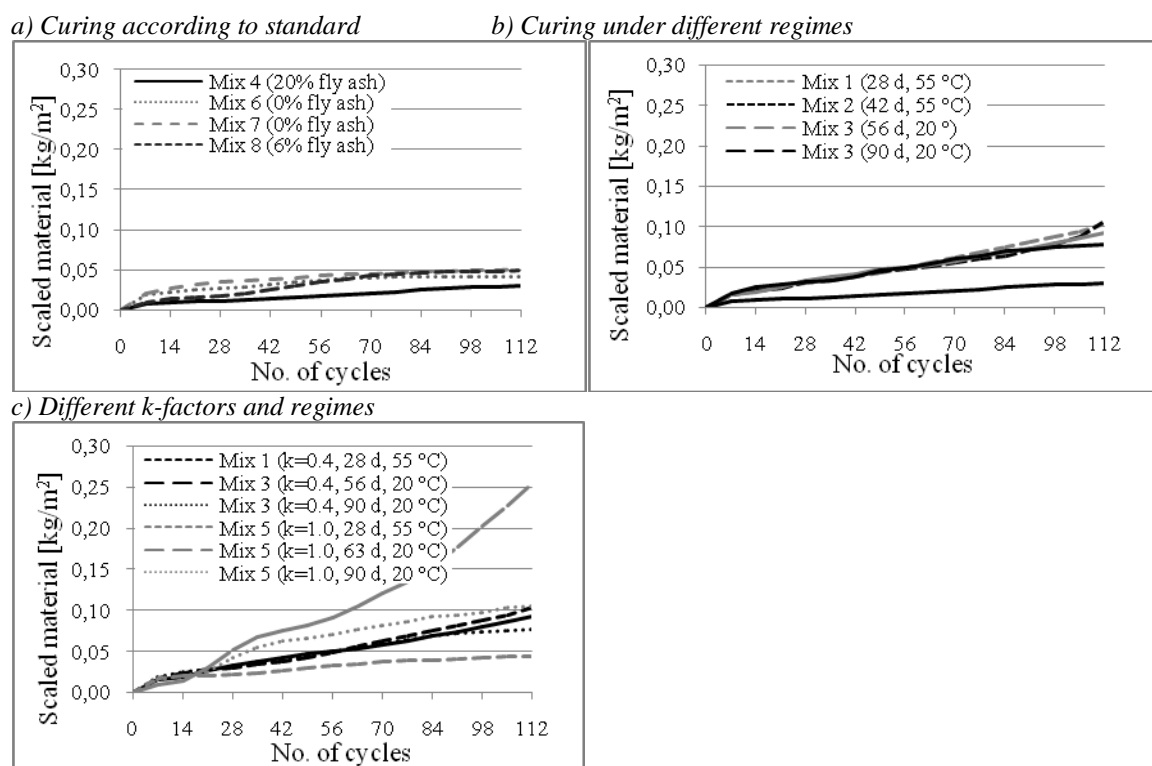


Figure 1 Mean values from scaling under freeze/thaw according to SS 13 72 44 (2005).

As can be seen in Figure 1a, the concrete containing 20% fly ash, did show slightly better durability regarding freezing and thawing, than the concrete with 6% and 0% fly ash. The resistance for the mixes with 6% fly ash and without fly ash was similar. However, larger amounts of air entraining agents were needed in concrete with fly ash compared to the concrete without to achieve the targeted air content, see Table 1.

Prolonged curing duration and elevated temperature at curing did lower the freeze/thaw durability for the concretes with k -factor equal to 0.4, see Figure 1b. This can be explained by the fact that the concrete with extended curing periods and/or cured at 55 °C had higher maturity degree than the one cured according to the standard, which would give denser capillary pores. These denser capillary pores can on the one side contribute to an increase in strength but on the other side result in an increased hydraulic pressure under the frost action, the latter may cause a slight increase in scaled material, as shown in Figure 1b, although with a limited low level ($\leq 0.1 \text{ kg/m}^2$ after about 112 freeze/thaw cycles)

The concrete with a k -factor equal to 1.0 showed to be less durable regarding scaling under freeze/thaw, than the concrete with a k -factor of 0.4, for concretes cured in 20 °C, see Figure 1c, to a great extent due to their different strength levels. The concrete from mix 5 ($k=1.0$), cured during 90 days showed better performance than the one cured during 63 days. This is attributed to that longer curing, gives more mature concrete, which significantly improves the strength and in return the resistance against freeze/thaw action. Since the standard test (28 d, 20 °C) was not planned for the concrete mix 5, the actual difference in the test results between mix 5 ($k=1.0$, 63 d, 20 °C) and mix 5 ($k=1.0$, 90 d, 20 °C) may involve large uncertainty.

3.2 Air void analysis

Air void analysis were performed on specimens from concrete mixes no. 3 (20% fly ash, $k=0.4$), 4 (20% fly ash, $k=0.4$), 5 (20% fly ash, $k=1.0$) and 7 (0% fly ash). The results from the analysis, which are presented in Table 3, shows that the air void structures of all four specimens tested, are acceptable.

Table 3 Results from the air void analysis performed according to SS-EN 480-11 (2005).

	Accuracy of measurement	Mix 3	Mix 4	Mix 5	Mix 7
Air content [vol-%]	± 0.7	5.1	4.0	2.9	5.9
Specific air void surface [mm^{-1}]	± 3	27	32	30	21
Spacing factor [mm]	± 0.015	0.19	0.18	0.22	0.22
Assumed paste content [vol-%]	-	31.6	31.6	31.6	31.6

4. CONCLUSIONS

The freeze/thaw durability of concrete with fly ash was similar or even slightly better than that of Portland cement concrete. All examined concretes were, however, properly air entrained. Curing for longer ages, or at elevated temperature, did not help for improvement of the freeze/thaw durability for the concretes with $(w/c)_{eq}$ of 0.45 and a k -factor of 0.4.

REFERENCES

1. Fagerlund, G. (1988): Effect of air-entraining and other admixtures on the salt-scaling resistance of concrete, *Durability of concrete: Aspects of admixtures and industrial by-products, International seminar*, April 1988, pp. 233-266.
2. Gebler, S.H., Klieger, P. (1986): Effect of Fly Ash on the Durability of Air-Entrained Concrete. Preprinted from *Proceedings, Second International Conference on the Use of Fly Ash, Silica Fume, Slag, and Other Mineral By-Products in Concrete*. April 21-25, 1986, Madrid.
3. Jepsen et al. (2001): Durability of Resource Saving "Green" Types of Concrete. *Green Concrete*. <http://www.gronbeton.dk/>. (26 Oct. 2010)
4. Li, B. (2009): *Chloride Transport in Concrete under Frost Action, An Experimental Study*. Lic. Department of Civil and Environmental Engineering, Chalmers University of Technology, Publication no. 2009:4, Göteborg, Sweden, 2009, 156 pp.
5. Müller, C., Severins, K. (2007-2009): Durability of concretes made with cements containing fly ash, *Concrete Technology reports, 2007-2009*, Vol. 31, 2010, pp. 7-17.
6. Rønning, T. F. (2001): *Freeze-Thaw Resistance of Concrete, Effect of: Curing Conditions, Moisture Exchange and Materials*. Ph.D. Thesis. Division of Structural Engineering, Concrete Section, The Norwegian Institute of Technology, Publication no. 6354, Trondheim, Norway, 2001, pp. 263.
7. Schießl, P. et al. (2001): *Neue Erkenntnisse über die Leistungsfähigkeit von Beton mit Steinkohlenflugashe (Teil 2)*. Beton, Verlag Bau + Technik, No. 2, pp. 9-13.
8. Pedersen, K.H. et al. (2008): A review of the interference of carbon containing fly ash with air entrainment in concrete. *Progress in Energy and Combustion Science*, Vol. 34, No. 2, pp 135-154
9. Zhang, D.S. (1996): Air entrainment in Fresh Concrete with PFA. *Cement and Concrete Composites*, Vol. 18, No. 6, pp.409-418, 185 pp.

Valuation of the 12 year old Concrete in the Ulkebugt Bridge, Sisimiut, Greenland



Christian Gottlieb
B.Eng., M.Sc. student
DTU Civil Engineering
Brovej, Building 118
DK – 2800 Kgs. Lyngby
cg@ishoejby.dk



Idar Olsen
B.Eng., M.Sc. student
DTU Civil Engineering
Brovej, Building 118
DK – 2800 Kgs. Lyngby
idar-olsen@hotmail.com



Jesper Frej Henningsen
B.Eng., M.Sc. student
DTU Civil Engineering
Brovej, Building 118
DK – 2800 Kgs. Lyngby
jesperfrej@gmail.com



Thomas Rohde
B.Eng., M.Sc. student
DTU Civil Engineering
Brovej, Building 118
DK – 2800 Kgs. Lyngby
thomas3x@msn.com



Co-author
Kurt Kielsgaard Hansen
Associate Professor
DTU Civil Engineering
Brovej, Building 118
DK-2800 Kgs. Lyngby
kkh@byg.dtu.dk



Co-author
Bent Grelk
M.Sc., Chief Consultant
Rambøll Denmark A/S
Hannemanns Allé 53
DK-2300 København S
bng@ramboll.dk

ABSTRACT

The Ulkebugt bridge is a vital connection for the town Sisimiut, as it is the only link between the airport and the town. The bridge is a box girder bridge with one central pillar. Most of the pillar's concrete surface is exposed to seawater, with a tide variation around 4 meters. In addition to the seawater the bridge is exposed to the rough arctic climate. Furthermore, the mean temperature is below 0 °C for two thirds of the year with many freeze-thaw passages in late autumn and early spring, which increases the opportunity for severe frost damages. The focus has been to evaluate the quality and condition of the concrete pillar in terms of composition and the extent of the present deterioration mechanisms, best represented by frost damage and chloride ingress. Results show critical chloride content in the concrete will be reached in approximately 10 years at the depth of the reinforcement bars. However, the results also reveal the presence of some surface defects which probably is related to problems with workmanship, i.e. placing and compaction of the fresh concrete.

Key words: Concrete, bridge pillar, arctic, chloride

1 CHLORIDE INGRESS

1.1 Severity of chloride ingress

The concrete pillar is exposed directly to seawater, as it is shown in Figure 1. The pillar is founded on the seabed, so a major part of the concrete surface is constantly under water and thereby exposed to chloride ingress by capillary suction and diffusion. The ingress is relatively slow under water in this dense concrete and due to lack of oxygen there is no real concern for chloride driven corrosion. The most critical part on the surface is in the splash-zone with tide and wave action. In the Ulkebugt the tide has a variation of around 4 meters. The chloride ingress in the splash-zone gives the best opportunity to estimate the lifetime on the concrete pillar.



Figure 1 - The pillar on the Ulkebugt Bridge.

1.2 Estimated lifetime

The chloride initiated corrosion is probably the greatest threat to concrete due to a relative large amount of chloride in the concrete (now and in the future).

A projection of the chloride ingress has been conducted by use of Fick's 2. Law of Diffusion and the results are presented in Figure 2.

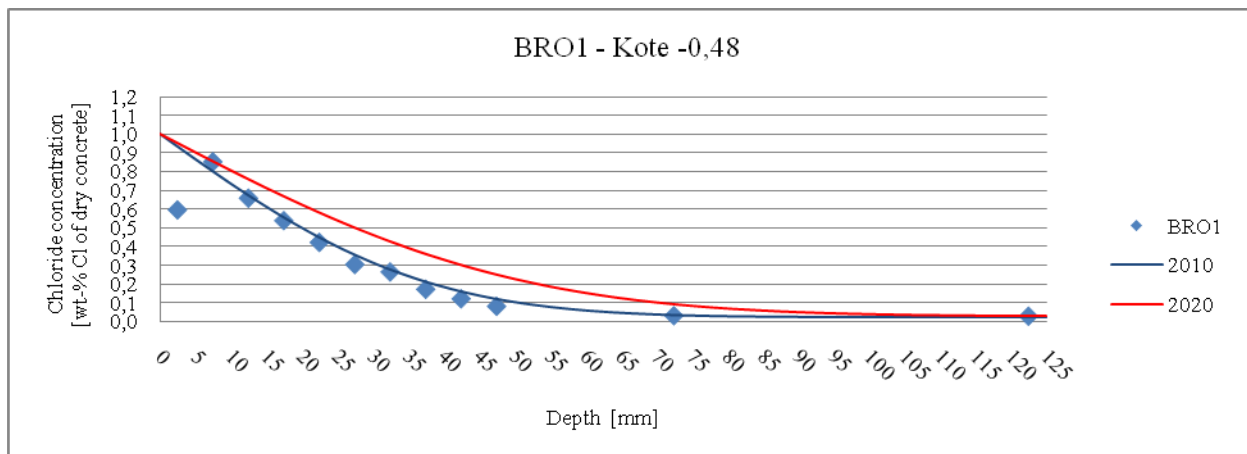


Figure 2 – Chloride profile of the concrete in the splash-zone. Year 2010 (blue) and 2020 (red). Measurement results are marked.

The lifetime of the concrete is limited by the chloride ingress. Corrosion of the reinforcement will initiate once the chloride level reaches 0.1 wt-% of the dry concrete. To make an estimated lifetime, it is important to know the thickness of the cover over the reinforcement. The requirement for the cover in the pillar in the splash-zone is 70 mm. Figure 2 shows that the critical chloride level at the depth of 70 mm will be reached in approximately 10 years.

2 ARCTIC CLIMATE

A part of this project's focus has been on the arctic climate, and what effects the climate would have on the concrete in the bridge pillar. Arctic climate are defined by having daily mean temperatures below 10 °C at the year's hottest month.

In Sisimiut the climate affects the temperatures in such way, that summers have low middle temperatures around 5 °C, and winters with temperatures almost reaching -20 °C. The mean temperature is below 0 °C for two thirds of the year with many freeze-thaw passages in late autumn and early spring, which increases the opportunity for severe frost damages

2.1 Frost damages

Frost damages are typically the first deterioration mechanism that comes into mind, when speaking about concrete constructions in cold areas with many freeze-thaw passages. Frost damages occur when water in concrete freezes. The focus on frost damages are temperatures below water's freezing point, and also the concrete water saturation, which is crucial for the extent of frost damages in concrete constructions.

The concrete core analysis show, that the concrete capillary porosity is relative low, which is giving the concrete a low permeability. This gives the concrete a good resistance against moisture and water ingress, reducing the risk for a critical water saturation of the concrete significantly and thereby minimizing the risk for frost damages. Furthermore, the concrete has a relatively high air content of approximately 10 – 11 % and a good distribution, which will almost eliminate the risk of frost damages. With these facts in mind, it is not surprising, that the different analysis shows no internal signs of frost damages.

However the concrete surface of the pillar shows in some areas signs (smaller and larger holes in the surface) which could indicate freeze-thaw damages. These holes are probably smaller and larger agglomerates of air voids, probably caused by an improper compaction of the fresh concrete in relation with a "closed" design of the formwork, which leads to a high amount of entrapped air voids (equal to agglomerates of air voids) along the form side. In places with larger holes, the seawater is allowed to enter far into the holes from start, making the concrete and reinforcement more vulnerable to chloride initiated corrosion. The result of insufficient compaction of the concrete is many deep holes in the concrete, which is contributing to the overall state of the concrete pillar.



Figure 3 – Deep holes into the concrete surface.

3 CASTING PROBLEMS

In order to obtain a high quality concrete, the concrete has to be proportioned correctly and the different constituents has to be of equally high quality. However, the final product is also greatly influenced by the execution of the concrete work, including mixing and casting of the concrete.

3.1 Casting below zero

Different conditions influence the concrete differently. Casting of concrete in the Arctic region is often done at temperatures below 0 °C, which can be executed with a good result and with the same quality as concrete casted at higher temperatures, if taken the right precautions.

When casting below zero it is essential to avoid water in the fresh concrete from freezing and hereby stopping the hydration process of the cement, resulting in a porous and low strength concrete. The concrete is, before having developed significant strength, also likely to develop cracks as a result of temperature differences between surface and the center of the structure.

In order to minimize the risk of the abovementioned damages different precautions has to be taken when casting below zero. Heating formwork and casting surfaces, such as dilatation joints, prior to casting, reduce temperature differences in the fresh concrete. The use of warm concrete and accelerators which speeds up the hydration of the concrete, reduce the risk of freezing of the water in the fresh concrete. The concrete must be covered and the form eventually heated after having finished the casting.

4 CONCLUSION

The concrete pillar is exposed directly to seawater. The most critical part on the surface is in the splash-zone with tide and wave action. Here the critical chloride level at the depth of the reinforcement bars will be reached in approximately 10 years.

The concrete surface of the pillar shows in some areas signs in form of smaller and larger holes in the surface which could indicate freeze-thaw damages. These holes are probably smaller and larger agglomerates of air voids, probably caused by an improper compaction of the fresh concrete in relation with a “closed” design of the formwork, which leads to a high amount of entrapped air voids along the form side. The seawater is allowed to enter far into the holes from start, making the concrete and reinforcement more vulnerable to chloride initiated corrosion.

REFERENCE

1. Gottlieb, C., & Henningsen, J.F., ”Ulkebugt Bridge”, Department of Civil Engineering, Technical University of Denmark, 2011 (In Danish).

Air void structure of produced frost resistant concrete – an on site study.



Dag Vollset
Concrete engineer
Product manager admixtures
Rescon Mapei AS
Vallsetvegen 6
N - 2120 Sagstua

dag.vollset@resconmapei.no



Øystein Mortensvik
M.Sc.
R&D Admixtures/Concrete
Rescon Mapei AS
Vallsetvegen 6
N - 2120 Sagstua

oystein.mortensvik@resconmapei.no

ABSTRACT

The quality of the air void system in concrete is of great importance to the frost resistance of concrete. It has been claimed that it is (extremely) difficult to produce an air-entrained concrete containing polycarboxylate-based superplasticisers that is both stable and frost resistant. Furthermore, the most common cements for ready-mixed concrete in Norway today contain 20% of fly ash. This is just one more element adding difficulties to the establishment of a quantitatively and qualitatively correct air void system.

Rescon Mapei has done extensive testing on fresh and hardened concrete, both in lab and on site.

The results from these projects show that it is possible to produce frost resistant concrete with a high quality air void system even in CEM II A/V. Air entraining agents with the ability to cope with some variations in the cement or the fly ash are now being produced.

An air void analyzer was placed on sites to make evaluation of the fresh concrete right after mixing, after transportation and after the concrete is placed in the mould. These results show good correlation with freeze/thaw-measurements and optical measurements on thin sections from equivalent hardened concrete.

Key words: polycarboxylates, air entraining agents, air void structure, freeze-thaw cycles.

1. INTRODUCTION

Outdoor concrete constructions will inevitably contain some humidity. A critically saturated concrete with more than 91% of its pores filled with water, is prone to freeze-thaw actions. Whenever concrete freezes, and water is transformed into ice, the volume increases by 9 %. If there is no space for this volume expansion, these forces might lead to spalling of the concrete. Any crack will also accelerate the corrosion process as the concrete cover is drastically reduced. Search on the internet on “freeze thaw damage +concrete” resulted in 386,000 hits. Concrete deterioration as a consequence of freeze-thaw cycles sums up to repair costs that probably exceeds initial building costs.

All concretes contain natural or entrapped air that is incorporated into the concrete during mixing operations. These air voids are relatively large, often irregular in shape and typically in the range of 1 to 10 mm or more in size. The volume of these bubbles can vary from 1 to 3-4 % of the volume of the concrete. If these air voids are filled with water and then freezes, their expansion will lead to severe consequences to the construction.

To protect concrete from freeze/thaw damage, it should be air-entrained by adding a surface active agent to the concrete mixture. This creates a large number of closely spaced, small spheric air bubbles in the hardened concrete. These air bubbles relieve the pressure build-up

caused by ice formation by acting as expansion chambers. The air-bubbles should be very small with a *specific surface* of more than 25 mm^{-1} , be well distributed and have a distance between each other, a *spacing factor*, of less than 0.20 mm in the cement paste. Traditionally, a volume of *micro pores* ($< 0,300 \text{ mm}$) of more than 2.0 % of the concrete will be sufficient to avoid spalling and scaling of the surface.

1.2 Air entraining agents

Over the last decade, the use of polycarboxylate based superplasticisers (PCE) has gradually increased and is today totally dominant in the production of all concretes – also frost resistant concretes. PCEs are also surface active agents that unless they are actively controlled by defoamers will produce air voids. The challenge for the admixture producer has therefore been to develop a sufficiently efficient defoaming system in the PCE that also is compatible with the addition of an air entraining agent and yielding not only the right amount, but also the right quality of the air voids. Standards on concrete admixtures (EN 934-2) specify requirements for the classification of different classes of admixtures, and the admixture must comply with these. But the admixtures are all tested separately. For instance, an air entraining admixture (AEA) is tested with a standard CEM I-cement, in a concrete with a fixed mix design aiming at a slump value of 50 mm and with 4 to 6 % air volume in the fresh concrete, measured with the air pressure method. This is not a concrete that will ever enter a construction.

In real life, the combination of plasticisers or superplasticisers and AEAs, with a workability that makes it possible to place the concrete, is used. Into this, there are also a number of parameters that for obvious reasons cannot be standardized: transport methods and distances, placing methods (pumping, vibration), construction size, curing conditions et cetera. What we are aiming at is for the concrete construction to withstand a number of freezing and thawing cycles. Consequently, the measurement of “realcrete” is of interest.

1.3 Testing of frost resistance

There are a number of test methods available, some to be performed on fresh concrete, some on hardened concrete. Throughout our project, we have used several methods and the measurements have been taken on real concrete with different combinations of admixtures, before and after transport and retempering, in addition also the effect of vibration has been measured.

Some comments on the different testing methods: In the air pressure-meter method on fresh concrete, only the *total air content* can be evaluated. Even this is not accurate, since the measurement is also operator-dependant. Furthermore; is the instrument calibrated, when is the sample collected, how is it compacted, is all air on the surface evacuated, et cetera. From our experience the method is nevertheless relatively reliable since repeated measurements give results within +/- 0.5 %. On the other hand, since the instrument only gives us the *quantity* of the air, it can not be a sufficient qualification of a frost resistant concrete. It is essential that the concrete sample can be said to be representative of the concrete in the construction!

The air void analyzer method, in which a sample is drilled out of the fresh concrete and thereafter placed in a column filled with water and a detraining agent, gives us in addition to the quantity of air (the bubbles are weighed) also the air void distribution. The principle is that largest bubbles have also the largest buoyancy and thus reach the weight first. Quantity of air combined with time recordings produce a quality analysis of the actual total air in the sample. Again, the question of whether the sample is representative can be discussed. In addition, we do

notice that a large number of tiny air bubbles is still evaporating from the concrete sample after the weighing is completed (the weight is too small to be registered) and these might very well contribute to the frost resistance of the concrete. What we have observed is therefore that the AVA results often are on the conservative side compared to other measurements, yielding results that might be too pessimistic.

The two tests performed on the hardened concrete both assume that the samples are representative of the actual concrete, which of course is question of sampling method, treatment of the fresh concrete, and also under which curing conditions they have matured. The Borås-method (SS 13 72 44 and now also EN 12390-9) can be performed both under a layer of de-ionised water, or a mix of 97 % tap water and 3 % sodium chloride. The test method is an actual quality test since the concrete undergoes “climate changes” through actual freeze/thaw conditions (from -20° to $+20^{\circ}$ in 24 hour cycles), but tests show that this treatment can give worse results in tests compared to real concretes if they are recorded on porous concrete, while very low permeable concrete withstands the swift temperature changes better than real life concretes that very seldom are exposed to such rapid drops/rises in temperatures. In the thin section analyses (NS-EN 480-11:2005), the numbers and sizes of air voids are collected by scanning two cut samples (100x150 mm) over a distance of 1200 mm of the concrete surface so one might assume that the results might be representative of the actual concrete specimens. The result is though based on the assumption that the voids are being spherical and that the sizes of the voids are evenly distributed.

From the above brief discussion it should be obvious that measurements of air void distribution and subsequent acceptance of concrete as “frost resistance” is highly uncertain, deriving from test sampling, treatment, curing and instrumental inaccuracy. Quite significant tolerances should therefore be given or acceptance criteria are stricter than necessary to be on the “safe side”.

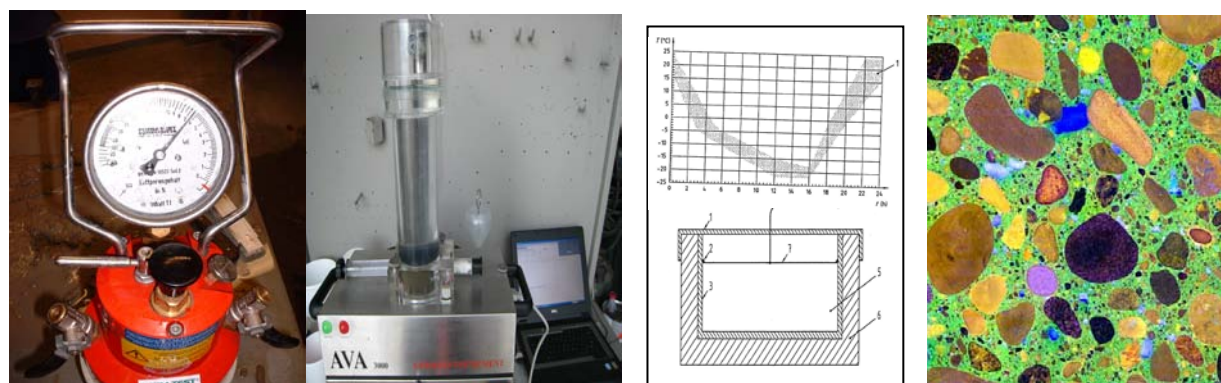


Figure 1. Methods in fresh concrete: a) air pressure-meter b) air void analyzer (AVA). Methods in hardened concrete: c) freeze-thaw cycles – temperatures and specimen set up(EN 12390-9) d) Thin section analyses of air void distribution (EN 480-11).

2. RESULTS

In one project, all concrete from 4 truck loads of concrete on site, in addition to two mixes in the laboratory were investigated by means of air pore volume, air pore structure and freeze-thaw resistance in addition to measurements of workability and compressive strength. Samples were taken out directly from the truck shortly after batching, then again after retempering after 1 hour, and also after forceful vibration of air-entrained and not-air-entrained concretes with water to cementitious ratios of 0.40 and 0.45. The results show that frost resistant concrete can only be

achieved by the use of air entraining agents. Larger quantities of measured air (with AEA) always yield excellent air pore structures, but have, as expected, negative effect on compressive strength.

The Air Void Analyzer (AVA) shows very good correlation to measured air pore structures in hardened concrete (thin sections). Spacing factor, specific surface and volume of micro pores are all relatively similar in the two measurements – AVA figures are in general more conservative than thin section analyses.

Table 1 – Concrete with Water to cementitious materials ratios 0.40.

<i>Test Method</i>	<i>Air pressure meter</i>	<i>Air Void Analyzer 3000</i>			<i>Microscopical Scanning</i>			<i>Freeze-Thaw cycles</i>
<i>Test sample #</i>	(% air volume)	(% air volume)	Specific surface	<i>Spacing factor</i>	(% air volume)	Specific surface	<i>Spacing factor</i>	Spalling (kg/m ²)
1A1	2.3	2.5	10.9	0,636	2.0	11.1	0,682	0,45
1A3	3.3	3.7	15.4	0,380	2.9	17.3	0,372	0,07
1B1	7.5	5.6	25.6	0,190	6.3	28.7	0,155	0,03
1B3	9.3	9.3	22.3	0,154	7.5	28.1	0,138	0,04
Lab3	1.5	0.7	9.9	1,200	0.6	17.0	0,745	2,59
Lab4	8.5	7.1	26.3	0,167	7.6	28.0	0,138	0,09

All concretes with 420 kg CEM II – 42.5 A/V, 4 % of silica and 1.0 % PCE, Sample A and Lab3 is without AEA, while sample B and Lab4 is added 0.2 % AEA. The differences between samples denoted 1 and 3 is 60 minutes transport, remixing and vibrated concrete

Table 2 – Concrete with Water to cementitious materials ratios 0.45.

<i>Test Method</i>	<i>Air pressure meter</i>	<i>Air Void Analyzer 3000</i>			<i>Microscopical Scanning</i>			<i>Freeze-Thaw cycles</i>
<i>Test sample #</i>	(% air volume)	(% air volume)	Specific surface	<i>Spacing factor</i>	(% air volume)	Specific surface	<i>Spacing factor</i>	Spalling (kg/m ²)
2A1	2,5	2,0	10,0	0,776	1,5	17,2	0,490	0,11
2A3	1,6	0,9	8,9	1,206	1,3	11,5	0,804	0,81
2B1	5,7	4,4	17,3	0,314	4,9	18,7	0,266	0,05
2B3	7,3	4,9	22,2	0,234	NA	NA	NA	0,06

All concretes with 410 kg CEM II – 42.5 A/V and 1,0 % PCE. Sample A is without AEA, sample B is added AEA. 1 and 3 denotes before and after transport/retempering and vibration

3. CONCLUSIONS

More full scale tests are performed and will be presented. It is obviously possible to combine polycarboxylates and air entraining agents in concretes containing fly ash. The variation of carbonic residuals has caused and will cause problems with air volume variations. To meet this, the further optimization of type of air entrainer is therefore needed. There are also projects ongoing in Norway including the participation of the Norwegian Road Administration to possibly obtain more qualified requirements for frost resistant concrete. The air pressure meter-method is a practical tool, but is the results to be trusted?

Freeze-thaw resistance of inert mineral powder concretes

Johanna Tikkanen,
M.Sc. Techn,
Research Scientist,
Building Materials Technology,
Technology,
School of Engineering,
Aalto University
johanna.tikkanen@tkk.fi

Hanna-Reea Välimäki,
M.Sc. Techn.
Research Scientist,
Building Materials

School of Engineering,
Aalto University

ABSTRACT

The freeze-thaw durability of inert mineral powder concretes was studied. Properties of a reference concrete produced by Portland cement were compared with corresponding inert mineral powder concretes made with either limestone or quartz powder replacing the binder in amounts of 10 or 20 %. CIF-test and a capillary suction test were performed on the concretes, thus, a basic understanding of the freeze-thaw durability of mineral powder concretes was obtained. It was determined that the water-binder ratio of the concretes must be kept constant i.e. the amount of mixing water has to be reduced when binder is replaced by inert fillers in order to achieve satisfactory freeze-thaw durability in mineral powder concretes.

Key words: Freeze-thaw resistance, CIF-test, capillary suction test, Environmental Scanning Electron Microscopy (ESEM), cement replacement, mineral powders, inert fillers.

1. INTRODUCTION

Micrometer sized (1–600 μm) mineral powders change the properties of fresh and hardened concrete and may allow the partial replacement of Portland cement. A partial replacement of cement by mineral powders can decrease the CO₂-emission burden of concrete due to smaller cement content, because producing one tonne of cement releases approximately one tonne of CO₂ into the atmosphere. This can have a significant impact on the production of ordinary Portland cement concrete (OPC) in the future and, thereby, to the entire global concrete construction industry. Mineral powder concretes could offer economic and ecological advantages for the concrete industry due to cement reduction. Recently, most of the research in the field of mineral powders has been focused on self compacting concretes (SCC), high performance concretes (HPC) and ultra high performance concretes (UHPC) [1], [2], [3], although a significant part of used concrete is actually OPC.

In general, mineral powders and micro fillers are considered to have a positive effect on concrete properties by decreasing the water demand in plasticized mixes and by improving the microstructure of concrete because particle packing in concrete is enhanced [4]. Micro fillers influence the microstructure and chemical composition of the interfacial transition zone (ITZ) between the larger aggregates and binder matrix through a nucleation mechanism which can be at least as important as the pozzolanic effect [5], [6].

In Finland and in the other Nordic countries, all outdoor structures are susceptible to freezing and thawing loads of varying intensity during the winter season. In order to be successfully used mineral powder concretes need to possess adequate fresh concrete properties and withstand cyclic frost attacks of our Nordic climate. In this study, the freeze-thaw durability properties and characteristics affecting air-entrainment of inert mineral powder concretes was investigated.

2. MATERIALS AND METHODS

2.1 Materials

Two different mineral powders were used: a limestone powder and a quartz powder. The cement was CEM II/ A-M(S-LL) 42.5 N. The used aggregate was a combination of 5 different fractions, one of which was crushed (#5-16 mm fraction). The used superplasticiser was a carboxylic ether polymer-based admixture commercially known as Glenium 51 and the air-entraining agent was a fatty acid soap commercially known as Ilma-Parmix. The mixture proportions are given in Table 1.

Table 1 – Mixture proportioning.

	A1	A2	A3	A4	A5
Cement (kg/m ³)	330,1	264,08	297,09	330,1	264,08
Limestone powder (kg/m ³)	-	66,02	33,01	66,02	-
Quartz powder (kg/m ³)	-	-	-	-	66,02
Aggregate (kg/m ³)	1701,0	1691,8	1696,4	1634,2	1692,2
of which crushed	426,6	424,5	425,5	421,7	424,9
Water (kg/m ³)	190	190	190	190	190
Air-entraining agent (kg/m ³)	0,048	0,048	0,048	0,048	0,048
Superplasticiser (kg/m ³)	1,4	1,4	1,4	1,68	1,4
Effective w/c -ratio	0,5498186	0,6861968	0,6104311	0,54983	0,6861968

2.2 CIF-test and capillary suction

The freeze-thaw testing was done according to [7]. CIF means "Capillary suction, Internal damage and Freeze-thaw test". In the test, CIF specimens were obtained by splitting a 150 mm cube mould with a centralised PTFE (Polytetrafluorethylene) plate and they were subjected to freeze-thaw attack by using de-ionised water. The freeze-thaw scaling resistance was evaluated by the measurement of mass scaled from specimens after 14, 28, 24 and 56 freeze-thaw cycles.

2.3 Ultrasonic pulse transit time (UPTT)

When a freeze-thaw attack occurs, cracks can develop inside concrete which may not be seen on the surface, but which lead to an alteration of concrete properties i.e. internal structural damage. This was investigated by means of ultrasonic pulse transit time (UPTT) described in [8]. Both internal damage and surface scaling were determined from the same specimen and were tested simultaneously.

2.4 Scanning electron microscopy (ESEM)

Scanning electron microscopy (SEM) can be used to observe the microstructure of concrete. It is capable of observing the microstructural scale which even includes capillary pores. When used

together with backscattered electron mode (BSE), pores appear dark which allows differentiation between pores, cement paste, and aggregate. At the age of 56 days, the specimens for the ESEM investigation were cut into approximately 2 mm thick slices with a diamond saw using alcohol as the lubricating and cooling liquid. The specimens were dried by using an alcohol exchange method [9] and they were impregnated with resin under vacuum. Finally, the impregnated samples were ground and polished using diamond spray (9, 4, 1 and 0.25 μm).

3. RESULTS

3.1 Scaling

Table 2 gives the scaling results of test concretes after subjected to the freeze–thaw cycles. The cyclic freezing and thawing rate in the laboratory conditions is much higher than that in the natural environment. Thus, it is reasonable to assume that the scaling observed during the tests was more severe compared to actual structures. According to the Finnish concrete code [10], the specified limit for concrete scaling in exposure class XF1 (exposure to freezing and thawing, moderate water saturation, without deicers) for service life of 50 years, is 500 g/m^2 . Only the reference concrete (A1) and concrete with 20 % limestone powder without cement reduction (A4) passed this criterion.

Table 2 – Air content, strength and scaling of test concretes.

	A1	A2	A3	A4	A5
Air content (%)	6,2	6,2	6,4	6	6,4
28 day strength (MPa)	33,4	24,5	28,0	35,0	23,8
Scaling after pre-impregnation (g)	0,00	0,00	0,00	0,00	0,00
7 d = 14 cycles (g)	1,66	1,77	1,77	0,71	1,49
14 d = 28 cycles (g)	0,90	1,83	2,21	0,91	2,44
21 d = 42 cycles (g)	0,82	2,36	3,06	1,22	2,39
28 d = 56 cycles (g)	1,04	3,14	2,02	1,47	3,39
Sum (g)	4,42	9,10	9,07	4,31	9,71
Scaling total (g/m ²)	267,82	551,37	549,62	261,09	588,71

3.2 Internal damage and water absorption

Results of the relative dynamic modulus (RDM) test and water absorption during the CIF test are presented in Figure 1. Contrary to scaling, very minor differences in the RDM result of the different concretes were observed.

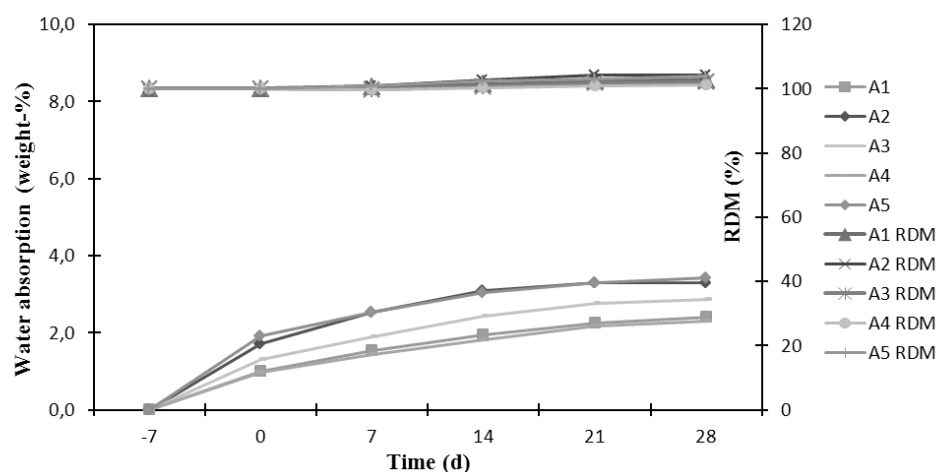


Figure 1 – Relative dynamic modulus (RDM) and water absorption during CIF test.

3.3 Microstructure

The results obtained from ESEM investigation did not show significant differences in the microstructure of the test specimens. Even though, for example, test concrete A2 had 66 kg less cement in cubic meter concrete than the reference test concrete (A1) and although their difference in compressive strength was almost 9 MPa, the porosity and microstructure of the samples were quite similar.

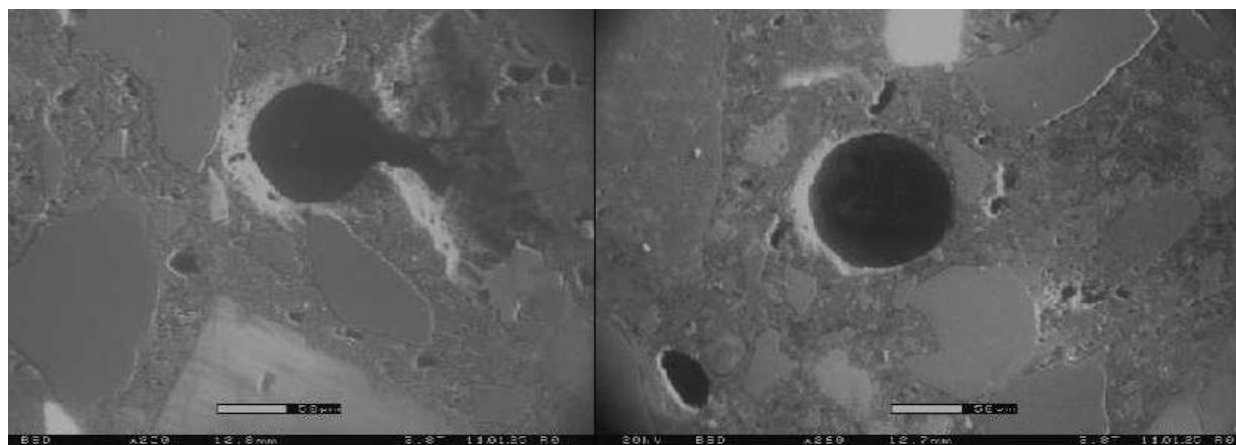


Figure 2 – Specimens A1 (on the left) and A2 (on the right) with similar microstructure.

4. CONCLUSIONS

It was found out that the water-binder ratio of the mineral powder concretes must be kept constant i.e. the amount of mixing water has to be reduced when binder is replaced by inert fillers in order to achieve satisfactory freeze-thaw durability in the mineral powder concretes. The type of mineral powder used did not seem to have an effect on the freeze-thaw durability of the concretes. The property most affected by the type of mineral powder was compressive strength which improved somewhat when limestone was used as inert filler when the cement amount was not reduced.

REFERENCES

1. Ghezal, A., Khayat, K. H. (2002). Optimizing self-consolidating concrete with limestone filler by using statistical factorial design methods. *ACI Materials Journal*. 99. No. 3, pp. 264.
2. Nehdi, M., Mindess, S., Aïtcin, P.-C. 1998. Rheology of high performance concrete: Effect of ultrafine particles. *Cement and Concrete Research*. 28. No. 5, pp. 687.
3. Bonavetti, V., Donza, H., Menéndez, G., Cabrera, O., Irassar, E. F. (2003). Limestone filler cement in low w/c concrete: A rational use of energy. *Cement and Concrete Research*. 33. No.6, pp. 865.
4. Goldman, A., and Bentur, A. (1993). Influence of microfillers on enhancement of concrete strength. *Cement and Concrete Research*, 23, No. 4, pp. 962.
5. Kjellsen, K.O., Wallevik, O.H. and Fjällberg, L., (1998). Microstructure and microchemistry of the paste-aggregate interfacial zone of high performance concrete. *Advances in Cement Research*, 10, No.1, pp. 33.
6. Detwiler, R.J. and Mehta, P.K., (1989) Chemical and physical effects of silica fume on mechanical behaviour of concrete, *ACI Materials Journal*. 86, No.6, pp. 609.
7. CEN/TS 12390-9 Testing hardened concrete - Part 9: Freeze thaw resistance - Scaling.
8. CEN/TR 15177 Testing the freeze thaw resistance of concrete - Internal structural damage
9. Cwirzen, A., (2004) Effect of the transition zone and ageing on the frost damage of high strength concretes. PhD thesis, Helsinki University of Technology.
10. BY 50 Betoninormit 2004 (Finnish concrete code), Suomen Betoniyhdistys r.y.

Moisture Transport in Concrete Structures in Swedish Hydro Power Plants



Martin Rosenqvist
M.Sc., Ph.D. student
Faculty of Engineering, Lund University
Vattenfall Research & Development
Älvkarlebylaboratoriet
SE – 814 26 Älvkarleby, Sweden
martin.rosenqvist@vattenfall.com

ABSTRACT

Concrete structures in hydro power plants exposed to harsh environment, such as non-frozen freshwater and long cold winters with freezing temperatures, are always in the danger-zone for suffering from concrete damages. Some existing concrete structures already suffer from different damages caused by high water content. The conditions regarding concrete quality, air entrainment, temperature and time will be investigated experimentally and theoretically in this doctoral study. The results could be of great help making better predictions of future degradation or represent a better basis when choosing repair methods and materials for concrete structures.

Key words: Moisture transport, frost resistance, degradation, hydro power plant.

1. INTRODUCTION

The environment surrounding a hydro power plant could be very harsh for the concrete structures regarding the presence of non-frozen freshwater and long cold winters with freezing temperatures combined with freeze/thaw-cycles. This description of the environment is also appropriate for bridges, harbours and other structures in contact with non-frozen freshwater.

Research has throughout times showed that high water content or a high moisture exposure could cause severe damages in concrete structures. For example concrete structures could be damaged by leaching, alkali silica reaction, frost and leakage in joints. In these examples the presence of water or moisture is of vital importance. The moisture transport in the concrete is also important for fully understanding what impact water could have on the degradation of concrete structures.

In late 2010 a new doctoral study was initiated with the purpose of studying frost resistance and effects of moisture transport in concrete structures in Swedish hydro power plants. The doctoral study will be executed at the Division of Building Materials at Lund University and on Vattenfall Research & Development.

2. BACKGROUND

The idea of this doctoral study was based on observations in experiments during a master thesis in 2009. The scope of the master thesis was to investigate the cause of observed scaling on concrete in the waterline on Porsi hydro power plant [1]. The damages could theoretically have

been caused by leaching, freeze/thaw-cycles or mechanical abrasion. The hypothesis was that freeze/thaw-cycles of concrete in contact with non-frozen freshwater were the dominant degradation mechanism. The experiments proved that it was possible to create similar scaling in the laboratory by exposing concrete specimens to freeze/thaw-cycles only.

Additional to the scaling in the waterline the specimens were also unexpectedly suffering from internal frost damages above the waterline. This internal degradation increased for every freeze/thaw-cycle. At the end of the experiment the degree of water saturation in the specimens was measured and it was exceeding the critical degree of water saturation of being frost resistant. This finding was interesting since a large moisture transport must have been occurred during the experiment. Unfortunately there was no time to investigate this finding.

3. RESEARCH PROGRAM

The doctoral study will resume the experimental work done during the master thesis and add theoretical work for the possibility of explaining the findings. The doctoral study will be divided into two parts, where each part consists of three research questions. The first part will experimentally and theoretically investigate the frost resistance and how moisture is transported and accumulated in concrete exposed to freshwater in combination with a temperature gradient.

The second part will experimentally and theoretically try to understand how concrete overlays could affect the frost resistance and the moisture content in concrete structures when repaired. Some repair methods or materials might be better compared to other methods or materials when evaluating how the moisture content could affect the risk of future degradation.

The theoretical work will be done by creating mathematical models for simulating the present and future behaviour of existing concrete structures exposed to non-frozen freshwater and freeze/thaw-cycles. The results from the experimental studies will be used to verify the models.

3.1 Part 1

The first research question concerns the risk for macroscopic ice lenses to form in the concrete, similar to frost heave in the roads in wintertime, see figure 1. Previous research has shown abnormal microstructural formations perpendicular to the direction of cooling in young cement paste specimens [2]. These results could indicate growth of ice lenses in the specimens.

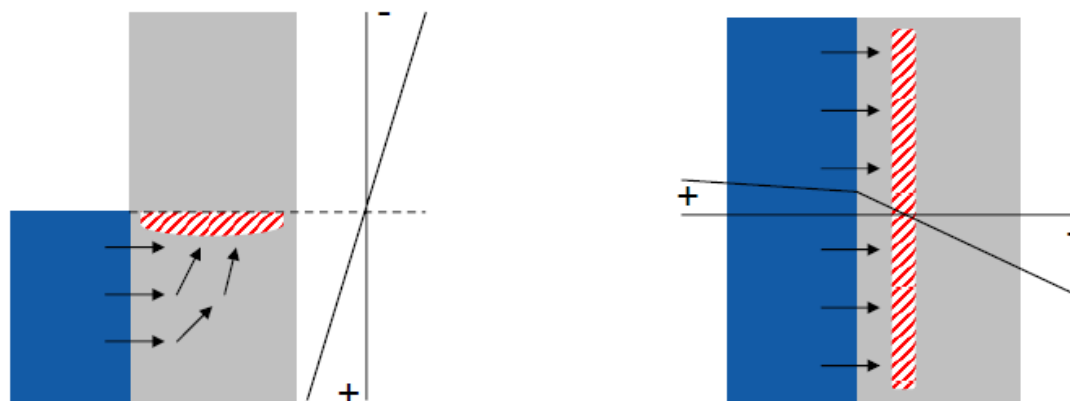


Figure 1 – Two examples of how macroscopic ice lenses theoretically could be formed.

The conditions – concrete quality, air entrainment, temperature and time – for the possibility to form macroscopic ice lenses in mature concrete are to be investigated in the upcoming study. The work will mostly be executed in the laboratory.

The second research question concerns the risk for scaling in the waterline and presence of internal frost damages above the waterline when the temperature is changing from freezing to thawing degrees, see figure 2. Meantime the moisture transport and accumulation in the specimens will be measured. The study will mainly be executed in the laboratory.

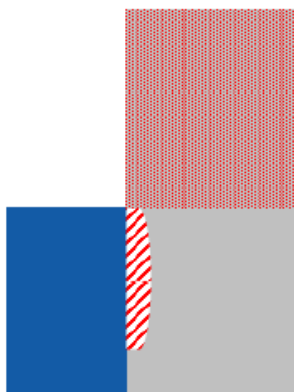


Figure 2 – Scaling in the waterline and internal frost damages above the waterline.

The third research question concerns the potential risk of frost resistant concrete to lose the frost resistance over time when being constantly exposed to non-frozen freshwater. It has been shown that concrete being completely water saturated, under no circumstances could withstand freeze/thaw-cycles [3]. Since a significant amount of water was present in the air voids, when the concrete was water saturated, the frost resistance was lost and the concrete was damaged.

The conditions – concrete quality, air entrainment and time – for the possibility of losing the frost resistance are to be investigated in the upcoming experimental study in the laboratory. The results from the laboratory study will be compared to field measurements from concrete structures having been exposed to similar conditions for either years or decades.

3.2 Part 2

The research questions 4-6 will investigate the effects on moisture transport and frost resistance when concrete structures are repaired with concrete overlays. Since these research questions are planned for the second part of the doctoral study no work has yet begun.

4. MATERIALS

For investigating the research questions, different concrete qualities have to be designed and cast. The combination and number of concrete qualities will vary due to the specific purpose of each experiment. Some experiments will only investigate if or when a phenomena or damage will occur. These experiments demand several different concrete qualities. Some other experiments will investigate the behaviour in terms of moisture transport and frost damages in existing concrete structures. In these cases fewer concrete qualities are needed.

The design of the different concrete qualities will be adapted to historically common concrete qualities. Old handbooks and guidelines for concrete manufacturing to hydro power plants will be of great value for this work. The final design of the concrete qualities will also be confirmed, if possible, by comparison with old records from different construction sites.

Since modern cements and additives differ from old cements and additives, this difference has to be accepted. By having this fact in mind the effects of the differences can be kept at a minimum.

5. DISCUSSION

The overall purpose of this doctoral study is to investigate the potential risk for frost damages, due to high water content, in concrete structures exposed to a very harsh environment. With an increased knowledge about how moisture is transported and accumulated in concrete during such conditions a better understanding could be obtained for the circumstances when concrete structures will get damaged by freeze/thaw-cycles during the winter.

An increased knowledge about frost resistance and moisture transport could also lead to better methods for the prediction of future degradation of concrete structures, such as Swedish hydro power plants. The increased knowledge would also make the work easier to investigate and evaluate old and existing concrete structures and choose appropriate repair methods and materials for each specific situation.

Being able to predict the demand or the effects of repair work the risk could be reduced for future damages or other problems related to frost resistance or moisture transport in concrete structures. This increased knowledge will hopefully be of great interest to the power industry and the society when maintaining a vast number of concrete structures of great value, such as hydro power plants, bridges, harbours and other concrete structures.

6. ACKNOWLEDGMENT

Thanks to Elforsk AB, Svenskt Vattenkraftcentrum (SVC) and Svenska Byggbranschens Utvecklingsfond (SBUF) for funding this doctoral study.

REFERENCES

1. Persson, M., Rosenqvist, M., "Frost damage in concrete dams", TVBM-5074, Division of Building Materials, Faculty of Engineering, Lund University, Lund, 2009. (In Swedish)
2. Corr, D., Monteiro, P., Bastacky, J., "Observations of ice lens formation and frost heave in young Portland cement paste", *Cement and Concrete Research* 33, 2003, pp. 1531 – 1537
3. Johannesson, B., "Dimensional and ice content changes of hardened concrete at different freezing and thawing temperatures", *Cement & Concrete Composites* 32, 2010 pp. 73 – 83

Ice abrasion by hydraulic pore pressure at rough concrete surface-ice indentation



Stefan Jacobsen
Professor.
COIN - Dept of Structural Eng.
NTNU
N-7491 Trondheim
stefan.jacobsen@ntnu.no

ABSTRACT

During short time indentation of a rough concrete surface into ice, widely differing concrete surface roughness may cause very high short-time contact pressure. Water between ice and concrete can then be pressed into the surface pores of the concrete. The indentation contact area determined as function of pressure, concrete surface roughness and mechanical properties of concrete and ice can be used to determine water penetration depth. When the hydraulic pressure is larger than concrete tensile strength fracture occurs. This paper shows the proposed model and that it can predict observed ice abrasion rates on real structures for realistic properties of concrete permeability, tensile strength, ice sheet movement, -pressure and number of ice-concrete contacts.

Key words: ice, concrete, abrasion, hydraulic contact pressure,

1. INTRODUCTION

Moving ice sheets can cause severe abrasion on concrete structures in spite of that the ice has inferior mechanical properties to the concrete. Several investigations have been made into this topic. The main work so far was by Huovinen [1] who studied the phenomenon and modelled the abrasion. The abrasion was ascribed to a two phase degradation of concrete; first cement paste, and then of protruding aggregate. The model does however not consider any effect of concrete permeability and water transport properties by ice contact. Hydraulic pressure that can arise as impacting ice forces water inwards is not taken into account. To develop ice abrasion resistant concrete, a new approach is presented with short time indentation of a rough concrete surface into ice causing high (Hertzian) contact pressure and water flow.

2. ICE ABRASION CALCULATION - COMPARISON WITH OBSERVATIONS

Figure 1 shows a simplified contact zone between ice and concrete with water pressed into the surface pores of the concrete according to Darcy by short-time elastic contact. Water can be available from the liquid-like layer on ice [2] from pressure melting according to Clausius-Clapeyron [3] and from sea-water.

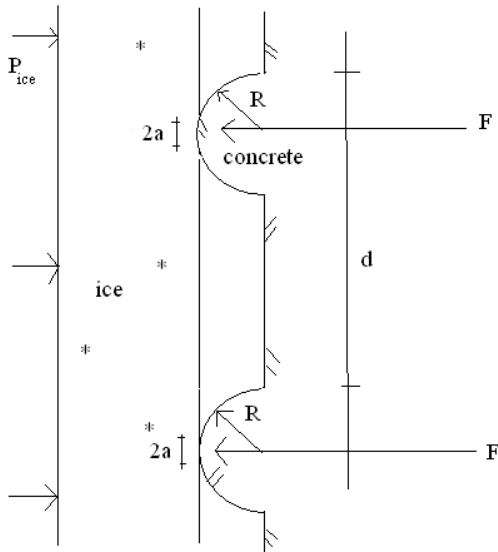


Figure 1 - Plane ice surface with average pressure P_{ice} towards rough concrete surface with half-spheres regularly spaced at distance d , reaction forces, F , and contact radii a .

The mean contact pressure p_m under the assumed elastic contact zone of radius a in figure 4 is 2/3 of the maximum contact pressure p_o [4]:

$$p_m = \frac{2}{3} p_o = \frac{F}{\pi a^2} \quad (1)$$

where the contact radius a is:

$$a^3 = \frac{3FR}{4E^*} \quad (2)$$

The reduced E-modulus E^* depends on Poissons ratios ν and E-modulii of ice and concrete:

$$\frac{1}{E^*} = \frac{1-\nu_i^2}{E_i} + \frac{1-\nu_c^2}{E_c} \quad (3)$$

If the contact and indentation of concrete in ice results in the local effective pressure p_{eff} , the depth of penetration, x , into the concrete surface during the time of indentation is given by a simplified solution to the non-steady state D'arcy flow [5,6]:

$$x(t_{ind}) = \sqrt{\frac{2p_{eff} t_{ind} K \cdot 10^6}{s \cdot g \cdot \rho_w}} \quad (4)$$

x [m]	depth of penetration
p_{eff} [MPa]	effective local hydraulic pressure in pore water at concrete surface
t_{ind} [S]	indentation time
s [m ³ /m ³]	pore volume fraction water filled by pressure ($\approx 0.02 - 0.06$ [5])
g	9.81 m/s ²
ρ_w	1000 kg/m ³

Figure 2 shows variation of depth of penetration, x , with concrete permeability, K , and time of indentation, t_{ind} for effective hydraulic pressure $p_{eff} = 30$ MPa. The air pore volume fraction, s , filled by pressure is assumed to be 0.06.

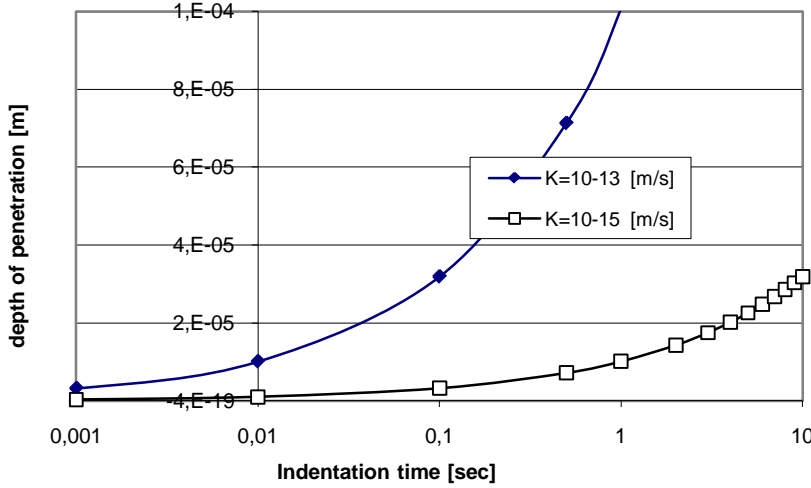


Figure 2 - depth of penetration as function of indentation time at 30 MPa contact pressure

Figure 2 shows that for typical high performance concrete and rock permeabilities the depth of penetration will be in the order of 1 – 10 microns during 0.01 s indents. Such a short indent time at ice crushing is realistic from time series of load and deformation analyzed in the frequency domain of ice sheets crushed against static vertical structures [7]. From this a relatively simple deterministic model is presented in the following using observations of maximum short time ice contact pressures from the literature in the order of 15 – 42 MPa. The indentation contact area between a rough concrete, here modelled as half-spheres on a plane as shown in figure 1, and ice is determined as function of concrete surface roughness (Radius R in figure 1) and mechanical properties of concrete and ice. The concrete-ice contact radius, a , for the chosen surface roughness radius can be determined from maximum pore water pressure p_{eff} by dividing eq (2) with πa^2 giving:

$$a = \frac{3\pi R p_{eff}}{4 E^*} \quad (5)$$

Then, from eq.(4) the depth where the hydraulic pressure is larger than concrete tensile strength, x_{crit} , is determined from penetration depth (eq.(4)) assuming a linear inwards pressure drop:

$$x_{crit} = x(t_{ind}) \left[1 - \frac{f_{c,t}}{p_{eff}} \right] \quad (6)$$

Where:

$f_{c,t}$ [MPa] concrete tensile strength

The number of contact points is determined based on figure 1 and assumptions and simplifications of the ice-concrete contact. This includes the square grid spacing (d), movement of the ice, maximum effective elastic contact pressure, size of crushed ice fragments and geometry of the fractured or abraded “pop-outs” (cylindrical) from the concrete:

$$ABR_c = \frac{L_{ice,ann}}{D_{fragment}} \cdot \frac{x_{crit} \cdot \left(\frac{\sqrt{A_s}}{d} + 1 \right)^2 \cdot a^2 \pi \cdot 1000}{A_s} \quad (7)$$

ABR_c [mm/year]	annual ice abrasion.
$L_{ice,ann}$ [m/yr]	annual ice movement
$D_{fragment}$ [m]	size of ice fragment after impact [7]
d [m]	length between individual indentation points in square grid (fig.1)
A_s [m ²]	concrete surface area exposed to ice (for simplicity 1m ²)

In table 1 below the abrasion calculation with eq.(7) is compared with observations of ice abrasion on the Canadian Confederation Bridge and a Finnish light houses.

Table 1 - Ice abrasion calculation compared with observations on marine concrete structures

Structure	K, f_i , d, R, E^* , D_{fragm} , L_{ice} , t_{ind} , P_{eff}	Measured	Calc. (eq.7)
		(mm/yr)	(mm/yr)
Confederation bridge [8]	$\approx 10^{-14}$, 8, 0.025, 0.008, 8200, 0.25, 2500, 0.01, 22.5	$\approx 0,3$	0,3
Lighthouse [1,9]	$\approx 5 \cdot 10^{-13}$, 5, 0.025, 0.008, 7555, 0.25, 1000, 0.01, 22.5	≈ 1	1,0

From table 1 we see that the model is capable of predicting ice abrasion of the right order of magnitude for these high-strength low permeability concretes. It can also be shown that this approach can be used to calculate scratching abrasion as ice is sliding over a concrete surface in stead of impacting. Finally it should be noted that the ice is effectively impermeable when there is no or very low brine pocket content (< 5 vol-%) [10,11] so that the flow can be assumed only in the concrete.

REFERENCES

1. Huovinen, S. (1990) Abrasion of concrete by ice in arectic sea structures, VTT Publications 62, (Doctoral thesis), Espoo, 110 p, app. 31 p.
2. Hobbs P.V. (1974) Ice Physics, Clarendon Press, Oxford, p.394
3. Barnes P., Tabor D. (1966) Plastic flow and pressure melting in the deformation of Ice I, Nature V210, 878-882
4. Fischer-Cripps A.C. (2007) Introduction to Contact Mechanics, Springer p.101
5. Neville A.M. (1995) Properties of concrete, 4th ed., Pearson Prentice Hall, p.495
6. Hoff, W. D. Hall, C.(2002): Water transport in brick, stone and concrete. Spon press London and New York, 318p
7. Timco, G.W. and Jordaan, I.J.(1987) "Time-series variations in ice crushing", Proc 9th Int Conf Port and Ocean Eng under Arctic Condit. (POAC), Fairbanks, V. 1, pp. 13-20.
8. Newhook J.P, McGuinn D.J. (2007) Ice abrasion assessment – piers of Confederation Bridge, Conf. Bridge Eng. Summit 1997-2007 Proc., Can Soc for Civ. Eng pp.145-157
9. Møen E. (2009) PhD Thesis in preparation, Norw. Univ of Science and Technology, Dept of Structural Engineering, Trondheim, Norway
10. Pringle D. Miner J. Eicken H. Golden K. (2009) J Geophys. Res V.114, C12017, 14 p.
11. Golden K. Eicken H. Heaton A. Miner J. Pringle D Zhu (2007) Geophys. Res Letters V.34, L16501, 6 p.

De-icing Salt Scaling Resistance of Concrete Containing New Composite Cement



Ali Akbar Ramezani pour
Ph.D.
Head of Concrete Technology and
Durability Research Center.
Amirkabir University of
Technology, Tehran, Iran.
aaramce@aut.ac.ir



Mohsen Jafari Nadushan
M.Sc.
Department of Civil Engineering.
Amirkabir University of
Technology, Tehran, Iran.
mohsen_djn@aut.ac.ir



Mansur Peydayesh
M.Sc.
Department of Civil
Engineering.
Amirkabir University of
Technology, Tehran, Iran.
peydyesh@aut.ac.ir

ABSTRACT

Salt scaling is a major damage problem for concrete pavements, so the phenomenon has been the subject of an extensive research effort in the world.

Effects of modified type II and composite Portland cements and air void on the de-icer scaling resistance of concrete were investigated in this paper. The specimens were tested for salt scaling resistance in accordance with ASTM C672.

Results reveal that the performance of type II Portland cement was more appropriate than composite cement in mixture without entrained air, but the mixture containing composite cement with entrained air has the best performance in salt scaling.

Key words: Salt Scaling, Entrained Air, Freezing – Thawing Cycle, Concrete Pavement.

1. INTRODUCTION

Concrete exposed to numerous durability issues that result in high maintenance costs. Salt scaling is a major damage problem for concrete and concrete pavements that is defined as superficial damage caused by freezing a saline solution on the surface of a concrete body. The damage is progressive and consists of the removal of small fragment of the concrete surface.

Replacement of cement with SCMs in the production of concrete not only improves the mechanical properties and durability of concrete but also decreases the amount of consumed cement, energy consumption and CO₂ emission. Hence for concrete pavements construction, a new composite Portland cement has been produced with natural pozzolana in Iran. The main objective of this work is to compare the effects of modified type II and composite Portland cements on mechanical and durability properties and de-icer scaling resistance of concrete.

According to the glue-spall theory, the damage results from cracking of the ice on the surface of concrete, when the thermal expansion mismatch stress exceeds the strength of the ice. It was

previously shown that cracks in the ice layer are expected to penetrate the underlying cementitious binder, and subsequently propagate into a path that is parallel to the composite interface, which results in the removal of a scallop [1].

2. EXPERIMENTAL PROGRAM

Modified type II and composite Portland cements were used in the concrete mixtures. The new composite Portland cement consists of 80% clinker and 18% natural pozzolan (volcanic ash, Tuff) and limestone. The rest of ingredient is gypsum. Chemical and physical characteristics of modified type II and composite Portland cements are shown in Table 1 and 2 respectively.

Table 1 - Chemical characteristics of cementitious materials.

	Modified Portland cement (type II)	Composite Portland cement
Chemical Components		
Calcium Oxide (CaO) (%)	62.4	59.23
Silicon Dioxide (SiO ₂) (%)	21.07	24.47
Magnesium Oxide (MgO) (%)	2.89	2.13
Aluminum Oxide (Al ₂ O ₃) (%)	4.99	5.54
Ferric Oxide (Fe ₂ O ₃) (%)	3.64	3.28
Sulphate Oxide (SO ₃) (%)	2.31	1.67
Potassium Oxide (K ₂ O) (%)	0.65	0.8
LOI (%)	2.02	6.2
Mineralogical composition		
C ₃ S (%)	49.41	-
C ₂ S (%)	22.83	-
C ₃ A (%)	7.07	-
C ₄ AF (%)	11.08	-

Table 2 - Physical characteristics of cementitious materials.

Physical properties	Modified Portland cement (type II)	Composite Portland cement
Blaine (cm ² /g)	3078	3240
Specific gravity (g/cm ³)	3.13	2.99
Initial setting time (min)	135	140
Final setting time (min)	187	195
Compressive strength (MPa)	3 days	19.6
	7 days	28.7
	28 days	37.0
	28 days	40.4

For all mix designs, coarse aggregates were crushed calcareous stone with a maximum size of 19 mm and fine aggregate was a natural sand. The coarse aggregates have a specific gravity and water absorption of 2560 kg/m³ and 1.75%, respectively, and the fine aggregate has water absorption of 2.3% and a specific gravity of 2570 kg/m³. Potable water was used for casting and curing all concrete specimens. A high range water reducing (HRWR) admixture based on modified polycarboxyl-ether was employed to achieve the desired workability in all concrete mixtures. A synthetic detergent air-entraining agent (Microair by BASF) was employed to achieve the desired air content in concrete mixtures. According to the ACI2012r-01 the values of air content in the concrete is considered 6%.

The mixture proportions for concrete specimens are summarized in Table 3. The concrete mixtures were prepared with a constant total binder (cement + SCMs) content of 375 kg/m³. Standard testing procedures were applied for determination of the air void content using a pressure method (ASTM C231).

Table 3 - Mix proportions of concrete.

Mix	Cement type	w/c	Concrete composition (kg/m ³)			Air content (%)	Air-entraining agent (%binder)	Superplasticizer (%binder)	Slump (mm)
			Cement	Water	Aggregate				
A-40-0	Modified Portland	0.4	375	150	1806.79	0	-	0.2	70 ± 20
B-40-0	Composite Portland	0.4	375	150	1806.79	0	-	0.2	70 ± 20
A-37-6	Modified Portland	0.37	375	139	1721.62	6	0.135	0.3	70 ± 20
B-37-6	Composite Portland	0.37	375	139	1721.62	6	0.135	0.3	70 ± 20

Concrete cubes of 100×100×100 mm dimension were cast for compressive strength. They were tested for compressive strength after 7, 28, 90 and 180 days of water curing. Salt scaling resistance of concrete was investigated according to ASTM C672 standard procedure [2], based on determination of concrete resistance to repeated freezing and thawing (F/T) in contact with 4% calcium chloride (CaCl₂) solution. Special specimens (300 × 200 × 75 mm) were used for this test. The specimens had been removed from moist storage at the age of 14 days and had stored in air for 14 days at 23±2 °C and 45 to 55 % relative humidity. The total number of freeze–thaw cycles was 50. Both visual examination according to ASTM C 672 and the mass of scaled material in salt scaling for every five cycles of freeze–thaw were considered.

3. RESULTS AND DISCUSSIONS

The compressive strengths of concrete specimens are presented in Fig. 1. In general, the concrete specimens containing type II Portland cement had higher compressive strength at various ages and up to 180 days when compared with the concrete specimens containing composite Portland cement. The reduction in compressive strength could be related to the degree of hydration, which is lower for composite Portland cement concrete than for type II Portland cement one at all ages. The reduction in degree of hydration of concrete specimens containing composite Portland cement is explained as the result of a clinker dilution effect. Entrained air caused a reduction in compressive strength at various ages and up to 180 days. Voids play a crucial role in determining the compressive strength of concrete. Existence of air

voids in concrete results in local intensification of stresses and a more rapid promulgation of either already existing microcracks or cracks crossing the air voids.

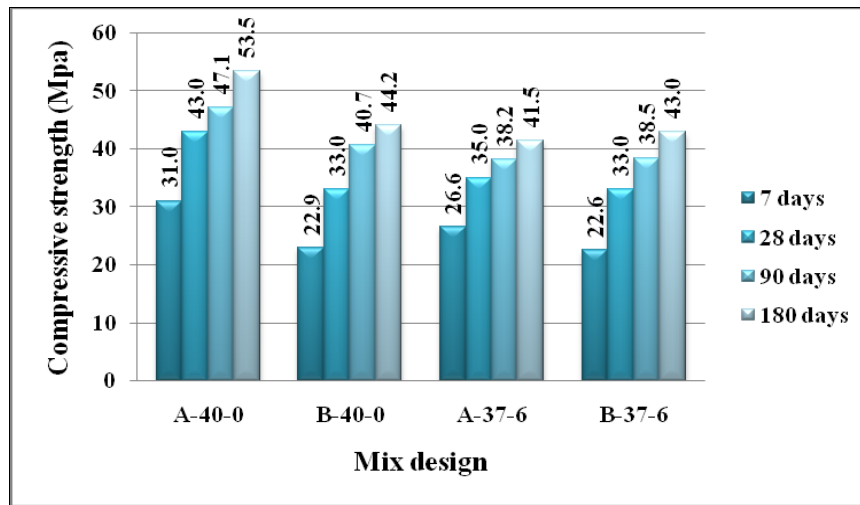


Fig. 1. The compressive strength at various ages.

The specimens under freeze–thaw scaling due to de-icing salt were inspected by visual examination according to ASTM C672- 98 [2]. Rating of the measured scaling for every five cycles of freeze–thaw is reported in Table 4.

Table 4 - Results of visual examination according to ASTM C 672-98.

Mix		Number of cycles									
Code	No	5	10	15	20	25	30	35	40	45	50
A-40-0	1	1	2	2	2	2	2	2	2	2	3
	2	2	3	3	3	3	3	3	3	3	3
A-37-6	1	2	2	2	2	2	3	3	3	3	3
	2	2	2	2	2	2	2	2	2	2	2
B-40-0	1	2	3	3	3	3	3	3	3	4	4
	2	2	3	3	3	3	3	3	3	4	4
B-37-6	1	2	2	2	2	2	2	2	2	2	2
	2	1	2	2	2	2	2	2	2	2	2

The mass of scaled material in salt scaling for every five cycles of freeze–thaw are presented in Fig. 2. It is clearly seen that the results of visual examination is consistent with the mass of scaled material. It can be found in Fig. 2 that the non-air-entrained concretes containing type II Portland cement performed significantly better than the non-air-entrained concretes containing composite Portland cement. For a concrete without air entrainment, one could expect 2.5% by volume of entrapped air voids. Tuff and limestone fills the cavities and pores in hardened concrete. Therefore there aren't any void for restraining the ice expansion. Results reveal that the mixture containing composite Portland cement with entrained air bubbles has the best performance in salt scaling test (See fig. 2).

The air content has a high significance on the salt scaling. Fig. 2 illustrates that the air-entrained concretes performed significantly better than the non-air-entrained ones. Entrained air could be beneficial to salt scaling resistance in three ways: (1) entrained air bubbles reduce bleeding [4]; (2) ice in the air voids sucks pore fluid from the surrounding matrix, which compresses the porous body [5] and (3) entrained air system caused a reduction in solution penetration depth in concrete.

Fig. 3 illustrates the relationship between compressive strength and mass of scaled material. The frost-salt scaling resistance of concrete was not correlated with increased compressive strength concrete.

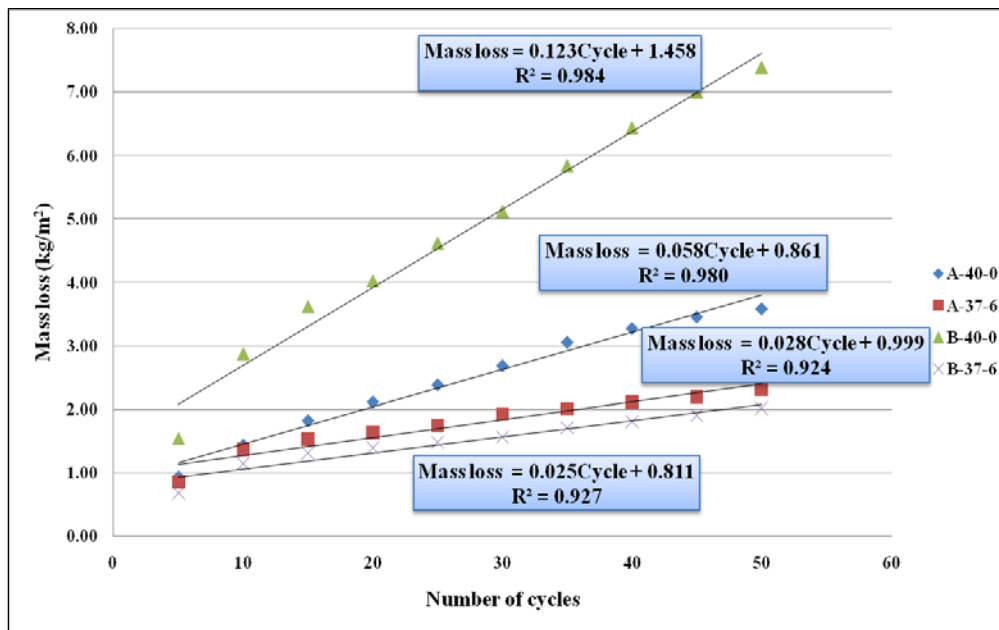


Fig. 2. The mass of scaled-off particles versus number of cycles for all mix designs

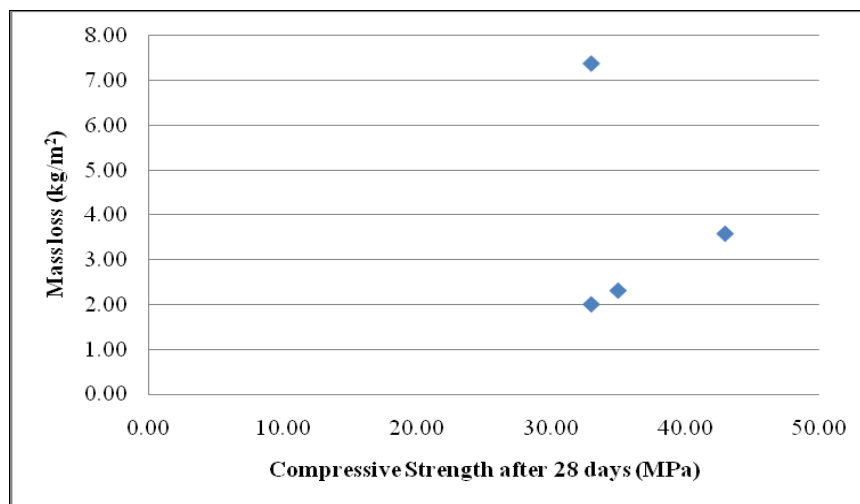


Fig. 3. The relationship between compressive strength and mass of scaled material.

As can be seen in Fig. 2, very good linear relationships between mass loss and number of cycles will be achieved for all concrete mixture. The results reveal that the mass of scaled material varies during the initial freeze/thaw cycles due to bleeding and finishing effects. Therefore, due

to the fact that the mechanical properties of the concrete do not vary significantly in the surface, each freezing cycle result in a relatively constant amount of damage.

CONCLUSIONS

From the results obtained in this investigation, the following conclusions are drawn:

1. The partial replacement of cement with tuff and limestone reduces the compressive strength of concrete. Entrained air caused a reduction in compressive strength at various ages for all concrete mixtures. Existence of air voids in concrete results in local intensification of stresses and a more rapid promulgation of either already existing microcracks or cracks.
2. Results reveal that the performance of type II Portland cement was more appropriate than composite cement in mixture without entrained air, but the mixture containing composite cement with entrained air has the best performance in salt scaling.
3. It is confirmed that entrained air can improve salt scaling resistance of concrete considerably. Entrained air bubbles reduce bleeding and therefore prevent reducing the strength of the surface. Also entrained air system caused a reduction in solution penetration depth in concrete. It is observed that, the most important parameter affecting the scaling resistance of the concrete is the air-entraining use.
4. The salt scaling resistance of concrete was not correlated with increased compressive strength concrete. The most effective parameter, after air-entraining use, is the surface strength.

References

- [1] G.W. Scherer, "Crystalization in pores", *Cem. Concr. Res.* 29, 1999, pp. 1347–1358.
- [2] American Society for Testing and Materials, "Standard test method for scaling resistance of concrete surfaces exposed to deicing chemicals", *ASTM Standard C672*, 1992.
- [3] G.W. Scherer, J.J. Valenza, "Mechanisms of frost damage", in: J. Skalny, F. Young (Eds.), *Materials Science of Concrete*, vol. VII, American Ceramic Society, 2005, pp. 209–246.
- [4] John J. Valenza, George W. Scherer. "A review of salt scaling: II. Mechanisms", *Cement and Concrete Research* 37, 2007, 1022–1034.
- [5] T.C. Powers, R.A. Helmuth, "Theory of volume changes in hardened Portland-cement paste during freezing", *Proc. Highw. Res. Board* 32, 1953, pp. 285–297.
- [6] John J. Valenza, George W. Scherer. "A review of salt scaling: I. Phenomenology", *Cement and Concrete Research* 37, 2007, pp. 1007–1021.
- [7] American Concrete Institute, "Standard Practice for Selecting Proportions for Normal, Heavyweight and Mass Concrete", *ACI Committee 211*, ACI 211.1-91, 2002.
- [8] American Concrete Institute, "Guide to Durable Concrete", *ACI Committee 201*, ACI 201.2R-01, 2001.

Session A7 – STRUCTURAL BEHAVIOUR

Reinforcement in tailor-made concrete structures



David Fall, M.Sc.,
Ph.D. Student
Department of Civil and
Environmental Engineering
Chalmers University of
Technology
SE-412 96 Göteborg, Sweden
E-mail:
david.fall@chalmers.se



Karin Lundgren, Ph.D.,
Associate Professor
Department of Civil and
Environmental Engineering
Chalmers University of
Technology
SE-412 96 Göteborg,
Sweden
E-mail:
karin.lundgren@chalmers.se



Kent Gylltoft, Ph.D.,
Professor
Department of Civil and
Environmental Engineering
Chalmers University of
Technology
SE-412 96 Göteborg, Sweden
E-mail:
kent.gylltoft@chalmers.se

ABSTRACT

The ability of making tailor-made concrete structures, utilizing the formability of concrete, in an effective manner is the aim of the ongoing European project TailorCrete (www.tailorcrete.com). With modern tools, such as industry robots, it is possible to mill a concrete mould in Styrofoam or molding sand directly from a 3D-modell. A fully developed automated production enables irregular shaped concrete at a lower cost than current production methods; this has until today been examined only for non-load-carrying concrete elements. This article presents possible reinforcement alternatives for implementation in such production process. Solutions such as conventional steel reinforcement, fibre reinforcement, fibre reinforced polymer bars and textile reinforcement are discussed. Each solution is associated with certain advantages and disadvantages. Furthermore, this article discusses the importance of developing rational design methods while working with tailor-made concrete elements.

Key words: reinforcement, complex concrete geometries

1. INTRODUCTION

Automated production of concrete elements is a very wide expression. It covers everything between machinery performing single production steps to advanced fully automated system for production of e.g. façade elements or concrete bricks. Most of the automated production seen today is developed for large production series. Each machine is designed and programmed to perform a few steps in the production e.g. reinforcement bending or welding. Generally, these machines only produce one type of element with very limited variations between series. In the project TailorCrete the aim is set at a general automation of all steps from 3D-model to finalized concrete element. Such general solution would allow unique elements to be produced while

retaining the economic benefits seen in large scale automated production; hence, tailor-made concrete structures could be used more commonly than as today, only in prestigious projects. More information about the project can be found at www.tailorcrete.com.

2 REINFORCEMENT ALTERNATIVES

The relatively high compressive stress capacity of concrete is well-known and the main reason for the wide use of concrete as a building material. However, tensile stress and shrinkage tends to cause cracks in the unreinforced material. Therefore, reinforcement is used. In the initial phase of the project different reinforcement alternatives were studied in order to evaluate which is suitable for automated production [1]. Conventional steel reinforcement has been widely used during the last century. During the last decades many alternative or complements have been developed e.g. fibre reinforcement, fibre reinforced polymer bars and textile reinforcement.

Conventional reinforcement provides the concrete element with high loading capacity and a well established design procedure. Thereby, the use of conventional steel reinforcement simplifies the implementation of tailor-made concrete elements with regards to regulations and standards. It is, however, important to stress that the need for development of the production method development is large. In order to fulfil the project aims the reinforcement bars must be formed, in an automated fashion, in arbitrary geometries and assembled with sufficient precision and robustness.

Fibre reinforcement is often described as short discontinuous fibres of varying length, thickness and material. Reinforcing fibres can be made of steel, glass, various synthetic materials (coal, polymer, etc.) or organic materials. Steel fibres can be used as primary reinforcement and have good durability with regards to corrosion. Glass fibres are most commonly used in thin, non-structural, concrete elements e.g. façade elements. The tensile strength of glass fibres is very high; however, it is heavily influenced of deterioration. Synthetic fibres can be produced from several materials with widely differing properties e.g. polyethylene, polypropylene, coal or aramid. The main benefit of using fibre reinforcement is that, in carefully chosen amounts, it offers a simple and rational production process well suitable for application in concrete elements of complex shape. Fibre reinforcement is mainly used as secondary reinforcement. However, in some applications it has been used as primary reinforcement with good result, as reported by Oslejs [2]. Further research is needed for such use to a larger extent. Furthermore, it is desirable to distribute and orient the fibres throughout the concrete structure in order to improve and optimize the reinforcing effect.

Bars made of fibre reinforced polymers (FRP-bars) could be a good alternative in tailor-made concrete element, especially in thin parts where the concrete cover demanded for conventional reinforcement could not be fulfilled. FRP-bars are made by continuous aramid, coal or glass fibres incorporated in a polymer matrix (e.g. polyester, epoxy or vinyl ester). The properties of the composite is affected by the fibre and matrix materials, but are generally characterized by lower weight, lower elastic modulus and higher tensile strength than conventional steel reinforcement [3]. Although FRP does not corrode, other deteriorating mechanisms affect the composite. Sea salt, de-icing salt, freeze-thaw cycles, UV – light and fresh water could all influence the durability [3]. In general the fracture is brittle; however, a more ductile material behavior could be obtained by combining several fibre materials within the matrix [4]. The big disadvantage with FRP-bars is the generally limited formability, i.e. the composite cannot be reshaped.

Textile reinforcement is made of continuous fibres arranged in several directions (e.g. nets or mats). In these textiles the fibre material is more effectively utilized than if the same material is scattered randomly in the concrete, which is the most common case for fibre reinforced concrete. However, the production and application process are very complex. Common fibre materials is AR-glass, coal or aramid but also thin steel or polymer threads can be used. The textile composites can be produced through hand lay-up, pultrusion or extrusion. While hand lay-up is a manual craftsmanship based production, pultrusion and extrusion techniques are more suitable to industrial production with large series. Textile reinforcement offers great flexibility and could therefore be considered as an alternative for tailor-made concrete elements; however, the production methods used today demands extensive development in order to be implemented in a fully automated production process.

Additionally, it should be mentioned that many of the presented alternatives can be used in combinations, e.g. conventional steel reinforcement and fibre reinforcement. The identified advantages and disadvantages of the discussed reinforcement alternatives are summarized in Table 1. In this table all fibre materials are generalized under the category fibre reinforcement. As mentioned, the fibre material influences the composite behaviour; however, the general features tabulated are common for all fibre materials.

Table 1. Summary of advantages and disadvantages with different reinforcement systems.

	+	-
Conventional reinforcement steel	Provides structural integrity. Conventionally used, i.e. easy to implement with regard to guidelines and design codes. Inexpensive	Might be difficult to produce effectively in arbitrary geometries. Certain concrete cover needed, i.e. not suitable for very thin concrete elements.
Fibre reinforcement	Can be added to the concrete during mixing.	Rarely used as primary reinforcement.
Fibre reinforced polymer	Good durability. Could be used in thin concrete members.	Rare technology which might lead to high costs. Fixed shape once produced.
Textile reinforcement	Could be applied in arbitrary geometries	Rare technology which might lead to high costs. Production method might need development

3 DESIGN METHODOLOGY

As previously mentioned, enabling the use of unique concrete elements at normal price levels is the purpose of developing an automated production process. For this to be used in practice, it is also important to improve the links between architects, structural engineers and producers. Furthermore, there is a need for a rational method for reinforcement design in complex geometries.

The process would start with creation of a 3D-model of the building (Figure 1, left). The structure can then be subdivided into producible concrete elements and analyzed to design a reinforcement layout or establish the amount and type of fibres needed. Once the reinforcement has been defined in the model, the final layout could be verified by additional analyses and then be produced (Figure 1, middle). The automated production, with great possibilities of producing

concrete elements with complex geometries, also allows for geometrical optimization. By adjusting the geometry, the material consumption could be decreased. Today, the process is divided in steps between architects, structural engineers and producers. One important possibility with the more automated process is that it enables a more easy-going interaction between the involved competences.

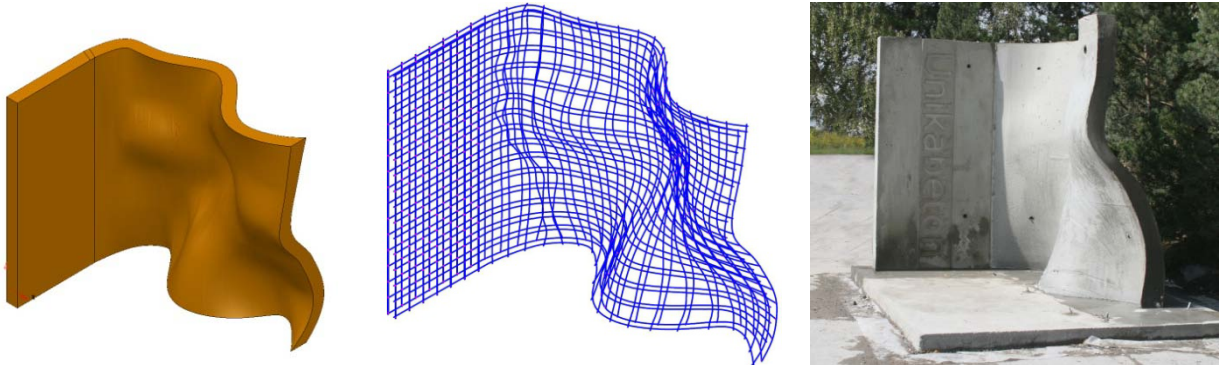


Figure 1- Architectural model of prototype element (left) and the corresponding reinforcement model (middle). Manufactured (unreinforced) prototype (right). Photo: Thomas Juul Andersen, Teknologisk Institut (DTI)

In order to simplify the production, the design shall aim at reinforcement bars bent only in one plane, even if the concrete element is double curved. While assembling it is likely that the bars will bend down by the self-weight. This change in position must be accounted for when the production is planned.

4 CONCLUSION

Good solutions to the problems associated with automated production of concrete structures are needed. The increased demand for unique concrete elements will also put demands on the production methods to be more cost effective than the time consuming and complex methods used, in prestigious projects, today. Possibilities of using the formability of concrete fully will not only make building more aesthetically attractive but also open up for utilizing the structural advantages with complex geometries.

ACKNOWLEDGEMENT

This research has received funding from the European Community's Seventh Framework Programme under grant agreement NMP2-LA-2009-228663.

REFERENCES

1. Fall, D. and C. Nielsen, *Concrete reinforcement solutions*. 2010, Chalmers University of Technology, pp. 27.
2. Oslejs, J., *New Frontiers for Steel Fiber-Reinforced Concrete*. Concrete International, 2008, May (1), pp. 45-50.
3. Dejke, V., *Durability of FRP Reinforcement in Concrete*, in *Department of Civil Engineering*, 2001, Chalmers University of Technology: Göteborg, 211 pp.
4. Karlsson, M., *Fiberkompositarmering*. 1998, FoU-Väst, 42 pp.

Corroded reinforced concrete structures: effects of high corrosion and corroded stirrups



Kamyab Zandi Hanjari
Ph.D.
Chalmers University of Tech
Sven Hultins gata 8
SE - 41296 Göteborg
kamyab.zandi@chalmers.se



Karin Lundgren
Associate Professor
Chalmers University of Tech
Sven Hultins gata 8
SE - 41296 Göteborg
Karin.lundgren@chalmers.se



Mario Plos
Associate Professor
Chalmers University of Tech
Sven Hultins gata 8
SE - 41296 Göteborg
Mario.plos@chalmers.se



Kent Gylltoft
Professor
Chalmers University of Tech
Sven Hultins gata 8
SE - 41296 Göteborg
Kent.gylltoft@chalmers.se

ABSTRACT

The influences of severe corrosion leading to extensive cover cracking and of corrosion of stirrups on the bond of corroded bars were studied through pull-out tests and detailed non-linear finite element analyses. The tests showed that when wide cracks develop, the favourable effect of rust flowing through cracks becomes significant. This considerably decreases the splitting stress and, consequently, the damage to the surrounding concrete. A previously developed corrosion model was extended to include this phenomenon and used in detailed three-dimensional analyses of the test specimens. The results indicated the favourable effect of rust flowing through cracks and also the important role of stirrups after cover cracking.

Key words: corrosion, stirrup, bond, pull-out test, finite element analysis.

1. INTRODUCTION

Many existing concrete structures, for example bridges, piers and parking garages, show significant corrosion. In the presence of high levels of corrosion it is not uncommon that cover cracking and spalling have occurred. The consequent reduction of bond strength can be a major problem for structures in the service and ultimate states. Earlier research by the authors has identified some of the uncertainties in the knowledge available today. The effect of corroded stirrups on bond strength has not previously been studied with pull-out tests or with detailed finite element analysis. A rather common approach in modelling the effect of the corroded stirrups is to take into account the loss of the cross-sectional area; this does not account for the volume expansion of rust around the corroded stirrups, which may lead to cover cracking. Another uncertainty is the remaining anchorage capacity in structures with severely corroded reinforcement, especially where extensive cracking has taken place. In this article, the two uncertainties outlined above are addressed. The effect of corroded stirrups and severe corrosion leading to extensive cover cracking were studied through pull-out tests. Thereafter, an earlier developed corrosion model was extended and used in detailed three-dimensional analyses of the test specimens.

2. EXPERIMENTAL PROGRAM

In collaboration between Chalmers University of Technology and Politecnico di Milano, a research program comprising both the study of corrosion cracking and bond strength deterioration was undertaken. The aim was to better understand the effects of large corrosion attacks and of corroding stirrups on cracking and bond strength in anchorage regions. Details about the tests are given in a test report [1], and two articles [2-3]. The eccentric pull-out specimens had the shape of a beam-end after inclined shear cracking. The influences of the location of the anchored bar, i.e. middle or corner placement; the presence or absence of transverse reinforcement; and the corrosion level were studied. The specimens were of three types: specimens without stirrups, where the main bars were corroded (type A); specimens with stirrups where the main bars were corroded and the stirrups were protected by insulating tape (type B); and specimens with stirrups where the main bars and stirrups were corroded (type C). All of the specimens were subjected to accelerated corrosion, with an average current density of $100 \mu\text{A}/\text{cm}^2$, for different time spans that caused a rebar weight loss up to approximately 20% in the main bars and 35% in the stirrups.

The tests showed that when the first corrosion crack took place, corrosion products started to flow through cracks and reached the outer surface of the concrete. For large corrosion penetrations, when several new cracks initiated and widened, the flow of rust became significant. This decreased the splitting stress around the bar and consequently reduced the damage to the surrounding concrete. The flow of rust not only depended on the number of cracks and crack width but also varied in time. During the time in which the specimens were subjected to corrosion, the flow of corrosion products took place continuously.

3. NUMERICAL ANALYSIS

The previously developed corrosion model, [4], was extended to include the rust flow effects. The extended model is briefly presented here; details concerning assumptions and the derivation of equations are given in Zandi Hanjari *et al.* [5] and Zandi Hanjari [6]. It was assumed that the volume flow of rust depends on the corrosion time interval, crack width and the normal stress in the rust layer. The corrosion time and corrosion rate were given as input to the model and corrosion penetration was determined theoretically based on Faraday's law. The crack width, w_{cr} , was computed from the nodal displacements across the crack, Figure 1. The section area of the crack, A_{cr} , through which rust flows, was calculated by $w_{cr} \cdot e$ where e is the element size along the crack. The total volume flow of rust, V , through a crack is calculated as the summation of the volume flow of rust in time steps, ΔV_i , as

$$V = \sum_{i=1}^k \Delta V_i \quad (1)$$

where index i is the time increment number. The volume flow of rust through a crack, within a time increment, Δt_i , was expressed by:

$$\Delta V_i = \left[v_{i-1} + \frac{1}{2} \left(\frac{A_{cr,i-1} \cdot \sigma_{n,i-1}}{\rho(V_{i-1} + \Delta V_i)} \cdot \Delta t_i \right) \right] \cdot A_{cr,i-1} \cdot \Delta t_i \quad (2)$$

where v is the velocity of the rust flow; σ_n is the splitting stress; and ρ is the density of rust. With respect to the volume flow of rust, the free increase of radius of the corroded bar was given from geometry by:

$$y_{ext} = -r + \sqrt{r^2 + (v_{rs} - 1)(2rx - x^2) - \frac{V}{\pi \cdot e}} \quad (3)$$

where y_{ext} is the free increase of the radius due to the remaining rust around the corroded bar, r is the original bar radius and v_{rs} is the volume of the rust relative to the uncorroded steel. Thereafter, the strain in the rust is calculated and the deformation in the interface layer, divided between the bond layer and the corrosion layer, is computed together with the condition for equilibrium using an iterative procedure.

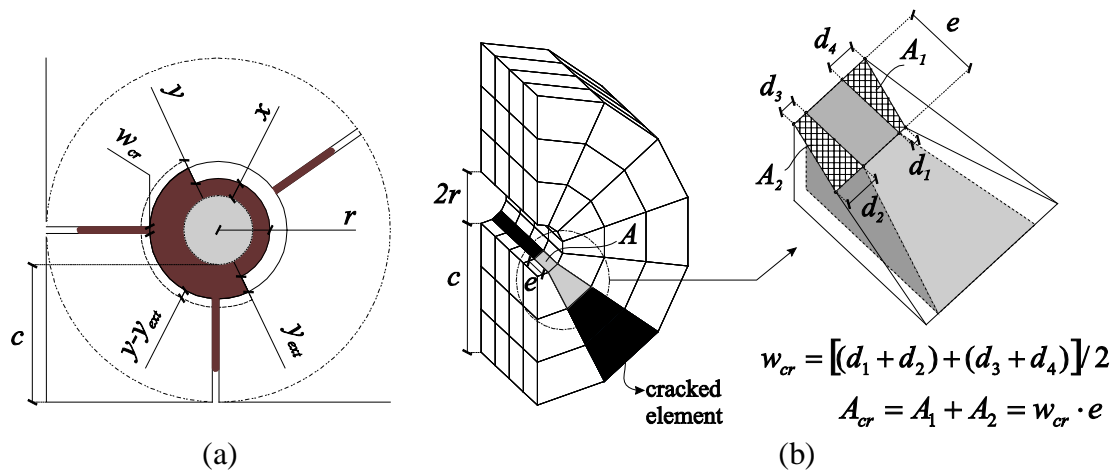


Figure 1 – (a) Physical interpretations of the variables in the extended corrosion model; and (b) section area of the crack through which rust flows.

4. RESULTS

The behaviour of the eccentric pull-out specimens in corrosion phase and pull-out tests was studied through three-dimensional non-linear finite element analyses with the original and the extended corrosion models. The modelling technique and material models are given in Zandi Hanjari *et al.* [5]. In the analyses with the extended corrosion model, for which the effect of rust flowing through cracks was included, the extensive cover cracking was reached at significantly larger corrosion penetrations compared with that in the analyses with the original corrosion model. In general, the crack pattern has changed slightly when the effect of rust flowing through the cracks was included, i.e. more cracks of smaller width were seen in the analyses with the extended corrosion model. This corresponds better to the measurements on the specimens.

The results from numerical analysis with the extended corrosion model, in terms of average bond stress versus free-end slip, are presented in Figure 2. The behaviour of the specimens without stirrups, type A, was relatively well predicted. The agreement was less good when the specimens had stirrups and especially when the stirrups were corroded. Generally, less bond capacity for the corroded bars was obtained in the analysis than that measured in the experiments.

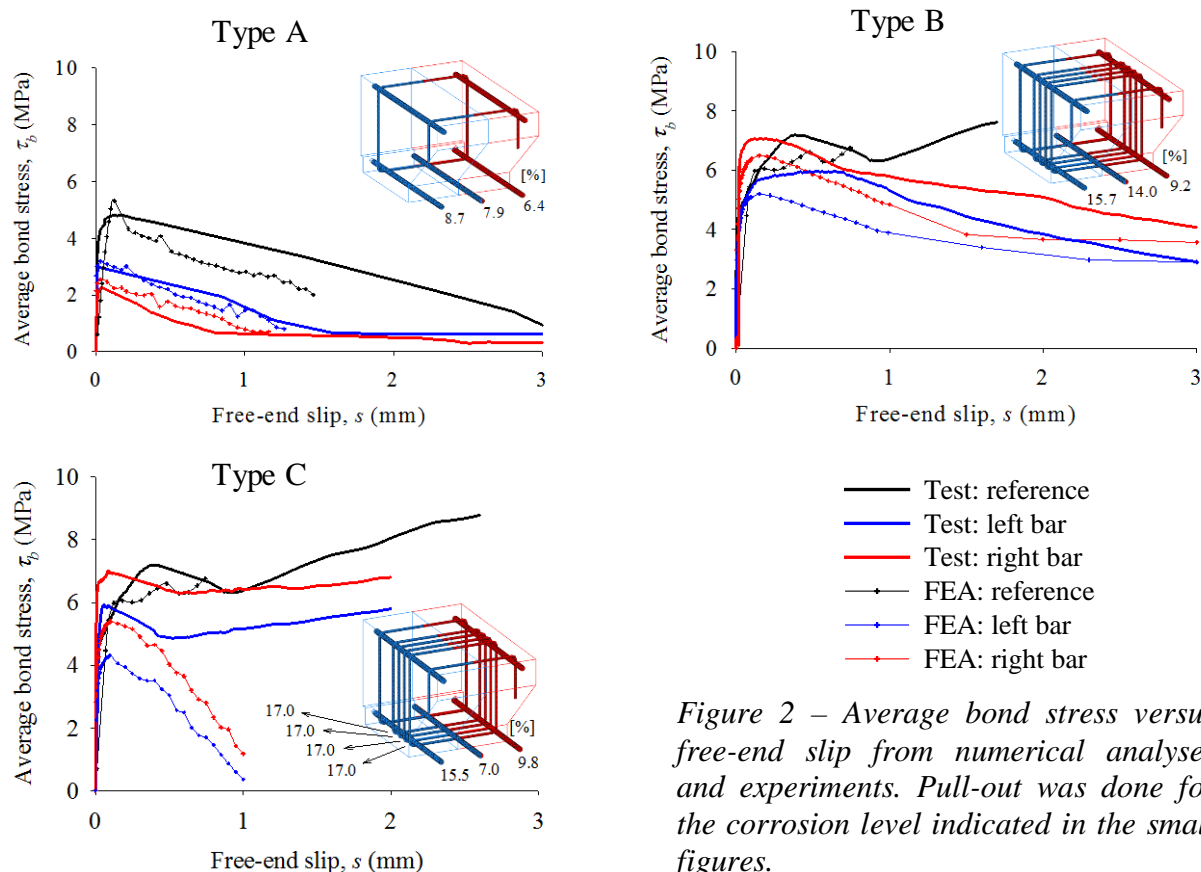


Figure 2 – Average bond stress versus free-end slip from numerical analyses and experiments. Pull-out was done for the corrosion level indicated in the small figures.

5. CONCLUSIONS

The following conclusions are drawn on the basis of this study.

- The tests and numerical analyses showed the significant influence of the stirrups, the position of the tested bar and the corrosion on the bond capacity and the failure mode.
- The extended corrosion model gave results that were consistent with what was observed in the experiments. The extended corrosion model, compared to the original corrosion model, resulted in more corrosion cracks with smaller crack openings.

REFERENCES

- Zandi Hanjari, K., Coronelli, D., “Anchorage Capacity of Corroded Reinforcement: Eccentric Pull-out Tests,” Report 2010-06, Chalmers Uni. of Tech, Politecnico di Milano.
- Coronelli, D., Zandi Hanjari, K. and Lundgren, K., “Severely corroded reinforced concrete with cover cracking,” submitted to *Materials and Structures*, 2010.
- Zandi Hanjari, K., Coronelli, D. and Lundgren, K. “Anchorage capacity of severely corroded bars with corroded stirrups,” submitted to *Magazine of Concrete Research*, 2010.
- Lundgren, K., “Bond between ribbed bars and concrete. Part 2: The effect of corrosion,” *Magazine of Concrete Research*, Vol. 57, No. 7, 2005, pp. 383-395.
- Zandi Hanjari, K., Lundgren, K., Plos, M. and Coronelli, D., “Three-dimensional modeling of corroded reinforcement in concrete,” submitted to *Structure and Infrastructure Engineering*, 2010.
- Zandi Hanjari, K., “Structural Behaviour of Deteriorated Concrete Structures,” Doctoral Thesis, Ny serie Nr 3142, Chalmers University of Technology, Gothenburg, 2010.

Punching Shear on Steel Edge Columns



Mikael Hallgren
Tekn.Dr., Docent
Tyréns AB
SE-118 86 Stockholm
Sweden
mikael.hallgren@tyrens.se

ABSTRACT

In the design of flat slabs supported on steel edge columns, the same design method for punching shear as for slabs on ridged concrete columns is usually adopted. This has been questioned, as a slender steel column cannot transfer the hogging moment of the slab which is normally assumed in punching shear design. An alternative design method based on beam shear analogy has been proposed and also been verified by non-linear finite element analyses.

Key words: Punching shear, slabs, edge steel columns, design, non-linear finite element analyses

1. INTRODUCTION

Punching shear failure on concrete edge columns has previously been studied in several investigations, e.g. [3][4], and the results are reflected in current codes, e.g. Eurocode 2. In these investigations, the columns are rigidly connected to the slab. Thus, the hogging moment of the slab over the column is transferred to the column. The punching shear failure at an concrete edge column in an in-situ cast flat slab structures hereby resembles an eccentric punching shear failure over an interior column.

However, in modern construction of building structures, the reinforced in-situ cast concrete is often combined with structural steel elements like beams and columns. These composite steel-concrete structures combine the speed and simplicity of steel structure erection with the robustness and stiffness of reinforced concrete. With its structural composite action, it also optimises the utilisation of materials. A popular method of construction of residential buildings is to cast concrete in-situ on precast floor plate elements which are supported on steel columns at the edges of the building.

The structural behaviour of flats slabs on slender steel edge columns differ a lot from that of flat slabs rigidly connected to concrete edge columns. Due to the low stiffness of the steel column compared to the stiffness of the concrete slab, and also due to the fact that the concrete slab usually is simply supported on the top end plates of the steel column, almost no hogging moment can be transferred from the slab to the column. The slab could be regarded as more or less pin supported over the steel column. However, in practise the concrete slab on edge steel columns is often designed for punching shear according to the same design procedure as for

slabs on rigidly connected concrete columns, which also requires tension reinforcement on the top side of the slab. Thus, the validity of the code rules regarding punching shear applied to the concrete-steel case has been questioned.

In a previous diploma work for the engineering degree at KTH [1], conducted and supervised at Tyréns, the behaviour of flat slabs supported on pinned edge supports has been studied in linear elastic finite element analyses and some recommendations to a modified design method and on modified detailing of reinforcement were given. In a later master thesis work at Chalmers [2], supervised by the author, the recommendations and the actual punching shear behaviour of the concrete slab to steel column connection were verified with non-linear finite element analyses. The present paper summarises the results from these studies and from on-going research.

2. PRESENT DESIGN PRACTISE AND SUGGESTED MODIFICATION

Based on the common method of designing flat slabs on rigid cast-in-situ concrete columns, present practise is that flat slabs on steel columns are designed in the same way. This means that at an edge column, the slab has to be checked for punching shear. The theory of punching implies that the top side of the slab above the column is in radial and tangential tension and that the bottom side of the slab close to the column is in radial and tangential compression. The ratio of flexural (top side) reinforcement is in most codes included in the design formula for punching shear strength. E.g. according to Eurocode 2, EN 1992-1-1, the punching strength is calculated from:

$$v_{Rd,c} = \frac{0.18}{\gamma_c} k \cdot (100 \cdot \rho_1 \cdot f_{ck})^{1/3} \quad (1)$$

Where γ_c is the partial safety factor for concrete, k is a coefficient considering the size effect, ρ_1 is the mean ratio of flexural reinforcement and f_{ck} is the characteristic compressive strength of concrete. The mean ratio of flexural reinforcement ρ_1 is computed by the geometrical average of the flexural reinforcement ratios in the two orthogonal directions above the column. At an interior column, the high bending moments in both directions would usually give sufficient reinforcement ratios to be used in equation (1). At edge columns rigidly connected with the slab, the hogging moment perpendicular to the slab edge would usually also require flexural reinforcement enough to satisfy equation (1). However, in the case with steel edge columns where there is almost no hogging moment perpendicular to the edge, extra top reinforcement is usually required just to give enough reinforcement ratio to satisfy equation (1) for the punching shear strength. The design then normally leads to an arrangement of the reinforcement as shown in Figures 1 and 2.

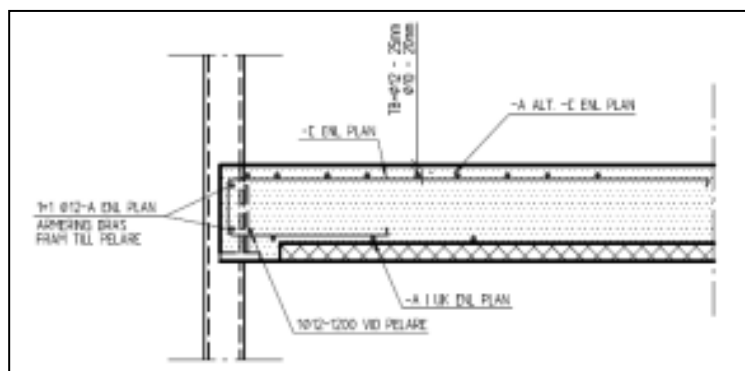


Figure 1 – Cross section of the steel column to concrete slab connection according to present practise [1].

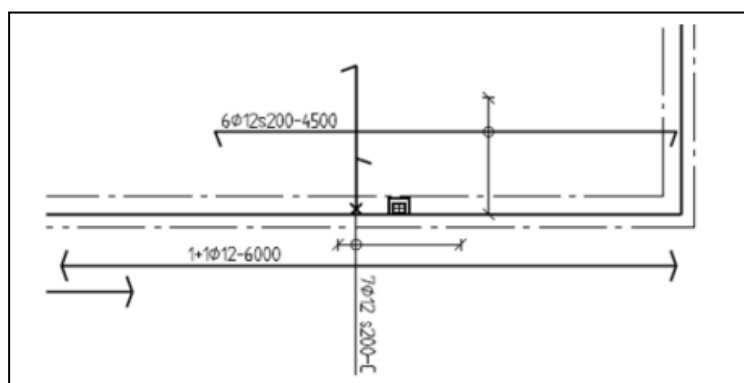


Figure 2 – Plan view of the steel column to concrete slab connection according to present practise [1].

However, this practise has been questioned. Why put in unnecessary rebars in the slab when there is no tension that requires that much reinforcement? The suggested modification according to [1] is that the failure mode is not classic punching shear but rather beam shear of the slab in perpendicular direction and simply supported at the edge, as shown in Figure 3. In the direction parallel to the edge, the slab should then also be design for beam action in the continuous slab strip over the edge column.

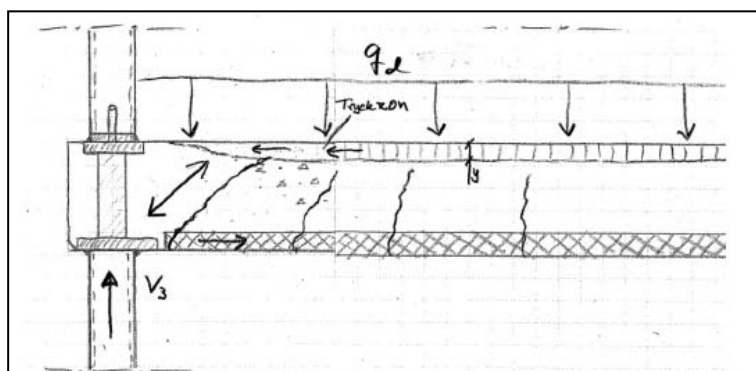


Figure 3 – Beam shear action perpendicular to the slab edge [1].

So based on the proposed theory for a modified design [1], the slab over the edge steel column should be checked for beam shear strength in perpendicular and parallel directions. Recommendations on the choice of cross sections to check and distributions of shear forces are further given in [1]. If required, shear reinforcement can be added and designed according to the applicable code. With Eurocode 2, the shear reinforcement would then be design according to the strut and tie method.

3. NON-LINEAR FINITE ELEMENT ANALYSES

The proposed theory described above has been tested with non-linear finite element analyses (NLFEA) [2]. The analyses were performed using the ATENA 3D software by Cervenka Ltd. which gives advanced concrete models, simulating the cracking and crushing of concrete as well as the yielding of steel and reinforcement.

In order to check the validity of the NLFEA and to calibrate the concrete model, some previous punching tests on slabs on concrete corner and edge columns [3][4] where modelled and simulated with the NLFEA program. The results from the analyses are in fairly good agreement with the measured behaviours of the test slabs, as shown in Figure 4.

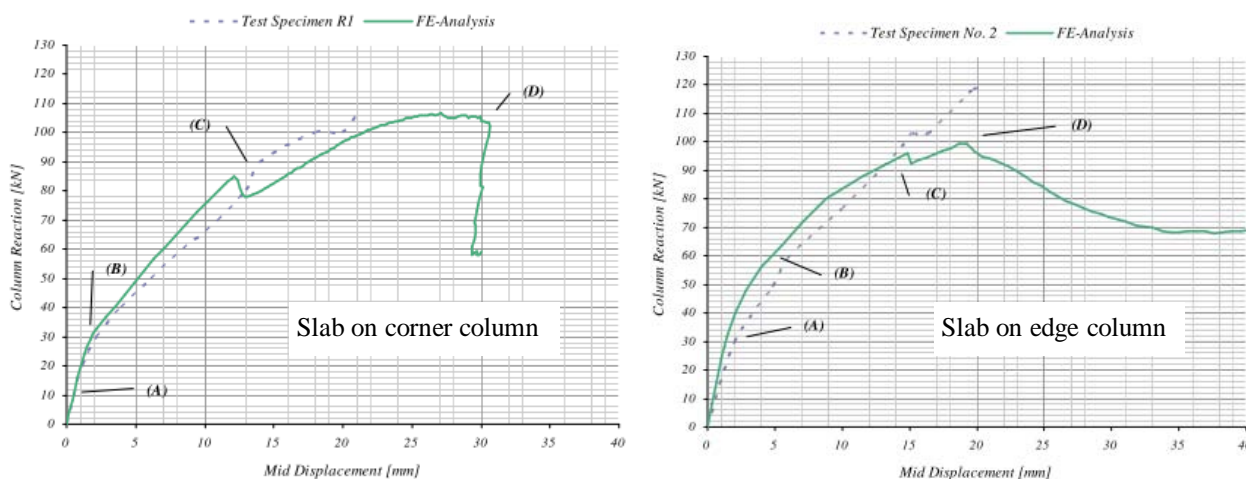


Figure 4 – NLFEA compared with test results from [3] and [4].

Three prototype models of slabs on edge steel columns were modelled and analysed with NLFEA. Due to symmetry, only the slab half on one side of the column had to be modelled. The reinforcement in the models were arranged as proposed in [1]. Slab dimensions and material properties were kept constant and only the amount of reinforcement was varied in the three analyses. The results from these analyses generally confirm the theory proposed in [1]. As shown in Figure 5, the shear cracks in the strip perpendicular to the slab edge evolve from flexural cracks on the bottom side of the slab. Hence, they more resemble shear in a simply supported beam than punching shear. However, some restraint still appears on the top side and the transition from shear in perpendicular direction to shear parallel to the edge is complicated.

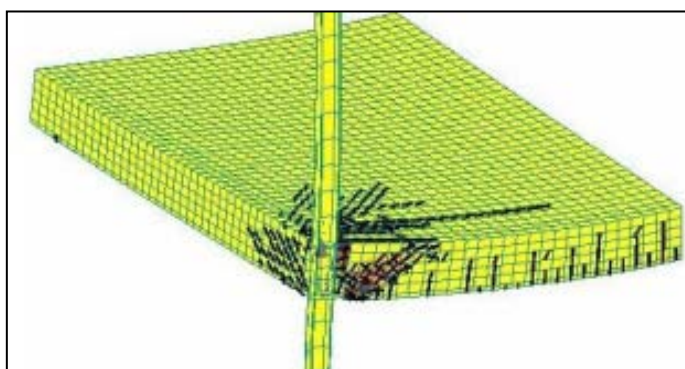


Figure 5 – Typical crack pattern from NLFEA of concrete slab on steel edge column [2].

4. FURTHER RESEARCH

Further studies with NLFEA are planned to be conducted. In those analyses, more parameters are to be varied in a parametric study. Furthermore, some analyses should also include shear reinforcement. Finally, the analyses should also be verified with some laboratory test.

REFERENCES

1. Jensen, M., *Dimensionering av betongbjälklag vid kant- och hörnpelare av stål*. TRITA-BKN Examensarbete 279, Betongbyggnad KTH, Stockholm 2009, 75 pp.
2. Ericsson, S. & Farahaninia K., *Punching Shear in Reinforced Concrete Slabs on Edge Steel Columns*. Examensarbete 2010:10, Betongbyggnad CTH, Göteborg 2010, 101 pp.
3. Ingvarsson H., *Betongplattors hållfasthet och armeringsutförande vid hörnpelare*. Meddelande Nr 122, Byggnadsstatik KTH, Stockholm 1977, 143 pp.
4. Kinnunen S., *Försök med betongplattor understödda av pelare vid fri kant*. Rapport R2, Statens institut för Byggforskning, Stockholm 1971, 103 pp.

Extreme Values of Climatic Thermal Stresses in Concrete Box Cross-sections



Oskar Larsson
M. Sc.
Lund University
Box 118
SE – 221 00 Lund
oskar.larsson@kstr.lth.se

ABSTRACT

The thermal stresses in a concrete bridge are affected by the surrounding climate. Varying temperature will produce movements which, if restrained, may induce stresses in the structure. To predict the thermal stresses in box cross-sections, FE simulations have been performed with extensive climatic input data to simulate the temperature and resulting stress fields in the hollow concrete arch of the New Svinesund Bridge. The results show that the thermal tension stresses can be above the tension strength of the concrete. A linear approach for estimating the thermal stresses may give an overestimation, due to non-linear effects.

Key words: FE-analysis, Solar radiation, Box cross-section, Climate data

1. INTRODUCTION

The temperature field in a concrete bridge is affected by complex interactions of climatic factors. Solar radiation, air temperature, wind speed and long-wave heat radiation all affects the temperature field in a concrete structure. The temperature field can be divided into different components; an average temperature, vertical and horizontal linear temperature differences and a non-linear temperature difference. Annual variations in air temperature mainly affect the average temperature of a structure, while the linear and non-linear temperature differences are mostly affected by solar radiation and long-wave heat radiation.

Varying temperature in a concrete structure will give rise to thermal movements. A change in average temperature will mainly give longitudinal movements while the linear as well as non-linear differences also produces transverse movements. In a rectangular hollow concrete section the movements in a wall are restrained by the adjacent walls, which can induce stresses and strains in the section. These stresses may, in combination with stresses from traffic loads, contribute to cracking.

During the latest 30 years, several investigations have been performed of thermal stresses in indeterminate concrete bridges [1]-[2]. These investigations have mainly been focused on longitudinal stresses, and transverse stresses have only been analysed and discussed briefly. Previous research on thermal actions has mainly been focused on the temperature levels and differences [3]. In most cases concerning long-term simulations general sets of data have been used; for example daily total solar radiation instead of using hourly data. The long-wave heat radiation, which is governed to a large extent by the cloud cover, is also treated in a simplified way.

In this research a FE-model is used to calculate temperature distributions and resulting thermal stresses in the cross-section of the New Svinesund Bridge. Extensive long-term climate data from two locations in Sweden is used for the temperature simulations. To get a more precise prediction of the temperature, hourly data is used for the climatic factors. The temperature profiles are used in a linear-elastic FE-model of the same cross-section to predict stresses induced from thermal expansion. Additional FE-simulations are performed using temperature components for the different walls extracted from the calculated temperature fields. The main objective of these simulations is to investigate if thermal stresses predicted from the use of linear temperature differences can be used in general situations for design purposes.

2. FE - SIMULATIONS

An FE-model was developed and validated using measurements performed on the New Svinesund Bridge, see figure 1 for the geometry of the used cross-section. The validation is described in Larsson & Karoumi [4], where the possibility to simulate the concrete temperature

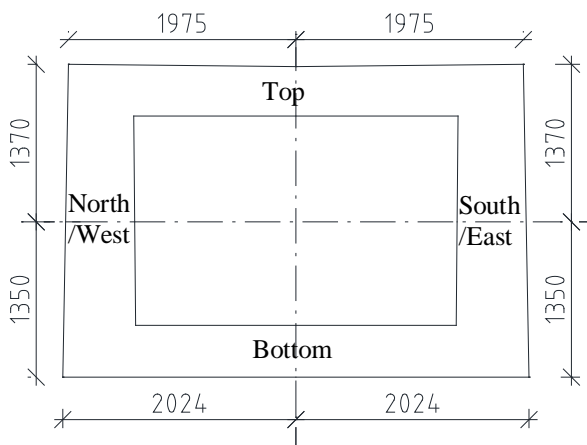


Figure 1 - The cross-section used in the FE-simulations, with labels for the walls. (mm)

in a hollow box cross-section was investigated. Measurements of solar radiation, long-wave radiation, wind speed and air temperature were used in a FE-model to simulate the temperature distribution. The results from the investigation showed that the FE-model can capture the temperature variation in an accurate way. The model was well suited to use for further studies of hollow concrete box cross-sections.

In the present research the FE-model is used with climate data from two meteorological stations in Sweden, the station in Stockholm in the middle part and the station in Luleå to the north. The number of years available for simulation was 15 years for both stations. The bridge is assumed to be located either east-west, with the vertical walls to the south and north, or north-south, with the vertical walls to the east and west.

The temperature distributions achieved from the heat transfer simulations are used as input in a FE-model to analyse thermal stresses. The level of thermal strains in a structure depends on the temperature difference and a thermal expansion coefficient, α , which, according to EN 1991-1-5 [5], can be set to $10^{-5} \text{ }^\circ\text{C}^{-1}$. If the structure, such as in our case, is not free to expand, varying temperature will cause stresses. The magnitude of the thermal stresses depends on the degree of restraint and the modulus of elasticity, which is set to 30 GPa in the FE-model. This corresponds roughly to a tensile strength of 2,7 MPa.

From the resulting temperature fields the average temperature and linear temperature difference have been calculated over each of the four walls. New static stress simulations using these temperature components as input over the different walls have been performed, both separately and combined. The results are compared to the results from original simulations. All results have also been compared to a FE-simulation using the recommended design value of a linear

temperature difference of 15 °C stated in EN 1991-1-5 [5]. This value is used for all the walls simultaneously.

3. RESULTS AND ANALYSIS

The annual maximum tension stress level has been extracted from different parts of the structure for all of the simulations. In figure 2 the annual maximum tension stress for the inside of the top wall using climate data from Stockholm is presented, the bridge located east-west. In the figure the results for the regular simulations (*Climate*) is compared to the results from the simulations using linear temperature difference (ΔT) separately and in combination with average temperature ($\Delta T+avg$) as input. The difference in stress level between *Climate* and ΔT is about 1 MPa for each year. The combination $\Delta T+avg$ gives a slightly lower stress level than for ΔT only, but the difference from the regular simulations is still large. The stress level is not depending on the direction of the bridge in this case, the stress level is similar when the bridge is located south-north. For the cases with climate data from Luleå the results for the annual maximum tension stress on the inside of the top flange are similar. The same difference of about 1 MPa is found between the regular climate simulations and the temperature components simulations.

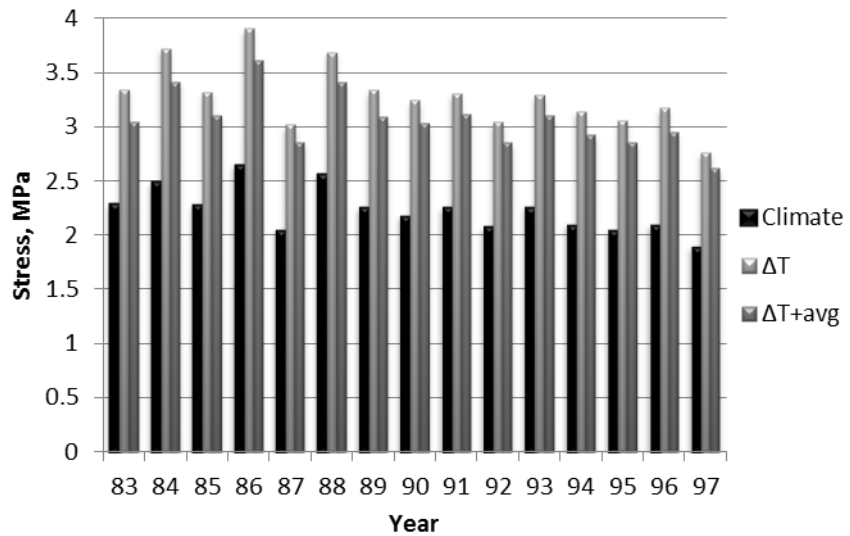


Figure 2 - Annual maximum tension stress on the inside of the top wall for Stockholm, bridge located east to west

If we instead look at the annual maximum tension stresses at the inside of the south wall for Stockholm, figure 3, it is clear that the linear approach is not suitable for this cross-section. The stress level is almost 3 times as large when ΔT is used as input compared to the regular simulation using climate data. This is due to the non-linearity of the thermal stress distribution, mainly caused by the differences in geometry and size between the horizontal and vertical walls in this cross-section.

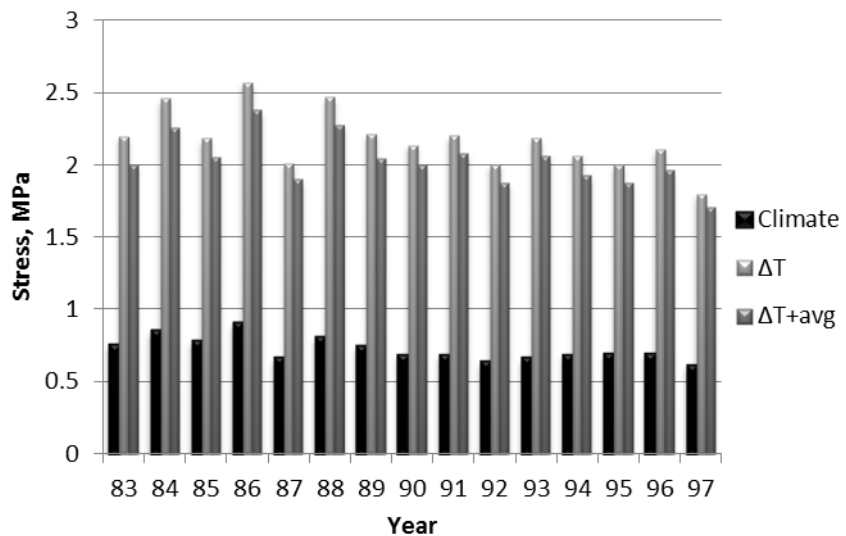


Figure 3 - Annual maximum tension stress on the inside of the south wall for Stockholm, bridge located east to west

From the extracted annual maxima, extreme values with a return period of 5 years have been extracted.

These values are presented in Table 1 together with the maximum inside tension stress from the simulation using the linear temperature difference from the Eurocode. The results show that the tension stress on the inside of the top wall is below the tension strength for the used concrete.

The results from the simulations using calculated linear temperature difference as input are close to the results from the simulations using Eurocode values. For Stockholm the 5-year values are almost equal to the Eurocode results. There is, however, a large difference compared to the simulations using climate data. This indicates that the recommended approach in the Eurocode overestimates the thermal tension stresses and that the non-linear effects are significant.

Table 1. Thermal transverse tension stresses on the inside of the respective walls with a return period of 5 years (MPa)

		Bridge located east-west		Bridge located north-south		
		Top	South	Top	East	West
Stockholm	<i>Climate</i>	2,39	0,79	2,22	0,84	0,67
	ΔT	3,52	2,33	3,26	2,12	1,97
Luleå	<i>Climate</i>	2,29	0,73	2,12	0,75	0,75
	ΔT	3,23	2,20	2,87	1,92	1,86
EN 1991-1-5	ΔT^*	3,51	2,35	3,51	2,35	2,35

*Independent of bridge direction

4. CONCLUSIONS

For the New Svinesund Bridge the annual maxima for the tension stress on the inside of the top wall are overestimated if a completely linear approach is used. A small reduction in stress level can be achieved if the difference in average temperature is included in the simulations, but it does not have a large impact. The annual maxima for the inside of the vertical walls are even more overestimated, due to the non-linearity of the stress distribution. The results indicate that the given value of a linear temperature difference of 15 °C in EN 1991-1-5 overestimates the thermal stresses if used in the design of bridges.

REFERENCES

1. Prakash Rao, D.S., "Temperature Distributions and Stresses in Concrete Bridges", *ACI Journal*, Title No. 83-52, 1986, pp. 588-596.
2. Elbadry, E., & Ghali, A., "Thermal Stresses and Cracking of Concrete Bridges", *ACI Journal*, Title No. 83-90, 1986, pp. 1001-1009.
3. Soukhov D., "Representative Values of Thermal Actions for Concrete Bridges", *Progress in Structural Engineering and Materials*, Vol. 2, No. 4, 2000, pp. 495-501
4. Larsson, O., & Karoumi, R., "Modelling of Climatic Thermal Actions in Hollow Concrete Box Cross-Sections", *Structural Engineering International*, No 1, 2011, pp. ??-??.
5. European Committee for Standardization, "ENV 1991-1-5: Actions on Structures - Part 1-5: General Actions - Thermal Actions", CEN, Brussels, 2005

Verifying the Behaviour of a Concrete Buttress Dam Subjected to Temperature Variations



Richard Malm
Ph.D., Researcher
KTH Royal Institute of
Technology
Division of Concrete Structures
SE-100 44 Stockholm, Sweden
richard.malm@byv.kth.se



Anders Ansell
Ph.D., Associate Professor
KTH Royal Institute of
Technology
Division of Concrete Structures
SE-100 44 Stockholm, Sweden
anders.ansell@byv.kth.se

ABSTRACT

Numerical simulations and experimental results are presented for a 60 year old buttress dam, subjected to temperature variations. The dam has several cracks, that likely have originated from temperature variations. The first step of the analyses was to recreate the current crack-pattern of the dam, by simulating cyclic seasonal temperature variations. After this, detailed simulations of the temperature variation were performed to compare the numerical results with the variations in crack widths and displacements measured for one year. The finite element model shows good agreement with the observed crack-pattern and the measured variations in crack widths and displacements.

Key words: Non-linear FEM, Concrete, Buttress dam, Cracks, Temperature variation

1. INTRODUCTION

The Storfinnforsen hydropower dam is one of the largest concrete dams in Sweden, with an 800 m long concrete section and a height of 40 m. The dam consists of 100 concrete monoliths, each consisting of a front-plate facing the water and is supported by a buttress as shown in Figure 1. After a few years, some of the largest monoliths showed horizontal cracks in the lower part of the front-plates, causing leakage of water from the reservoir. Besides this, freeze-thawing damage was found on the upstream side of the front-plates. Due to this, strengthening was conducted where the cracks were grouted. An insulating wall was also installed to create a temperature-controlled area, within the monolith, between the insulating wall and the front-plate. However, some years after the installation of the insulation wall, new cracks were found on the monoliths that were believed to affect the structural safety of the dam. One diagonal crack had propagated from the inspection gangway towards the front-plate, which could potentially reduce the safety margin for an overturning failure of the monolith. An Elforsk-project was initiated to explain the cause of the cracks and evaluate the safety of the dam, [1] - [3]. Before planning a new strengthening of the dam, thorough investigations were conducted. Temperatures, displacements and variation in crack widths were measured. In combination with this, finite element analyses were performed for the condition assessment of the dam.

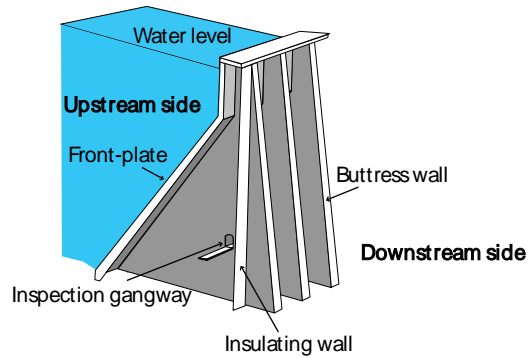


Figure 1 – Sketch of the three monoliths of the Storfinnforsen hydropower dam.

2. CRACKING DUE TO TEMPERATURE VARIATIONS

In this project the seasonal temperature variations of the dam were simulated with a non-linear finite element (FE) analysis. The purpose was to describe the development for 60 years of service life of the dam to capture the crack-pattern found in-situ. The initial design of one monolith was simulated, subjected to cyclic seasonal temperature variations, assuming $-15\text{ }^{\circ}\text{C}$ in the winter and $+25\text{ }^{\circ}\text{C}$ during the summer. After simulating a few years of the original structure, the insulation wall was introduced in the model where an updated temperature distribution was included. This was done numerically, by first simulating three years of thermal steady state by changing from summer to winter conditions respectively for the case without the insulation wall and followed by two additional years with the insulation wall. At this point, the cracking observed in-situ had been accurately captured with the finite element model, as seen in Figure 2. Further description of the analyses and the results can be found in [3] - [5]. It is shown that seasonal thermal variation initiates cracks in the same regions that were found on the Storfinnforsen dam. A stabilised crack-pattern, i.e. when no new cracks initiate or propagate, was reached after two years in the FE analyses. At this point, the front-plate and the buttress wall of the dam had extensive cracking. When these cracks were found on the real dam, an insulation wall was installed to reduce the temperature gradient over the front-plate. This was also included in the FE analysis and it is shown that this insulation wall is the cause of several new cracks. The final crack-pattern that occurs in the FE analysis after years of cycling the temperature corresponds with the pattern observed in-situ.

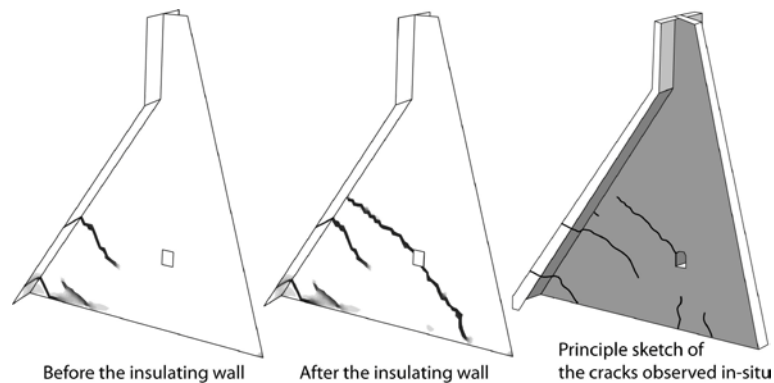


Figure 2 – Calculated and observed crack-pattern on the largest monoliths.

The previous model showed that it was possible to capture the cracking in the dam that have occurred until its current status. The next phase was to compare one year of measurements of

deflections and variation in crack width with the results obtained from the FE model. This simulation was made as a restart analysis of the previous model, i.e. the cracked dam in the centre of Figure 2, [3] - [5]. A detailed simulation with transient heat transfer analysis based on the measurements was performed, where the mean temperature for each week was used as predefined fields in the non-linear FE model.

A description of the measurement set-up and results is found in [2]. The measurements performed on the dam included temperature gauges, pendulum measurements of the crest displacement and variations in crack width obtained with LVDT-sensors. The two largest monoliths, called no 42 and 43, were monitored. There is a slight difference in geometry of these two monoliths, and the FE-model is most similar to monolith no 42. Measurements of the outside air temperatures at Storfinnforsen hydropower dam were unfortunately not complete since the thermal gauges failed to record the temperature at some periods of time, as seen in the upper graph in Figure 3. To receive complete signals, the measured temperatures were updated with temperatures for the same period at Östersund, obtained from an on-line database, www.temperatur.nu, [6].

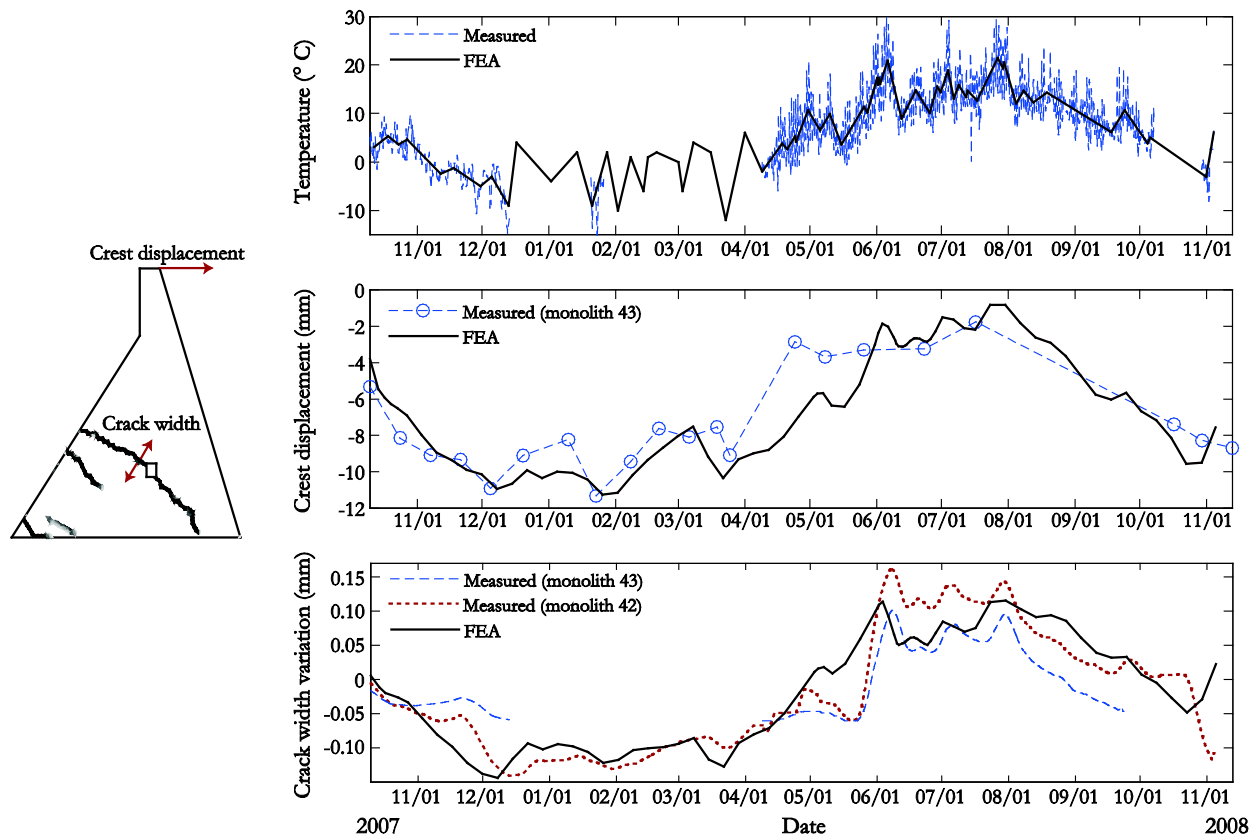


Figure 3 – Calculated and measured crest displacement and variation in crack width.

The calculated and the measured crest displacements are illustrated in the centre graph in Figure 3. The displacement when the measurements started is initially defined as the zero level in the measurements. It is unknown at exactly which position the dam crest was at this time. Therefore, the measured displacement has been added a constant value so that it has the same average value as obtained from the FE model. Thereby, the zero level is defined according to the design drawings. The measured total displacement during a year is 9.6 mm while the peak-to-peak value from the FE analysis is 10.4 mm. A positive displacement is defined in the downstream direction, i.e. when the dam is moving away from the water.

The variation in crack width is shown in the bottom graph of Figure 3. The initial value of all curves is adjusted so that their average value is equal to zero. It is only the variation in crack width that is measured and hence only the variation is compared. The measured variation in crack width, especially in monolith 42, and the calculated variation shows good agreement. During the summer, the measured crack width on monolith 42 is slightly higher and the calculated crack width variation is in closer agreement with the measured on monolith 43. The peak-to-peak variation of the measured crack width on monolith 42 is 0.34 mm while it is 0.26 mm in the simulation. Due to the incomplete measured signal of monolith 43 within this period, the minimum crack width variation that occurred in the winter was not measured. Considering the minimum value measured during the previous winter, a peak-to-peak variation of 0.24 mm for monolith 43 was obtained.

3. CONCLUSION

The results showed that the insulation wall had most probably led to increased mechanical stresses in the buttress, as a result of the contraction and expansion due to the seasonal temperature changes. The finite element model shows good agreement with the observed crack-pattern and the measured variation crack widths and displacements. There are today approximately 25 large concrete dams in Sweden and most of these are old structures. Their conditions need to be maintained, in some cases through costly upgrading and repairs. Advanced finite element analysis will be an important tool in the condition assessment of these dams and similar dams around the world.

4. ACKNOWLEDGEMENT

This project has been performed with financial support of Elforsk AB, the Swedish Power Companies R&D Association. Manouchehr Hassanzadeh (Vattenfall Power Consultant) was the project manager and Tomas Ekström (EnergoRetea AB) was responsible for the measurements of the dam.

REFERENCES

1. Björnström, J.; Ekström T., and Hassanzadeh M., “Cracked concrete dams – overview and calculation methods”, Report 06:29, Elforsk AB, Stockholm, 2006, 114 pp.
2. Ansell, A.; Björnström, J.; Ekström, T.; Hassanzadeh, M. and Unosson, M., “Cracked concrete buttress dams – Part I”, Elforsk Report 08:21, Stockholm, 2008, 97 pp.
3. Ansell, A., Ekström, T., Hassanzadeh, M. and Malm, R. “Cracked concrete buttress dams – Application of non-linear models – Part II”, Elforsk Report 10:69, Stockholm, 2010, 43 pp.
4. Ansell, A. and Malm, R., “Modelling of thermally induced cracking of a concrete buttress dam”, Nordic Concrete Research 38 (2/2008), 2008. pp 69-88.
5. Malm, R. and Ansell A. 2011. Cracking of a Concrete Buttress Dam Due to Seasonal Temperature Variation. ACI Structural Journal 108 (1), pp 13-22.
6. Malm, R., “Predicting shear type crack initiation and growth in concrete with non-linear finite element method”, Bulletin 97, Department of Civil and Architectural Engineering, KTH, Stockholm, 2009. 43 pp.

Loading Tests of Concrete Monoblock Railway Sleepers

Olli Kerokoski, Dr. Tech.
Department of Civil Engineering,
Tampere University of Technology,
P.O. Box 527, FI-33101 Tampere, Finland

Tommi Rantala, M.Sc.,
Department of Civil Engineering,
Tampere University of Technology,
P.O. Box 527, FI-33101 Tampere, Finland

Antti Nurmikolu, Dr. Tech.
Department of Civil Engineering,
Tampere University of Technology,
P.O. Box 527, FI-33101 Tampere, Finland

ABSTRACT

Prestressed concrete monoblock sleepers have served Finnish railways well for several decades. The main reason to launch a comprehensive research project was to investigate the deterioration mechanisms that primarily determine the life cycle of sleepers. This paper presents the results of the first phase of the project including static and dynamic loading tests on concrete sleepers. The loading tests complied with European standard EN 13230. Several 30 to 40 year old sleepers removed from Finnish railway lines were loaded. The behaviour of unused sleepers from two manufacturers was compared to the behaviour of old sleepers. The tests targeted both the sleeper centre and the rail seat section. All old sleepers had cracks underneath at the rail seat sections. These cracks did not affect ultimate bending moment capacity. An estimate of the structural performance and typical failure mechanisms of the sleepers was given.

Key words: Concrete sleeper, loading test, damage, crack.

1. INTRODUCTION

Currently nearly 70 per cent of the Finnish rail network is equipped with prestressed concrete monoblock sleepers. The most important functions of sleepers are to transfer rail forces to the ballast bed, to serve as a support and mount for the rail foot and fastenings and to preserve track gauge. The Finnish Transport Agency's (FTA) need to better understand the life cycle of sleepers installed in various decades launched a comprehensive research programme at the Department of Civil Engineering of Tampere University of Technology (TUT). The focus of this study was on structural behaviour during static and dynamic loading of different types of concrete sleepers with different service histories.

2. LOADING TEST ARRANGEMENTS AND TESTED SLEEPERS

Loading tests were performed both on unused and used railway sleepers according to European standard EN 13230 [2]. The used sleepers had been removed from the tracks for various reasons. The testing programme comprised static tests on the rail seat section and sleeper centre as well as dynamic tests on the rail seat section. Despite not being specified in the EN standard, dynamic tests were also performed on the sleeper centre. The test programme is presented in Table 1. Besides the requirements set in the standard, vertical sleeper deflections and concrete strains were also measured during the tests. The aim of the loading tests was to compare differences in the behaviour of unused (new) and used (old) sleepers. A loading frame (Figure 1) was constructed at Tampere University of Technology for both the static and the dynamic tests.

Table 1. Number of performed loading tests [1].

Test type	New sleeper (unused)	Used sleeper
Static, rail seat section	4	10
Static, sleeper centre	4	10
Dynamic, rail seat	2	2
Dynamic, sleeper centre	2	2



Figure 1. Loading frame. Test on rail seat section (left) and test on sleeper centre (right) [1].

Two new and unused sleeper types were tested: BP99 (date of manufacture 30.11.2009) and B97 (13.3.2009). The sleepers had 12 strands 6.5 mm in diameter.

Three old and used sleeper types were tested: B63, B75 and BV75. Types B63 and B75 have almost identical dimensions, type B75 is only 5 mm higher at the rail seat section. These types were manufactured by the post-tensioning method using $\text{Ø}9.4$ mm steel bars. Type BV75 was manufactured by the pre-tensioning method using 12 pieces of 7-wire strands 6.4 mm in diameter. Both damaged and undamaged sleepers were tested.

A loop-shaped strain gauge model developed at TUT was used to measure concrete strains during the loading tests. Four traditional strain gauges were glued on the inner surface of the loop. The gauge measures strain over a 100 mm distance. It was attached to the sleeper with two bolts. The advantage of this measurement method is that the gauge is able to continue measuring after cracking has started. Strains were measured directly below the point of loading.

Four of the vertical displacement transducers were installed precisely in the middle of the two support lines. Two of the displacement transducers were installed 105 mm from the point of the loading force.

The support arrangements for static loading tests on rail seat sections were as shown in Figure 2 where the distance L_c between the centrelines of supports was 600 mm. The supports were 100 mm wide. Resilient pads required by the standard were placed between the supports under the sleepers and the undersides of sleepers.

In dynamic loading tests on rail seat sections the location of supports was the same as in static loading tests. The sleepers were also provided with lateral and longitudinal supports that prevented lateral and longitudinal movement of sleepers during dynamic loading tests.

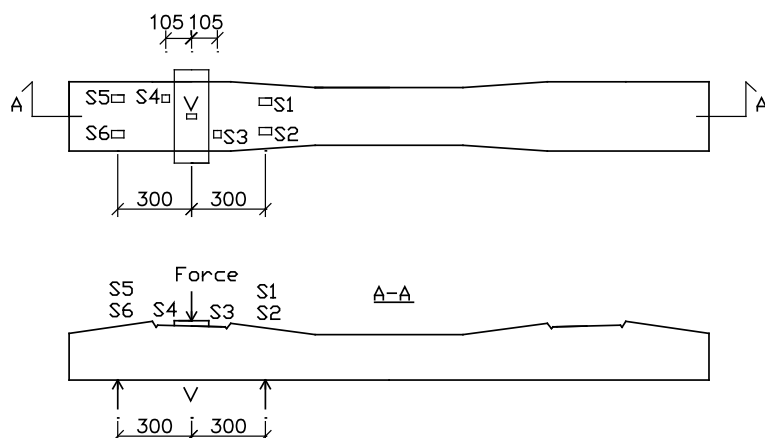


Figure 2. Locations of sleeper strain gauge (V) and vertical displacement transducers (S) for the rail seat section tests.

In loading tests on sleeper centres the sleeper was loaded upside down from the middle of the sleeper, the distance between supports L_c being 1600 mm.

European standard EN 13230-2 [2] gives guidelines for calculating reference test loads and criteria for different concrete sleeper types. The criteria are presented in the test result table. The minimum force during dynamic loading tests, which loads never go under during the cycles, was 50 kN and the first load step equalled the reference test load. Load step increments were 20 kN, and the loading cycle was repeated 5000 times for each step. The frequency of loading used in loading tests was 2 Hz.

3. RESULTS

The general condition of used sleepers was good. The sides of the sleepers had occasional 50-300 mm long longitudinal cracks, and small pieces of concrete had chipped off. Only the B63 sleepers appeared to be in poor condition visually.

Each loaded used sleeper already had a vertical crack in the rail seat section. The cracks were almost fully closed and often could only be noticed when looking at the sleepers from the side during loading. No abnormal signs of corrosion were observed in the prestressed reinforcement at the crack.

Deflections measured during tests on sleeper centres indicate that a deflection of about 1 mm is enough to produce a crack in the middle of a new sleeper.

According to the criteria of Standard EN 13230-2, a sleeper must be able to take the reference test load without cracking. In the static loading tests on rail seat sections the unused sleepers clearly met this criterion. The standard also sets a criterion for a permanent crack 0.05 mm in width. Table 2 shows that sleepers BV75, B97 and BP99 meet the criterion well. B75 sleepers only just meet the criterion, but the degraded B63 sleeper does not meet it at all. Moreover, the standard sets a criterion for the maximum load that a sleeper must be able to take. The various sleeper types clearly meet the criterion with the exception of a single B63. The bending moments corresponding to the formation of the first crack and failure were added to the table.

The failure mode of loaded rail seat sections was most often bending failure or shear-bending failure where the prestressed reinforcement finally yielded to the tensile loads and broke.

Table 2. Results of static loading tests on rail seat sections [1].

Tested sleepers	First crack		Crack width $\geq 0,05$ mm when unloaded		Failure	
	Force [kN] (Criterion > 128 kN)	Moment [kNm]	Force [kN] (Criterion > 230 kN)	Force [kN] (Criterion > 320 kN)	Moment [kNm]	
BV75 (test 3)	-	-	450	530	80	
BV75 (test 6)	-	-	430	548	82	
BV75 (test 7)	-	-	420	484	73	
BV75 (test 8)	-	-	400	465	70	
BV75 (test 9)	-	-	410	477	72	
BV75 (test 10)	-	-	370	465	70	
BV75 (test 11)	-	-	460	503	75	
B97 (test 2)	170	26	310	565	85	
B97 (test 12)	180	27	370	511	77	
BP99 (test 4)	180	27	340	509	76	
BP99 (test 13)	190	29	400	480	72	
B63 (test 1)	-	-	200	300	45	
B75 (test 14)	-	-	250	387	58	
B75 (test 5)	-	-	250	397	60	

In the static loading tests on sleeper centres the unused sleepers of type B97 and BP99 clearly met the criteria set for the first crack. Based on the tests on sleeper centres, sleepers BV75 are at least as durable as B97 and BP99 sleepers presently being procured for the Finnish rail network. Sleepers B63 and B75 also passed the loading tests on sleeper centres surprisingly well considering their observed condition.

The results of dynamic loading tests on rail seat sections were lower than those of static tests. Results of dynamic loading tests on sleeper centres did not differ significantly from those of static loading tests on the centres. Despite the small number of tests, it can be estimated that the impact of dynamic loads on sleeper centres is not as significant as on rail seat sections.

4. CONCLUSIONS

Loading tests revealed that there was a crack on the underside of every used sleeper at the rail seat. The cracks were almost fully closed and thus difficult to notice before loading. Based on the results of the loading tests, it can be estimated that occasional cracks are largely insignificant when a sleeper is subjected to static loading. Sleepers B97 and BP99 met the criteria of standard EN 13230-2 well, and sleepers BV75 very well considering their age, in rail seat section loading tests. Sleepers B63 and B75 fared clearly worse than other sleeper types, but based on visual inspection their load bearing capacity was at least satisfactory considering their condition.

REFERENCES

1. Rantala, T. Betoniratapölkyn vaurioitumismekanismit (Damage mechanisms of a concrete sleeper). Master of Science Thesis. Tampere University of Technology. 2011.
2. EN 13230 Railway applications. Track. Concrete sleepers and bearers. Parts 1 & 2. European committee for standardization. 2009.

Shear Strength of High Strength- High Performance Reinforced Concrete Beams



Shuaib H. Ahmad
Ph.D.
NED University of
Engineering &
Technology,
Karachi-Pakistan
sahmad@neduet.edu.pk



S.F.A. Rafeeqi
Ph.D.
NED University of
Engineering &
Technology,
Karachi-Pakistan
pvc2@neduet.edu.pk



Shamsun Fareed
dM.Engg.
NED University of
Engineering
& Technology,
Karachi-Pakistan
sfareed@neduet.edu.pk

ABSTRACT

The shear strength of reinforced concrete members is a function of shear capacity of concrete (V_c), which in turn depends on influencing parameters including concrete compressive strength (f_c), ratio of tension reinforcement (ρ), shear span to depth ratio (\bar{a}), size effect or depth factor (ξ), size of the aggregate in relation to the minimum size of the member (aggregate interlock aspects).

In this paper a relational database using ACCESS software is developed and is populated with experimental results of 2145 shear critical reinforced concrete beams without web reinforcement using both normal as well as high strength –high performance concrete. An evaluation was conducted to assess the predictive accuracy of shear design equations of ACI Code and Euro Code EC2. The results indicate that both the Codes do not adequately address the size effect or the depth factor effect on the shear capacity, with Euro code EC2 exhibiting reduced factor of safety and ACI Code becoming unconservative for large or deeper reinforced concrete members.

Key words: database, shear strength, concrete compressive strength, shear span to depth ratio.

1 INTRODUCTION

Many different definitions have been proposed for High Performance Concrete (HPC) including the Strategic Highway Research Program (SHRP), the American Concrete Institute (ACI), and the Federal Highway Administration (FHWA). For majority of structural design for buildings, attribute of compressive strength and the associated stiffness (modulus of elasticity) of concrete are the primary design parameters used by the designers and relatively less attention is given to the durability associated attributes of concrete. In this paper, HPC is considered to be high strength concrete as this attribute is the principal driver for other enhanced attributes of concrete

in structural applications and also this attribute is influenced by water-cement ratio which in turns influences durability and workability of concrete.

Euro Code EC2 and ACI Code [1,2] of practice provide empirical equations to predict the shear capacity of reinforced concrete beams. These empirical equations are derived from set of reinforced concrete beams without web reinforcement and are limited by the range of variables and the breadth and depth of variables considered in their respective experimental programs.

In a this study relational ACCESS shear database is developed and populated with test data of shear critical reinforced concrete beams without web reinforcement made with normal as well as high strength concrete. This database is used to assess the predictive accuracy of design equations of the Euro Code EC2 and ACI Code [1,2]

2. COMPARISON WITH DESIGN EQUATIONS

2.1 Euro Code EC2

The design equation in Euro Code EC2 (Eq.6.2a) [1], Eq. 1 for predicting the shear capacity of reinforced concrete beams without web reinforcement is:

$$V = \left(\frac{0.18}{\gamma_c} K (100 \rho_l f_{ck})^{1/3} + 0.15 \sigma_{cp} \right) b d \geq \left(0.035 k^{3/2} f_{ck}^{1/2} \right) b d \quad (1)$$

Where γ_c = material constant, $k = 1 + \sqrt{\frac{200}{d}} \leq 2$, ρ_l = longitudinal steel ratio and σ_{cp} = Axial stress in case of pre-stressed members.

Figure 1 shows the effect of effective depth (d) on the Margin of Safety $\left(\frac{V_{exp}}{V_{pre}} \right)_{EC2}$.

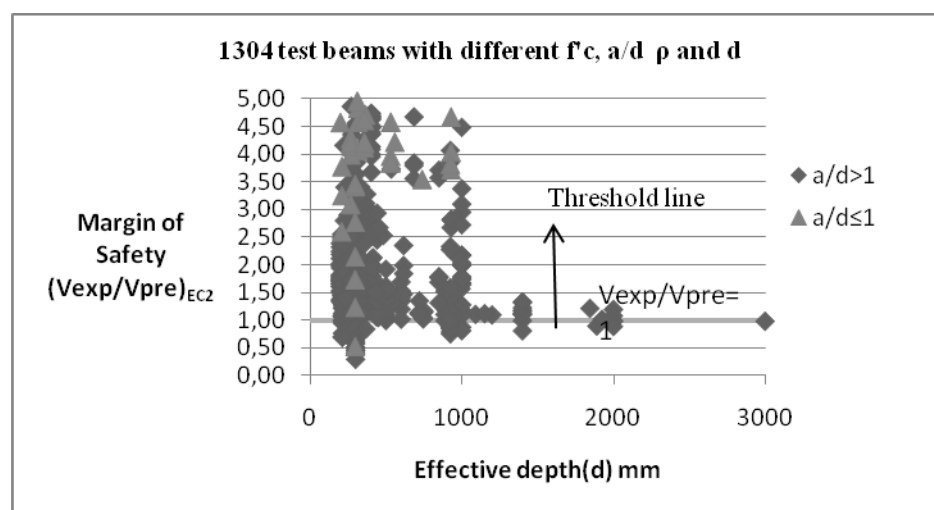


Figure 1 Influence of d on $\left(\frac{V_{exp}}{V_{pre}} \right)_{EC2}$.

It can also be seen from Figure 1, that irrespective of ratio of tension reinforcement ρ , shear span to depth ratio $\frac{a}{d}$ and concrete compressive strength f_c , Euro Code (Eq.6.2.a) is conservative (with reduced margin of safety) for shear capacity of reinforced concrete beams having effective depth (d) > 1200 mm without web reinforcement and hence safe (with reduced margin of safety) for reinforced concrete beams with $d > 1200$ mm.

2.2 ACI Code equation

The expression used in ACI Code [2] (ACI Eq-11-6) Eq-2 for predicting the shear strength of reinforced concrete beams with shear span to depth ($\frac{a}{d} > 1.0$) is:

$$V = (0.16\sqrt{f_c} + 17.2\rho Vd/M) bd \quad (2)$$

and expression used in ACI Code (ACI Eq-11-29) Eq-3 for predicting the shear strength of reinforced concrete beams with shear span to depth ($\frac{a}{d} \leq 1.0$) is:

$$V = (3.5 - 2.5 a/d)(0.16\sqrt{f_c} + 17.2\rho Vd/M) bd \quad (3)$$

In order to evaluate the predictive accuracy of ACI Code (Eq-11-6) and (Eq-11-29), respective data from the ACCESS shear database was selected in which 1994 reinforced concrete beams were with shear span to depth ratio ($\frac{a}{d} > 1.0$) and 151 reinforced concrete beams were with shear span to depth ratio ($\frac{a}{d} \leq 1.0$).

The issue of size effect or the depth factor on the shear strength of reinforced concrete members have been addressed by number of researchers [3-11]. Figure 2 shows the effect of effective

depth (d) on the Margin of Safety $\left(\frac{V_{exp}}{V_{pre}}\right)_{ACI}$ and it can be seen that the margin of safety of ACI Code (Eq-11-6) decreases with increase in the effective depth of beam which indicates that the ACI Code (Eq-11-6) does not accurately reflect the depth effect or the size effect. It can also be seen from Figure 2, that irrespective of ratio of tension reinforcement ρ , shear span to depth ratio $\frac{a}{d}$ and concrete compressive strength f_c , the ACI Code (Eq. 11-6) overestimates the shear capacity of reinforced concrete beams having effective depth (d) > 1200 mm without web reinforcement and hence un conservative for reinforced concrete beams with $d > 1200$ mm.

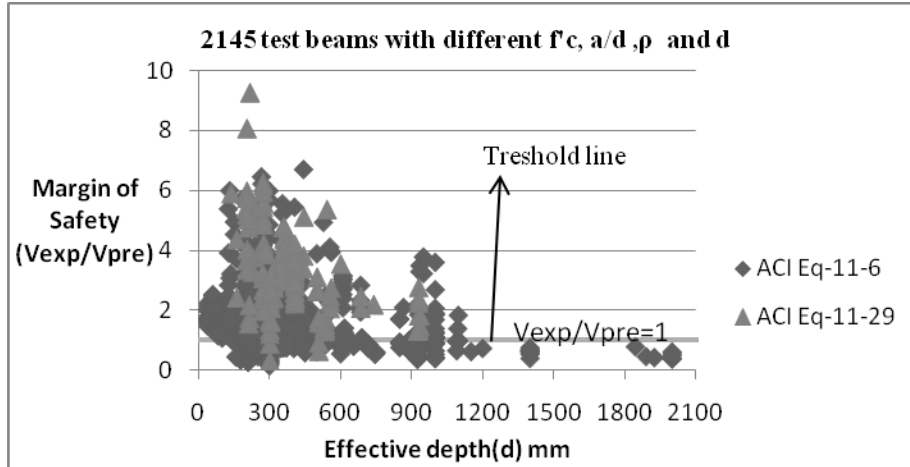


Figure 2 - Influence of d on $\left(\frac{V_{exp}}{V_{pre}}\right)_{ACI}$.

Table 1 shows the summary of results for the comparison of the Margin of Safety's $\left(\frac{V_{exp}}{V_{pre}}\right)_{avg}$ for the prediction of the shear capacity as per the equations of the Euro Code EC2 and the ACI Code. The number of beams varies for each case, because of the relative constraints or the limits in the respective empirical equations of the Codes.

Table 1- Summary of results for the Margin of Safety for the predictions of shear capacity as per the Euro Code and ACI Code Equations.

Concrete Type	Shear span to depth ratio (a/d)	No. of beams in the Shear Database, used for the comparisons		Avg, Margin of Safety $(V_{exp}/V_{pre})_{Avg}$	
		Euro Code EC2	ACI Code	Euro Code EC2	ACI Code
NSC and HSC	All a/d's	1036	2145	2.27	1.69
Normal strength concrete (NSC)	a/d > 1	623	1403	1.89	1.67
	a/d ≤ 1	87	117	6.94	3.22
High strength concrete (HSC)	a/d > 1	305	591	1.51	1.36
	a/d ≤ 1	21	34	5.45	3.12

4. SUMMARY AND CONCLUSIONS

On the basis of the results of the evaluation study of Euro Code EC2 and ACI code equations for the shear capacity, the following conclusions can be drawn;

1. For reinforced concrete beams without web reinforcement, having effective depth (d) > 1200 mm, the shear capacity as predicted by Euro Code (Eq. 6.2.a) is conservative with reduced margin of safety as compared to the predictions of ACI Code (Eq-11-6) which are un-conservative. Thus the depth factor is not adequately addressed in the ACI Code.
2. For normal strength reinforced concrete beams having shear span to depth ratio $\frac{a}{d} > 1.0$, the Margin of Safety for Euro Code EC2 (Eq. 6.2.a) is 1.89 and the Margin of safety for

ACI Code (Eq-11-6) is 1.67, hence both Euro Code EC2 (Eq.6.2.a) is little more conservative.

For normal strength reinforced concrete beams having shear span to depth ratio $\frac{a}{d} \leq 1.0$, the Margin of Safety for Euro Code EC2 (Eq. 6.2.a) is 6.94 as compared to 3.22 for ACI Code (Eq-11-6), hence Euro Code EC2 (Eq. 6.2.a) is significantly more conservative.

3. For high strength-high performance reinforced concrete beams having shear span to depth ratio $\frac{a}{d} > 1.0$, the Margin of Safety for Euro Code EC2 (Eq. 6.2.a) is 1.51 as compared to about 1.36 for ACI Code (Eq-11-6), hence Euro Code EC2 (Eq. 6.2.a) is more conservative.

For high strength-high performance reinforced concrete beams having shear span to depth ratio $\frac{a}{d} \leq 1.0$, the Margin of Safety for Euro Code EC2 (Eq. 6.2.a) is 5.45 as compared to about 3.12 for ACI Code (Eq-11-6), hence Euro Code EC2 (Eq. 6.2.a) is more conservative.

REFERENCES

1. European Committee for Standardization, Eurocode 2: Design of Concrete Structures - Part 1-1: General rules and rules for Buildings, Revised Final Draft, April 2002, 226 pp.
2. ACI Committee 318, "Building Code Requirement for Reinforced Concrete (ACI 318-08)," American Concrete Institute, Detroit, 2008, 447 pp.
3. Zsutty, Theodore C., "Beam Shear Strength Prediction by Analysis of Existing Data," ACI Journal Proceedings V. 65, No.11, Nov. 1968, pp. 763-773.
4. Evan C. Bentz, Empirical Modeling of Reinforced Concrete Shear Strength Size Effect for Members without Stirrups, ACI Structural Journal, V. 102, No. 2, March-April 2005, pp.232-241.
5. G. N. J Kani, How Safe Are Our Large Reinforced Concrete Beams? ACI Journal, March 1967 pp.128-141
6. K.N. Smith, and A.S. Vantsiotis, Deep Beam Test Results Compared with Present Building Code Models, ACI Journal, Jul-Aug 1982, pp.280-287.
7. Michael P. Collins and Daniel Kuchma, How Safe Are Our Large, Lightly Reinforced Concrete Beams, Slabs and Footing? ACI Structural Journal, V.96, No.4, Jul-Aug 1999 pp.482-490.
8. Prodromos D. Zararis & George Ch. Papadakis, Diagonal Shear Failure and Size Effect in RC Beams without Web Reinforcement, Journal of Structural Engineering, July 2001, pp.733-742.
9. Shioya, T.; Iguro, M.; Nojiri, Y.; Akiayma, H.; and Okada, T., 1989, "Shear Strength of Large Reinforced Concrete Beams, Fracture Mechanics: Application to Concrete," *Fracture Mechanics: Application to Concrete*, SP-118, V. C.
10. Zdenek P. Bazant & Hsu- Huei Sun, Size Effect in Diagonal Shear Failure: Influence of Aggregate Size and Stirrups, ACI Materials Journal, Jul- Aug 1987, pp.259-272.
11. Zdenek P. Bazant & Jin- Keun Kim, Size Effect in Shear Failure of Longitudinally Reinforced Beams, ACI Journal, Sep- Oct 1984, pp.456-468.

Session A8 – MODELLING AND TESTING

Chloride Ingress into Concrete under Water Pressure



Mia Schou Lund
B.Sc, M.Sc. student
DTU Civil Engineering
Brovej, Building 118
DK - 2800 Kgs. Lyngby
s071963@student.dtu.dk



Bent Grell
M.Sc, Chief Consultant
Bridge Maintenance & Materials Technology
Ramboll Denmark A/S
Hannemanns Alle 53
DK - 2300 København S
bng@ramboll.dk



Lotte Braad Sander
B.Sc, M.Sc. student
DTU Civil Engineering
Brovej, Building 118
DK - 2800 Kgs. Lyngby
s071972@student.dtu.dk



Kurt Kielsgaard Hansen
Associated professor, Ph.D.
DTU Civil Engineering
Brovej, Building 118
DK - 2800 Kgs. Lyngby
kkh@dtu.dk

ABSTRACT

The chloride ingress into concrete under water pressures of 100 kPa and 800 kPa have been investigated by experiments. The specimens were exposed to a 10% NaCl solution and water mixture. For the concrete having $w/c = 0.35$ the experimental results show the chloride diffusion coefficient at 800 kPa (~ 8 atm.) is 12 times greater than at 100 kPa (~ 1 atm.). For $w/c = 0.45$ and $w/c = 0.55$ the chloride diffusion coefficients are 7 and 3 times greater. This means that a change in pressure highly influences the chloride ingress into the concrete and thereby the life length models for concrete structures.

Key words: Concrete, w/c -ratios, water pressure, chloride diffusion coefficient

1. INTRODUCTION

It is important to be aware of the chloride concentration inside concrete structures. If the chloride concentration at the reinforcement reaches a critical level it will start to corrode. This will reduce or influence the durability of the concrete structure.

Large constructions such as tunnel elements and foundations for bridges can be placed on large sea water depths where the water pressure is fairly different from the pressure in the splash zone. When the life length for such a concrete structure on a large sea water depth is estimated using the normally used models, the concrete test specimens is typically exposed to sea water at atmospheric pressure, i.e. 100 kPa, which corresponds to the pressure in the splash zone. Therefore chloride ingress into concrete under water pressures of 100 kPa and 800 kPa is investigated to see if there is a significant difference in the obtained chloride diffusion coefficient [1].

2. METHODS

2.1. Types of concrete

The chloride ingress experiments were conducted on concretes with three different w/c-ratios – 0.35, 0.45 and 0.55. All concretes were cast without additives (pure Portland cement (CEM I)) to avoid any influence of these. However, a superplasticizer was used to cast concrete with w/c = 0.35 to improve the workability. By choosing the above mentioned w/c-ratios, the experiments were conducted on concretes with almost the same maturity (~30 days). The concrete with w/c = 0.35 is self desiccating whereas the concretes with w/c = 0.45 and 0.55, respectively, contain excess water. Concrete with w/c = 0.55 has such a high capillary porosity that the chlorides are expected easily to penetrate into this concrete. For comparison the experiments were also conducted on the actual concrete mix from the Great Belt Tunnel in Denmark. This concrete has a w/c-ratio of approximately 0.35 and contains puzzolans (fly ash and microsilica).

2.2 Experimental procedure

The experiments were conducted at a pressure of 100 kPa (~1 atm.) and 800 kPa (~8 atm.). A pressure of 100 kPa corresponds to the pressure in the splash zone. A pressure of 800 kPa corresponds to the water pressure that concrete structures on large depths (80 meters = theoretical depth of the tunnel under Great Belt) are exposed to.

All of the experiments have been made on cylindrical concrete specimens with a height of 8 cm and a diameter of 10 cm. The curved sides of the specimens were painted with epoxy resin so that the chloride ingress could only take place through the top or the bottom of the cylinders. Before exposure of salt water all specimens were dried at 40 °C in 5 days. The specimens were exposed to a 10% NaCl¹ solution and were submerged into the salt solution through the experiments. At 100 kPa the specimens were exposed to salt water for 23 days. At 800 kPa the time for exposure depended on the w/c-ratio. Specimens at w/c = 0.35 were exposed for 1 day and specimens at w/c = 0.45 and w/c = 0.55 for 5 days. Figure 1 shows the water pressure equipment used for the experiments at 800 kPa.



Figure 1 – The water pressure equipment at Rambøll Danmark A/S.

¹ 10 % NaCl solution is used in other accelerated chloride diffusion test such as NT Build 492 [2]

After exposure of salt water the amount of chlorides in the concrete were measured by means of titration on powder samples.

3. RESULTS AND DISCUSSION

The measured chloride content through the specimens made it possible to draw chloride profiles of the chloride variation through each specimen. Hereby the chloride diffusion coefficient was estimated by using the Error Function solution to Fick's 2. Law of Diffusion. Figure 2 shows an example of the chloride profile for concrete with $w/c = 0.35$ used to estimate the chloride diffusion coefficient.

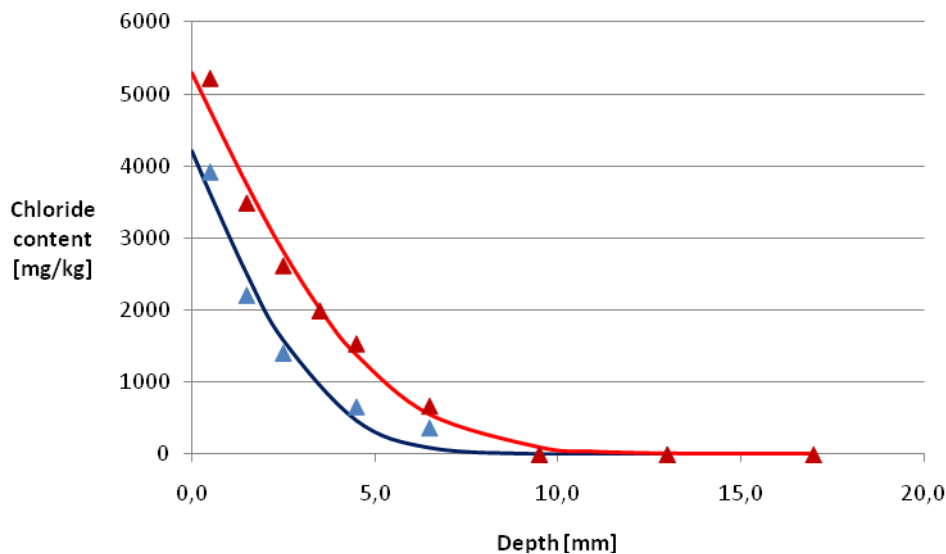


Figure 2 – Chloride profile of concrete with $w/c = 0.35$ at 100 kPa (red) and 800 kPa (blue). Measurement results are marked.

From Figure 2 it is seen that the Error Function solution to Fick's 2. Law of Diffusion fits the experimental data fairly good and therefore the chloride diffusion coefficient can be estimated by using the Error Function solution.

Table 1 summarizes the chloride diffusion coefficients for the different concretes.

Table 1 – Chloride diffusion coefficients for concretes with different w/c -ratios at different pressures. * = Values are subject to some uncertainty, see text.

	Pressure [kPa]	Time [days]	Chloride diffusion coefficient $D \cdot 10^{12}$ [m ² /s]
Great Belt Concrete	800	1	28
w/c = 0,35	100	23	4,0
w/c = 0,35	800	1	46
w/c = 0,45	100	23	7,3
w/c = 0,45	800	5	50*
w/c = 0,55	100	23	12
w/c = 0,55	800	5	38*

In Table 1 some values are marked with a ‘*’. These values are subject to some uncertainty. For the concretes with $w/c = 0.45/0.55$ chlorides were measured all the way through the specimens at 800 kPa. This means that the chloride ingress from the two absorption surfaces has affected each other. The conditions for using the Error Function solution then haven’t been met since the solution is build on the assumption that the concrete can be understood as a half infinite medium. Therefore it has been more difficult to fit the Error Function solution to the experimental data for the concretes with $w/c = 0.45/0.55$.

The chloride diffusion coefficient describes how open a concrete is to chloride ingress. A low chloride diffusion coefficient corresponds to a low diffusion of chlorides through the concrete and reverse. From Table 1 it is seen that the chloride diffusion coefficient in general increases with an increase in w/c -ratio. This indicates that an increase in w/c -ratio causes a reduction in the resistance to chloride diffusion.

The experiment at 800 kPa was also conducted for concrete used at The Great Belt Tunnel in Denmark. As this concrete contains puzzolans the chloride diffusion coefficient is about half the value as for the concrete with the same w/c without puzzolans. However it is important to note that the concrete specimens from The Great Belt Tunnel have a maturity of approximately 15 years which of course influence the pore structure and the chloride ingress in the concrete.

If the chloride diffusion coefficients at 100 kPa and 800 kPa are compared it is seen that for concrete with $w/c = 0.35$ the chloride diffusion coefficient at 800 kPa is 12 times greater as at 100 kPa. For the concretes with $w/c = 0.45$ and $w/c = 0.55$ the chloride diffusion coefficient is increased 7 and 3 times, respectively. That the increase isn’t as pronounced as for the concrete with $w/c = 0.35$ can be explained by the fact that the conditions for the Error Function solution haven’t been met.

Despite the fact that there have been some uncertainties on the results, there is no doubt of the tendency that the results show. An increase in water pressure does clearly affect the chloride diffusion in concrete for both low and high w/c -ratios.

4. CONCLUSION

The chloride diffusion coefficient is a transport parameter, which is used when estimating the life time of concrete structures. The coefficient is according to our results increased with a factor up to 12 compared at water pressures of 800 kPa and 100 kPa. This means that the water pressure has a great influence on the chloride diffusion and thereby on the life length models which are to be used for concrete structures.

REFERENCES

1. Sander, L.B. & Lund, M., “Water and Chloride Ingress in Concrete under Pressure”, Department of Civil Engineering, Technical University of Denmark, 2010 (In Danish).
2. Nordtest method, NT Build 492, “Concrete, mortar and cement-based repair materials: chloride migration coefficient from non-steady-state migration experiments”, 1999.

Updated Temperature-Stress-Testing-Machine (TSTM): Introductory test results and determination of material properties development



Terje Kanstad
Professor
COIN, Department of
Structural Engineering,
NTNU
NO-7465 Trondheim
terje.kanstad@ntnu.no



Gunrid Kjellmark
M.Sc.
COIN, SINTEF
Building and Infrastructure
NO-7465
gunrid.kjellmark@sintef.no



Anja B. E. Klausen
Ph.D-student
COIN, SINTEF
Building and Infrastructure
NO-7465 Trondheim
anja.klausen@sintef.no



Øyvind Bjøntegård
Ph.D
COIN, Norwegian Public Roads
Administration
NO-0033 Oslo
oyvind.bjontegaard@vegvesen.no

ABSTRACT

To be able to follow up the topic property development and crack risk assessment in the hydration period, which is an important topic for large infrastructure projects, the experimental equipment at the concrete laboratory at NTNU and SINTEF in Trondheim is expanded and modernized. The updated version of the TSTM-machine may simulate the behaviour of real concrete structures, because pre-calculated temperature- and stress histories can be prescribed to the steering system of the TSTM. The first results are presented to show how the system works, and E-modulus development curves are determined directly from the test results. Furthermore, future plans and test possibilities are shortly described.

Key words: Concrete, Early Age, Stresses, Cracking, Temperature, Experiments

1. INTRODUCTION AND OBJECTIVE

To be able to follow up development of new cement and concrete types within the research topic “Crack assessment of early age concrete in large infrastructure projects”, the experimental equipment in the Concrete Laboratory at NTNU and SINTEF has been expanded and modernized, see also [1]. Early age concrete cracking is caused by restrained volume changes (i.e. autogenous shrinkage and thermal dilation) in hardening concrete structures, and may be a serious threat to aesthetics, tightness and durability. For decades it has been well known that use of low heat cements, including slag and fly-ash, reduce the cracking risk at early ages. However, today the situation is different because the cements seem to be continuously changing and because materials as fly-ash are being frequently used in a much broader range of cement types mainly due to environmental aspects. To prevent unwanted cracking in hardening concrete structures and to be able to predict the property development it is therefore a need for updating the material data bases and the general knowledge continuously as materials are changing.

The upgrading of the test equipment, and belonging research activities, is a part of COIN’s Focus area 3.1: Crackfree concrete structures. The main objectives are to map the most relevant properties for the new materials, to contribute to better understanding of the involved

mechanisms and the role of the different material properties, more efficient materials testing, and more reliable and user-friendly calculation methods.

The role of the different major effects, volume changes, structural system and stiffness properties, involved in the stress development is illustrated in Figure 1 below. In the modernized TSTM, the new features are that arbitrary degree of restraint may be prescribed, and that both the E-modulus development and the creep properties may be directly deduced from the test results. Before doing tests in the TSTM the temperature history and the degree of restraint may be calculated for the critical point in the structure, and afterwards the TSTM cross section can be given the same stress and temperature history as this critical point in the structure. The term degree of restraint is thoroughly considered in [4].

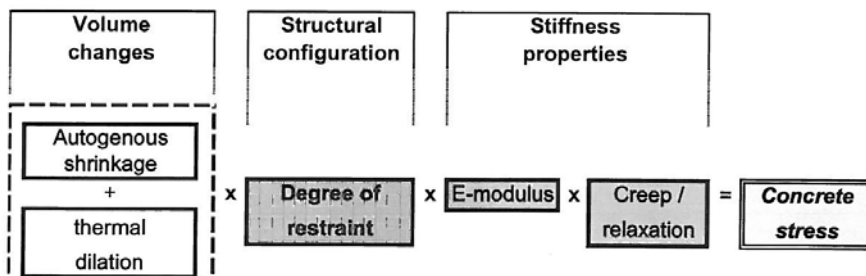


Figure 1: Stress development during the hardening phase – schematic program[2]

2. EXPERIMENTAL EQUIPMENT AND TEST PROCEDURES

The experimental set-up, illustrated in Figure 2, consists of a concrete dogbone specimen which is cast directly in the steel formwork of the testing machine. The rig is located in a conditioned room which holds 20 °C and 50 % relative humidity.

The total length of the specimen is 1200 mm while the length that is controlled by the steering system is 700 mm. On the formwork surface 6 mm copper pipes are placed and connected in series to a cooling/heating simulator (Julabo FP33). This system provides that a fluid circulates through the rig, and the temperature can be regulated from a computer or by manual programming. Thus, realistic or isothermal temperature histories can be prescribed and applied to the concrete specimen. Afterwards, the concrete surfaces are covered with plastic film, an aluminium foil before the whole system is isolated.

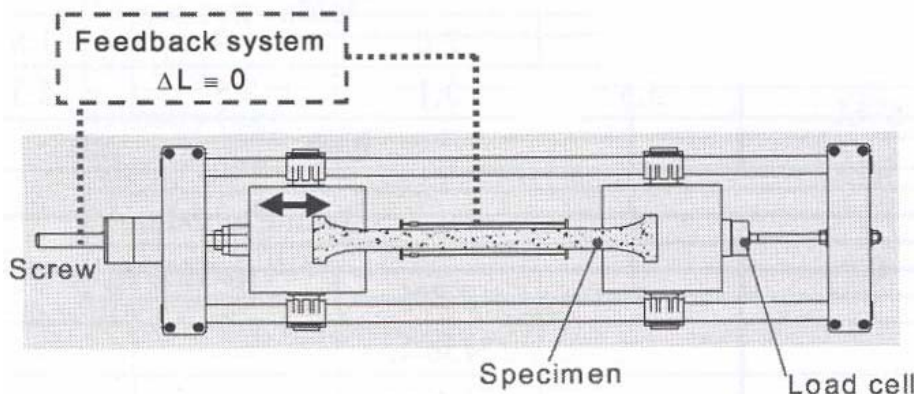


Figure 2: Temperature-stress-testing-machine (TSTM). Principle sketch.

3. TEST RESULTS, PROPERTY DEVELOPMENT AND FUTURE PLANS

Figure 3a presents stress and strain development for two test specimens where the temperature varied between 19 and 25°C, i.e. a realistic temperature history for a slender structure, for example a slab cast in indoor climate. Both tests were carried out under 100% restrained conditions. In the tests the strain varied within specified limits, while the stress is constant in short time intervals. When the sum of time dependent strains, i.e. thermal dilation, autogenous shrinkage and creep together, reach the strain limit, the rig moves the specimen back in accordance with the specified degree of restraint. If 100% restraint is specified as in the present tests, the specimen is pulled back to zero strain, and if 50% restraint is specified, 50% of the strain is pulled back etc. The result is stepwise varying stress development, and gradual and stepwise varying strain curves as shown in the figure.

For each stress step the E-modulus may be determined as $E = \Delta\sigma / \Delta\varepsilon$, and therefore determined automatically through the entire interesting time period. The results from the two first tests are shown in Figure 3b). The lowest E-modulus from these tests is about 4000 MPa determined about 7,5 hours after concrete mixing, which is much earlier than what is possible by conventional E-modulus tests. By extrapolating the curve down to zero stiffness the starting point of stress calculations, t_0 discussed in [1,3], may be determined in a reliable way.

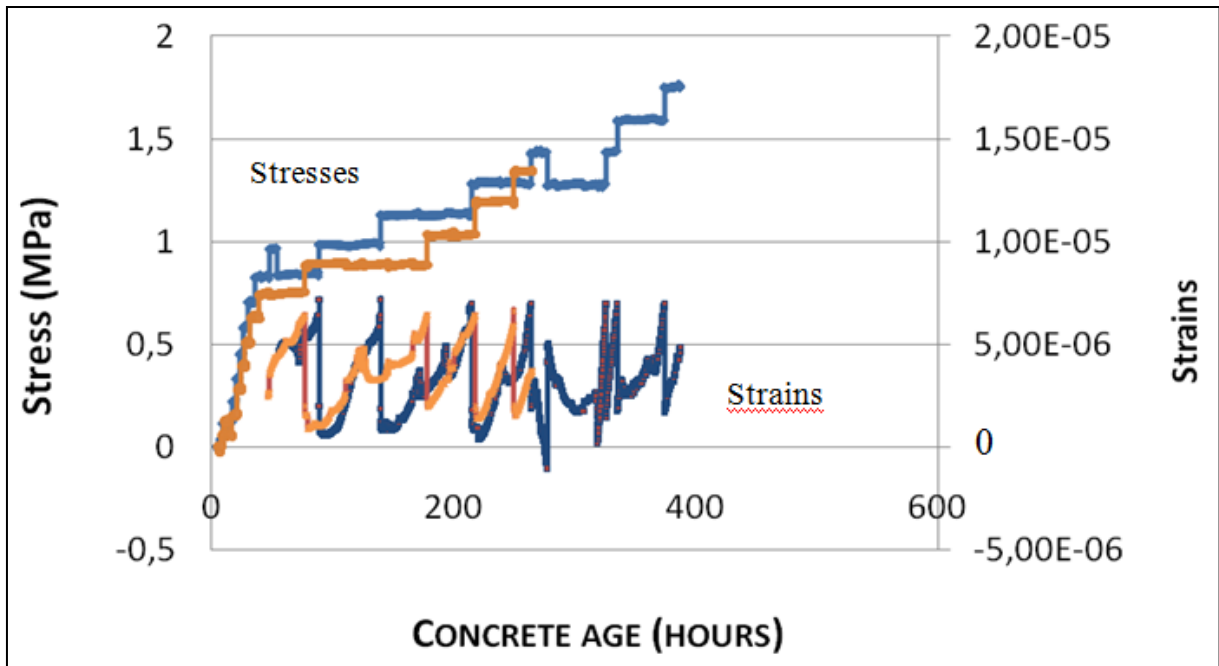
Furthermore may the creep properties be determined from the time periods where the stresses are constant. In these periods, the total strain consists of thermal dilation, autogenous deformation and creep, and since the two first terms are stress independent components which can be measured by companion dilation rig specimens, the creep strains can be determined by subtracting the two first components from the total strain.

ACKNOWLEDGEMENTS

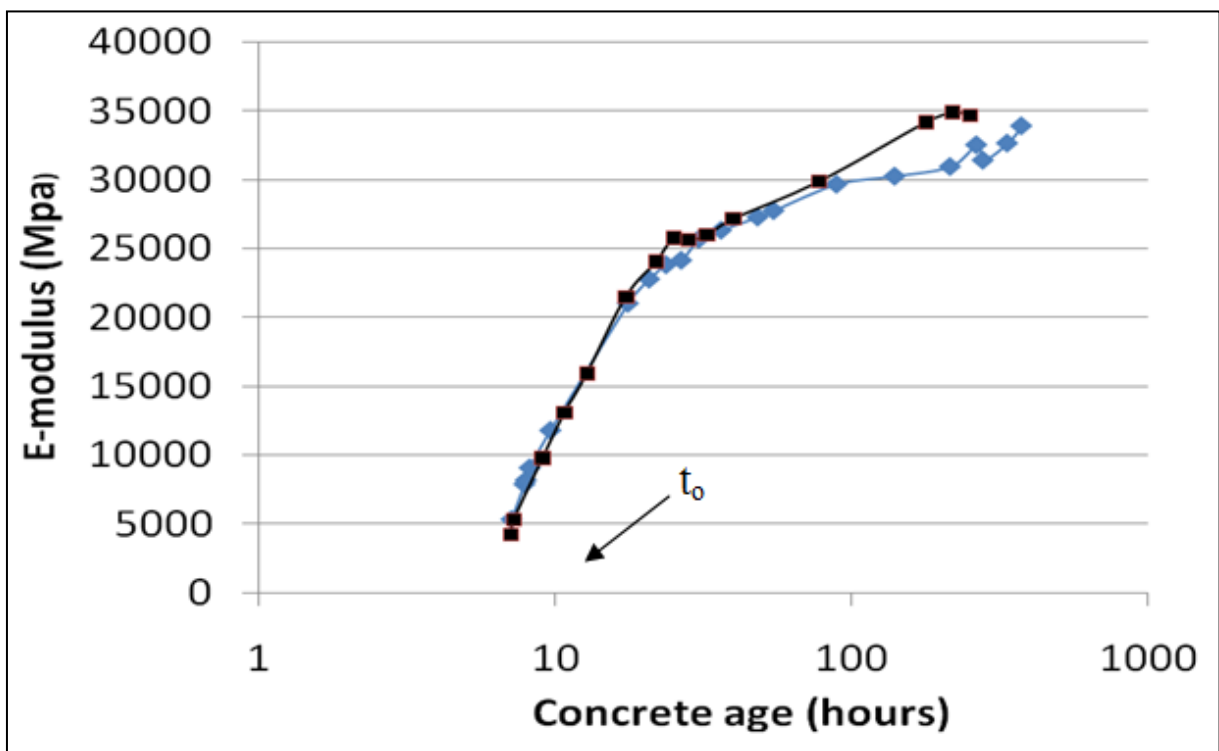
The paper is based on the work performed in COIN - Concrete Innovation Centre (www.coinweb.no) - which is a Centre for Research based Innovation, initiated by the Research Council of Norway (RCN) in 2006. The Centre is directed by SINTEF, with NTNU as a research partners and with the present industrial partners: Aker Solutions, Norcem, Norwegian Public Roads Administration, Rescon Mapei, Skanska, Spenncon, Unicon, Veidekke and Weber Saint Gobain.

REFERENCES

1. Kjellmark, G. et al NCR-paper
2. Bjøntegård, Ø. (2009) *Volume changes and cracking tendency in concrete*. Technology report no. 2565, Norwegian Public Roads Administration, Road Directorate. 2009-09-07, ISSN 1504-5005
3. Bjøntegård, Ø., Kanstad, T., Sellevold, E.J. (2000), t_0 – *The startpoint of stress calculations*, in IPACS TASK 2 + 3 Memo meeting in Delft 20-21 March
4. Kanstad, T. et al (2005) Verification of three different stress calculation methods for early age concrete. Proceedings of the Nordic mini seminar: Crack risk assessment of hardening concrete structures. ISBN 82



a)



b)

Figure 3: (a) Recorded stress- and strain development, (b) E-modulus development.

Development of New Method for Determination of Concrete Setting Time



Lasse Frølich Kristensen
M.Sc., Civil Engineer
Aalborg Portland A/S
Rørdalsvej 44, DK-9100 Aalborg
E-mail: lasse.f.kristensen@aalborgportland.com

ABSTRACT

Correlation between heat development and penetration resistance test for determination of concrete setting time have been studied. Opposite to penetration resistance tests the heat development measurement is performed semi-automatic and is independent of the skills of the operator. Furthermore the heat development provides information on the course of hydration. A correlation factor of 0.99 between the two methods has been found and the study demonstrates that slump concrete penetration tests correlates with the same factor to heat development compared to self compacting concrete.

Key words: Setting time, heat development, penetration resistance, self compacting concrete

1. INTRODUCTION

Concrete setting time is theoretically very difficult to predict. This is caused by the fact that setting time is governed by a complex interaction of several parameters such as w/c-ratio, cement type, water reducer type, other admixtures, aggregate shape ect. Therefore experimental work is usually required in order to determinate concrete setting time.

The standard method for determination of concrete setting time is penetration resistance. In Denmark these tests are performed according to [1]. Outside Europe [2] is the most common used standard. The results from penetration resistance tests are well documented and considered in good agreement with reality – despite the fact that there might be some dependency on the skills of the operator. The procedure of a penetration test is as follows: Concrete is mixed and sieved on an 8 mm mesh. The mortar is filled into at least two containers of approximately 2.5 litres of volume. From this point the specimen is monitored by manually pressing a piston into the sample at different times and calculating the resistance to penetration. Setting time is given by 3.5 MPa penetration resistance.

Concrete setting time is an important parameter to ready mixed concrete and precast concrete. Ready mixed concrete plants need information of setting in order to ensure that no setting occur during transport and casting (regardless of temperature and humidity). Also knowledge of when to start finishing the concrete surface is important especially when casting floors and other horizontal structures. In the precast industri setting time is used to plan the day of production – this determines when the workers can finish the surface and get off from work.

In Denmark there has been an increasing use of self compacting concrete (SCC) with low to moderate strength – typically 28 days compressive strengths in the area of 25-30 MPa.

SCC contains high dosages of admixtures relative to the content of cement, which have a retarding effect, and does therefore have a significantly longer setting time compared to regular

slump concrete. The admixtures are typically lignosulphonate based water reducers and polycarboxylic ether based superplasticizers.

Measurement of setting time using the penetration method is done manually and the concrete is monitored from mixing till setting. Therefore the test of SCC becomes exceptionally demanding regarding time consumption and costs. For research and development purposes it is also a restraint that it is difficult to perform more than one measurement per day.

Others methods of determining concrete setting time have been proposed. Among these are electrical resistance [3] and ultrasound [4]. The advantage of the penetration test is that measurement is done relatively direct to the examined property. But as mentioned above there are also a number of disadvantages. As will be demonstrated in the following a method based on heat development correlates superb to penetration tests but do not have the disadvantages. Furthermore information of the hydration process is gained with this test method.

2. EXPERIMENTAL

2.1 Setup

Initially the concrete is sieved on an 8 mm mesh (analogous to the penetration test) and filled into a sample cylinder with a volume of approximately 0.1 litres. The sample is mounted with a thermo sensor and placed into a insulated container. From this point temperature is measured continuously during 24 hours or more. The data is collected via a datalogger and transferred to a PC. Using the temperature data and taking into account the heat loss a curve of heat development (dQ/dt) and accumulated heat development (Q) is constructed. The procedure is schematically illustrated in figure 1.

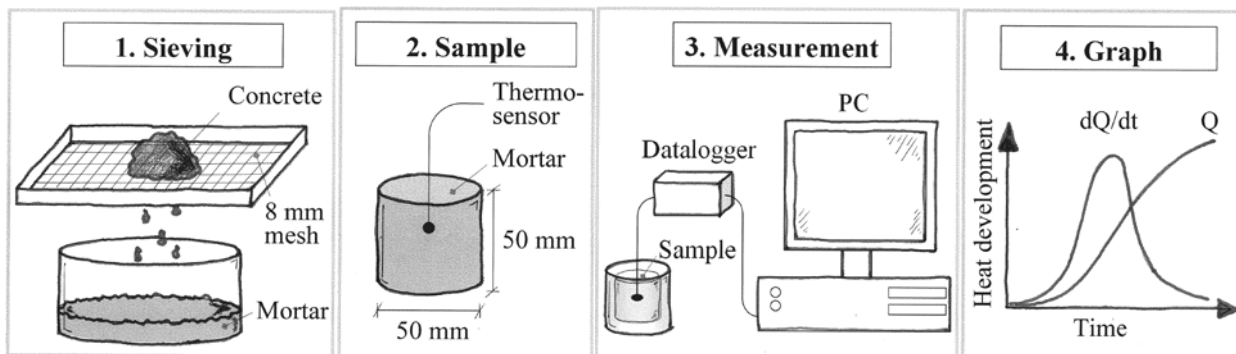


Figure 1 – Schematically illustration of heat development measurement.

2.2 Mix designs

Seven different concretes have been prepared. These concretes are typically Danish ready mix concretes and cover the normal area of setting time. In order to achieve a wide range of setting times an accelerator has been used in one mix design and a retarder in another. The mix designs contain three different types of cement and workability ranging from slump 120 mm to slump flow 550 mm for the SCC's. The mix designs are given in table 1.

Table 1 – Mix designs. Workability 120 refers to slump while 550 refer to slump flow. Strength class refers to cylinder strengths

Mix designation	1	2	3	4	5	6	7	8
Strength class	C35	C35	C35	C40	C40	C25	C25	C25
Setting time [Hours]	3.5	5.0	8.0	9.5	10.5	10.0	11.5	18.5
Workability [mm]	120	120	120	120	550	550	550	550
Cement type	CEM I 52.5 N	CEM I 52.5 N	CEM I 52.5 N	CEM I 42.5 N	CEM I 52.5 N	CEM I 52.5 N	CEM II 52.5 N	CEM I 52.5 N
Cement [kg/m ³]	360	330	330	370	350	250	250	250
Eq. w/c-ratio [-]	0.40	0.42	0.42	0.35	0.40	0.51	0.51	0.51
Remarks	Accele- rator	Non re- tarding water red.	Retarding water red.	Sulphate resistant cement	SCC	SCC	Portland- limestone cement	Retarder

A few of the mixes have been repeated several times with different cement and admixture samples and therefore the total number of tests that forms the basis of the study are actually 18.

3. RESULTS AND DISCUSSION

In figure 2 selected interrelated heat development measurements and penetrations setting time measurements of each mix design are shown.

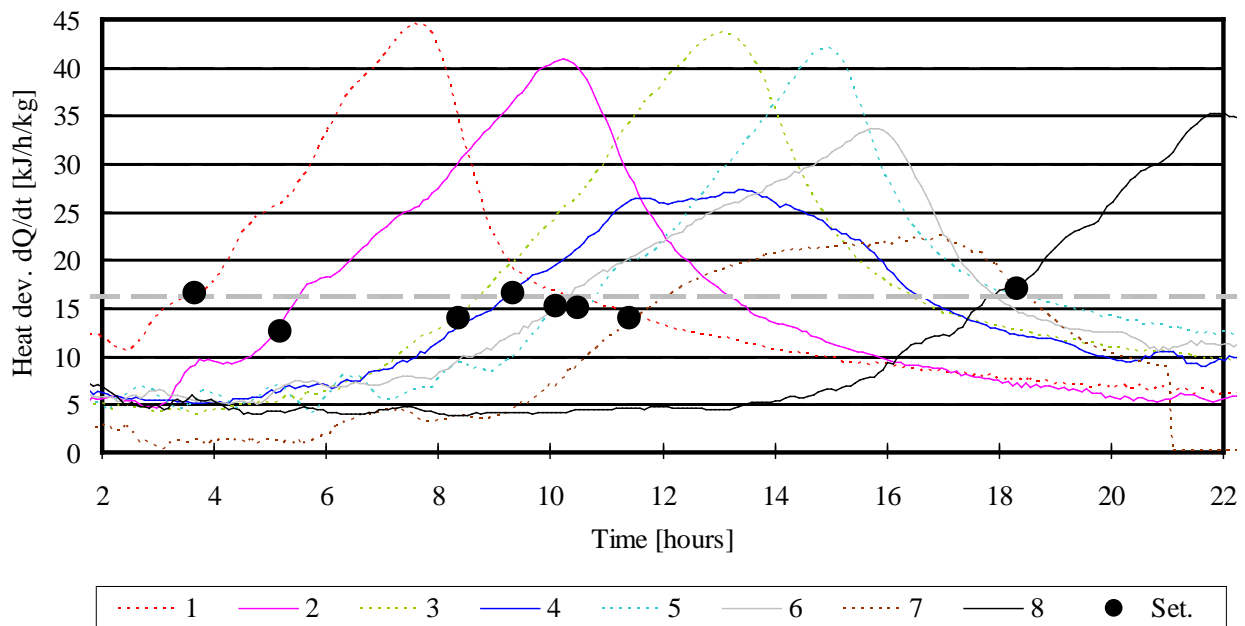


Figure 2 – Interrelated heat development and penetration resistance measurements

It is seen that penetration resistance setting time approximately correspond to $dQ/dt = 16$ kJ/h/kg cement (value marked with grey horizontal line in figure 2). This value is used as set-point throughout this paper. From figure 2 it is also seen that workability of the fresh concrete does not effects the correlation between heat development and penetration resistance.

In figure 3 penetration setting time and $dQ/dt = 16$ kJ/h/kg are plotted and the coefficient of correlation from linear regression is seen to be 0.99. The mean deviation between the estimate

from heat development and penetration resistance test is 19 minutes. The experience at Aalborg Portland is that the penetration method itself has a reproducibility of approximately 30 min.

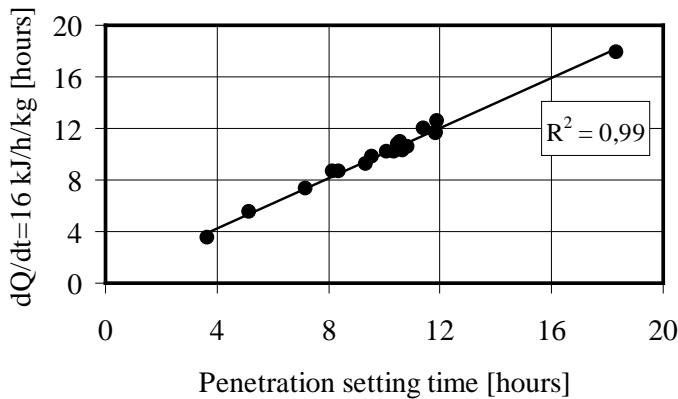


Figure 3 – Correlation between penetration resistance and heat development

Besides correlation to penetration resistance the curves in figure 2 also contains information on the course of hydration. It is for instance seen that mix number 5 and 7 has significantly lower dQ/dt peak values compared to the other curves. The reason for this is in both cases that the cement type differs with more coarsely ground clinker in the cement.

Neither the penetration test nor the heat development test takes into account the proportion of coarse aggregate in the concrete since the stones are removed from the concrete before testing. A “stone-rich” concrete might have a different setting time as compared to a concrete which primarily is mortar.

4. CONCLUSIONS

Using heat development to determinate concrete setting time has a number of advantages compared to penetration test as is normally used. It has been shown that when the velocity of the heat development reaches a certain level it corresponds to setting time determined with penetration test. A correlation factor of 0.99 has been found between the two methods and therefore the heat development method is considered good in agreement with the penetration method. No difference in correlation from slump concrete to SCC has been found.

REFERENCES

1. DS 423.17:1984, “Testing of concrete - Fresh concrete - Hardening”, Danish Standards, 1984
2. ASTM C403, “Standard Test Method for Time of Setting of Concrete Mixtures by Penetration Resistance, 2008
3. Zongjin, L., Xiao, L., Wei, X. “Determination of concrete setting time using electrical resistivity measurement”, Journal of materials in civil engineering, May 2007 pp. 423-427
4. Robeyst, N., Gruyaert, E., Grosse, C.U., Belie, N.D. “Monitoring the setting of concrete containing blast-furnace slag by measuring the ultrasonic p-wave velocity, Cement and Concrete Research 38, 2008 pp. 1169-1176

Experimental Methods for Consideration of Concrete Cracking in Service Life Design



Brad J. Pease, Ph.D.
Tech. Univ. of Denmark, Dept. of
Civil Engineering (DTU Byg),
Brovej, DK-2800 Kgs. Lyngby,
Denmark bjp@byg.dtu.dk



Mette Geiker, Ph.D.
Tech. Univ. of Denmark, Dept. of Civil
Engineering (DTU Byg), Kgs. Lyngby,
Denmark mge@byg.dtu.dk
Norwegian Univ. of Sci. and Tech.
(NTNU), Trondheim, Norway
mette.geiker@ntnu.no



Henrik Stang, Ph.D.
Tech. Univ. of Denmark, Dept. of
Civil Engineering (DTU Byg),
Brovej, DK-2800 Kgs. Lyngby,
Denmark hs@byg.dtu.dk



Jason Weiss, Ph.D.
Purdue University School of Civil
Engineering, 550 Stadium Mall Dr.,
West Lafayette, IN 47907 USA
wjweiss@purdue.edu

ABSTRACT

Prediction of service life of reinforced concrete structures using corrosion initiation as the controlling limit state and assuming homogeneous concrete has become commonplace. However, advancements are needed to progress service life models to consider initially non-pristine concrete (i.e., concrete with cracks at start of service) and to more accurately estimate time-to-cracking due to reinforcement corrosion based on experimental measurements. This paper presents two non-destructive measurement techniques with potential to quantify the impact concrete cracks have on service life of reinforced concrete.

Keywords: X-ray attenuation; instrumented rebar; non-destructive techniques; cracking; service life modelling

1. INTRODUCTION

To advance service life models to consider more realistic initial concrete conditions in the form of cracked concrete as well as the impact of reinforcement corrosion, advanced experimental techniques and results are needed. Monitoring moisture ingress and local environmental aggressivity in cracked concrete could provide vital information on the initiation phase of reinforcement corrosion. The propagation phase could be modelled based on knowledge of the reinforcement corrosion process and subsequent corrosion-induced cracking. This paper describes two experimental techniques/setups, x-ray attenuation measurements and an instrumented rebar, for monitoring of movements of moisture and corrosion products and assessment of aggressivity of local environment, respectively.

2. X-RAY ATTENUATION MEASUREMENT TECHNIQUE

Figure 1(a) shows the x-ray system which consists of a shielded environmental control chamber housing an x-ray source and a 252 x 256 pixel (25 x 25 mm²) x-ray camera mounted on a

programmable x,y frame [1]. Figure 1(b) illustrates a typically used composite representation of an x-ray attenuation measurement [2-4], in the case of moisture ingress measurements. As shown in Figure 1(b), the x-ray source produces a beam with initial intensity, I_0 [counts], which interacts with a conditioned sample. The sample attenuates (absorbs and scatters) a portion of the x-rays according to the Beer-Lambert law ($I_{dry} = I_0 \cdot e^{-\mu \cdot t}$, where μ [cm^{-1}] is the linear attenuation coefficient and t [cm] is thickness of the sample) resulting in a transmitted intensity, I_{dry} [counts]. Moisture ingress, represented in the model as a water layer with thickness, t_w and linear attenuation coefficient, μ_w , attenuates additional x-rays. Using the Beer-Lambert law, I_{dry} , and I_{wet} , the change in moisture content, Δw [g/cm^3] is directly measured [2]:

$$\Delta w = -\frac{\rho_w}{\mu_w t} \left(\frac{I_{wet}}{I_{dry}} \right) \quad (1)$$

where ρ_w [g/cm^3] is the density of water. Equation 1 may be modified using densities and linear attenuation coefficients of other materials and other ‘dry’ and ‘wet’ conditions to determine concentration changes of e.g. corrosion products. The following sections present two applications of x-ray attenuation measurement to monitor movement of water and corrosion products in concrete.

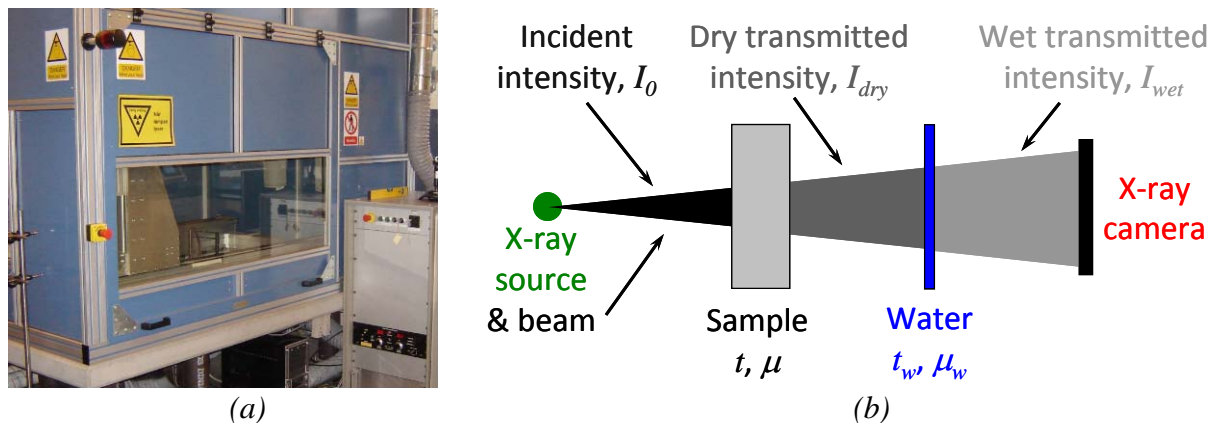


Figure 1 – (a) X-ray attenuation equipment and (b) schematic of moisture ingress measurement described as a composite system of a conditioned sample and a thickness of water.

2.1 Monitoring moisture ingress in cracked/uncracked concrete

In [2,3] x-ray attenuation measurements were utilized to monitor moisture ingress in concrete wedge split test (WST) specimen, loaded to varying load level or crack mouth opening displacements (CMOD's; unloaded, peak load, 0.10, 0.15, 0.20, 0.40 mm CMOD) and conditioned to 50% relative humidity. Figure 2 shows the 100 x 100 x 50 mm³ WST specimen geometry and a typical result of the x-ray attenuation measurements. As seen, an area of approximately 45 x 75 mm² was monitored, necessitating the use of the programmable x,y frame to sweep and record x-ray images at 15 locations. At each location, 10 images were recorded with an integration time (similar to shutter speed in visual imaging) of 5 seconds. Individual images were averaged and tiled to create a 1057 x 658 pixel image, meaning moisture changes were monitored at 695,506 points. A complete measurement (i.e., 15 measurements) took approximately 28 minutes.

The dry transmitted intensity, I_{dry} was initially recorded from the conditioned sample followed by ponding with water and measurements of wet transmitted intensities at various times after exposure. The contours shown in Figure 2 indicate the change in moisture content after one hour of exposure, for a 0.15 mm CMOD sample, normalized to the maximum moisture content change after 24 hours. This normalization is necessary due to variations in cement paste content.

Results indicated that as CMOD increased water moved more rapidly into the depth and laterally in the WST specimens [2,3]. It was concluded that cracks may be divided into two portions, one that has free surface for sorption behaviour and a second portion with consistent length that inhibits ingress.

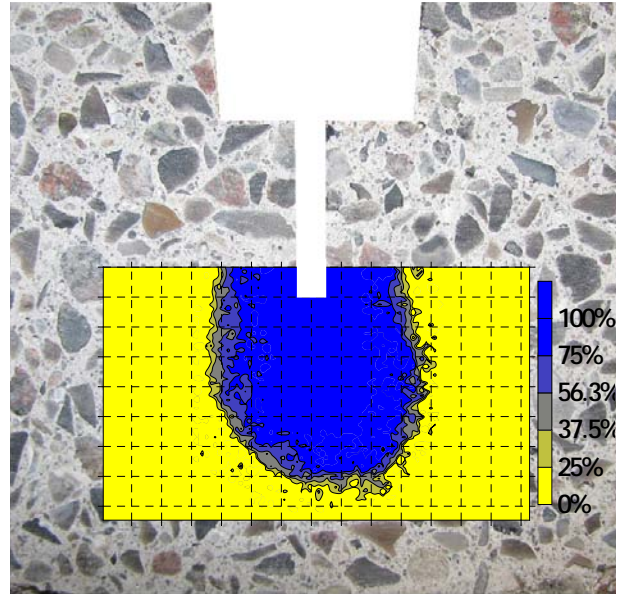


Figure 2 – WST specimen with overlay of x -ray attenuation measurements after one hour of exposure to liquid water for a 0.15 mm CMOD. Grid lines at 5 mm increments.

2.2 Monitoring penetration of reinforcement corrosion products and time-to-cracking

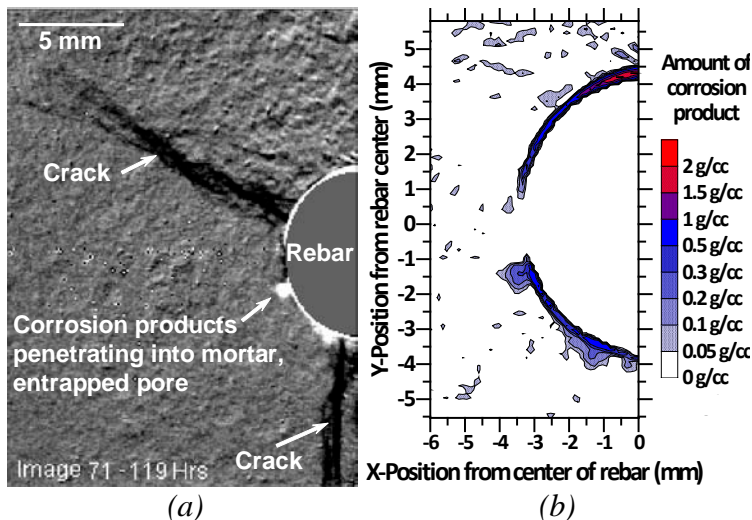


Figure 3 – (a) Computed x -ray image (Equation 1) and (b) contour plot of location, concentration of corrosion products after 119 hours of corrosion testing, from [4]

X-ray attenuation measurements have also been used to monitor accelerated corrosion testing (application of direct current) [4]. Figure 3(a) shows corrosion products (white) penetrate the mortar around a smooth corroding rebar; the corrosion induced two cracks (black). The circular region of corrosion products likely is the result of filling entrapped air. The contour plot in Figure 3(b) provides details on the location and amount of corrosion products. Continuous monitoring provides measures of time-to-cracking, concentration of corrosion products needed to induce cracking, and penetration depth of

corrosion products into the surrounding concrete.

3. INSTRUMENTED REBAR FOR LOCATION-DEPENDENT ASSESSMENT OF CORROSION STATE

Figure 4 illustrates an instrumented rebar, consisting of a hollowed rebar with 17 protruding steel pin sensors, which is capable of carrying loads, inducing realistic concrete cracks, and

measuring location-dependent open circuit potential (OCP) measurements – indicating where

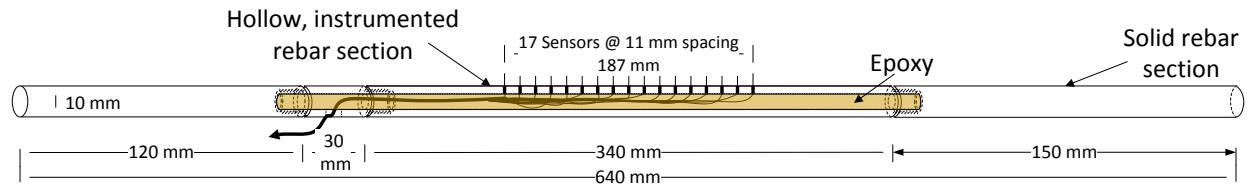


Figure 4 – Schematic of instrumented rebar (deformed bar used, ribs not shown). From [2, 5]

and when a risk of reinforcement corrosion exists [2,5]. Figure 5 provides a typical measure from an instrumented rebar placed in for the first 7 days of exposure to a 10% chloride solution. The white broken isoline ($-200 \text{ mV}_{\text{SHE}}$) indicates active corrosion is thermodynamically favoured based on the local environmental conditions. After approximately 0.75 days of exposure the OCP at the crack dropped below $-200 \text{ mV}_{\text{SHE}}$ and with additional time the corrosion risk area increased. After testing, the instrumented rebar (I.R.) and an adjacent standard rebar (S.R.) were removed and inspected to determine locations of anodic regions, as shown in the sketches in Figure 5. In all cases anodic sites were located within the corrosion risk area; however, anode sites were significantly smaller, likely due to formation of corrosion macrocells.

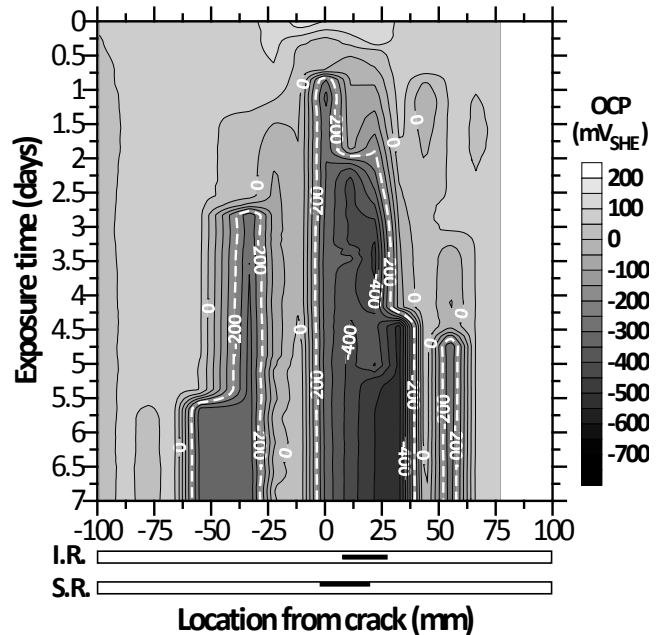


Figure 5 – Contour plot of OCP's measured from instrumented rebar cast in a three point bending beam with 0.6 mm crack width. Sketches indicate locations of anode sites. From [2,5]

4. SUMMARY AND CONCLUSIONS

Two experimental techniques, x-ray attenuation measurements and an instrumented rebar, and sample results were presented. These techniques provide useful data for the verification and refinement of current or development of new, fundamentally sound service life models.

REFERENCES

1. GNI X-ray Absorption Systems, www.gni.dk, Denmark, 2008
2. Pease, B., "Influence of concrete cracking on ingress and reinforcement corrosion," *Ph.D. thesis*, Technical University of Denmark, Kgs. Lyngby, Denmark, 276 pp. In press
3. Pease, B., Couch, J., Geiker, M., Stang, H., Weiss, J., "Assessing the Portion of the Crack Length Contributing to Water Sorption in Concrete Using X-Ray Absorption," *Proceedings: ConcreteLife'09*, Haifa, Israel, September 2009, pp. 1-8
4. Michel, A., Pease, B., Geiker, M., Stang, H., Olesen, J., "Monitoring reinforcement corrosion and corrosion-induced cracking using non-destructive x-ray attenuation measurements," Submitted to *Cement and Concrete Research*

5. Pease, B., Geiker, M., Stang, H., Weiss, J., "The design of an instrumented rebar for assessment of corrosion in cracked reinforced concrete," *Materials and Structures*, in press

Numerical Study of Shotcrete as Rock Support on Irregular Tunnel Surfaces



Anders Ansell
Ph.D., Associate Professor
KTH Royal Institute of Technology
Division of Concrete Structures
SE-100 44 Stockholm, Sweden
anders.ansell@byv.kth.se

ABSTRACT

Effective rock support in tunnels often depends on the performance of load carrying shotcrete systems. Tunnels and underground openings in hard rock are often constructed with arch-shaped ceilings and complicated three dimensional geometries arise at intersections and crossings. This is further complicated due to the often irregular shape of the rock walls and the uneven shotcrete thickness. The project will deal with the interaction between rock and reinforcement consisting of shotcrete and rock bolts, including variations in rock geometries, shotcrete thickness and material compositions. The objective is to obtain an understanding of the behaviour of shotcrete as a construction material, from spraying until possible failure.

Key words: Shotcrete, Tunnel, Irregular geometry, Finite element model, Non-linear materials.

1. INTRODUCTION

Tunnels and underground openings in hard rock are often constructed with arch-shaped ceilings designed to carry the weight of the above rock. At intersections with cross tunnels and other openings complicated three dimensional (3D) geometries will arise making it difficult to accurately calculate and determine the stresses that must be carried. This is further complicated due to the often irregular shape of the rock walls. Shotcrete (sprayed concrete) is together with rock bolts the most common elements in rock reinforcement which interacts with the supported rock. The irregular tunnel walls also results in an uneven shotcrete thickness, resulting in a highly irregular shell that bonds to the rock. The load carrying capacity of bolt anchored shotcrete on rock was discussed by Nilsson [1] who concluded that a further, detailed study of the interaction in 3D between an irregular, rough rock surface supported by bolts and shotcrete with varying thickness is of great interest. The numerical investigation must be made using FE (finite element) models with non-linear material formulations capable of describing large deformations as well as concrete cracking and crushing. There is little published research on numerical studies of rock supported with shotcrete and bolts where non-linear material formulations for concrete and steel are used [2]. The focus is often set on the properties of the rock and the reinforcement is often given only elastic deformation properties. This recently initiated research project was started to obtain a basic understanding of the performance of load carrying shotcrete systems for rock support. Of special interest is the load carrying contribution from the bonding between rock and shotcrete. The main objective is to understand the behaviour of shotcrete as a construction material, with a focus on the entire life cycle from spraying until possible failure occurs.

2. IRREGULAR ROCK SURFACES

A rock surface with sharp edges, peaks and depressions will affect the load carrying capacity of rock support systems as it provides good anchorage between rock and shotcrete. This unevenly distributed bond lead to varying degrees of interaction and constraint as increasing load and stresses in the shotcrete approach the ultimate stress of the material. The curved geometry of tunnel ceilings and cross tunnels also has a noticeable effect on the load carrying capacity through the build-up of compressed arches and the effects of dome action. The situation is further complicated by the often irregular shape of the rock walls and the varying shotcrete thickness which is a result of this. Shotcrete fills out holes and depressions in the rock resulting in a shotcrete surface that is smoother (harmonic-shaped) than the underlying rock. This can lead to the formation of thin, critical shotcrete sections with lower load carrying capacity and an increased risk of crack initiation. Fotieva & Bulychev [3] concluded that variation in shotcrete thickness leads to stress concentrations and an increased risk of crack initiation. This has also been observed in situ [4] during failure mapping of shotcrete within the traffic tunnels of the Southern Link (Södra länken) in Stockholm. If rock bolts with washers (plates) are used together with shotcrete may these cause stress concentrations in the shotcrete. It is therefore interesting to further study how the placement and properties of the bolts and washers affects the overall stress situation in the shotcrete, especially in combination with varying mechanical bond between rock and shotcrete.

3. FINITE ELEMENT MODELS

Studies of the interaction between rock, shotcrete and other support must thus be made using models capable of describing details in 3D. One basic model is a horizontal shotcrete slab that carries a severely cracked rock mass, which gives a uniformly distributed load on the slab. The outer section of the rock will in this case thus only be present as a load and not contribute to the load carrying capacity. The model must contain rock bolts as hangers between the shotcrete and the intact rock, above the cracked rock mass. The easiest way to approximate irregularities is to apply harmonic (sine-shaped) variations in two orthogonal directions to the surface of this otherwise plane and horizontal slab. The result is shown in Figure 1(a) and can be seen as a part of a shotcreted horizontal tunnel ceiling. These types of shell structures were modelled by Nilsson [1] who studied slabs with freely supported and fixed edges. The effect of one or many rock bolts was also included by restricting the vertical movements for a small number of nodes before the load was applied. It should be noted that this shape is a good approximation of the outer surface of the shotcrete. In this first study were not different geometries of the upper and lower surfaces considered resulting in a constant shotcrete thickness. A further development of the plane slab is a curved shotcrete shell with a semi-circular cross-section, also with a constant thickness and harmonic irregularities, such as shown in Figure 1(b). A more sophisticated version is shown in Figure 1(c) where the outer surface of the curved shell is given a highly irregular, randomly distributed shape. The inner surface of the shell is similar to that of shell (b), approximating the outer surface of shotcrete that fills out depressions in the rock. Such a shell will have a varying thickness and is a reasonable approximation of what can be observed in situ. For rock bolts and shotcrete, described using concrete material models, the stress-strain relations must be non-linear to account for plastic deformation in steel and cracking in concrete materials. The analyses within this project are carried out using the general finite element program Abaqus/Standard [5] containing non-linear material formulations suitable for concrete, here the “smeared crack approach” is used.

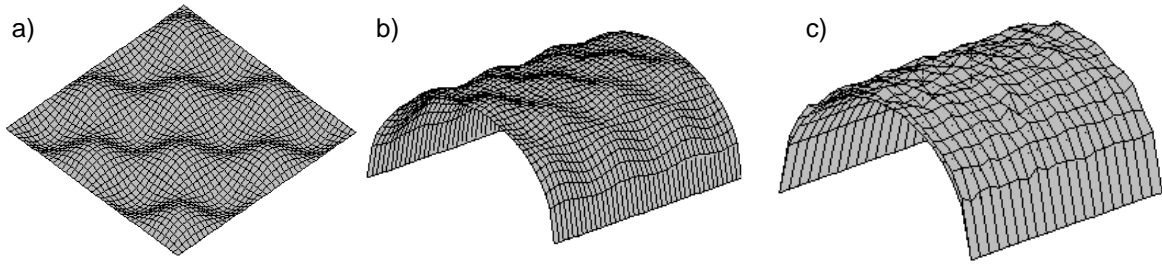


Figure 1 – Finite element models of (a) a plane shotcrete slab with harmonic irregularities, (b) a shotcrete shell with harmonic irregularities and (c) a shotcrete shell with a highly irregular outside and a smooth inside.

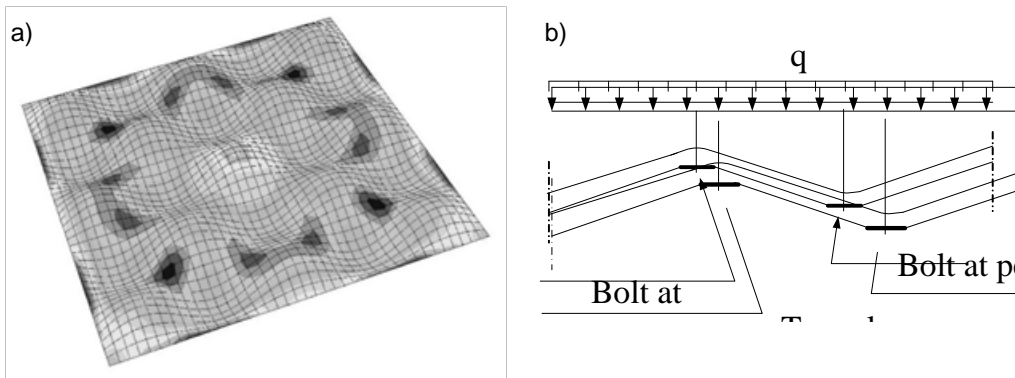


Figure 2 – High tensile stresses around the bolt placed in a depression on an 80 mm thick shotcrete slab (a). Placement of rock bolts at peaks or in depressions (b). From [1].

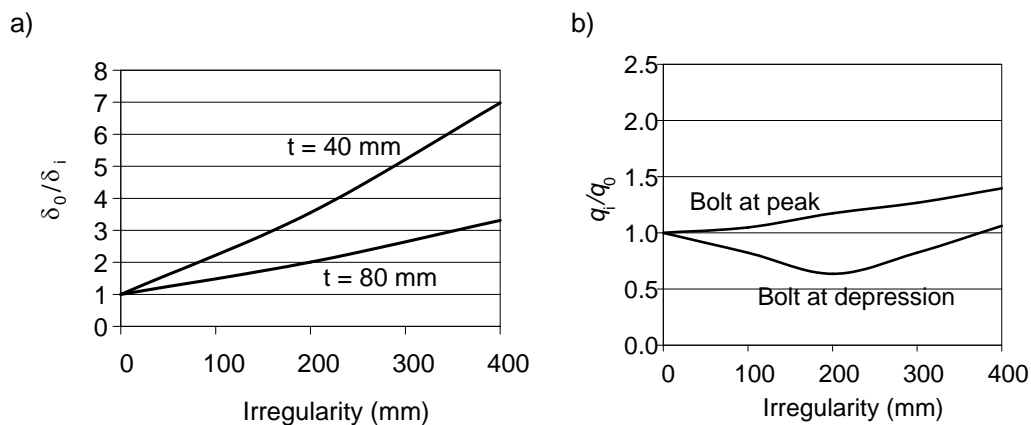


Figure 3 – Irregularity vs. (a) relative stiffness and shotcrete thickness and (b) failure load for an 80 mm thick shotcrete slab, with respect to placement of the rock bolt. From [1].

4. PRELIMINARY RESULTS

The first part of the project summarizes preliminary results based on the work by Nilsson [1] who studied the importance of placement of rock bolts with respect to the load carrying capacity and risk of early shotcrete failure. The examples studied so far include a horizontal, quadrilateral section of shotcrete suspended with single or multiple rock bolts. The thickness of the shotcrete was set to 40 or 80 mm and the irregular surfaces were as described in Figure 2. The finite element model of the shotcrete lining was built up with 3D shell elements with four nodes and nine integration points through the thickness. The uniformly distributed load from the weight of the rock was applied as vertical point-loads at every node of the model. The example presented here consists of a $4 \times 4 \text{ m}^2$ shotcrete section with a “wave length” of 1.6 m and a bolt placed at the centre. The rock bolt is assumed to have a quadrilateral washer which is represented by nodes that are fixed in the vertical direction. The two possibilities of either placing the bolt at a peak or a depression in the slab were compared. For the results in Figure 3 the relative stiffness is the ratio between the deflection δ_0 of a plane and δ_i of an irregular slab, respectively. The relative load carrying capacity is obtained from the corresponding distributed loads at failure.

5 CONCLUSIONS AND FURTHER RESEARCH

The presented project has recently been initiated and this far is the preliminary results from a pilot-study available. However, these results demonstrate some of the important aspects that are studied in detail within the ongoing project. It has been shown that the irregularities have a greater effect on the stiffness of a shotcrete slab than on its load bearing capacity. The structural response of the slab is affected by the thickness in relation to the irregularities so that a thin slab becomes relatively much stiffer with increased irregularity compared to a thicker slab. The reason for this is the relatively large change in bending stiffness as a function of irregularity for the thinner slab [1]. It has also been seen that when the bolts are placed at peaks on the tunnel surface the major load will be carried by the shotcrete acting as compressed domes between the bolts, thereby increasing the load bearing capacity. It is also pointed out that these high values increase the risk of tensile failures in the bolts and punching failures of the bearing plates. The project will focus on the interaction between rock and reinforcement consisting of shotcrete and rock bolts. Detailed finite models in 3D will include variations in rock geometries, shotcrete thickness and material composition. The applied loads, the geometries and size of tunnel sections studied will be chosen on basis of conditions that are common in tunnelling and civil engineering.

REFERENCES

1. Nilsson, U., “Structural behaviour of fibre reinforced sprayed concrete anchored in rock”, Doctoral thesis, KTH Structural Engineering, Stockholm, 2004.
2. Ansell, A., “3D-Modelling of the interaction between rock and shotcrete”, Report K33, Befo, Stockholm, 2009. (In Swedish).
3. Fotieva, N.N., & Bulychev, N.S., “Design of sprayed concrete tunnel lining upon static and seismic effects”, Proceedings of the second International Symposium on Sprayed Concrete, Gol, 23–26 September 1996.
4. Ansell, A., & Slunga, A., “Investigation of cracked shotcrete on drains in the Southern Link – Mapped cracks”, PM 2004-01-20, Vägverket, Stockholm, 2004. (In Swedish).
5. Simulia, http://www.simulia.com/products/abaqus_standard.html. 2009.

Fine Particles - a Fracture Mechanical Approach



Anna Kronlöf
Dr. (Tech.), Senior Research Scientist
VTT Technical Research Centre of
Finland
anna.kronlof@vtt.fi

ABSTRACT

The work is a closer analysis of Kronlöf's earlier work [1994] and thesis [1997]. It is also related to Björn Lagerblad's and Carsten Vogt's work [2004] as well as Vogt's theses [2010], all dealing with the unexplained substantial strengthening in the presence of large amounts of fine quartz. In this analysis the strengthening effect was up to 20 MPa but could be also negative. At the age of 7 days the effect depended on the average distance between particles as well as on the water to binder ratio, while at the age of 91 days it only depended on the average distance, being independent of the water to binder ratio over the wide range from 0.22 to 2.0. It was concluded that in the later case the effect was mechanical. An empirical model was made and fracture mechanical explanation given to describe the strengthening effect.

Key words: fracture mechanics, modelling, filler effect, optimising OPC content, compressive strength, fine particles

1. MATERIALS AND METHODS

The aggregate was 100% well crystallised quartz and its maximum size was 6 mm. The particle size distributions (PSD) did not vary from 0.5 – 6 mm, but varied widely below this range. The specific surface area of the three fine fractions was determined from their PSDs measured with the X-ray sedimentation method and was in the range of OPC: 993, 584 and 306 m²/kg. The binder comprised 90% of relatively coarse OPC (P40/91 LH SR) and 10 % of silica fume. The aggregate to binder ratio with each of the aggregate mixes varied over a wide range from 1.7 to 22. The water requirement was determined by adding a sufficient amount of water to give a workability flow value of roughly 13 cm by the Haegermann method. All mixes were plasticized. The mixes were tested for compressive strength at the ages of 7 and 91 days. The experimental details are given elsewhere (Kronlöf 1994).

2. MODELLING

The compressive strength was estimated with a modified rule of mixtures (Equation 1, 2 and 3).

$$f = V_{Paste} \cdot f_{Paste} + f(Aggr) \quad [1]$$

$$f(Aggr)_{7d} = 6.80 \cdot V_{Aggr} \cdot f_{Paste}^{0.60} \quad [2]$$

$$f(Aggr)_{91d} = 15.54 \cdot V_{Aggr} \cdot f_{Paste}^{0.48} \quad [3]$$

Equation 1 provided a good description of the strength of mixes made without fine quartz (R^2 va= 0.994 at 7 d and 0.998 at 91 d), but when fine fractions were introduced to the aggregate the

experimental strength was upto 20 MPa higher than the estimation. The difference is shown in Figure 1.

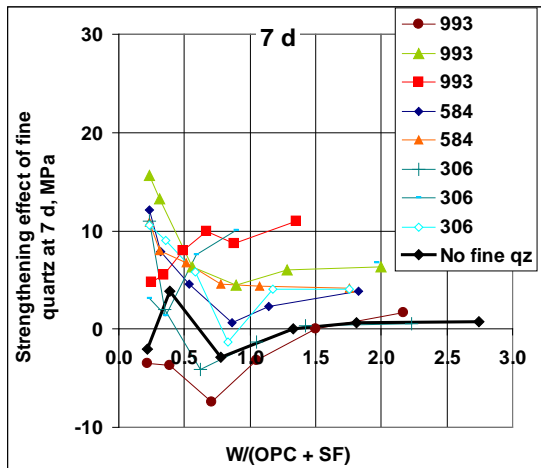


Figure 1a.

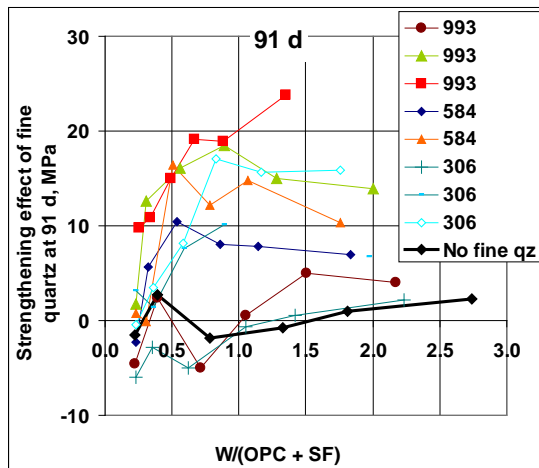


Figure 1b.

The strengthening effect of fine quartz (the difference between experimental results and Equation 1) plotted against the water-to-binder ratio for 7 and 91 days results. The symbols give the SSA of the fine quartz. W denotes water, OPC cement and SF silica fume as weight units.

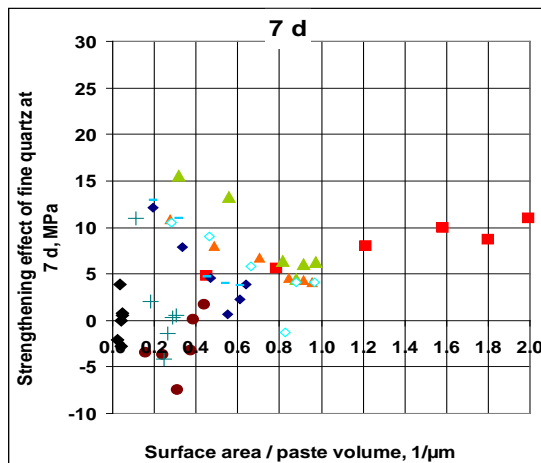


Figure 2a.

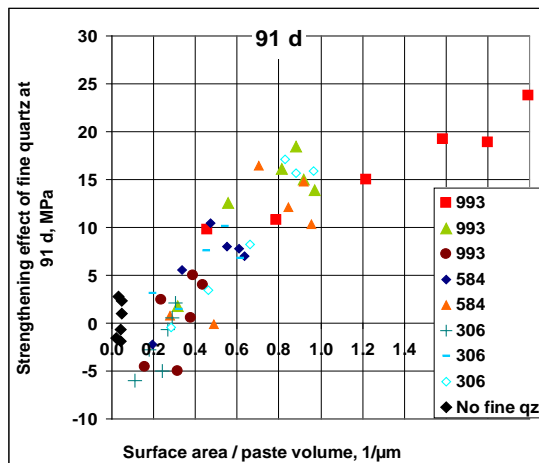


Figure 2b.

The strengthening effect of fine quartz (the difference between experimental results and Equation 1) as a function of the ratio between the total quartz surface area (the area of the interfacial transition zone) and the paste volume (ITZ ratio) for 7 and 91 days results.

Attempts were made to relate the above mechanism to some kind of chemical effect by applying the cement equivalent concept. It showed that the chemically identical quartz particles in the chemically identical environment and rheologically stable conditions could either strengthen or weaken the material. A hypothesis was made that the strengthening/weakening mechanism is not chemical in nature in the sense of binding reaction products but mechanical. According to the hypothesis quartz particles could be either strengthening components or flaws depending on the overall mix composition structure. This was also supported by the fact that quartz is a very inert material. The net strength was given the formulation given in Equation 4.

$$f = V_{Paste} \cdot f_{Paste} + f(Aggr) + f(Fine quartz)$$

[4]

In this equation the third term ($f(\text{Fine quartz})$) represents the strengthening effect of fine quartz powder. This was examined in terms of mix composition geometry (volume fractions and distributions) of the two phases, paste and quartz. It was found that at the age of 91 days the most dominating quantity was the ratio between the total quartz surface area (the area of the interfacial transition zone) and the paste volume (ITZ ratio). The larger was the ITZ ratio, the larger was the strengthening effect. When the ITZ ratio was lower than 0.25 ($1/\mu\text{m}$), indicating that the average distance was larger than $8 \mu\text{m}$ between quartz surfaces, the quartz particles weakened the concrete structure and thus indicating that they behaved as flaws. However, at the age of 7 d the previous tendency was more diverged (Figures 2 and 3). This finding was modelled with Equations 5 and 6.

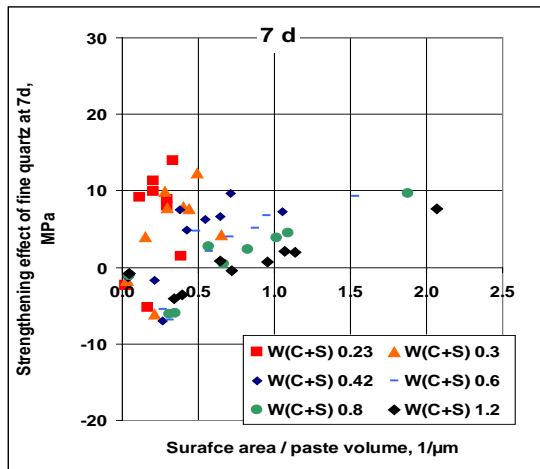


Figure 3a.

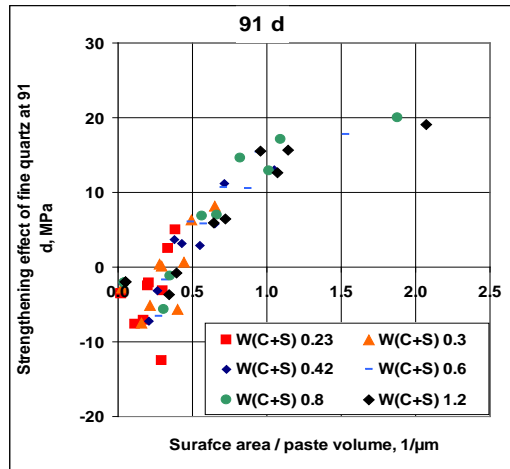


Figure 3b.

Interpolated fine quartz strengthening effect as a function of ITZ ratio for 7 and 91 days results. The interpolated values are the values of the previous figures interpolated and calculated to show the water-to-binder ratio effect in the range from 0.23 to 1.2. The legends denote the water-to-binder ratios.

A fracture mechanical explanation of the found behaviour can be given as follows: The compressive strength of concrete is controlled by the initiation and subsequent coalescence of a large number of individual cracks. If the number of quartz particles is small, i.e. the distance between particles is larger than some effective grain size of concrete, the particles only enhance the probability of crack initiation. The resulting crack sizes and coalescence are here controlled by the paste properties. The quartz particles have in this case a detrimental effect on concrete strength. Besides acting as crack initiators, the particles may also act as microcrack arresters in the paste. With an increasing number of particles, the interparticle spacing decreases and at some point begins to control the coalescence process. The crack driving force is roughly controlled by the square root of the crack size and in this case the crack size will be a function of the interparticle spacing. The end-result will be the behaviour described by Equations [5] and [6] (Figure 4).

$$f(\text{Fine quartz})_{7d} = 5.24 \cdot \ln(A_{\text{Aggr}} / V_{\text{Paste}}) + 0.19 \cdot f_{\text{Paste}} + 4.27 \quad [5]$$

$$f(\text{Fine quartz})_{91d} = 10.68 \cdot \ln(A_{\text{Aggr}} / V_{\text{Paste}}) + 14.80 \quad [6]$$

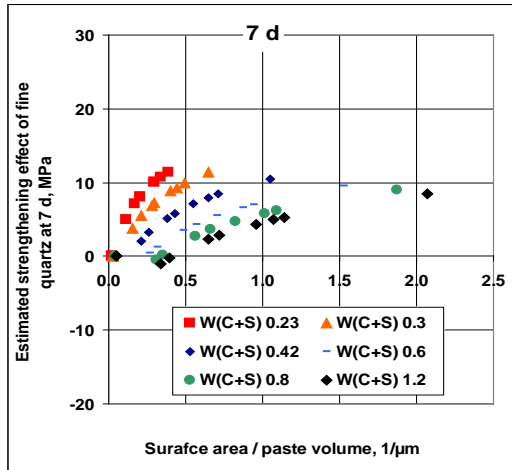


Figure 4a.

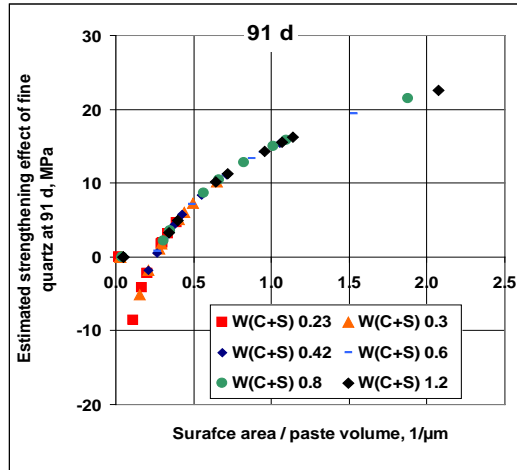


Figure 4b.

Estimated fine quartz strengthening effect for 7 and 91 days results by Equations 5 and 6.

3. SUMMARY AND CONCLUSIONS

The binding effect of substituting materials in OPC is often explained by their chemical activity such as pozzolanic reaction or surface nucleation of CSH while their mechanical effect is overlooked. This study examined strengthening effect which was mainly mechanical. The experimental result showed that powder was detrimental to strength if used in small quantities and if it was coarser than cement. However, if the powder was very fine and its potential for improving particle packing was utilized as reduced paste content, the positive strengthening effect was up to 20 MPa. At the age of 91 days the positive effect was not dependent on the water to binder ratio. It depended only on the ratio between the total aggregate surface area which is the area of the interfacial transition zone and the paste volume (ITZ ratio). This ratio is inversely proportional to the distance between the quartz particles. At the age of 7 days the strengthening effect depended also on the water to binder ratio. Also when reactive powders are used the mechanical effect is a part of the under-laying mechanism whenever a part of the particle remains un-reacted. This is the case also with pure OPC in high strength mixes. In addition to the geometry addressed here, the significance of the particle surface bond to the surrounding paste as well as the options to modify it should be further studied.

This research was done as a part of the project SIPI (Internal surfaces of mineral based functional materials), in collaboration with VTT, Aalto, and Åbo Akademi, funded by VTT, TEKES, Nordkalk Oy Ab, Cements Ab and Tikkurila Oyj.

REFERENCES

- Kronlöf, A., "Effect of fine aggregate on concrete strength," *Mat. Struct.* 1994, pp.15 – 25.
 Lagerblad, B., Vogt, C., "Ultrafine Particles to Save Cement and Improve Concrete Properties," Swedish Cement and Concrete Research Inst., Stockholm, 2004, 40 pp.
 Vogt, C., Ultrafine particles in concrete - Influence of ultrafine particles on concrete properties and application to concrete mix design, Thesis, The Royal Institute of Technology 2010.

Session A9 – FIELD TESTING OF DURABILITY

Issues Related to the Use of Portland-Limestone Cements in Sulphate Exposure



R. Doug Hooton
B.A.Sc., M.A.Sc., Ph.D.
University of Toronto
Dept. of Civil Engineering
Toronto, Ontario, Canada, M5S 1A4
hooton@civ.utoronto.ca



Amir Ramezaniapour
B.A.Sc, M.A.Sc.
University of Toronto
Dept. of Civil Engineering
Toronto, Ontario, Canada, M5S 1A4
amirmohammad.ramezaniapour@utoronto.ca



Reza M. Ahani
B.A.Sc., M.A.Sc.
University of Toronto
Dept. of Civil Engineering
Toronto, Ontario, Canada, M5S 1A4
reza.mohammadiyahani@utoronto.ca

ABSTRACT

Portland-limestone cements (PLC) contain up to 15% interground limestone have been recently adopted in Canada. They are required to have equivalent performance to Portland cements, but due to concerns with increased potential for the thaumasite form of sulphate attack, the Canadian concrete standard, currently does not allow their use in sulphate exposures. Research to resolve this concern resulted in development of a modified version of the ASTM C1012 test exposing mortar bars to sodium sulphate at 5 °C instead of the standard 23 °C. Results from this modified 5 °C test have shown that damage due to thaumasite can occur if PLC are used as the sole cementing material, but also that it can be prevented by using the same levels of Class F fly ash, ground-granulated blast-furnace slag, metakaolin, and ternary blends with silica fume normally used to prevent the ettringite form of sulphate attack that occurs at 23 °C. As a result, CSA is considering removal of the current restrictions.

Key words: limestone cement, thaumasite, sulphate attack, test methods

1. INTRODUCTION

Portland-limestone cements (PLC), already popular in Europe, have been recently adopted in Canada. Canadian PLCs contain up to 15% interground limestone and have to meet the same set time, strength development and other physical requirements as portland cements of the same type. While they are working well in most applications, currently they are not allowed for use in

concrete subjected to sulphate exposures due to concerns about the increased potential for the thaumasite form of sulphate attack (TSA).

2. EXPERIMENTAL

The test currently used to evaluate sulphate resistance of cementitious binders in North America is ASTM C1012. In this test, 25x25x285 mm mortar bars are cured until reaching 20 MPa, and then are exposed to a 5% sodium sulphate solution at 23 °C, while monitoring length and mass changes. In both ASTM and CSA specifications, high sulphate resistance (HS) is when expansions after 6 m are < 0.05% (or less than 0.10% at 12m) and moderate sulphate resistance (MS) is when expansions are < 0.10% at 6m. However, this test is not suited to determination of the risk for TSA which preferentially forms at temperatures of 5-10 °C. As a result, in this work, a modified version of the ASTM C1012 test was developed [1, 2] where the same mortar bars are exposed to sodium sulphate at 5 °C. This modified test was adopted in Canadian standard CSA A3000 [3] in 2010 for blended cements made using Portland limestone cements and sufficient levels of supplementary cementitious materials. The expansion limits adopted for the 5 °C test are 0.10% at 18m, but with a secondary limit of 0.10% at 24m if the increase in expansion between 12 and 18m exceeds 0.03%.

The mixtures evaluated in this study include a high C₃A clinker ground with different levels of limestone to produce PLC with 0, 2.4, 10.6, 12.7 and 21.8 % limestone. Chemical compositions are shown in Table 1. Mortar bars using these cements were then mixed using 0, 30 and 50% slag replacements. Both the 5 and 23 °C versions of the ASTM C1012 test were performed.

Table 1- Chemical compositions of Cementing Materials

Cement Type (CSA)	Interground Limestone %	SiO ₂ %	Al ₂ O ₃ %	Fe ₂ O ₃ %	CaO %	MgO %	SO ₃ %	LOI %	Blaine m ² /kg	Na ₂ O _{eq.} %
GU	0	20.61	5.52	2.19	63.36	2.41	4.17	0.58	402	1.03
GU	2	19.67	5.35	2.13	62.72	2.40	4.73	1.43	391	1.02
GUL	11	18.46	4.97	1.98	61.34	2.35	4.39	5.23	515	0.96
GUL	13	18.88	5.06	2.02	61.86	2.31	4.31	4.47	507	0.97
non-spec	22	17.44	4.64	1.86	59.79	2.29	4.07	8.90	562	0.90
Slag	-	38.14	7.18	0.74	40	10.6	1.08*	-	~450	0.63

* sulphide sulphur

In 2010, concrete prisms were cast from over 40 mixtures at w/cm = 0.40 and 0.50 using PC and PLC of differing C₃A contents and different levels of replacement by slag, fly ash, metakaolin, and slag plus silica fume. After 28 day, they were subjected to both ambient and cool temperature laboratory and field exposures to different concentrations (0, 1,500, and 15,000 mg/l SO₄) and forms (Mg and Na) of sulphate. The laboratory prisms are 50x50x285 mm while the field prisms are 75x75x285 mm. The field prisms were buried in solution 2m underground to maintain average temperatures of ~10 °C. The lab prisms are being measured monthly and the field specimens monitored annually.

3. RESULTS

The mortar bar expansions are shown in Table 2 for mortar bars exposed at 23 and 5 °C.

Table 2. ASTM C1012 Sulphate Resistance Expansions at 23 and 5 °C

Temperature (°C)	% Slag	Time of Exposure (Days)	Average Expansion (%)				
			Plain Portland Limestone	Type GU	GUL 11	GUL13	GUL22
			0	2.4	10.6	12.7	21.8
23	0	6 months	0.188	0.267	0.271	0.485	0.562
		12 months	1.69	1.554	1.854	2.978	1.479
		18 months	X	X	X	X	X
	30	6 months	0.04	0.036	0.031	0.029	0.03
		12 months	0.053	0.044	0.038	0.038	0.039
		18 months	0.064	0.054	0.05	0.048	0.049
	50	6 months	0.025	0.023	0.016	0.018	0.018
		12 months	0.032	0.028	0.021	0.022	0.022
		18 months	0.04	0.036	0.03	0.031	0.031
5	0	6 months	0.067	0.097	1.26	X	X
		12 months	1.42	X	X	X	X
		18 months	X	X	X	X	X
	30	6 months	0.028	0.031	0.031	0.032	0.036
		12 months	0.038	0.042	0.044	0.072	0.19
		18 months	0.065	0.063	0.093	0.237	0.642
	50	6 months	0.016	0.014	0.01	0.011	0.016
		12 months	0.025	0.024	0.018	0.019	0.023
		18 months	0.027	0.027	0.021	0.022	0.026

X = bars completely deteriorated

As expected, the high C₃A clinker PLCs all failed when used as the sole cementing material in both temperature exposures, however, the types of deterioration were different. By XRD analysis after 12m, the bars exposed at 23 °C formed ettringite, while those exposed at 5 °C formed mainly thaumasite and disintegrated. Higher levels of limestone in the cement shortened the time to onset of expansion at both 23 and 5 °C. Expansions were significantly reduced with 30% slag replacement of PLC but it was not sufficient to prevent all signs of expansion and visual deterioration at 5 °C. In those samples, thaumasite was detected by XRD but the visual signs of deterioration were more similar to the damage observed in bars stored at 23 °C. However, with this source of cement, 50% slag has been found to provide high sulphate resistance of concrete in Ontario for over 30 years. The data in Table 2 shows that 50% slag is also able to prevent deleterious expansion or signs of deterioration in both temperature exposures. XRD analysis did not show any evidence of thaumasite formation in any of the 50% slag mixtures stored at 5 °C after 18 months exposure.

4. CONCLUSIONS

Standard sulphate resistance tests where specimens are stored at laboratory temperatures will not predict the potential for deterioration due to the thaumasite form of sulphate attack. Results from a modified ASTM C1012 sulphate resistance test with bars exposed at 5 °C have shown (a) that damage due to thaumasite can occur in the presence of sufficient quantities of limestone interground with the Portland cement and, (b) that it can be prevented by using the same levels of slag replacement of normal Portland cement normally used to prevent the ettringite form of sulfate attack that occurs at 23 °C. While thaumasite was found to be presenting all the Portland and PLC bars stored at 5 °C, there was no evidence of thaumasite in PLC plus slag mixtures when stored at 5 °C. Similar testing by R. L. Day at University of Calgary and M.D.A. Thomas at University of New Brunswick resulted in the same conclusions when pozzolans were used. As a result, the Canadian CSA A3000 cement standard was amended in 2010 to allow blended cements made with PLC to be used in sulphate exposures if they also contain at least 25% Class F fly ash, 40% ground-granulated blast-furnace slag, 15% metakaolin, and ternary blends with 5% silica fume and either 25% slag or 20% Class F fly ash. In addition to these prescriptive limits, ASTM C1012 bars stored in 5% sodium sulphate solution at 5 °C must have expansions of less than 0.10% at 18 months (with a supplemental limit of 0.10% at 24 months if the increase in expansion between 12 and 18 months exceeds 0.03%). These requirements are in addition to previous requirements, for the ettringite form of sulphate attack, that standard ASTM C1012 bars stored at 23 °C have expansions of less than 0.10% at 12 months. Sulphate exposure tests of a wide range of concretes outdoors at cool temperatures are underway to confirm the laboratory results.

REFERENCES

1. Hooton, R.D. and Brown, P.W., "Development of Test Methods To Address the Various Mechanisms of Sulfate Attack," RILEM Proceedings, PRO63, Concrete in Aggressive, Aqueous Environments, June 3-5, 2009, Toulouse, Vol. 2, pp.280-297.
2. Hooton R.D., Ramezaniapour A., and Schutz, U., "Decreasing the Clinker Component in Cementing Materials: Performance of Portland-Limestone Cements in Concrete in combination with Supplementary Cementing Materials", CD Proceedings, 2010 Concrete Sustainability Conference, NRMCA, Tempe, Arizona, April 12-15, 2010.
3. CSA A3000 Cementitious Materials Compendium, Canadian Standards Association, Toronto, Canada (2008 Edition, updated Oct. 2010). www.csa-international.org

Concrete Durability Based on Coupled Laboratory Deterioration by Frost, Carbonation and Chloride



Erika Holt
Ph.D., Senior Research
Scientist
VTT Technical Research
Centre of Finland
P.O. Box 1000
FI-02044 VTT, Finland
erika.holt@vtt.fi



Markku Leivo
Dr. (Tech.), Senior
Research Scientist
VTT Technical Research
Centre of Finland
P.O. Box 1000
FI-02044 VTT, Finland
markku.leivo@vtt.fi

ABSTRACT

Concrete performance is typically based on deterioration caused by one mechanism alone. The service life of a structure is linked to reaching limit states that are estimated from models based of laboratory data. Accelerated laboratory tests are conducted as independent studies of performance, such as single assessments of frost, frost-salt, chloride ingress or carbonation induced corrosion acting alone. Yet in real field performance, concrete is actually being affected by simultaneous environmental and conditional exposures. This paper presents a new approach to evaluating durability: by coupling deterioration mechanisms within laboratory testing to more accurately predict long-term performance.

Key words: durability, frost, frost-salt, carbonation, chloride, service life, field stations

1. INTRODUCTION

When durability of concrete is evaluated, many types of exposure or attack may be considered to influence the structural performance. Yet tools for predicting the lifetime of concrete materials are typically based on one driving force of the deterioration, such as spalling due to de-icer salt with frost exposure or cracking caused by chloride ingress and subsequent reinforcement corrosion. Accelerated laboratory tests are used to test these individual deterioration mechanisms and correlate the results to real-time performance of structures. In reality, existing structures are subjected to numerous and sometimes simultaneous forms of deterioration in their relative environments. Thus laboratory simulations and deterioration predictions should take into account these multiple, interacted deterioration parameters when modelling service life.

A three year Finnish research project has recently been completed investigating deterioration when concrete is subjected to multiple attacks. For instance, evaluating how cracks resulting from frost attack influence chloride ingress, or how carbonation changes the surface properties and thus may affect frost-salt scaling. The project builds on 30+ years of concrete durability research, including 10 years of field station studies. The latest project's laboratory program has been based on standardized test methods, taking into account the affects of ageing and repeated exposure cycles to different conditions as well as field studies [1]. The final stage of the project addressed improving service life prediction tools based on the laboratory coupled deterioration

results [2]. The project results have quantitatively supported the hypothesis that a holistic approach should be taken to predicting deterioration.

2. MIX DESIGN AND TEST PROGRAM

About 30 different normal strength concrete mixtures have been evaluated with coupled deterioration attack with a range of cementitious binders and air contents. The mix designs were chosen to represent prevailing ready-mix and pre-cast production. Common Finnish cements, blast furnace slag (BFS) and fly ash (FA) were used along with Glenium superplasticizer and Ilma-Parmix air entrainment. The compressive strengths were up to 60 MPa and the effective water-to-binder ratio ranged from 0.40 to 0.60. Some concretes were intentionally produced with no or only inadequate air entrainment, to allow for more rapid deterioration and thus modelling a range of behaviours. Full details of the mixture designs are detailed within the project reports and public database. The coupled deterioration testing has included the following combinations:

- 1) carbonation and frost (effect on water ingress and internal damage),
- 2) carbonation and frost-salt (effects on scaling),
- 3) carbonation and chloride (effects on corrosion),
- 4) frost and chloride (effects of internal cracking on chloride penetration).

In the first two cases of carbonation and frost, testing was done on newer samples as well as ones aged one year and dried at 65% RH, with or without surface carbonation. In the first three of the four series, the reverse order of testing was also done, for instance either carbonation followed by frost, or then first frost followed by carbonation, as shown above. Frost and frost-salt was tested for at least 56 cycles using the Borås slab test (CEN/TC 51 N 722) to assess internal damage and surface scaling. Accelerated carbonation was tested at both 1% and 4% CO₂ compared to normal (non-accelerated) carbonation at 60% RH and 20°C and the field. The chloride diffusion was measured with the CTH method (NT Build 492) at various ages as well as using chloride profiling of field samples by grinding. Carbonation depth was measured using phenolphthalein indicator solution (EN 13295). In some cases, it was possible to subject the samples to repeated cycles of the same two attack types, for instance carbonation and frost attack, followed by additional round(s) of carbonation and frost exposure in lab conditions. Microscopic studies and real-time exposure at field stations have supplemented the lab results.

3. RESULTS

The selected project results reported here are focused on examples of the influence on durability when replacing cement with by-products of fly ash or blast furnace slag, for both individual and combined deterioration attack. Investigations of interacted deterioration caused by frost-salt combined with carbonation have shown the influence of the surface layer and pore structure properties when assessing scaling, or vice-versa. These tests were done on reference samples were aged for 1 year, dried and then the sample surface layers were cut away (any possible carbonated layers removed) before exposure to 56 cycles of the slab test with NaCl solution. The second series of combined deterioration had atmospheric exposure to carbonation for one year (65% RH storage), followed by the same frost-salt test.

An example of how the mix design and mineral admixtures affect coupled durability performance is shown in Figure 1. These results are for mixtures with either 50% slag or 24% fly ash ($w/b_{\text{eff}}=0.42$ and 5% air). For single deterioration exposure of frost alone, both mixtures containing by-products had less damage than the reference mix. Yet when exposed to coupled attack of carbonation with frost, the performance of the fly ash mixture was worse than the reference and slag mixtures. This indicates that the pore structure of the fly-ash containing mixtures was detrimentally altered due to carbonation and/or the 1 year of drying at 65% RH, and thus showed worse durability performance. When examining the same test series with respect to internal damage during the frost-salt test, there was no significant damage or variation in the mixtures with or without the carbonation exposure.

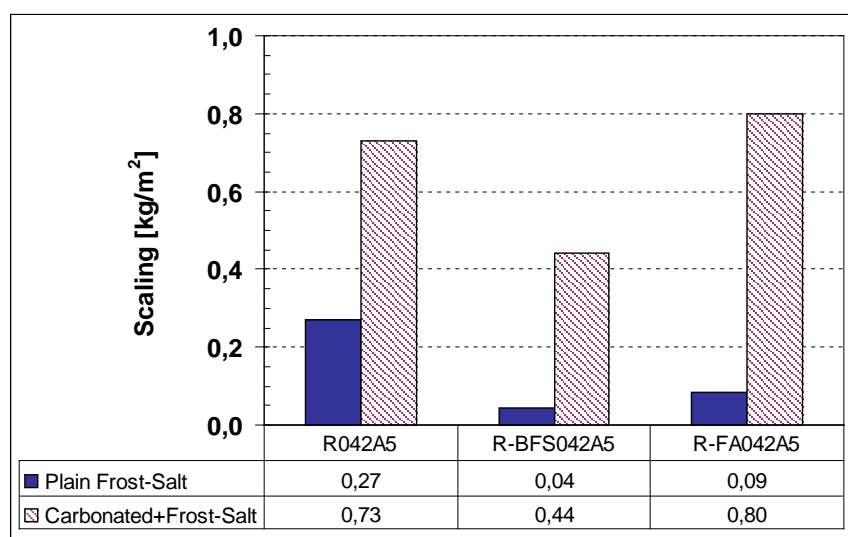


Figure 1 - Influence of carbonation on scaling from frost-salt testing, for reference mix with Rapid cement (R) compared to mixtures with 50% slag (BFS) or 24% fly ash (FA) mixtures.

In another test series of combining chloride attack with carbonation in the interacted durability study, the goal was to see what influence the surface and pore structure properties have on the carbonation. In this series of tests, the pore structure and thus surface layer properties were altered by exposing the samples to a rapid chloride migration test prior to strong carbonation exposure of 4% CO_2 for 56 days. An example of the carbonation test results are shown in Figure 2, with the standard deviation of the measurements indicated by the error bars. The left side solid bar indicates the carbonation measured after CO_2 exposure alone (with no chloride exposure). The other results are from after the chloride plus carbonation exposure, on both the non-chloride side of the sample (exposed to NaOH, indicated by the middle lined bars) and on the chloride exposure side (Cl indicated by the right side dotted bars). The results show a significant drop in the level of carbonation depth for samples that had been exposed to chlorides.

Comparing the effect of cement type, the sulphate resistant cement (mix SR05A2) had the lowest amount of carbonation in both cases of individual or combined influence with chloride ingress. After the combined deterioration exposure, there was extremely low carbonation, showing great durability. The mixture with a higher air content (Y05A5 compared to Y05A2) had the highest level of carbonation in both cases as well. Including blast furnace slag (mix R-BFS05A2) showed the most benefit in reducing carbonation depth alone, though the impact was insignificant in the case of combined deterioration of carbonation and chloride. After chloride exposure, the carbonation levels were nearly equivalent for the reference (mix Y05A2) mixture compared to mixtures containing either fly ash or blast furnace slag.

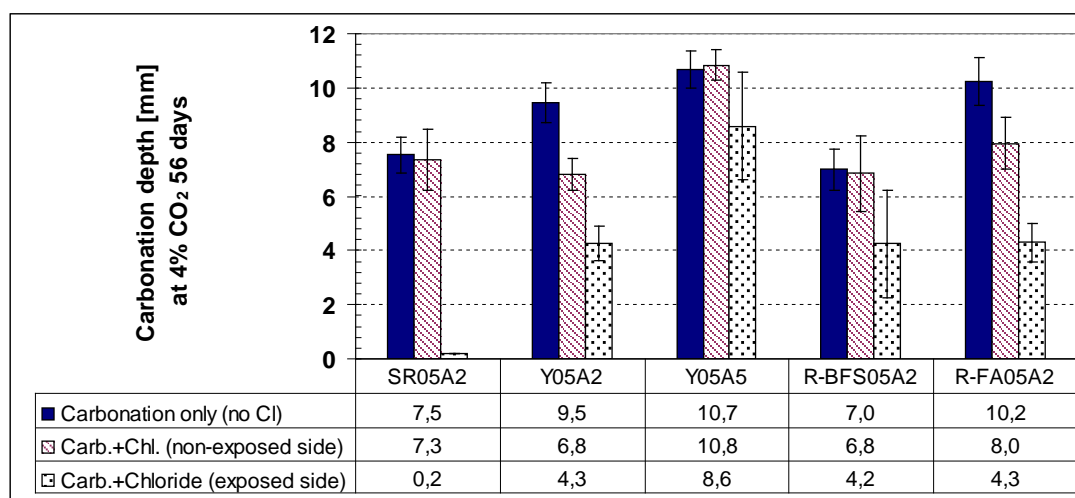


Figure 2 - Influence of chloride ingress on carbonation depth (cements: SR= sulphate resistant, Y=Yleis XX cement, R=Rapid cement; binders: BFS=blast furnace slag, FA= fly ash; air: A2=2% air, A5= 5% air)

Within the scope of the project, new testing procedures have been tried on mortars to evaluation the effects of carbonation on chloride ingress. Additional test results are shared within the scope of the presentation, including further results of chloride-carbonation interaction and the impact of moisture content on chloride ingress.

4. SUMMARY

These results presented here give a small example of the wide range of laboratory investigations that have been a part of the Finnish interacted deterioration project. All of the results of this project as well as two earlier Finnish durability projects in cooperation with Aalto University are available on a public database for evaluation and future cooperative studies. The research has shown that single attacks tested in laboratory conditions yield different results than what may actually be experienced in field applications or in-situ concrete structures, where multiple degradation types are occurring simultaneously. The new interacted durability laboratory results have been combined with field studies to improve durability models and service life prediction tools. The results have had an impact on Finnish concrete practice and durability guidelines.

REFERENCES

1. Kuosa, H., "Concrete Durability Field Testing in Finland," *Proceedings of Nordic Concrete Research Symposium*, Finland, June 2011, 4 p.
2. Vesikari, E., "Modeling of Carbonation and Chloride Penetration Interacted by Frost Damage in Concrete," *Proceedings of Nordic Concrete Research Symposium*, Finland, June 2011, 4

Effect of NaCl and different CO₂ concentrations on the mineral compositions of a hardened cement paste



Fahim Al-Neshawy
Lic.Sc.
Aalto University
School of Engineering
Department of Structural
Engineering and Building
Technology
P.O.Box 12100,
FIN-00076 Aalto, Finland
fahim.al-neshawy@aalto.fi



Esko Sistonen
Ph.D., Act. Professor
Aalto University
School of Engineering
Department of Structural
Engineering and Building
Technology
P.O.Box 12100,
FIN-00076 Aalto, Finland
esko.sistonen@aalto.fi



Jukka Piironen
M.Sc.
Aalto University
School of Engineering
Department of Structural
Engineering and Building
Technology
P.O.Box 12100,
FIN-00076 Aalto, Finland
jukka.piironen@aalto.fi

ABSTRACT

Carbonation of concrete is often at the origin of the corrosion of the steel reinforcement which is actually one of the main causes for the degradation of concrete structures. The degradation might be more significant in the case of chloride ingress. The objective of this paper is to determine the relationship between the chemical change of the hardened cement paste and accelerated carbonation using different CO₂ concentrations with the presence of chloride ions. For this purpose, cement paste samples was prepared and stored in different environmental conditions. The chemical changes of the cement paste were analyzed by using X-Ray diffractometry and thermal analysis.

Key words: cement paste, carbonation, sodium chloride, chemical analysis.

1. INTRODUCTION

1.1 General

Carbon dioxide (CO₂) in the air can penetrate into the concrete; dissolve in the pore solution, and react with calcium hydroxide, leading to water formation and calcium carbonate precipitation. The carbonation is a diffusion based phenomenon, where the carbonation front moves inwards the concrete at a rate proportional to the square root of time. The rate of the reaction of the hardened cement pastes with CO₂ is known to depend strongly on the w/c of concrete, mixture composition, pore structure, temperature and curing conditions of concrete and its internal humidity. [1]

1.2 Carbonation mechanism

Carbonation of hydrated cement compounds, i.e. essentially calcium hydroxide (Ca(OH)_2) and calcium silicate hydrate (C-S-H) is a chemical reaction of neutralisation of bases by an acid, the carbon dioxide in the air, which can be represented by the simple equations (1) and (2):



These reactions take place in solution and the reactants have to dissolve before reacting. The solubility of calcium hydroxide is reduced by sodium and potassium hydroxides. These reactions induce a reduction of the pH of the pore solution to such a value that the steel reinforcement is no longer protected against corrosion. [2]

1.3 The interactions between chloride and concrete

When concrete is in contact with a chloride solution, chloride ions penetrate in the pore solution. They appear in concrete both as free Cl^- ions (meaning water-soluble ions) in the pore interstitial solution and as chemically bound component of hydrate phases (e.g., Friedel's salt $\text{Ca}_2\text{Al(OH)}_6\text{Cl}\cdot 2\text{H}_2\text{O}$). Free chloride ions are the most dangerous because of their capacity to diffuse towards the steel bars [3].

2. MATERIALS AND TEST PROCEDURE

Cement paste samples were prepared by mixing the cement with water at a water cement ratio (w/c) of 0.5. The cement use was a Rapid cement type CEM II/A -LL 42.5 R, produced by Finnsementti OY. The chemical analysis of the cement is shown in Table 1. The cement paste was filled into 8 plastic bottles, which were sealed then rotated for 8 hours and allowed to cure for 28 days at room temperature (22°C). The procedure of preparing the cement paste samples is shown in Figure 1.



Figure 1. Preparation of the cement paste samples

Table 1 Chemical analysis of the type I cement used in this study

CaO	SiO ₂	Al ₂ O ₃	Fe ₂ O ₃	C ₃ S	C ₂ S	C ₃ A	C ₄ AF	MgO
65 %	1 %	5,3 %	3,1 %	68 %	9 %	9 %	10 %	2,7%

After curing, the specimens were demoulded. One reference sample was kept sealed to avoid carbonation. As shown in Figure 2, samples were exposed either to a combination of 4% CO_2 -concentration and 10%-NaCl solution or pure carbonation at 1%, 4% or normal CO_2 -concentrations. One sample was exposed to 10%-NaCl solution only. The relative humidity during carbonations was kept at a 65%.

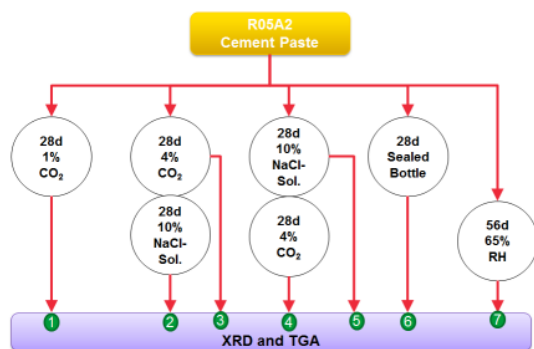


Figure 2. Test procedure for the cement paste samples

The chemical changes of the cement paste were analyzed by using X-Ray diffractometry and thermal analysis.

3. RESULTS AND DISCUSSION

The summary of the contents of the crystalline compounds in the samples is presented in Table 2. The estimates presented for the amounts of the minerals are based on the relative intensities of the reflections observed in the XRD diagrams (shown in Figure 3) of the samples. Thus, they are only valid for each sample separately, and the estimates cannot be compared with each other.

Table 2. The content of the crystalline compounds in the cement pastes (XRD).

	28 d Sealed bottle	28d 1% CO ₂	28d 4% CO ₂	28d 4% CO ₂ + 28d 10% NaCl	28d 10% NaCl	28d 10% NaCl + 28d 4% CO ₂	56d RH 65%
calcite	++++	+++++	+++++	+++++	+++++	+++++	+++++
aragonite	-	++	++	++	++	++	++
vaterite	-	++	++	++	-	++	++
portlandite	+++++	++	++	-	+++	-	+++
C ₂ S	(+)	+++	++	++	++	+++	+++
C ₄ AF	(+)	(+)	(+)	(+)	(+)	(+)	(+)
ettringite	+++	++	+	-	++	+	+
gypsum	+++	-	-	++	-	-	-
halite	-	-	-	+++++	++	+++	-
	+++++	very high	+++	medium	+	very low	
	++++	high	++	low	-	not detected	

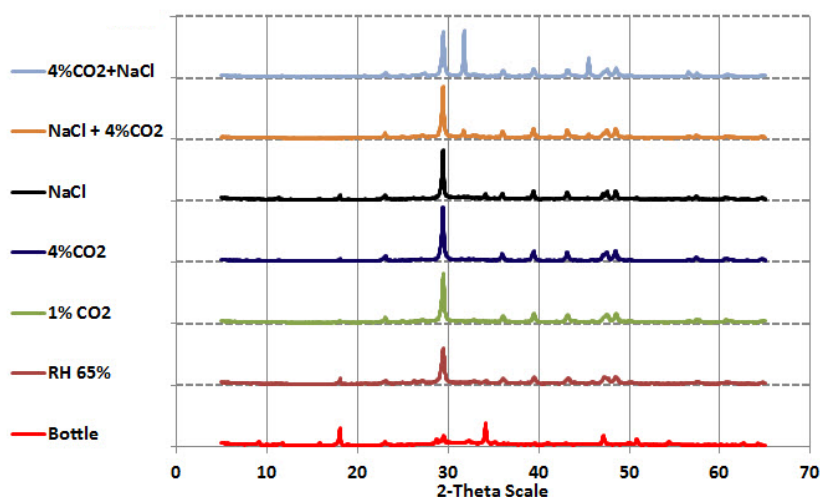


Figure 3. X-ray diffraction diagrams for the samples analyzed.

The thermal behaviour of the paste samples (bottle), (1% CO₂), (4% CO₂) and (RH65%) was very similar. The thermal behaviour of the paste samples (4% CO₂ + 10% NaCl), (10% NaCl) and (10% NaCl + 4% CO₂) was somewhat different from the behaviour of the four other paste samples. However, their behaviour could also be divided into eight successive phases during which degradation reactions causing mass loss were detected. The thermal curves of the cement pastes are shown in Figure 4.

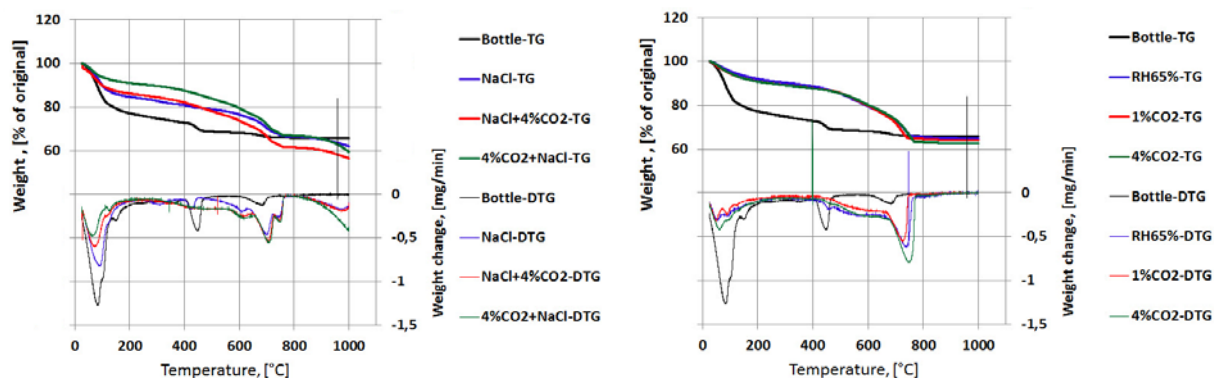


Figure 4 TG and DTG curves for the different samples

4. CONCLUSION

In this paper, a study on the chemical changes and phase analysis of cement paste due to accelerated carbonation and chloride penetration has been carried out by XRD and Thermo gravimetric analysis.

The results indicate that the content of the crystalline compounds and the thermal behaviour of the cement paste were similar to all of the samples exposed to accelerated carbonation regardless of the CO₂-concentration. The chloride penetration caused a difference in the content of the crystalline compounds and the thermal behaviour of the cement paste.

REFERENCES

1. Castellote, M., Fernandez, L., Andrade C. and Alonso C. (2008). Chemical changes and phase analysis of OPC pastes carbonated at different CO₂ concentrations. RILEM, Materials and Structures, Volume 42, Number 4, pp. 515-525.
2. Houst, Y. F. (1996). The role of moisture in the carbonation of cementitious materials. International journal for restoration of buildings and monuments, Volume 2, pp. 49-66.
3. Barberona, F., Baroghel-Bounya, V., Zannib, H., Bressonc, B., Cailleric, J-B., Malosseb, L. and Gan, Z. (2005). Interactions between chloride and cement-paste materials. Elsevier, Magnetic Resonance Imaging 23, pp. 267-272
4. Bertos, M.F., Simons, S.J.R., Hills, C.D. and Carey, P.J. (2004). A review of accelerated carbonation technology in the treatment of cement-based materials and sequestration of CO₂. Elsevier, Journal of Hazardous Materials B112. pp. 193-205.

Concrete durability field testing in Finland



Hannele Kuosa
M.Sc. (Tech.), Research Scientist
VTT Technical Research Centre of Finland
P.O. BOX 1000
FI-02044 VTT, Finland
E-mail: hannele.kuosa@vtt.fi

ABSTRACT

There are three Finnish concrete field testing stations containing approximately 90 different concrete mixture designs that have been placed over a 10 year period. There is no other method as reliable as field testing to get reference data for service life models. In field testing all interacted deterioration is included - e.g. chloride penetration is interacting with carbonation and frost deterioration. Field testing includes e.g. moisture, salt exposure, temperature and solar radiation variations and effects of carbon dioxide and hydration with time. This presentation is mainly concentrated on relatively new highway field testing and sheltered carbonation testing in Finland. Some field results and comparison with laboratory testing results are presented [1].

Key words: Field testing, durability, frost-salt, frost, chloride, carbonation, interacted deterioration, ageing

1 INTRODUCTION

Of the Finnish field stations, two are without salt and one highway testing field has salt exposure. The fields without salt exposure are in southern and northern Finland. Several test series with different binding materials have been prepared during three different projects at the EU, Nordic and Finnish levels. Some parallel highway field concretes are located in field stations in both Borås, Sweden, and in Kotka, Finland, to find out possible differences.

All field testing results for the mixes prepared after 2007 in the national DuraInt project as well as all the updated field testing data for the former field testing projects in Finland - CONLIFE (2001-04) and a parallel national project YmpBetoni (2002 - 04) with Finnish ecological binding materials are today summarized in an Excel-format database. This data will be updated for the service life modelling work together with other available field testing data, such as the longer-term BTB-project data (Borås, 1996). All of the above projects have included extensive laboratory testing programs. Here only the most recent DuraInt field testing results and comparison with laboratory testing is presented. Field testing has included also e.g. collection of weather data and data on highway salting. At the highway field there has also been specimen for concrete temperature and humidity follow up and a novel study on the use of optical fibres for the measurement of concrete moisture content (Englund/Fortum R&D).

This presentation is in connection with separate presentations on interacted laboratory (Holt & Leivo, VTT) and service life prediction studies (Vesikari, VTT).

2 CHLORIDE PENETRATION STUDIES

The aim was to get long term field testing data and understand the effect of binding material, w/b ratio, air content and specific concrete surface treatments (impregnation, form lining) on chloride penetration. Field specimen (300 x 300 x 500 mm³, 2/concrete) were placed mainly at a distance of 4.5 m from the road lane on wooden stands. For some parallel specimen this exposure distance is also 6 m, 8 m and 10 m. Four parallel concretes are at Borås testing field in Sweden. For field chloride analysis, cylinders (ø100 mm) were cored from the field specimen. Powder samples were taken from these cylinders for chloride content analyses by a profile grinding method and by dry-slicing. Chloride profiles have so far been created after the 1st and mostly also after the 3rd winter. These profiles represent the vertical surfaces facing towards the highway. In the laboratory chloride migration coefficients (D_{nssm}) were measured at 3 months age by the CTH-method (NT Build 492). In Figures 1 and 2 there are some examples on the results to date.

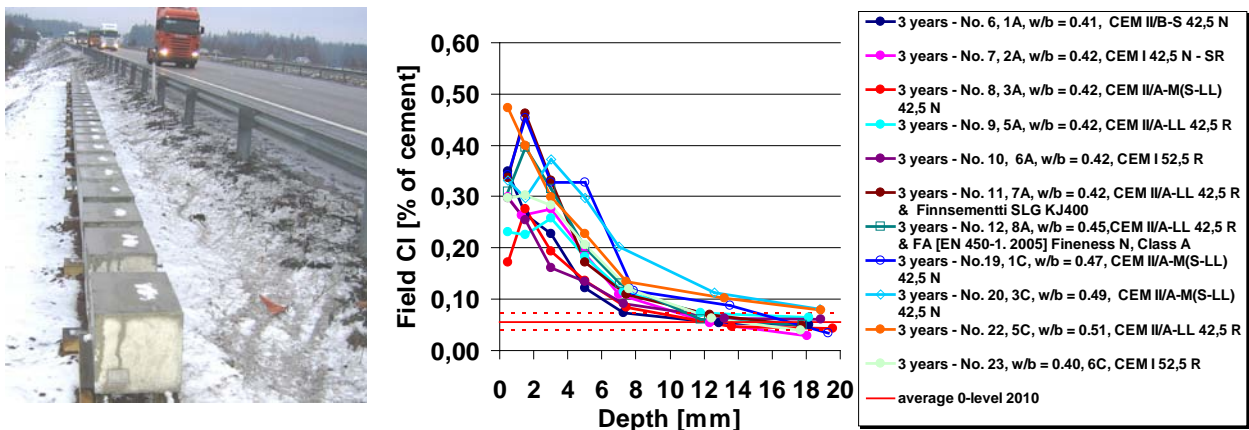


Figure 1. Field specimen for chloride penetration studies at highway testing field and chloride ingress profiles after three winters (2007-2010) for specimen with different binding materials and w/b ratios. All these specimens are at 4.5 m from the highway lane.

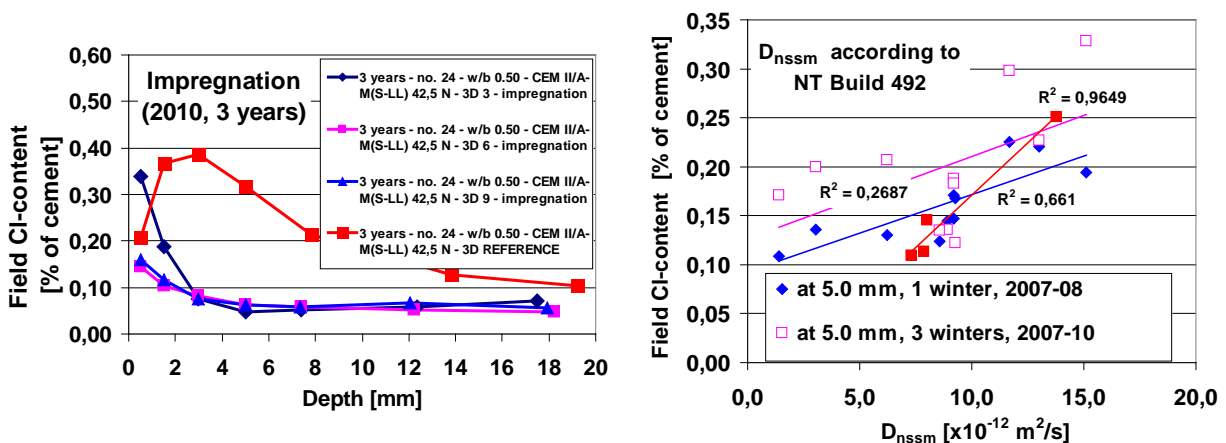


Figure 2. Left chloride ingress profiles after the 3rd winter season for the specimen with impregnation and for the reference, and right chloride content at field at 5.0 mm from the specimens surface after the 1st and 3rd winter season as a function of D_{nssm} (NT Build 492). Good correlation only after the 1st winter season.

3 CARBONATION STUDIES

After de-moulding at 1 d, carbonation specimen (beams 100x100x500 mm³) were cured in water. At 7 d they were moved to a climatic room with RH 65 % (+ 20 °C). Measurement of carbonation depth was done essentially as described in [EN 13295]. Testing in the field and laboratory after 7 d age was otherwise as below:

- Carbonation continued in laboratory climatic room with RH 65 % (+20 °C).
- Field carbonation sheltered was started at about concrete age 28 d.
- Accelerated carbonation in a sealed cabinet with 1 % CO₂, RH 60 % and 21°C was started at concrete age 28 d.

The average field carbonation times are 268 days and 772 days (January 2011). The coefficients for carbonation (k-values) were calculated by the common equation: Carbonation [mm] = $k\sqrt{t}$, where t is the carbonation time [d] and k is the coefficient for carbonation [mm/d^{0.5}]. Some examples from the field and laboratory results are presented in Figures 3A - D. There is quite good general correlation between field, laboratory RH 65 % and 1 % CO₂ accelerated carbonation (Fig. 3A). The effect of e.g. w/b, compressive strength (Fig. 3C) or CO₂-diffusion coefficient, binding materials and air content (Fig. 3D) should be included in the modelling of field carbonation, as well as all the exposure factors.

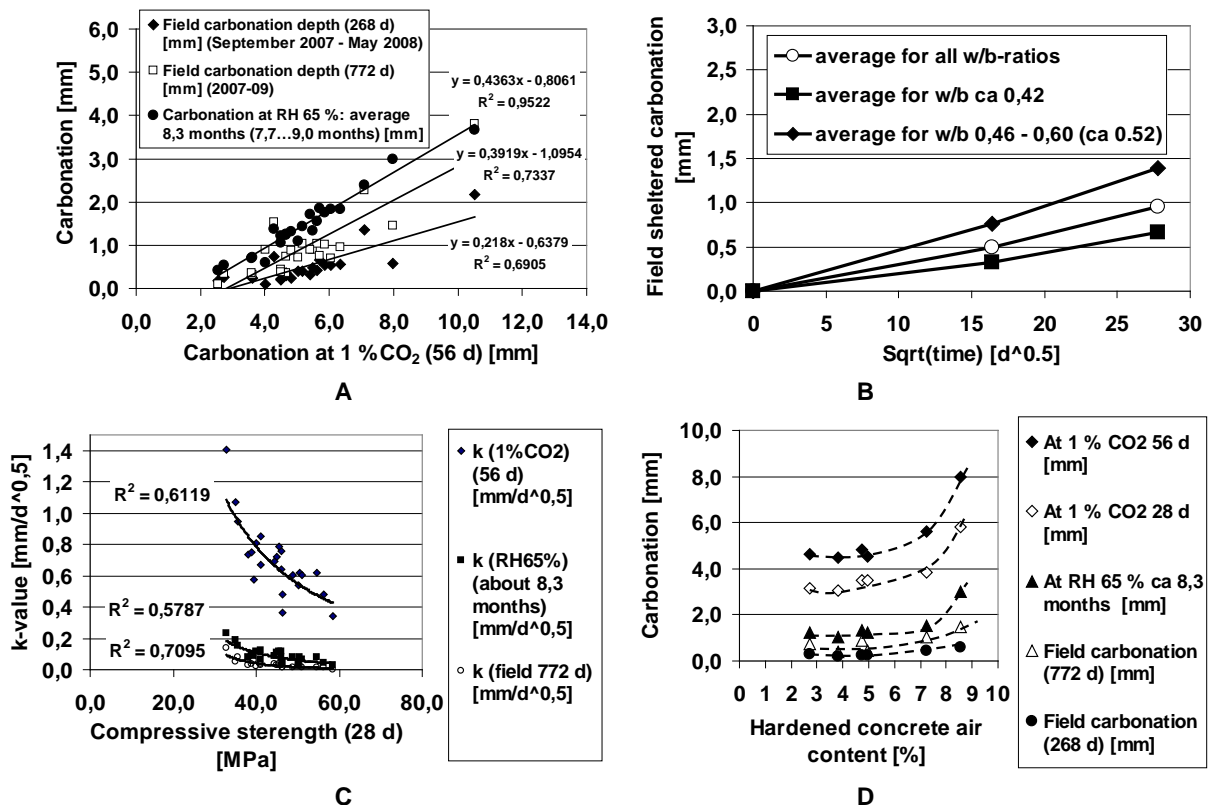


Figure 3 A) Carbonation at RH 65 % and at field sheltered (772 d) as a function 56 d carbonation at 1 % CO₂ (at RH 60 %). B) Field carbonation sheltered as a function of square root of time for concretes with w/b ca 0.42 (14 mixes), with w/b 0.46 – 0.60 (9 mixes, average w/b ca 0.52) and the average carbonation for all the concretes (14 + 9 = 23 mixes). C) Carbonation k-value as a function of compressive strength. D) Carbonation as a function of air content, when the binding material (CEM II/A-M(S-LL) 42,5 N) and w/c ratio (0.42) is the same for all the mixes.

4 FROST-SALT AND FROST STUDIES

The aim was to get field testing data as well as versatile laboratory testing results on the effect of binding material, w/b ratio, air content and air pore structure on freeze-thaw durability with and without salt exposure. Field specimen (75x150x150 mm³), (3+1)/concrete) were situated in wooden stands in the field with no salt exposure and in addition in metal racks at the highway field with salt exposure (Fig. 4A). Frost- or frost-salt scaling (volume change) and internal deterioration (RDM by ultrasound and fundamental frequency) have been monitored. There was an extra field specimen for future thin section studies on e.g. cracking, scaling and carbonation. After three winters (2007-10) there has been no major deterioration yet. Even the concretes with no air entrainment have managed well so far (3 winters) beside the highway.

In all 21 mixes the frost-salt/frost testing was done in laboratory after three curing conditions:

- By the standard Slab test method at 28 d [CEN/TR 15177, CEN/TS 12390-9].
- As 'aged and carbonated' after ca 1 year at RH 65%, i.e. including also surface drying at RH 65 % (+20 °C).
- As 'aged but not carbonated' (>1 year at RH 65 %). In this case at RH 65 % partly carbonated surface layer (10 mm) was sawed off. Sawing off the surface layer also meant that the final testing surface drying degree was smaller than in the case b) above.

Testing was always started in the normal way, by re-saturation of the specimens. Frost-salt scaling after 56 cycles is presented in Fig. 4B. It can be seen that carbonation and ca 1 year drying at RH 65 % clearly affected the frost-salt scaling. Hydration, carbonation and drying will have an effect on frost-salt scaling. Thus all ageing should be included in the models for frost-salt scaling. Concrete composition will have an effect on the significance of ageing.

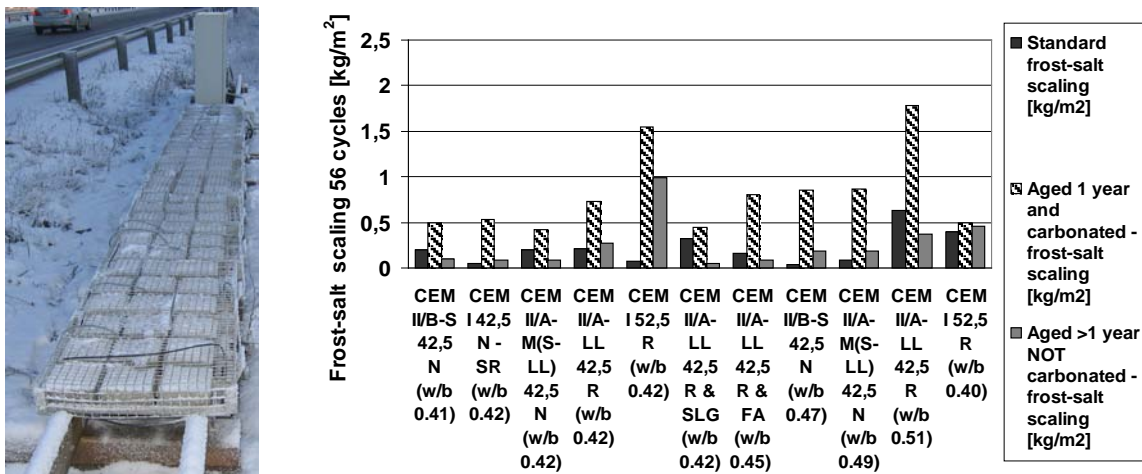


Figure 4. Specimen for frost-salt scaling at highway testing field and laboratory Slab test frost-salt scaling (56 cycles) by standard method (at 28 d), after 1 year surface drying and carbonation at RH 65 % and after no carbonation and lower surface drying degree at RH 65 % (age over 1 year, 10 mm surface layer was sawed off before testing).

REFERENCES

- Kuosa, H. 2011. Concrete durability field testing. Field and laboratory results 2007 - -2010. Research Report VTT-R-00482-11.

Impact of Hydrated Cement Paste Content and Entrained Air-Void System Parameters on the Durability of Concrete



Karl Peterson, Ph.D.
University of Toronto
35 Saint George Street,
Toronto, Ontario M5S 1A4
Canada
karl.peterson@utoronto.ca



Lawrence Sutter, Ph.D.
Michigan Technological Univ.
1400 Townsend Dr.,
Houghton, Michigan 49931
USA
llsutter@mtu.edu

ABSTRACT

A comprehensive investigation of the effects of hydrated cement paste quality and air-void system parameters on freeze-thaw durability was conducted. Fresh concrete testing such as ASTM C231, physical testing such as ASTM C666, and microscopical evaluation were combined to assess these effects. As a result of this study, a relationship between hydrated cement paste content, air-void system spacing factor, and air content was observed. Even without detailed measurements of the air void size distribution, the ASTM C231 air content results and paste content estimates perform just as well as the spacing factor calculation at predicting F-T performance.

Key words: freeze-thaw durability, spacing factor, paste content, air content.

1. INTRODUCTION

In cold climates, concrete used in pavements and bridges must be able to withstand cyclic freezing and thawing (F-T). The larger study from which this work is drawn [1] is designed to examine whether traditional limits used to describe the air-void system still apply to concrete prepared with currently available materials and admixtures. Overall this research examines the relationship(s) between F-T durability and the quality of hydrated cement paste (HCP) integral to the concrete. This paper describes the results of characterization and F-T testing of a series of laboratory concrete mixtures that represent a variety of HCPs and air-void systems. Specifically, it examines the relationship between hydrated cement paste content, air-void system spacing factor, and air content with respect to predicting freeze-thaw performance.

2. METHODOLOGY

2.1 Mixture Design

The breadth of the mixture design matrix is too large to be presented in this short paper and is therefore only summarized. A total of 80 different concrete mixtures were prepared and each mixture was prepared in replicate. The mixture parameters used included three target air contents: (i.e. 2 and 3 % vol. air, both $\pm 1\%$, and 6 % vol. air, $\pm 1.5\%$) two air entraining admixture (AEA) types (i.e. one vinsol resin, one synthetic), supplementary cementitious materials (SCM) were included in some mixtures (i.e. Class C fly ash at 25% replacement level, ground blast furnace slag (GBFS) at 40% replacement level, four different total cementitious

material contents (CMC) (i.e. 335 kg/m³, 307 kg/m³, 291 kg/m³, 279 kg/m³), three water-cementitious ratios (*w/cm*): (i.e. 0.45, 0.50, and 0.52), one coarse aggregate (limestone), two different fine aggregate sources, and the aggregate gradings of the low CMC mixtures (291 kg/m³, 279 kg/m³), were optimized using the Shilstone Method [2].

2.2 Fresh Concrete Tests

A variety of fresh concrete tests were performed to assess the quality of the mixtures. The single test discussed in this paper is ASTM C231 *Standard Test Method for Air Content of Freshly Mixed Concrete by the Pressure Method*.

2.3 Hardened Concrete Tests

Several standard hardened concrete tests were performed on all mixtures. Those discussed in this paper include ASTM C666 *Standard Test Method for Resistance of Concrete to Rapid Freezing and Thawing* and ASTM C457 *Standard Test Method for Microscopical Determination of Parameters of the Air-Void System in Hardened Concrete*. One non-standard hardened concrete test was performed on all mixtures, *Hardened Air Content by Means of Flat-Bed Scanner* [3]. This test accomplishes the same measurements specified in ASTM C457.

3. RESULTS AND DISCUSSION

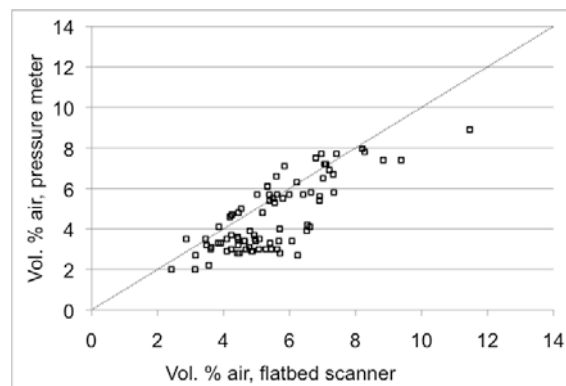


Figure 1 - Air content measured by flatbed scanner compared to that measured by ASTM C231 (pressure meter).

As shown in Figure 1, for the concrete mixtures prepared, the total air contents measured by flatbed scanner agree well with those measured by ASTM C231 (pressure meter). Likewise, but not shown, the spacing factor and specific surface measured by ASTM C457 and the flatbed scanner were in good agreement. The flatbed scanner has been demonstrated as an acceptable means of establishing the air-void system parameters.

However, adequate total air does not always guarantee adequate F-T performance. Alternatively, concretes with inadequate total air content can often perform well in a F-T environment. Therefore, guaranteeing F-T performance is clearly related to more than total air. Producing a concrete with an air-void system having a spacing factor of 0.1-0.2 mm or specific surface of 24-43 mm⁻¹, and a paste to air ratio of 4-10 is considered the best approach for guaranteeing F-T performance [4]. However, accurately and reproducibly measuring anything other than total air content in the field has not been demonstrated as being possible. One element of this research was to examine other approaches to measuring air-void system parameters or otherwise evaluating the F-T performance.

The pressure meter is the most common quality control test used to verify that an adequate air-void system has been produced in a concrete.

For the concrete mixtures prepared, Figure 2 shows the measured specific surface and spacing factor by flatbed scanner in terms of the target air content (Figure 2a) and in terms of durability factor as determined by ASTM C666 (Figure 2b). A durability factor less than 85% after 300 cycles was considered indicative of a non-F-T durable concrete. Figure 2a illustrates that in general, a minimum total air content of 6% results in a concrete mixture that has both an adequate air-void-system spacing factor and specific surface. Figure 2b illustrates that in general, an adequate air-void-system spacing factor and specific surface results in a concrete mixture that is F-T durable.

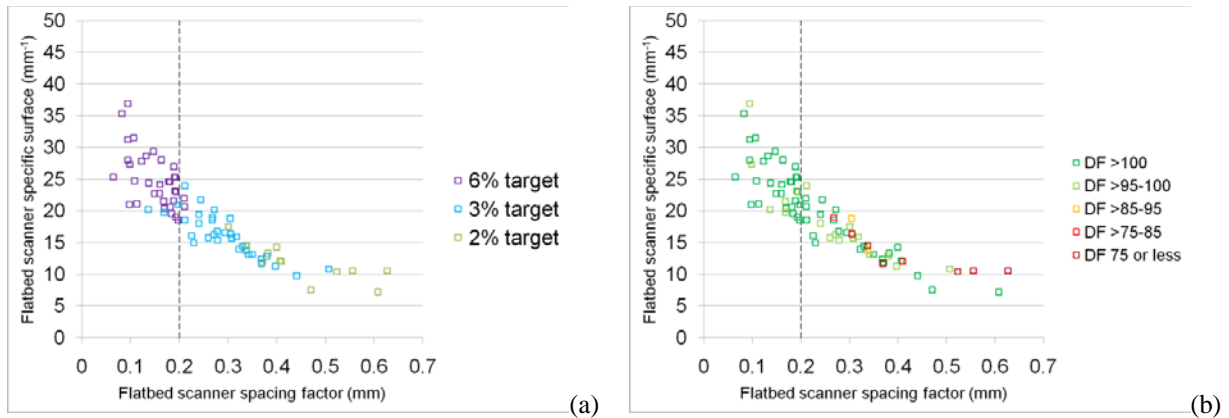


Figure 2 - Measured specific surface and spacing factor by flatbed scanner. Figure 2a shows the relationship in terms of the target air content and Figure 2b in terms of DF. Dashed line shows traditional spacing factor threshold at 0.2 mm.

Figure 3 shows the relationship between paste content and total air content for all concrete mixtures plotted according to ASTM C666 durability factor, CMC, and w/cm . A trend in F-T performance is noted indicating that paste content and total air content, together, could provide a reliable means of predicting F-T performance. For these mixtures the paste content was calculated from the mixture design. Paste content is defined as total concrete volume minus aggregate volume and pressure meter air volume.

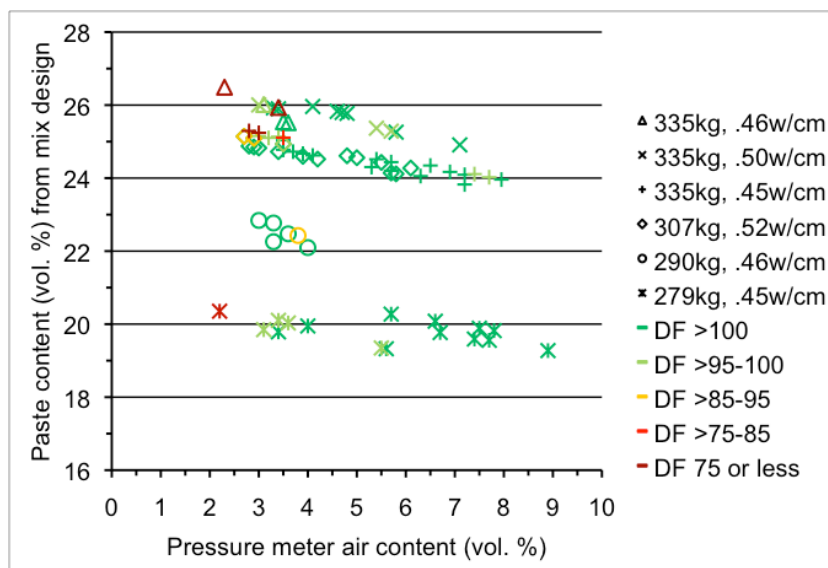


Figure 3 - Paste content vs. ASTM C231 (pressure meter) air content for all concrete mixtures plotted according to ASTM C666 durability factor, CMC, and w/cm .

Figure 4 plots the spacing factor, air content, and paste content in a 3-dimensional plot that illustrates in most cases, the combination of air content and paste content can be used to predict F-T performance consistent with the conventional approach of using the spacing factor alone.

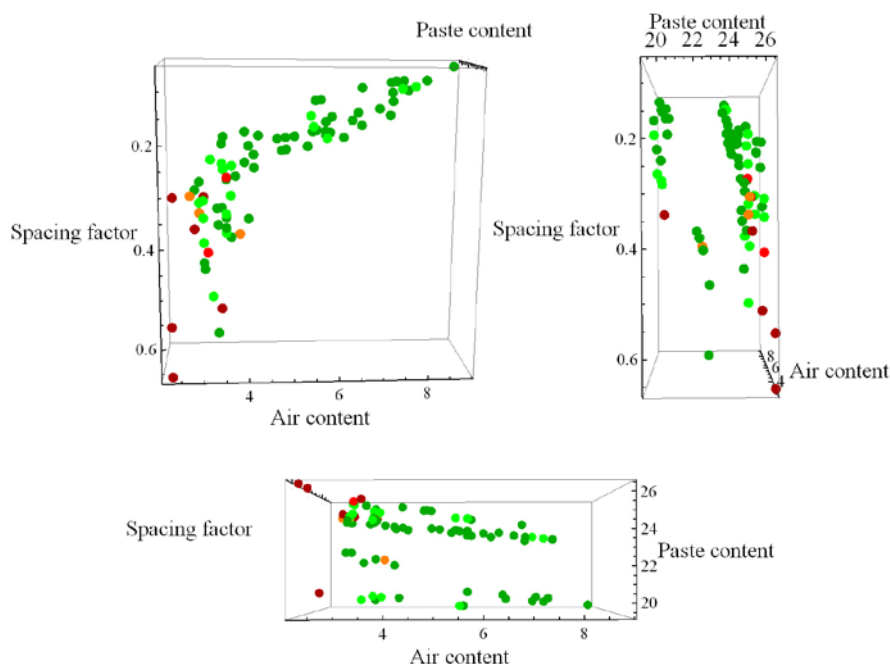


Figure 4 - Views of 3-dimensional plot of spacing factor, pressure meter air content, and paste content where points are color coded according to ASTM C666 Procedure B durability factor, dark red = DF 75 or less, red = DF >75-85, orange = DF >85-95, light green = DF >95-100, and green = DF >100.

4. CONCLUSIONS

The classic limitation of an air-void system spacing factor less than or equal to 0.2 mm is still a safe value to ensure F-T durability, but evidence exists that concrete mixtures with a spacing factor greater than 0.2 mm can also be F-T durable. Even without detailed measurements of the air void size distribution, the pressure meter air content results and paste content estimates perform just as well as the spacing factor calculation at predicting F-T performance.

REFERENCES

1. Sutter, L., & Peterson, K., "Impact of Hydrated Cement Paste Quality and Entrained Air-Void System on the Durability of Concrete: Final Report," *Michigan Department of Transportation*, in review.
2. Shilstone, J., "Concrete Mixture Optimization," *Concrete International*, American Concrete Inst., Farmington Hills, Michigan, USA, June 1990, Vol. 12, No. 6, pp. 33-39.
3. Peterson K., Sutter L., Radlinski M., "The Practical Application of a Flatbed Scanner for Air-Void Characterization of Hardened Concrete," *Journal of ASTM International*, Vol. 6, No. 9, 15 p., 2009.
4. American Concrete Institute Committee 201, "Guide to Durable Concrete, ACI Manual of Concrete Practice," ACI 201.2R-08, American Concrete Inst., Farmington Hills, Michigan, USA.

Modelling of Carbonation and Chloride Penetration Interacted by Frost Damage in Concrete



Erkki Vesikari
Lic. Tech.
VTT Technical Research Centre of Finland
P.O. Box 1000
FI - 02044 VTT, Finland
erkki.vesikari@vtt.fi

ABSTRACT

The main objective of this research was to analyse the results of laboratory and field tests on frost attack and the effects of frost attack on the rate of carbonation and chloride penetration. Both internal frost attack and frost scaling were studied. Differential equations for interacted degradation were developed. The results of carbonation and chloride penetration tests with internally damaged concrete samples were utilised in quantification of carbonation and chloride penetration rate. The process of simultaneously proceeding frost attack, carbonation and chloride penetration could be reproduced by computer simulation.

Key words: carbonation, chloride penetration, frost attack, interaction.

1. INTRODUCTION

The main focus in the project was laid on the field test results of frost attack (both internal and surface scaling) and the effects of frost attack on the rate carbonation and chloride penetration. As it was desired to apply these findings to practical service life design, a special effort was made to produce “interaction factors” for service life models based on the “factor approach”. By the interaction factors the accelerating effect of frost attack on carbonation and chloride penetration is taken into account.

The research consisted of the following parts: (1) theoretical study, (2) analysis of laboratory test results, (3) determination of service life factors, and, (4) computer simulation.

2. RESEARCH AND RESULTS

2.1 Theoretical study

This study was an attempt to develop a theoretical basis for practical service life models with respect to carbonation and chloride penetration in concrete with the interaction of frost attack.

In the case of concrete exposed to frost attack, the carbonation coefficient is increasing with the increased internal damage in concrete. In that case the total carbonation depth is determined as the sum of incremental carbonation depths which are determined from Equation 1. The carbonation coefficient $k_{ca;IntFr}$ increases with time with increased frost deterioration in concrete. Likewise the depth of frost scaling increases with time [1]:

$$x_{ca;Fr} = \sum \Delta x_{ca;Fr} \quad (1)$$

$$\Delta x_{ca;Fr}(t + \Delta t) = \frac{k_{ca;IntFr}^2(t)}{2} \cdot \frac{1}{x_{ca;Fr}(t) - x_{FrSc}(t)} \cdot \Delta t$$

where $k_{ca;IntFr}$ is the carbonation coefficient of concrete exposed to internal frost action,
 x_{ca} depth of carbonation as interacted by frost attack, and,
 x_{FrSc} depth of frost scaling.

Using the analogy with carbonation the depth of critical chloride content (with respect to corrosion initiation) can be determined from the Equation 2 [1].

$$x_{cl;Fr} = \sum \Delta x_{cl;Fr} \quad (2)$$

$$\Delta x_{cl;Fr}(t + \Delta t) = \frac{k_{cl;IntFr}^2(t)}{2} \cdot \frac{1}{x_{cl;Fr}(t) - x_{FrSc}(t)} \cdot \Delta t$$

where $k_{cl;IntFr}$ is the coefficient of chloride penetration in concrete exposed to frost action ,
and
 x_{cl} depth of critical chloride content.

2.2 Analysis of test results

To evaluate how the carbonation coefficient and the coefficient of chloride penetration ($k_{ca;IntFr}$ and $k_{cl;IntFr}$) depend on the of internal damage in concrete carbonation and chloride penetration tests with internally cracked concrete specimens were made. The residual dynamic modulus (RDM) was adjusted by freeze-thaw tests and ultrasonic measurements to predefined values, ranging between 0 – 100%, before starting the carbonation and a chloride penetration tests. The carbonation test was an accelerated test in a carbonation chamber with 1% CO₂. The chloride migration test was made using the standard NT Build 492.

According to the test results the depth of carbonation increases with increased internal frost damage (RDM) as presented in Figure 1a. In Figure 1b the increase of chloride migration coefficient with internal frost damage is presented [2].

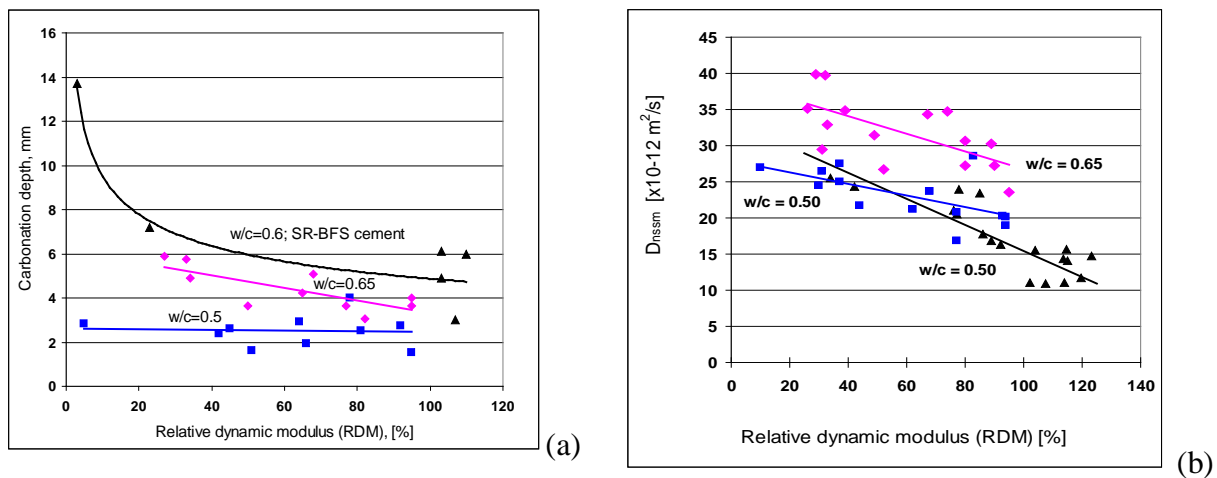


Figure 1 - The effect of internal frost damage (RDM) on (a) the depth of carbonation and on (b) the chloride migration coefficient of concrete.

Using the test results the average trend of the carbonation and chloride penetration coefficients as a function of RDM could be modelled as presented in Equations 3 and 4.

$$\frac{k_{ca;IntFr}(t)}{k_{ca0}} = 1 + 0.64 \cdot \left(1 - \frac{RDM(t)}{100}\right)^{1.32} \quad (3)$$

$$\frac{k_{cl;IntFr}(t)}{k_{cl0}} = 1 + 0.30 \cdot \left(1 - \frac{RDM(t)}{100}\right)^{0.93} \quad (4)$$

where k_{ca0} is the carbonation coefficient of undamaged (original) concrete, and k_{cl0} chloride penetration coefficient of undamaged concrete.

2.3 Determination of the interaction factors for service life

The RDM value 66.7% was assumed to be to the limit state of service life with regard to internal frost damage, $t_{L;IntFr}$. To determine the interaction factors for service life the RDM value was assumed to change linearly with time, as presented in Equation 5.

$$RDM(t) = 100 - 33.3 \cdot \frac{t}{t_{L;IntFr}} \quad (5)$$

where $t_{L;IntFr}$ is the service life with regard to internal frost damage.

Using the Equations 1, 2, 3, 4 and 5 the interaction coefficients for the initiation time of corrosion could be determined and tabulated as a function of $t_{L;IntFr}$ and the initiation time of corrosion without internal frost attack $t_{0;ca}$ and $t_{0;cl}$ respectively.

The interaction factors of frost scaling for the initiation time of corrosion could also be determined. A linear rate of frost scaling was assumed. The interaction factors in this case are the same for both carbonation and chloride initiated corrosion but they depend on the depth of concrete cover. Table 1 shows the interaction factors for the cover depth of 25 mm [2].

Table 1 - Interaction factors of frost scaling for the initiation time of corrosion (apply to both carbonation and chloride initiation). Concrete cover = 25 mm.

t_0	$t_{L;FrSc}$									
	20	40	60	80	100	120	140	160	180	200
10	0.90	0.90	1.00	1.00	1.00	1.00	1.00	1.00	1.00	1.00
20	0.85	0.90	0.95	0.95	0.95	0.95	0.95	0.95	0.95	0.95
30	0.77	0.87	0.90	0.93	0.93	0.93	0.97	0.97	0.97	0.97
40	0.73	0.85	0.88	0.90	0.93	0.93	0.95	0.95	0.95	0.95
50	0.69	0.82	0.88	0.92	0.92	0.94	0.96	0.96	0.96	0.96
60	0.64	0.80	0.85	0.88	0.92	0.93	0.93	0.95	0.95	0.95
70	0.59	0.75	0.83	0.87	0.90	0.91	0.93	0.93	0.94	0.94
80	0.56	0.73	0.81	0.85	0.87	0.90	0.91	0.92	0.94	0.94
90	0.53	0.71	0.79	0.83	0.87	0.89	0.90	0.91	0.92	0.93
100	0.49	0.68	0.77	0.82	0.85	0.87	0.89	0.90	0.91	0.92
110	0.47	0.65	0.74	0.80	0.83	0.86	0.88	0.89	0.91	0.92
120	0.45	0.63	0.73	0.78	0.82	0.85	0.87	0.88	0.90	0.91
130	0.42	0.61	0.71	0.77	0.81	0.84	0.86	0.88	0.88	0.90
140	0.40	0.59	0.69	0.76	0.80	0.83	0.85	0.86	0.88	0.89
150	0.38	0.57	0.68	0.74	0.79	0.81	0.84	0.85	0.87	0.88
160	0.36	0.55	0.66	0.72	0.77	0.81	0.83	0.85	0.86	0.87
170	0.35	0.54	0.64	0.71	0.76	0.79	0.82	0.84	0.85	0.87
180	0.34	0.52	0.63	0.70	0.75	0.78	0.81	0.83	0.84	0.86
190	0.32	0.51	0.62	0.69	0.74	0.77	0.80	0.82	0.84	0.85
200	0.31	0.49	0.60	0.67	0.72	0.76	0.79	0.81	0.83	0.84

The updated initiation time of corrosion is obtained by multiplying the original initiation time by the factor in the table.

2.4 Computer simulation

Computer simulation software (developed in VTT in 1990's) was used to illustrate the interaction of degradation modes. The simulation program was updated with the developed degradation models for frost scaling, internal frost attack, carbonation and chloride penetration. Computer simulation software (1) emulates the real climatic conditions, (2) calculates the temperature and moisture contents in a cross-section of a concrete structure (exposed to weather), and (3) applies temperature and moisture sensitive degradation models so that the degradation over time and the service life can be predicted

The Equations 1, 2, 3 and 4 were inserted to computer simulation. In computer simulation the value of RDM and the depth of frost scaling were evaluated by specific models with the time step of 1 hour. Figure 2 shows an example on how the internal frost attack and the frost scaling effect on the depth of carbonation with time [2].

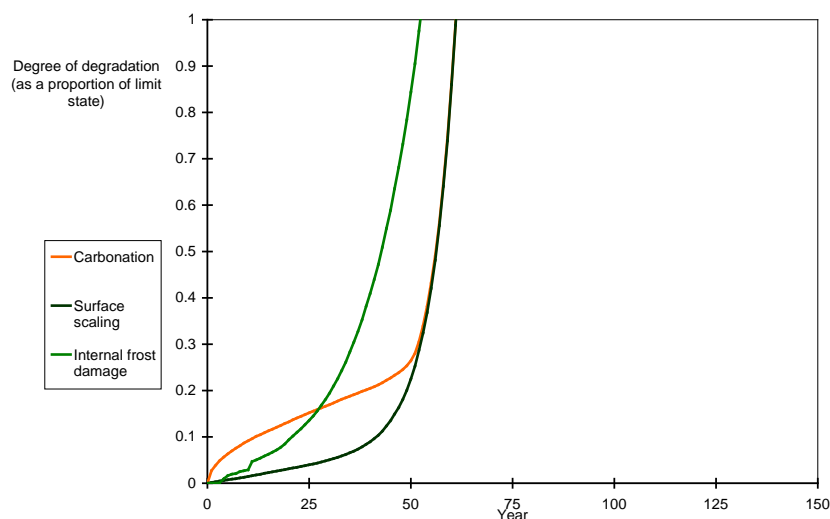


Figure 2 - Computer simulation of carbonation depth together with simultaneous internal frost attack and frost scaling.

3 CONCLUSIONS

The effect of frost attack on carbonation and chloride penetration may be substantial and should be taken into account when evaluating the service life of concrete structures exposed to frost attack. The interaction can be simulated by a special software. Interaction factors for the service life prediction by the factor approach were determined.

REFERENCES

1. Vesikari, E., "Carbonation and Chloride Penetration in Concrete with Special Objective of Service Life Modelling by the Factor Approach". *VTT Technical research Centre of Finland*. VTT-R-04771-09, 2009, 38 p.
2. Vesikari, E., "Frost Deterioration Process and Interaction with Carbonation and Chloride Penetration – Analysis of Test Results". *VTT Technical Research Centre of Finland*. 2011 (publication in progress).

The Effect of Cracking on Chloride Migration in Concrete



Jukka Piironen, M.Sc.
Aalto University
School of Engineering
Dept. of Structural Engineering
and Building Technology
P.O.Box 12100,
FIN-00076 Aalto, Finland
jukka.piironen@aalto.fi



Esko Sistonen, Act. Professor
Aalto University
School of Engineering
Dept. of Structural Engineering
and Building Technology
esko.sistonen@aalto.fi

Olli-Pekka Kari, M.Sc.
Aalto University
School of Engineering
Dept. of Structural Engineering
and Building Technology
olli-pekka.kari@aalto.fi

Professor Jari Puttonen
Aalto University
School of Engineering
Dept. of Structural Engineering
and Building Technology
jari.puttonen@aalto.fi



Fahim Al-Neshawy, Lic.Sc.
Aalto University
School of Engineering
Dept. of Structural Engineering
and Building Technology
fahim.al-neshawy@aalto.fi

ABSTRACT

Corrosion of reinforcement due to chloride penetration is one of the major deterioration mechanisms in concrete structures. The focus of this research was to investigate the comparison between the crack width and length and the non-steady-state chloride migration in concrete with artificial cracks. One concrete was used. The experimental results were compared with diffusion simulations. There was indication of consistency between the length and width of cracks and between the length of cracks and migration. The migration depth below the end of crack was independent from the width of crack. The simulation of chloride diffusion was similar to migration tests.

Key words: Concrete, cracking, rapid chloride penetration, non-steady-state chloride migration.

1. INTRODUCTION

1.1 General

Chloride-induced steel reinforcement corrosion is one of the major worldwide deterioration problems for reinforced concrete structures. The high alkaline environment of concrete forms a passive film on the surface of the embedded steel which normally prevents the steel from corroding. The passive film is disrupted or destroyed under chloride attack and the steel corrodes spontaneously. Yet the corrosion of the steel reinforcement may be accelerated due to the cracking of the concrete cover, because the chloride ions may drift through the crack. There

are several different transport mechanisms into concrete for chloride ions. These can be divided into the groups of diffusion, permeation, convection and migration, [1]. A diffusion coefficient is generally assessed to describe chloride penetration into concrete. Chloride penetration rarely happens purely by diffusion; this can only happen in permanently water-saturated concrete. It often happens through difficult-to-model mechanisms such as the exposure of dry concrete containing chloride to water, followed by dry and wet periods. Chloride transport in concrete is a rather complicated process, [2]. Migration is the movement of a charged substance under the action of an electrical field. As with diffusion, only free chloride ions in a solution are able to contribute to the flow of migration. Migration hardly exists in a pure form because the migration process is always coupled with the diffusion process as a result of a concentration gradient, [3].

2. EXPERIMENTAL

The objective of this research was to seek parameters that have significance for chloride migration in cracked concrete [4]. The main focus is on the size of the crack.

2.1 Preparation of the specimens

One concrete was used in the tests. The mix proportion used and properties of the concrete are presented in Table 1.

Table 1 – Mix proportion used and properties of concrete

Cement and Additive	Mix Proportions (kg/m ³)			Air Content (%)	Compressive Strength 28d (MPa)
	Cement and Additive	Eff. Water	Aggregate		
CEM II/A-M(S-LL) 42.5N	333	170	1899	3.0	54.1

The concrete was cast into 150 x 150 x 150 mm³ moulds. The cubes were stored in a climatic room after curing at a relative humidity of 65% and a temperature of 20°C for about a year before testing. The final specimens were cylinders with a diameter of 98 mm and height of 50 mm. Artificial crack without splitting the specimens into two pieces were made. The cracking of the specimen was limited to the desired width. The specimens were cracked by first sawing a small start notch. Steel plates were attached to the both sides of the notch. Tensile stress was applied to these plates. The time, pulling force, displacement between the plates during the pulling and the final displacement (telltale width) after releasing the pulling force were recorded. After the cracking the attached steel plates were removed by sawing the start notch of the crack off. The production of the specimens is shown in Figure 1. The crack widths on the top of the specimens and the crack lengths on both sides of the specimens were optically measured.

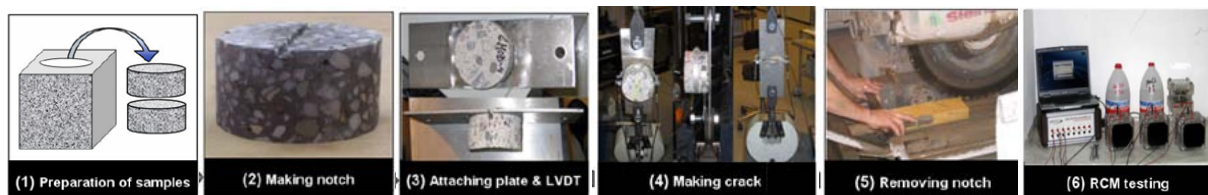


Figure 1 – Production of the specimens.

After measuring the specimens were exposed to non-steady-state rapid chloride migration (RCM) experiments according to the NT BUILD 492 [5]. The specimens were exposed to a vacuum treatment for three hours. The container was then filled with a saturated Ca(OH)₂

solution. The specimens were fully exposed. The specimens were kept in the $\text{Ca}(\text{OH})_2$ solution for 18 ± 2 hours.

The migration tests were performed with the PROOVE'it rapid chloride migration test equipment. The specimens were sealed between two cells filled with the NaOH- and NaCl-solutions and the cells were attached to the main power unit. The voltage used, testing time and passed adjusted charge during the experiment was recorded. The temperature and passing charge were also recorded. The specimens were split in half after the chloride migration experiment. The freshly split surface was sprayed with silver nitrate that makes the chloride migration visible. The surfaces were photographed. The migration depth of chloride was measured from the crack to both edges of the specimen at intervals of 5 mm (experiment) and also from photos (actual).

3. RESULTS

The principle for the measurements and the results for the crack width and length and chloride migration measurements trough the crack zone of the specimens are presented in Figure 2.

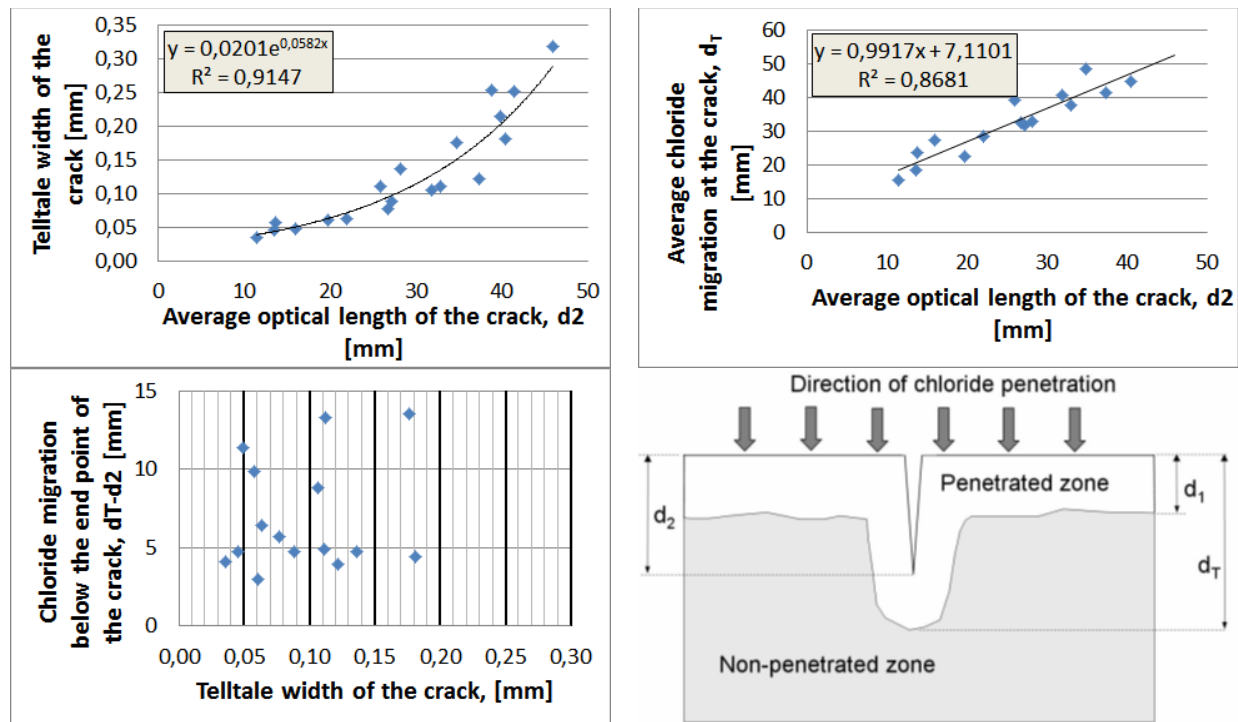


Figure 2 – Chloride penetration through the crack zone.

The experimental test results were compared with numerical simulations made with Comsol Multiphysics software. The results of the experimental tests made the baseline for the numerical simulation values. The diffusion coefficient was calculated from the average chloride migration depth of the intact edges of the specimens. Chloride diffusion was simulated with four crack widths. The fitted crack lengths were estimated from the results of the crack width and length measurements shown in Figure 2. The cracks were assumed to be wedge-shaped. An example of the comparisons between the experimental, actual and simulated chloride migration is presented in Figure 3.

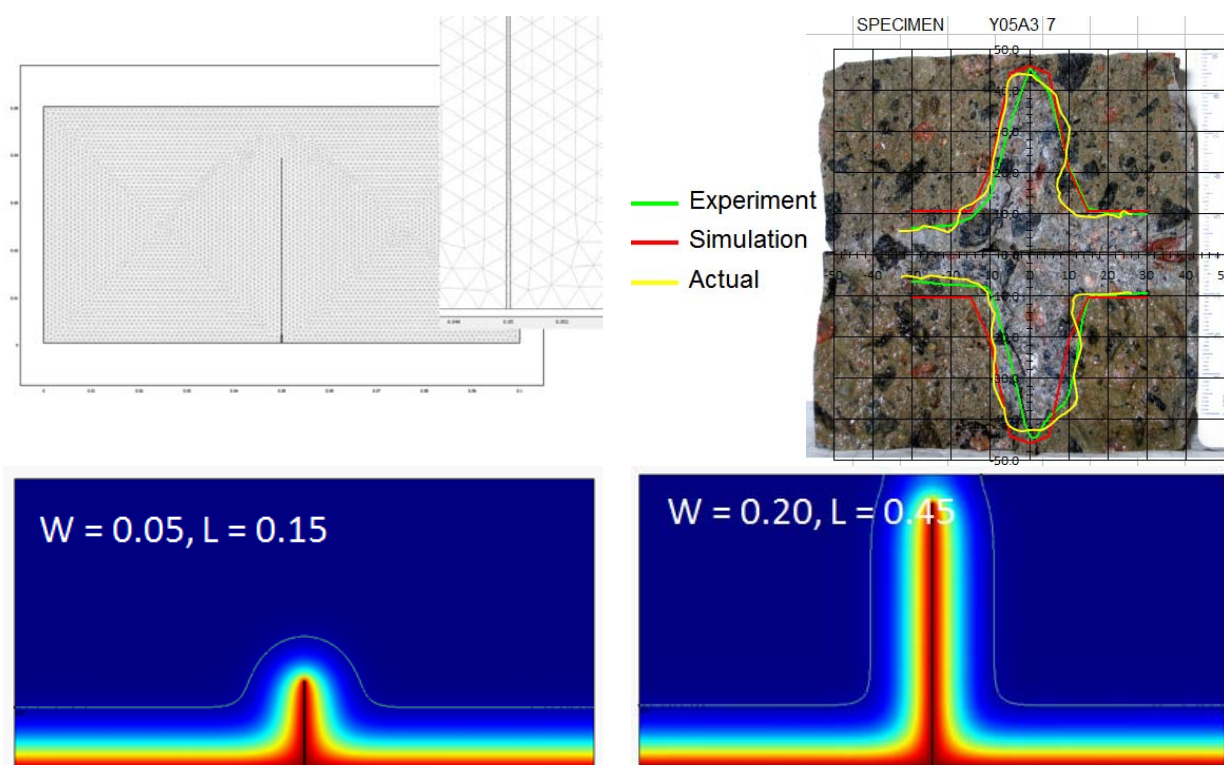


Figure 3 – Mesh used in the calculations and a comparison between the calculated, experimental and actual chloride migration.

4. DISCUSSION AND CONCLUSION

There was some indication of consistency between the measured length and telltale width of a crack and also with the length of a crack and chloride migration depth at the crack. But then the chloride migration depth below the end point of a crack was independent from the telltale width of a crack. The calculated simulation of chloride diffusion is similar to the experimental migration test, even though the experimental test is based on migration and the calculations are made by using only diffusion and without migration.

REFERENCES

1. Poulsen, E., and Mejlbro, L. (2006), Diffusion of Chloride in Concrete, Theory and Application, Modern Concrete Technology 14, Editor Taylor & Francis, 442 pp., 2006, ISBN13 9-78-0-419-25300-6.
2. Boddy A., Bentz E., Thomas M.D.A, Hooton R.D. An overview and sensitivity study of a multimechanistic chloride transport model. Cement and Concrete Research 29 (1999), pp. 827-837.
3. Tang, L., Chloride Transport in Concrete – Measurement and Prediction; Doctoral thesis, Dept. of Building Materials, Chalmers University of Technology, Publication P-96:6, Göteborg (1996) ISSN 1104-893X.
4. Sillanpää, M., The effect of cracking on chloride diffusion in concrete, Master thesis, Faculty of Engineering and Architecture, Aalto University, 2010, pp.(80+54).
5. NORDTEST METHOD NT BUILD 492. Concrete, mortar and cement-based repair materials: Chloride migration coefficient from non-steady-state migration experiments. NORDTEST (Espoo), 1999, ISSN 0283-7153.

Session B1 – BINDERS AND ADMIXTURES

A new type of accelerator for Portland cement



Leif Fjällberg
MSc (chemical engineering)
Swedish Cement and Concrete Research Institute
SE-100 44 Stockholm
E-mail: leif.fjallberg@cbi.se



Björn Lagerblad
Ph.D., Prof.
Swedish Cement and Concrete Research Institute
SE-100 44 Stockholm
E-mail: bjorn.lagerblad@cbi.se

ABSTRACT

A new type of accelerator called X-seed for Portland cement has been studied. It consists of C-S-H particles in nano scale in a suspension. The particles act as nucleation sites for cement hydration between and on the surface of cement grains. The accelerator is effective at room temperature as well as at lower temperatures eg. 10°C.

The accelerator was added in amounts of 2-4 % of the cement weight. The acceleration effect was higher with the higher dosage.

To evaluate the hydration development calorimetric measurements, XRD, pore solution and SEM analysis were performed and setting time was measured.

A CEM I and a CEM II cement were tested. The effect of the accelerator was greater in CEM I which also is a coarser cement.

Key words: accelerator, early hydration.

1. INTRODUCTION

The aim of the project was to study the effect of a new type of accelerator on the early cement hydration and the reaction mechanisms.

This paper summarises the part of the study where the accelerating effect of a new type of accelerator called X-seed was used with different Portland cements. The research project is one of the long term programs at CBI, where the effect of accelerators on the early hydration is studied.

2. EXPERIMENTS

An isotherm calorimeter, TAM Air, was used for measuring the heat evolution for cement pastes. Also some XRD-, SEM- and pore solution analysis were made. The cements used were the Swedish moderate heat cement CEM I 42.5 N and the Swedish ordinary cement CEM II/A-LL 42.5 R. Cement pastes with water/cement ratio 0.4 were made.

3. RESULTS

3.1 Calorimetry

The calorimetric measurements were made at both 20°C and 10°C. As comparison also CaCl₂ was used. The amount of accelerator (X-seed) is the total amount of accelerator in suspension in % of the cement weight. Calculated as dry content 4 % of suspension is about 0.7 % as dry content. The effect of accelerators in CEM II at 20°C and at 10°C is illustrated in figure 1.

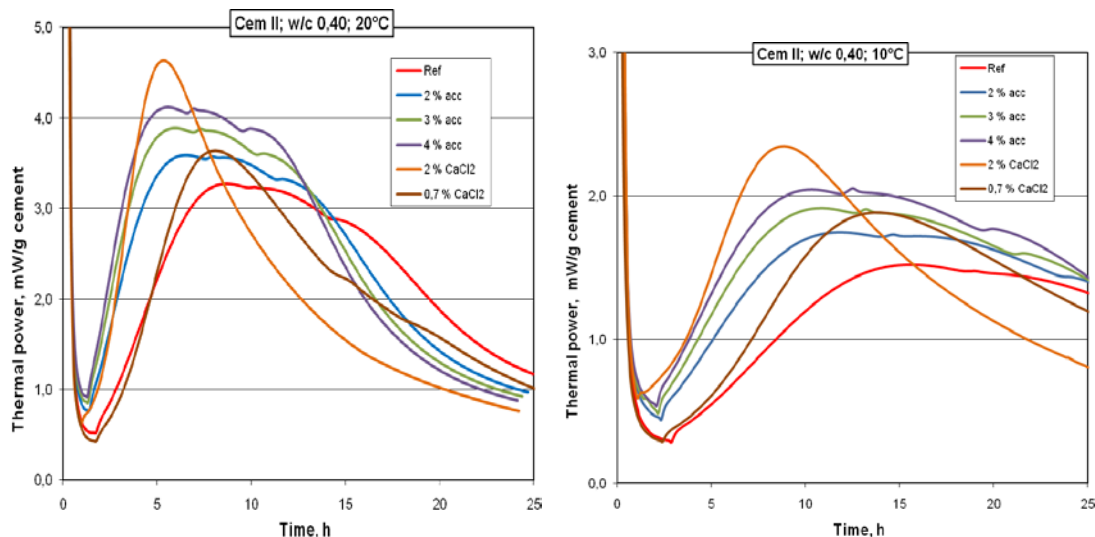


Figure 1. The effect of different amounts of accelerator in CEM II at 20°C and at 10°C.

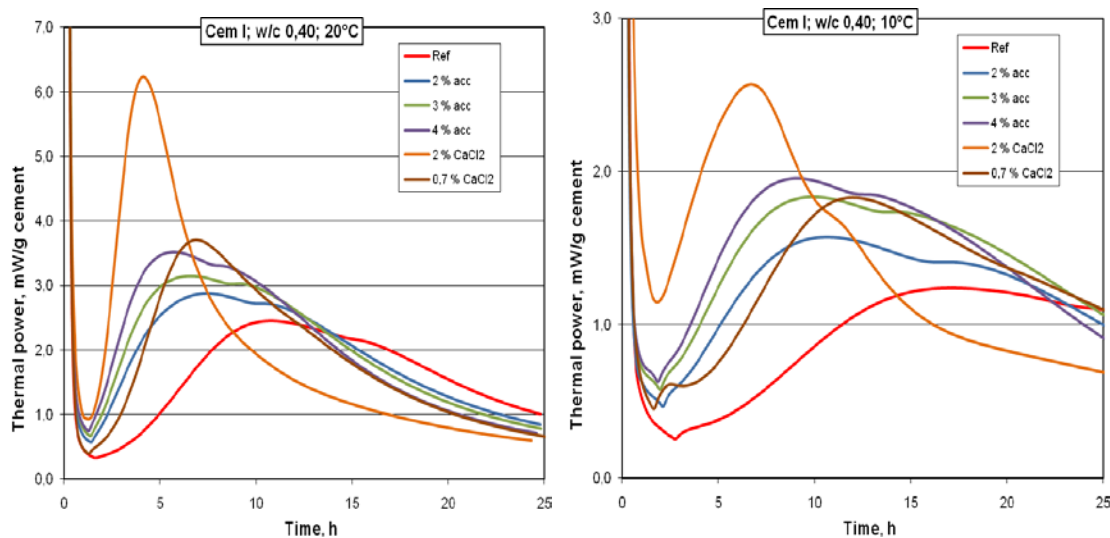


Figure 2. The effect of different amounts of accelerator in CEM I at 20°C and at 10°C.

For CEM II the time for the maximum of the main hydration peak was reduced from 8 hours to 5 hours at 20°C and from 15 hours to 10 hours at 10°C with a dosage of 4 % X-seed. For CEM I the time for the maximum of the main hydration peak was reduced from 11 hours to 5 hours at 20°C and from 17 hours to 8 hours at 10°C with the same dosage of X-seed. The slope of the hydration curve also became steeper and the maximum of the main hydration peak became higher with increasing amount of accelerator for both cements and at both temperatures. This indicates that more hydration products are formed in a shorter time. With 2 % CaCl_2 the main hydration peak becomes much higher and sharper than with X-seed, which means that the reaction mechanisms for these two accelerators are quite different. X-seed is effective also at low dosages and at low temperatures. The dosages of X-seed as dry content of the cement weight varied between about 0.4 and 0.7 %.

3.2 X-ray diffraction

A semi quantitative XRD-method was used where the peak areas for different components were calculated. For calculating the degree of hydration for alite the peak area of the hydrated sample was compared to the peak area of unhydrated sample.

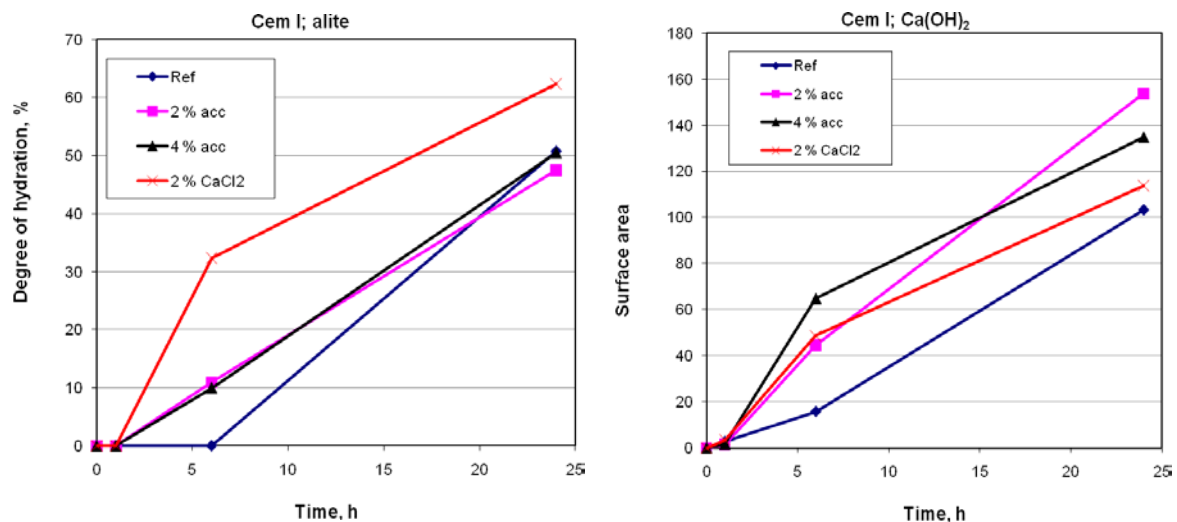


Figure 3. The degree of hydration for alite and the $\text{Ca}(\text{OH})_2$ development with different amounts of accelerator (X-seed and CaCl_2) in CEM I.

A clear effect of acceleration can be seen after six hours of hydration. The alite has reacted more and more $\text{Ca}(\text{OH})_2$ has developed compared to the reference sample without accelerator.

3.3 SEM-analysis

SEM-analysis of a cracked surface of three hours old cement paste with or without accelerator (X-seed) is seen in figure 4. In the picture to the left small ettringite needles can be seen on the cement grains. In the picture to the right clusters of small particles can be seen between the cement grains.

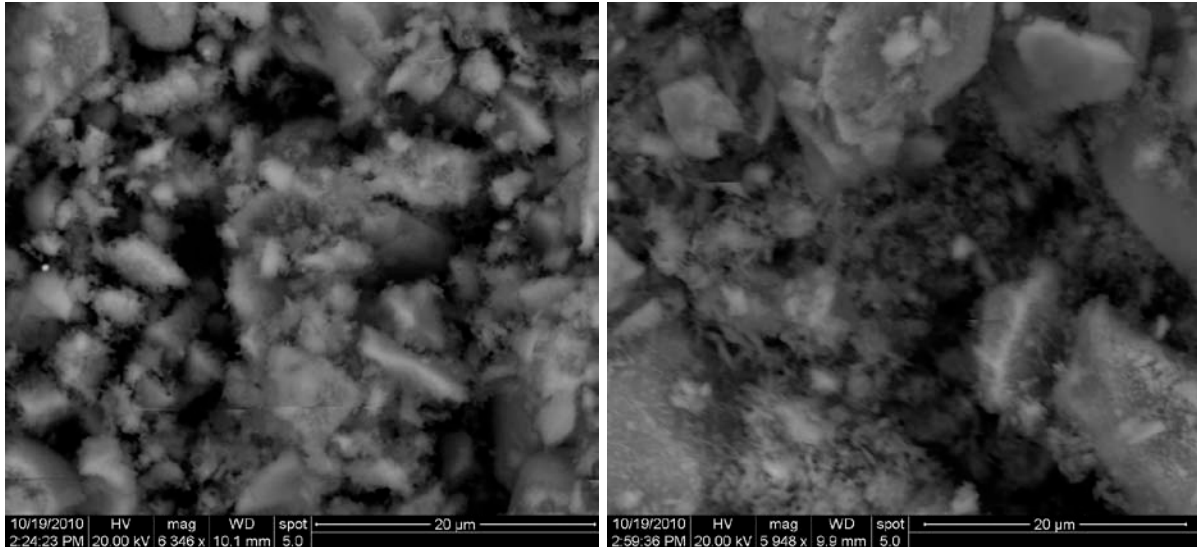


Figure 4. Reference sample to the left, 4 % X-seed to the right at the age of three hours. Cracked surface and CEM I.

3.4 Pore solution analysis and setting time

The most obvious effect for the pore solution is that the sodium content increases with increasing amount of X-seed, which means that the accelerator contains a considerable amount of sodium. Another effect is that the Ca-ion concentration drops faster during the six first hours of hydration, indicating that nucleation of hydrates are accelerated.

The setting time was much more reduced in CEM I than in CEM II, where the effect was very little. 2 % CaCl_2 was the most effective accelerator. For CEM I the start of the setting time was reduced from 4⁰⁰ h to 2⁵⁰ h with 4 % X-seed and to 2⁰⁰ h with 2 % CaCl_2 . For CEM II the start of the setting time was hardly affected at all with 4 % X-seed and it was only 10 minutes shorter with 2 % CaCl_2 . The end of the setting time was more reduced.

4. CONCLUSIONS

The calorimetric measurements show a clear acceleration effect of X-seed both at 10°C and 20°C for the two cements used. The effect is greater in CEM I both with X-seed and CaCl_2 . This cement is coarser, which means that the accelerators easier can reach the surfaces of the cement grains. The effect is obvious also with the lowest dosage of X-seed.

From the XRD-analysis a clear acceleration effect could be seen after six hours hydration. The alite hydration and the amount of formed Ca(OH)_2 were higher than for the reference sample without accelerator.

Also the setting time was more reduced in CEM I than in CEM II with accelerator.

The main effect of the pore solution was that the sodium content increased markedly and that the calcium content decreased faster with X-seed.

A study of early-age Ordinary Portland Cement Hydration according to Autocatalytic Reaction Model



Tapio Vehmas
M.Sc. Research Scientist
VTT Technical Research
Centre of Finland
Kemistintie 3, Espoo
FI-02044 VTT, Finland
tapio.vehmas@vtt.fi



Anna Kronlöf
Dr.(tech) Senior Research Scientist
VTT Technical Research
Centre of Finland
Kemistintie 3, Espoo
FI-02044 VTT, Finland
anna.kronlof@vtt.fi

ABSTRACT

Early-age hydration of Ordinary Portland Cement was studied with semi-adiabatic calorimeter in the presence of limestone and calcium-silicate-hydrate (C-S-H) coated limestone. The calorimetric data was analyzed as an autocatalytic reaction. Early age hydration followed the principles of autocatalytic reaction and the rate controlling phase was the initially nucleated C-S-H. Addition of limestone did not increase it, whereas C-S-H coated limestone had a massive impact to the hydration reaction.

Key words: Early-age hydration, seeding, autocatalytic reaction, calorimeter.

1. INTRODUCTION

Attempts to reduce the CO₂ emissions of cement have increased the use of supplementary materials in blended cements. Their draw back is slow early age strength development. In order to enhance it, the rate controlling mechanisms need to be recognised. According to present understanding [1] the old concept of cement hydration's autocatalytic nature has remerged [2]. In the present study the early age hydration Ordinary Portland Cement (OPC) was studied in paste with semi-adiabatic calorimeter and scanning electron microscope in the presence of various finely ground limestone fillers as well as fillers coated with calcium-silicate-hydrate (C-S-H). The calorimetric data was analyzed as an autocatalytic reaction (*Equations 1 and 2*) to distinguish reaction rate (k) and number of initially formed hydration nuclei ($[B_0]$). The latter are nuclei formed in supersaturated solution and precipitated through heterogeneous nucleation on surfaces [5]. The hydration heat was evaluated also to estimate the early-age and overall cement hydration degree.

2. MATERIALS AND METHODS

The cement used was CEM I 52,5 R, white cement from Aalborg. The limestone was jet-mill grounded to different finesses from Nordkalk's SB63 -calcite filler a commonly used limestone filler in Finland. Particle distributions were measured with a Beckman Coulter LS particle size analyzer (Figure 2). Calcium-silicate-hydrate (C-S-H) coated limestone was produced by vigorously mixing Na₂(SiO₂)_{3,3} and Ca(OH)₂ respectively to water in the presence of limestone. The amount of C-S-H was defined to produce a uniform layer with respect to the surface area of limestone. Extra water was evaporated from C-S-H coated limestone slurry by drying in 40°C. The uniform coverage of limestone with CSH was verified by JEOL Scanning Electron Microscope (Figure 2). Cement pastes were mixed with a Hobart mixer. The dry materials were first mixed for 1 min, tempered

water was added to during 30s period and the total mixing time was 5 minutes. Samples were placed into the calorimeter approximately 15 min after mixing. It was assumed that initial heat of dissolution was lost and heat observed originated from silicate reactions [3]. Heat capacities were calculated and the experiments conducted according to [4] with two parallel samples. Increased temperatures during semi-adiabatic calorimeter experiments were normalized to constant temperature with Arrhenius equation using the value of 33 kJ/mol for activation energy. The autocatalytic reaction model (*Equation 2*) was fitted to the normalized calorimeter curves using the Excel solver function. Assuming that observed hydration heat was proportional to the formation of C-S-H, $[B]$ represented the formed calcium-silicate-hydrate and $[B_0]$ the quantity of the initially formed C-S-H. $[A_0]$ was chosen arbitrarily as a value of 400 kJ. Fitting was done by letting both constants (number of initial C-S-H nuclei $[B_0]$ and reaction rate constant k) change freely until the point where the calorimeter curve and the autocatalytic model significantly deviated.

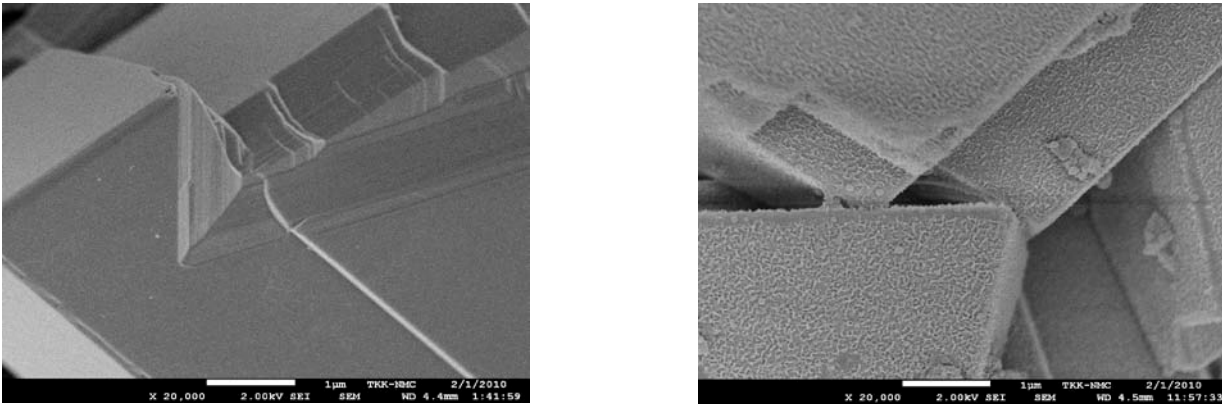


Figure 1. Scanning electron microscope images of C-S-H coating. left: uncoated calcite surface right: C-S-H coated calcite surface. (Vehmas, Kronlöf, Anoshkin).

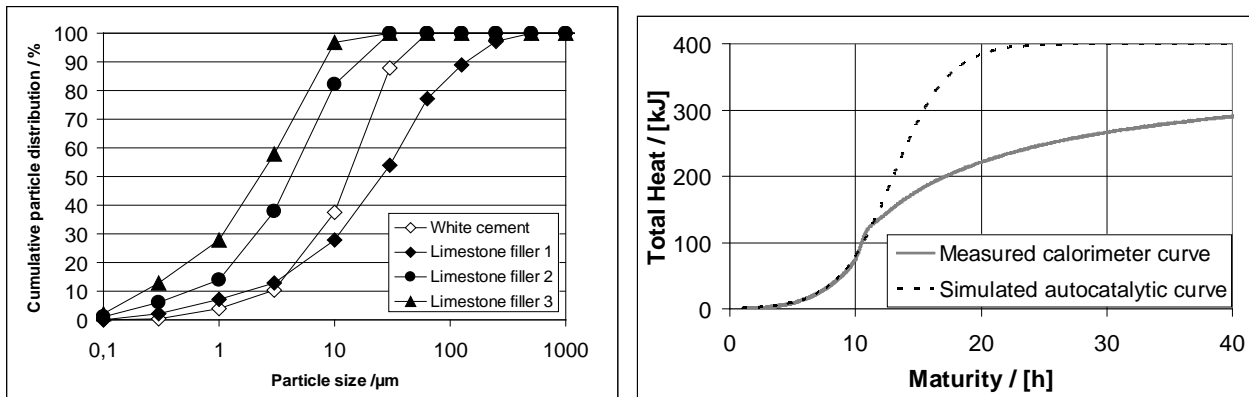


Figure 2. left: Particle size distributions of white cement and limestones. right: Measured calorimeter curve (grey, solid line) and simulated autocatalytic curve (black dashed).



$$[B] = \frac{[B_0] + [A_0]}{1 + \frac{[A_0]}{[B_0]} e^{-([A_0] - [B_0])kt}} - [B_0] \quad (2)$$

3. RESULTS

The fitting revealed that number of initial C-S-H nuclei was clearly increased as water/cement – ratio (w/c) increased. The observed limestone filler’s ability to enhance hydration did not significantly increase number of initial C-S-H nuclei for its effect was not dominating until a few hours after the time span discussed here. The effect of C-S-H coated limestone was remarkable. The number of initial C-S-H nuclei up to 4.5 fold compared to the effect of increased w/c.

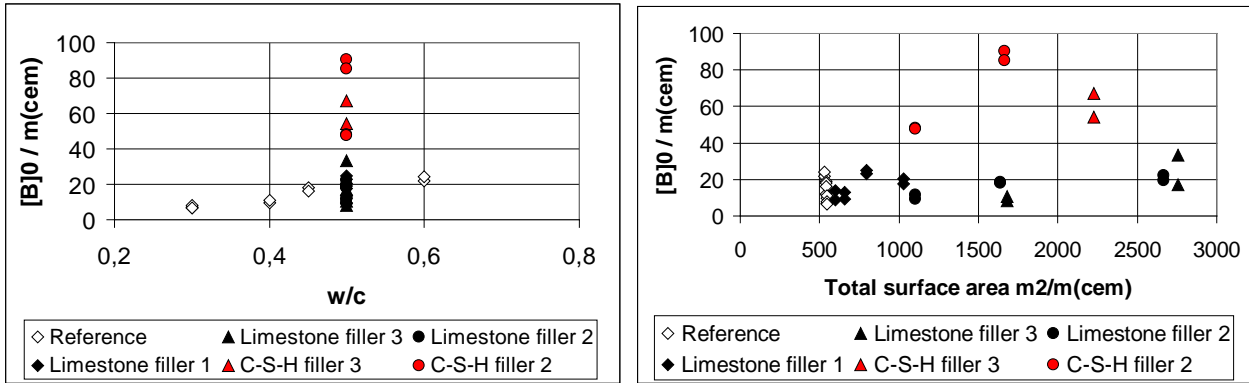


Figure 3. Modelled number of initial nuclei in function of a) water/cement –ratio b) total surface area of cement+ limestone filler divided by cement weight.

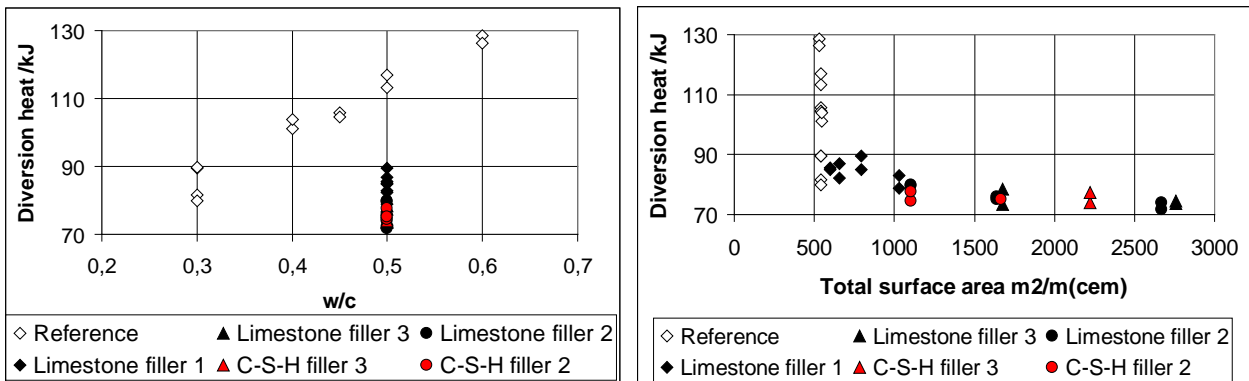


Figure 4. The point where modelled autocatalytic reaction and observed calorimeter curve started to differ in function of a) water/cement –ratio b) total surface area divided by cement weight.

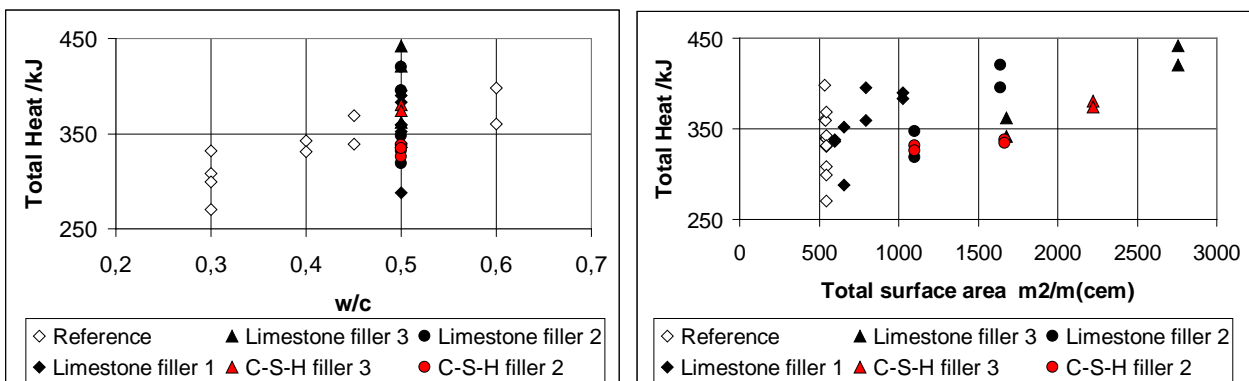


Figure 5. Total heat evolved during 100h observation time in function of a) water/cement –ratio b) total surface area divided by cement weight.

The point where the heat release rate begins to decrease equals to the point where autocatalytic model diverges from calorimeter data. The heat evolved at this point (diversion heat) increased as

w/c ratio increased. As limestone or C-S-H coated limestone was added, the diversion heat decreased nearly to a constant level. No difference between limestone and C-S-H coated limestone was detected. Total heat evolved in 100h observation time increased as the w/c ratio increased. Addition of limestone or C-S-H coated limestone increased total heat at higher dosages.

4. CONCLUSIONS AND DISCUSSION

Cement hydration followed the autocatalytic reaction principles within the first hours. The number of the initial nuclei increased as the w/c -ratio increased. This is in line with [5] stating that the number of initial C-S-H depends on amount of supersaturated silicon present in the solution.

Addition of limestone surface did not change the dominant mechanism. The shape of calorimeter curves indicated that the addition of limestone surface did not increase the number of the initial nuclei. The length of dormant period was still depended of number of initial C-S-H nuclei. However, the fact that the addition accelerated the reaction after the first hours give reason to postulate that limestone may enhance C-S-H nuclei production later during hydration process.

C-S-H coated limestone significantly accelerated the reaction and according to the autocatalytic reaction, increased the number of the initial C-S-H nuclei. It was concluded that the C-S-H coating served as initial C-S-H nuclei for the reaction. Regardless of the surface area of the C-S-H coated limestone introduced to the paste, the heat evolved at the point where calorimetric curve diverged from the model (diversion point) was observed to be relatively constant. This point has been anticipated to be the transition point of the reaction mode from the dissolution controlled into the diffusion controlled stage. The value rather decreased than increased as the total surface area increased (Figure 4) indicating that the amount of produced C-S-H needed to change the reaction mode was smaller the larger the surface area introduced to the paste. This observation contradicts with the basic concept of “diffusion barrier”. The concept indicates that larger area would lead to thinner product layer per CSH produced and therefore to higher amount of C-S-H at the point of the mode change.

This research was done as a part in of the project SIPI (Internal surfaces of mineral based functional materials), collaboration with VTT, Aalto University and Åbo Akademi, funded by VTT, TEKES, Nordkalk Oy Ab, Cementa Ab and Tikkurila Oyj.

REFERENCES

1. Jeffrey W. Bullard, Hamlin M. Jennings, Richard A. Livingston, Andre Nonat, George W. Scherer, Jeffrey S. Schweitzer, Karen L. Scrivener, Jeffrey J. Thomas, “Mechanism of Cement Hydration”. *Cement and Concrete Research* In Press. Available online 29 October 2010.
2. Thomas J., Jennings H., Chen J., “Influence of Nucleation Seeding on the Hydration Mechanism of Tricalcium Silicate and Cement” *Journal of Physical Chemistry C*. Vol 113 2009 pp.4327-4334
3. Hesse C. Goetz-Neunhoeffer, Neubauer J., “ A new approach in quantitative in-situ XRD of Cement pastes: Correlation of heat flow curves with early hydration reactions” *Cement and Concrete Research* Vol 41 2011 pp.123-128
4. RILEM TC 119-TCE: “Avoidance of thermal cracking in concrete at early-ages” *Materials and Structures* Vol. 300 1997 pp451-464
5. Garrault S., Nonat A., “Hydrated layer formation on Tricalcium and Dicalcium Silicate Surfaces: Experimental Study and numerical simulations” *Langmuir* vol 17 2001 pp. 8131-8138.

Effect of chemical admixtures on the early strength development of fly ash blended cement at low temperature



Kien Dinh Hoang, PhD student
Norwegian Uni. of Sci. & Tech.,
7491 Trondheim, Norway
Email: kien.hoang@ntnu.no



Mette Rica Geiker, Dr., Prof.
Tech. Univ. of Denmark
Norwegian Uni. of Sci. & Tech.,
7491 Trondheim, Norway
Email: mette.geiker@ntnu.no



Harald Justnes, Dr., Adj. Prof.
SINTEF Building & Infrastructure
Norwegian Uni. of Sci. & Tech.,
Richard Birkelandsvei 3,
7465 Trondheim, Norway
Email: harald.justnes@sintef.no



Roar Myrdal, Dr., Adj. Prof.
Norwegian Uni. of Sci. & Tech.,
7491 Trondheim, Norway
Email: roar.myrdal@normet.fi

ABSTRACT

The effect of sodium sulphate Na_2SO_4 and calcium nitrate $\text{Ca}(\text{NO}_3)_2$ (CN) on the strength development up to 28 days of fly ash blended cement (OPC-FA) at low temperature (5°C) was investigated. The addition of Na_2SO_4 increased the compressive strength at all ages, particularly at early ages. The presence of CN in the system also increased the strength but is less effective than Na_2SO_4 at early ages. The hydration temperature evolution was also examined through calorimeter tests. The results indicated that Na_2SO_4 has both setting and hardening accelerating effects while in the case of CN the setting effect seems to predominate over the hardening one.

Key words: Portland cement, fly ash, compressive strength, accelerator, low temperature.

1. INTRODUCTION

It is believed that the slow pozzolanic reaction of fly ash at early stage is the main reason for low early strength of OPC-FA system. To counteract this, the efficiency of mechanical, thermal and chemical treatment methods have been investigated [1]. Among them, the chemical method was observed to an effective and economic way to obtain this target [1].

Na_2SO_4 was tested as a chemical activator for fly ash-lime system at 23°C and showed an efficiency in increasing both the early and later strengths [2]. Na_2SO_4 was also reported to significantly increase the early strength of OPC-FA at 20°C [3].

CN was investigated with different OPCs at low temperature ($5\text{-}7^\circ\text{C}$) and was declared as a setting accelerator [4]. CN also was reported to increase the early strength of OPC at 20°C [5].

The study of chemical activation on OPC-FA system at low temperature is limited and very few results related to this subject have been reported [6]. In this study, the effect of Na_2SO_4 and CN on the early hydration of OPC-FA at low temperature (5°C) was investigated.

2. MATERIALS AND EXPERIMENTS

Cement (OPC) and fly ash (FA) used in this investigation were supplied from Norcem. The chemical and mineral compositions are given in Table 1 and Table 2. Natural sand with size distribution from 0 to 4 mm supplied by Norstone was used as aggregates for preparing mortars. Chemical reagents Na_2SO_4 and $\text{Ca}(\text{NO}_3)_2$ were used as chemical admixtures.

Table 1: Chemical composition

Oxide	Cement (%)	Fly ash (%)
SiO_2	20.55	54.40
Al_2O_3	4.53	22.01
Fe_2O_3	3.53	5.83
CaO	62.43	4.80
MgO	2.65	2.22
SO_3	3.20	0.52
K_2O	0.94	2.21
Na_2O	0.50	1.15
Carbon (C)	-	3.64

Table 2: Mineral composition

Mineral	Cement (%)
C_3S	62.43
C_2S	11.83
C_3A	6.04
C_4AF	10.74

Every mix investigated in this study had OPC/FA ratio of 7/3 by weight. Mixes were mixed according to NS-EN-480-1:2006 with water to binder ratio of 0.5 and binder to sand ratio of 1/3. Chemical admixtures were dissolved in mixing water before adding to the mixes. Different dosages of chemicals in percent based on the total mass of cement and fly ash were used, see Table 3.

Table 3: Mixes investigated

Mix	Na_2SO_4 (%)	CN (%)
M1	0	0
M2	2	0
M3	4	0
M4	0	0.5
M5	0	1

Compressive strength of mortar prism 40x40x160 mm was tested according to NS-EN-1015-11. Immediately after mixing and casting, prisms were stored in 5°C room. After 24 hours, prisms were demoulded and compressive strength was determined. For testing at higher ages (2 and 28 days), prisms were further cured in sealed plastics at 5°C until the testing ages were attained.

Temperature evolution recordings during the hydration process were performed on approximately 3 kg samples using a semi-adiabatic calorimeter; Quadrel iQdrum300. The measurements were carried out at 5°C for a period of 5 days.

3 RESULTS AND DISCUSSIONS

3.1 Compressive strength

The addition of Na_2SO_4 resulted in an increase in strength at all ages, especially at early ages as shown in Figure 1. At 2% dosage, the strength was increased by about 45%, 30% and 10% at the ages of 1 day, 2 days and 28 days, respectively. A similar tendency was observed with the dosage of 4%, but the strength was increased more strongly at early ages, by about 125% at 1

day and 55% at 2 days. These results might be explained as the effect of Na_2SO_4 increasingly the alkalinity of the solution and thereby enhancing the dissolution of fly ash at initial stages and its pozzolanic reactivity [7]. At the same time, a large amount of Aft was probably formed due to the presence of SO_4^{2-} ions [2].

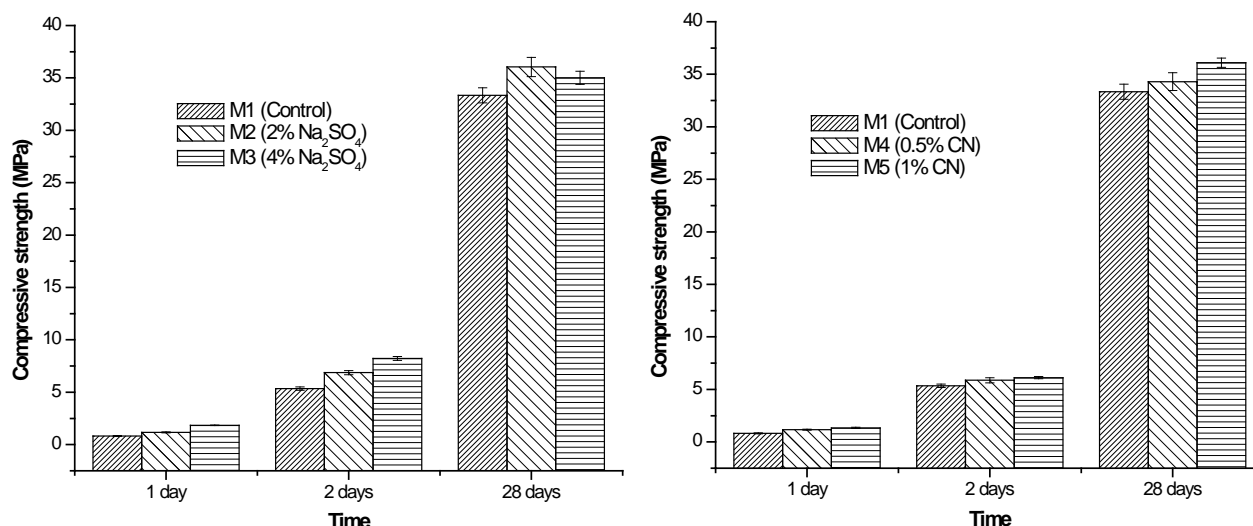


Figure 1: Compressive strength of mortar prisms with $\text{OPC}/\text{FA} = 7/3$ and varying amounts of Na_2SO_4 and CN.

In the presence of CN, the compressive strength was also enhanced at all ages (Figure 1). Similar to Na_2SO_4 , the efficiency of CN in promoting strength development was higher at early ages. With dosage of 0.5%, the strength increased by about 40%, 10% and 5% at 1, 2 and 28 days. A similar observation was attained with dosages of 1%, the increase in strength was about 65%, 15% and 10% at 1, 2 and 28 days. CN has been demonstrated as a setting accelerator for OPC at low temperature [4]. The increased hydration rate of cement probably provides more calcium hydroxide for the pozzolanic reaction of fly ash resulting in higher early strength.

3.2 Hydration temperature evolution

The calorimeter tests were done on four mixes including M1, M2, M3, and M5. The results of these measurements are presented in terms of temperature evolution versus time (Figure 2).

It can be seen that all temperature vs. time curves had similar profiles, but temperature developed at different rates. The addition of Na_2SO_4 resulted in higher temperature evolution at early ages. The main peak, which corresponds to the main reactions taking place during the hardening stage, reached higher temperature for mixes M2 and M3 than for the control mix (M1), indicating a hardening accelerating effect of Na_2SO_4 . In addition, mix M3 with highest dosage of Na_2SO_4 has higher main peak than mix M2. Another aspect which can be observed is that mixes M2 and M3 have shorter induction periods, i.e. the main peaks of these curves occurred earlier than that of the sample M1, showing the setting accelerating effect of Na_2SO_4 . Again, higher dosage of Na_2SO_4 was observed to be more effective with respect to this effect.

In the presence of CN (mix M5), the main peak had similar intensity but occurred earlier than for mix M2. This indicates that CN has both setting and hardening accelerating effects in which the setting effect seems to dominate.

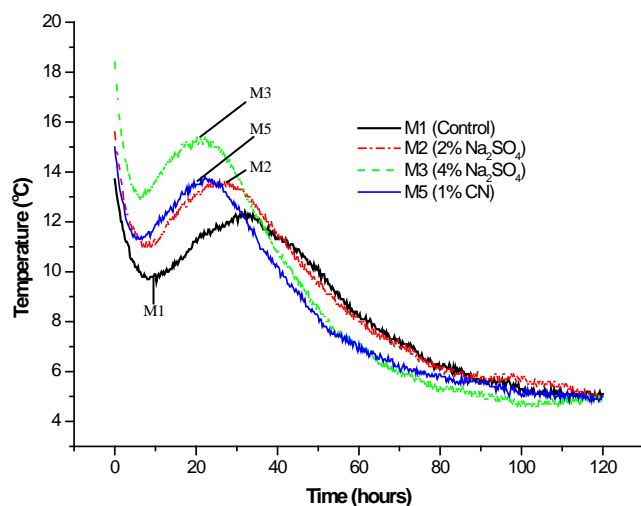


Figure 2: Temperature evolution versus time

4 CONCLUSIONS

The addition of Na_2SO_4 increased the compressive strength of OPC/FA at low temperatures at all ages (1, 2 and 28 days) but stronger at early ages. A higher dosage of Na_2SO_4 was more effective with respect to both hardening and setting accelerating effects. The presence of CN also improved the compressive strength at all ages at low temperature, particularly at early ages. However, it seems that the setting accelerating effect of CN contribute to the early strength enhancement of the blended system.

ACKNOWLEDGEMENTS

The paper is based on the work performed in COIN - Concrete Innovation Centre - which is a Centre for Research based Innovation, initiated by the Research Council of Norway (RCN) in 2006. COIN has an annual budget of NOK 25 mill, and is financed by RCN (approx. 40 %), industrial partners (approx 45 % of which $\frac{1}{4}$ is cash) and by SINTEF and NTNU (in all approx 15 %). The Centre is directed by SINTEF, with NTNU as a research partners and with the present industrial partners: Aker Solutions, Norcem, Norwegian Public Roads Administration, Rescon Mapei, Skanska, Spenncon, Unicon, Veidekke and Weber Saint Gobain.

REFERENCES

1. Shi, C., Day, R.L., "Comparison of different methods for enhancing reactivity of pozzolanas", *Cement and Concrete Research*, 31, 2001, pp. 813-818.
2. Shi, C., "Early microstructure development of activated lime-fly ash pastes" *Cement and Concrete Research*, Vol. 26, No. 9, 1996, pp. 1351-1359.
3. Quian, J., Shi, C., & Wang, Z., "Activation of blended cements containing fly ash" *Cement and Concrete Research*, 31, 2001, pp. 1121-1127.
4. Justnes, H., Nygaard, E.C., "Technical calcium nitrate as set accelerator for cement at low temperature" *Cement and Concrete Research*, Vol. 25, No. 8, 1995, pp. 1766-1774.
5. Aggoun, S., Cheikh-Zouaoui, M., Chikh, N., & Duval, R., "Effect of some admixtures on the setting time and strength evolution of cement pastes at early ages" *Construction and Building Materials*, 22, 2008, pp. 106-110.
6. Terzo, L.J., "Concrete admixture and use in low temperatures", U.S. Patent No. US20050172863A1, August 2005.
7. Fraay, A.L.A, Bijen, J.M., de Haan, Y.M, "The reaction of fly ash in concrete. A critical examination", *Cement and Concrete Research*, Vol. 19, 1989, pp. 235-246.

Reactive magnesium oxide as alternative secondary binder for Portland cement



Andrzej Cwirzen
Docent, Ph.D.
Aalto University
andrzej.cwirzen@aalto.fi



Karin Habermehl-Cwirzen
Ph.D.
Aalto University
Karin.habermehl-
cwirzen@aalto.fi

ABSTRACT

Reactive magnesium oxide which is produced using low oxidation temperatures is characterized by higher reactivity in comparison with regular magnesium oxide. Its hydration rate is claimed to be similar to Portland cement. The test results showed that the addition of a moderate amount of up to 20 wt% of cement resulted in the enhancement of the compressive strength by 20%. No micro cracking was observed. The hydration products appeared to contain in addition to CSH, Portlandite also Brucide which is directly related to the reaction between magnesium oxide and water. No hybrid phases have been detected. The microstructure of the binder matrix was densified by formation of brucide.

Key words: magnesia, ESEM, compressive strength, microstructure

1. INTRODUCTION

Presence of magnesium oxide in Portland cement is limited to 1% due to problems with expansion related to its slow hydration rate. Magnesium oxide was also used to produce “sorel” cements which hydration products are based on magnesium oxychlorides, [1]. Harisson et al. showed that lowering the oxidation temperature to 800 °C increases significantly its reactivity. As a result the hydration rate is claimed to be similar to Portland cement [2] and thus problems related to later expansions should be excluded. The produced magnesium oxide was called as “reactive”. It was also claimed that addition of the reactive magnesium oxide (magnesia) to Portland cement would enhance its mechanical properties as well as durability due to formation of stabile brucite. More recent tests results by Vandeperre [3] showed that there is no interaction between the formed magnesium hydroxide and any of the hydration products related to Portland cement.

The present paper includes preliminary results of research on reactive magnesium oxide used as secondary binder.

2. EXPERIMENTAL SETUP

Mortar specimens were used to determine mechanical properties and to study microstructure. The mix compositions are given in Table 1. All mixes contained 1/1 ratio of fine sand to total binder content. The amount of reactive magnesium varied from 0 to 80 wt% of cement. CEM I produced by Finsementti was used in all mixes. Addition of polycarboxylate based

superplasticizer varied from 0 to 2.5 wt% of the binder. Water to binder ratio was 0.4, 0.55 and 0.7. Additional samples used in XRD studies were prepared as pastes having identical as corresponding mortar mixes water to binder ratio and amount of superplasticizer. The specimens were stored in water until the compressive and flexural strengths were measured after 28 days. Microstructure was characterized using Environmental Scanning Electron Microscope (ESEM) type Electroscan E3. The operating parameters were: accelerating voltage 20 keV, chamber pressure 1.8 torr and working distance 13.3 mm. All measurements were done on 28 days old resin impregnated and polished mortar specimens. Preparation procedure for polished specimens included cutting of samples using diamond saw and alcohol as a lubricant. In order to remove capillary water all specimens were stored for 24 hours in alcohol, followed by vacuum resin impregnation. In the final stage samples were grinded and polished using diamond pads (125 and 25 μm) and diamond spray (6, 3, 1 and 0,25 μm). Chemical composition was studied using EDX analyser combined with ESEM produced by Electroscan – Kevex. The counting rate of the analyser was kept at around 1500 cps with counting time of 60 s. Additional study of the chemical composition of the binders before and after hydration was done using an XRD diffractometer PW1830 produced by Philips. The XRD analysis was done on grinded hydrated paste samples at ages of 24 hours, 4 days and 28 days.

Table 1 Mix composition.

Mix	Cement [wt% of total binder]	MgO [wt% of total binder]	sand [wt% of total binder]	SP [g]	W/B ratio
Ref	100	0	100	0	0.4
Mg20	80	20	100	0.75	0.4
Mg30	60	40	100	1	0.40
Mg60	40	60	100	2.5	0.55
Mg60	20	80	100	2.5	0.7

3. TEST RESULTS AND DISCUSSION

The compressive strength values appeared to be improved only when magnesium oxide replaced 20% of portland cement, Figure 1. Lower strength recorded for 60 and 80% replacements can be linked to higher water to binder ratio which increased from 0.4 to 0.55 and 0.7 required due to worsening workability and lower strength of brucide. Addition of 20 and 30% of reactive magnesium oxide did not affect significantly the workability of the produced mixes which enabled to use the same as in the case of the reference mortars water to binder ratio. Mix MG20 and MG30 containing respectively 20 and 30% of magnesia had similar to the reference mix MG0 microstructure and chemical composition. The ESEM-BSE-EDX test results shown in Figure 2 indicated less porosity especially in the ITZ (interfacial transition zone). In addition to anhydrous cement, portlandite and C-S-H inclusions of brucide have been observed.

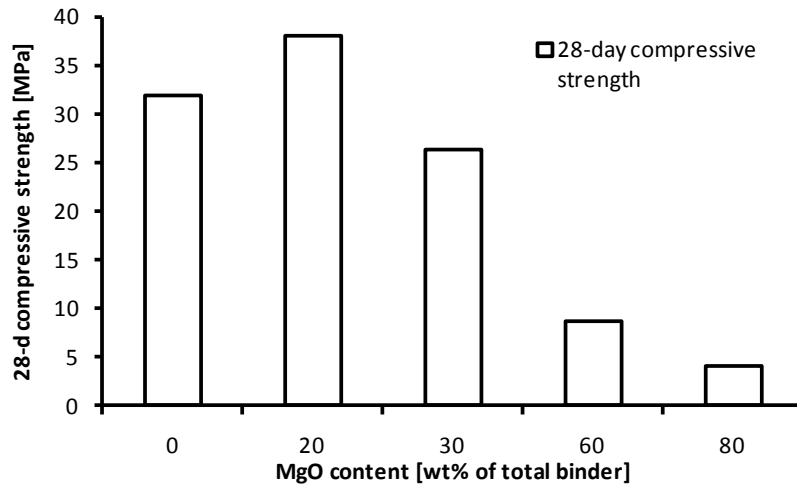


Figure 1. 28-day compressive strength values

Addition of magnesia appeared to have a significant effect on microstructure of binder matrix. At higher additions of 60-80% ESEM-BSE study revealed very low capillary porosity, Figures 2. Furthermore, the interfacial transition zone (ITZ) characterized by higher porosity was not detected, even despite significantly higher water to binder ratio of 0.7. Similar effect of magnesia on micro porosity was observed by Lawry et al [4] who detected slight decrease of porosity already by 20% replacement.

The densification of the binder matrix can be attributed to creation of additional nucleation spots by magnesia particles and formation of brucide. Lawry at al [4] observed that magnesia promoted precipitation of Portlandite crystals.

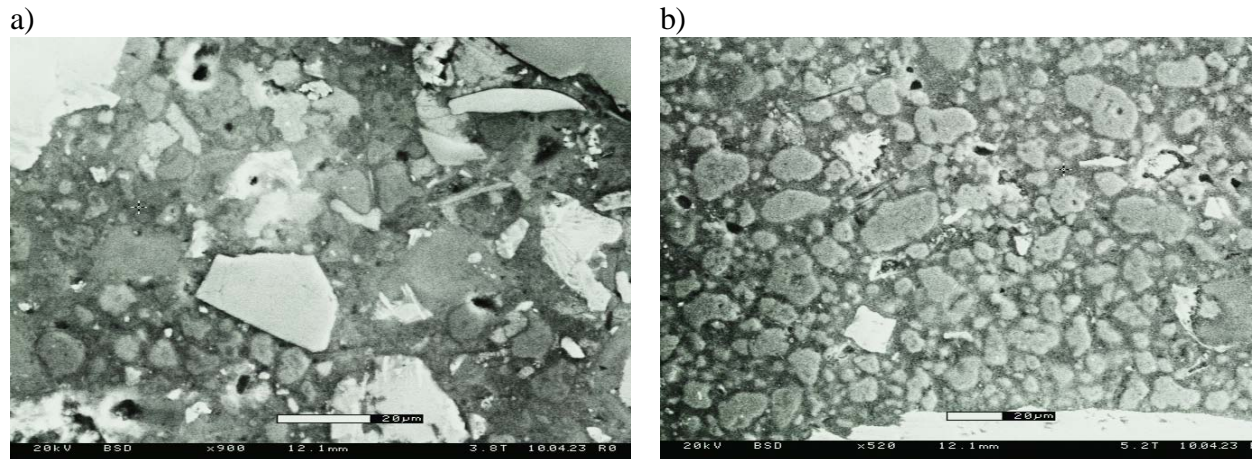


Figure 2. ESEM-EDX of 28-day old samples. a) 30% replacement, b) 80% replacement

The XRD spectra for 28-days old paste specimens of mixes containing 20 and 80% of magnesia are shown in Figure 3. Both mixes showed significant amount of Portlandite, some anhydrous cement as well as ettringite. Traces of calcite have been found in all samples which can be related to drying method using acetone. In the case of 80% replacement brucide was a dominant hydration product. Based on these test results no intermediate phases have formed which complied with results and conclusions of others, [3].

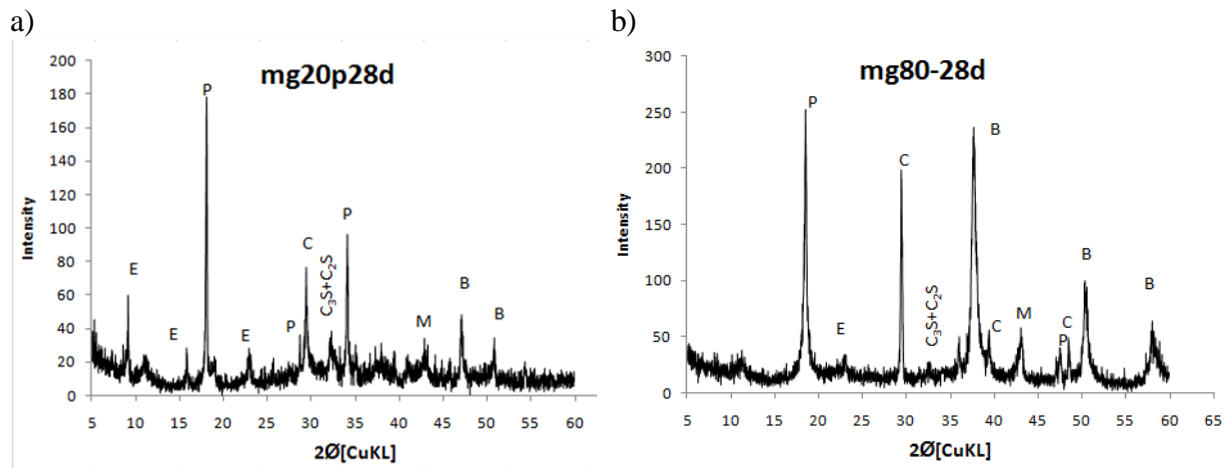


Figure 3. XRD spectra of paste containing: a) 20 and b) 80 wt% of Magnesium. E-ettringite, P-portlandite, C-calcit, M-magnesia, B-brucide

4. CONCLUSSIONS

The obtained results showed that reactive magnesia produced at lower temperatures has a hydration rate much higher in comparison with magnesia present in Portland cement and with regular magnesia produced at higher oxidation temperatures. The main hydration product of magnesia added to Portland cement is brucide. Brucide appeared to densify the binder macrostructure and increased 28-day compressive strength when added at lower amounts. More detailed studies on the effects of magnesium oxide on durability are certainly required.

REFERENCES

1. Zongjin Li1 and C. K. Chau, Reactivity and Function of Magnesium Oxide in Sorel Cement, JOURNAL OF MATERIALS IN CIVIL ENGINEERING © ASCE / MARCH 2008 / 239
2. Harrison J. Reactive magnesium oxide cements, In: W.I.P. Organisation (Ed.) Australia 2001
3. L.J. Vandeperre, , M. Liska, A. Al-Tabba, Microstructures of reactive magnesia cement blends, Cement & Concrete Composites 30 (2008) 706–71
4. Lawry, J., Thermal characterisation of Portland cement-magnesia blends, Journal of Thermal analysis, Vol. 80, (2005), 637-641

A Novel Cellulose Based Stabilizing Admixture for Self Compacting Concrete



Tapio Vehmas
M.Sc. Research Scientist
VTT Technical Research
Centre of Finland
Kemistintie 3, Espoo
P.O Box 1000
FI-02044 VTT, Finland
tapio.vehmas@vtt.fi



Markku Leivo
Dr.(tech) Senior Research Scientist
VTT Technical Research
Centre of Finland
Kemistintie 3, Espoo
P.O Box 1000
FI-02044 VTT, Finland
markku.leivo@vtt.fi

ABSTRACT

A Novel Cellulose Based stabilizing Admixture (NCBA) with unique rheological properties was introduced. Rheological effects of NCBA were studied in cement paste, mortar and self compacting concrete. It was observed that NCBA increased only the mixes yield stress, whereas commercial melamine sulphonate based stabilizer increased mixes' yield stress and plastic viscosity. This phenomenon made it possible to produce a good quality self compacting concrete with relatively low performance aggregates and a high water /cement –ratio.

Key words: Self compacting concrete, stabilizing admixture, rheology, Bingham model

1. INTRODUCTION

Self compacting concretes (SCC) have shown great promises in their usability in various casting processes. Economically, the use of SCC is not greatly favoured because low cost and robust SCC is not easily achievable. Therefore SCC has been identified as potential development target for nanotechnology-based materials [1]. Today, low cost SCC usually demands higher water/cement- ratios, where the use of supplementary cementitious materials or stabilizing agents is forced. This study introduces a novel stabilizing agent based on unique properties of cellulose-based materials. Adding a small portion (dry weight <1 %) of cellulose-based stabilizing admixture forms a stabile gel-like structure with water. This structured gel has a high yield stress and a considerably low viscosity with thixotropic nature. In this study, it was shown that some of these properties can be attained in SCC mixes having a moderately low cellulose based admixture addition. These qualities build a foundation for a new type of SCC stabilizer, which modifies only the mixes' yield stress value.

2. MATERIALS AND METHODS

The cement used was CEM II/A-M(S-LL) 42,5N, Yleissementti from Finnsementti. Standard sand according DIN EN196-1 was used in mortar experiments. In concrete experiments, natural aggregates and filler were used. Two grades of Novel Cellulose Based stabilizing Admixtures (NCBA) were received from UPM and were used as received. The used superplasticizing agent was polykarboxylate ether –type Glenium 51 (17.5 %) from BASF. Commercial melamine sulphonate -based stabilizer was used as a reference stabilizer. Paste and mortar mixes were prepared in a small Hobart mixer. Concrete mixes were produced with a normal laboratory mixer (Zyklos).

Cement pastes were mixed during a 5 min mixing period. Extra water was added to NCBA pastes, in order to produce equal yield stress for each sample. In mortar samples, the aggregate/cement –ratio was 1 and the superplasticizer dosage was 0.37 % of cement weight. Various water / cement –ratio mortars were studied. Concrete samples were produced for a constant water/cement –ratio 0.6 with- and without the NCBA admixture.

Rheology of NCBA was measured with a RHEOTEST RN4 -rheometer with a coaxial cylinder geometry (S1). In paste mixes, serrated (1mm grooves) S1 geometry was used. Mortar rheology was measured with a Rheotest VK –geometry, specially designed for cementitious materials. Rheology of concrete was evaluated with Mk II impeller [2] in Tattersal -apparatus. According to the Bingham model, values for yield stress and plastic viscosity were calculated.

3. RESULTS AND DISCUSSION

3.1 Cement pastes

Cement pastes were proportioned experimentally for equal yield stresses (according Bingham model). The reference paste was pure cement paste with a w/c –ratio 0,4. Addition of NCBA increased the pastes' yield stress which was compensated with water addition. In Figure 1, it can be seen that appropriate NCBA + water addition produced pastes with relatively equal yield stresses compared to the reference paste. If the w/c –ratio was increased without NCBA, lowering of yield stress values was observed (Fig. 1 top left). Plastic viscosities of NCBA stabilized cement pastes followed the same w/c –ratio dependency as the reference paste without NCBA (Fig.1 top right). This phenomenon was especially pronounced with NCBA type 1 – stabilizers. Type 2 stabilizers had a slight increase in plastic viscosities. The commercial stabilizer was observed to increase both yield stress and plastic viscosity of the paste samples (Fig.1 top). Approximately five times larger NCBA type 2 -dosage was needed compared to NCBA type 1 stabilizers (fig. 1 lower left).

3.2 Mortar mixes

Rheology of mortar mixes was studied with a VK- measuring geometry. Absolute values for yield stress and plastic viscosities of mortar mixes are not possible to calculate with this measuring geometry. For approximately values, linear regression for torque (mNm) and speed of rotation (rpm) were done. Figure 2 presents “yield stress” torque and “plastic viscosity” for torque –values for the studied pastes. Similar behaviour of NCBA –stabilized mortars was observed comparing to cement paste results. It can be seen from Figure 2 that “yield stresses” of mortars can be affected, without a large effect to “plastic viscosity”. This phenomenon could be especially seen with NCBA type 1 –stabilizer and dosage 0.15%. It was possible to increase w/c-ratio from 0.35 to over 0.5 with equal yield stress, but significantly lower “plastic viscosity

3.3 Concrete

In concrete experiments a similar approach was applied as in mortar studies. Pressure and revolution rate were approximated as shear stress and shear rate. Rheology measurements with Tattersal -apparatus are presented in Figure 3. Concrete rheology studies were done with w/c –ratio 0.6 and relatively coarse natural filler. It was impossible to proportion a mix with SCC -type slump flow, with usual good concrete qualities (no bleeding and segregation). With an appropriate NCBA dosage, it was possible to produce a good quality SCC. If the NCBA –

dosage was increased, the “yield stress” was observed to increase, whereas no significant changes in “plastic viscosity” were seen. A rough estimate of values for these qualities can be estimated by comparing ratio of angular coefficients and intersection points in the Tattersal apparatus measurements. The ratio of angular coefficients was 1.4 and for intersection points 2.3. It can be concluded that similar behaviour of NCBA in paste and mortar studies can also be detected at the concrete scale.

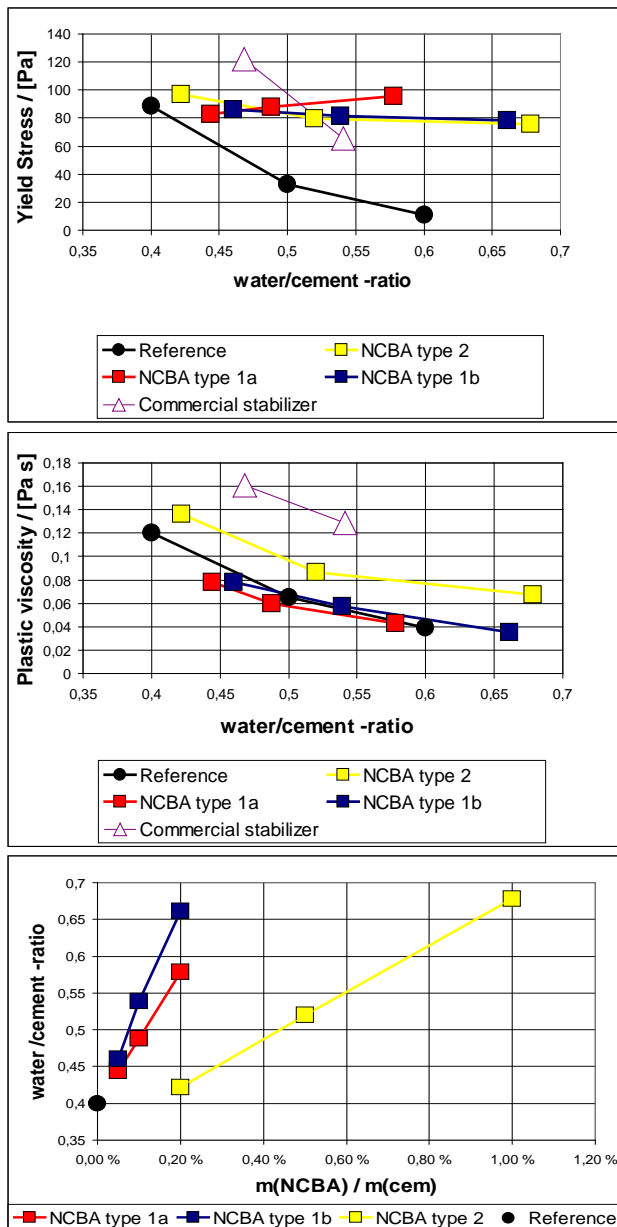


Figure 1. Results from rheological studies of cement pastes. Top left: Yield stresses of cement pastes as function of w/c -ratio. Top right: Plastic viscosities of pastes as function of w/c -ratio. Lower left: w/c -ratio as function of NCBA dosage.

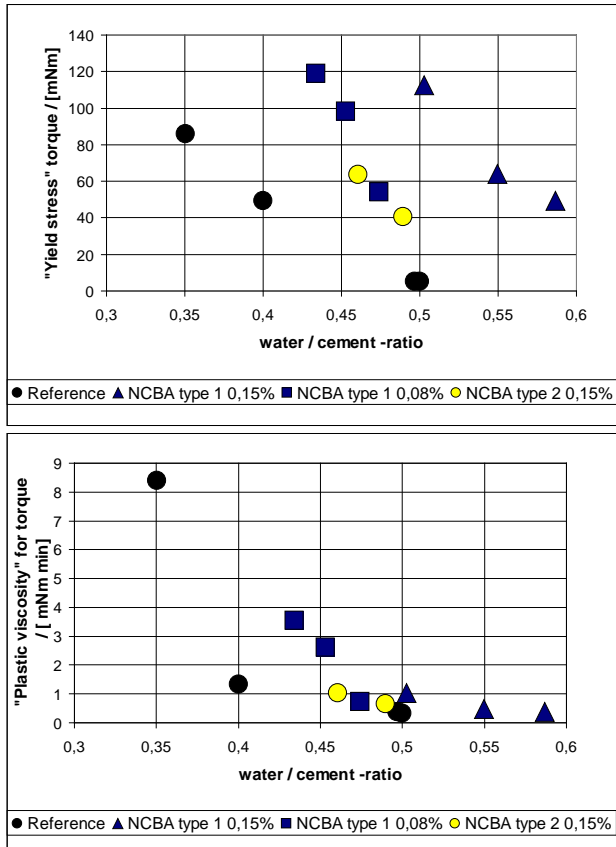


Figure 2. Results from rheological studies of mortar pastes. Left: “yield stress” –values as function of w/c –ratio. Right: “plastic viscosity” values as function of w/c –ratio.

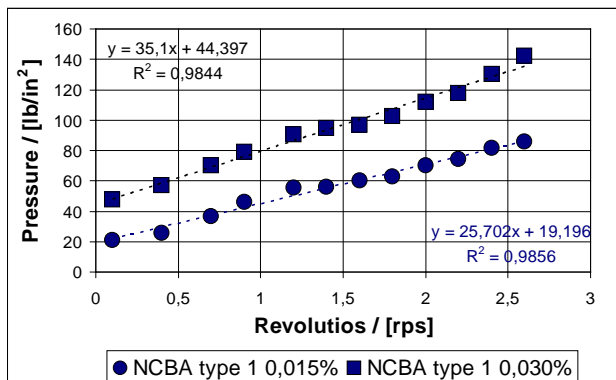


Figure 3. Rheology of NCBA type 1 –stabilized self compacting concretes. Addition of NCBA –stabilizer increased concretes’ yield stress. Without NCBA –stabilizer, it was impossible to prepare SCC.

4. CONCLUSION

Effects of Novel Cellulose Based stabilizing Admixture (NCBA) were introduced. Rheological properties of NCBA stabilized cement paste, mortar and self compacting concrete (SCC) were studied. It was observed that NCBA increased mixes yield stress and thus made it possible to produce high water / cement –ratio self compacting concretes with low performance aggregates and fillers. In comparison to a commercial melamine sulphonate –based stabilizing admixture, a

different mechanism was observed. With NCBA it was possible to modify yield stress independently without affecting plastic viscosity.

A complementary study of robustness qualities of Novel Cellulose Based stabilizing Admixture is also available [3].

REFERENCES

- [1] Birgisson B., Taylor P., Armaghani J., Shah S., “American Road Map for Nanotechnology-Based Concrete Materials” *Journal of the Transportation Research Board*, No. 2142 Vol.2 2010 pp.130-137.
- [2] Tattersall G., Banfill P., “The rheology of fresh concrete”, Pitman books limited, ISBN 0-273-08558-1, 1983
- [3] Kuosa H., “High water-cement ratio SCC robustness with novel cellulose based admixture”, *Nordic Concrete Research* 2011.

Session B2 – AGGREGATES AND ADDITIVES

Engineered Air-entrainment of Concrete



Sara Laustsen
M.Sc, B.Sc.
Technical University of Denmark
Department of Civil Engineering
Brovej, Building 118
2800 Kgs. Lyngby
Denmark
SAL@BYG.DTU.DK

ABSTRACT

Superabsorbent polymers (SAP) have been used to create voids in concrete. Salt frost damage seems to be dominated by the amount and type of the SAP particles rather than the size of the SAP particles. Internal frost damage is shown to propagate through the concrete specimens starting from the exposed surfaces. Furthermore, internal frost damage seems to occur before salt frost scaling. The compressive strength values are on the same level until a given amount of SAP. Calculated water absorption values based on computed tomography (CT) scanning indicate that the absorption decreases with increasing amount of SAP in concrete mixes.

Key words: SAP, salt frost scaling, internal frost damage, compressive strength, CT scanning.

1. INTRODUCTION

In the 1940's and the 1950's it was shown that air-entrainment of concrete improved the freeze-thaw resistance of concrete [1,2]. A chemically air-entraining agent (AEA) is mostly used to incorporate air into the concrete. The relative low cost related to the use of AEA is one of the advantages using AEA. However, the use of AEA has disadvantages. Some of the major disadvantages are mentioned below.

- The dosage of AEA is not clearly correlated with the air content in concrete [3].
- The air void system is unstable in fresh concrete. The air voids tend to coalesce to bigger air voids due to the lower free energy of big air voids compared to small air voids. This results in a poor distribution of air voids. Furthermore, the efficiency of air voids with respect to frost protection of concrete is higher for sub-mm air voids than mm-sized air voids.
- The density difference between air voids and the surrounding concrete may cause redistribution of the air void system and air loss. This is especially an issue at long mixing time and at long transportation time.

The concrete producer often has to entrain more air than necessary as a consequence of the above mentioned disadvantages. This is done to ensure fulfilment of the requirements regarding air content in concrete. The increased air content results in a higher strength reduction than necessary. Consequently, the concrete producer often uses a trial-and-error approach [3] for obtaining the optimum air content. The trial-and-error approach implies waste of concrete and thus money.

Superabsorbent polymers (SAP) have shown to counteract autogenous change of relative humidity [4] and were suggested as air entrainment by e.g. Jensen and Hansen [5]. A previous study indicates that SAP incorporates air into concrete [6]. SAP is a type of polymer able to absorb a large quantity of water relative to its own mass. SAP swells due to the water absorption. An example of SAP from everyday life is gummi bears. Dry, spherical SAP particles are added to the concrete during mixing. During mixing, the SAP particles absorb water and swell. Around setting time, the SAP particles are drained due to the concrete hydration. This results in air-filled or partly air-filled SAP voids containing the initial SAP particle. Some of the major advantages using SAP for incorporation of air into concrete are given below.

- Possibility of designing the air void system with respect to the amount of air and the size of the voids. This is based on knowledge about the amount of added SAP particles, size of added SAP particles and the swelling due to water absorption.
- The water-filled SAP particles will not coalesce and thus form a stable system.
- SAP particles are water-filled in fresh concrete and their densities are of the same magnitude as the density of water. This implies that the water-filled SAP particles do not redistribute to the same extent as air voids made by AEA.

The mechanisms of freeze-thaw deterioration have been studied for more than 60 years. Still, researchers are not agreeing on the mechanisms. However, it seems widely accepted that freeze-thaw deterioration composes of two kinds of deterioration: Internal frost damage and salt frost scaling damage. The internal frost damage occurs inside the concrete structures and is not visible on the outside. Salt frost scaling damage occurs on the concrete surface and is visible.

The present paper summarizes some of the results presented in the PhD thesis *Engineered air-entrainment of concrete* [7]. In total, 44 concrete mixes with water-cement ratio 0.45 were tested. Four types of SAP were used. Furthermore, washed SAP particles from one of the SAP types were used. All concrete mixes with SAP contained only one type of SAP. Four different sizes and 13 different amounts of SAP particles were tested.

2. CONCRETE PROPERTIES

Slump value and air content in fresh concrete were measured for all 44 concrete mixes. The air contents in fresh concrete seemed correlated with the amount and the type of added SAP. Similar tendency was not observed regarding slump values. The air contents of fresh concrete were lower for concrete mixes containing washed SAP particles than the corresponding concrete mixes with non-washed SAP particles. This indicated that residual surfactant on the SAP particles from the production caused entrainment of additional air into the concrete mixes. The amount of additional air depended on the amount and type of added SAP particles.

3. SALT FROST SCALING

All 44 concrete mixes were test with respect to salt frost scaling tests according to DS/CEN/TS 12390-9:2006 [8]. DS/CEN/TS 12390-9:2006 is similar as SS 13 72 44:2005 called the Borås method [9]. The results showed that the salt frost resistance was dominated by the type and the amount of SAP rather than the size of SAP particles. Furthermore, the results showed that the salt frost scaling resistance was higher of concrete mixes containing non-washed SAP than

concrete mixes containing washed SAP. The salt frost scaling resistance was, however, improved for concrete mixes containing washed SAP particles compared to reference concrete mixes (without SAP).

The theory for salt frost scaling described by Lindmark [10] fits the results best compared to the osmotic pressure theory presented by Powers [11,12] and the glue-spall theory presented by Scherer and Valenza [13]. Correlation between internal frost damage and salt frost scaling damage is possible according to the theory described by Lindmark. However, Lindmark seems to focus on water movement due to ion concentration differences. The more general explanation regarding water movement towards places at a lower energy state may be more suitable. This explanation includes water movement due to ion concentration differences and movement of super-cooled water towards ice.

4. INTERNAL FROST DAMAGE

The degree of internal frost damage was evaluated by use of photos of impregnated vertical cross sections of salt frost scaling specimens after 0, 14 and 56 freeze-thaw cycles. The specimens were taken from a reference concrete mix (without SAP) and concrete mixes with different amount of the same type of SAP. The photos showed that internal frost damage propagated through the specimens starting at the test surface for salt frost scaling. This indicates that the mechanisms of internal frost damage and salt frost scaling damage are correlated or similar. Furthermore, the photos indicated that internal frost damage occurred prior to salt frost scaling.

5. ABSORPTION OF SAP

Computed tomography (CT) scanning was conducted on approximately 20^3 mm^3 specimens from the concrete mixes containing washed SAP particles and the corresponding concrete mixes with non-washed SAP particles. Furthermore, CT scanning was conducted on cement paste specimens similar to the concrete mixes. The air void distributions of mixes containing SAP had a dominating peak unlike the air void distributions of the reference mixes (without SAP). The absorption values were calculated based on swollen diameter of the SAP particles. The swollen diameter corresponded to the position of the dominating peak. The calculated absorptions values were independent whether or not residual surfactant is present on the SAP particles. The calculated absorption values pointed to a lower absorption of SAP particles in concrete mixes than SAP particles in cement paste mixes. Furthermore, the calculated values indicated that the absorption decreased with increasing amounts of SAP in concrete mixes. Manual analyses of the air void systems supported the air void distributions based on CT data.

6. COMPRESSIVE STRENGTH

All 44 concrete mixes were tested with respect to compressive strength according to DS/EN 12390-3:2002 [14]. The compressive strength of concrete was reduced if the air content was increased. However, the results from compressive strength indicated that the strength was of the same magnitude as reference concrete mixes (without SAP) until a given amount of SAP. Subsequently, the strength loss was of the same magnitude as using AEA for incorporation of air into concrete.

REFERENCES

- [1] T. C. Powers, *The Air Requirement of Frost-Resistant Concrete*, Highway Research Board, Vol. 29, Portland Cement Association Bulletin 33, 1949.
- [2] T. C. Powers, *Void Spacing as a Basis for Producing Air-Entrained Concrete*, Journal of The American Concrete Institute, Vol. 25, No. 9, page 741-760, 1954.
- [3] M. Pigeon, J. Marchand and R. Pleau, *Frost resistant concrete*, Construction and Building Materials, Vol. 10, No. 5, page 339-348, 1996.
- [4] O. M. Jensen and P. F. Hansen, *Autogenous deformation and change of relative humidity in silica fume-modified cement paste*, ACI Materials Journal 93, No. 6, page 539-543, 1996.
- [5] O. M. Jensen and P. F. Hansen, *Water-entrained cement-based materials - I. Principles and theoretical background*, Cement and Concrete Research 31, No. 4, page 647-654, 2001.
- [6] S. Laustsen, M. T. Hasholt and O. M. Jensen, *A new technology for air-entrainment of concrete*, RILEM Proceedings PRO 61, page 1223-1230, Proceedings of the First International Conference: Microstructure Related Durability of Cementitious Composites, Edited by W. Sun, K. van Breugel, C. Miao, G. Ye and H. Chen, 2008.
- [7] S. Laustsen, *Engineered air-entrainment of concrete*, PhD thesis, Technical University of Denmark, Department of Civil Engineering, Section of Building Materials, 2011 (In preparation).
- [8] DS/CEN/TS 12390-9, *Testing hardened concrete - Part 9: Freeze-thaw resistance - Scaling*, 1st edition, Danish Standards, 2006.
- [9] SS 13 72 44, *Concrete testing – Hardened concrete – Scaling at freezing*, 4th edition, Swedish Standards Institute, 2005.
- [10] S. Lindmark, *Mechanisms of salt frost scaling of portland cement-bound materials: Studies and hypothesis*, PhD thesis, Report TVBM 1017, Lund University, 1998.
- [11] T. C. Powers, *The mechanism of frost action in concrete*, National Sand and Gravel Association, Stanton Walker Lecture No. 3, 1965.
- [12] T. C. Powers, *Freezing effects in concrete*, American Concrete Institute, ACI Publication SP 47-1, 1975.
- [13] G. W. Scherer and J. J. Valenza II, *Mechanisms of frost damage*, Materials Science of Concrete, Vol. VII, American Ceramic Society, page 209-246, 2005.
- [14] DS/EN 12390-3, *Testing hardened concrete - Part 3: Compressive strength of test specimens*, 1st edition, Danish Standards, 2002.

Accuracy of sand flow cone in characterizing fine aggregates



Olli Skyttä
M. Sc.
Consolis Technology Oy
PL 72
FI-21291 Rusko
olli.skytta@consolis.com

ABSTRACT

The problems related to characterizing sands in concrete production have increased lately as lower quality aggregates, especially the need to use manufactured sand have become the commonplace reality in many countries and locations due to environmental issues.

A fairly simple sand flow cone measuring the flow time and loose packing has been found able to give useful information for sand selection and quality control purposes with excellent accuracy. Sand flow cone was used to measure the effect of manufactured sand replacement of natural sand in two different cases with materials from two completely different geographical and geological locations.

Key words: fine aggregates, characterizing, accuracy, sand flow cone.

1. INTRODUCTION

Cost-efficiency has been governing the production in concrete industry until recent times when environmental issues have began to have an increasing role in the industry. The main solution to fulfil both of these requirements has been to reduce the amount of cement in concrete production by optimising the aggregate mix. However, most of the available tools to measure the aggregate properties, especially those of fine aggregate are either labour demanding, inaccurate or useful only for lab purposes requiring expensive equipment and highly educated specialists. The problems have increased lately as lower quality aggregates, especially the need to use manufactured sand have become the commonplace reality in many countries and locations.

A fairly simple and low cost sand flow cone measuring the flow time and loose packing has been tested for sand selection and quality control purposes. The target was to find a practical tool for sand characterization for aggregate mix optimization in full scale concrete production. Sand flow cone was used to measure the effect of manufactured sand replacement of natural sand in two different but typical cases, where the studied materials were from two completely different geographical and geological locations.

2. EXPERIMENTS

As the concrete industry is facing the need to replace natural sands with crushed sand - often called manufactured sand – the target of the test was to find out how well this test could differentiate the sands containing a varying percentage of crushed material. Generally the

crushed sand will have unfavourable particle shape and texture leading to lower packing density and longer flow times. In practise it would mean higher water demand leading to higher cement contents, which is not acceptable from environmental reasons. The particle shape can to a certain limit be controlled by the crushing procedure, thus the sand flow cone method could perhaps be useful for the characterization of sands crushed with different equipment.

2.1 Test method

The selected sand flow cone was the New Zealand sand flow cone, which was considered more interesting than other similar methods based on the experiences in Australian ready mix concrete industry (1, 2).



Figure 1 – New Zealand Sand Flow Cone.

The NZ cone uses a 1 kg sample of sand, which is allowed to flow through the funnel into a cylinder of known volume and weight. The surface of the cylinder is stroked even and the weight of the cylinder with the sand in it measured. As the specific gravity of the sand is known, the loose packing density of the sand can be calculated. The average of three measurements is calculated. The measured flow time in seconds and packing as a percentage of voids are the parameters describing the properties of the sand.

2.2 Test procedure

The sand flow cone test was performed first with 0/4 mm natural sand, after this 10 percent of the sand was replaced with 0/4 mm crushed sand, which had been sieved into small fractions and then combined again to have the same grading as the natural sand. Thus the particle size distribution was tried to be maintain the same through the tests, the only variable being the particle shape. The test procedure was repeated with the natural sand being replaced in 10 percent steps till the final test contained 100 percent crushed material. The replacement was by volume as the specific gravity of crushed aggregate – especially of limestone - was higher than that of natural sand. In both cases the crushed material was produced by standard crushing equipment without special attention to the obtainable particle shape of fine aggregate.

The first test series was with Finnish glasifluvial sand, which was replaced by crushed bedrock silicate aggregate consisting mainly of large crystals of feldspars, quarts and mica minerals.

The second test series was done with Dutch river sand, which was replaced by crushed Belgian limestone.

3. TEST RESULTS

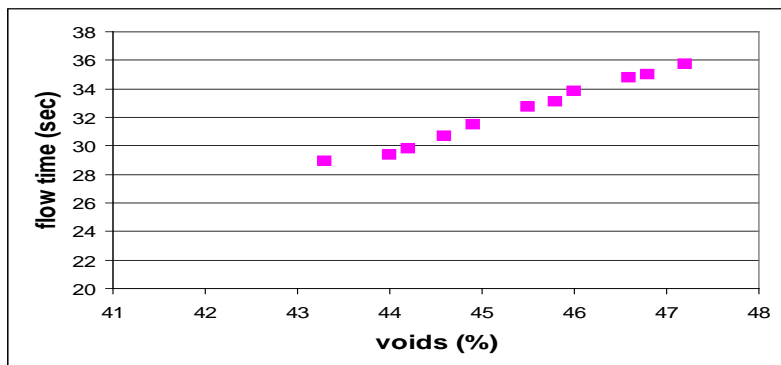


Figure 2 – Test results with natural Finnish sand replaced by crushed granite

The measurement with plain sand gave the best packing and shortest flow time as expected. The effect of increasing replacement with crushed material was surprisingly linear. Experience with rodded packing of aggregates would have suggested markedly larger variation. Now the variation between packing measurements was less than 0.5 volume percent, which compares to a variation of void space of less than 5 litres per cubic meter of packed material.

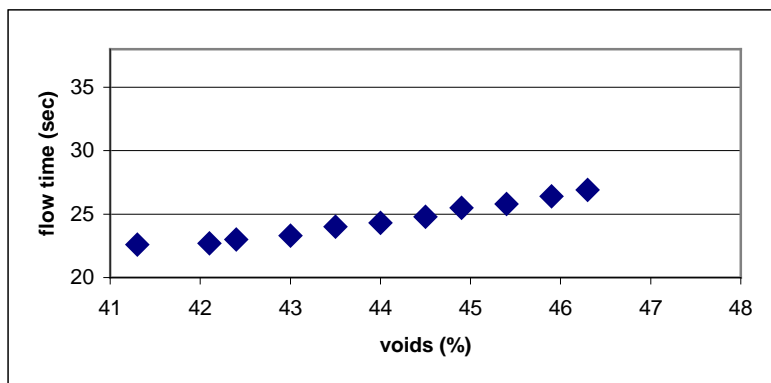


Figure 3 – Test results with natural Dutch river sand replaced by crushed limestone

The results with Dutch river sand replaced by crushed limestone gave even more linear response (Fig. 3).

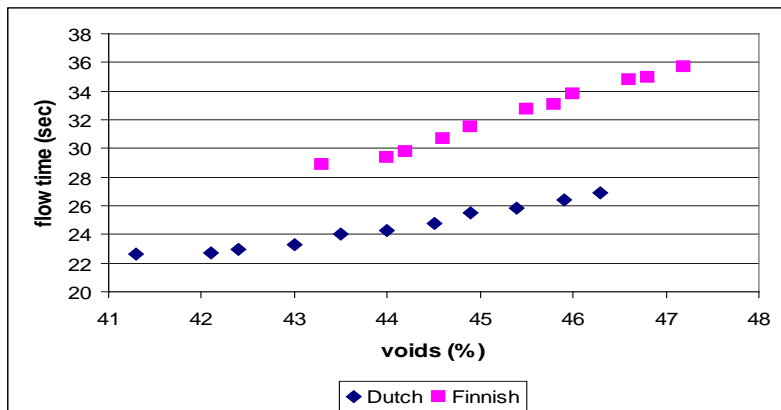


Figure 4 – Difference between aggregates from different sources.

The difference in packing and void space measurement between Finnish aggregates and Dutch aggregates can be explained by the more cubical shape of minerals, especially of feldspars, of Finnish aggregates.

4 CONCLUSIONS

A fairly simple and low cost sand flow cone measuring the flow time and loose packing has been found to be able to give useful information for sand selection and quality control purposes with excellent accuracy. Sand flow cone was used to measure the effect of manufactured sand replacement of natural sand in two different but typical cases, where the studied materials were from two completely different geographical and geological locations. The obtained results have led to the use of sand flow cone as a standard tool for fine aggregate characterizing and concrete mix optimization in full scale concrete production.

REFERENCES

1. Day, K., "Concrete Mix Design, Quality Control and Specification", E & FN Spon, 2006, 357 pp.
2. Finnish Standards Association, SFS-EN 933-6, "Tests for geometrical properties of aggregates. Part 6: Assessment of surface characteristics. Flow coefficient of aggregates", 2002-03-04
3. NZS 3111 "The Sand Flow Test", 1986

Synergetic effect between fly ash and limestone powder in Portland composite cements



Klaartje De Weerd
PhD student
SINTEF Building and
Infrastructure
NO-7465 Trondheim
Klaartje.De.Weerd@sindef.no



Harald Justnes
Chief Researcher
SINTEF Building and
Infrastructure
NO-7465 Trondheim
Harald.Justnes@sindef.no



Knut O. Kjellsen
Adjunct Professor
NTNU departement of
Structural Engineering
NO-7491 Trondheim
Knut.Kjellsen@norcem.no

ABSTRACT

Replacing 5% fly ash with 5% limestone powder in a fly ash blended cement (35% fly ash), gives rise to an increase in strength both after 28 days and 1 year of curing at 20°C. This strength increase coincides with changes in the nature of the hydration products, observed using both XRD and TGA. Combining both fly ash and limestone powder to replace ordinary Portland cement yields a higher strength than when using either one of them. This is referred to as the synergetic effect between fly ash and limestone powder.

Key words: carboaluminate hydrates, XRD, TGA.

1. INTRODUCTION

The objective of this study was to contribute to the design of an all-round Portland composite cement with increased clinker replacement (about 35%) using materials available on the Norwegian market. It was opted to use fly ash which is currently used for the production of the fly ash blended cement, and limestone powder available at the quarry used for the production of the clinker.

A synergetic effect between fly ash and limestone when replacing ordinary Portland cement (OPC) was postulated at the XX NCR symposium 2008 [1]. Limestone is known to interact with the AFm phases and leads to the formation of hemi- and monocarboaluminate hydrate instead of monosulphate [2]. The ettringite is thereby stabilized, which might result in an increase in solid volume and a decrease in porosity. This on its turn might result in an enhanced compressive strength. The impact of this on the properties of OPC is however limited due to the low aluminate content of the OPC (5%). Fly ash, on the other hand, is richer in aluminates (about 20%). During its pozzolanic reaction, the fly ash liberates additional aluminates and might thereby enhance the effect of the limestone powder.

The aim of this study is therefore to investigate this postulated synergetic interaction between fly ash and limestone when replacing OPC, and its impact on the compressive strength.

2. EXPERIMENTAL

The materials used in this study are: ordinary Portland clinker, a class F siliceous fly ash (FA), limestone powder (L), and natural gypsum. The chemical composition determined by XRF and the physical properties of the clinker, fly ash, and limestone are given in Table 1. The clinker was interground with 3.7% of natural gypsum and is further referred to as ordinary Portland cement (OPC).

Table 1 - Chemical composition and the physical characteristics of the clinker, fly ash and limestone powder

	Clinker	Fly ash	Limestone
SiO ₂	20.0	50.0	12.9
Al ₂ O ₃	5.4	23.9	2.7
Fe ₂ O ₃	3.1	6.0	2.0
CaO	60.6	6.3	42.3
MgO	2.9	2.1	1.8
SO ₃	1.5	0.4	-
P ₂ O ₅	0.1	1.1	-
K ₂ O	1.2	1.4	0.6
Na ₂ O	0.5	0.6	0.5
LOI	0.3	3.6	37.7
Carbon	-	3.1	-
Chloride	0.05	0.0	-
Free CaO	1.85	-	-
Gypsum	3.7	-	-
Blaine surface [m ² /kg]	450*	450	810
Density [kg/m ³]	3150*	2490	2740
d ₅₀ [μm]	11*	14	4

* For OPC = clinker + gypsum

The compressive strength was tested on three mortar prisms (40×40×160 mm) prepared with a water-to-binder weight ratio of 0.50 and binder-to-sand weight ratio of 1:3. The samples were cured at 20°C, in a saturated Ca(OH)₂ solution.

Paste samples were prepared with a water-to-binder ratio of 0.50. The pastes were stored under sealed conditions at 20°C. At the age of testing the samples were crushed and the hydration was stopped by solvent exchange using isopropanol and ether. The resulting powders were examined by thermogravimetric analysis (TGA) using a Mettler Toledo TGA/SDTA851 and by X-ray diffraction (XRD), using a PANalytical X'Pert Pro MPD diffractometer in a θ -2 θ configuration with an incident beam monochromator and CuK α radiation ($\lambda=1.54\text{\AA}$).

3. RESULTS

Figure 1 show the compressive strength measured on mortar after 28 days and 1 year of curing of composite cements containing 65% OPC and 35% of a combination of fly ash and limestone powder, and limestone cements. It can be seen that both replacing 5% fly ash with 5% limestone in a 65%OPC + 35% fly ash cement, or 5% of OPC in an 100% OPC results in a slight increase in compressive strength at both tested ages. In the case of the composite cements containing fly

ash, the effect was greatest after 28 days and seems weakened after 1 year, whereas for limestone cements the effect seems to increase with time.

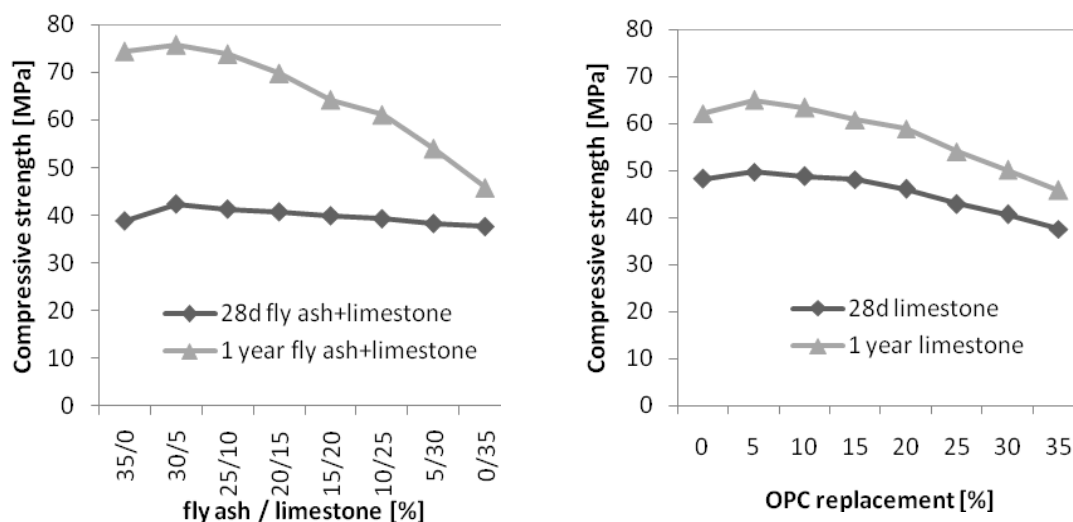


Figure 1 - Compressive strength measured on mortar prisms after 28 days and 1 year of curing at 20°C; Left: composite cements containing 65%OPC and 35% a combination of fly ash and limestone powder; Right: OPC replaced by limestone powder.

Figure 2 shows the thermogravimetric (TG) curves with the corresponding derivative curves (DTG), and the X-ray diffraction patterns (XRD) for four mixes: 100% OPC, 95%OPC+5%L, 65%OPC+35%FA and 65%OPC+30%FA+5%L. The presence of limestone powder results in a change of the hydration products. In the DTG curves this is reflected by changes at about 120°C and 180°C which correspond to changes in respectively the AFt and AFm phases.

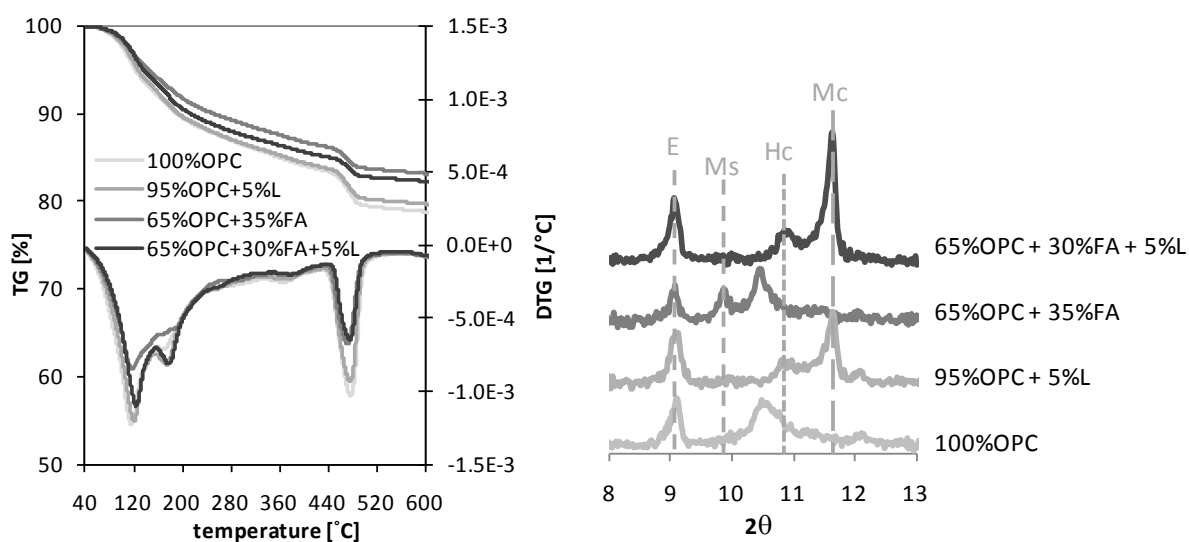


Figure 2 - Left: Thermogravimetric (TG) curves and their derivatives (DTG) for pastes cured for 90 days at 20°C. Right: XRD spectra for pastes cured for 90 days with E=ettringite, Ms = monosulphate, Hc = hemicarbonat and Mc = monocarbonat.

These changes are confirmed by the XRD patterns at low diffraction angles: in the presence of limestone ettringite (E) is stabilized and hemi- and monocarbonat (Hc and Mc) form instead of monosulphate (Ms). The broad peak between Ms and Hc is most likely an Ms-like phase in

which part of the sulphate is replaced by hydroxides and/or carbonate. It should be noted that more AFm phases are formed in the composite cements containing fly ash compared to their OPC equivalents, indicating that additional aluminates are supplied by the fly ash.

The strength increase when 5% fly ash or 5% OPC is replaced with 5% limestone is most likely due to the observed changes in the hydration products, as discussed previously [3, 4].

3 CONCLUSION

The synergetic effect when combining fly ash and limestone powder to replace OPC has been confirmed. A combination of fly ash and limestone powder showed a higher compressive strength than using only one of them. Furthermore the strength increase coincides with a change in hydration products which is observed by XRD and TG.

The commercial fly ash blended cement currently produced at Norcem Heidelberg cement (<20% fly ash) does not contain limestone powder. Combining fly ash with limestone powder to replace the clinker enables to increase the clinker replacement. In future commercial cements this synergetic effect between fly ash and limestone powder might be used. In 2010, trial projects such as the Meteorological Institute in Oslo, and the Science Center in the county, Østfold, using a cement consisting of 65% OPC, 30% fly ash and 5% limestone powder have been performed by Norcem Heidelberg cement [5].

4 ACKNOWLEDGEMENTS

The paper is based on the work performed in COIN - Concrete Innovation Centre (www.coinweb.no) - which is a Centre for Research based Innovation, initiated by the Research Council of Norway (RCN) in 2006. COIN has an annual budget of NOK 25 mill, and is financed by RCN (approx. 40 %), industrial partners (approx 45 % of which ¼ is cash) and by SINTEF and NTNU (in all approx 15 %). The Centre is directed by SINTEF, with NTNU as research partner and with the present industrial partners: Aker Solutions, Norcem, Norwegian Public Roads Administration, Rescon Mapei, Skanska, Spenncon, Unicon, Veidekke and Weber Saint Gobain.

REFERENCES

1. De Weerd, K. and H. Justnes. The reactivity of fly ash and limestone in cementitious systems. in Proceedings Nordic Concrete Research. 2008. Bålsta: p. 104-105.
2. Lothenbach, B., et al., Influence of limestone on the hydration of Portland cements. *Cement and Concrete Research*, 2008. 38(6): p. 848-860.
3. De Weerd, K., et al., Synergy between fly ash and limestone powder in ternary cements. *Cement and Concrete Composites*, 2011. 33(1): p. 30-38.
4. De Weerd, K., et al., Hydration mechanisms of ternary Portland cements containing limestone powder and fly ash. *Cement and Concrete Research*, 2010. In review.
5. Mathisen, E., *Green cement for the house of the future (in Norwegian)*, in *Cement Nå*. 2009, Norcem HeidelbergCement Group Oslo, Norway. p. 3-6.

Feasibility of Optical Moisture Measurement in Concrete Aggregates



Taisto Haavasoja
M.D., Ph.D. (Phys.)
Teconer Ltd
Runopolku 1b,
FI - 00420 Helsinki
taisto.haavasoja@teconer.fi

ABSTRACT

We have studied feasibility of using optical means to measure aggregate moisture content. We measured optical response of some commonly used aggregates at around 1.5 μm wavelengths. The results suggest that this wavelength range enables nominal accuracy of about 0.1% in moisture by weight. One of the major benefits in optical technology is a noncontact measurement allowing practically a onetime calibration procedure and a long lifetime of the sensor due to solid state design. On the challenge side there is a need to protect the sensor window from dust and condensing of moisture. These issues have been field tested in concrete plants and a long term accuracy of 0.3% is realistic in practise. We also measured the optical response to a maximum variation in aggregate grading.

Key words: Aggregate, moisture, water content, optical sensor, infra-red spectroscopy.

1. INTRODUCTION

Coarse aggregates can contain 0-2% surface moisture by weight and fine aggregates even up to 10%. These numbers exclude absorbed water, which ranges typically from 0.5 to 4% according to Ref. [1]. Ultimately, wet aggregates may contain moisture more than is desirable to preserve the water-cementitious material ratio (w/cm) in design limits and not overdosing cement. In practise, moisture content of aggregates must be known to fractions of percent to minimise variability in concrete quality and to enable optimal usage of cement. Accurately measured moisture in aggregates allows optimising strength, durability and shrinkage of concrete products. Also knowing the right moisture content prior to mixing permits faster mixing times, when there is no need to add water during mixing.

There are a number of means to arrange measurement of aggregate moisture in concrete plants. The traditional measurement by weighing and drying a sample is satisfactory only in plants, where the aggregates are well mixed by the time of loading to silos so that variation of moisture is minimal between batches. Few plants have this strategy in practise and thus in many plants an automatic measurement is highly recommended.

Currently the most widely used automatic moisture measurement in concrete industry seems to be based on capacitive or microwave sensors. These sensors are installed typically in direct contact with the aggregates in silos or silo feeders. The dipole nature of water molecule implies a high dielectric constant of water enabling simple detection in aggregates by coupling to a sensing electromagnetic field. Since the dielectric constant of most aggregates is fairly small compared to water, capacitive sensing produces often a fairly stable result. Nevertheless, direct

contact to sample causes mechanical wearing of the sensor requiring occasional recalibration and finally replacement of either the sensor plate or the whole sensor. Few concrete plants have personnel capable to calibrate or maintain the sensor.

Optical detection of material moisture would allow noncontact detection with clear advantages for concrete industry. Optical moisture sensors are based on absorption peaks by water molecules at near infra-red wavelengths. There have been optical moisture sensors available for process industry over tens of years, but they have not been widely used in concrete plants due to their high price compared to microwave sensors. However, development of optoelectronic components thanks to optical communication technology has enabled designing more optimal sensors for measuring surface moisture in aggregates.

In the following chapters we present a new optical sensor designed for detection of moisture and discuss the challenges of applying the sensor for optical detection of aggregate moisture.

2. WATER CONTENT MONITOR WCM411

Optical moisture sensors have an active light source, which transmits preselected wavelengths of light on the sample, and a detector, which collects the reflected light for analysis. There are typically two or more wavelengths selected so that one is on an absorption peak of water molecule and the other are used for a reference signal. The reflected amount of light at each wavelength bears information about surface moisture on the sample studied.

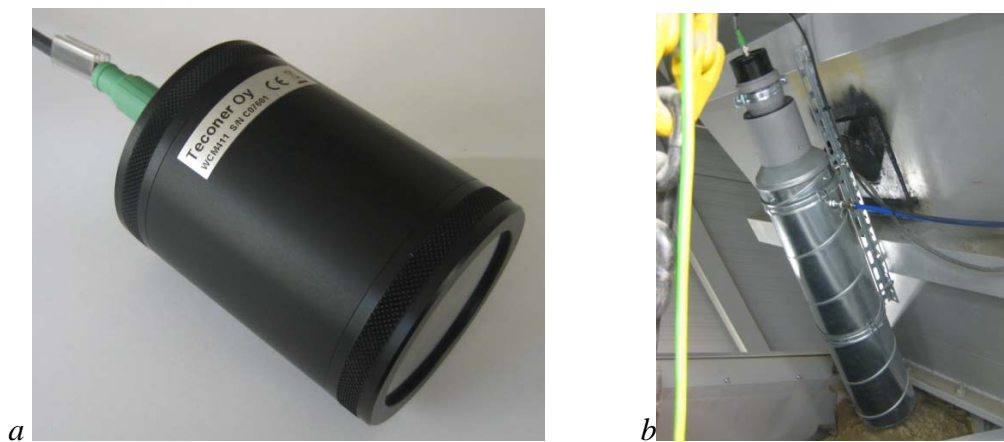


Figure 1 – (a) A photograph of the WCM411 sensor on the left and (b) an example of an installation with a dust protection tube on the right.

The new optical sensor is called Water Content Monitor WCM411 (Teconer Ltd.). A photograph of the sensor and an example of installation over a silo feeder are shown in Figure 1. The sensor is installed typically within 0.5 – 0.8 meters from the sample surface with a dust protection tube as shown in Figure 1b. The sensor is supplied with a cable for power (9-30 VDC) and communication (RS-232, 4-20 mA current loop). Repeatability and short time stability of the sensor is about 0.1% by weight. An absolute accuracy of about 0.3% is reachable with a careful calibration and this accuracy can be maintained for extended periods assuming dust protection of the sensor window is effective. The sensor does not have any moving parts and uses a long lifetime LED light source allowing an extensive maintenance free service life.

3. PERFORMANCE

The response of an optical sensor to moisture comes from the sample surface. Some aggregates may be partially transparent and in that case the response may come from some depth beneath the upper surface, typically a few millimetres. Since the detection area is fairly small, less than 0.1 m at 1 m distance, the sample area is often not optically homogeneous, which prevents accurate measurements with static samples. Thus it is better to use a moving sample and calculate an average value to represent the whole lot. To calibrate a given sample of aggregate, we use a micro mixer to mix the sample continuously and add water, e.g., in steps of 1%. Figure 2 shows an example of a calibration response with a 0-4 mm fine aggregate.

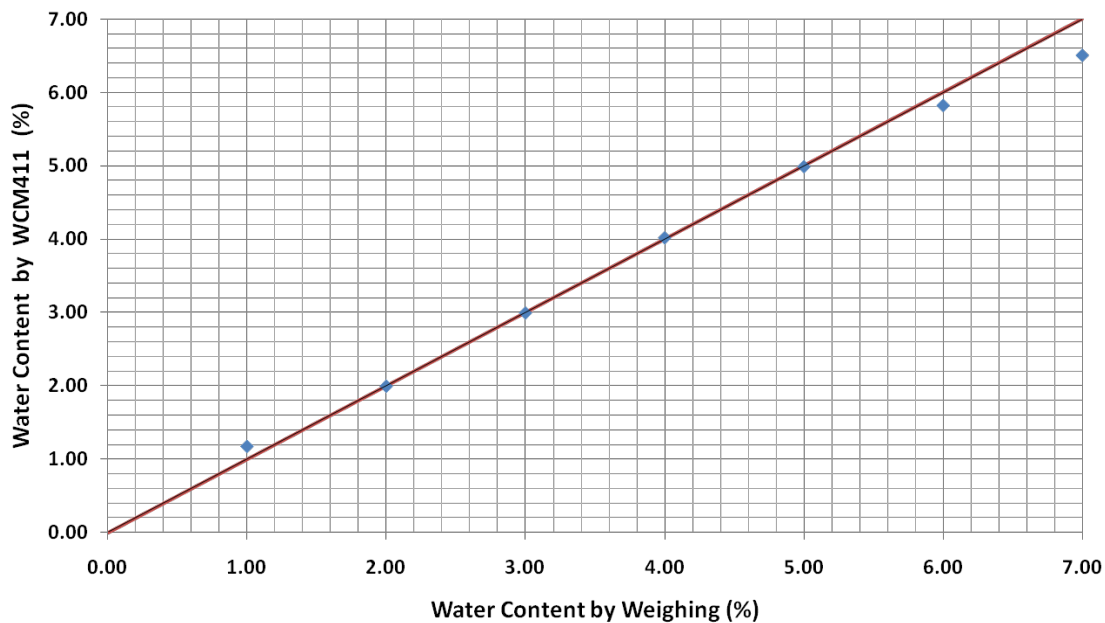


Figure 2 - A typical calibration line for a 0-4 mm fine aggregate. The blue dots represent response to addition of water content in steps of 1%. The red line is just a guide to the eye for an ideal response. The deviations at 1%, 6% and 7% come from an incomplete mixing of the micro mixer, which can be proved by employing another kind of a mixing technique.

As Figure 2 implies an optical sensor can have an extremely high nominal accuracy, fractions of 0.1% at typical moisture contents. However, there are a number of reasons why this level of accuracy is not reachable in practise. Those reasons include variation in grading of the aggregate, challenges in sampling reference values of moisture and stability of the measurement environment. The last concern can be taken care by the dust protection tube and secure fixing of the sensor as shown in Figure 1b.

We tested the sensitivity to variation in grading in a 0-8 mm fine aggregate. The grading was changed by adding fine particle fractions up 0.25 mm sieve as much as the norm [2] allows. This corresponded to an increase of about 15 units in fineness number and 8.7% in formal surface area. If the optical measurement interacts only with the top layer of the sample, we would expect the slope of the calibration curve to decrease by the increase of surface area. The change was clearly smaller, from 1.000 to 0.952, corresponding on the average to a reduction of only 0.20%

units in moisture (Figure 3a). The result supports the interpretation that the aggregate is to some extent transparent at near infrared wavelengths.

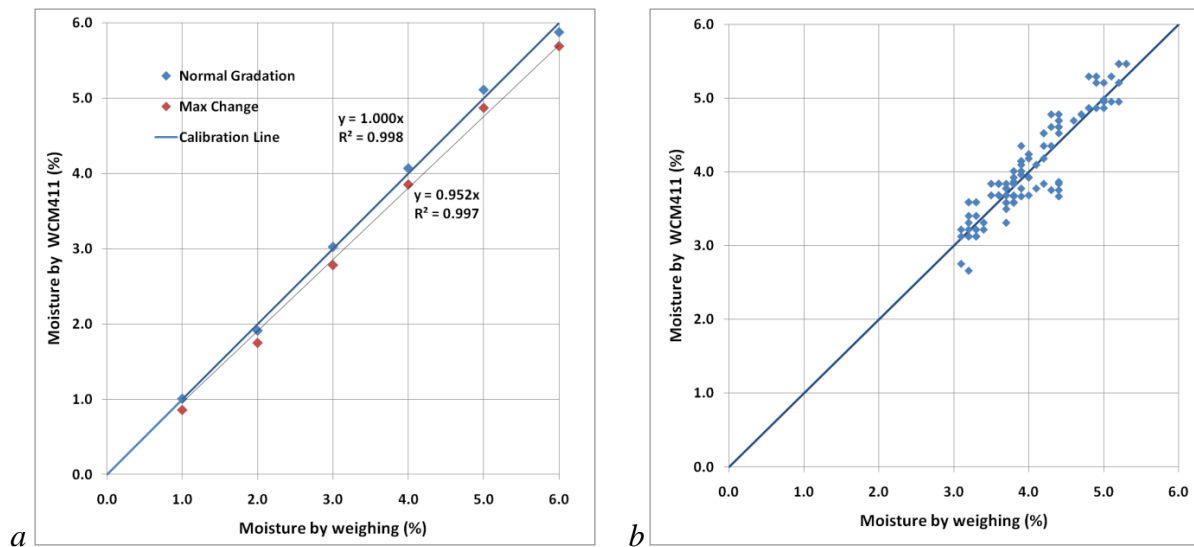


Figure – 3 (a) Response of a calibrated sensor (blue dots) to a maximum increase in fine gradation (red dots) and (b) comparison to a reference in a long term plant test.

Figure 3b shows the results of a long term test in a plant environment. The apparent differences in the data have clearly increased as compared to calibration data. However, the standard deviation, 0.25% in moisture, is still fairly low. Surprisingly, the most significant reason for the scatter is not related to the performance of the sensor but instead to manual sampling problems of the weighed reference data.

4. CONCLUSION

Optical sensing of moisture in concrete aggregates has been available for some time but it has not been competitive with capacitive and microwave technologies so far. Recent advances in solid state light sources and detectors have enabled designing price competitive optical sensors which can be optimised for a given specific task. We have shown that the performance of an optical moisture sensor competes with microwave technologies. The challenge to keep the optical window clean can be solved with simple arrangements. Noncontact measurement, long lifetime due to solid state design, easy calibration, high accuracy and low need for maintenance will help to deploy optical sensing to measure aggregate moisture.

REFERENCES

1. Aggregates for Concrete, [ACI Education Bulletin E1-07](#), developed by ACI Committee E-701, American Concrete Institute 2007.
2. BY43 Betonin kiviainekset 2008, Betoniyhdistys ry, Suomen Rakennusmedia Oy 2008.

How to evaluate crushed rocks for concrete production



Björn Lagerblad
PhD. Senior Researcher
Swedish Cement &
Concrete Research Inst.
100 44 Stockholm Sweden
bjorn.lagerblad@cbi.se



Mikael Westerholm
Techn. Lic., Researcher
Swedish Cement & Concrete
Research Inst.
100 44 Stockholm Sweden
mikael.westerholm@cbi.se



Hans-Erik Gram
PhD. Project Leader
Cementa AB
Box
hans-
erik.gram@cementa.se

ABSTRACT

Crushed granitic rocks as fine aggregate can be used to produce concrete but the suitability varies. In general the crushed aggregates contain too much fillers but this can be adjusted with wind sieving. Some products can almost directly replace natural aggregates while others are almost impossible to use without an excess of cement. In much this depends on the quality of the fines. The fines are normally made up of mineral grains and the shape of these minerals defines the quality. Cubic feldspars give good fines while flaky micas give fines of poor quality. There are several indirect test methods that indicate the quality of the fines.

Key words: Concrete, manufactured sand, grain shape, micas, granites, rheology,

1. INTRODUCTION

Natural aggregates must be saved for environmental reasons and thus aggregates from crushed rocks must be utilized in concrete production. In Sweden most stone quarries are situated in granitic rocks and products from this rock type has been investigated. Fragments of crushed rocks are more rugged and flaky and according to traditional proportioning more cement is needed to get proper rheology and workability. Larger grains can easily be screened and cubitized but it is more difficult with the fine aggregates. The most important parameters in proportioning of concrete are sorting and grain shape. The sorting must be adjusted for grain shape and texture. To be able to do this the properties of all fractions must be evaluated and problems identified.

Cement production has a large environmental impact and thus methods to decrease the amount of cement in the mixes must be found. The problem is to identify where the problem is and to find methods of comminution, screening and separation to get better sorting and grain shape.

1.1 Concrete proportioning with crushed rocks as aggregate

Fresh concrete is a particle suspension. In the fresh concrete cement is also a particle. Larger particles mainly roll on smaller particles. As a general rule flaky and rough particles need more fine material. This is valid all the way down to the finest particles, the filler. In general the effect on workability of large flaky or elongated particles can be compensated by increasing the amount of fine material. Thus, for a given workability and quality, the more flaky and rough fragments of crushed rocks has to be compensated for by a larger amount of cement or other fine particles.

2 EVALUATION OF FINES

The workability of the concrete has been measured with the classical methods like Abrams slump cone but the data becomes more accurate when measured in a viscometer. It divides the workability in yield stress and plastic viscosity. The yield stress measures the force needed to set the concrete in motion, while the plastic viscosity describes how easily it flows when the yield stress has been exceeded.

Even with the same concrete recipe there is a large variation in workability and rheology depending on the properties of the 0/2 mm fraction. The performance of the aggregates have been analyzed in concrete 0-16 mm, mortar (0-2 mm) and micro mortar (0-0.25 mm). The results show that the quality of the 0/2 mm fraction and the fines are most critical when it comes to the workability and rheology of concrete. The problem increases with decreasing aggregate size. Thus most work was concentrated on the material passing the 2 mm sieve.

Figure 1 shows the rheological properties of mortar with different 0/2 mm material. The mortar has a fixed composition between aggregate, cement and water. A fine aggregate with low water demand and good particle shape gives a mortar or concrete with relatively low yield stress and plastic viscosity. The red area shows the rheology of the mortar with aggregate as delivered. These aggregates gave mortars with a very large spread in rheology, mainly, due to high contents of fine material and filler. Thus to be able to compare the effect of particle shape and quality the material was resorted to the grading of the natural aggregate. By resorting the material the rheology can be improved but there are still differences that are due to different basic properties. Some of the aggregates have a yield stress similar to natural aggregate (green symbol) but the plastic viscosity is always higher.

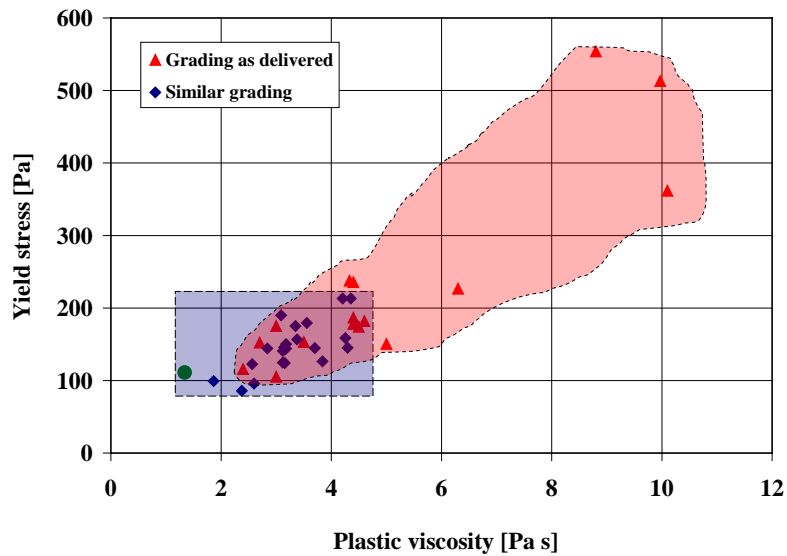


Figure 1. Influence of different fine aggregates (0/2 mm) on the rheology of mortar. No superplasticizer used. The mortar with the green symbol is the reference aggregate (natural aggregate). The red symbols are from crushed aggregates as it arrived. Blue symbols are from crushed aggregate resorted to the grading of natural aggregate.

More refined rheological studies [1] with finer fractions (micro mortar) show that the problems mainly are due to bad properties in fractions less than 0.25 mm. The yield stress and plastic viscosity can be lowered further by the use of super plasticizer (see later) but the superplasticizer (SP) is not able to fully compensate for poor particle shape and thus the viscosity will always be higher. There may also be problems with water separation and cohesion if overdosed with SP.

Figure 2 shows the results of a series of concrete mixes with decreasing amounts of cement and increasing amount of fines. The results show that by keeping the water/cement ratio constant it is possible to reduce the amount of cement and increase the strength. This, however, demands an increase in the amount of superplasticizer.

By increasing the amount of fines (micro mortar) in concrete it is possible to minimize the effect of more troublesome coarser particles but this in turn demands good quality of the fines and thus the quality criteria of the fines has to be defined.

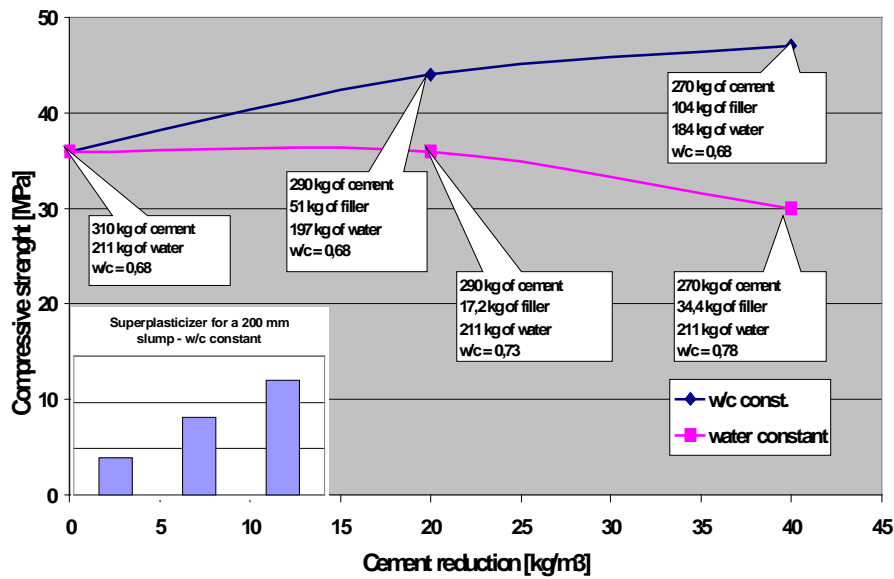


Figure 2. Test of compressive strength of concrete (0/16 mm) with increasing amount of good quality fines and decreasing amount of cement [2]. The slump is adjusted to 200 mm by superplasticizer. The relative amount of SP is indicated in the inset figure. The blue line is with constant w/c and the red line with cement replacement and constant amount of water. The fines is the fine fraction of wind sieved material, mainly < 0.2 mm.

The major problem with the fines from granitic crushed rocks is the grain shape. This can be analyzed by image analysis of microscopic picture from cut sections, either from thin sections in polarizing microscope or scanning electron microscope [1]. The two dimensional picture from a cut sample can, however, not divide between an elongate and a flaky particle. Thus analyses were also performed on lying particles that can divide between these two. The results showed that the flaky geometry was domination over the elongated.

In most cases the flakiness diminishes with increasing grain size. Comparison with petrography showed that the flakiness could be correlated with the amount of free mica and that this in turn was correlated with bad rheology, especially viscosity (Figure 3). The improvement in grain shape with larger grains is due to that with larger size the micas are bound to other minerals and the composite is more cubic than the mica itself. With more coarse grained rocks free mica is found in coarser fractions.

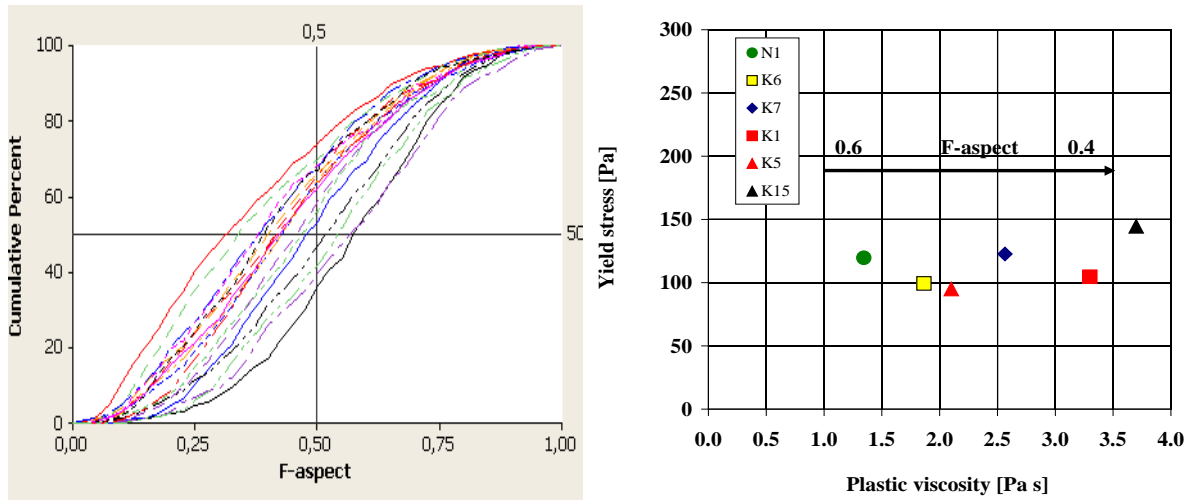


Figure 3a show the particle shape (*F-aspect*) in the 0.125/0.25 mm (sieve) fraction from different granite fine aggregates. A majority of the crushed aggregate are flakier than the natural aggregate (curve to the right).

Figur 3b shows the effect of the aggregate shape on the rheology of mortar (0/2 mm). The *F-aspect* comes from 0.125/0.25 mm (sieve) grains.

In routine quality control of fine aggregate it is not possible to run petrographic analyses, image analyses or rheological tests. Other and simpler methods, apart from standard sieve analysis, are needed.

Other methods to characterize fine sands include loose packing, determination of flow time, flakiness index besides above mentioned rheological methods. Loose packing showed that angular and flaky particles packed less and thus this can be used as criteria. Flow of dry particles (and mortar) showed that more flaky particles passed a funnel slower and can thus be used as quality criteria.

REFERENCES

1. Lagerblad, B., Westerholm, M., Fjällberg, L., Gram H-E, (2008). Bergkrossmaterial som ballast i betong, 121pp, CBI-rapport 1:2008 (in Swedish with English summary.)
2. Horta, A., Environmental Implications of replacing natural sand into crushed rocks in concrete. Master thesis KTH, To be published 2011.

The work has been financed by the Swedish Energy Agency (Pnr 30491-1), the consortium for financing basic research at CBI and Cementa AB.

The final report will be published 2011.

Finland's Emerging Alkali-Aggregate Reaction Problem?



Hannu Pyy
Lic. (Tech), Senior
Research Scientist
VTT Technical Research
Centre of Finland
P.O. Box 1000
FI-02044 VTT, Finland
hannu.pyy@vtt.fi



Erika Holt
Ph.D., Senior Research
Scientist
VTT Technical Research
Centre of Finland
P.O. Box 1000
FI-02044 VTT, Finland
erika.holt@vtt.fi

ABSTRACT

Finland is known as a country having very durable granitic aggregate that is used in a wide range of construction applications. Yet recent field results from existing concrete structures have shown evidence of alkali aggregate reactions (AAR). In Finland there is a need to have a better understanding of what causes AAR and from what aggregate sources, how to identify it or separate it from other deterioration mechanisms and guidelines about how to avoid AAR in future construction. This paper shares information about a few of the Finnish structures where AAR has been detected.

Key words: deterioration, durability, alkalinity, aggregate, alkali aggregate reaction

1. BACKGROUND

Certain aggregate types have a high risk of dissolution when interacting with the alkalis released during the hydration of portland cement. In wet conditions, this reaction causes a gel around the aggregate particles that can crack the concrete and provide further paths for deleterious materials. The reaction is referred to as Alkali Silica Reaction (ASR) for concrete or aggregate containing silica, or more commonly Alkali Aggregate Reaction (AAR). It has often been believed that the chemical reaction between Finnish aggregates and their surrounding environment is quite low. In this regard, the risk of AAR has been considered negligible in Finland. Yet recent in-situ structural concrete assessments have shown otherwise.

The three conditions required for AAR to occur include: 1) reactive silica (from aggregate), 2) sufficient alkalis (mainly from portland cement), and 3) sufficient moisture. Without a high moisture content (>80% RH), ASR will not occur. Higher temperature also accelerates AAR. Thus southern European climates often report a much higher incidence of AAR in concrete compared to Nordic environments. In Finland, the highest risk environment would be a very moist and warm environment, exemplified by modern indoor spa and pool facilities. Exterior concrete structures in Finland are also at risk of AAR, though the deterioration may take longer to appear. On the other hand, concrete exposed to a permanently dry or a heated indoor environment is considered not at risk of AAR, independent of aggregate type or binder composition.

The rate of AAR reaction is also very dependent on an aggregate's geological composition. The first sign of an AAR problem is usually random- or map-cracking on the concrete surface caused by excessive internal expansion. Internally, the gel causing the internal expansion can dry to form a white amorphous deposit, apparent as a reaction rim around individual aggregate

particles. In addition to the aesthetic problem, such fractures and expansion due to AAR further accelerate other deterioration mechanisms, such as chloride ingress and/or frost damage. The structures most at risk for AAR damage are bridges, hydraulic structures, exposed frames (i.e. open multi-storey car parks) and foundations.

The reason why AAR has become a problem in recent years is because of changing materials, such as binders with higher alkalis and use of different aggregate sources, and also that we have better tools to identify when AAR is occurring. We have understood that in many cases in Finland it has been difficult to differentiate between damage initiated by frost action or AAR, especially because it is widely believed that AAR does not occur in Finland. In both cases the result that can be seen in the field is cracking on the surface of a structure. On the basis of crack patterns, a skilled person can make a quite good estimate on the cause of cracking. And sometimes it is possible to even see AAR gel that has moved out to the exposed concrete surface. This is the most distinguishing factor between frost damage and AAR: the appearance of gel within interior cracks. In frost damage, the cracking is normally heaviest near the surface and weakens deeper, whereas in AAR the reaction causes expansion inside the structure causing a homogeneous cracking network in the whole structure. In this way AAR can be more harmful than frost action. The only way to identify AAR from an existing structure is analyze the interior of the concrete, such as by petrographic analysis.

The suggested routes for testing the potential risk of AAR when selecting materials for new construction are: 1) petrographic analysis of aggregate alone, 2) accelerated expansion test of mortar bars (14 day test, i.e. by RILEM AAR-2 or ASTM C1260), or 3) one year expansion test of concrete prisms (i.e. by RILEM AAR-3 or ASTM C1293).



Figure 1. Areas in Finland where AAR has been found in structures.



Figure 2. Finnish bridge with side beam having signs of AAR.

2. FINNISH EXPERIENCE

The geology of Finnish bedrock and soil is well studied and therefore there is a good general view of the composition of aggregates in different parts of Finland. This helps to estimate the potentiality of AAR. Though earlier not viewed as a deterioration concern, AAR has been found more recently in Finnish bridges when investigating other types of deterioration attack, such as chloride ingress and frost-salt exposure.

AAR in Finnish structures has been investigated at VTT by the use of petrographic thin section microscopy. Such studies have been integrated with studies of in-service structures for 25 years. It is during the past 10 years that AAR has been identified in about 10 bridges from various locations around Finland (Figures 1 and 2). This represents about 2 % of all concrete durability assessments by thin-section microscopy on bridges done at VTT in the past 10 years. In these cases the level of damage varies from low to high. Often the role of AAR has been smaller than the role of other damaging forces. In 2 – 3 of these cases, AAR has played a major role. In these cases initial thin section studies gave a warning about high levels of AAR and a heavier damage than was recognized on site. The studies were completed with additional thin section studies, where strong AAR was found on the bridge decks. Bridge decks are more favoured to AAR than other structures (like columns), because of the use of de-icing salts and occurrence of rain that pools on the decks.

The age of Finnish bridges where AAR has been found has varied from 31 years to over 50 years. In most cases the age of the bridge has been between 40-50 years when studied. AAR has not been found in bridges under the age of 30 years. In general frost action is the most important damaging force in Finnish exposed structures, yet when it hits together with AAR, severe damage is to be expected.

The appearance of AAR has been seen in thin section studies as a gel in the interfacial transition zone between the cement paste and aggregate, as well as in gel filling in cracks running from the reacted aggregates as a result of expansion and as cracked aggregates (Figure 3). The appearances are in-line with international guidelines [1]. During one petrographic study at VTT, it was even possible to see clear AAR gels coming out from the cored concrete surface a few days after the samples were taken.

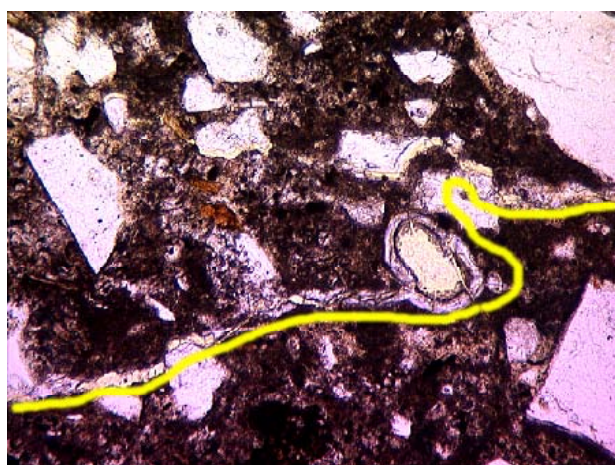


Figure 3a. Cracks and AAR gel in concrete (marked with yellow) from a Finnish bridge.

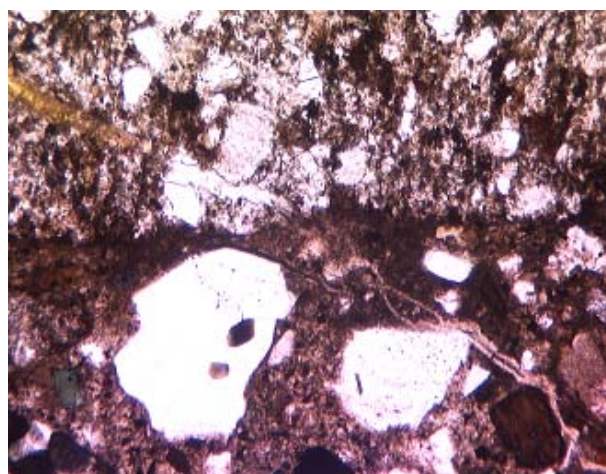


Figure 3b. Cracks and AAR gel in concrete from a Finnish paper mill.

In Finland AAR is more connected to certain rock types than to certain geographical areas. The Finnish rock types associated with AAR are in most cases fine grained stressed and strained mica bearing quartz rich shists and quartzites. The grain size is very often under 0.1 mm. Also some fine grained cataclastic and other rock types have shown AAR. In these cases the AAR is dependent on the structure of the quartz.

In addition to bridges, AAR has also been found in other Finnish structures. For instance, AAR has been seen in industrial indoor structures where the conditions are favoured, i.e. the temperature is high (even 30-40 °C) and the relative humidity is high. In the case of a Finnish swimming pool and in a paper mill (Figure 3b), the concrete structures have been wet during the use or manufacturing processes respectively.

3. FUTURE

Looking towards the future, there is a risk that AAR in Finnish concrete structures will continue to be found and could potentially accelerate. This could be a costly problem for real estate and structural owners if it is not addressed.

Our concrete industry knows that it is becoming necessary to use new aggregate sources of potentially lower quality. Recycling concrete and building materials may become more common as landfill costs rise. Use of new or alternative binders and cements with higher alkali contents will also have an affect on AAR risk. It is necessary for Finland to have knowledge [2] and guidelines about how AAR may contribute to structural durability as our construction practice adopts concrete materials with a wider range of properties.

The future needs for minimizing AAR in Finland include:

- geological mapping where potentially reactive aggregate are located in Finland.
- concrete structural mapping of locations where AAR has been found in Finland. This could also include identifying the concrete mix design and aggregate sources in these locations, if known.
- assessing test methods that can be used for AAR, with Finnish materials.
- clearly defining how to distinguish AAR from other deterioration mechanisms.
- establishing acceptance limits for AAR test results.
- educating concrete owners and testing companies on how to identify AAR.
- educating the concrete industry on how to avoid AAR.

It is hoped that by establishing guidelines about how to identify AAR and set limits on concrete material properties, it will be possible for Finnish concrete designers and owners to make well informed choices about mixture design and aggregate sources during the material specification and acceptance stages to minimize AAR risk. AAR in Finland is a deterioration risk that can be avoided but also should not be ignored.

REFERENCES

1. Durable concrete with Alkali Reactive Aggregates. Publication no. 21. Norwegian Concrete Association. 2008. 16 p. + app. 16 p.
2. Pyy, H., Holt, E., "Does Finland have an Alkali-Aggregate Reaction Problem?", *Betoni* journal, Vol. 4, 2010, pp. 46-48, in Finnish.

An investigative study on the effects of silica flour, zeolite and silica fume on the water absorption of Roller compacted concrete

N. Salehi¹, R.Khosravian²

¹*Department of Civil Engineering Isfahan University of Technology. Address; no.131, Malek blind alley, Aineh Khaneh Boulevard, Isfahan, Iran. Postal code:*

816365455.tel:09133684863.fax:03116244766

E-mail: salehi.n.navid@gmail.com

²*Department of Civil Engineering Isfahan University of Technology. Address; No.188 Khayyam Quarter Keshavarz*

Street, Isfahan, Iran.PostalCode:8174853487

E-mail: khosravian.reza@gmail.com

ABSTRACT:

Due to the high maintenance expenditure as well as production costs of conventional asphalt pavements in recent years, the substitution of concrete pavements has been taken into account. One important factor of such pavements is long term performance such as durability. Freeze & thaw cycles effects on the structures in the vicinity of roads are among the most destructive elements of concrete. Regarding this factor, the substitution of pozzolanic materials with existing cement in concrete mixture is a common choice. The desired performance of these materials is decreasing the water absorption rate. To achieve this goal we've substituted a partial amount of cement with three pozzolanic materials as follows: zeolite, silica flour and silica fume. Therefore we are looking for the optimum material among these 3 types and its percentage of substitution to have the best results in long and short term performance. Related to this parameter we performed the tests on the samples with the ages of 4 and 12 weeks to analyze the performance of these materials in long term reactions.

Keywords: silica fume, zeolite, silica flour, roller compacted concrete (RCC)

INTRODUCTION

RCC is a concrete with zero slump, which is compacted with roller. The use of RCC is rather new and has been developed significantly during recent years. [1,2].until recently many experimental studies were performed relating to the effect of cementitious materials containing pozzolanic properties .regarding these fact we can point to: choi and groom developed a method for RCCP mix designs on the basis of soil mechanics point of view .this method was suitable for small and medium scale projects. From the out coming results of this research a specific graph for RCCP aggregate grading was obtained. This graph is generally used for highways [3].Atis and colleagues investigated the stability of RCC containing fly ash that has large amount of calcium. On the basis of these results it is concluded:

1) RCCP containing fly ash has good 3-day strength.

2)28-day strength of RCC containing 15% fly ash is equal to the samples containing cement alone.

3)90-day strength of RCC containing 30% fly ash is better than the samples containing just cement. At the end the use of Afsin-Elbiston for pavement construction is recommended [4].cao

and colleagues investigated the pavements containing large amounts fly ash. According to the results of their research the effects of fly ash is gradual and is suitable for flexural strength. Meanwhile by increasing the amount of fly ash its effect in the long term curing was more noticeable[5].sun and colleagues investigated the effects of fly ash on the fatigue phenomena in RCCP.according to the results they carried a relation regarding the fatigue in RCCP and for the conditions of presence and absence of fly ash .this relation can be applied in the design of RCCP.the use of fly ash improved the strength of RCCP against the fatigue for about 40-50 percent in proportion to RCCP without fly ash[6].kasravi and colleagues investigated the strength and durability of RCCP under circumstances of heavy loads and warm weather conditions specifically for middle east. In these conditions the RCCP is exposed to high range of pressure and cracking. Also the effect of changes in mix designs of RCCP in warm weather was evaluated. These variations included type and amount of cement, the ratio of coarse aggregates to cement & w/c ratio and grade of compaction.

The effect of these parameters on the specific weight, compressive and flexural strength was investigated. According to this research the suggested w/c ratio for warm regions is (0.4 - 0.5).for better compaction and improvement of tensile strength this range is limited to 0.45.in spite to conventional concretes the decrease in w/c ratio doesn't lead to higher strength [7].

Applying different mix designs and uses supplementary cementitious materials with different percentages, in order to improve the mechanical and durability properties of RCCP of a remarkable importance. To achieve this goal lab tests based on the analysis and comparison of limestone powder (s12) and khash natural pozzolan was performed .in this research the use of cementitious materials as much as 12and 15 % of aggregates amount was considered. Also the substitution of cement with pozzolan and s-12 was applied. This substitution is equal to 10, 15 and 20 percent of total cementitious, materials. Meanwhile for obtaining the final mix designs tests were performed related to finding the optimum humidity. Finally the selected mix designs were prepared by compacting the samples in 3 layers.

1 MIX DESIGNS:

In this research at the first we analyzed the available grading of our aggregates, including 10-20 mm and 5-10 mm gravels and 0-5 mm sand. Then we combined them in a way that the resultant grading graph of aggregates will locate in the range of standard graph of ACI 211.3R-02. By selecting 10% of (10-20) ^{mm} gravel, 20% of (5-10) ^{mm} gravel and 70% of (0-5) ^{mm} sand the resulting grading graph is acceptable. We have chosen two amounts of 12% and 15% of cementitious material for our mix designs. Also we used silica fume, silica flour and zeolite as substitute of cement as much as 10%, 15% and 20% of total cementitious materials. By this mean we obtained 18 mix designs for 28 and 90-day water absorption tests separately. (Table1)

Table1. Selected Mix Designs

No. of Mix Design	Mix Design Name	water	Cementitious material	Aggregates
1	c12-m10	130.0	240.75	1981.35
	c12-f10			
	c12-z10			
2	c12-m15	130.0	240.75	1981.35
	c12-f15			
	c12-z15			
3	c12-m20	130.0	240.75	1981.35
	c12-f20			
	c12-z20			
4	c15-m10	119.0	293.0	1965.85
	c15-f10			
	c15-z10			
5	c15-m15	119.0	293.0	1965.85
	c15-f15			
	c15-z15			
6	c15-m20	119.0	293.0	1965.85
	c15-f20			
	c15-z20			

2 TEST RESULTS

The result of 28 and 90-day water absorption test of samples which are contained silica fume are tabulated in Table2 and 3 respectively. The trend variation also is shown in Fig.1 and 2. It is deducible from the performed tests:

The 28-day water absorption test results shows, without regard to the percentage of cement used, by increasing silica fume from 10% to 20% the water absorption ratio increases incessantly, so the maximum water absorption ratio is assessed by samples containing 20% silica fume. The percentage of increase in samples with 12% cement is equal to 20 but this value is raised to 81 by adding 15% cement.

The 90-day test shows similar outcomes. The results reveal that in both case, samples containing 12% and 15% cement, increasing silica fume is followed by increasing water absorption ratio. The augment percentage for both amount of cement is 32%.

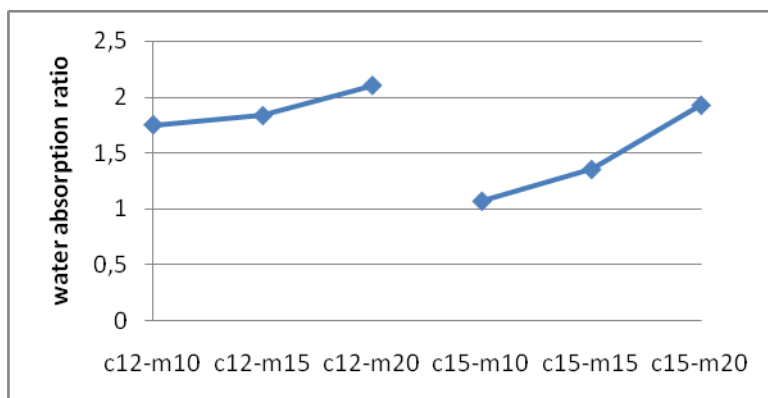
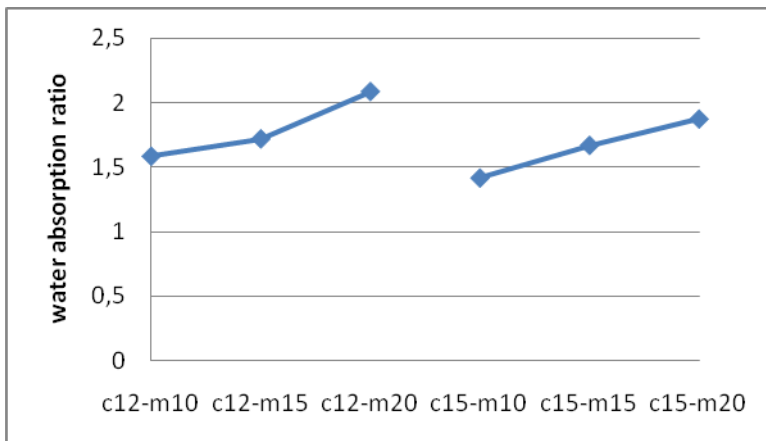


Fig.1. 28-day water absorption of samples containing silica fume

Table2. 28-day water absorption of samples containing silica fume

mix design	28-day water absorption ratio
c12-m10	1.753
c12-m15	1.835
c12-m20	2.106
c15-m10	1.067
c15-m15	1.352
c15-m20	1.928

*Fig.2. 90-day water absorption of samples containing silica fume**Table3. 90-day water absorption of samples containing silica fume*

mix design	90-day water absorption ratio
c12-m10	1.583
c12-m15	1.719
c12-m20	2.088
c15-m10	1.413
c15-m15	1.668
c15-m20	1.873

The result of 28 and 90-day samples water absorption containing silica flour are brought in Table4 and 5 and the trend variation is shown in Fig.3 and 4. From these it can be conclude that: when samples containing 12% cement, by increasing silica flour from 10% to 15% the water absorption increases by 10 percent, but when the percentage of cement increase up to 20% the water absorption decreases by 22 percent, so by adding silica flour in samples containing 12% cement the water absorption has the maximum value in sample c12-f15. In samples which contain 15% cement, the trend variation becomes unvarying as though by increasing silica flour water absorption reduces. The water absorption has the minimum value in c15-f20.

For 90-day the results does not demonstrate a different changing trend. When samples containing 12% cement, by increasing silica flour from 10% to 20% the water absorption has a rise and fall trend so by adding silica flour in samples containing 12% cement the water

absorption has the maximum value in sample c12-f15. In samples which contain 15% cement, the trend variation becomes unvarying as though by increasing silica flour water absorption reduces. The water absorption has the maximum value in c15-f10.

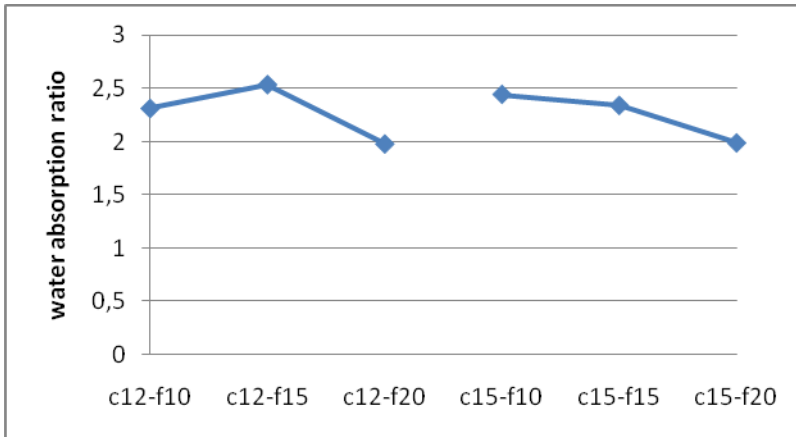


Fig.3. 28-day water absorption of samples containing silica flour

Table4. 28-day water absorption of samples containing silica flour

mix design	28-day water absorption ratio
c12-f10	2.315
c12-f15	2.538
c12-f20	1.983
c15-f10	2.447
c15-f15	2.344
c15-f20	1.993

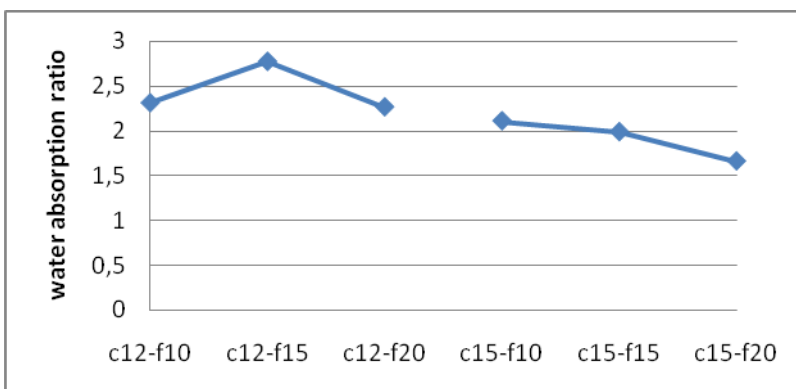


Fig.4. 90-day water absorption of samples containing silica flour

Table5. 90-day water absorption of samples containing silica flour

mix design	90-day water absorption ratio
c12-f10	2.311
c12-f15	2.775
c12-f20	2.265
c15-f10	2.109
c15-f15	1.987
c15-f20	1.659

The result of 28 and 90 days samples water absorption which are contained zeolite are tabulated in Table6 and 7 respectively. The trend variation also is shown in Fig.5 and 6. It is deducible from the performed test results that:

When samples containing 12% cement, by increasing zeolite from 10% to 20% the water absorption has an increasing trend, so in samples containing 12% cement the water absorption has the maximum value in sample c12-z20. Once again in samples which are contained 15% cement the test results shows the same trend, but in less moderate way that by increasing silica fume from 10% to 20% the water absorption augment by 29 percent, therefore the sample c15-z20 has the uttermost water absorption ratio.

In 90-day test, in case of adding 12% cement water absorption shows an inverse changing trend so that increasing in zeolite is followed by reduction in water absorption. However in condition of 15% cement the variation trend pursue as the same before but the scale of variation becomes more inclement as if increasing in percentage of zeolite from 10 to 20 culminates in augmenting water absorption of 57%.

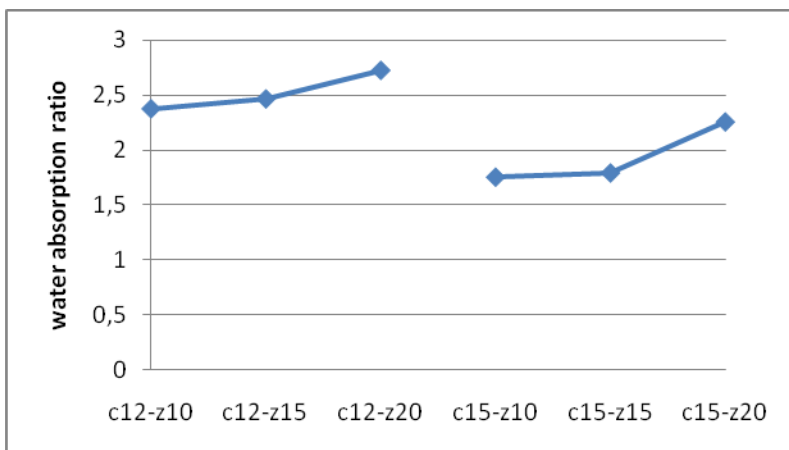
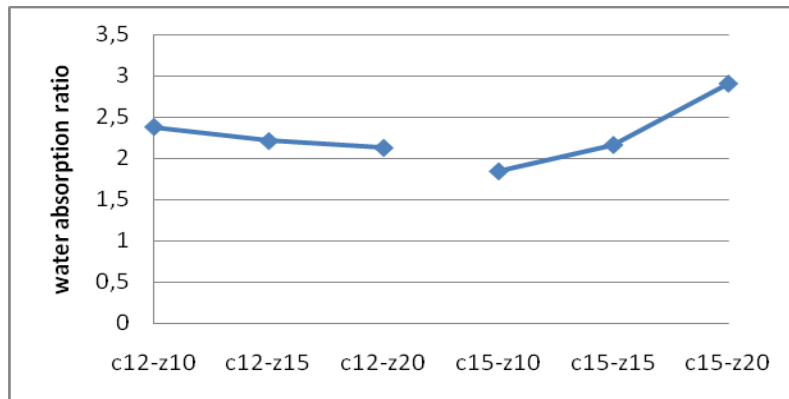


Fig.5. 28-day water absorption of samples containing zeolite

Table6. 28-day water absorption of samples containing zeolite

mix design	28-day water absorption ratio
c12-z10	2.371
c12-z15	2.46
c12-z20	2.719
c15-z10	1.751
c15-z15	1.789
c15-z20	2.252

*Fig. 6. 90-day water absorption of samples containing zeolite**Table7. 90-day water absorption of samples containing zeolite*

mix design	90-day water absorption ratio
c12-z10	2.382
c12-z15	2.212
c12-z20	2.129
c15-z10	1.846
c15-z15	2.165
c15-z20	2.907

Comparing the effect of passing time on reaching the maximum water absorption ratio by adding silica fume is shown in Table8 and Fig.7. As you can see in this figure the variation trend for 28-day water absorption is as the same as 90-day test. However in case of 12% cement added the 28-day test shows better results but long time water absorption of samples containing 15% cement is more.

Table8. Comparing 28-day and 90-day water absorption samples containing silica fume

mix design	28-day water absorption	90-day water absorption
c12-m10	1.753	1.583
c12-m15	1.835	1.719
c12-m20	2.106	2.088
c15-m10	1.067	1.413
c15-m15	1.352	1.668
c15-m20	1.928	1.873

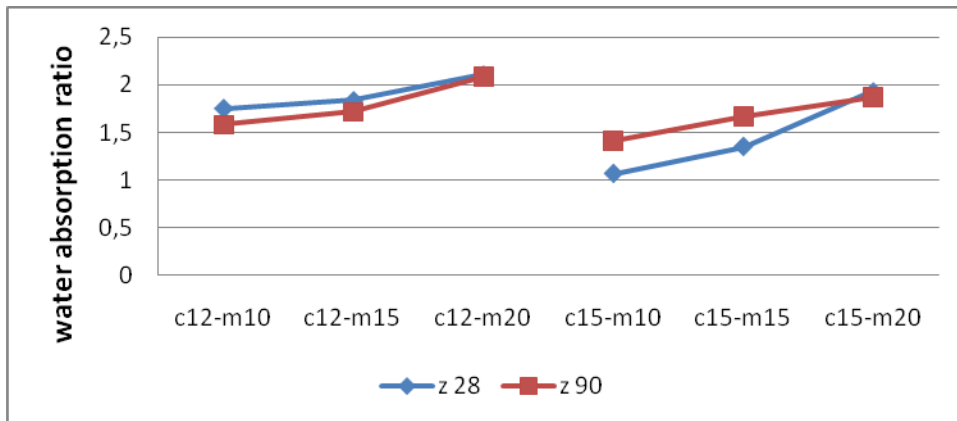


Fig.7. comparing 28-day (blue) and 90-day (red) water absorption samples containing silica fume

Table9 and Fig.8 compare 28-day with 90-day water absorption samples containing silica flour. As you can see in this figure the variation trend for 28-day water absorption is similar to 90-day test but in condition of 12% cement the 90-day test shows better results but in long time, samples containing 15% cement perform worse in aspect of water absorption.

Table9. Comparing 28-day and 90-day water absorption samples containing silica flour

mix design	28-day water absorption	90-day water absorption
c12-f10	2.315	2.311
c12-f15	2.538	2.775
c12-f20	1.983	2.265
c15-f10	2.447	2.109
c15-f15	2.344	1.987
c15-f20	1.993	1.659

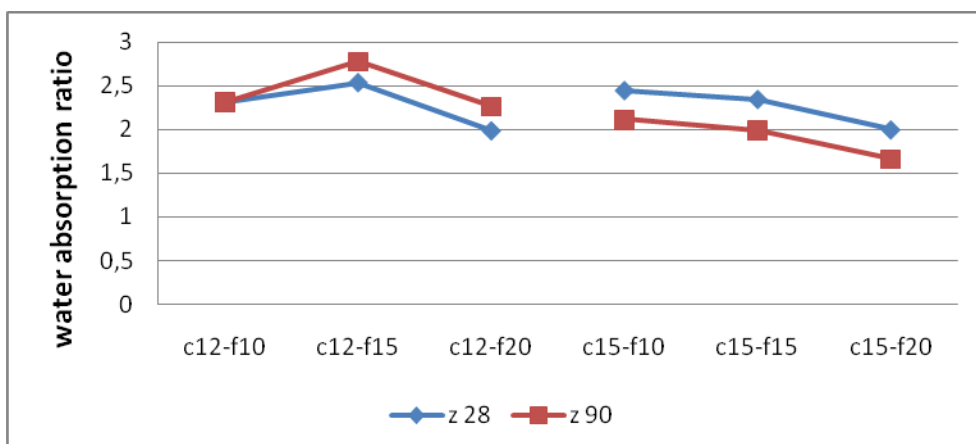


Fig.8. comparing 28-day (blue) and 90-day (red) water absorption samples containing silica flour

Table10 and Fig.9 compare 28-day with 90-day water absorption samples which are contained zeolite. As it is shown in the figure the variation trend for 90-day water absorption does not

change in compare with 28-day test also it is deducible from the table that when samples contain 15% cement, more water absorption ratio is assessed.

Table10. Comparing 28-day and 90-day water absorption samples containing zeolite

mix design	28-day water absoption	90-day water absorption
C12-z10	2.371	2.382
C12-z15	2.46	2.212
C12-z20	2.719	2.129
C15-z10	1.751	1.846
C15-z15	1.789	2.165
C15-z20	2.252	2.907

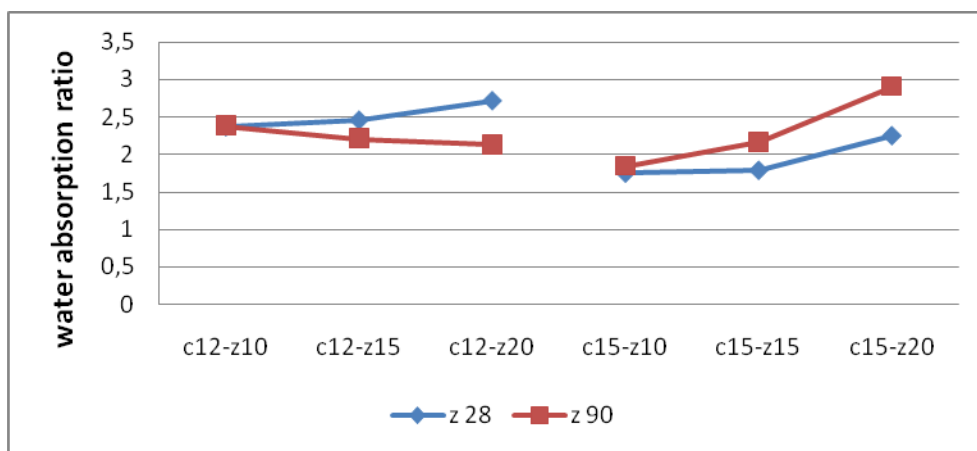


Fig.9. Comparing 28-day and 90-day water absorption samples containing zeolite

The result of 28 and 90-day water absorption of samples to evaluate and compare the effect of adding different cementitious materials, used in this study, are shown in Fig.10 and 11 respectively and the results are tabulated in Table11 and 12. It is deducible from the figure that: In case of 28-day test, by adding 12% cement zeolite has better performance. In addition silica flour can be an alternative zeolite except when the percentage of is equal to 20 because water absorption in sample c12-f20 reduces considerably. On the other hand, when 15% cement is used silica flour has the best action. Also it can be replaced by silica fume when the 20% cementitious material is used, although in this condition zeolite act better.

For 90-day test, silica flour has the best performance as if it reaches higher water absorption in compare with silica fume and zeolite, although in case of using 12% cement and 20% cementitious material there is no difference between these 3 type of materials. In addition, in case of using 15% cement, the test results reveal that using zeolite gains more water absorption ratio considerably at percentage of 20.

Table 11. The effect of type cementitious material on 28-day water absorption

mix design	28-day water absorption ratio		
	silica fume	silica flour	zeolite
1	1.753	2.315	2.371
2	1.835	2.538	2.46
3	2.106	1.983	2.719
4	1.067	2.447	1.751
5	1.352	2.344	1.789
6	1.928	1.993	2.252

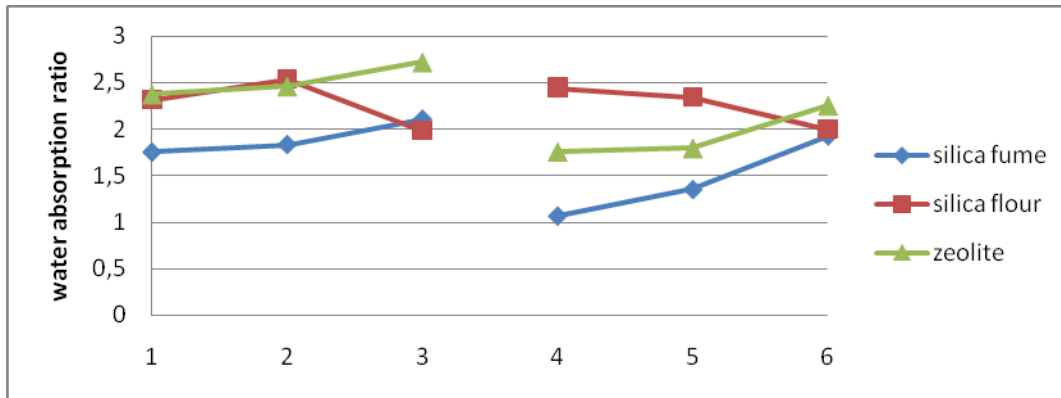
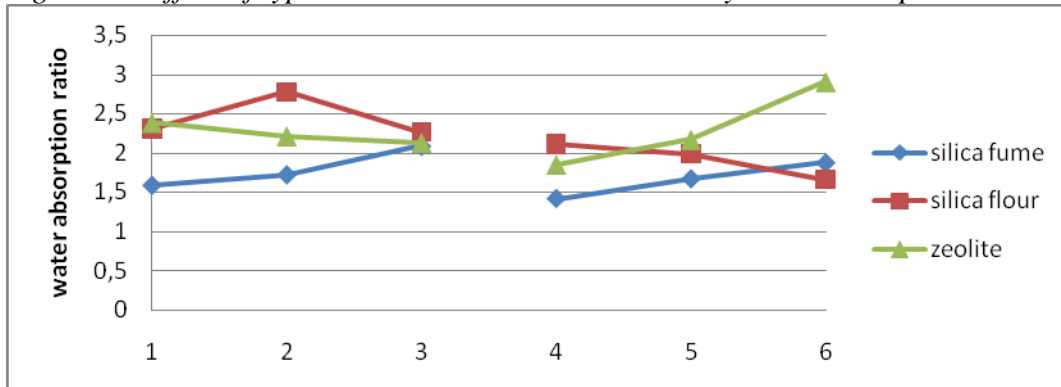


Fig 10. The effect of type cementitious material on 28-day water absorption

Table 12. The effect of type cementitious material on 90-day water absorption

mix design	90-day water absorption ratio		
	silica fume	silica flour	zeolite
1	1.583	2.311	2.382
2	1.719	2.775	2.212
3	2.088	2.265	2.129
4	1.413	2.109	1.846
5	1.668	1.987	2.165
6	1.873	1.659	2.907

Fig 11. The effect of type cementitious material on 90-day water absorption



3 CONCLUSION:

After analyzing the data it is concluded that:

- 1) The silica fume has the best performance, since it has the least water absorption.
- 2) By having 12% CM and 20% substitution of pozzolanic materials, it is observed that the rate of water absorption converges during 90 days.
- 3) By having 15% CM and 20% substitution of pozzolanic materials, it is observed that the rate of water absorption converges at the age 28 days.
- 4) Higher amount of silica fume causes a similar behavior during the time, So that the mix designs including c12-m20 and c15-m20 have no change in their water absorption from the age of 28 to 90 days.
- 5) Increase of silica fume and zeolite causes more water absorption however, the increase of silica flour leads to lower water absorption rate.
- 6) Generally the increase of cementitious materials decreases the water absorption.
- 7) In the case of time, the increase of zeolite increases the difference of water absorption among the mix designs .
- 8) Generally, time has diverse effects on samples containing 12% CM in proportion to ones containing 15% CM.

Totally we can say that: in the case of using silica fume and zeolite, it is recommended to use them just in samples containing 12% cementitious materials. Because, as the result of the time at the 90-day age water absorption in samples with 15% CM increases .in spite of zeolite and silica fume it is suggested to use silica flour just with 15% cementitious materials. Basically it should be considered that the water absorption is a factor of durability therefore, the materials were compared on the basis of having the best long term performance.

REFERENCES:

- [1] ACI 207/5R-99, "Roller compacted concrete", ACI manual of concrete Practice, author, USA, p.47, (1999).
- [2] ACI 325.10R, "state of the art Report on roller compacted concrete Pavements", ACI Manual of Concrete Practice, Author, USA, p.32, (1999).
- [3] Choi, Y.K, and Groom, J.L, "RCC Mix Design-soils Approach", Journal of Materials in civil Engineering Vol.13, No.1, PP.71-76, (2001).
- [4] Atis, C.D., Sevim, U.K., Qzcan, F Bilim, O., Karahan, A.H, and Eksi, A., "Strength Properties of Roller Compacted Concrete Containing a Non-standard High Calcium Fly Ash", Materials Letters, Vol.58, PP.1446-1450, (2004)
- [5] Cao, C., Sun, W, and Qin, H., "The Analysis on Strength and Fly Ash Effect of Roller compacted concrete with high volume Fly ash", Cemeny and concrete Research, V.30, No.1, PP.71-75, (2000).
- [6] Sun, W., Liu, L, Qin, H., Zhang, Y., Jin Zand Qian, M., "Fatigue performance and Equations of Roller Compacted Concrete with Fly Ash", Cement and Concrete Research, V.28, No.2, PP.309-315, (1998).
- [7] Qasravi, H. Y., Hisham, Y., Asi, I.M., Ibrahim, M., Al-Abdol Wahhab, H.I., "Proportioning RCCP Mixes Under Hot Weather Condition for A Specified Tensile Strength", Cement and Concrete Research, 2004.

Evaluation of Curing Effect of Blast-Furnace Slag Concrete by Using Odor Sensor



Mako to KAGAYA
D. Eng.
Akita University
JP 1-1, Tegata-Gakuencho, Akita
makokaga@gipc.akita-u.ac.jp



Noritoshi SAITO
B. Eng.
Akita University
JP 1-1, Tegata-Gakuencho, Akita
nori@gipc.akita-u.ac.jp



Yoshitsugu SHIROKADO
D. Eng.
Akita University
JP 1-1, Tegata-Gakuencho, Akita
shiro715@gipc.akita-u.ac.jp

ABSTRACT

The odor strength and compressive strength of ordinary concrete and blast-furnace slag concrete with 6000 cm²/g fineness slag were measured. The difference between odor strength in the standard curing and the other curing condition was defined as difference in odor strength. It has been shown that the difference in odor strength decreased and compressive strength increased with prolonging the period of water curing before starting the exposure test. There existed the linear relationship between the difference in odor strength at the age of 14 days and compressive strength at the age of 180 days in outdoor exposure test starting at winter season.

Key words: Blast-furnace slag powder, Difference in odor strength, Compressive strength

1. INTRODUCTION

The effective utilization of blast-furnace slag powder for replacement cement materials is very important from the view point of saving resources. It is necessary to develop simple method of evaluation of curing effect of the concrete containing by-product since arid and low-temperature environment in the early ages lowered the compressive strength and durability of the concrete in comparison with standard curing [1]. We notice that the odor emits from the crushed specimen in case of concrete strength test [2].

The odor strength was measured at the age of 14 days in concrete specimen of slag concrete

cured in water curing (standard curing) for different period before exposing in outdoor atmosphere in winter season. The difference between odor strength in the standard curing and that in outdoor curing condition was defined as the difference in odor strength, and the relations between the difference and the length of water curing (standard curing) period and compressive strength at the age of 180 days were examined for slag concrete comparing with ordinary concrete.

2. MEASUREMENT OF ODOR STRENGTH

The instrument equipped with odor sensor which consists of two types of highly sensitive metallic oxide semiconductors was used in this study. One semiconductor is sensitive to the odor molecule with relatively high molecular weight and another one is to that with relatively low molecular weight. When the reduction of oxidation reaction of the metallic oxide is caused by the absorption of the odor molecule, internal electrical resistance value of the semiconductor is changed. The change of resistance is converted to dimensionless numerical value as odor strength.

The calcium hydroxide was hard to dissolve in water, but some high level concentration of calcium hydroxide solutions were positively used to clarify the relationship between concentration of calcium hydroxide solution and odor strength. The aerial odor strength in the measurement environment was subtracted from the tested odor strength. The relation has showed clear increasing trend of odor strength with an increase in the concentration of calcium hydroxide solution. It therefore was judged that the measurement of the odor strength in the concrete could evaluate the difference of the amount of the crystallized calcium hydroxide formed by the difference of the progression of hydration reaction due to different curing condition.

3. RESULTS AND DISCUSSION

Figure 1 shows the compressive strength development of ordinary and blast-furnace slag concrete cured in 20 °C water and 2 °C aerial atmosphere. The compressive strength of blast-furnace slag concrete cured in 20 °C water exceeded that of ordinary concrete at the age of 14 days. This compressive strength development is caused by the accelerated latent hydraulicity of the blast-furnace slag with 6000 cm²/g fineness used in the concrete. On the other hand the strength of the slag concrete cured in 2 °C aerial atmosphere was considerably lower than that in 20 °C water, and the strength development was not observed after 28 days. Since these results

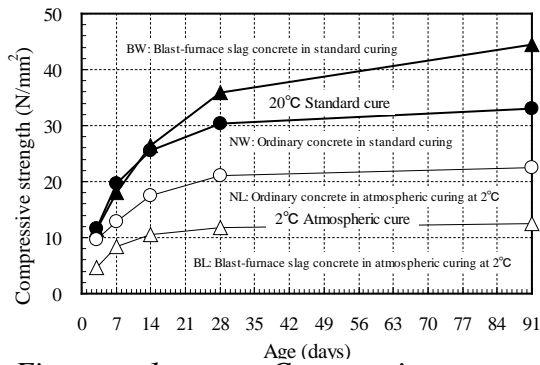


Figure 1 – Compressive strength development of ordinary and blast-furnace slag concrete at standard and 2 °C atmospheric cured specimen

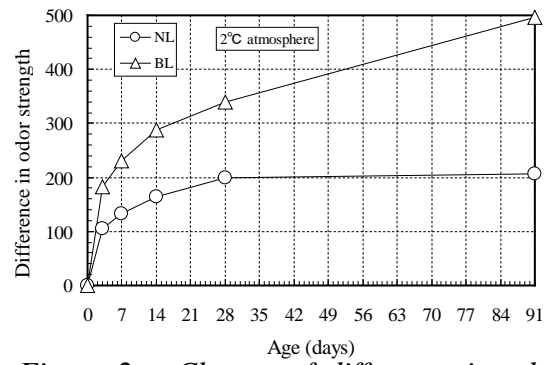


Figure 2 – Change of difference in odor strength between standard and 2 °C atmospheric cured concrete specimen

show the requirement of appropriate curing temperature and humidity to develop the strength of blast-furnace slag concrete, the evaluation of the requirement by using odor sensor was applied.

Figure 2 shows the age dependent change of the difference in the odor strength cured in 20 °C water standard curing and 2 °C aerial atmosphere in case of ordinary and blast-furnace slag concrete. The difference in odor strength of both concrete increases with the age, and the value of blast-furnace slag concrete is 77 to 290 higher than that of ordinary concrete at the age of 3 to 91 days. It therefore is judged that the curing effect of blast-furnace slag concrete is lower level than that of ordinary concrete in 2 °C aerial atmosphere curing. This result of curing effect is the same with the result of compressive strength development in 2 °C aerial atmosphere curing as shown in Figure 1 and it is considered that the difference in the odor strength shows the curing effect. The smaller the difference in odor strength is, the closer to standard curing the curing condition is.

Figure 3 shows the relationship between 20 °C water curing period and the difference in odor strength of the specimen in outdoor atmosphere at the age of 14 days in winter time. The

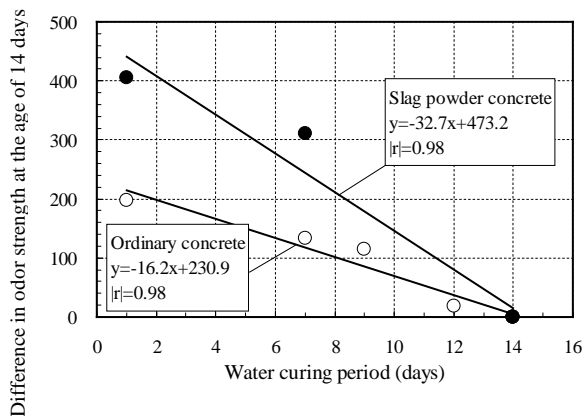


Figure 3 – Relationship between water curing period and difference in odor strength at the age of 14 days

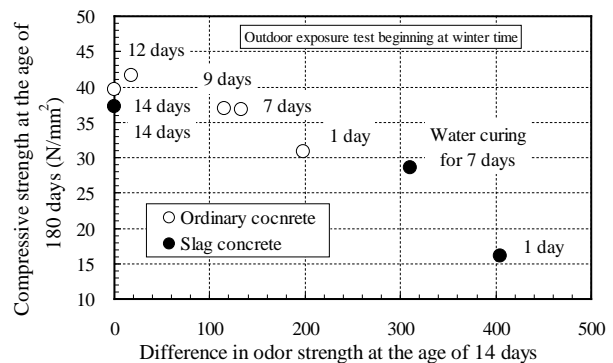


Figure 4 – Relationship between difference in odor strength at the age of 14 days and compressive strength at the age of 180 days in outdoor exposure test

difference in odor strength decreases with an increase in the period of water curing. As shown in this figure, it is necessary to prolong the water curing period for the slag concrete compared with ordinary concrete to obtain a given difference in odor strength in winter time. It is generally accepted that an increase in the period of water curing produces curing effect. It therefore is considered that the decrease in the difference in the odor strength with an increase in the period of water curing evaluates the curing effect of the slag concrete.

Finally, the relationship between the curing effect and long term compressive strength (180 days) was examined. Figure 4 shows the relationship between difference in odor strength at the age of 14 days and compressive strength at the age of 180 days in outdoor exposure test beginning at winter time. The numerical values in the figure show water curing period before starting the outdoor exposure test. The compressive strength at the age of 180 days in outdoor exposure test decreases with an increase in difference in odor strength at the age of 14 days. From these results, it is considered that the level of the difference in odor strength measured at initial age evaluates the quality such as long term strength of the slag concrete cured in different condition.

4. CONCLUSIONS

The following results were obtained.

- (1) The difference between odor strength in the standard curing and that in each curing condition was defined as the difference in odor strength. The difference in odor strength of slag concrete decreased with an increase in the water curing period before exposing in outdoor atmosphere.
- (2) There existed the close relation between the difference in odor strength measured at initial age and long term compressive strength of slag and ordinary concrete cured in different condition.

REFERENCES

1. Iyoda, T. and Uomoto, T. : Progress of hydration and amount of free water in hardened cement in arid condition continuously on early curing, Cement Science and Concrete Technology, No.54, 2000, pp.167-173 (in Japanese).
2. Shirokado, Y., Chang, D. and Kagaya, M. : Evaluation of curing effect of fly ash cement concrete by using odor sensor, Proceedings of the Japan Concrete Institute, Vol.30, No.2, 2008, pp.217-221 (in Japanese).

An Investigative Study on the Effects of Natural Pozzolan and Limestone Powder on the Mechanical Properties of Roller Compacted Concrete



Navid Salehi
No.131, Malek blind alley
Aineh Khaneh Boulevard
Isfahan, Iran.
Postal code: 816365455.
salehi.n.navid@gmail.com



AmirHossein Khodaeeyan
No.160, Nowbahar.2 alley,
Mehran street, mehr street
Isafahan Iran
Postal code:
akhodaeen@gmail.com



MohammadReza Vafaie
No.105, Arman blind alley, Mir Overpasses Bridge
Sheikh Saddough St, Isfahan. Iran.
Postal code: 8163754171
mova3d@gmail.com

ABSTRACT

Due to the high maintenance expenditure as well as production costs of conventional asphalt pavements in recent years, the substitution of concrete pavements has been taken into account. One important factor of such pavements is long term performance. Regarding this factor, the substitution of pozzolanic materials with existing cement in mixture is a common choice in order to improve the durability factors and a better long term compressive strength. Owing to this change in cementitious materials, it is a general anticipation of the pozzolanic behavior to be observed that the early age compressive strength is decreased. On the other hand somehow this defect will be compensated in long term compressive strength. Further than that, due to conventional loads of road pavements the tensile and flexural strength have their own importance. Therefore, regarding these two factors the related tests were also performed and the results were analyzed. Consequently the main purpose is finding the optimum material among these 2 types of pozzolanic supplements and its percentage of substitution. The preference basis is having the best average strength in both long and short term performance and other mechanical properties. Altogether the natural pozzolan has a better performance than limestone powder.

Keywords: limestone powder(s-12), natural pozzolan, roller compacted concrete (RCC)

1. INTRODUCTION

RCC is a concrete with zero slump, which is compacted with roller. The use of RCC is rather new and has been developed significantly during recent years. [1,2].until recently many experimental studies were performed relating to the effect of cementitious materials containing

pozzolanic properties .regarding these fact we can point to: Choi and Groom developed a method for RCCP mix designs on the basis of soil mechanics point of view .this method was suitable for small and medium scale projects. From the out coming results of this research a specific graph for RCCP aggregate grading was obtained. This graph is generally used for highways [3]. Atis and colleagues investigated the stability of RCC containing fly ash that has large amount of calcium. On the basis of these results it is concluded:

1. RCCP containing fly ash has good 3-day strength.
2. 28-day strength of RCC containing 15% fly ash is equal to the samples containing cement alone.
3. 90-day strength of RCC containing 30% fly ash is better than the samples containing just cement.

At the end the use of Afsin-Elbiston for pavement construction is recommended [4]. Cao and colleagues investigated the pavements containing large amounts fly ash. According to the results of their research the effects of fly ash is gradual and is suitable for flexural strength. Meanwhile by increasing the amount of fly ash its effect in the long term curing was more noticeable [5].sun and colleagues investigated the effects of fly ash on the fatigue phenomena in RCCP. According to the results they carried a relation regarding the fatigue in RCCP and for the conditions of presence and absence of fly ash .this relation can be applied in the design of RCCP. The use of fly ash improved the strength of RCCP against the fatigue for about 40-50 percent in proportion to RCCP without fly ash[6]. Kasravi and colleagues investigated the strength and durability of RCCP under circumstances of heavy loads and warm weather conditions specifically for Middle East. In these conditions the RCCP is exposed to high range of pressure and cracking. Also the effect of changes in mix designs of RCCP in warm weather was evaluated. These variations included type and amount of cement, the ratio of coarse aggregates to cement & w/c ratio and grade of compaction.

The effect of these parameters on the specific weight, compressive and flexural strength was investigated. According to this research the suggested w/c ratio for warm regions is (0.4 - 0.5).for better compaction and improvement of tensile strength this range is limited to 0.45.in spite to conventional concretes the decrease in w/c ratio doesn't lead to higher strength .

Applying different mix designs and uses supplementary cementitious materials with different percentages, in order to improve the mechanical and durability properties of RCCP of a remarkable importance. To achieve this goal lab tests based on the analysis and comparison of limestone powder (s12) and Khash natural pozzolan was performed .in this research the use of cementitious materials as much as 12and 15 % of aggregates amount was considered. Also the substitution of cement with pozzolan and s-12 was applied. This substitution is equal to 10, 15 and 20 percent of total cementitious, materials. Meanwhile for obtaining the final mix designs tests were performed related to finding the optimum humidity. Finally the selected mix designs were prepared by compact the samples in 3 layers.

2. MIX DESIGN

in this research at the first we considered the available grading of our aggregates including 10-20 mm and 5-10 mm gravels 0-5 mm sand. Then we combined them in the way that the resultant grading graph of our aggregates will locate in the range of standard graph of ACI 211.3R-02. By selecting 10% (10-20) ^{mm} gravel, 20% (5-10) ^{mm} gravel and 70% (0-5) ^{mm} sand the resulting grading graph is acceptable. We have chosen two amounts of 10% and 15% of cementitious material for our mix designs. Also we used Khash pozzolan and limestone powder as substitute of cement as much as 10%, 15% and 20% of total cementitious materials. By this mean we

obtained 12 mix designs for the optimum humidity test and after that we prepared the final mix designs according to the best w/c ratios which are shown in the Table 1.

Table 1 – Selected Mix Designs

Water	Cementitious material	Aggregates	Mix design name
107/4	209/583	1747/5288	C12S10 C12P10
102/5	210/859	1757/276	C12S15 C12P15
104/1	210/54	1754/243	C12S20 C12P20
104/1	210/54	1754/243	C15S10 C15P10
104/5	210/54	1753/377	C15S15 C15P15
104/1	210/54	1754/243	C15S20 C15P20

3. TESTS

3.1 Compressive Strength Experiment

For assessing 28 and 90 days strength of cubic sample with 150×150×150 mm dimensions we use Tectonic device with compressive capacity of 300 ton. The result of 28 and 90 days samples compressive strength which are contained s12, pozzolan, are written in Table 2 and 3.

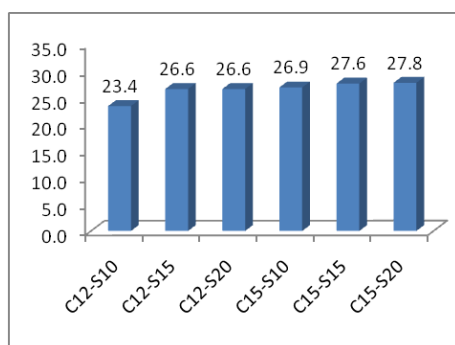


Fig 1 - 28-day strength of samples containing S-12(MPa)

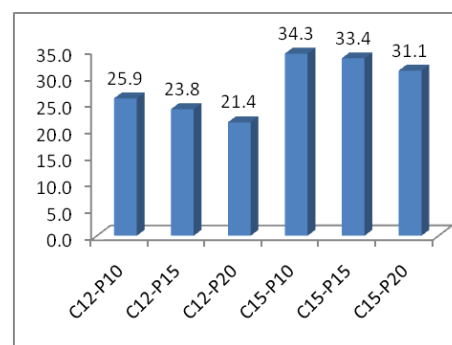


Fig 2 – 28-day strength of pozzolan samples

It is deductable from the performed tests that:

By increasing cement from 12 to 15 percent in samples which contained limestone powder the compressive strength show 4% rise. By increasing s12, 28-days strength shows an approximate rise about 3%.By increasing cement percent in samples which contained pozzolan, 28-days strength increase by 4%.Increasing pozzolan followed by decline in 28-day strength as it can be seen that with 10 -20 % rise in pozzolan in samples which contained 12% cement, compressive strength decrease by 20% and in 15% cement samples decrease by 10% Adding pozzolan in contrast to 28-days strength could increase the 90-days strength. As an example, increasing

pozzolan from 10 to 20% could cause up to 30% increase in 90 days strength. The effect of varying limestone powder percent in 90-days strength is relatively slighter than 28-days strength as an example, adding limestone reduces 90-days strength less than 28-days strength. Samples with 20% pozzolan have highest 90-days strength. Samples with limestone and 12 % cement in age of 28 days could not reach the minimum required strength. The results of samples containing s-12 and pozzolan are shown in Tables 4 and 5 respectively.

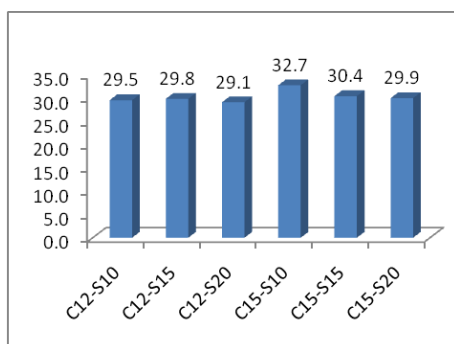


Fig 3- 90-day strength of samples containing s12 (MPA)

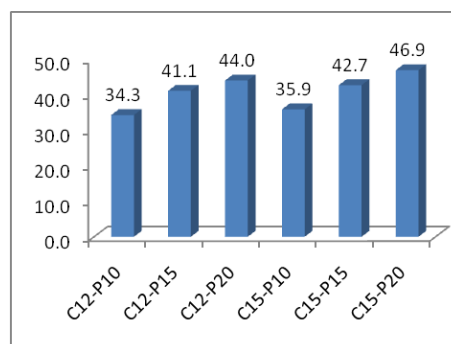


Fig 4- 90-day strength of pozzolan samples (MPA)

3.2 Flexural Strength Experiment

For evaluating 28-days flexural strength of prismatic samples with $100 \times 100 \times 350^{\text{mm}}$ according to ASTM c78 with tri-axial device of 50 KN (tri-test 50). The result of flexural strength on samples containing s12 and pozzolan are written in Tables 6 and 7. The following results can be concluded from flexural strength:

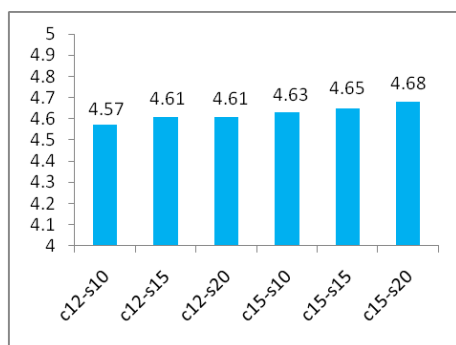


Fig 5 – Flexural strength of S-12 samples (MPA)

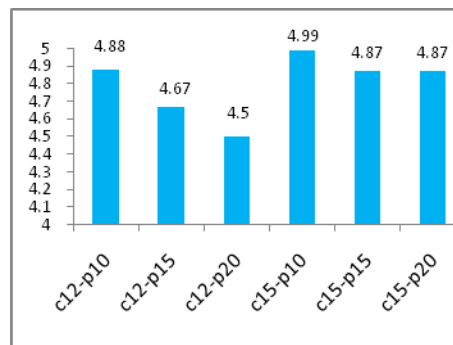


Fig 6 – Flexural strength of pozzolan samples (MPA)

The variation ranges of 28-days flexural strength are compatible with 28-days compressive strength. By increasing cement content flexural strength increase. In pozzolan samples increasing pozzolan content followed by decrease flexural strength. In limestone powder samples increasing limestone caused slight increase in flexural strength that we can ignore it in 28-days samples.

3.3 Tensile Strength Experiment (Brazilian Method)

Cylindrical samples with dimensions of $150 \times 300^{\text{mm}}$ are used to assess tensile strength. The results of tensile strength test on pozzolan and limestone samples are brought in Table 8 and 9. The variation trend of tensile strength are compatible with other 28-days mechanical strength. Increasing cement content lead to increase tensile strength like other mechanical strength. In samples with pozzolan by increasing pozzolan tensile strength is decrease. In samples which contained limestone by increasing limestone tensile strength experience a slight rise.

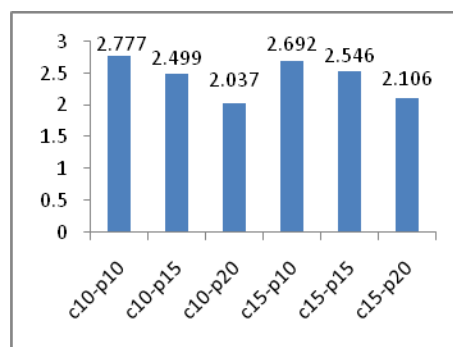
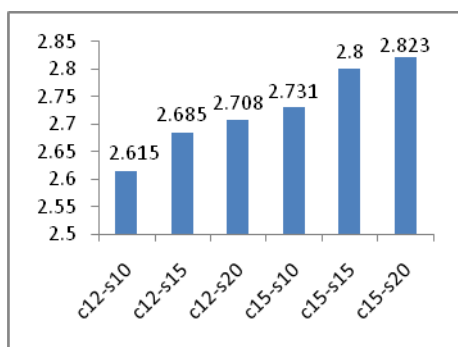


Fig 7 – Flexural strength of S-12 samples (MPa) Fig 8 – Flexural strength of pozzolan samples (MPa)

4. CONCLUSION

At the end by processing all data we can come to the following conclusions:

- 1) By increasing cement percent mechanical strength of RCC improved.
- 2) Those samples with pozzolan and 15% cement show acceptable strength, however; samples with 12% cement reach the minimal strength of 28 days.
- 3) Compressive strength of pozzolan samples is better than limestone samples.
- 4) Among all samples that reach the compressive strength limit with the same age and cementations materials the strength of pozzolanic samples are better than limestone ones.
- 5) The effect of alternative cementation strength can be take into account mechanical strength because the variation trend of tensile and flexural strength in the age of 28 days are the same as 28-days compressive strength
- 6) Pozzolan can improve the long-term gaining strength of RCC.
- 7) Using pozzolan lead to increase of long period strength of pavement and increasing pozzolan up to 20% is the suggested amount for use.

REFERENCES

1. ACI 207/5R-99, "Roller compacted concrete", ACI manual of concrete Practice, author, USA, p.47, (1999).
2. ACI 325.10R, "state of the art Report on roller compacted concrete Pavements", ACI Manual of Concrete Practice, Author, USA, p.32, (1999).
3. Choi, Y.K, and Groom, J.L, "RCC Mix Design-soils Approach", Journal of Materials in civil Engineering Vol.13, No.1, PP.71-76, (2001).

4. Atis, C.D., Sevim, U.K., Qzcan, F Bilim, O., Karahan, A.H, and Eksi, A., "Strength Properties of Roller Compacted Concrete Containing a Non-standard High Calcium Fly Ash", *Materials Letters*, Vol.58, PP.1446-1450, (2004)
5. Cao, C., Sun, Wand Qin, H., "The Analysis on Strength and Fly Ash Effect of Roller compacted concrete with high volume Fly ash", *Cemeny and concrete Research*, V.30, No.1, PP.71-75, (2000).
6. Sun, W., Liu, L, Qin, H., Zhang, Y., Jin Zand Qian, M., "Fatigue performance and Equations of Roller Compacted Concrete with Fly Ash", *Cement and Concrete Research*, V.28, No.2, PP.309-315, (1998).

Session B3 – MIX DESIGN AND RHEOLOGY

Production of concrete for the Fehmarn Belt Fixed Link exposure site



Claus Pade
M.Sc., Senior Consultant
Concrete Centre, Danish Technological Institute
Gregersensvej, DK-2630 Taastrup
E-mail: cpa@teknologisk.dk



Martin Kaasgaard
M.Sc., Consultant
Concrete Centre, Danish Technological Institute
Gregersensvej, DK-2630 Taastrup
E-mail: mkaa@teknologisk.dk

ABSTRACT

Femern A/S, the Owner of the coming Fehmarn Belt Fixed Link, has through an open tender process selected the Concrete Centre at Danish Technological Institute as its external concrete laboratory. As part of a testing program supporting the preparation of material requirements the Concrete Centre's HighTech Concrete Laboratory produced 30 concrete blocks and a large number of small test specimens from fifteen different mix designs. An extensive testing program was initiated comprising documentation of both fresh and hardened concrete, and large concrete blocks (2 x 1 x 0.2 m) were placed partly submerged in the harbour of Rødbyhavn. These blocks will be monitored at least until the end of the construction period (2020). The batching, mixing and casting of the concrete are described, including how the required maximum 1 %-wt batching deviation was obtained, and the testing program for the documentation of the fresh and hardened concrete properties is provided.

Key words: Concrete production, Batch-to-batch variation, Exposure site, Durability.

1. INTRODUCTION

In order to compare the performance of different concrete binder systems it is pivotal to control the w/c-ratio rather accurately, so that differences between different binder systems are not being over or under estimated merely because of differences in the w/c-ratio of the concrete samples being compared. A typical modern concrete mixing station operated in a normal production sequence is not able to produce concrete with greater accuracy on the water content than ± 10 l/m³, corresponding to a variation of the w/c-ratio of $\pm 0,02 - 0,03$ [1], which is probably why most concrete is produced with a target w/c-ratio of 0,02 to 0,03 below the maximum allowable w/c-ratio. As an example a concrete having a nominal w/c-ratio of 0,400 at a water content of 140 l/m³ may vary in w/c-ratio between 0,371 and 0,429 if the water content varies by ± 10 l/m³. Such variation in w/c-ratio corresponds to variations in chloride migration coefficient of roughly 12 - 16·10⁻¹² m²/s for pure Portland cement concrete [2] – of course assuming that the concrete specimens tested was cast exactly at the nominal w/c-ratio. Therefore, if test specimens are cast with the typical variations in w/c-ratio during industrial

concrete production comparison of e.g. chloride migration coefficient of different binder systems will be ambiguous and may lead to erroneous conclusions.

A much better batching accuracy complying with the required maximum 1% deviation can be achieved in smaller scale laboratory mixers. However, it is impractical to use such mixers when having to cast concrete specimens of 0,4 m³.

Thus the solution adopted in the Fehmarn testing program was to use an industrial scale concrete mixer and introduce working procedures that ensure high accuracy of the w/c-ratio.

2. MATERIALS

The range of materials acquired for the project is shown in Table 1. Samples of all constituent materials have been subjected to a test program exceeding existing EN requirements. The project involved 15 different concrete compositions that each had to be trial mixed adjusting admixture content in order for the concrete meet requirements to consistency and air void system, and finally four batches of each concrete, i.e. in total 60 batches of 230 liter of concrete had to be produced in order to make the necessary test specimens.

Table 1. Materials acquired for completion of test program.

Constituent	Portland cement	Portland cement	Slag cement	Fly ash	Microsilica	Blast furnace slag	Fine aggregate 0/1	Coarse aggregate 4/8	Coarse aggregate 8/16	Coarse aggregate 11/22	Air entraining agent	Superplasticizer
Description	CEM I 42,5 N	CEM I 52,5 N	CEM III/B 42,5 N	EN 450-1 type N	Slurry	EN 15167-1	Sea dredged, quartz	Crushed, granitic	Crushed, granitic	Crushed, granitic	Synthetic	PCE
Amount	12,6 t	2,1 t	5 t	3,2 t	2,8 t	1,7 t	50 t	18 t	18 t	31,5 t	200 kg	500 kg

3. BATCHING, MIXING AND CASTING OF CONCRETE

The mixing station at DTI is equipped with a 375/250 liter counter-current mixer from Haarup A/S, five aggregate silos and four powder silos. Water can be batched either based on weight or on volume (flowmeter). For the current project only weight based water batching was used. The mixing station is operated using process control software from Skako A/S. Just before initiation of the project all weight cells were calibrated using traceable weights.

The aggregate, the powder except silica fume, and water were batched “manually” one by one using the process control software in a special mode. Silica fume slurry and admixtures were prepared in beakers using a laboratory balance.

The main challenge in complying with the requirement of less than 1% batching deviation was to control the moisture content in the aggregate. Therefore, to obtain best possible control over aggregate moisture, in connection with the production of each batch of concrete the moisture content in the individual aggregate fraction was determined on three samples of approximate 1 kg each taken from the material actually batched, i.e. from the material on the conveyor belt.

This procedure also allowed to batch exactly the nominal amount of aggregate as material could be added or removed from the conveyor belt to equal the desired amount. The moisture content was determined using microwave ovens as the average of the weighted average of the three measurements. The total time required to get the moisture content of four aggregate fractions was approximately 25 minutes. During this time the aggregate was resting in closed confines of the mixer, i.e. no moisture loss took place. Based on the measured moisture contents the exact amount of water needed was calculated and subsequently batched. Based on the data for the 60 batches of concrete produced, the minimum, maximum, average and standard deviation obtained for the individual material is shown in Table 2. As can be seen maximum deviation was less than 1% as required. The maximum deviation on the w/c-ratio was 0,86 % corresponding to between 0,397 - 0,403 for a nominal value of 0,400, i.e. much better than the 0,371 - 0,429 typical of industrial concrete mixing stations. The improved batching accuracy translated into an expected deviation on the chloride migration coefficient of between 14 - 14,4·10⁻¹² m²/s rather than 12 - 16·10⁻¹² m²/s, i.e. a 10-fold improvement.

Table 2. Batching deviations of constituent materials and of corresponding w/c-ratio.

Material/Property		Cement	Fly ash	Microsilica	Slag	Fine aggregate 0/1	Coarse aggregate 4/8	Coarse aggregate 8/16	Coarse aggregate 11/22	Air entraining agent	Superplasticizer	Water	w/c-ratio
Deviation (%)	Min	0,00	0,00	0,00	0,00	0,00	0,00	0,00	0,00	0,00	0,00	0,01	0,00
	Max	0,56	0,42	0,22	0,28	0,99	0,32	0,37	0,35	0,98	0,87	0,72	0,86
	Average	0,18	0,08	0,04	0,01	0,28	0,09	0,08	0,09	0,32	0,39	0,29	0,26
	Standard	0,15	0,13	0,06	0,04	0,27	0,07	0,07	0,10	0,30	0,26	0,18	0,21

The applied mixing sequence was 1) the aggregate already in the mixer was mixed for 30 seconds, 2) powder was added from the powder pre-silo and mixing continues for 30 seconds, 3) water was added over a period of 20 - 30 seconds while mixing, 4) air entraining agent was added and with a 30 second delay the superplasticizer was added, 5) mixing was continued for 120 seconds after addition of superplasticizer.

The fresh concrete properties were then tested and if in accordance with target ranges the concrete was discharged to a 500 liter crane bucket, and used to cast test cylinders and cubes or a small concrete block of 1 x 1 x 0,2 m.

For the production of a large concrete block (1 x 2 x 0,2 m) two batches of concrete were required. For SCC concrete both batches had to meet fresh concrete requirements, while for slump concrete the two batches had to be homogenized and the combined batch had to meet fresh concrete requirements. Homogenization was performed in a 500 liter pan mixer discharging the concrete back into the crane bucket.

Casting of slump concrete was performed in layers of 30 - 40 cm each vibrated according to the HETEK guidelines [3]. SCC was cast at a target rate of 20 m/hr.



Figure 1. Concrete mixing station (left), SCC casting (middle), Measuring slump flow (right).

4. CONCRETE TEST PROGRAM

Both the fresh and hardened concrete was subjected to an extensive test program. The fresh concrete was tested for slump, density, air content, air void system parameters using the AVA 2000, bleeding and initial setting time. For slump concrete the target consistency range was set at 140 - 180 mm slump, and for SCC the slump flow target range was 550 – 610 mm. The target air content range was 3,5 - 5,5 % as measured by pressuremeter. No targets were set on bleeding and initial setting time.

The hardened concrete was tested for compressive and splitting tensile strength development from 0.5 – 56 days of maturity. The air void system parameters, frost resistance, chloride migration coefficient, chloride diffusion coefficient (only selected concrete types) and petrographic analysis was determined according to relevant standards.

5. CONCLUSION

With the adoption of some special working procedures designed to provide better control of moisture content in aggregate the production of the concrete for the Fehmarn test program was successfully completed meeting the requirement to maximum 1% batching deviation on all constituents. As a result highly reliable documentation of the tested concrete types could be obtained and very well-documented and characterized concrete blocks are now exposed to sea water in Rødbyhavn, where their continued monitoring will hopefully serve as valuable input to the future Fehmarn maintenance and repair strategies, while also providing the basis for future research on long term durability aspects of different binder system.

REFERENCES

1. Cazacliu, B., and Ventura, A.: “Technical and environmental effects of concrete production: dry batch versus central mixed plant”, Journal of Cleaner Production, No. 18, 2010, pp. 1320-1327.
2. “The effect of the w/c ratio on chloride transport into concrete – immersion, migration and resistivity tests”, HETEK, report No. 54, Vejdirektoratet, 1997, 35p.
3. “Stavvibrering – Høj kvalitetsbeton, Entreprenøren teknologi - anvisning” HETEK, rapport No. 74, Vejdirektoratet, 1994, 32p.

Concrete with superabsorbent polymers (SAP) - experience from the Fehmarn field exposure station in Rødbyhavn



Marianne Tange Hasholt
Assistant professor,
M.Sc., Ph.D.
Department of Civil
Engineering
Technical University of
Denmark
E-mail: matah@byg.dtu.dk



Claus Pade
Senior consultant, M.Sc.
Concrete Centre
Danish Technological
Institute
E-mail:
cpa@teknologisk.dk

ABSTRACT

A field exposure station has been established in Rødbyhavn Harbour. One of the concrete types tested is with superabsorbent polymer (SAP) - a new type of additive, which can be used to mitigate self-desiccation and to control air void structure.

This paper presents results from the extensive laboratory test program, which was conducted before test panels were placed in Rødbyhavn Harbour. Results show that when using SAP, it is possible to produce concrete with a pre-defined air void structure. Strength and transport properties are comparable to the properties of a reference concrete, but results are inconclusive as regards frost resistance.

Key words: Superabsorbent polymer (SAP), Rødbyhavn field exposure station.

1. INTRODUCTION

Superabsorbent polymer (SAP) is the generic name for a group of substances. They are first and foremost known for their ability to absorb and store water - up to 1000 times their own weight or even more, depending on the type of SAP and the purity of the water [1]. If SAP is added to concrete during mixing, it will also absorb water and swell. This results in a large number of small internal water reservoirs in the fresh concrete. During subsequent hydration, the cement paste imbibes water from the SAP-particles. When the SAP particle is drained, its volume decreases, and it leaves an air-filled void.

As preliminary work for the coming Fehmarn Belt Fixed Link, a field exposure station has been established in Rødbyhavn Harbour. Along with 14 panels made of more conventional types of concrete, concrete with SAP is exposed to the marine environment. This is the first time concrete with SAP is tested under such conditions, outside the laboratory.

The idea of mixing SAP into concrete was originally conceived to reduce autogenous shrinkage, because the internal water reservoirs will work as internal curing [2, 3]. However, in this project the objective is to obtain an engineered air void structure by using SAP particles of a specific size. Contrary to air voids created by a chemical air entraining agent, SAP voids are presumably more stable during mixing and placing of the fresh concrete, because they are water-filled.

2. TEST PLAN

One of the other types of concrete placed at Rødbyhavn is used as reference concrete (REF). This is a conventional type of concrete, which satisfies all requirements for concrete in environmental class E according to DS 2426. The characteristics of this concrete are:

- $w/c_{eq} = 0.40$, where $w/c_{eq} = w / (c + \frac{1}{2} \cdot fa + 2 \cdot sf)$
- CEM I cement and 4 % silica fume b.w. of binder
- frost resistance ensured by use of air entraining agent,
target air content: 4.5 %

Concrete with SAP (denoted SAP) is produced without air entraining agent. Instead is added 2.0 kg dry SAP pr. m³ concrete and extra mixing water equivalent to the expected absorption of SAP. The SAP used is a suspension-polymerized covalently cross-linked acrylamide/acrylic acid copolymer with particle size in the range 90-150 µm. It is known from previous experiments [e.g. 3] that this particular type of SAP absorbs approximately 12.5 g water pr. g dry SAP, when it is mixed in concrete. Assuming 2 % natural air, the void volume of the two types of concrete are expected to be very similar.

The two types of concrete, REF and SAP, are compared as regards fresh concrete properties, development of strength, chloride migration, and frost resistance, see the following section.

3. RESULTS

3.1 Properties of fresh concrete

The properties of the fresh concrete are listed in table 1:

Table 1 – Properties of the fresh concrete.

	Slump* EN 12350-2 [mm]	Air content* EN 12350-7 [%]	Bleeding DS 423.18 [vol. %]	Hardening DS 423.17 [h]
REF	120-150	4.5-4.8	0.0	4.44
SAP	130-160	1.4-1.7	0.1	7.12

* measurements for 4 batches

Workability of the two types of concrete is very similar. The air content differs, but that it because pores created by SAP are water-filled in the fresh concrete.

3.2 Strength development

The strength development is pictured in figure 1:

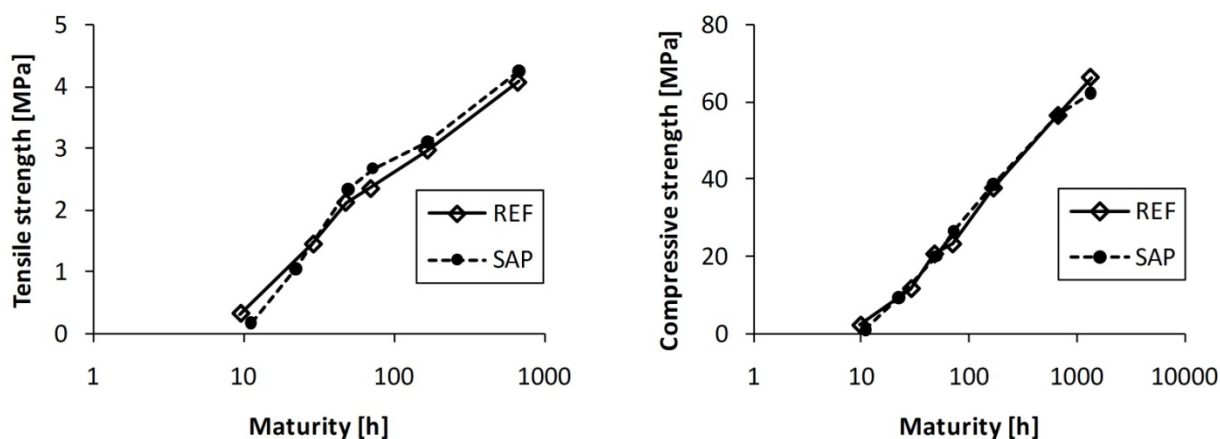


Figure 1 – Strength development. Left: tensile strength. Right: compressive strength

SAP addition affects strength development in two ways [4]: When voids are created, this reduces strength. At low w/c (< 0.42), internal curing increases degree of hydration at later ages and thereby increases the strength. In the present case, w/c = 0.43, so the internal curing has no effect on strength development. As REF and SAP have approximately the same void volume, they are expected to have equal strength, and this seems indeed to be the case.

3.3 Durability

Chloride migration

The chloride migration coefficient has been measured for both types of concrete according to NT BUILD 492. The two types of concrete had exactly the same migration coefficient, i.e. $D_{nssm} = 11.6 \cdot 10^{-12} \text{ m}^2/\text{s}$.

Air void structure and frost resistance

Air void analysis has been conducted according to EN 480-11. The histogram in figure 2 (left) shows how the air content is distributed depending on air void size. For SAP, there is a sharp peak at 300 μm . This is expected, as a 120 μm dry SAP particle, given the absorption capacity, will swell to 280 μm . For REF, the air content is in a much broader range of sizes, primarily from 50-300 μm . The spacing factor is 0.14 mm for REF and 0.24 mm for SAP, respectively.

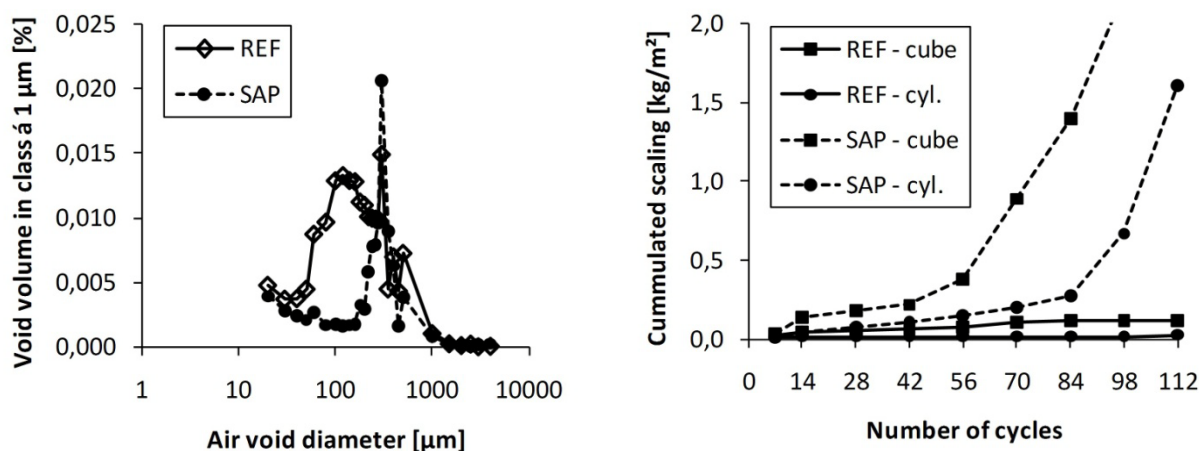


Figure 2 – Left: Histogram showing air content for different classes of void size. Right: Results of accelerated freeze/thaw testing according to SS 13 72 44.

Cast cubes and cylindrical specimens (cores drilled from test panels) have been subject to freeze/thaw testing according to SS 13 72 44. Results are shown in figure 2 (right). Up to 56 cycles, both types of concrete show relatively low scaling. For REF, the frost resistance of both cubes and cylinders can be classified as “very good”. For SAP at 56 cycles, the frost resistance for cylinders are “good”, and the cubes are close to getting the same label, but $m_{56}/m_{28} = 2.1$, where it is not allowed to exceed 2 in this category. However, after 56 cycles, scaling for SAP accelerates. There may be two different reasons for this: First, due to internal curing, the initial moisture content for SAP is higher, and the concrete may therefore more easily become critically saturated. Second, the air void structure in SAP is coarser and therefore it does not offer sufficient frost protection. According to DS 2426, the accept limit for the spacing factor is 0.20 mm. If concrete had been produced with smaller SAP particles, then the spacing factor could have fulfilled this demand with the same volume of SAP voids. The limit of 0.20 mm is based on experience with concrete with air entraining agent. We need to test if the same evaluation criterion is suitable for concrete with SAP (and other types of concrete, where the air void structure is very different from concrete with air entraining agent).

4. CONCLUSION

It is possible with the SAP technology to produce concrete with a designed air void structure, also when concrete is produced on an industrial scale. Fresh concrete properties and mechanical properties of concrete with SAP are comparable to properties of the reference concrete. As regards frost resistance, laboratory test results are not clear whether concrete with SAP is frost resistant or not. In the coming years, results from the Rødbyhavn field exposure station will tell us if it is in real life or not. More research is needed to prescribe how SAP is used to design an air void structure that will provide adequate frost protection.

ACKNOWLEDGEMENT

Femern A/S has funded setting-up of the Rødbyhavn field exposure station, including casting of concrete panels and initial laboratory testing, and the next 10 years Femern A/S also finances frequent examinations of the exposed concrete. Femern A/S has accepted concrete with SAP as part of the field exposure project. In the coming years, the field exposure station will give us invaluable experience with the long-term performance of concrete with SAP. This support from Femern A/S is greatly acknowledged.

REFERENCES

1. Buchholz, F.L., & Graham, A.T. (eds.): “Modern superabsorbent polymer technology”, Wiley VCH, New York, 1998.
2. Jensen, O.M., and Hansen, P.F.: “Water-entrained cement-based materials. I. Principles and theoretical background”, *Cem Conc Res* no. 31, 2001, pp. 647-654.
3. Jensen, O.M., and Hansen, P.F.: “Water-entrained cement-based materials. II. Experimental observations”, *Cem Conc Res* no. 32, 2002, pp. 973-978.
4. Hasholt, M.T., Jespersen, M.H.S., & Jensen, O.M.: “Mechanical properties of concrete with SAP. Part I: Development of compressive strength”, proceedings, International RILEM Conference on Use of Superabsorbent Polymers and Other New Additives in Concrete, Lyngby, Denmark, August 2010, pp. 117-126.

X-ray characterisation of early-age cement structuration for phase kinetics



Tom C. Lundin,
DSc (Tech),
Academic Lecturer,
Åbo Akademi University,
Laboratory of Physical
Chemistry. Porthaninkatu 3,
20500 Turku/Åbo, Finland
tom.lundin@abo.fi



Kristian R. Gunnelius
MSc (ChemEng),
Doctoral student,
Åbo Akademi University,
Laboratory of Physical Chemistry.
Porthaninkatu 3,
20500 Turku/Åbo,
Finland kristian.gunnelius@abo.fi



Jarl B. Rosenholm,
PhD, Professor,
Åbo Akademi University,
Laboratory of Physical
Chemistry. Porthaninkatu 3,
20500 Turku/Åbo, Finland
jarl.rosenholm@abo.fi

ABSTRACT

During the hydration of cement the phase transformations affect the final strength, and a simple way of monitoring these on a structural basis is required. X-ray diffraction (XRD) analysis provides a non-invasive method to characterise the time dependency of hydration white Portland. Upon wetting the cement phase transformation was initiated and reflected as exponential decreases in the amount of starting phases. Cement hydration created new amorphous and crystalline cement phases under the first 21–28-hours of the hydration period. The qualitative method requires further refinement in order to provide quantitative data.

Key words: early-age, phase identification, hydration kinetics, white Portland cement, XRD

1. INTRODUCTION

The most abundantly produced material by mankind is cement and despite its long history the mechanisms behind the hydration reactions are yet not fully understood. The cement performance is determined by its phase composition [1, 2, 3] as well as its strength [4, 5]. In order to further tailor the cement and its end-properties, more basic knowledge on the phases, their formation and composition-determining reaction conditions is required. In this study wet cementitious systems were characterised for enhanced understanding of the chemistry during the sol-gel-transitions stages in the hydration phase. Our tools provide nano-scale information of the early-age cement phase composition. The hydration of cement can be classified as a sol-gel

transition reaction. Upon hydration the free pore water is continually being replaced by growing solid phases. Their increasing volume will at some instance render a 3D wall-to-wall network structure. Up to this stage also significant changes in the cement flow properties occur that greatly affect its workability. These can be readily characterised e.g. by rheological methods.

2. MATERIALS AND METHODS

The hydration of Aalborg white Portland cement (WPC) was monitored during the first 103 h at 35°C by X-ray diffraction using a Bruker-AXS D8 Discovery system equipped with a primary Göbel mirror and a 2D HI-STAR[®] detector. The liquid sample (60 mL, w/c=0.4) was wetted and mixed by a 5-min ultrasonication and analysed *in vivo* conditions as covered by a 7.5 µm thick polyimide (Kapton[®] by Chemplex) film. The XRD spectra were collected every 40 min in the 2θ range of 5.7° to 100.1°. A CuKα radiation of wave length 1.54184 nm with a slit and collimator of 0.5 mm were used. The 2θ step size was 0.020° and the scanning speed was 300 s/step of 30° 2θ. During operation the electric voltage and current of the X-ray tube were 40 kV and 40 mA respectively. Prior to analysis the x-ray device was calibrated with a Bruker AXS certified corund (Al₂O₃) standard. For phase identification a PDF-2 database (2010) was utilized. The phase areas were integrated on basis of the detector counts per second (cps) over the peak width (2θ).

3. RESULTS

An estimation of the cement phase compositions during hydration was done for selected phases. The dry WPC, as measured prior to wetting, displayed a XRD pattern where the phase Calcium Magnesium Aluminum Silicate (54CaO·16SiO₂·Al₂O₃·MgO) was identified, Figure 1 (insert). Immediately after wetting the phases detected in the WPC changed, Figure 1. It was seen that some phases disappeared during wetting while new ones were formed during hydration. The phase identification on the data turned out to be unreliable and exact phase data was left out.

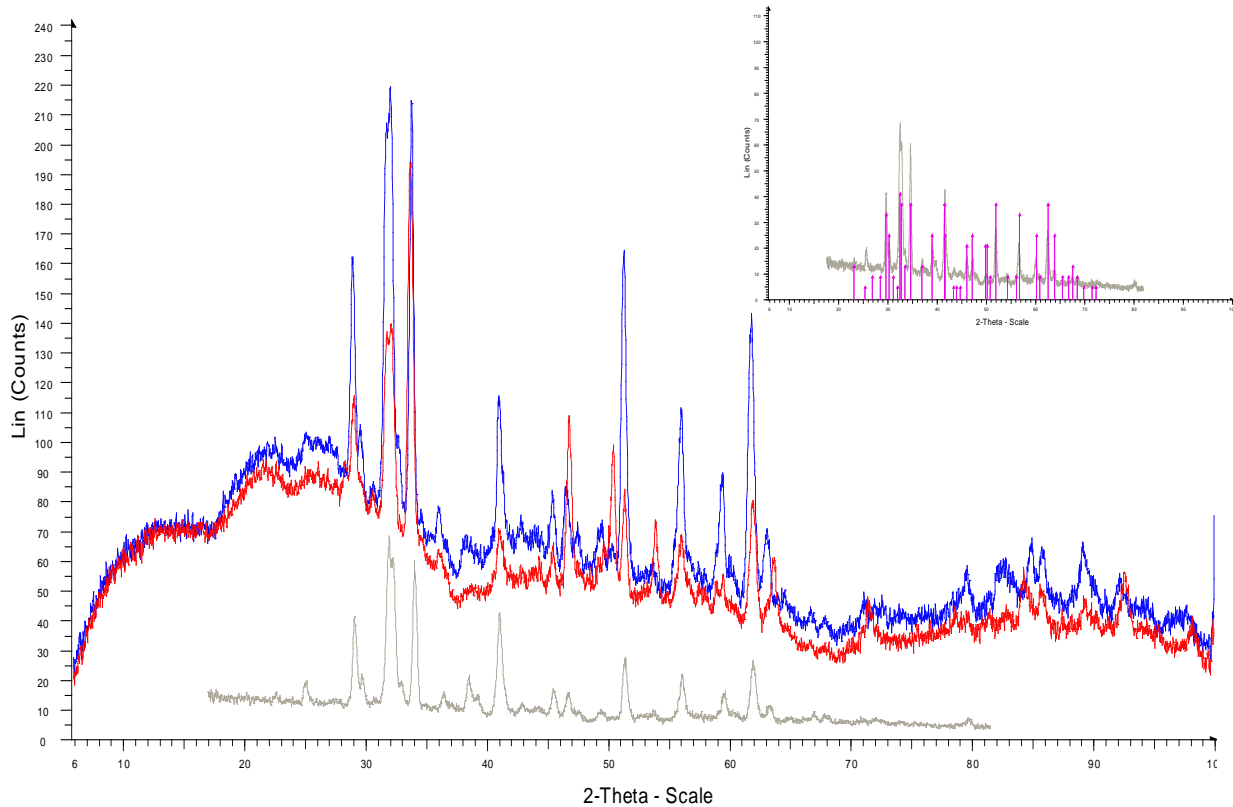


Figure 1. X-ray diffraction patterns of the dry, wetted and hydrating cement samples coloured in gray, red and blue respectively. In-set graph with the XRD pattern of dry WPC powder with the peaks for CaMgAlSi indicated.

A sequential plot of the XRD patterns recorded for the first 103 hours was used to illustrate the hydration rate of the WPC, Figure 2. New phases were detected after 0.15-2.2 h. Beyond this point specific phases displayed a steady increase as determined from their relative peak areas. The kinetics of phase formation could be estimated on basis of the phase conversion data. It was apparent that the initially abundant C, E, F and G phases decreased during the first 4 hours. This represents the chemically balanced precipitation reactions creating new solid structures – the key principle behind the cement hydration reactions. Scattering arising from calcium-based phases (C3S, C2S and C-S-H) was present from the first moment as the specific peak scattering increased upon hydration. For practical reasons the measurement was started 15 min after wetting the WPC powder. A variety of scattering signal from at least two amorphous phases was detected at the lower 2Θ -values in the range $5.7\text{--}27^\circ$ (smaller in-set graph in Figure 2). This was probably arising from the freshly created and structurally amorphous C-S-H components.

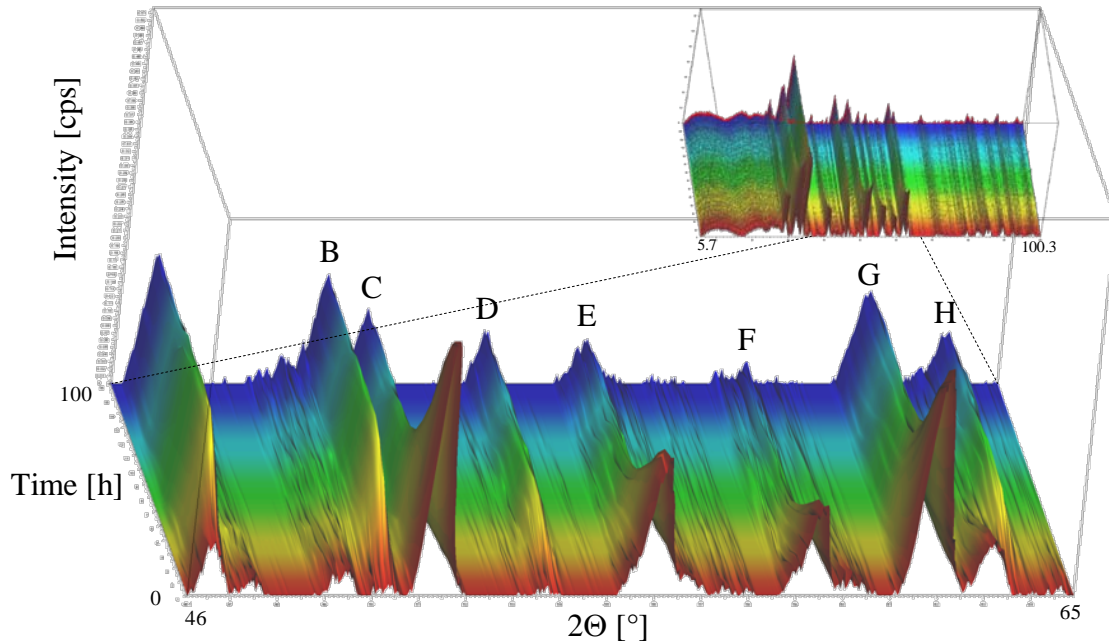


Figure 2. Subsequent X-ray diffractograms with background removed revealing kinetics of phase formation in the hydration of early-age WPC. The plot displays 2Θ ($46-65^\circ$) on x-, scatter signal counts (pcs) on y- and reaction time ($0.2-103.0$ h) on z-axis, respectively. The peaks indicated phase dissolution and structurisation. The initial phase formations were detected after $0.2-2.2$ h when hydrating at 35°C with $c/w=0.40$. The insert graph data display the full 2Θ range ($5.7-100.1^\circ$) of all XRD data.

The different cement phases were judged by their relative peak areas. A set of peaks were chosen from the 2Θ range above in Figure 2. These were given arbitrary names due to the number of conflicting phase ID's provided by the PDF2-database. It may be that the x-ray analysed sample surface has changed from the original alignment during the analysis time due to the hydration. However, the peak raw areas of the selected phases were compared as a function of hydration time, Figure 3. It is known that some of the initial phases (e.g. tricalcium silicate, tricalcium aluminate, dicalcium silicate and calcite) are dissolved in the cement hydration [6]. The current study indicated an exponential decrease of the phases as driven by their component dissolution. It is known that the phases created are calcium silica hydrate (C-S-H) components [1, 2, 3]. Upon wetting the new phases started to form as indicated by the increase in their peak areas. A levelling-out in these values appeared after about 21-28 h of hydration, as judged by their respective raw peak areas, Figure 3. This indicated a clear decrease, or even cease, in the crystal growth rate of the respective phase, as the precipitation reaction was significantly reduced. This implies that a majority of the ion mobility would have been lost by this time. Mobile ions are a prerequisite for the precipitation reactions creating the new cement phases. Beyond this point the subsequent hydration reactions would to a greater degree involve restructurisation of the phases created in the early hydration stages: the thermodynamically instable as well as the amorphous ones. [7]

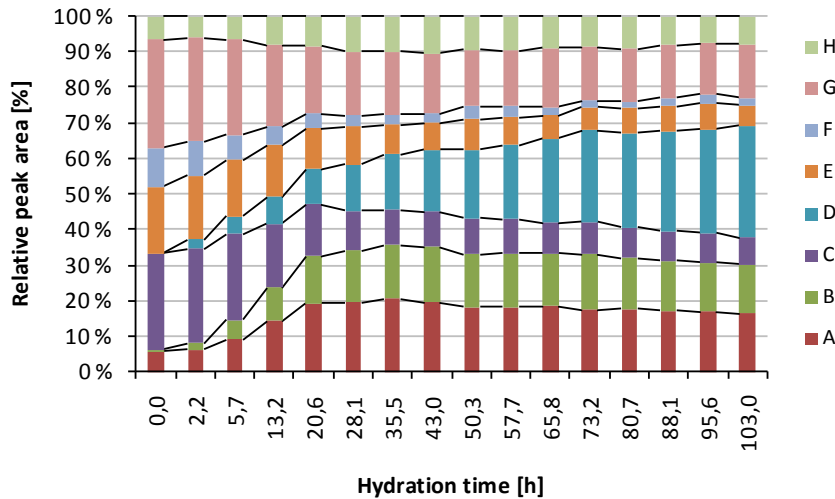


Figure 3. Example of selected peak areas as function of hydration time for the different phases indicating their relative amount in the 2Θ -range $46-65^\circ$. The amorphous phase contributions were not accounted for in these calculations.

4. CONCLUSIONS

The results indicated that the used x-ray system with a 2D-detector was successful in this type of non-invasive material characterisation, provided a suitable and stable sample carrier. For reliable phase identification a properly aligned surface of the beamed sample is required. The cement phases responsible for the cement hydration were readily distinguished from the XRD-data. Also information on the behaviour of the structurally important C-S-H phase could be identified. From the results it was seen that the original phases initially were dissolved and decreased in amount as their relative peak area were declining. The data imply that several phases were present from the start as also that new phases were formed after 0.15-2.2 h of hydration. The phase amounts were increased until 21-28 h of hydration. Further work will reveal specific qualitative information on hydration cement systems.

REFERENCES

- [1] Taylor, H.F.W., "Cement Chemistry", Academic Press Limited, London, 1990
- [2] Stutzman, P.E., "Guide for X-Ray Powder Diffraction Analysis of Portland Cement and Clinker", NISTIR 5755, National Institute of Standards and Technology, Gaithersburg, 1996
- [3] Bezjak, A. and Jelenić, I., "Quantitative Determination of Major and Minor Phases in Portland Cements from X-Ray Diffraction Patterns Represented by Fourier Series," *Cement and Concrete Research*, Vol. 1, pp. 475-492, 1971
- [4] Hewlett, P.C. Ed., "Lea's chemistry of cement and concrete," 4th ed. London, Great Britain: Elsevier Butterworth Heinemann, 2003.
- [5] 2. De La Torre, Angeles, et al. "Full Phase Analysis of Portland Clinker by Penetrating Synchrotron Powder Diffraction," *Analytical Chemistry*, vol. 73, no. 2. pp. 151, 2001
- [6] Scherer, G.W. et al. "Effect of pressure on early hydration of class H and white cement," *Cement and Concrete Research*, Vol. 40 pp 845-850, 2010

[7] Mitchell, L.D. et al. "Quantitative Rietveld analysis of hydrated cementitious systems," *Powder Diffraction*, Vol 21, No 2, pp 111-113, 2002

Rheological and Structural Characterization of Early-age Cement Pastes



Kristian R. Gunnelius
MSc (ChemEng),
Doctoral student,
Åbo Akademi University,
Laboratory of Physical
Chemistry.
Porthaninkatu 3,
20500 Turku/Åbo,
Finland
kristian.gunnelius@abo.fi



Tom C. Lundin,
DSc (Tech),
Academic Lecturer,
Åbo Akademi University,
Laboratory of Physical Chemistry.
Porthaninkatu 3,
20500 Turku/Åbo, Finland
tom.lundin@abo.fi



Jarl B. Rosenholm,
PhD, Professor,
Åbo Akademi University,
Laboratory of Physical
Chemistry. Porthaninkatu 3,
20500 Turku/Åbo, Finland
jarl.rosenholm@abo.fi

ABSTRACT

The rheology of cement pastes containing two different types of limestone microfiller particles was characterized. We used two limestone-based fillers, A and B. They were found to have somewhat different electrokinetic properties, and were thus expected to affect the rheology and hydration of cement slightly differently. XRD-analysis was used to identify the phases in the fillers. Filler A lowered the cohesive energy of the paste at low additions, while B raised the cohesive energy of the paste immediately. Both fillers raised the cohesive energy significantly when larger amounts were added. Both fillers accelerated the initial reactions, A more than B.

Key words: wet cement, rheology, early-age, XRD, phase identification

1. THEORY

Rheology is a powerful tool for characterising suspensions, including wet cementitious systems, for enhanced understanding of colloidal-level interface chemistry during sol and initial gel-transformation stages. Rheological tools provide flow and structural properties following quantitative information on specific particle-particle interactions. The liquid state is traditionally characterised by its workability properties and, the hydration phase, by cement setting kinetics [1] [2]. Previously Calcium carbonate has been seen to accelerate initial cement reactions [3] [4]. The parameters of interest are the particle interactions, their packing, arrangement and agglomeration tendency that govern the behaviour of cement paste. The rheological method

developed by Ramsay et al [5] and Tadros [6] was used to calculate the internal cohesive energy U_c of the wet cement paste according to

$$U_c = \int_0^{\widehat{\gamma}_c} \sigma d\gamma = \int_0^{\widehat{\gamma}_c} \gamma_0 G' d\gamma = \frac{1}{2} \widehat{\gamma}_c^2 G' \quad (1)$$

where G' is the elastic modulus, $\widehat{\gamma}_c$ is the critical amplitude and σ is the measured shear stress. This method allows for discrete identification of the shear rates where particle flocculation, segregation and sedimentation take place.

2. EXPERIMENTAL

The materials consisted of a white Portland cement (Finnsementti Aalborg white cement) and two different ground limestone samples A and B. Zeta potentials were measured with a colloidal dynamics Acoustosizer 2 using 1M NaOH and 1 M HCl to perform titrations. XRD analysis of the powder samples attached onto amorphous silica was performed with a Bruker D8 Discovery® x-ray diffractometer.

Rheological experiments were performed using solids to water ratio of 0.4. The cement was mixed with the filler in powder form. Water was added and the paste was mixed manually in a Finnsonic ultrasonic bath for 2 minutes at ambient temperature. A wet cement paste sample was placed in the measuring system and the rheological measurement was started 6 minutes after the water addition. The rheological experiments were performed using a Bohlin VOR rheometer using serrated plate-plate geometry to eliminate wall slip. Amplitude sweeps were performed at 1 Hz oscillation was from 0.01 to 20 mrad. Kinetic experiments were performed at 1 Hz and 0.2 mrad.

3. RESULTS

XRD analysis of the fillers illustrated in figure 1 showed that A contained mainly CaCO_3 in the form of calcite while B contained calcite and dolomite phases. The latter containing Mg, implies a tendency towards formation of Brucite phase at contents above 1%. Due to volumetric expansion this may be structurally detrimental for the final cement strength development. This can occur as cracks when phase formations occur at different rates [7].

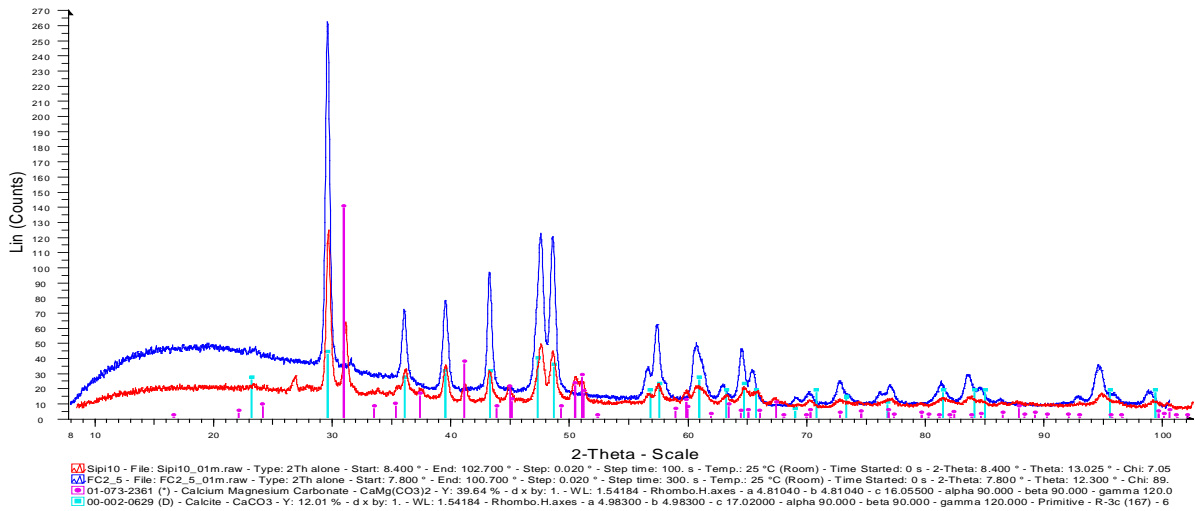


Figure 1 – X-ray diffraction patterns of filler A (Calcite; above in blue) and filler B (Calcite/dolomite; below in red) with respective phase ID's.

Figure 2 shows data of the elastic modulus of the cement paste as a function of addition of filler A having a wide size distribution. It was seen that the elastic modulus of the paste increased when a large portion of the cement was replaced with filler A. Often a plateau, the LRV (linear region of viscoelasticity) was observed at small amplitudes, where the elastic modulus was largely unchanged with increasing amplitude. The point where the elastic modulus started to drop was identified as the critical amplitude. This is illustrated in the figure for the paste with 50% filler A. Here the critical amplitude was estimated to be 0.3 mrad.

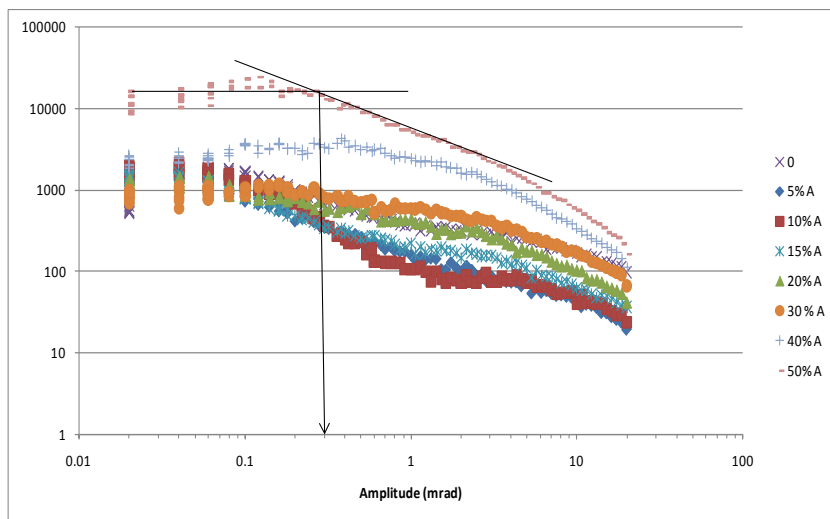


Figure 2- Elastic modulus as a function of the amplitude at 1 Hz for the cement pastes containing 0-50wt% A of the solids at 40 vol% solids/water.

Data in figure 3 describe the cohesive energy as a function of the filler fraction. Filler A showed a drop in the cohesive energy at lower additions. The paste containing filler B on the other hand raised the cohesive energy slightly at low additions. Replacing the cement beyond 25vol % with filler raised the wet paste cohesive energy substantially.

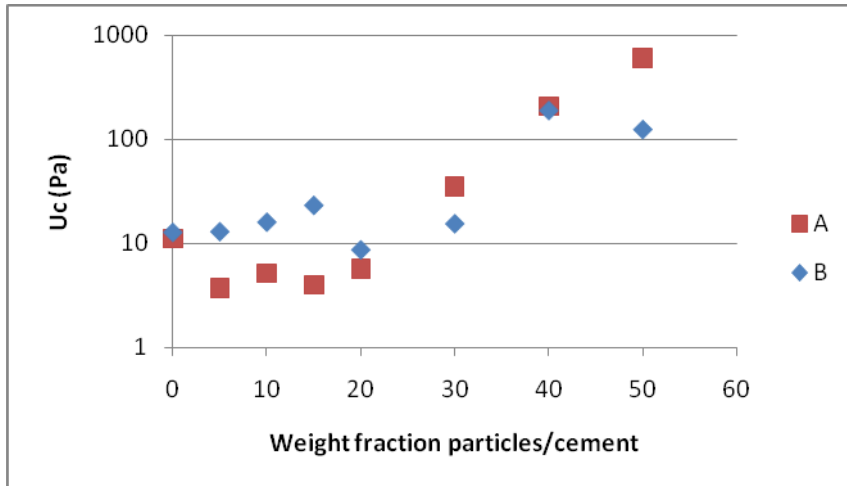


Figure 3- The wet cement paste's cohesive energy as a function of the fraction added filler.

Oscillatory tests were performed at constant frequency and amplitude. The first hour results are illustrated in figure 4. The cement samples in these tests were chemically identical (containing the same mass cement/water), and had a different volume fraction of solids. There was a systematic drop in the measured loss modulus (G'') in conjunction with a levelling-off in the storage modulus (G'). This may suggest a type of stabilisation occurring at this point. It may be so that a plane of shear was induced within the sample not allowing force transmission. The paste containing A came to the stable area faster than the paste containing B, while the pure cement was the last to reach this state. This suggests that filler A speeded up the setting reactions more than filler B as the pure cement was observed to react slowest.

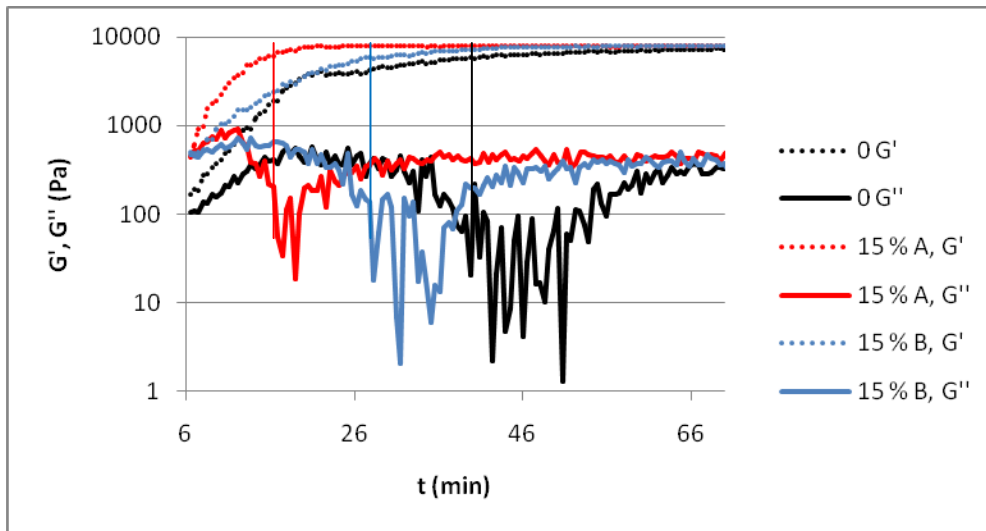


Figure 4- The storage modulus G' and the loss modulus G'' as a function of setting time for cement pastes with filler A and B.

5. CONCLUSIONS

The rheology of wet cement pastes can be modified by the addition of different fillers. By selecting suitable particles for a cementitious system the rheological properties can be tuned so that the cement behaves e.g. without spatial segregation taking place during setting. When filler A, containing calcium carbonate, was introduced into the paste the cohesive energy initially dropped, only to rise at higher concentrations. The data analysis implies that quantification of

the internal cohesive energy for cement paste systems is made feasible. Furthermore the kinetic experiments showed that both fillers accelerated the initial setting reactions.

REFERENCES

1. Nehdi, M., & Al Martini S., "Estimating time and temperature dependent yield stress of cement paste using oscillatory rheology and genetic algorithms." *Cement and Concrete Research*, Vol. 39, 2009, pp. 1007-1016.
2. Rössler, C., Eberhardt, A., Kucerová, H., & Möser, B., "Influence of hydration on the fluidity of normal Portland cement pastes," *Cement and Concrete Research*, vol. 38, 2008, pp. 897-906.
3. Kadri E.H., Aggoun S., De Schutter G., & K. Ezziane, "Combined effect of chemical nature and fineness of mineral," *Materials and Structures*, vol. 43, 2010, pp. 665-673.
4. J Péra, S Husson, & B. Guilhot, "Influence of finely ground limestone on cement hydration," *Cement and Concrete Composites*, vol. 21, 1999, pp. 99-105.
5. Ramsay J.D.F., Daish S.R., & Wright C.J., "Structure and Stability of Concentrated Boehmite Sols," *Faraday Discuss. Chem. Soc.*, vol. 65, no. 65, 1978.
6. Th. F. Tadros, "Correlation of viscoelastic properties of stable and flocculated suspensions with their interparticle interactions," *adv. colloid iterface sci.*, no. 68, 1996, pp. 97-200.
7. P. C. Hewlett, Ed., *Lea's chemistry of cement and concrete*, 4th ed. London, Great Britain: Elsevier Butterworth Heinemann, 2003.

Rheology of matrix with different crushed mineral fillers and admixtures



Rolands Cepuritis, MSc student
Dept of Structural Eng.
NTNU
N-7491Trondheim
rolands.cepuritis@hcb.lv



Stefan Jacobsen, Professor.
COIN Dept of Structural Eng.
NTNU
N-7491Trondheim
stefan.jacobsen@ntnu.no

Bård Pedersen, PhD
Norstone, NPRA, Norwegian
Public Roads Administration
baard.pedersen@vegvesen.no



Hedda Vikan, PhD,
Senior Principal Engineer
NPRA, Norwegian Public
Roads Administration
Hedda.vikan@vegvesen.no

Espen Rudberg,
Rescon Mapei,
Norway

Klaartje DeWeerd,
Sintef,
Norway



Ya Peng, MSc, PhD student
COIN Dept of Structural Eng.
NTNU
N-7491Trondheim
ya.peng@ntnu.no

Børge Wigum, PhD,
Professor II
Norstone, NTNU
borge.wigum@norstone.no

ABSTRACT

The effect of 7 widely different fillers on rheology of filler modified paste (= matrix) was investigated at w/b = 0.50 and 0.60 and 0.4 % superplasticizer (SP) of fly ash cement. Two replacement levels $V_{\text{filler}}/V_{\text{powder}} = 0.20$ and 0.33 were used at constant volume fraction of solid particles $\phi = 0.459$ in all mixes (equal to the cement volume fraction in the reference with w/b = 0.40 without filler). Two different types of co-polymeric SP were used. A Physica MCR300 Rheometer was used for flow tests (yield stress, plastic viscosity), static tests (yield stress, shear modulus) as well as for oscillatory tests (viscoelastic properties). The main effects observed were highest consistency for natural filler compared to crushed filler, that the magnitude of the effect of SP-type on rheology seemed to be similar or perhaps larger than the magnitude of the effect of filler type. The consistency increased as filler replaced cement at increasing w/b and constant volume fraction of particles, even as volumetric amount of SP reduced.

Key words: crushed aggregate, filler, admixture, matrix, rheology.

1. INTRODUCTION

The aggregate is important for most concrete properties. Due to depleting resources the concrete industry is experiencing a transfer from natural to crushed aggregates. Some major differences between natural and crushed aggregates are: a) Particle size distribution of crushed aggregates usually have denser, Fueller-type, curves b) Less rounded particle shape in crushed material, c) Considerably higher filler content compared to natural sand. This latter point is an important one and leads to the following problem; How much of the filler do we need to remove from the

sand? By using new technology such as air classification it is even possible to modify the filler itself, for example by removing only particles below a certain size). Important questions for the concrete producer then are; How is the concrete mix design affected compared to concrete with natural aggregate? And to what extent can we use admixtures to modify "unwanted" properties caused by the crushed fillers?

For fresh concrete, the main factors affecting rheology can be simplified into quality and volume fraction of aggregate (Φ) and of cement paste ($1-\Phi$). The effect on rheology of the filler depends largely on its specific surface [1], mineral composition and some other factors. In concrete the effect of filler becomes more important the larger its volume fraction. Furthermore, the correlation between the rheology of filler modified paste (= matrix) and concrete is probably closer the higher the volume fraction of matrix [2]. On the other hand, the maximum packing, Φ_{\max} , which is also an important parameter, becomes more difficult to measure the finer the particles. Thus it could be useful to investigate the rheology of matrix as a first step in the assessment of filler- and admixture effects on properties of fresh concrete.

The particle-matrix method for proportioning regards all particles > 0.125 mm as a particle phase dispersed in a lubricating matrix made up of all fluids and particles (binder, filler etc) < 0.125 mm [2,3]. The method has been used in Norway by many practitioners for more than a decade and has proven very useful. However, the size limit between lubrication- and particle phase when dividing between particles at 0.125mm is somewhat arbitrary. It has been observed that cement paste may work just as well as lubricating phase [4].

In the question of how to obtain stable and robust SCC there are mainly two means; powders and admixtures, unless smaller aggregate size and reduced density difference can be chosen. In Norway the rock industry is quite large with a number of quarries producing aggregates to meet the future increased demand for industrial aggregate. One important output from this industry is fines (or filler) representing an important source of value. In this paper we present parts of a study on the effect of different types of filler on the rheology of matrix, always keeping the fraction of solids, Φ , constant to develop more sustainable concrete. The objective has been to investigate the combined effects of fillers and admixtures (and eventually also cements) for the implementation of manufactured sand in concrete.

2. MATERIALS AND TESTING

7 fillers and two types of admixtures were investigated. The fillers (0-0.125 mm) were natural or from crushing of different types of rock in various processes including limestone. They were mixed with cement, SP and water in a high speed blender. The resulting matrices had constant $w/b = 0.40, 0.50$ and 0.60 . Properties such as particle size, specific surface and particle shape of several of these fillers are given in [5]. Two different co-polymeric superplasticizers were used; Rescon Mapei SP-130 and SR-N where the first has longer side-chains than the second one. Both were used at a constant dosage = 0.4% of fly ash cement weight. The cement was the standard Norwegian CEM II with 20% low lime fly ash ground with the clinker. All mixes were made with constant solid volume fraction $\Phi = 0.459$ (or $V_{\text{water}}/V_{\text{solid}}$ (=voids ratio) = 1.18). This is the solid volume fraction of the reference cement paste with $w/b = 0.40$ without filler. The 7 fillers were used at two replacements; $V_{\text{filler}}/V_{\text{powder}} = 0.20$ and 0.33 . Rheology was studied with a Physica MCR300 Rheometer with parallel plate configuration utilizing its advanced programming capacities in a 23 minute test cycle for each material. The gap was adjusted at 1

mm and all tests were run at 20°C. This included flow parameters (flow curves, yield stress τ_0 and plastic viscosity μ), thixotropy (hysteresis of flow curves [6], time dependant viscosity under shear), static/elastic behaviour from rest at both controlled shear and stress as well as viscoelastic properties in oscillatory amplitude sweeps at 1 s⁻¹ frequency. Some repeatability tests as well as different shear histories were also investigated. Also some other powder materials (colouring agents) and a few mixes at other powder replacements than those shown in table 1 were tested. However, here we only show the results of the tests where all 7 fillers were tested at 2 different replacements (20 and 33 volume-% of cement replaced by filler) with 2 different types of copolymeric SP.

3. RESULTS

Table 1 shows a compilation of some main rheology results for matrices with $\Phi = 0.459$, SP = 0.4 % of fly ash cement at w/b = 0.50 and 0.60 where the replacement levels of filler were $V_{\text{filler}}/V_{\text{powder}} = 0.20$ and 0.33, respectively.

Table 1 – Rheology, min-max (mean,) of matrices, 7 filler types, $\Phi = 0.459$, SP = 0.4 % of c

		w/b = 0.50 ($V_{\text{filler}}/V_{\text{powder}}=0.20$)		w/b = 0.60 ($V_{\text{filler}}/V_{\text{powder}}=0.33$)	
		SP 130	SR N	SP 130	SR N
Flow curves	τ_0 Bingh.(Pa)	14-24 (18)	17-28 (22)	7-21 (13)	7-25 (16)
	μ (Pa.s)	0.19-0.28 (0.23)	0.33-0.58 (0.44)	0.13-0.28 (0.19)	0.19-0.48 (0.33)
	τ_0 Her.-Bulkl.	6-10 (8)	-25 - -11 (-17)	-4 - +5 (1)	-18 - -1 (-9)
	Hyst.ar.(Pa/s)	151-587 (285)	262-1274 (731)	85-588 (275)	325-805 (549)
Static	τ_0 Gel str.	2-8 (5)	5-10 (8)	2-7 (3)	1-7 (4)
	τ_0	7-19 (12)	19-34 (26)	4-18 (9)	4-22 (13)
	$\tau_0 + 10$ min	8-22 (14)	25-44 (33)	5-22 (11)	6-26 (19)
	G_τ (Pa)	857-1819 (1356)	2925-4651 (3816)	788-1556 (1117)	1992-3450 (2487)
	G_γ	92-352 (183)	391-2066 (1227)	53-404 (167)	71-828 (535)
Visco-elastic	G^*	44-155 (102)	26-151 (58)	15-68 (44)	26-158 (60)
	γ_{crit} (s ⁻¹)	0.003-0.004 (0.003)	0.001-0.012 (0.008)	0.002-0.006 (0.004)	0.002-0.012 (0.006)

Table 1 show that the differences in flow properties for different fillers seem to be relatively small at constant Φ and SP-type and -dosage. This is seen by comparing the mean values (in parentheses) with the min and max values in each of the four columns of table 1. Furthermore, the variation between different types of fillers is probably of the same order as the variation due to replacing fly ash cement with filler and associated w/b-increase. For SP 130 the variation of μ between matrixes with different fillers was 0.19 – 0.28 Pa.s for w/b = 0.50 and $V_{\text{filler}}/V_{\text{powder}} = 0.20$. The variation was slightly higher; 0.13 – 0.28 Pa.s, at w/b = 0.60 and $V_{\text{filler}}/V_{\text{powder}} = 0.33$. This variation is only slightly larger than between 4 parallel tests on a single material (0.13 – 0.20 Pa.s for matrix with limestone filler at w/b = 0.50).

The clearest effect on rheology was when changing w/b while keeping the type of SP, and also when changing the type of SP and keeping w/b constant. Furthermore, the two fillers with natural material gave higher consistency than the crushed fillers as expected. The increased w/b with filler replacement seemed to slightly increase consistency at the actual reduction of total SP (SP constant dosage as percentage of cement) when keeping Φ constant.

The static tests showed highest gel strength and static yield stress at highest age as expected. The static shear moduli, G , were determined as tangent at 50 % of maximum stress. Highest G was observed in the stress controlled test with lower rate of shear than in the measurements at constant rate of shear. It seems that static shear moduli G were increased more by the short side-chained SR-N than the rheological properties taken from the flow curves (Bingham yield, plastic viscosity, thixotropy).

The reference paste ($w/b = 0.40$, $\Phi=0.459$, 0.4 % SP, no filler) was tested a number of times with different types of SP and test sequences. Generally, higher values for most rheological properties shown in Table 1 (i.e lower consistency) were obtained compared to when using filler. That is, when filler replaces fly ash cement (but keeping total particle volume fraction constant ($\Phi = 0.459$)), the consistency increases even if the SP-content of the mix-volume reduces. Thus all fillers showed a positive effect by increasing the consistency when replacing cement and keeping SP-percentage as a constant dosage of cement.

The complex modulus G^* was determined as function of time dependant shear stress and shear rate: $G^* = \tau(t)/\dot{\gamma}(t)$ at increasing strain amplitude. We used oscillatory amplitude sweeps at 1 s^{-1} frequency that gave storage- (G') and loss- (G'') modulus at the critical strain amplitude where $G' = G'' = G^*$. Starting from very low oscillatory shear deformations this usually is taken as the transition from solid or gel to liquid behaviour at the end of the linear viscoelastic range. The G^* - values were all significantly lower than the static G -values. There was a tendency of lowest G for the natural fillers whereas no such effect could be seen on G^* .

A further analysis of the most reliable parameter will be made. In table 1 The H-B model gave best flow curve fit ($R^2 = 0.995-0.995$) compared to the Bingham model ($R^2 = 0.924-0.958$) due to shear thinning. On the other hand this often gave negative yield stress so the H-B model is probably not applicable to describe yield. Also the determination of static G could be uncertain due to the nature of the stress-strain curves. (A fourth rheologic sequence aimed at relating to stability was also used where the evolution of apparent time dependant viscosity was recorded in consecutive tests at high, low and high shear rate. This also gives information about thixotropy. These results have not been analyzed yet but will be published with an enlarged analysis of the present results. The analysis will also give implications for further research, such as relation to specific surface, particle shape, maximum packing density (Φ_{\max}), proportioning principles and stability.

4. ACKNOWLEDGEMENT

The work was part of COIN task groups TG 2.1 and 2.3 and was financed by Norbetong and COIN.

REFERENCES

1. Pedersen B. (2004) PhD Norw Univ of Sc and Tech 2004:92, 198 p.+app
2. Mørtzell E (1996) Dr.ing 1996:12 Norw.Univ.Sc.&Tech (1996) 310 p. (In Norw.)
3. Smeplass S., Mørtzell E.(2001) Proc 2nd Int. Symp SCC, Tokyo, 267-276
4. Jacobsen S., Arntsen B.(2008) Materials and Structures (41) 703-716
5. Wigum B.(2010) Classification and particle properties of fine aggregates, NTNU, 29 p.
6. Vikan H (2005) PhD Norw Univ of Sc and Tech 2005:189, 332 p

An appraisal of the strength to water cement ratio relations



Ganesh Babu. K
Professor
Dept. of Ocean Engineering,
IIT Madras, Chennai.
Kgbabu18@yahoo.com



Durga Prasad. R
Research Scholar,
Dept. of Ocean Engineering,
IIT Madras, Chennai
prasadiitproject@gmail.com



Chandra Sekhar. B
Research Scholar,
Dept. of Ocean Engineering,
IIT Madras, Chennai
sekharbhojaraju@gmail.com

ABSTRACT

Historically the strength to water cement ratio relationship is well recognised, though the different national provisions indicate a substantial variation. The paper is an appraisal of the existing water cement ratio to strength provisions presently. Also the data available from the various sources are compiled to understand the efficacy of these relationships. A brief appraisal of these studies indicate that while there is a significant variation in the strength results to justify these variations in the provisions, an effort should be to maximize the strength at any level.

Key words: Concrete mix, Compressive strength, Water cement ratio, Codal provisions

1. INTRODUCTION

1.1 General

Provisions relating to concrete mix design essentially try to ensure economical mixes with a reasonable confidence level on strength and workability. However, even a cursory examination of these provisions indicates that there is a significant variation in these provisions. It is obvious that these variations do stem from parameters like cement type and strength, type size and gradation of aggregates, water content and workability, fines content, ratio of fines to coarse aggregates, super plasticizers and other mineral and chemical admixtures. It is thus felt by a few that it is difficult to arrive at any unique or even acceptable relationship.

1.2 Mix design methodology

In a properly designed normal concrete mix it is necessary to have an appropriate grading of aggregates (both fine and coarse) forming a near dense structure (not certainly the maximum possible to allow for hydration), which is then bound by the cementitious hydration products. This ensures that an optimum amount of cement is utilized to achieve minimum voids in the concrete mass. The specifications for normal concrete mix design require that the properties of the constituent materials available- cement, aggregates and water are evaluated. Based on the required design strength and workability the water cement ratio and water content are

established. From these the cement content is obtained and the total aggregate content or the fine and coarse aggregate contents are evaluated based on absolute volume method, taking into consideration the bulk density and fineness modulus. While a comprehensive discussion on all these parameters is not possible within the limited focus of the present paper, it attempts to have a close look at the various national provisions concerning the water cement ratio to strength relationships.

2 WATER CEMENT RATIO TO STRENGTH RELATIONSHIP

For a specific cement quality, the strength of the concrete composite depends primarily on the water cement ratio only; if a proper compaction is assured. In normal concretes this compaction is assured through the workability criteria which defines the water content required. Modifications relating to the effect of superplasticizers and mineral admixtures could be taken into account by an appropriate understanding of the effects of these materials on workability and the strength of the cementitious binder part. The starting point for the basic water cement ratio strength relation is the Abrams report [1] of 1920, which was redrawn and presented in Figure 1.

3 EXISTING NATIONAL PROVISIONS

In their much later observations Shilstone [2] and Kosmakta [3] pointed out that the ACI relation is similar to the old Abram's equation, however, taking into consideration the change in the volume to weight relationship required. In more recent times these relations have undergone significant changes due to the improved strengths resulting from the production processes like dry process and more effective grinding of both raw meal and cement clinker.

This paper is an effort to understand the provisions in the various national standards presently [4-10], and compare them with the results from available literature, so that the effectiveness of each of these is ascertained. The national standards compared have been chosen with a view to represent the present status, both in terms of the changes over the years and also the latest status. Figure 2 presents the water cement ratio to strength relations used in the American [4,5], British [6], Euro [7], German [8], and Indian standards [9,10]. The original Abram's relation is also presented in the same figure for a comparison, which obviously predicts the lowest strength at any water cement ratio as it was based on the cements of the bygone era.

It is also clear from Figure 2 that amongst the relations suggested by various national provisions the IS: 10262-1982 (earlier Indian standard) and ACI 211.1-91 (for normal concretes) predict very low strengths in comparison to the other provisions. The relationships suggested by the British, German and Euro provisions predict the highest strengths, with only marginal differences between them. Also, the German method tries to clearly depict even the effects of compaction at the lower water cement ratios. However, the water cementitious materials ratio to the strength relationship recommended by the ACI 211.4R-93 (for high strength concretes containing fly ash, with or without HRWR) predicts a strength values which are midway between these two extremes. The advantage in terms of the higher workability, better cement distribution and compaction resulting in an increase in strength compared to the concrete without the HRWR is clearly reflected in Figure 2. The revised Indian standard IS: 10262-2009 does not propose any specific water cement ratio to strength relation, may be due to the

considerable differences in the various national provisions of today, and suggests that the design be based on the past experience.

After a critical appraisal of these relationships recommended by various national provisions, the next step was to check the efficacy of these with a broad spectrum of experimental results available in literature. While it is possible to look at this efficacy through a limited experimental investigation to validate, which any way was attempted, it is best to look for a large data base to understand the total problem scenario. A literature search in this direction showed two data bases. The first one was the “Database for Mechanical Properties of Concrete”, from the Building Material Engineering Laboratory of the Department of Architecture, Graduate School of Engineering, University of Tokyo [11] and the second the “Concrete data”, for the Machine Learning Repository exercise from the University of California, Irvine [12]. Figure 3 shows the water cement ratio to strength relation plotted with the University of Tokyo data. It may be noted that we filtered the data related to only the normal concretes with OPC (Type 1 cement) without any admixtures, either chemical or mineral. The one surprising fact that can be seen is that there are several concretes at a specific water cement ratio, but showing a wide variation in the strengths obtained. One could easily observe that this variation is contained in the upper bound and lower bound relations, though this was not given exclusively for limiting the number of curves in the plot. The average curve that fits the above data was however shown in Figure 3. The various national provisions were then superposed on this data. Once again for clarity only the Euro relation (representing the best possible estimate from the previous Figure 2 and the ACI 211.4R-93 (though only relevant for concretes with fly ash and HRWR, being the maximum in ACI guidelines) were superimposed on the data points. Also, the relation that was derived based on the strengths of concretes that were optimised for strength and compaction by ensuring the best grading and good cement was also superposed on the data as can be seen. It can be seen that even the best from ACI as already stated is only near the average of the data presented. The Euro and the author’s laboratory relations more or less are close to the upper bound of the data. The second data bank is little more coherent and resulted in a good fit. The author’s laboratory relation was also superimposed on this to see the maximum possible. It is seen that the author’s laboratory predicts higher strengths than that were obtained in the university of California data. It is felt that probably the best possible strength is predicted by the author’s laboratory relation, and for practical application a reduced strength (may be about 10%) could be assumed for convenience.

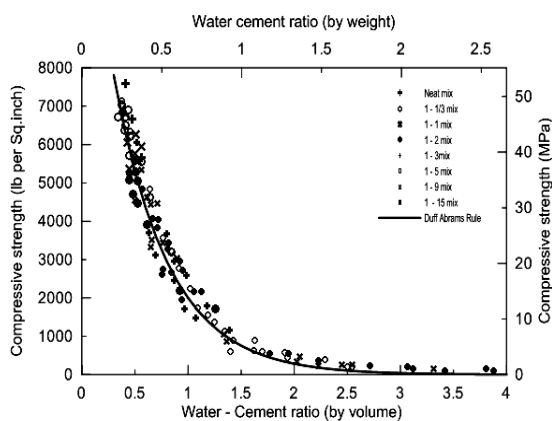


Figure 1 –Strength to water cement ratio relation (after Abram’s -1920)

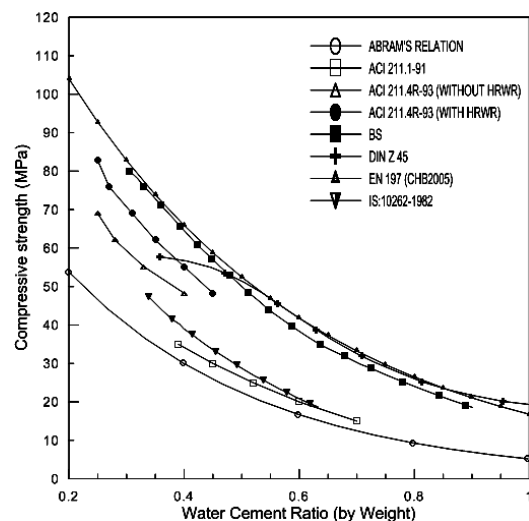


Figure 2 – Comparison of the strength to water cement ratio relations.

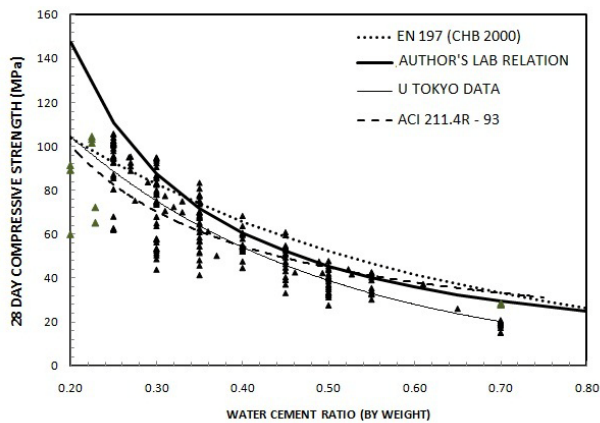


Figure 3 – strength to water cement ratio relations (U. Tokyo data)

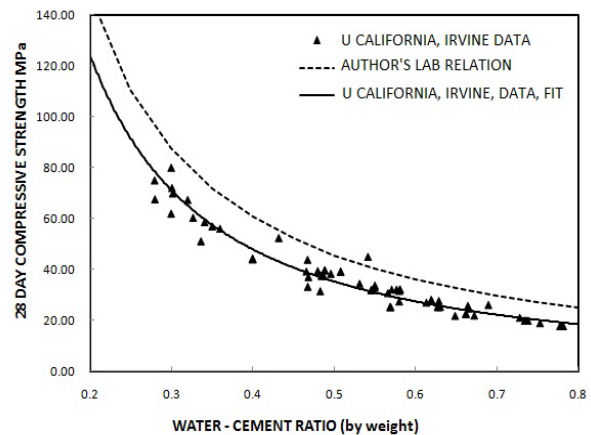


Figure 4 – strength to water cement ratio relations (U. California data)

REFERENCES

1. Abrams, D A. "Design of concrete mixtures", Bulletin No.1, Structural Materials Research Laboratory, Lewis Institute, Chicago, pp.20.
2. Shilstone, J. M, "The water-cement ratio – which one and where do we go?" *Concrete International*, Vol.64, September 1991, pp. 64-69.
3. Kosmakta, S. H, "In defense of the water cement ratio," *Concrete International*, Vol.64, September 1991, pp. 65-69.
4. ____ACI 211.1-91, "Standard Practice for Selecting Proportions for Normal Heavyweight, and Mass Concrete", ACI Committee 211, Reapproved 1997.
5. ____ACI 211.4R – 93, "Guide for Selecting Proportions for High-Strength Concrete with Portland Cement and Fly Ash", ACI Committee 211, Reapproved 1998.
6. Neville. A.M, "Properties of Concrete", Longman Scientific & Technical, Harlow (1987).
7. Sika Concrete Handbook, Sika Services AG Corporate Construction, CH-8048 Zürich, Switzerland, December 2005.
8. ____ DIN 1045, "Beton und Stahlbeton", Beton Verlag GMBH, Koln, 1988.
9. ____ IS:10262-1982, "Recommended Guidelines for Concrete Mix Design", Bureau of Indian Standards, New Delhi, 1983.
10. ____ IS:10262-2009, "Recommended Guidelines for Concrete Mix Design", Bureau of Indian Standards, New Delhi, 1983.
11. Noguchi. T, "Database for Mechanical Properties of Concrete", Building Material Engineering Lab., Department of Architecture, Graduate School of Engineering, Univ. of Tokyo. <http://bme.t.u-tokyo.ac.jp/researches/detail/concreteDB/download.html>
12. ____ "Concrete_data.xls", Machine Learning Repository, Univ. of California, Irvine. <http://archive.ics.uci.edu/ml/machine-learning-databases/concrete/compressive/>
13. Ganesh Babu, K., Raja, G. L. V., Srinivasa Rao, P, "Concrete mix design – An appraisal of the current codal provisions," *The Indian Concrete Journal*, Vol.66, No.2, February 1992, pp. 87-102.
14. Gilkey, H.J., "Water-Cement ratio versus strength – Another look", *ACI Journal*, Vol.57, 1961, pp. 1287-1312.

**Session B4 – EXECUTION OF CONCRETE STRUCTURES
AND SURFACES**

Tailormade Concrete Structures with the use of Digital Fabrication and Self Compacting Concrete



Thomas Juul Andersen
Cand.arch.
Danish Technological Institute
Gregersensvej, DK-2630 Taastrup
tja@dti.dk



Tine Aarre
Civil Engineer, PhD
Danish Technological Institute
Gregersensvej, DK-2630 Taastrup
taa@dti.dk

ABSTRACT

August 2009 a huge European project under FP7 was launched called New Industrial Technologies for Tailor-made Concrete Structures at mass customized Prices (acronym: TailorCrete). The research and development within the project introduces a radically new concept of producing unique, tailor-made concrete structures with complex geometries using an industrialized and cost-effective approach based on robots, ICT and advanced concrete technology. The innovative aspect is to produce formwork and reinforcement for concrete directly from the architects 3D CAD drawings, and thereby allow new and front-end architecture in normal housing with no extra costs for the citizen.

Keywords: Digital architecture, digital fabrication, self compacting concrete, robot technology, non-standardized formwork, reinforcement

1. INTRODUCTION

The motivation for the new concept comes from the successes already achieved in the manufacturing industry through the integration of new advanced technologies including computer aided design (CAD) and robot technology. In the construction sector, the availability of digital architecture gives designers wide ranging possibilities to produce intricate geometric designs that add uniqueness and value to the finished structures. However, the link between the digital architecture and the creation of complex formwork and reinforcement is missing. Thus today, the creation of complex concrete structures is extremely costly as the fabrication and processing of formwork and reinforcement is still a very labor intensive process. The main idea behind the TailorCrete concept is to close this gap by introducing robots, programmed from the 3D CAD designs via advanced ITC technology, for the processing of formwork and reinforcement.

2. RESEARCH CHALLENGES

In order to utilize the 3D data from the designers, digital manufacturing techniques are necessary to implement in the future manufacturing of non-standardized concrete. This is a natural step for the concrete industry in order to exploit the full potential of concrete and at the same time lower the costs. One of the most promising techniques with already some experience is the usage of robot technology to fabricate both formwork and reinforcement.

2.1 Non-standardized formwork

One of the major challenges in the future manufacturing of non-standardized concrete structures is to introduce new and more cost-effective ways to manufacture the needed non-standardized formwork. Automated installations in the concrete industry like robot installations represent a very small part of all robot installations. These installations mostly cover shuttering robots used in pre-cast concrete plants in the production of plain concrete elements [1]. In order to optimize the production of non-standardized concrete structures, there is a need for development of new methods to produce non-standardized formwork by the usage of digital fabrication techniques.

2.2 Tailor-made reinforcement

Another major challenge within the area of non-standardized concrete structures is to optimize both production and usage of reinforcement. Conventional steel reinforcement is used in connection to almost every concrete structure, and it will most likely also be a necessary solution in connection to non-standardized concrete structures of the future. The main challenge is to optimize the production by introducing new digital manufacturing techniques and thereby be able to shape the reinforcement precisely at a lower price. Besides traditional reinforcement, the usage of alternative reinforcement like e.g. textile reinforcement and different types of fiber reinforcement (steel, glass, synthetic) will have an important role in the construction of future concrete structures.

2.3 Self-compacting concrete (SCC)

For Tailor-made concrete structures with complex geometries, it is absolutely essential to use self-compacting concrete (SCC), due to poor accessibility in connection to complex formwork. The fluid nature makes handling of SCC more complicated than conventional concrete, often leading to costly construction errors. Thus, an understanding and control of the rheological properties (flow properties) of SCC becomes the most critical issue in its production and usage.

3. PRELIMINARY RESULTS

The TailorCrete project has now been underway for just over a year, and some interesting results have already been achieved.

3.1 Non-standardized formwork

There is a need for new and more flexible formwork solutions if the non-standardized formwork of the future shall be manufactured using digital fabrication techniques. The properties required from the formwork solution and especially the property of actual formwork material that defines the final shape of the concrete are very crucial for the choice of digital fabrication technique. The objective of the research is to develop new formwork solutions for concrete structures cast on site. Within the project two different approaches have been chosen – one additive approach and one subtractive approach.

One method is the usage of a digitally controlled adjustable pin-bed model. Automatically, based on a 3D model, actuators arranged in a grid can adjust their length according to control points in the model. On top of the actuators, a flexible membrane defines the final shape and serves as a mould. This method allows to cast the actual formwork parts which can be transported to the construction site. For this solution different wax types have been tested in terms of melting point, softening point, shrinkage, handling etc. It has proved that certain wax types are actually very promising – and when the wax is cast in honeycomb structures it is both possible to reduce material consumption and weight for easier assembling on-site.

Another method is milling using robot technology. Using this method, the final shape of the formwork parts are achieved by milling in a solid block. The parameters that characterize the potential new block materials are a low price, great flexibility in the shaping process, sustainability and low weight. Thus, lightweight foam like expanded polystyrene has proved to meet these demands and has been tested during several robot millings. To make formwork processing using the combination of robot milling and light weight foam materials an innovative and cost-effective method, several challenges have been faced. First challenge is to reduce the milling time, which has lead to a series of tests where a combination of developed milling tools and advanced 5-axis robot milling strategies has been used. Second challenge is to achieve more homogeneous surfaces of the concrete and acceptable release between formwork and concrete. These demands have been met by introducing different types of coatings to the milled formwork parts in foam. The most promising results have been achieved using liquid epoxy coatings and solid, elastic rubber skins.

To ensure the compatibility between the digitally fabricated formwork parts and existing load bearing systems, a new formwork system is being developed. It consists of standard blocks in a modular system applying both to the wax and foam formwork parts and the existing load bearing systems available today. The blocks are very easy to assemble without the use of heavy lifting equipment.

3.2 Tailor-made reinforcement

The research in reinforcement has focused on both traditional reinforcement and alternative reinforcement types.

Concerning traditional reinforcement, the research has focused on the possibilities to automate the production using digital fabrication techniques. Thus, the research has explored the potential of using robots to bend and assemble traditional reinforcement. Initial tests have been performed on a robot installation leading to the development of a method where the robot automatically

could bend reinforcement bars in 2 dimensions. The method will now be used both to bend in all 3 dimensions and to assemble the bars by welding.

As regards alternative reinforcement, an investigation on reinforcement methods suitable for non-standardized concrete structures has been made. So far the research has focused on flexible reinforcement types like fibers (steel, synthetic, carbon etc.) and textile reinforcement. Together with research in flow patterns of self compacting concrete using Computational Fluid Dynamics, prediction of e.g. the final position of fibers in the concrete will be investigated. This will give better opportunities to calculate the properties of the non-standardized concrete structures.

3.3 Self-compacting concrete (SCC)

It has been shown that flow patterns, filling time and final position and geometry of free surfaces can be predicted with reasonable accuracy based on information on rheological properties and form geometry as well as filling technique using CFD (Computational Fluid Dynamics) [2]. Initial simulations of SCC flow have been carried out. Simulations show the free surface flow in the laboratory scale beam formwork. Using measured rheological parameters, the results will be compared to the experimental observations. Some of the future challenges of flow simulations are to be able to simulate the flow through reinforced sections in a computational cost effective way.

In order to have full control of the flow behavior for verification of the flow models, a formwork has been designed for the experimental observations. The formwork is made of transparent acrylic sheets to allow visual observations of flow. Initially, castings have focused on SCC with and without steel fibers.

4. CONCLUSIONS

A completely new approach for producing geometric advanced concrete structures of high aesthetic quality at mass customized prices is being developed in the TailorCrete project. This approach is based on a combination of front-edge knowledge on concrete technology, robot technology and ICT.

Initial tests have shown both the potential of the new concept but also some of the future challenges. In order to meet these challenges the research in both formwork, reinforcement and self-compacting concrete have to be verified via full-scale prototype tests. Thus, both element-scale prototypes and later building-scale prototypes will be made, and these prototypes will reveal the full potential of the TailorCrete-concept.

REFERENCES

1. Hansen, Christian et al., Dynamic high-precision multi-functional shuttering robot (MFSR), BFT 08/2006.
2. Thrane, L., Form Filling with Self-Compacting Concrete, PhD Thesis, Department of Civil Engineering, Technical University of Denmark, 2007.

Double curved concrete surfaces with precisely embedded optical fibres displaying live images.



Johannes Rauff Greisen
Consultant, M. Arch.
Industrial Ph.D.-scholar
RASA, CINARK
DTI, Gregersensvej 4
DK-2630 Taastrup
Denmark
jrg@dti.dk



Lars Nyholm Thrane
Consultant, Civ. Eng.,
Ph.D.
DTI, Concrete
Gregersensvej 4
DK-2630 Taastrup
Denmark
lth@dti.dk



Claus Pade
Senior consultant
Danish Technological
Institute, Concrete
Gregersensvej 4
DK-2630 Taastrup
Denmark
cpa@dti.dk



Christoffer Dupont
CTO
Dupont Lightstone ApS
Forskerparken 10
DK-5230 Odense
Denmark
cd@dupontlightstone.com

ABSTRACT

Optic fibres for light transmission through concrete can be used to show live images on concrete surfaces. The technology has been developed by Dupont Lightstone for planar concrete screens. Using the technology on double curved surfaces involves a major challenge in achieving accurate fibre positioning and formwork rigidity maintaining fibres orthogonal to the surface during casting *and* allowing reasonable deforming. This paper describes the development of the next generation of optic fibre formwork featuring three and five axes robotic operations and finished cast items, which are used to evaluate the precision and feasibility of the technology.

Key words: Advanced formwork, Optic Fibres, Robotics, CAD, CAM, Concrete Surface, , Complex Shape, Double curved.

1. INTRODUCTION

The experiment described in this paper is pursuing to make concrete building show light driven live images on freely formed curved surfaces. It is building upon existing production technology based on DTI [1] and display technology developed by Dupont Lightstone [2]. The latter is based on metal sheets with two axis laser cut fixing holes for positioning of optic fibres. This technology can only produce planar surfaces, because in this only case the fibres are *parallel*. They have the same direction in which the formwork and the cast item can be removed from each other, referred to as 'deforming'. A soft formwork material seems to be an option, but cast in optic fibres must be positioned precisely and angled orthogonally to provide sufficient image quality, i.e. the formwork must be rigid enough to keep the optic fibres fixed in place and angle during casting. A curved cast concrete item have optic fibres pointing out into the formwork in

non-parallel directions (Fig. 3, middle) as a result of them being orthogonal to the curved surface geometry at the point, where they penetrate the surface. This results in a mechanical interlocking making non-destructive deforming impossible, requiring a new formwork technology delivering precision at a cost permitting destructive removal.

Six formwork concepts were developed, three was tested towards feasibility and one was chosen to be developed to full scale. This successfully resulted in two spheric concrete objects with approximately 3000 optic fibres embedded and evenly distributed.

2. MATERIALS AND METHODS

The development of the double curved concrete screen was broken down into three phases.

- 1) The image consist of pixels (the end of an optic fibre represents one pixel), so a pattern that is able to transfer the 2D-interface input to a 3D-surface output must be defined.
- 2) Produce 3Dformwork where a significantly large amount of optical fibres can be mounted efficiently, and be kept precisely fixed with a tolerance less than 1mm(position) and 2 degrees(angle) during the casting.
- 3) Define a concrete mix that envelopes the optical fibres without blocking the 10mm voids between them. The concrete must be self compacting and result in a bubble free surface.

In general for all three phases iterative methods were used for problem solving, qualitative methods was used to evaluate the appearance of the cast concrete surface and quantitative methods for evaluating the efficiency and precision of the process.

2.1 Pattern

First phase was solved with a triangular pattern. The interface consists of a circular plane with a 60 degrees grid of interface-pixels, with an equal distance. The concrete screen consists of the same triangular grid of surface pixels with varying angles and distances. The two grids are connected with optical fibres, so any optic fibre endpoint in the interface (interface-pixel) refers to the same optic fibre endpoint in the surface (surface-pixel).

Our triangular pattern offers 2D-3D connection but varies from traditional triangulation (also known as polygonal tessellation) by the limitation that the amount *and* position of triangles must be identical in the 2D interface as in the 3D surface, in order to obtain image correspondence.

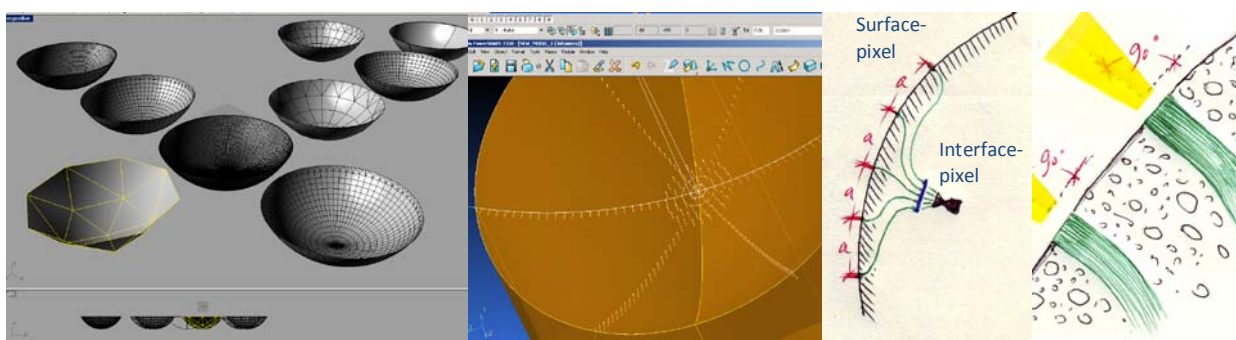


Figure 1 - Surface with experimental surfacepixel grids (left), final positioning and angle of the holes in the formwork (middle) and concept of orthogonally cast in fibres with equal dist. 'a'.

2.2 Formwork

The three formwork concepts tested were based on: a) Casting sand, b) Plastic sheet vacuum coated Expanded Polystyrene (EPS) and c) Epoxy resin coated EPS. The latter, c, was chosen

for full scale development. The form is manufactured removing material from the EPS with a 40mm ball nose milling tool and numerical controlled (NC) three axes operation. The milled form is coated and strengthened in 10mm depth with a thin penetrating epoxy resin. The coated formwork is reinstalled in the robot cell and carefully aligned according to the robots coordinate system, and a specially made tool with a diameter of slightly less than one millimetre, are drilling in the mounting holes for the optic fibres using NC five axes operations. 3000 optic fibres 1mm i diameter are manually inserted in the formwork and connected to the interface. One by one - specific surfacepixel corresponding to specific interfacepixel.



Figure 2 - Robot drilling holes(left), Optic fibres inserting (middle), Final formwork (right).

2.3 Concrete

A certified self levelling dry-mix mortar was chosen. Surface grinding and wet polishing was done manually with flexible rotating diamond discs (Roughness 60 for grinding, 120 and 200 for polishing).



Figure 3 - Casting(left), Cast screen before surface finishing (middle) - and after (right).

Distances between surfacepixels in the cast concrete item were measured with a flexible steel ruler (Fig. 4) and compared to respective distances in the digital model. Furthermore the alignment of surfacepixels is measured.

The polished concrete surface is visually evaluated in different light conditions and in wet and dry condition. The surface is soaked in water and when drying out micro cracks were identified.

3. RESULTS

The formwork produced proved to be rigid enough to control concrete and optic fibres during casting and yet relatively easy to remove after curing without damaging fibres and concrete.

The distances between the optic fibres corresponds with the distances defined in the CAD model within one millimetre, and the displacement from their average line is less than half a millimetre.



Figure 4 - Measuring(left), surface with unlighted fibres (middle) and light fibres (right)

The final surface appears smooth and delicate, and the micro cracks have no constructive implication and will not become visible due to the final hydrophobic surface treatment.

4. DISCUSSION, CONCLUSIONS AND OUTLOOK

Variations in measures and alignment appears to be randomly distributed to both sides of the reference, so it is concluded to derive from the interaction between the epoxy coatings uneven surface and flexibility of the drilling tool, rather than from CAD-CAM errors. The variations and micro cracks are not considered to represent a functional problem, so it is concluded that robot manufactured expanded polystyrene formwork can be made with a rigidity and precision enabling replacement of traditional metal sheet based formwork, and thereby provide hitherto unseen geometrical freedom for concrete surfaces with embedded optic fibres.

Due to the fact that the amount of surface pixels will grow exponentially with the size of the cast concrete surface [3], the manufacturing process embraces the need for project specific adjustments when going into architectural scale: Pixel size can be changed by altering the diameter of the fibre and of the drilling device. The amount of pixels and distance between them (dot pitch) can be changed in the Computer Aided Design (CAD). The formwork can be physically divided in Computer Aided Manufacturing (CAM) to enable fast manual mounting of optic fibres, because the final polish will insure a seem-less surface.

The manufacturing process (Fig. 2 and 3) combines digital and manual skills: CAD-CAM delivers spatial precision and the sensitive human hand delivers flexible, careful mounting within a narrow working envelope. With a few adjustments the demonstrated manufacturing process can deliver mass customization [4] for high end concrete building.

REFERENCES

1. Thrane, L.N., Andersen T.J., Mathiesen, D. "The use of robots and self-compacting concrete for unique concrete structures". *Tailor Made Concrete Structures* – Walraven & Stoelhorst (eds) © 2008 Taylor & Francis Group, London, ISBN 978-0-415-47535-8
2. Dupont, C. "Display system integrateable into a building structure", 2008 Patent nr. WO/2008/049432
3. Scheurer, F. "Size Matters: Digital Manufacturing in Architecture". *Dimension, 306090 Books, Vol 12* – © 2008 Princeton Architectural Press, New York, ISBN 978-0615182025
4. Jørgensen, T. R. "Arkitektur & Mass Customization" © 2007 Centre for Industrialized Architecture, The Royal Danish Academy of Fine Arts, School of Architecture. Copenhagen, ISBN: 978-87-7830-148-2

The Effect of Damage and Repair to carrying Capacity of a Bridge



Olli-Pekka Tynkkynen
M.Sc
Destia Oy
Heidehofintie 2
01300 Vantaa
olli-pekka.tynkkynen@destia.fi

ABSTRACT

Because of the age distribution of Finnish bridges and the growth of heavy traffic axle weights, bridge repair and strengthening are presently important issues in Finland. With a mandate from the Finnish Transport Agency we have carried out extensive research which aims to generate a concrete bridge repair design manual [1]. This manual covers structural repairs of reinforced concrete bridges and pre-stressed concrete bridges, as well as the challenge of widening bridges.

Key words: Concrete Bridges, Pre-stressed Bridges, repair, capacity.

1. INTRODUCTION

1.1 General

Three theses has been made as a part of this research, two of which have been made at Tampere University of Technology in Finland and one of which has been made in Sweden at Lund University on Technology. All theses were directed by Lic.Sc Torsten Lunabba from Destia.

One of the theses made in Finland is written by Eetu Väisänen and it deals with the issue of widening bridges. The other Finnish thesis is written by Olli-Pekka Tynkkynen and it deals with structural repair of reinforced concrete bridges. The Finnish theses have both been supervised by professor Ralf Lindberg. The Swedish thesis was written by Daniella Odendaal and it deals with structural repair of pre-stressed concrete bridges. This thesis has been supervised by professor Sven Thelandersson.

Problems which have been of particular interest are the effects of the bridge's own weight and hydration heat when new structurally functional concrete is cast alongside existing concrete.

1.2 Project Schedule

The first two master's work was launched in early 2009 and ware completed in late 2009. The last thesis began in the autumn of 2009 and was completed in early 2010. After finishing the thesis began the making of the actual guidance. At the moment guidance is under work and should be introduced during year 2011.

2. CONTENT OF THE GUIDANCE

Here is a summary of the content of the forthcoming manual:

2.1 The Strength of the old Concrete Structure

This chapter includes a short-simplified definition of how the strength of the old structure is defined. If the old concrete strength obtained from the drill samples exceed the original design strength at least 10% will the old design strength be used in carrying capacity calculations. If the measured strength of the concrete is between 95 and 110% of the original design strength should the concrete strength in calculations be reduced at 5Mpa. If the strength of the concrete is lower than 95% or if there are internal frost damage we should use lower design strength in calculations.

If the main steel parts are rusted we should reduce their calculative strength and tenacity. Corrosion rate will be evaluated according to regulations of the Finnish Transport Agency [2]. If the corrosion rate is 1 (hardly any corrosion) we can use the original strength and steel area. If the corrosion rate is 2, corrosion must be stopped and we can use max 95% of the steel area in calculations. If the corrosion rate is 3 or 4 steel surface area reduction should be evaluated case by case basis and the tenacity should be reduced. If the corrosion rate is 4 (which means heavy corrosion) the yielding ability must be evaluated as zero.

Capacity evaluation of the tendon cables goes roughly like with reinforcement. If the corrosion rate is 1 we can use the original strength and steel area. If the corrosion rate is 2, corrosion must be stopped and we can use max 90% of the steel area in calculations. If the corrosion rate is 3 or 4 steel surface area reduction should be evaluated case by case basis and the tenacity should be reduced. If the corrosion rate is 3 or 4 and the area of the cable is minimum 90% of the original, cable elongation is reduced to 10%. If the area of the cable is lower than 90% of the original the yielding ability must be evaluated as zero.

2.2 Effects of the hydration heat

When a massive casting is made can there be problems with the temperature difference between the inner parts of the structure and the surface of the structure. In the new guidance there will be charts which can be used to evaluate the temperature difference. The temperature difference must be limited to 15°C. The most important way to limit the temperature difference is to isolate the surface or protect it from wind. Isolation reduces the temperature difference but it hardly effects the maximum temperature of a massive casting.

While widening a bridge we sometimes cast massive parts directly onto the old structure. While the new concrete solidifies its temperature is usually much higher than the temperature of the old structure. For this reason there will be long term tension in the new structure and shear stress in the seam. These forces must be considered when designing the new part and its reinforcement.

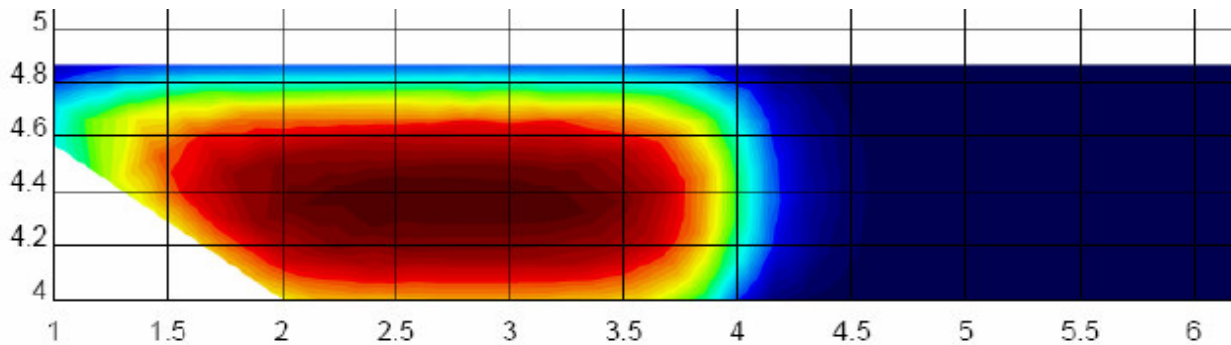


Figure 1 – Heat distribution in a widened bridge 24 hours after casting [3].

2.3 Load distribution between the old and the new structure

In a repaired structure forces are not distributed the same way as in the new structure. Repair technique affects a lot on how the forces are divided during and after the work. Sometimes a new concrete does not carry the load at all while sometimes it works just as effectively as the original concrete. Decisive factors are support during work, the age of the old concrete, creep of the old concrete and shrinkage in the old and new structure.

For example the case where new concrete is cast directly onto the old structure so that the holders are hanging from the old structure. In this case the weight of the structure will first go entirely to the old structure. New concrete will start to carry loads only after the old concrete creeps.

In the guide forces are distributed using load factors and effective elastic coefficients.

2.4 Repairing of a post-tensioned bridge

In her thesis Daniella Odendaal investigated repair of pre-stressed bridges. As a summary of the results we can say that when we are repairing a normal T-cross-section, the most critical parts are work time stress in the old concrete and long term tensile stress in the new concrete. The long-term tensile stress is caused by the cooling of hydration heat and new concrete shrinkage. Cable tension in the structure hardly decreases due to work.

REFERENCES

1. Finnish Transport Agency "Betonisiltojen korjaussuunnitteluohje" Not yet published
2. Finnish National Road Administration, "Raudoitteiden korroosioasteen määrittely" Helsinki, Finland, 2003
3. Väisänen E., Thesis "Sillan vaurioiden ja korjaamisen vaikutus kantavuuteen, sillan leventäminen". Tampere, Finland, September 2009 pp.65

Danish Expert Centre for constructions to the infrastructure

Mette Glavind
Centre Manager M.Sc., Ph.D.
Danish Technological Institute
Gregersensvej
DK – 2630 Taastrup
meg@teknologisk.dk

Henrik Stang
Professor, M.Sc., Ph.D.
Technical University of Denmark
Brovej, Building 118
DK-2800 Lyngby
hs@byg.dtu.dk

Claus Pade
Team leader, M.Sc.
Danish Technological Institute
Gregersensvej
DK – 2630 Taastrup
cpa@teknologisk.dk

Dorthe Mathiesen
Teamleder, B.Sc.
Danish Technological Institute
Gregersensvej
DK-2630 Taastrup
dma@teknologisk.dk

Henrik E. Sørensen
Teamleder, M.Sc., Ph.D.
Danish Technological Institute
Gregersensvej
DK-2630 Taastrup
hks@teknologisk.dk

ABSTRACT

In 2010 a new Expert Centre for constructions to the infrastructure was established. The Centre's activities are focused on durability aspects of reinforced concrete constructions exposed to severe environmental conditions, e.g. tunnels and bridges subjected to sea water, de-icing salts and freeze/thaw. The Centre is a close cooperation between Danish Technological Institute and Technical University of Denmark. The research initiated in 2010 include: Seawater affected long-term durability, models for chloride binding, the influence of casting defects and chloride threshold values. Examples of preliminary results of these are presented together with a gross list of new research to be initiated in the future.

Key words: Expert Centre, Durability, Infrastructure constructions, Chlorides.

1. INTRODUCTION TO THE EXPERT CENTRE

1.1 Background

In 2010 an expert centre for constructions to the infrastructure was established. The Center's activities are focused on durability aspect of reinforced concrete constructions exposed to severe environmental conditions, e.g. tunnels, bridges and off shore windmills subjected to sea water, de-icing salts and freeze/thaw. These structures are difficult and costly to construct and maintain. Denmark as well as other European countries face huge future challenges not only regarding the construction of new infrastructure, but also with respect to maintenance and repair

of the existing worn down infrastructure. It is estimated that the annual turnover in EU related to the physical infrastructure is around 0,3 trillion EURO, corresponding to 2-3 % of the GDP, [1].

1.2 Facts

The Expert Centre is based on a close cooperation between the Concrete Centre at Danish Technological Institute and the Department of Civil Engineering at the Technical University of Denmark. The aim is to combine and utilize complementary competences and laboratory facilities and to carry out collaborative PhD, post-doc and master projects.

A number of external cooperation partners are related to the expert center with an advisory role. These are the Femern Belt building owner, the Danish Road Directorate, Banedanmark, Metroselskabet, Cowi, Grontmij Carl Bro, RAMBØLL, MT Højgaard, Pihl, Aalborg Portland and Dansk Konstruktions og Betoninstitut A/S.

The Expert Centre is co-financed by the Danish Agency of Science, Technology and Innovation for 2½ years. It is the ambition is to continue the cooperation based on funding from EUs 7th and 8th framework programme after the national grant period. The Expert Centre will seek influence from an active participation in official EU lobby networks related to the infrastructure (current working title: Refine).

More information can be found in [2].

2. CURRENT RESEARCH TOPICS

The research initiated in 2010 include: Long-term durability of seawater affected concrete, models for chloride binding, determination of chloride threshold values and the influence of casting defects on durability. Examples of preliminary results of within these topics are presented.

2.1 Long-term durability of sea water exposed concrete structures

The aim of this project is to improve the understanding of the long-term durability of Danish sea water exposed concrete constructions made with different types of concrete by characterizing the microstructure of young as well as old concrete under the optical microscope and in the scanning electron microscope. Particularly, the effect of different binder combinations on the resistance to sulphate attack and chloride ingress is investigated.

Danish coastal bridges covering the period from 1930 when concrete was made with pure Portland cement to the Øresund Link completed in 2000 made with silica fume concrete and 3-powder concrete are investigated. Further, input from the Femern exposure site is included. Results will hopefully give valuable scientific input aiding the specification of concrete for future infrastructure constructions. This is illustrated in figure 1.

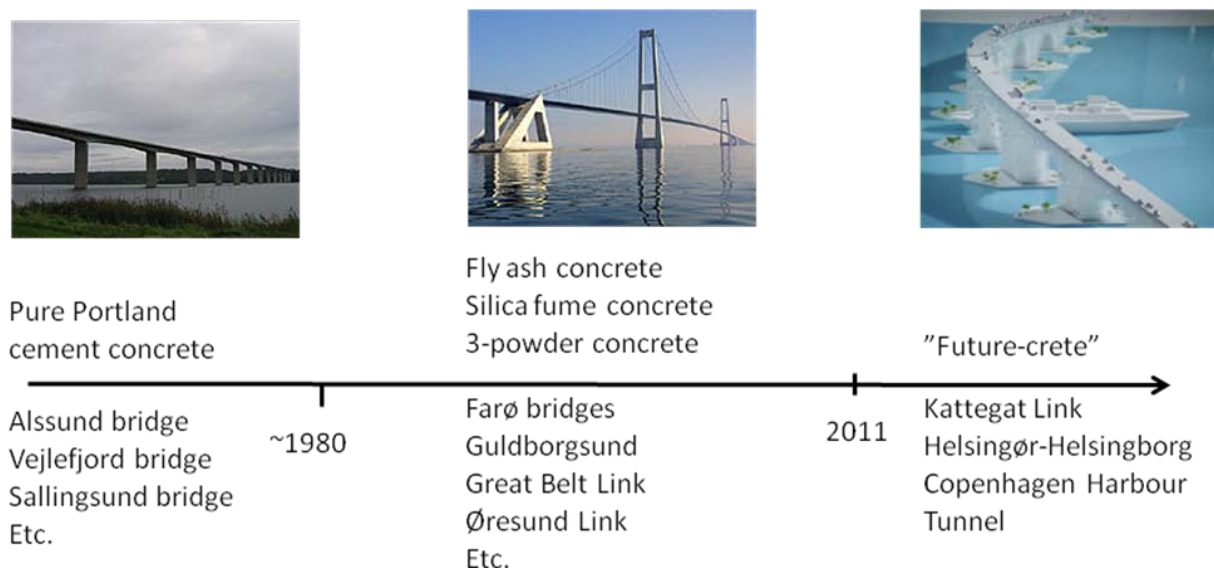


Figure 1 Development in binder combinations for Danish coastal bridges

2.2 Casting defects and unavoidable structural weaknesses

A testing programme has been initiated investigating the influence of casting defects and unavoidable structural weaknesses on durability, e.g.: Cold and "warm" casting joints, poker vibrator tracks and different types of reinforcements spacers. Test methods to evaluate the durability include: Petrographic analysis, chloride migration, frost resistance, tensile strength and rheological measurements.

Figure 2 shows a fluorescent impregnated plane section of a 2 hour old invisible "warm" SCC joint. Chloride migration results indicate that two layers of SCC can safely be cast on top of each other without creating something that has cold joint character.

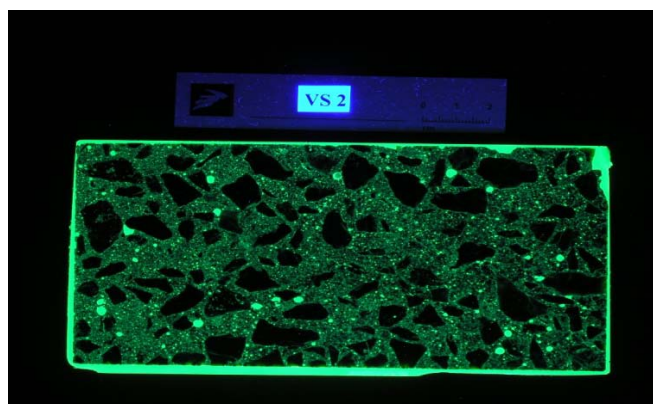


Figure 2 Fluorescent impregnated plane section of a 2 hour old "warm" SCC joint

Further, it is investigated how self compacting concrete (SCC) performs compared to slump concrete. Preliminary results show that it is necessary to be able to mix the SCC with a variation in water content of less than $\pm 5 \text{ l/m}^3$ in order to be able to obtain acceptable small variations in rheology.

2.3 Chloride binding and chloride threshold levels

This is a major research topic within the Expert Centre where the primary aim is to develop models for chloride binding, i.e. where in the microstructure the chlorides are bound and which parameters affect the chloride binding and how the binding affects the chloride threshold levels. A literature survey shows that the chloride ingress in concrete is more complicated than presently known. The starting hypothesis for the work is that the chlorides are bound in the inner hydration product which has been observed in SEM-EDX analyses.

Another aim of this research is to get a better understanding of the parameters governing the chloride threshold levels, so that as a minimum result concrete with different binder compositions can be ranked and as an ultimate vision absolute figures can be measured and/or estimated. Part of the work is to develop a new test set up taking all important parameters into account. The work will take its basis in e.g. the RILEM group working with this subject.

A PhD at Technical University of Denmark as well as approximately 2 VIPs at Danish Technological Institute will focus on this research subject the coming years.

3. GROSS LIST OF RESEARCH TOPICS

A gross list of other research topics has been prepared and discussed with the external reference group. From this list new research topics are to be selected and research initiated. This is at the time of writing in process, but the list below shows the most probable projects to be initiated in 2011.

- Models for cracks, including understanding damage formation in and through the interface between reinforcement and concrete. This will be carried out by a PhD and a Post Doc .
- Numerical service life models based on chloride driven reinforcement corrosion.
- Influence of hardening temperature on the development of durability properties and input parameters for hardening simulations based on new binder types.
- The effect of micro defects/cracks on carbonation, chloride and sulphate ingress.
- Initial development of service life models.

REFERENCES

1. "Building Up Infrastructure Networks of a Sustainable Europe, Initiative of European Construction, Technology Platform, refine, www.ectp.org.
2. www.concreteexpertcentre.com.

New Innovations in Finnish Prestressed Concrete Production



Eeva Kaataja
M.Sc., Project Engineer
Parma Oy
Mäkrinteentie 19,
FI - 36220 Kangasala
eeva.kaataja@parma.fi



Juha Rämö
M.Sc., Design Director
Parma Oy
Hiidenmäentie 20,
FI - 03101 Nummela
juha.ramo@parma.fi

ABSTRACT

Steel reinforced concrete piles are widely known and used in the world. Problems related to their shortness and brittleness in handling, have created a need for more durable and longer piles. Compared to precast concrete piles, the cable duct is a quite similar concrete product, which has problems in usability.

Extrusion technique enables to manufacture prestressed concrete piles with hollow cores. With this new production technology for prestressed piles and cable ducts almost the same machinery as in the hollow core slab production can be utilized. New piles and cable ducts are more durable and longer, and in addition, the amount of concrete and steel can be reduced.

Key words: prestressed, precast, pile, cable duct

1. INTRODUCTION

In construction technology piles are used in the foundations of buildings and infra structures. When soil is not suitable for construction purposes, piles are used to transfer loads from the surface layer deeper into a denser soil layer. Parma Oy is a Finnish company specialized in design, production and supply of prefabricated concrete elements. The company belongs to Consolis Group. In collaboration with Consolis, Parma invests in research and development. The company has launched on the market two new products based on prestressed, extrusion technique in production. The first is a prestressed concrete pile (*Figure 1*) and the second a prestressed concrete cable duct which is an application of the new pile (*Figure 2*).

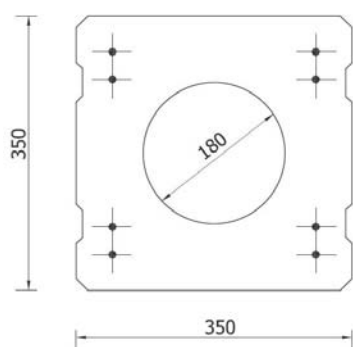


Figure 1. The cross section of Parma prestressed concrete pile, 350mm x 350mm. The diameter of the hollow core is 180 mm.

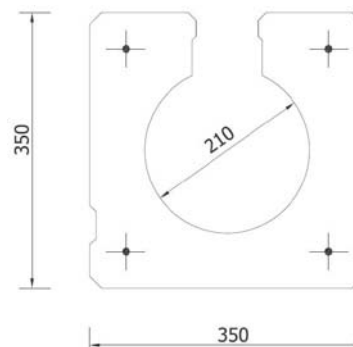


Figure 2. The cross section of Parma prestressed cable duct, 350mm x 350mm. The diameter of the hollow core is 180mm.

2. HISTORY

Prestressed concrete piles are not totally new in Finland. There used to be prestressed concrete pile production in Finland from the 1950s to the early 1970s when piles were cast in moulds and prestressed. One specific reason, why the production was ceased in the 1970s, was not given but some technical problems in the production were named as well as breaking problems during assembly.

Concrete piles are widely known and used in many countries, especially in the United States where prestressed concrete pile production has continued from the 1950s until today. [1]

3. TRADITIONAL AND NEW PILES

3.1 Traditional piles

In Finland the piles are usually either reinforced precast concrete piles or steel piles.

Reinforced precast concrete piles are quite fragile to handle and due to low resistance to tensile strength the bearing capacity of concrete piles needs to be reduced. The impact during pile driving causes tension forces in the pile when an impact wave reflects from the bottom end of the pile back upwards. [1]

The length of precast piles is normally limited to 15 metres and thus time-consuming pile joints are necessary.

3.2 Benefits of prestressed and extruded concrete piles

The new prestressed concrete piles are manufactured by the extrusion technique on the same casting line as hollow core slabs. The extrusion technique enables better use of material. The pile has a hollow core and therefore it is lighter in weight than the traditional pile. In addition, the straightness and unity may be checked after assembly.

The size of the first application of Parma prestressed concrete pile is 350mm x 350mm and the diameter of the hollow core is 180mm. The maximum length of the new pile is 20m.

The main advantages of the new production technology in the pile production are that almost the same machinery as in the hollow core production can be utilized and a large production volume is enabled (*Figure 3*). The start-up investments of the prestressed concrete pile production are low due to existing facilities at hollow core slab factories. Thanks to the manufacturing technique also the cement content in concrete can be reduced, which decreases material costs. The production method is fast, cost-effective and thanks to the extrusion technique, the quality of products is very good.



Figure 3.
The prestressed pile production.



Figure 4.
Prestressed piles in construction site.

The main properties of prestressed concrete piles are durability, stiffness and high resistance to cracking. The concrete strength class is C55 for the new pile. The prestressing force has been specified to avoid tension stresses during handling and piling. The steel strands in piles are symmetrically stressed. [2]

The increase in bearing capacity reduces the amount of required piles. Additional cost benefit can be achieved through longer piles and decreased amount of pile joints. When pile joints can be avoided, the piling is faster to accomplish, and the installation costs are lower.

3.3 Tests and first pilot project

A number of studies and tests were carried out in co-operation with the Tampere University of Technology (TUT) during the years 2007-2010. Some test pile driving and pile driving analysis were performed as well as some impact tests and tests according to the standard SFS-EN 129764 +A1. After these tests the same piles were in bending and shearing strength tests. Using the test

results, the TUT has specified capacity graphs and calculations according to Eurocode and National Standard. According to these tests and calculations, the highest permissible axial compression capacity in serviceability limit state for the 350mm x 350mm pile is 1105 kN. [2] Correspondingly the permissible axial compressive stress is 11,6 MPa for the 350mm x 350mm pile. [3] That signifies that the capacity-cost ratio is much higher in comparison with traditional concrete piles.

The first full-scale pilot project of 75 piles was delivered and piling was performed successfully in December 2010 (*Figure 4*).

3.4 Ongoing research and development

The manufacturing technique for the pile joints and rock points in extrude production have been developed and tested. At the moment, the patent for these methods is pending. In addition, the design of smaller cross sections for prestressed concrete piles is under development. Moreover, the CE mark is pending for the prestressed concrete pile.

One possibility to utilize the hollow core in the pile is to install geothermal pipes inside the hollow core. This has been tested once, but no actual customer projects have been executed yet.

4. CABLE DUCT

Compared to concrete piles, cable duct is a quite similar precast concrete product. The contractors have expressed a wish for a more durable element as well as lighter concrete covers which are needed for manual installation. An application of the prestressed pile was invented with an open gap of 80mm on top of the product and a covering strip, which is made of a lightweight material and is easy to install. A “running over” -test was performed by a wheel loader and no damage was discovered in the cable duct after the test. Also the products were tested in a test site in southern Finland in October 2009 when 19 cable ducts 6 metres in length were installed along the railway. [4]

After these accepted tests, the Finnish Transport Agency granted a licence for the prestressed cable duct to be used along the railways. [5]

REFERENCES

1. Kerokoski, O., “Jännitetyt betonipaalut - esiselvitys,” Tampere University of Technology, Earth and Foundation Structures, Tampere 2007, 67 pp.
2. ”Parman ecopaalut, Suunnittelu- ja asennusohje,” Parma Oy, 7.9.2010, 12pp.
3. Kerokoski, O., ” Jännitetty betonipaalu, sallittu aksiaalinen kuorma, laskelma,” Tampere University of Technology, Department of Civil Engineering, Tampere 10.6.2010, 2pp.
4. Nieminen, J., “Kirkkonummi-Karjaa-rataosalla tehtävä kaapelikanavaelementtitestaus,” The Finnish Transport Agency, Rail Department, 8.12.2009, 6 pp.
5. Viitala, T., “Esijännitetty ja liukuvalettu betoninen kaapelikanavajärjestelmä,” The Finnish Transport Agency, Rail Department, Dnro 4857/1043/2010, 6.9.2010, 3pp.

Effect of temperatures on the accelerated curing of concrete



Ganesh Babu. K
Professor
Dept. of Ocean Engineering
IIT Madras, Chennai - 600036
kgbabu18@yahoo.com



Chandra Sekhar B
Research Scholar
Dept. of Ocean Engineering
IIT Madras, Chennai - 600036
sekharbhojaraju@gmail.com



Durga Prasad R
Research Scholar
Dept. of Ocean Engineering
IIT Madras, Chennai - 600036
durgakind@gmail.com

ABSTRACT

The increased pace of construction activities necessitated methods for assessing the quality of concrete almost immediately so that effective correction can be made before it is too late. The present effort is to bring together all this information along with the experimental investigations and correlate the various options available, their relative advantages and disadvantages towards a reliable establishment of the accelerated concrete testing.

Key words: Concrete, Temperature effects, Accelerated curing, Quality control.

1. INTRODUCTION

1.1 General

The traditional 28 day strength of the concrete is still being used to define the quality of the concrete and its performance. However, it is now well understood that the quality of concrete cannot be defined by this simple compressive strength alone, even accepting that the compressive strength in itself is a good measure of the quality of the concrete, with specific recommendations towards the materials like cement and aggregates, the water-cement ratio and workability, the compaction procedures etc. It is necessary to evaluate the strength at the earliest possible time for an appropriate correction, if required. Such an evaluation will not only provide guidance for construction process but will also aid in predicting the long term behavior.

There have been several attempts to assess the 28 day compressive strength of concrete through accelerated curing methods for a long time. The fundamental principle in most of these attempts is to look at either a direct comparison of the 28 day strength with a specified accelerated curing procedure or to look for a more general methodology like the maturity concept. The first type has been favoured to a large extent by the industry and field practitioners. One main advantage of this is that it helps to calibrate the concretes for a specific application, may be even a ready mixing plant. In principle the relationships are project specific and over a period of time have led to certain direct equations.

Exhaustive literature survey shows that there have been several researchers who have worked in this particular area and some of these have led to the various existing national provisions. This paper tries to bring some coherence to the results available in literature and compare the same with the laboratory experimental results. Finally the paper attempts to recommend a simple and viable methodology for field practice.

2. ACCELERATED CURING

2.1 Literature survey

Saul [1] suggested that the combined effect of time and temperature on the hardening process is related to the strength development of concrete. He also stated that relatively good results can be obtained when the specimen was steam cured at 100⁰C using a moderate rate of temperature rise. AL Rawi [2] observed a significant increase in the one day compressive strength when the curing temperature increased from 50⁰C-70⁰C, but there was no significant variation found for the range 70⁰C-90⁰C. Yokomichi [3] did not obtain a significant increase in the 1 day strength when the curing temperature was increased from 60⁰C to 80⁰C. Higginson [4] stated that the 28 day strength of concretes steam cured at 71⁰C or steam cured at 54⁰C was about the same.

2.2 National Provisions

Of the many national standards available, the provisions in the American [5], British [6], and the Indian [7] standards, which practically encompass almost all the other national provisions are discussed in the present paper. Table 1 presents a comprehensive overview of the different provisions in the above codes. These concrete standards suggest methodologies which can be used to provide an indication of the 28-day strength of concrete after about 24 hours itself. ASTM C 684 presents four methods in which the accelerated curing is attempted by just ensuring that the concrete cures by either its own heat of hydration or by thermal acceleration. The warm water method is said to be in principle a procedure to preserve the heat of hydration. However, it is necessary to keep the specimen in a water bath at 35⁰C for a period of almost 24 long hours. A similar approach of conserving the heat of hydration by insulation for almost 48 hours from the time of casting is required in autogenous curing. Knowing the fact that temperatures inside a concrete mass can reach almost 70⁰C or even higher through heat of hydration the above statements do not appear to be appropriate. The high temperature and pressure method is more sophisticated and requires specific expertise and equipment. Lastly, the boiling water method which uses an already set concrete specimen to be exposed to boiling water for a relatively brief period of 3.5 hours appears to be the most practicable. The British standards utilize curing temperatures of 35, 55 and 82⁰C with the corresponding acceleration periods of 24, 20 and 14 hours. The earlier discussions regarding the difficulties associated with maintaining the above temperature over the relatively long period required compared to the boiling water method of ASTM appears to be applicable here also. Finally the Indian standard specifications appeared to be a mix of both, with the warm water method being at 55⁰C for a period of 20 hours, similar to the BS code and boiling water method for a period of 3.5 hours as in the ASTM.

3 EXPERIMENTAL INVESTIGATIONS

Concrete mixtures designed for compressive strengths varying from 20-70 MPa (at 25 – 50 mm slump) were studied at temperatures of 27⁰C (laboratory), 55⁰C and 100⁰C. It is to be

emphasized that these concretes were not modulated to achieve the highest strength possible through the utilization of either higher strength cements or optimal packing of aggregate through specific grading.

4 RESULTS AND DISCUSSIONS

Figure 1 presents the strength results of the above concretes after different time periods of acceleration at 55⁰C. Figure 2 is a presentation of the variations in the strengths of the above concretes at the two accelerated strength methodologies in the Indian standards (one similar to the British and the other similar to the American), at 55⁰C and 100⁰C. To have a relative comparison the 28 day strength values at the laboratory temperature of 27⁰C were also presented in the same figure. The compressive strength variations of different cements with age after an accelerated curing at a temperature of 70⁰C were studied by Al Rawi (8) earlier. Figure 3 presents these strength variations in a graph similar to the earlier ones. All these figures show a trend similar to the normal water cement ratio to the strength relationship presented. The variation of the relative compressive strength (relative to the strength at 0.5 water cement ratio) with water cement ratio for the different concretes at the different temperatures (Figure 4) clearly shows barring the minor variation the relationship could be nearly unique, defined by the equation :

$$[f_{28} / f_{28(0.5)}] = 0.40[w/c]^{-1.334}$$

Also, from Figure 4 it can be seen that the relative strength estimate by using this relation is almost the same as the strength estimate at 70⁰C, while the similar estimates at the 55⁰C and 100⁰C are overestimated and underestimated respectively, as was also observed by a few other researchers in the earlier studies.

Table 1 – Specifications for the accelerated curing of concrete based various national provisions

National standard	Test method	Curing medium	Curing		Age at test
			Start (after casting)	Duration / temperature	
ASTM C684-99 (2003) (20-30 ⁰ c)	Warm water	Hot water	Immediate	23.5 h ± 0.5h (35 ± 3 ⁰ C)	24 h ± 0.25h
	Boiling water	Boiling water	23h ± 0.5h	3.5 h ± 0.08h (100 ⁰ C)	28.5 h ± 0.25h
	Autogenous	Heat of Hydration	Immediate	48 h ± 0.25h (45 ± 4 ⁰ C)	49 h ± 0.25h
	Autoclaving	Steam and pressure	Immediate	5 h ± 0.08h (149 ⁰ C)	5.25 h ± 0.08h
BS 1881: Part 112: 1983 (20 ± 2 ⁰ c)	35 ⁰ C method	Insulating water	Immediate	24 h ± 0.25h (35 ± 2 ⁰ C)	25 h ± 0.25h
	55 ⁰ C method	Heating by water	1.5 h	19 h 50 m ± 0.33h (55 ± 2 ⁰ C)	22 h 30 m ± 0.25h
	82 ⁰ C method	Heating by water	1 h	14 h ± 0.25h (82 ± 2 ⁰ C)	16 h ± 0.25h
IS:9013 - 1978 (27 ± 2 ⁰ c)	Warm water	Heating by water	1.5 h to 3.5 h	19 h 50 m (55 ± 2 ⁰ C)	22 h 50 m
	Boiling water	Heating by water	23 h ± 0.25h	3.5 h ± 0.25h (100 ± 3 ⁰ C)	29.5 h ± 0.25h

5 CONCLUSIONS

The investigations clearly reveal the fact that the accelerated curing of concrete resulted in the strength to water cement ratio relations similar to the normal curing results. There is a lot of variation in the strengths of concrete specimens cured at the different temperatures in an accelerated curing process. It was observed that the relative strength estimate by using this relation is almost the same as the strength estimate at 70°C, while the similar estimates at the 55°C and 100°C are overestimated and underestimated respectively, while these were nearly the same at a curing temperature of 70°C, as was also observed by a few other researchers in the earlier studies. However, the strengths looking at the simplicity of maintaining the bath temperature at 100°C the boiling water method is more suitable for field applications.

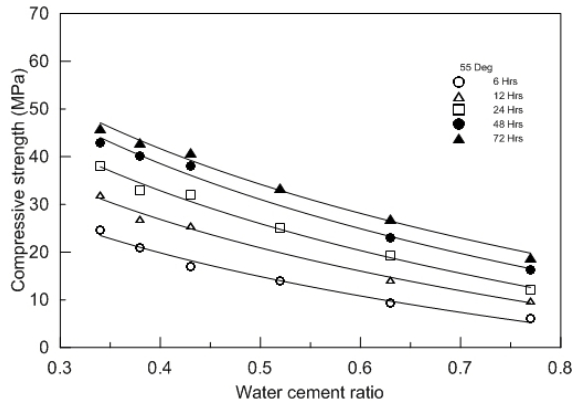


Figure 1- Strength variation with age (55°C)

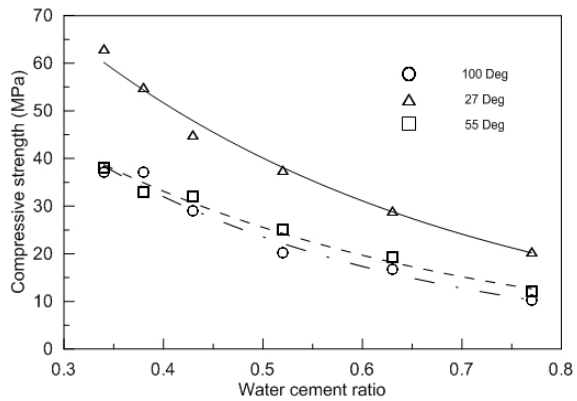


Figure 2- Strength variation at with temperature

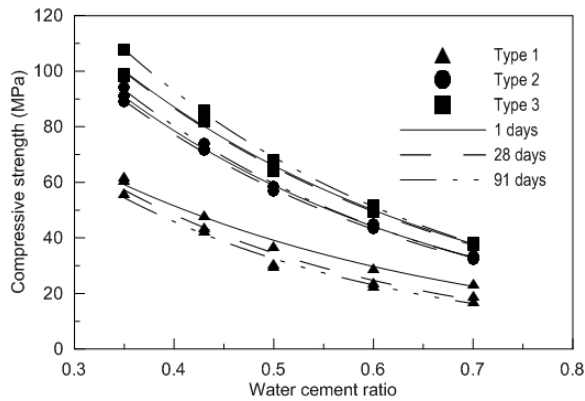


Figure 3- Strength variations with age for different cements at 70°C (8)

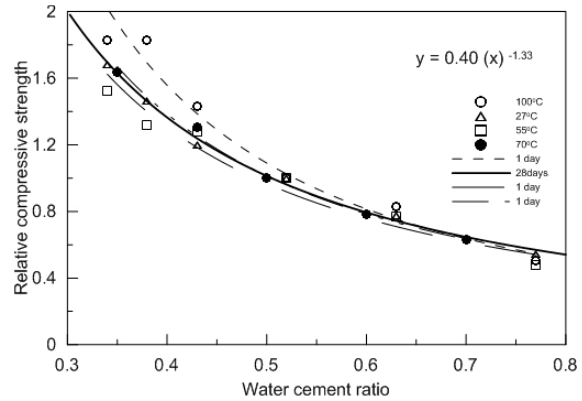


Figure 4- Relative strength variation at different temperatures

REFERENCES

1. Saul.A.G.A., Magazine of Concrete. Res. 2, 27 (1951).
2. Al-Rawi R. S., Cement and Concrete Research, Vol.6, pp. 603-612, 1976.
3. Yokomichi.H and Hayashi.M., RILEM Bull. Vol 3, pp. 309 (1966).
4. Higginson.E.C., J. American. Concrete. Institute. 5_88, 281 (1961).s
5. ----ASTM C 684 – 99 (2003), ASTM International.
6. ----BS 1881: Part 112: 1983, British Standards Institution, 1983.
7. ----IS: 9013 – 1978, (December 1998), Bureau of Indian standards.
8. Al-Rawi R. S., Cement and Concrete Research, Vol.7, pp. 312-322, 1977.

Session B5 – USE OF FIBRES

Ductile High Tensile Strength Concrete



Terje Kanstad
 Professor
 COIN
 Department of Structural Engineering, NTNU
 NO-7465 Trondheim
 E-mail: terje.kanstad@ntnu.no



Sindre Sandbakk
 M.Sc.
 COIN
 SINTEF Building and Infrastructure
 NO-7465 Trondheim
 E-mail: sindre.sandbakk@sintef.no

ABSTRACT

During the first 4 years of COIN, several fibre reinforced concrete research activities have been carried out within the three sub-projects: (1)Materials development, (2)Guidelines for design, execution and control and (3)Field and full scale laboratory testing. Both synthetic and steel fibres have been used in several concrete types ranging from superlight concretes with compressive strength as low as 3MPa to high performance concrete with 120 MPa compressive strength. A proposal for Norwegian design-guidelines is made, and much effort has been paid to test method investigations. The full scale tests include amongst others prefabricated beams in lightweight and ordinary concrete, beams with simplified reinforcement layout, hybrid concrete beams, and post-tensioned flat slabs.

Key words: Concrete, steel fibre, synthetic fibre, design, test methods, load carrying structures

1. INTRODUCTION AND OBJECTIVE

The project includes the fibre reinforced concrete activities within the Norwegian centre of research based innovation, COIN, and has the following major objectives: (1)To do R&D work which stimulates and makes use of fibres possible in load carrying concrete structures. (2) Further development and verification of ductile high tensile strength concrete with target tensile strength: 15MPa. The research partners are SINTEF and NTNU, while Veidekke, Consolis, Unicon, Rescon-Mapei, St Gobain Weber and the Norwegian directorate of roads are involved industrial partners.

The following three sub-projects are established: (A) Materials development, incl. fibre type investigations and performance of structures to achieve the target concrete. (B) Guidelines for design and execution, and (C) Field - and full scale laboratory testing.

2. MATERIALS DEVELOPMENT

A major task so far has been to map the properties of various fibre and concrete types, as basis for further development and improvement of the fibre concrete technology. Synergies between fibre reinforcement and self compacting concrete (SCC) were clearly shown several years ago [1], and therefore SCC is given high priority. So far focus has been towards concrete for ordinary construction projects, which means that UHPC not has been a prioritized topic. Despite for this, materials with residual bending strengths as large as 17 MPa has been made using ordinary part materials and steel fibre content in the range 2-3 volume % (160-240 kg/m³). In this material even a 3 meter long model of the famous Leonardo da Vinci bridge has been built.

Some typical results from uniaxial tensile strength testing of a lightweight aggregate concrete (self-weight 1100kg/m³ and compressive cylinder strength about 20 N/mm²) are presented in Figure 1a) and b). It is experienced that steel fibre volumes of this size increase the tensile strength several times, while synthetic fibres do not have this effect at all. Furthermore it has been shown that even moderate amounts of both fibre types improves the quality of LWAC considerably regarding residual tensile strength, ductility in compression and tension, and bond between ordinary reinforcement and concrete. Another experience is that steel fibres give more than two times larger residual strength than synthetic fibres when mixes with the same fibre volume are compared [2].

Figure 1 c) shows results from three-point bending tests (NS-EN 14651) of a relatively low-strength SCC made to achieve FRC with high ductility [3]. It is interesting to observe that the combination of 0,5% synthetic and 0,5% steel fibres gave a rather good ductility and a residual strength at 2,5 mm crackwidth close to the concrete with 1,0% steel fibres only.

3. GUIDELINES FOR DESIGN, EXECUTION AND CONTROL

The guideline proposal is published as a COIN-report [4], and covers the following topics: Material related topics for concrete and fibres, test methods, verification and execution, design methods, and reinforcing rules. Ongoing activities are establishment of relations between the most common test methods for the residual strength [5], test method investigations for characterization of the fresh concrete properties, and verification of the shear design formula and the crack-width rules.

The guidelines hold for both ordinary concrete and SCC, and are written for application of both synthetic and steel fibres. The basic design material property is the residual tensile strength which should be determined from the three-point bending test described in NS-EN14651. Alternative methods might be used, but then their relation to the NS-EN14651 test should be known. A test regime for the concrete producer's verification of residual strength class is specified, and furthermore procedures for control of fibre content at the building sites are described. The rules are prepared for consideration of different fibre orientation in the standard test method specimens and the real concrete structures.

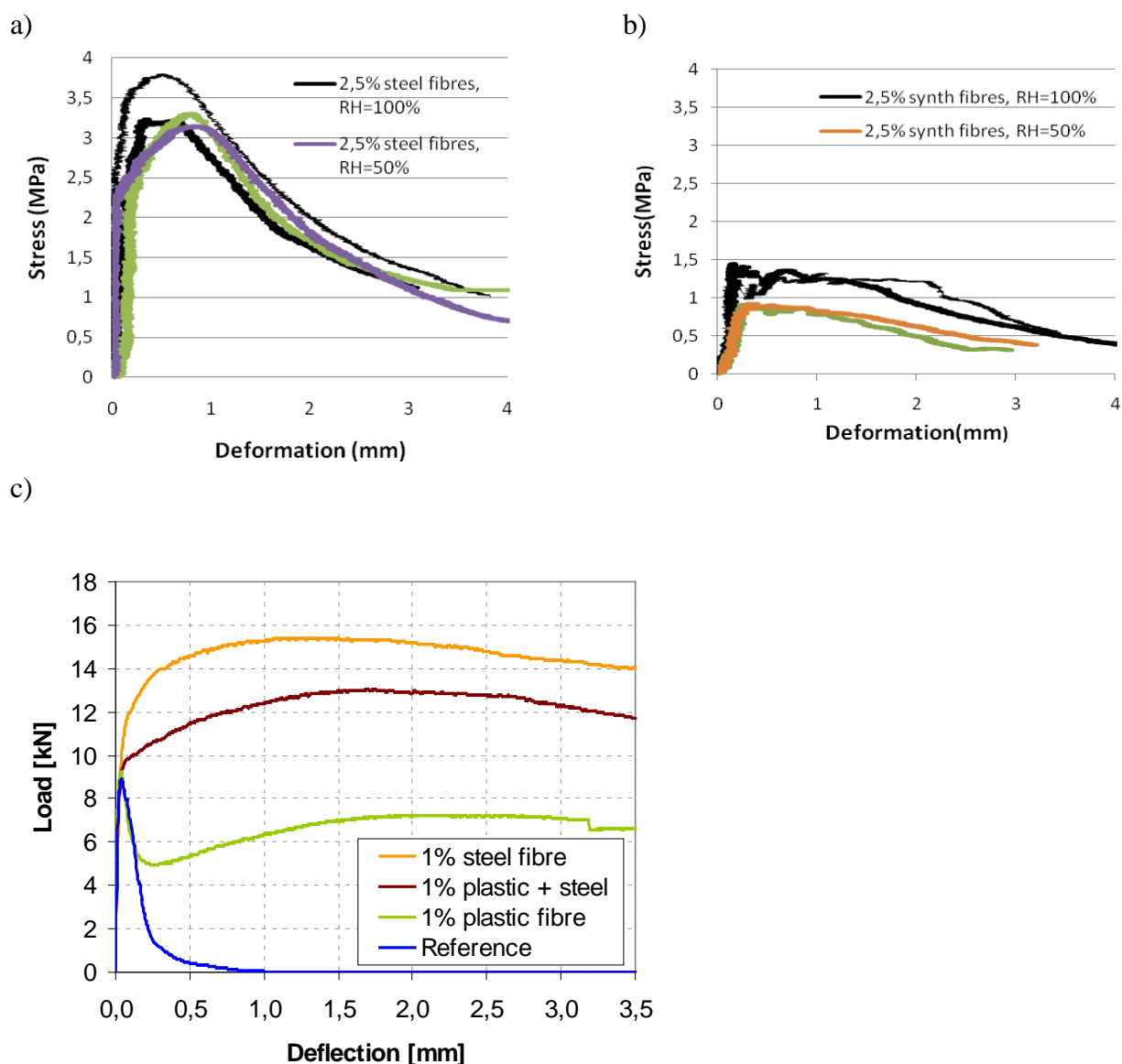


Figure 1: a) Typical results from uniaxial tensile tests of various Lightweight aggregate(LWAC) concrete specimens. 2,5% end hooked steel fibres, (b) Typical results from uniaxial tensile tests of various LWAC specimens. 2,5% synthetic fibres (embossed surface), (c) Results from three-point bending tests (EN14651) of low strength self compacting concrete (B20, $d_{max}=8mm$)

4. FIELD - AND FULL SCALE LABORATORY TESTING

The field test project includes a series of full scale post-tensioned and fibre reinforced flat slabs, walls and slabs cast on construction sites, several series of slab and beam elements cast in the laboratory, and precast beam elements cast in both lightweight and ordinary concrete. As part of the evaluation of the results, control of the fibre content in the critical sections have been carried out, and one major observation is that while the fibre content seems to have rather small variations in the structures, the variations in fibre orientation within the structures may be rather large, and probably the main explanation of the large scatter we often observe in test results for fibre reinforced concrete structural elements. This is also the reason why the present guideline proposal is prepared for taking fibre orientation deviating from isotropic conditions into account.

In a beam series made by LWAC (1100 kg/m³) without fibres, the failure typically started as an anchorage failure with a major horizontal crack at the height of the ordinary tensile reinforcement in the shear span and towards the support. It was shown that both synthetic and steel fibres improved the bond strength and the tensile robustness significantly so the anchorage failure type did not occur in any of the fibre reinforced beams. For these beams the final failure instead was moment or shear failure after comprehensive diagonal cracking.

Within the PhD-project of Grepstad [6] hybrid concrete beams made by combinations of ordinary concrete and lightweight aggregate concrete are tested, and both materials are fibre reinforced to improve their strength and ductility.

Finally, it should be mentioned that control of fibre content in the fresh concrete, at the building sites, is an important topic which the contractor and COIN-partner Veidekke has paid much attention to [7].

ACKNOWLEDGEMENTS

The paper is based on the work performed in COIN - Concrete Innovation Centre (www.coinweb.no) - which is a Centre for Research based Innovation, initiated by the Research Council of Norway (RCN) in 2006. The Centre is directed by SINTEF, with NTNU as a research partners and with the present industrial partners: Aker Solutions, Norcem, Norwegian Public Roads Administration, Rescon Mapei, Skanska, Spenncon, Unicon, Veidekke and Weber Saint Gobain.

REFERENCES

- 1 Døssland, Å.L. Fibre Reinforcement in Load Carrying Concrete Structures. Doctoral Thesis. Department of Structural Engineering, NTNU 2008:50. Trondheim, Norway.
- 2 Kanstad, T. (2009) Fibre Reinforced Superlight Concrete: Testing of Materials and Full Scale Beams. SINTEF Building and Infrastructure 2009 (ISBN 978-82-536-1122-8)
- 3 Vikan, H., Sandbakk, S. and Kanstad, T. Residual bending strength of concretes with variable content of two different fibre types. COIN-report, 2011
- 4 Kanstad, T. et al. Proposal for Norwegian Guidelines for Design, Execution and Control of Fibre Reinforced Concrete. COIN-report, 2011
- 5 Sandbakk, S. and Kanstad, T. Panel- and Beam testing of Fibre Reinforced Concrete. Proceedings of the XXI Nordic concrete research symposium, Helsinki, June 2011.
- 6 Nes, L.G, Øverli, J.A. Hybrid Concrete Beams. Proceedings of the XXI Nordic concrete research symposium, Helsinki, June 2011.
- 7 Nikolaisen, E.B. Fibre content in fresh concrete at building sites. Master thesis , UMB Ås, Norway, June 2010. (In Norwegian).

Panel- and Beam testing of Fibre Reinforced Concrete



Sindre Sandbakk
M.Sc., Ph.D. fellow
SINTEF Byggforsk
Richard Birkelandsvei 3
NO - 7465 Trondheim
sindre.sandbakk@sintef.no



Terje Kanstad
Ph.D, Professor
Department for Structural
Engineering, NTNU
NO - 7491 Trondheim
terje.kanstad@ntnu.no

ABSTRACT

Beam- and panel tests on fibre reinforced concrete specimens have been performed according to different codes to investigate whether it is possible to establish relations between the different test methods. The most important findings are that it seems possible to establish such relations, and that moderate amounts of fibre reinforcement may have the same resistance to bending as the required minimum reinforcement according to Eurocode 2.

Key words: Fibre reinforced concrete, beam tests, panel tests, flexural residual tensile strength.

1. INTRODUCTION

Within the COIN project, experimental and theoretical work has been carried out in order to understand in which way the results from panel tests and beam tests performed according to different codes may be compared. Circular panels with diameter 600 mm and 800 mm, and thickness 75 mm and 100 mm have been tested according to the Norwegian Concrete Association Publication nr 7 (NB7) and a method quite similar to ASTM C 1550. The only difference was that the supports were allowed to slide outwards together with the panel, while ASTM C 1550 describes that the panel shall slide on the support [1]. Beams have been tested according to NS-EN 14651 and the Norwegian Sawn Beam Test (NSBT) method, a method which deviates from NS-EN 14488-3 only by the dimension of the beams. This work shows that when the test results are analyzed as *flexural bending stress vs. crack mouth opening displacement* (CMOD) it is possible to establish relations between the different test methods.

2. CALCULATIONS

If the moment capacity of a beam or a slab is known, and by using stress distributions based on the theory of linear elasticity, it is straightforward to calculate the residual flexural tensile strength, $f_{R,j}$ at different deformation stages [3]. For beams, the relationship between applied load and bending moment is easy to calculate, and even described in NS-EN 14651 for beams

tested according to this code [3]. For panel tests, however, the relationship between a centrally located point load and the bending moment is more complicated. As shown by Johansen [4] it is possible to calculate the moment capacity for slabs using yield line theory. Furthermore, by counting the number of cracks in a panel after testing, it is possible to calculate the moment capacity per unit length of cracks, and finally the residual flexural tensile strength can be calculated also from panel testing.

Panels tested according to the ASTM 1550 with three supports shall at least have three cracks; otherwise the panel shall be discarded [1]. To calculate the relationship between the CMOD and the deflection, δ , it is assumed that the panel sectors are of equal size and that they move as rigid bodies, with a contact point between the sectors at the top surface. Similar assumptions are used by Bernard & Xu in calculation of crack widths in these panels, and they have shown that their rigid plate model slightly overestimates the crack widths compared to experiments, and that the crack widths at large deflections are wider near the centre and more narrow near the edge of the panel than predicted by the rigid plate model [5]. Another point is, as reported by Sandbakk et al [6], that the crack growth is not equal in all cracks in a panel test according to ASTM C 1550. However, if the abovementioned model is used to calculate the CMOD from the deflection, it is anyway quite close to the measured value. Panels tested at continuous support, as described in NB7 [7] and NS-EN 14488-5 [8], normally crack in four or more sectors. Also for these panels the assumption of equally sized sectors and rigid body movement has been used.

The relationship between deflection and CMOD for beams tested according to NS-EN 14651 is described in the code [3]. The CMOD vs. deflection relationship for the results shown in this paper is found by the same assumption as for the panels, namely a contact point at the top of the beam and rigid body movement and therefore not exactly as described in NS-EN 14651. This is done to calculate the CMOD for beams and panels as similarly as possible. For beams tested in four-point bending, similar to the description in NS-EN 14488-3 [9], the crack offset from the mid section will influence the relationship between CMOD and deflection, as described by Bernard et al [10]. This effect is included for the beams tested according to the NSBT-method.

3 RESULTS

The results from the panel tests presented in Figure 1 a) and b) and the beam tests presented in Figure 1 c) are from a test series performed in 2008, and all panels are made with the same concrete mix design. One important result from both panel test methods is that the panel dimension has no significant effect on the flexural tensile stress vs. CMOD relationship, a matter that also may be shown analytically. Bjøntegaard [11] has shown that the energy absorption capacity from square and round panels correspond well, which means that also panels tested according to NS 14488-5 should be independent of the dimensions if evaluated as flexural tensile stress vs. CMOD. Another important result is that the flexural tensile stress vs. CMOD relationship is nearly identical for both panel test methods. The CS-condition most likely gives larger friction than the present 3P-condition [11], which may explain that the calculated flexural stress is larger for the CS-panels than for the 3P-panels. The results from the beam tests shown in Figure 1 c) show that NSBT-tests gives approximately the same flexural tensile stress at cracking, but that the calculated stress is less after cracking and the scatter is larger than for the panels. An explanation for the first observation may be that the beams will crack at the weakest point, while the support system decides where the 3P-panels will crack and the friction effect gives increased capacity for the CS-panels, while the latter finding may be explained by the relatively small crack area of the beams compared to the panels.

From the beam tests presented in Figure 1 d) to g), it is shown that the test method in NS-EN 14651 gives larger flexural tensile stress than the NSBT-method, so that it is actually possible that beam tests according to NS-EN 14651 gives approximately the same flexural tensile stress vs. CMOD relationship as the panel tests.

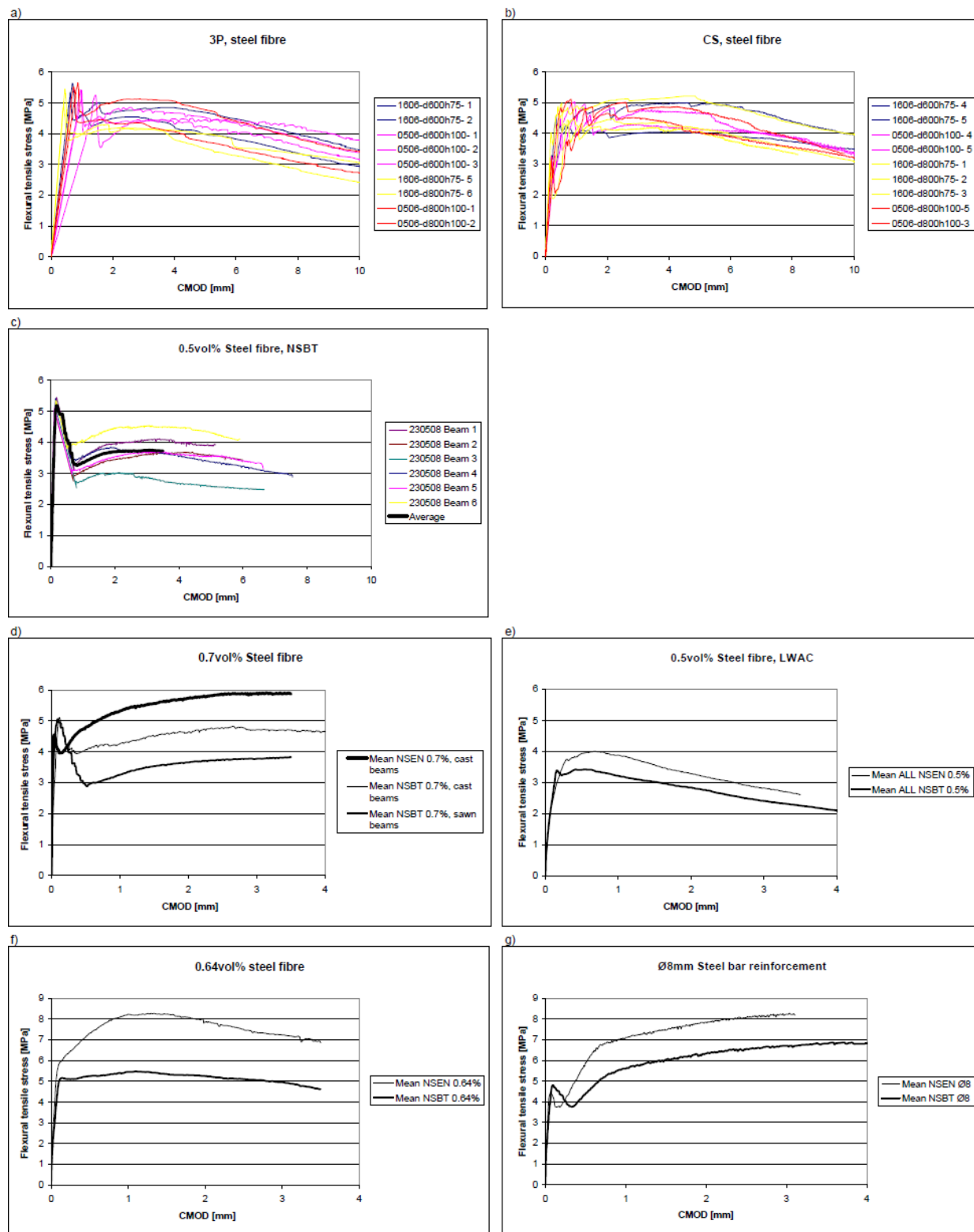


Figure 1 – Flexural tensile stress vs. CMOD, panel and beam tests

The most interesting observation from the results is actually that relatively moderate amounts of fibre reinforcement may be as effective as the required minimum reinforcement area according to Eurocode 2 (one 8mm bar has a cross section area of 50 mm² while $A_{s,min}$ is 25 mm² and 32 mm² NSEN-beams and NSBT-beams, respectively).

ACKNOWLEDGEMENT

The paper is based on the work performed in COIN - Concrete Innovation Centre (www.coinweb.no) - which is a Centre for Research based Innovation, initiated by the Research Council of Norway (RCN) in 2006. COIN has an annual budget of NOK 25 mill, and is financed by RCN (approx. 40 %), industrial partners (approx 45 % of which ¼ is cash) and by SINTEF and NTNU (in all approx 15 %). The Centre is directed by SINTEF, with NTNU as a research partners and with the present industrial partners: Aker Solutions, Norcem, Norwegian Public Roads Administration, Rescon Mapei, Skanska, Spenncon, Unicon, Veidekke and Weber Saint Gobain.

REFERENCES

1. ASTM C 1550-08, "Standard Test Method for Flexural Toughness of Fiber Reinforced Concrete (Using Centrally Loaded Round Panels)", October 2008.
2. NS-EN 199-1-1, "Eurocode 2: Design of concrete structures. Part 1-1: General rules and rules for buildings", December 2004 + NA November 2008.
3. NS-EN 14651, "Test method for metallic fibre concrete. Measuring the flexural tensile strength (limit of proportionality (LOP), residual)", August 2007.
4. Johansen, K. W., "Yield-line formulae for slabs", *Cement and Concrete Association*, 1972
5. Bernard, E.S. & Xu, G. G., "Crack widths in ASTM C-1550 panels", *Shotcrete: Elements of a System*, 2010
6. Sandbakk, S., Kanstad, T., Bjøntegaard, Ø., Vandewalle, L., Parmentier, B., "International Round Robin Testing of Circular FRC Slabs", COIN Project report 23-2010, 2010
7. Norwegian Concrete Association, "Publication nr 7, Sprøytebetong til fjellsikring", 2003
8. NS-EN 14488-5, "Testing sprayed concrete. Part 5: Determination of energy absorption capacity of fibre reinforced slab specimen", 2006
9. NS-EN 14488-5, "Testing sprayed concrete. Part 3: Flexural strengths (first peak, ultimate and residual) of fibre reinforced beam specimens", 2006
10. Bernard, E. S. Tutlu, E., Diamantlidis, D., "Crack Offset Corrections to Post-crack Performance Parameters Obtained from Third-point Loaded Fiber Reinforced Shotcrete Beams", *Cement, Concrete and Aggregates*, Vol. 25, No. 2, 2003
11. Bjøntegaard, Ø. "Technology report 2534, NRPA, Energy absorption capacity for fibre reinforced sprayed concrete. Effect of friction in round and square panel tests with continuous support (Series 4)" Norwegian Public Road Administration, 2009

High-Performance Steel Fibreconcrete Strength



Andrejs Krasnikovs
Dr.Sc.Ing, Professor
Concrete mechanics lab.
Institute of Mechanics
Riga Technical University
Riga, LV 1658, LATVIA
e-mail: akrasn@latnet.lv



Olga Kononova
Dr.Sc.Ing, Assoc. Professor
Institute of Mechanics
Riga Technical University
Riga, LV 1658, LATVIA
e-mail:
olga.kononova@gmail.com



Videvuds Lapsa
Dr.Sc.Ing,
Assoc. Professor
Concrete mechanics lab.
Riga Technical University
Riga, LV 1658, LATVIA
e-mail: valapsa@latnet.lv



Andrejs Pupurs
Ph.D. Student
Concrete mechanics lab
Riga Technical University
Riga, LV 1658, LATVIA
e-mail: pupurs@rtu.lv

ABSTRACT

Steel fibres are bridging the crack in the reinforced high-performance (SFRHPC) concrete providing resistance to crack propagation and crack opening before being pulled out. Structural SFRHPC fracture model was created; material fracture process was modelled, based on single fibre pull-out law. Different geometry and size steel fibres were added to concrete matrix (fibre cocktail) was modelled and investigated experimentally. As the load carried by each fibre at a constant crack opening is known from micro mechanical investigations, the corresponding total bending load P for a beam was obtained through equilibrium conditions. Prediction results were discussed.

Key words: steel fibres, high-performance concrete, strength, fracture

1. INTRODUCTION

The use of short steel fibres instead a steel rebars in conventional concrete is beneficial due to a simpler casting procedure. In a high performance (HP) concrete dispersed fibres use can be observed as an approach is reducing material brittleness when material load bearing capacity and strength are increasing. At the same time, a large content of steel fibres negatively affects the mix workability. Therefore for the aim of good workability of the mix, steel fibres are limited both by their maximal content, geometry (chemical bond between steel fibre and concrete matrix is weak and fibres are anchoring in the matrix mainly geometrically and by frictional forces) and length. Increasing applied load, micro cracks in SFRHPC are growing and coalescent forming macro crack (or macro cracks). Steel fibres are bridging the crack providing resistance to crack propagation and crack opening before being pulled out (main mechanism for majority of commercially available fibres), that determines the load bearing capacity of the

cracked material. Therefore it is important to perform a detailed micro-mechanical investigation of fibre pull-out process in order to understand and characterize the behaviour and crack propagation in SFHPRC structural elements.

2. PULL-OUT EXPERIMENTS

Follows types of steel fibres were used in investigation – straight fibres, fibres with end hooks (Dramix), and corrugated form fibres (Tabix) [1, 2]. The pull-out test samples were manufactured in plywood moulds with configuration and moulded specimen dimensions given in Fig.1.a. The parameter L shows the embedded length of the fibre (that will be subjected to pull-out) and α shows the orientation angle of the fibre with respect to the load direction. A thin plastic film was used also as a separator between the two halves of the specimen as shown in Fig.1.a (shown as a thick line on the specimen middle). All pull-out specimens were tested in

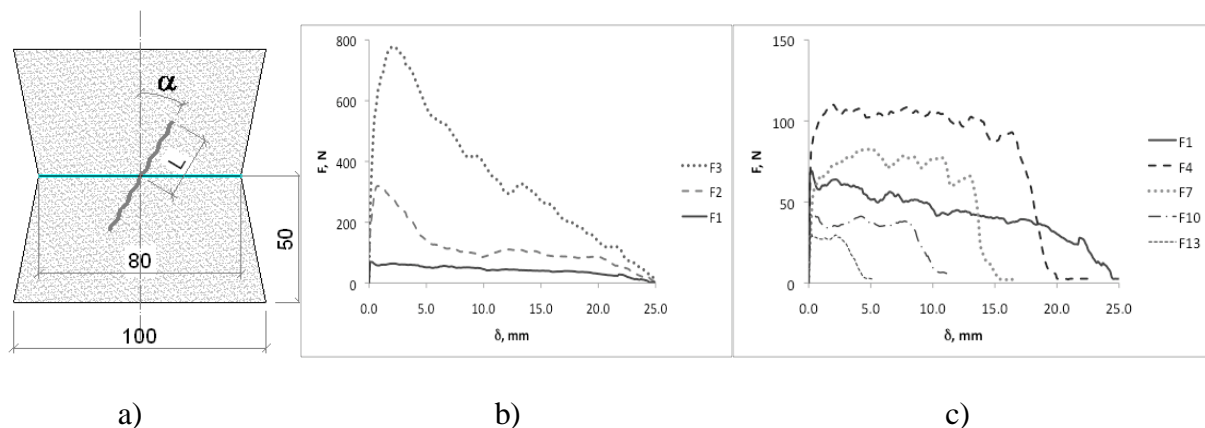


Fig.1. a) a pull-out test specimen, L - embedded length, α - orientation angle; b) pull-out curves ($L=25$ mm, $\alpha=0^\circ$) for : F1 – straight (lower curve); F2 – hooked-end (middle curve); F3 – corrugated (upper curve); c) pull-out curves for straight fibers embedded in different depth: F1 - $L=25$ mm; F4 - $L=20$ mm; F7 - $L=15$ mm; F10 - $L=10$ mm; F13 - $L=5$ mm

tensile testing machine Zwick/Roell Z150 (grips with 1kN dynamometer was used), combined with video extensometer “Messphysik” (for displacement measuring). Experiments were realized for fibre embedment lengths $L=5$ mm; 10mm; 15mm; 20mm; 25mm and orientation angles $\alpha=0^\circ$; 10° ; 20° ; 30° ; 45° ; 60° (the results patterns are shown in Fig.1.b,c). Because of an experimental data scatter nine specimens were tested with the same geometry and concrete matrix properties (three different compressive strength matrixes were investigated) and average values and data dispersions were obtained.

3. MACRO-SCALE MODELING

The construction member cracking and post cracking behaviour was investigated experimentally testing notched SFHPRC prisms (15x15x60cm) under 4-point bending (till macro-crack mouth opening displacement (CMOD) reaches 6-10mm) and obtaining applied load – CMOD diagrams. The same process was simulated numerically on the base of elaborated structural macro-crack (bridged by fibres) opening model. Elaborated model takes into account the types of fibres used and also the quantity of each fibre type in the concrete mix. It had been shown by

many research papers [see references in 2-5] that the amount and type of fibres used in FRC mix significantly influence the load bearing capacity and behaviour of the FRC structural element.

3.1. Description of the model

A SFRC beam with chaotic fibre orientation subjected to four point bending was modelled. The geometry (length, form and diameter) and amount of each fibre type is included in fibre-cocktail mix is given. A random distribution function is applied to assign location and orientation angle of each fibre. Monte-Carlo simulations were performed to obtain fibre distribution in every particular SFRHPC prism. After that, weakest (critical) cross section was recognized as the cross section with the smallest amount of fibres crossing it. In the critical cross-section the number and distribution of each fibre type is known. By known fibre distribution it is meant to state that orientation angle and embedded length are known with respect to the plane of cross-section. The crack starts to open (this procedure in the model is happened step by step increasing crack mouth opening displacement (CMOD)). At every step (known value of CMOD) every fibre crossing the crack starts to pull out. Information about such every fibre location orientation, type and embedment length is known previously from the distribution procedure and is keeping in the model. Then the corresponding data from the database file which contains all information from pull-out experiments must be correctly read and applied (see Fig.2). Load is

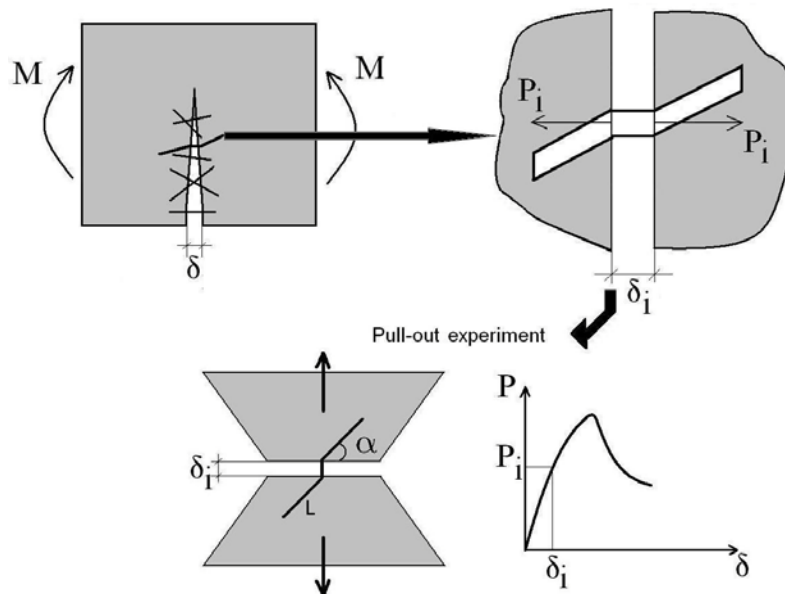


Fig.2. Model description

bearing by every particular fibre is crossing the crack, denotes depending on fibre location and its location point opening δ_i (see Fig.2). Summarizing all local loads we are obtaining bending moment working in the crack plane and corresponding value of external force. Performing numerical simulation of above mentioned crack opening process we are obtaining theoretical applied load- CMOD curve.

3.2. Model verification

The proposed model was applied for SFRC and SFRHPC behaviour prediction with various

fibre types and concentrations. SFRC mixes with fibre concentration within the range from 50 kg/m³ to 450 kg/m³ and still high workability were studied. In Fig. 3 is shown model prediction comparison with experiment for SFRHPC having fibre cocktail: Tabix 50 -125 kg/m³; Dramix 30-35 kg/m³; Straight (13mm long) -25 kg/m³; Straight (6 mm long) -10 kg/m³.

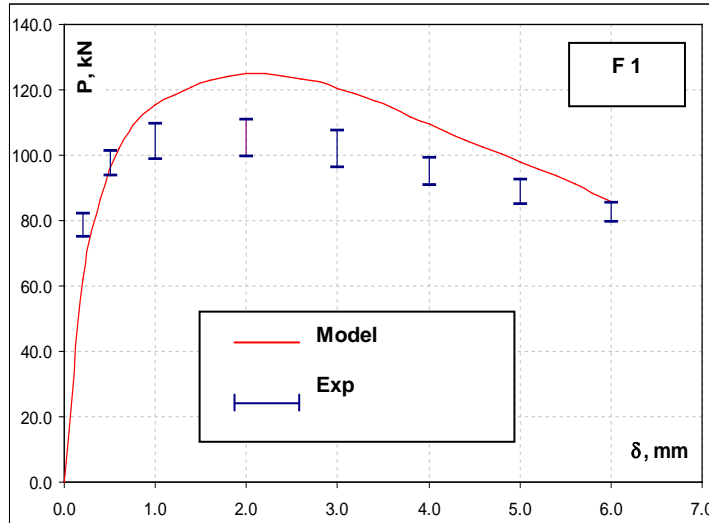


Fig.3. Model predicted load- CMOD (mm) dependence in comparison with experiment for SFRHPC containing 293kg/m³ different type steel fibres. Beam size is 15x15x60 cm.

CONCLUSIONS

Detailed structural SFRHPC post-cracking behaviour model was elaborated and numerically analyzed. The validity of the proposed model has been proved for SFRC and SFRHPC beams with fibre concentrations up to 450 kg/m³. Prediction results comparison with experiments was allowed to appreciate such factors as: fibres distribution, orientation, and way of anchoring as well as matrix strength influence on non-linear post-cracking SFRC mechanical behaviour.

REFERENCES

1. Krasnikovs A., Kononova O. & Pupurs A., "Steel Fiber Reinforced Concrete Strength," *Sc. Proceedings of Riga Technical University. Transport and Engineering*, 6, vol.28, Riga, 2008, pp. 142-150.
2. Krasnikovs A. & Kononova O., "Strength Prediction for Concrete Reinforced by Different Length and Shape Short Steel Fibers," *Sc. Proceedings of Riga Technical University. Transport and Engineering*, 6, vol.31, 2009, pp.89-93.
3. Naaman A.E., "Engineered Steel Fibers with Optimal Properties fro Reinforcement of Cement Composites," *J. of Advanced Concrete Technology*, Vol.1, No3, 2003, pp. 241-252.
4. Victor C. Li., "On Engineered Cementitious Composites a Revue of the Material an it's Applications," *J. of Advanced Concrete Technology*, Vol.1, No3, 2003, pp. 215-230.
5. Banthia N. & Sappakittipakom M., "Toughness Enhancement in Steel Fiber Reinforced Concrete through Fiber Hybridization," *Cement & Concrete Research*, 37, 2007, pp.1366-1372.

Fibre Reinforced Concrete (FRC) (with Glass, Steel and Carbon Fibres) Strength



Andrejs Krasnikovs
Dr.Sc.Ing, Professor
Concrete mechanics lab.
Institute of Mechanics
Riga Technical University
Riga, LV 1658, LATVIA
e-mail: akrasn@latnet.lv



Amjad Khabbaz
Dr.Sc.Ing, Researcher
Concrete mechanics lab.
Riga Technical University
Riga, LV 1658, LATVIA
e-mail: amjad.khabbaz@rtu.lv



Angelina Galushchak
Ph.D. Student
Institute of Mechanics
Riga Technical University
Riga, LV 1658, LATVIA
e-mail: shapulja@inbox.lv



Arturs Machanovskis
Ph.D. Student
Institute of Mechanics
Riga Technical University
Riga, LV 1658, LATVIA
artursmacanovskis@inbox.lv

ABSTRACT

An AR glass carbon and steel fibre concrete strength and post cracking behaviour was investigated experimentally. Detailed micromechanical investigation for single fibre and few fibres pull-out micromechanical mechanism were performed numerically (using FEM modelling) as well as experimentally. Fiberconcrete fracture (and post-cracking) behaviour were investigated (experimentally under three and four point bending) depending on concrete matrix strength (conventional and high performance), fibre amount and fibre length in strands (for non-metallic fibres). Numerical model, based on fibre bundle pull-out mechanism in concrete was used to predict fiberconcrete post cracking behaviour. Theoretical results were compared with the data obtained in experiments.

Key words: short fibres, glass fibre, carbon fibre, concrete, strength, fracture

1. INTRODUCTION

If we want to predict fibre concrete material cracking and post-cracking behaviour, and the same time are looking for tensile strength increase and quasi-plastic (with few % deformation without losing load bearing capability) material post-cracking behaviour, the study of single fibre and fibre bundle pull-out mechanisms out of cement matrix is important. Publications discussed this problem are described in [1-4]. Fracture experimental investigation for glass, steel and carbon short fibre concretes [1, 2] was recognized main micro-mechanisms of fibre bridging cracks in material. In present paper, investigation of single and few non-metallic fibres micro-mechanics embedded into concrete matrix under external loads were performed numerically (using FEM approach) and experimentally. Micromechanical data were used for fiberconcrete cracking and post-cracking behaviour based on elaborated structural model. Prediction results were validated by fiberconcrete bending tests.

2. MICRO-MECHANICS

2.1 Single fiber pull out

Single fibre is oriented orthogonal to concrete surface and is pulling out. Our and another authors experimental observations shown four main stages of such procedure:

a) fibre and concrete matrix are bonded together (perfect bond), all deformations in system are elastic; b) cylindrical delamination crack is starting from the outer concrete block surface propagate into material between fibre and concrete matrix. Crack is growing mainly by mode 2; c) when fibre embedment is small (short fibre or pulling out the shorter end of fibre which is bridging the crack) delamination is reaching all length of fibre after that fibre with friction is pulling out. If fibre embedment is large, fibre is breaking at the length L in concrete, after what free fibre end with friction is pulling out of matrix; d) stretched fibre breaks out of concrete.

Fibers breaking in material according scenario a-c are responsible to fiberconcrete post-cracking quasi-plastic behaviour and are the subject of present investigation. Simulations have been done by ANSYS. Three numerical 2D models were investigated: 1) single glass (or carbon, or straight steel) fibre is embedded into concrete matrix with perfect bond between them and subjected to external pulling load; 2) the situation, when between pulling out fiber and matrix is growing delamination. In delaminated area fiber and matrix are debonded. Each mutual motion in this zone performs with friction. Numerically this situation was simulated incorporating soft interlayer between fiber and matrix (Fig.1 left picture). Stresses in fiber along the line parallel to fiber axis in vicinity to interface with matrix (0.98 of fiber radius) are shown in Fig.1 (right picture). Peaks on the lines (going from left to right) corresponds to: a) fiber end in concrete

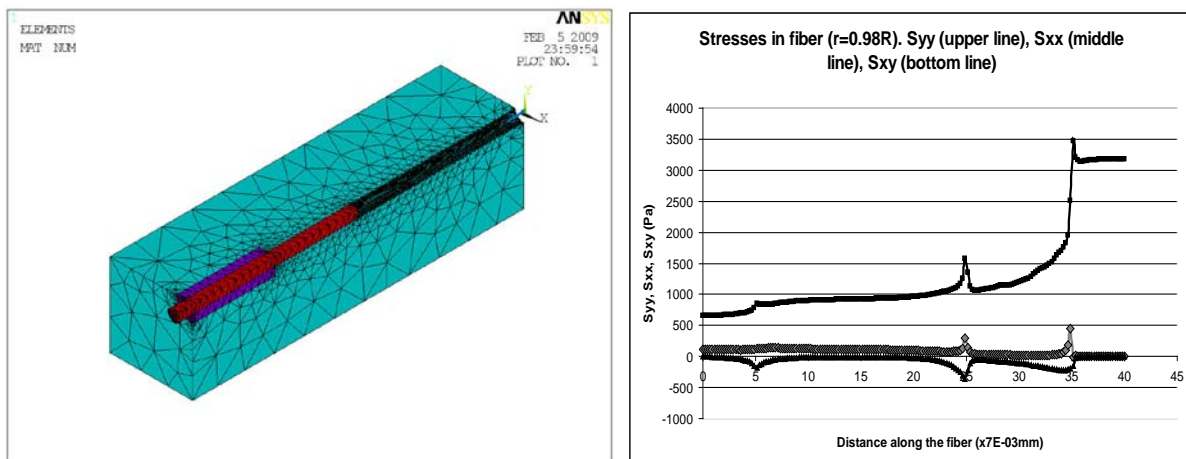


Fig.1. Fiber is partially debonded in concrete (left picture). Stresses in the fiber on the line parallel to fiber direction ($r=0.98R$) (right picture). Stress in y direction along the fiber S_y (upper line), stress in x direction –direction orthogonal to fiber direction S_{xx} (middle line) and shear stress S_{xy} (bottom line).

(small peaks); b) beginning of delamination zone (middle peaks); c) outer surface of concrete block (right peaks). Stress peaks at the front of delamination zone (corresponds to singularities in classical solution) are explaining mechanism of fiber break at some distance in concrete volume, because during delamination growth elevated overstress is crossing different fiber crosssections in concrete till the weakest is reached. Simultaneously overstress is decreasing with the distance from the crack (outer surface of concrete block) surface and increasing with fiber/matrix interface friction increase (corresponds to concrete matrix with higher compressive

strength). At the same moment overloads in the matrix are rising into concrete body micro-cracks formation around the fiber. These cracks were observed experimentally; 3) numerical model were elaborated to describe fiber end sliding motion after the break in the concrete matrix or in the case when delamination reach the embedded end of fiber. FEM model with contact elements between fiber and matrix were exploited.

2.1 Fiber bundle pull out

Three above mentioned models were realized for fiber bundle with 2, 3, 12 and 800 fiber in a bundle. Traditionally non-metallic (glass, carbon) short fibers, are ready for concrete mix, are available in a form of fiber bundles (chopped strands) with 600 to 1200 filaments in each bundle. During fiberconcrete mixing cement paste is penetrating into bundles only partially, forming external shell (composite - fibers in cement paste) and the core (fibers without paste between them). Such bundle bridging the macro-crack is failing by rupture of the fibers in a composite shell and consequent core sliding out (this process governs by friction between adjacent fibers) and easily can be recognized in Fig.2.

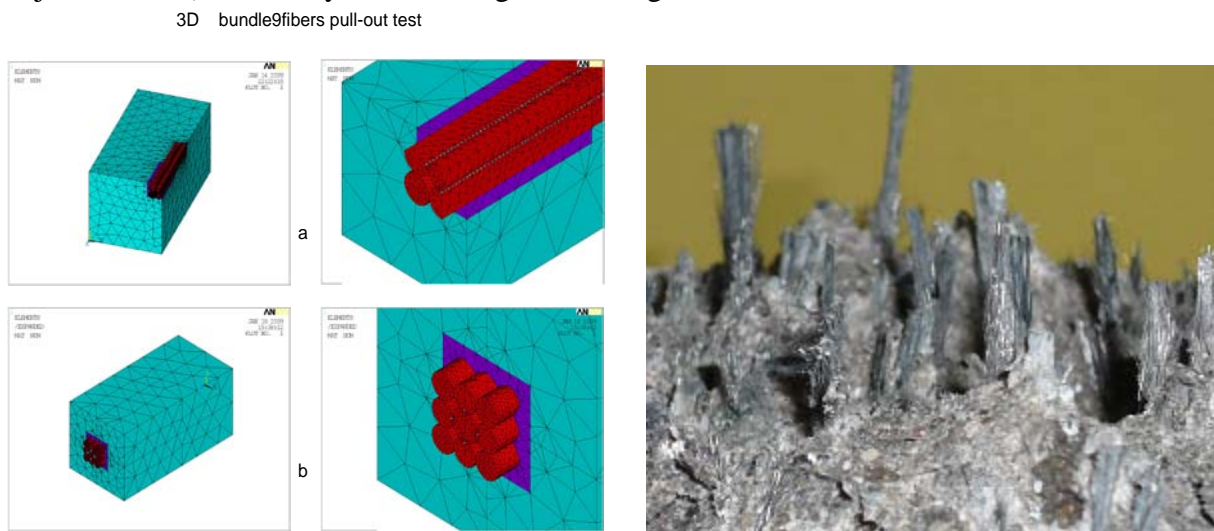


Fig.2. Partially debonded 9 fibers in concrete (FEM model for pull-out investigation) (left picture); pulled out carbon fiber bundles. Bundle has external composite shell (fibers with cement paste between them) and internal core (fibers without cement paste) (can be recognized on right picture).

2.2 Single fiber and fiber bundle pulling out experimental validation

Obtained numerical results were validated by performed experimental tests for single two and 600 fibers (bundle). Main fiber and matrix failure mechanisms were recognized. Single glass and carbon fibers were embedded into concrete matrix on the depth 10mm and 20mm, pulling out such fibers for one part of samples fail out of concrete. Fibers, in other samples, fail in concrete and after that were pulled out. Pulled out part of each fiber haven't exceeded 1.5mm. This mechanism directly corresponds to models b, c. For bundles having 600 filaments, fibers in outer shell fails according mechanisms b, c. Bundle central core were pulled out and had full length (this effect depends on how many concrete paste penetrated bundle embedded end).

2.2 Macro-scale modeling and experimental validation

Fiberconcrete prismatic samples with the size 10x10x40cm were elaborated. Fully computer driven testing machine Zwick -150 (with ultimate force 150kN) were used. Stress- prism midpoint deflection diagrams for glass fiber and carbon fiber concrete were obtained. Experimentally obtained pull-out laws were used as the main input data for the proposed structural FRC fracture model [2] and non-linear behavior of FRC beams under bending loads were predicted. Predictions were compared with experimental test data for prismatic samples (with the size 10x10x40cm) 4 point bending.

CONCLUSIONS

Numerical investigation for glass, carbon and straight steel single fibre and fibre bundles (glass and carbon) pull out of concrete matrix micromechanics (detailed micro-stresses and micro forces) were performed. Results were compared with performed pull out experiments. Main fibre and bundle load bearing and rupture micro-mechanical mechanisms were recognized. On the base of experimentally obtained pull-out data fiberconcrete fracture and post-cracking behaviour prediction for prisms under 4-point bending loading conditions were done. Prediction results were compared with experimental data.

REFERENCES

1. A.Krasnikovs, A.Khabaz & Kononova O. " Numerical 2D Investigation of Non-metallic (glass and carbon) Fiber Micro-mechanical Behaviour in Concrete Matrix,)," *Sc. Proceedings of Riga Technical University. Transport and Engineering*, 2, vol.10, 2009, pp. 67-78.
2. A. Krasnikovs, A. Khabaz, I. Telnova, A. Machanovsky & J. Klavinsh, "Numerical 3D investigation of non--metallic (glass, carbon) fibre pull-out micromechanics (in concrete matrix)," *Sc. Proceedings of Riga Technical University. Transport and Engineering*, 6, vol.33, 2010, pp.103-108.
3. Bentur, A., Wu, S.T., Banthia, N., Baggott, R., Hansen, W., Katz, A., Leung, C.K.Y., Li, V.C., Mobasher, B., Naaman, A.E., Robertson, R., Soroushian, P., Stang, H. & Taerwe, L.R. In *High Performance Fiber Reinforced Cementitious Composites*; Naaman, A.E. & Reinhardt, H. Eds.; Chapman and Hall: London, 1995; P.149-191.
4. Victor C. Li & Stang H., "Interface Property Characterization and Strengthening Mechanisms in Fiber Reinforced Cement Based Composites," *Advanced Cement Based Materials*, 6, 1997, pp.1-20.
5. Banholzer B., Brameshuber W. & Jung W., "Analytical simulation of pull-out tests – the direct problem," *Cement & Concrete Composites*, 27, 2005, pp.93-101.

Development of Cardboard Fibre Engineered Cementitious Composite (CFECC)



Karin Habermehl-Cwirzen
Dipl.-Ing., Dr. Tech.
Senior Research Scientist
Aalto University
Rakentajanaukio 4
FI-00076 Aalto
karin.habermehl-cwirzen@tkk.fi



Vesa Penttala
Dr. Tech, Professor
Aalto University
Rakentajanaukio 4
FI-00076 Aalto
vesa.penttala@aalto.fi



Andrzej Cwirzen
Dr. Tech., Docent
Aalto University
Rakentajanaukio 4
FI-00076
andrzej.cwirzen@tkk.fi

ABSTRACT

The present study is focused on the extraction of fibres from cardboards and their incorporation into Portland cement-based binder matrices. The effects of the cardboard amount on the mechanical properties and microstructure were studied. One single source of cardboard was used to eliminate possible variations in the cardboard fibre morphology. The studied mixes contained cement and sand. The w/c ratio was chosen to be 0.8. The obtained results showed that the rheology of the fresh mixes depended strongly on the amount of added cardboard. The compressive strength value was around 11 MPa and the flexural strength was around 2.5 MPa for 5-10% of added paper.

Key words: cardboard, concrete, renewable resources, sustainability.

1. INTRODUCTION

CFEFF is a part of a project funded by the Academy of Finland, called “renewable-resources (micro/nano)-fibre engineered cementitious composites (RRFECC)”. This project is aiming to tackle the carbon footprint problem of cementitious composites and to produce sustainable concrete, by incorporating materials from renewable resources into cementitious matrices. In CFECC we study the cardboard fibre extraction, their incorporation into the matrices, and their influences on the cementitious materials properties.

Application of fibres in building materials has been used for hundreds of years. For instance, in the Middle Ages it was common to utilize animal hairs to reinforce mortars used for brick walls, [1]. More recently a number of types of materials have been used to produce fibres incorporated into concretes and mortars. The most common fibre materials are steel, glass, carbon and synthetic fibres such as polyethylene or polypropylene. The newest development in fibre technology is downsizing of the fibre diameter to nanometer dimension. Some research has been

done on carbon nanofibres and carbon nanotubes, [2, 3]. Recently, there is also a considerable interest in bio-fibres [4]. The present paper deals with the mechanical properties of concrete equipped with bio-fibre, which were easily obtained from recycled cardboard.

2. MATERIALS AND METHODS

2.1 Materials

The applied cardboard came from one single source of cardboard; recovered juice boxes. A single source was used to eliminate possible variations in the cardboard fibre morphology. The mixes showed that pre-cutting of the cardboard was not necessary. The boxes were plainly rolled to tubes to fit into the inlet of the mixer.

Portland cement CEM II 42.5 produced by Finnsementti Oy was used in the mixes. Sands of sizes # 0.5-1.2 mm were added to all mixes.

As known from former studies of our group, cementitious materials containing paper or cardboard additions, need a higher amount of mixing water than regular mix designs, therefore, the w/c ratio was chosen to be 0.8.

2.2 Mixer and Mixes

Mixing was done by a fully automated and digitally controlled intensive mixer by Eirich. The mixes were kept as simple as possible to diminish the number of variables which could influence the concrete properties. Therefore, no superplastizer or air-entrainment agents were added to the cardboard-cement mixes.

Due to the high-speed mixing properties of the mixer and the alkalinity of the paste, the cardboard did not need to be shredded beforehand. The rheology of the mixes depended strongly on the amount of added cardboard and it varied from dry to fluid. The compressive strength varied between 11-50 MPa, while the minimum bending strength was around 2.5 MPa.

3. RESULTS AND DISCUSSION

All mixes contained 20 kg of cement, 20 kg of sand, and 16 l of water (w/c 0.8). In this study, we used several cardboard dosages in the mixes, varying from 0-4 kg of cardboard. Small amounts of cardboard (0.5 kg) resulted in a very fluid mix, in which cardboard did not disintegrate sufficiently. High amounts of cardboard (4 kg), made the mix very dry and, therefore, also in this situation the cardboard did not disintegrate. The other mixes worked well. Mixes with 1 kg of cardboard were liquid, but the concrete did not segregate. After 24 hours, demoulding of the concrete cubes was possible. Addition of 1.5 kg cardboard resulted in a easily workable mix. The mix containing 2 kg of cardboard appeared to be relatively dry, but it still had a satisfactory workability. The reference mix without cardboard having a water-to-cement ratio of 0.8 had a too liquid-like consistency to be cast. Therefore, the w/c ratio of the reference mix was eventually lowered to 0.45.

The ESEM investigations of the papercrete microstructure were performed with an Electroscan E-3 microscope. The environmental scanning electron microscope offers the possibility to study cementitious materials in an easy way, because the vacuum restrictions and problems with a normal SEM are avoided. The acceleration voltage was 15 keV and the chamber pressure 5 Torr. Fractured samples were used. Some examples of obtained images are shown in Figure 1. The results revealed that the mixing process provided a significant decomposition of the original cardboard structure into micro-sized cellulose fibres. The diameter of the fibres ranged from 1 to 10 μm , the fibre length extended to tens of millimetres. ESEM investigation revealed the formation of hydration products, including C-S-H and Portlandite, on the cellulose fibres.

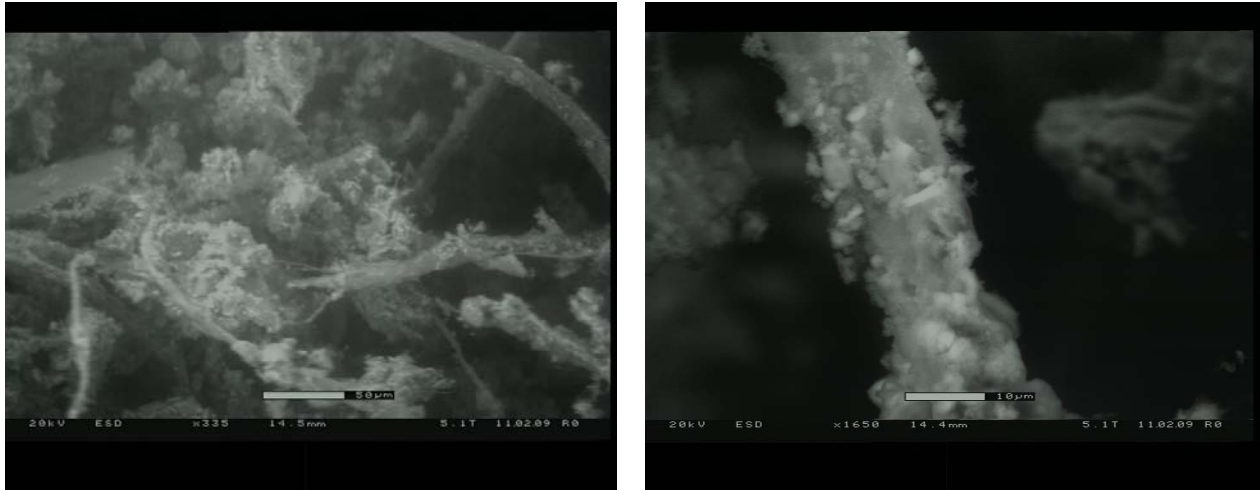


Figure 1. ESEM images of fractured specimens

The compressive strength was tested with standard $10 \times 10 \times 10 \text{ cm}^3$ cubes, while the flexural strength was measured with standard beam sizes of $10 \times 10 \times 50 \text{ cm}^3$. The density of the reference concrete was about 2200 kg/m^3 , with the addition of cardboard to the mix the average density decreased to 1850 kg/m^3 . The compressive and flexural strength results of 28 days old specimens are shown in Figure 2. The average compressive strength of the reference samples was about 50.8 MPa. Obtained results showed that an addition of 5 to 10 % of paper (according to cement weight) resulted in nearly the same compressive strength of about 11 MPa and flexural strength of about 2.5 MPa.

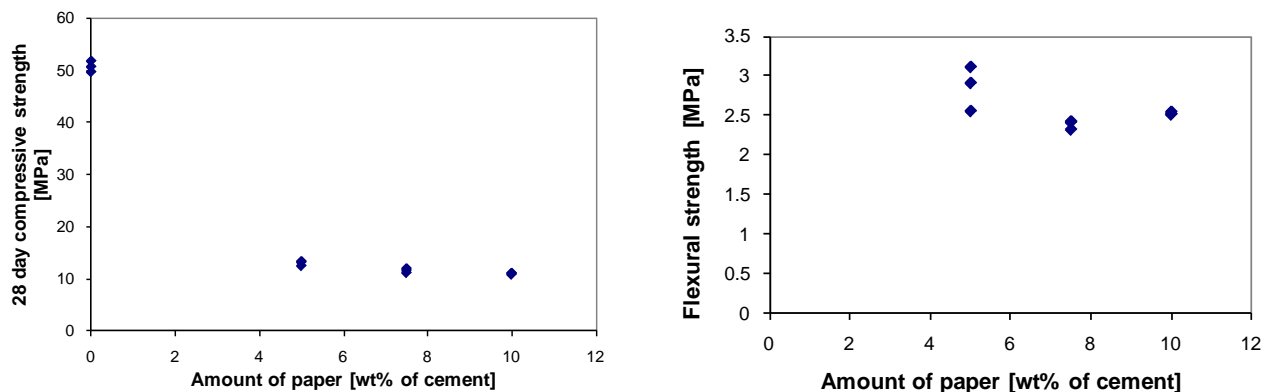


Figure 2. The 28-day compressive and flexural strength results of the test concretes

4. CONCLUSION

The presented study revealed that the application of relatively simple processes enabled to obtain a high degree of disintegration of cardboard into micro-sized cellulose fibres. Their addition into a Portland cement based matrix resulted in decreased compressive and flexural strength. The workability of the mix varied widely and, in some cases, perfect consistency behaviour could be achieved. Possible applications of cardboard-concrete can be as insulation material, e.g. as sandwich structure between walls. The main scientific challenge will be to modify the cardboard fibres in such a way, that the mechanical values will be comparable to concrete. Incorporation of recycled cardboard lowers the cost of the material, avoids land filling, and results in an environmentally friendlier cementitious material.

5. ACKNOWLEDGEMENT

K.M.E. Habermehl-Cwirzen acknowledges gratefully the support by the Academy of Finland to this research project. The help of Mr Pertti Alho in the production of the test concretes is also gratefully acknowledged.

REFERENCES

1. Cwirzen, Andrzej; Habermehl-Cwirzen, Karin; Flege, S.; Balogh, A.G., Characterization of Mortars and Plasters of Palatium and Einhard Basilica in Seligenstadt, Germany. HMC 08. 1st Historical Mortars Conference, Lisbon, Portugal 24-26. September 2008. p.46
2. Kowald, T., Trettin, R., Improvement of cementitious binders by multi-walled carbon nanotubes, Nanoscale modification of cementitious materials, Nanotechnology in Construction, Edited by Bittnal et al, Springer, 2009, pp. 261-266
3. A. Cwirzen, K. Habermehl-Cwirzen, V. Penttala, D. Shandakov, L.I. Nasibulina, A.G. Nasibulin, E.I. Kauppinen, Properties of high yield synthesized carbon nano fibres / Portland cement composite, Advances in Cement Research, Vol.21, No. 2, 2009, pp.141-146
4. Bhatnagar, A., Sain, M., Processing of Cellulose Nanofiber-reinforced Composites, Journal of Reinforced Plastics and Composites, 25, 2005, pp.1259

Formulations of Electrically Conductive Cement-based Composites



René Čechmánek
Research Institute
of Building Materials, JSC
Hněvkovského 30/65
CZ – 617 00 Brno
cechmanek@vustah.cz



Pavel Šteffan
Brno University of Technology
Faculty of Electrical Engineering
and Communication
Údolní 53
CZ – 602 00 Brno
steffan@feec.vutbr.cz



Jiří Junek
Research Institute
of Building Materials, JSC
Hněvkovského 30/65
CZ – 617 00 Brno
junek@vustah.cz

ABSTRACT

It is possible to achieve specific electrical properties by addition of certain components into a cement matrix. It was found that to enhance electrical conductivity of cement composites carbon particles of micro or nano-size are mostly suitable. Structurally-technical elements made of these newly composed fibre inorganic composites are able to shield against electromagnetic fields, to transform electricity to heat or to scan the weight of moving vehicles. This paper deals with design and selection of appropriate formulations for cable shielding or pavement heating.

Key words: Cement composite, carbon, conductivity, electromagnetic shielding, heating.

1. INTRODUCTION

Thin walled cement composites reinforced with dispersed fibres find today increasing markets in all spheres of building industry: especially facing panels, U-shaped channels for high-voltage cables and variously shaped architectural elements. Such composites minimize production, transport and assembly costs and have high resistance to weather. One of targets is to achieve electrical conductivity of these composites by the means of carbon particle additions.

2. CARBON PARTICLES SUITABLE FOR CONDUCTIVITY IMPROVEMENT

2.1 Selection of carbon particles

In the course of searching for suitable components there were selected mainly various kinds of micronized graphite with particle size in micro- or nanometres, which is characterized by excellent electrical properties as well as good compatibility with a cement matrix, except of higher demand of batch water due to its bulk specific surface. As secondary compounds carbon black and expanded graphite with similar properties as micronized graphite were used.

2.2 Properties of carbon particles

The particle size of micronized and expanded graphite is in micrometres, while the particle size of carbon black is in nanometres. Micronized graphite has carbon content $> 80\%$, carbon black has high carbon content (99 %). Expanded graphites have lower carbon content (60 - 96 %). Some compounds were modified to decrease interfacial tension and increase surface wettability for achievement of better mixture workability of cement composites by the means of surface treatment of nickel or Teflon.

3. CEMENT COMPOSITES WITH ADDITION OF CARBON PARTICLES

3.1 Test mixtures

Glass fibre reinforced concrete (GFRC) was taken as a standard for further modifications. Fine-grained matrix consists of cement, sand, and microsilica and it is reinforced by alkali-resistant glass fibres of length 12 mm in amount of 3 % per dry mixture weight. All mixtures were prepared in a mixer with a stationary drum and forced movement of paddles.

The proportion of carbon particles was expressed as a percentage of a dry mixture weight (cement + sand + microsilica) as a substitution of a part of sand in range of 4 - 10 % per weight. In the case of electromagnetic shielding metal parings were used in proportion of 3 - 10 % per weight. Considering an application based on a relation between electrical behaviour and mechanical strain and reverse deformation of concrete elements, two types of fibre reinforcement (carbon and metal) were chosen as a substitution for glass fibres as well.

3.2 Influence on workability of fibre-cement mixtures

Fibre-cement mixtures were prepared in order to achieve optimal workability and minimal impedance, i.e. maximal electrical conductivity. Carbon origin as well as particle size both affect impedance properties of the final composites, and as well the particle size affects workability of fresh mixtures. It was found that the finer carbon powder, the lower was the impedance and the worse its workability. Appropriate mixture workability was achieved by the addition of various kinds of polycarboxylate-based superplasticizers. For wettability improvement addition of ethyl alcohol was used as well.

3.3 Influence on physical-mechanical characteristics of composites

All samples were cured in laboratory conditions close to real manufacture conditions with temperature 25 °C and humidity 55 %. The physical-mechanical properties of composites were tested on standard samples for thin-walled GFRC elements with dimensions 250 × 50 × 10 mm in age of 28 days. Higher water/cement factor causes significantly higher water absorption and lower bulk density, associated with low flexural strength and impact strength of the final composites. Generally bulk density is 1750 - 1800 kg/m³, water absorption 15 - 20 %, flexural strength 10 - 12 N/mm² and impact strength 3 - 5 kJ/m².

4. MEASUREMENT OF ELECTRICAL PROPERTIES

Conduction of electrical current in cements and concretes is essentially electrolytic. In order to avoid the problems of polarization, alternate currents are often used for determining resistivity of electrolytes and therefore also of cements and concretes. Electrical resistance is monitored, and expressed as impedance [1]. Influence of A.C. frequency on calculated values of impedance was found to be reasonably significant. A lot of factors with significant influence on measured values had to be taken into account. Internal factors include the mixture composition and method of its preparation. External factors are moisture and temperature of environment.

According to our measurements following statements could be concluded. The addition of carbon particles induces good electrical properties in cement-based composites. Though carbon fibres are less conductive than metal fibres, composites with carbon fibres were evaluated as better current conductors than the composites with metal ones. It is supposed that this is due to extremely fine size of carbon fibres which provides more effective inter-fibre continuity.

5. APPLICATIONS OF PROPOSED COMPOSITES

5.1 Application of electromagnetic shielding

Electromagnetic field is assumed to be a problem in the so called “sick house syndrome”. External electromagnetic fields can cause problems both in human health and in industry, where it can interfere with production of electronic equipment. Standard GFRC elements inhibit electromagnetic field up to approximately - 5 dB but our modified fibre-cement composite is able to achieve a level up to - 35 dB. In comparison to a massive steel reinforced concrete the same shielding effect is achieved with using of incomparably less structural thickness.

In order to approach real conditions as much as possible the measurement was carried out in a special electromagnetic chamber. Shielding efficiency was proven by the non-availability of any communication network inside the chamber [2]. A fibre-cement channel was manufactured to demonstrate the application of electromagnetic shielding. It contains three chambers to separate electric cables with different voltage so that they do not interfere with each other.

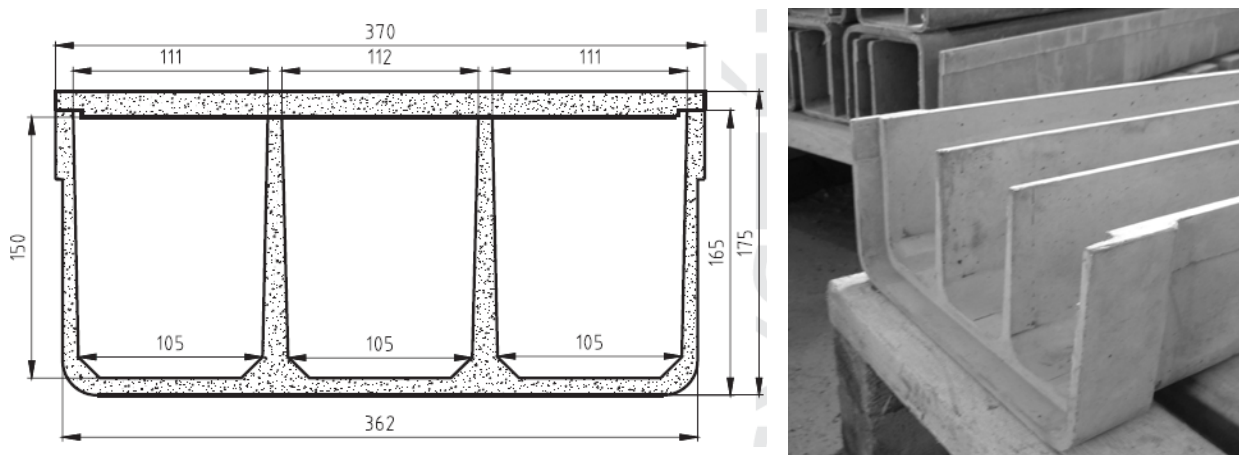


Figure 1 – Channel for electromagnetic shielding between cables.

5.2 Application of concrete heating

Electric heating of pavements is carried out by using of heating cables built into a concrete panel or a sand bed under a pavement made of asphalt or cobble-stone. The main disadvantage of the heating cables is a difficult and time-demanding cable fixing to a defined position. On the other hand embedding a heating fibre-cement composite slab directly in-situ is very easy.

A fibre-cement slab with dimensions $1800 \times 1400 \times 20$ mm and circle openings with diameter 110 mm for better incorporation into a concrete panel was cast with the designed composition. An initial setting of openings in square lattice caused heating to occur only in stripes and not across the whole surface, therefore an optimisation had to be done for uniform heating ability. As a prototype element a trafficable steel reinforced concrete panel was made with the ability to thaw snow cover or to defrost ice for reduction of slipping hazard on pavements or access ramps in front of buildings. The proposed element combines the advantages of the solid bearing steel reinforced concrete and those of a thin fibre-cement slab with the required heating capacity.

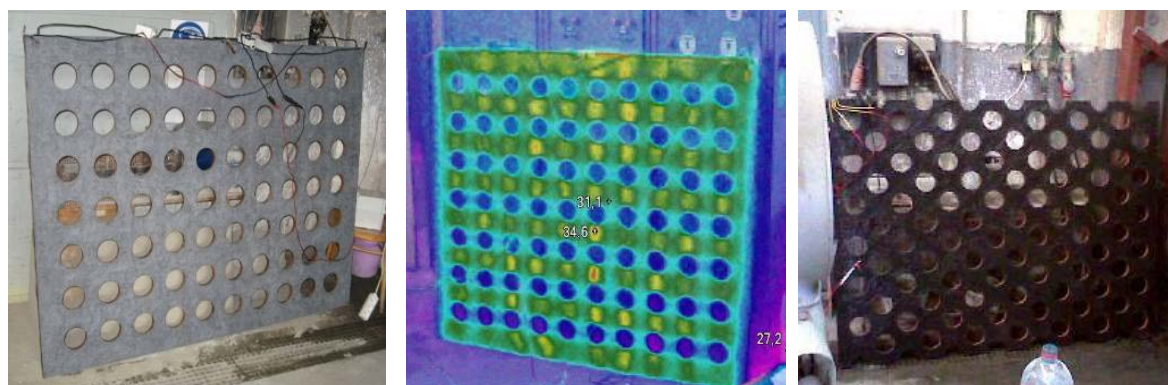


Figure 2 – Initial and final setting of openings.

6. CONCLUSION

It was found that electrical properties of cement composites are possible to achieve by the means of carbon particles. Because conduction of electrical current in concretes is essentially electrolytic, it is necessary to use alternating current for determining the resistance of concretes. By the means of the field test it was approved that these newly composed fibre inorganic composites are able to shield against electromagnetic fields or to transform electricity to heat.

ACKNOWLEDGEMENTS

This contribution was based on results of the research programme MPO ČR FT-TA3/027 Multifunctional composites of extraordinary properties on base of inorganic nano-components.

REFERENCES

1. Nikkanen, P., “On the Electrical Properties of Concrete and Their Applications”, *Valtion Teknillinen Tiedotus*, Sarja III, Rakennus 60:1962, 77 pp.
2. <http://www.computer.org/portal/web/csdl/doi/10.1109/ICONS.2010.39>

Deformability of high strength concrete



Magureanu Cornelia
Prof., Ph.D.
Technical University
of Cluj Napoca, Romania
magureanu.cornelia@bmt.utcluj.ro



Heghes Bogdan
Lecturer, Ph.D.
Technical University
of Cluj Napoca, Romania
bogdan.heghes@bmt.utcluj.ro

ABSTRACT

The paper presents experimental investigation regarding deformability of high strength concrete elements realised with concrete class C80/90 subjected to flexure. The elements were subjected to four point bending test and flexural response is investigated through displacement ductility.

Key words: high strength concrete, deformability, flexural response, ductility.

1. INTRODUCTION

High performance concrete is a brittle material and its brittleness increase proportionally with increase of its strength. It is necessary to provide a greater ductility on elements realised with high performance concrete in order to apply them in seismic prone areas.

The study report in this paper mainly investigates the implications of using high strength concrete (C80/95) in reinforced concrete flexural members.

2. EXPERIMENTAL PROGRAM

The experimental program contained a number of six simple reinforced concrete beams, tested at 4 point bending. The beams were realised with concrete with mean compressive strength determined on cubes of 150mm, was about 103MPa. The beams were realised with constant length of $L=3200\text{mm}$ and a cross section of $125\times 250\text{mm}$. The longitudinal percentage of reinforcement was 1.35%, 1.86% and 2.31%, for each longitudinal percentage 2 beams were made. Stirrups were localised only on shear zone of the beam, the behaviour under pure bending moment was the main focus of the test.

For longitudinal reinforcement S500 steel type was used and OB37 steel type for stirrups.

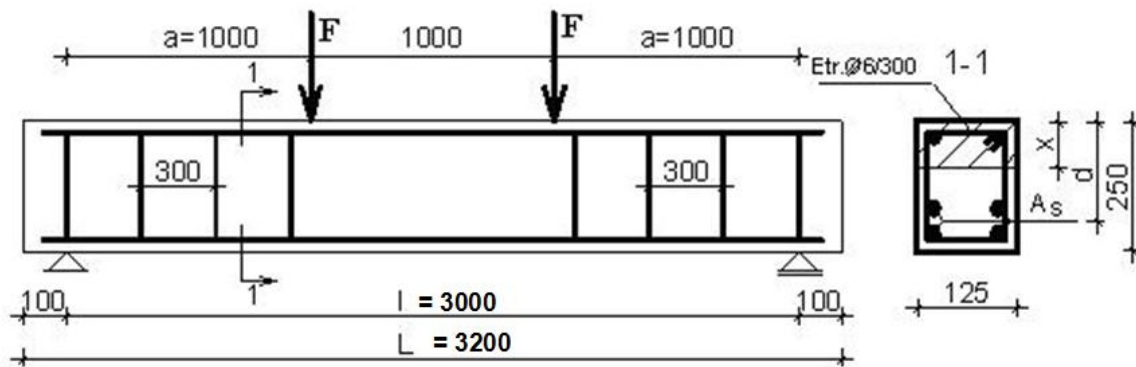


Figure 1 – Loading scheme

Figure 2 presents the relation between ultimate bending moment and reinforcement percentage and also between ultimate deflection value and reinforcement percentage. It can be observed that a linear behaviour exists between ultimate bending moment and longitudinal reinforcement percentage, bending moment is directly proportional with reinforcement ratio. This is also true for relation between ultimate deflection and longitudinal reinforcement percentage, deflection value from flexure diminishes with the rise of the longitudinal reinforcement percentage value.

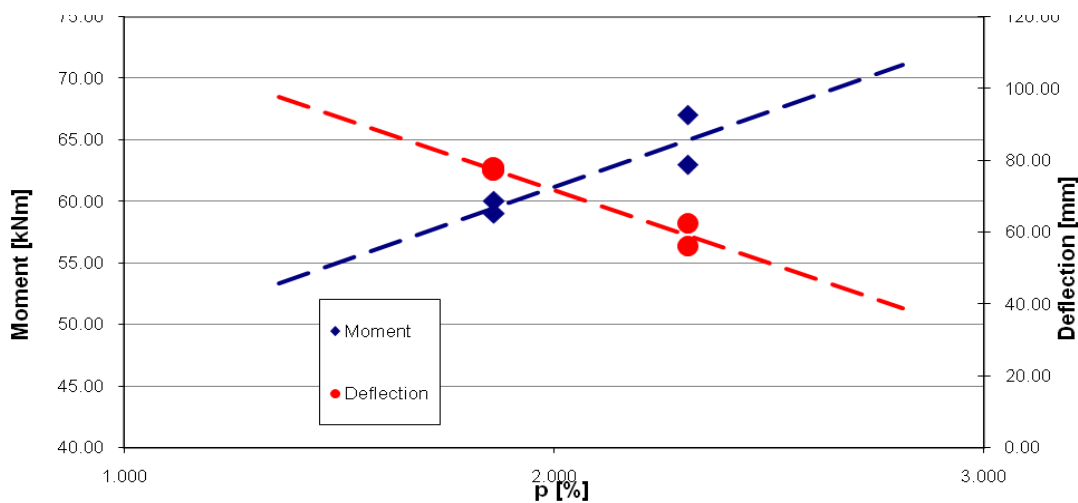


Figure 2 – Ultimate bending – reinforcement percentage and deflection-reinforcement percentage relations

Two displacement ductility were defined:

- $\mu_{\Delta 0,2}$ - ratio between ultimate deflection Δ_u^{exp} and deflection at the yielding of longitudinal reinforcement $\Delta_{y0,2}^{\text{exp}}$;
- μ_{Δ} - ratio between ultimate deflection Δ_u^{exp} and deflection at the point between elastic and plastic behaviour of the beam, determined from moment-displacement diagram $M - \Delta$.

It was remarked that for beams realized with high strength concrete and type S500 longitudinal reinforcement ratio, the displacement values are very closed (see Fig. 3), fact that can be related to the behaviour of the component materials of reinforced concrete elements. In case of high

strength concrete elements, both high strength concrete and steel type S500 are high performance materials which behaves linear up to 85% of their ultimate strength.

Using this type of steel in reinforced concrete elements subjected to flexure one can conclude that plastic behaviour of the elements in flexure occurs close after yielding of the longitudinal reinforcement. This can indicate the necessity of using high strength concrete with superior types of steel like S500, thus eliminating the fragile rupture of the concrete.

For different types of concrete class and different steel types, is widely regarded that is better to use mechanical reinforcement coefficient, defined by:

$$\omega = \frac{A_s \cdot f_{yd}}{A_c \cdot f_{cd}} \tag{1}$$

where A_s is longitudinal reinforcement area, f_{yd} is dimensioning value of reinforcement, A_c are concrete area and f_{cd} is dimensioning value of concrete strength.

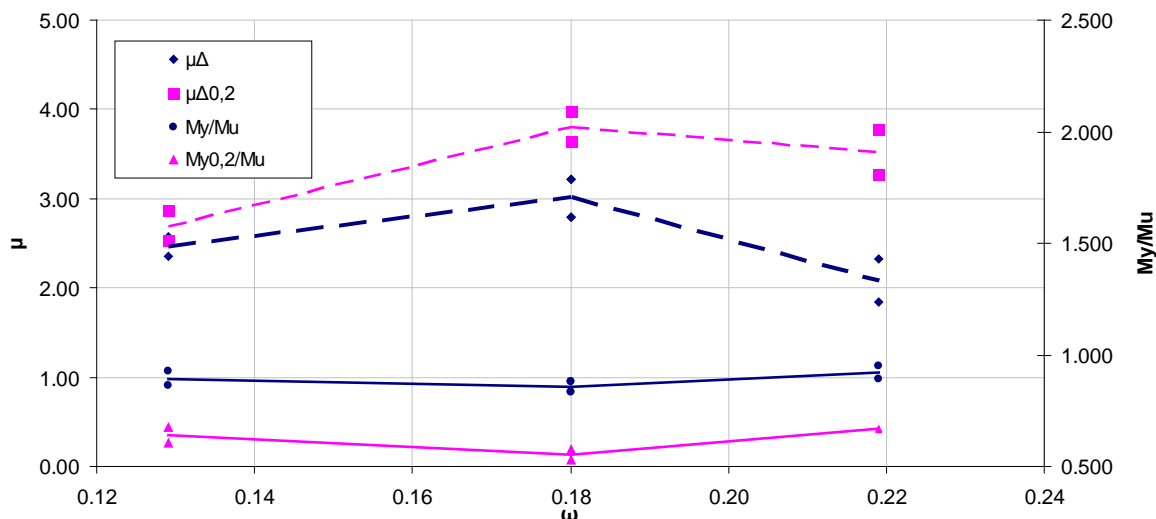


Figure 3 – Displacement ductility-mechanical reinforcement coefficient

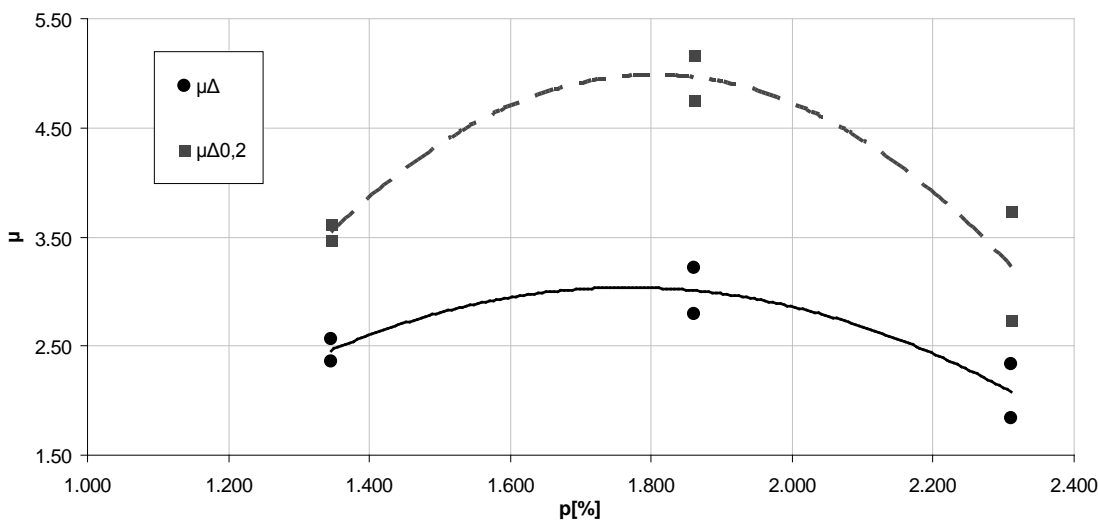


Figure 4 – Displacement ductility-reinforcement percentage relationship

It can be observed from Figure 3 two behaviour patterns considering ductility in relation with mechanical coefficient of reinforcement ω :

- for values of $\omega \leq 0.19$ ($p \leq 2.0\%$), the two ductility defined ($\mu_{\Delta 0,2}$ and μ_{Δ}) are rising with mechanical coefficient of reinforcement ω or reinforcement percentage p ;
- for values of $\omega > 0.19$ ($p > 2.0\%$), the two ductility defined ($\mu_{\Delta 0,2}$ and μ_{Δ}) are shrinking with the rise of coefficient of reinforcement ω or reinforcement percentage p .

This behaviour is also presentment considering the influence of reinforcement percentage p , in Figure 4. It can be observed the same behaviour type like in case of mechanical coefficient of reinforcement.

Displacement ductility index is situated between 3.5-4.75 for μ_{Δ} and 2-3 for $\mu_{\Delta 0,2}$ [1].

CONCLUSIONS

Linear behaviour is observed in case of high strength concrete beams realized with steel type S500 up to 85% of failure load and good post-elastic behaviour regarding flexure displacement.

Ductility displacement index is growing up to about 1.85-2.00% reinforcement percentage p , and then an opposite behaviour is observed.

Optimal behaviour regarding ductility index is obtained for a value of about 0.180-0.200 of mechanical reinforcement percentage ω .

Flexure displacement ductility index at failure is about 3.5-4.75, resulting in good ductility for high strength concrete beams, dismissing the theory of sudden failure (explosive failure) of high strength concrete. This is not the case for reinforced concrete elements subjected to flexure.

ACKNOWLEDGEMENTS

The research that is the subject of this paper was funded by CNCSIS Romania, through the PNII program, CNCSIS Code TD_280, for which the authors gratefully acknowledge this support.

REFERENCES

1. Heghes, B., "Ductility of high strength concrete – PhD Thesis", Technical University of Cluj Napoca, Romania, 2008.
2. Magureanu, C., Heghes B., Negrutiu, C., "Deformability of high strength concrete elements", Conferința Națională Tehnico-Științifică "Tehnologii Moderne pentru Mileniul III, Oradea, 5-6 noiembrie 2010, publiche on Analele Universității din Oradea, Fascicula Construcții și Instalații Hidroedilitare, ISSN 1454-4067, Vol. XIII-2, Supliment 1, pp. 249-254.
3. Heghes, B., "Deformabilitatea grinzilor realizate cu betoși otel de inalta performanta", National Symposium: Noile reglementari pentru beton, Bucuresti, 2009.

Session B6 – NUCLEAR AND FIRE SAFETY

Concrete and Fire – Swedish Recommendations for Preventing Spalling in Civil Engineering Structures



Johan Silfwerbrand
Professor, Managing Director
Swedish Cement & Concrete Research Institute
Drottning Kristinas väg 26
SE-100 44 Stockholm
johan.silfwerbrand@cbi.se

ABSTRACT

Explosive spalling may occur in moist, impermeable concrete structures exposed to fire. In 2003, the Swedish Concrete Association established a committee to develop recommendations for preventing explosive spalling in concrete structures exposed to fire. The recommendations contain both a chart indicating when polypropylene fibres or other measures are needed in order to prevent spalling and a table expressing the amount of fibres needed for different cases. The recommendations are limited to civil engineering structures with a focus on concrete members in tunnels where the need for recommendations is most urgent. The recommendation report is concluded with a list of research needs.

Key words: Concrete, fire, polypropylene fibres, spalling, recommendations.

1. INTRODUCTION

Concrete is a material that have good fire properties, superior to timber, steel, and asphalt. However, recent fires in the tunnels through Great Belt, English Channel, and Mont Blanc have shown that spalling may occur in moist, impermeable concrete structures exposed to fire. The deterioration process leads to reduction of the cross section, spalling of the concrete cover, and exposure of the reinforcement. If the fire has direct access to the reinforcement, the reinforcement temperature is increased dramatically leading to a substantial strength decrease. Present knowledge implies that conventional concrete usually does not spall whereas high performance concrete (HPC) and self-compacting concrete (SCC) usually do since they normally are impermeable. An increased use of HPC and SCC demands more research in this area and recommendations to prevent explosive spalling. In 2003, the Swedish Concrete Association established a committee to develop recommendations for preventing explosive spalling in concrete structures exposed to fire. In May 2004, the committee published the first preliminary recommendations [1]. From 2004, the committee has carefully followed the progress of two large experimental research programs on concrete exposed to fire. The test results were available in 2008, and the committee has used them to develop the recommendations [2].

2. SUMMARY OF RESEARCH RESULTS

Fire Technology at SP Technical Research Institute of Sweden has conducted several fire test projects during recent years [3-8]. Since the problem of fire spalling has been identified in

modern tunnels where high performance concrete and self-compacting concrete have been used, the projects have also been focused on these types of concrete. A total of more than 300 small and 60 large test specimens of more than 50 different cement mixes have been tested. This paper is too short for providing a detailed summary. However, we know that several factors influence the risk and magnitude of fire spalling of concrete. The following ones have been identified as most important:

- Moisture content (higher content increases spalling)
- Permeability usually expressed as w/c or an equivalent w/c (lower w/c increases spalling)
- Powder content (powder: particles < 0.063 mm, higher content increases spalling)
- Compressive stresses (also small stresses increase spalling)

Experience shows that conventional concrete of strength class C25/30 and lower (i.e., approx. equivalent $w/c > 0.60$), containing conventional cement for housing (in Sweden: CEM II/A-LL) without supplement of limestone filler, does not spall if cured indoors during 6 months. For conventional concrete, there is threshold value for the moisture content equal to approximately 3 % [9-10]. Beyond this value, there is no spalling. The problem with dense concrete (HPS and SCC) is that the time to obtain such a value takes very long time, in [5, 8], more than 12 months were not sufficient. The critical powder content in the concrete is dependent on several factors and is difficult to determine. Increased powder content leads to a denser concrete with less permeability for water and vapour in turn resulting in increased spalling risk. This was obvious in a test series on columns [3]. In the preliminary recommendations [1], compressive stresses up to 15 MPa were never considered as a problem. However, in the new fire test results [5, 8] spalling was obtained also at lower stress levels. Tensioned concrete specimens and unloaded specimens are significantly less prone to spalling.

3. RECOMMENDATIONS

The recommendations are limited to concrete members in civil engineering structures. The reasons are (i) that tunnel fires have triggered the question on spalling, (ii) that there is no indication of any severe fire spalling in concrete buildings, and (iii) that the fire tests have been focused on concrete for civil engineering structures. All concrete structures for civil engineering structures are not vulnerable to fire spalling. Four exceptions have been identified (Table 1).

Table 1 – Cases where fire spalling can be neglected.

Case No.	Description	Example
I	The risk of fire can be excluded or is negligible.	Dam structures in contact with water.
II	The concrete structure will – at least in a long-term perspective – desiccates to a state defined by a moisture content below 3 %.	Thin concrete members in an arid climate.
III	The consequences of fire spalling, if any, are negligible.	Concrete members that are reinforced or detailed in such a way that spalling of the concrete cover can be accepted. Concrete bridges may belong to this group.
IV	The risk of human injuries due to debris from fire spalled concrete is negligible or non-existing.	Concrete pavements.

Based on the test results, a flow chart has been drawn (Figure 1). It defines the cases where measures are needed in order to prevent spalling. The addition of polypropylene fibres is likely to be cost-efficient and the most common measure, but there are also other alternatives: thermal insulation, special investigation, and fire testing. If polypropylene fibres are selected, Table 2 shows required content. This content is dependent on security class, economical, environmental and societal consequences, equivalent w/c , and powder content. Automatic control of the fibre dosage is encouraged.

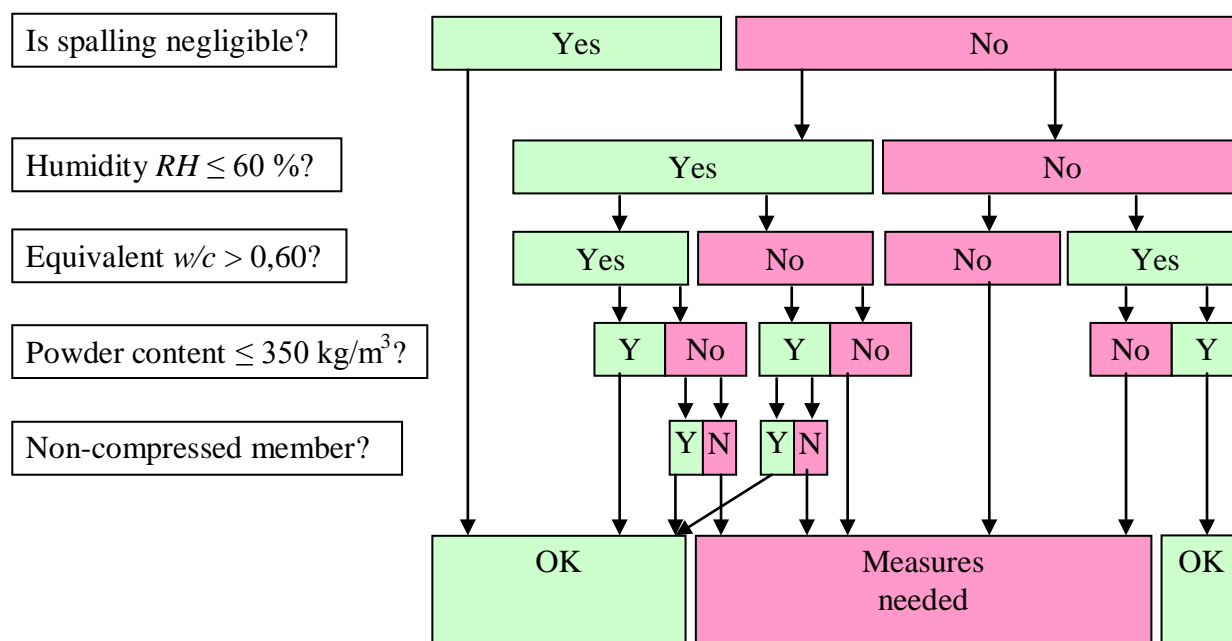


Figure 1 – Flow cart showing when polypropylene fibres, other measures or a special investigation are needed to prevent fire spalling or guarantee that fire spalling cannot occur.

Table 2 – Required minimum polypropylene fibre content (in kg/m^3) to prevent spalling.

Does the actual case belong to any of the cases I-IV above?	Security class	Economical, environmental or societal consequences	Equivalent w/c			
			0.50 – 0.60		< 0.50	
			Powder content $\leq 350 \text{ kg/m}^3$	Powder content $> 350 \text{ kg/m}^3$	Powder content $\leq 350 \text{ kg/m}^3$	Powder content $> 350 \text{ kg/m}^3$
Yes	1 – 3	Minor to major	0	0	0	0
No	1	Minor	0	1.0	1.0	1.0
No	2	Moderate	1.0	1.0*	1.0*	1.4*
No	2	Major	1.0	1.0*	1.0*	1.4*
No	3	Moderate	1.0*	1.4*	1.4*	Other measures**
No	3	Major	1.4*	Other measures**	Other measures**	Other measures**

* The amount of fibres has to be guaranteed by using automatic dosage equipment an adequate quality assurance system. If not the amounts have to be increase with 0.3 kg/m^3 to 1.3 and 1.7 kg/m^3 , respectively.

** Other measures are needed, e.g., fire testing according to EN 1363-1 of the candidate concrete, insulating and fire testing, or a special investigation according to an agreement between client, material producer, and contractor.

4. RESEARCH NEEDS

Among 14 identified research needs, the following ones ought to be mentioned: (i) the mechanism and causes of spalling in concrete with or without polypropylene fibres and the influence on spalling of (ii) moisture content, (iii) reinforcement, (iv) air content, and (v) filler content (especially fillers other than limestone). Investigations on moisture content effects have to be conducted on concrete specimens with representative cross sections and modern mixes. The specimens have to be cured sufficiently long in order to reach moisture contents close to 3 %.

5. CONCLUDING REMARKS

The Swedish Concrete Association has developed recommendations for preventing fire spalling in concrete for civil engineering structures. For the first time, there are recommendations providing required polypropylene fibre contents for different cases. More research is needed in order to generalize the recommendations to buildings and to study effects of moisture content, reinforcement, air content, and various fillers.

REFERENCES

1. Swedish Concrete Association: "Preliminary Recommendations to Prevent Explosive Spalling in Concrete Structures Subjected to Fire". The journal *Betong*, No. 2, May 2004, pp. 21-24. (In Swedish).
2. Swedish Concrete Association: "Concrete and Fire. Recommendations to Prevent Spalling in Civil Engineering Structures". Concrete Report No. 16, 2011. Interimistic edition.
3. Boström, L., "The Performance of Some Self Compacting Concretes when Exposed to Fire". SP Report No. 2002:23, SP Fire Technology, Borås, Sweden, 2002.
4. Boström, L., "Innovative Self-Compacting Concrete – Development of Test Methodology for Determination of Fire Spalling". SP Report 2004:06, SP Fire Technology, Borås, Sweden, 2004.
5. Boström, L., & Jansson, R., "Self-compacting Concrete Exposed to Fire". SP Report 2008:53, SP Fire Technology, Borås, Sweden, 2008.
6. Jansson, R., "Material Properties Related to Fire Spalling of Concrete". Licentiate Thesis, Report TVBM-3143, Lund Institute of Technology, Div. of Building Materials, Lund, Sweden, 2008.
7. Jansson, R., & Boström, L., "Spalling of Concrete Exposed to Fire". SP Report 2008:52, SP Fire Technology, Borås, Sweden, 2008.
8. Nilsson, H., & Saleh I., "Self-Compacting Concrete with Good Fire Spalling Properties – Final Report". SBUF Reports 11522, 11801 and 12013, Brandforskprojekt 331-041 & 301-061, SBUF, Stockholm, Sweden, 2009. (In Swedish).
9. Meyer-Ottens, C., "The Question of Spalling of Concrete Structural Elements of Standard Concrete under Fire Loading". PhD Thesis, Technical University of Braunschweig, Braunschweig, Germany, 1972.
10. Copier, W. J., "The Spalling of Normalweight and Lightweight Concrete on Exposure to Fire". *Heron*, Vol. 24, No. 2, 1979, pp. 1-92.

Ageing of Cementitious Materials for Storage of Nuclear Waste



Arezou Babaahmadi
PhD candidate
Division of Building
Technology
Chalmers University of
Technology
SE-412 96 Gothenburg,
Sweden
Arezou.babaahmadi@chalmers.se



Tang Luping
Professor
Division of Building
Technology
Chalmers University of
Technology
SE-412 96 Gothenburg,
Sweden
tang.luping@chalmers.se



Zareen Abbas
Associate Professor
Department of Chemistry
University of Gothenburg
Kemivägen 4,
SE-412 96, Gothenburg,
Sweden
zareen@chem.gu.se



Gunnar Gustafson
Professor
Department of Geology
and Geotechnics
Chalmers University of
Technology
S-412 96 Gothenburg,
Sweden
gunnar.gustafson@chalmers.se

ABSTRACT

This paper presents an on-going research project dealing with ageing process of cementitious materials in a perspective of hundreds and thousands years. As it is risky to use empirical models for extrapolation of performance data from relatively short term experiments, a mechanism-based (chemo-mechanical coupled) model for safer prediction of longevity of concrete in storage facilities for nuclear waste is needed. The project work involves thermodynamic modeling, development of accelerated aging tests, physical, chemical and mineralogical characterization of young and aged cementitious materials, including mechanical, transport (diffusivity) properties, binding (adsorption) capacities and surface complexation (charging) behavior.

Key words: Ageing, cement, concrete, diffusion, leaching, nuclear waste

1. INTRODUCTION

Deposition of low and intermediate level radioactive waste (LILW), involves processes with duration of up to 100000 years. Radioactive ions having long half life, especially ^{14}C , can contaminate the groundwater if leached from the repository. The repository for nuclear waste in Sweden is called SFR and is situated under the Baltic in Forsmark. It has a building structure with extensive use of concrete. Performance analysis as well expansion plans regarding this facility involves understanding of the longevity of concrete structures.

Study of the service life prediction of concrete structures has been a major topic since 1980's [1-3]. However, it has been limited to durability analysis of normal concrete structures designed with a service life not more than hundred years such as bridges, tunnels, nuclear power plants, etc. Empirical modifications based on experience and predictions cannot provide understanding of physical or chemical processes such as internal and external diffusion of ions, interaction between these ions and re-deposition of the interacted products. A recent review of service life modelling can be found in the state-of-the-art report of RILEM TC 205-DSC "Durability of self-compacting concrete [4]. There are also computational models in which thermodynamic and mechanical equilibrium are coupled [5-7], but model based predictions cannot be verified due to uncertainties in the input data. A mechanism based approach using PhreeqC with the tool box of multi-component diffusion (MCD), has been used to model the long time stability of the engineered barriers of SFR including concrete and the surroundings [8]. However, the input parameters used in that study were preliminary. In this paper the overall thoughts and plans regarding an ongoing project dealing with ageing of cementitious materials are discussed. This project aims to combine thermodynamic modelling results with good quality input parameters in order to correlate the modelled outputs to the mechanical behaviour of concrete.

2. METHODOLOGY

Experimental and modelling plans in this project are directed towards compensating the lack of valid data and information regarding longevity of concrete structures. A brief summary about some of the preliminary experiments and the ideas behind them is presented below.

2.1. Accelerating hydration process

In order to accelerate the hydration process of cement particles in concrete specimens it is possible to use elevated temperatures (oven cured) or microwave treatment. These methods are often used as of accelerating the early strength but not the durability since they cause coarser pore structure and micro-cracks. Elevated temperatures don't have accelerating factor more than 2-3 according to Arrhenius law since the temperature has to be below 50-60°C in order to avoid the substantial changes in the structure of hydrates. On the other hand through microwave treatment 28 days strength of cement and mortar cured at 40°C for 120 min or 60°C for 48 min can be reached without degradation of specimens [9]. An experiment using a 3D microwave oven (JT 366, Whirlpool), is designed in a way that the optimized power and duration of microwave curing while keeping the temperature less than 50-60°C can be attained. Thermo couples are embedded inside three dummy specimens and placed at the centre and also at about 20-30 mm from the bottom of the specimens. Specimens are immersed in the water to keep water saturation during treatment and also as of having a thermal buffer to reduce the possible temperature fluctuations. The aged specimens can be used in other chemical or electrochemical tests without waiting for a long time of curing hydration.

2.2. Accelerated ageing tests

Two Effective factors enhancing the dissolution of solid phase and degrading the solid cement matrix are pH and surface area. The pH-stat leaching test is designed to enhance the dissolution of solid matrix in a controlled way at a specific pH. This is a possibly quick way to finding information regarding chemical and mineralogical compositions of cementitious materials at different aged stages (different pH conditions). The test involves using fine particles in a

solution with constant pH so as to release ions like Ca^{2+} , in the sample. Paste specimens cured for about 6 months were ground to the powder with size of about 0.1 mm (0.075-0.125) under non- CO_2 condition (wet crushing, grinding, sieving and afterwards vacuum drying). The powder is stored in the sealed container with CO_2 absorbent until the test with the solutions of pH 12, 10 and 8. The pH of the solution is adjusted by adding nitric acid to the solution, which is controlled by computer software called TIAMO. After the equilibrium (no further addition of acid solution is needed) the solid material will be separated from the solution by filtering. The filtrate will be analyzed for cations and anions by ICP and IC, respectively. The solid material will be analyzed for chemical and mineralogical compositions by X-ray diffraction and IR. The remained solid parts will be analyzed for chemical and mineralogical compositions by X-ray diffraction and IR.

Moreover a flush column leaching test was designed to accelerate the leaching of cement paste particles of 0.075-0.125 mm in a flash column with a water flow through the column from the bottom to the top so as to try to make the particles under the suspension condition. Demineralised water and groundwater from the real exposure field will be used in the test under the circulated flow system with the liquid volume of 5 litres. When the pH in the circulated water is over 10, the water will be refreshed and the replaced water will be analyzed for cations and anions in the similar way as in the pH-stat leaching test. After the equilibrium (no more increase in pH), the remained solid parts will be analyzed for chemical and mineralogical compositions in the similar way as in the pH-stat leaching test.

Another leaching experiment is to use external electrical field in order to accelerate leaching of Ca^{2+} ions. Migration test is done using cement specimens with the size of $\text{Ø}50 \times 50\text{-}75$ mm under the potential of 60-100 V DC. Lithium ions are used to substitute the leached calcium ions in the pore solution in order to keep the electrical neutrality of the pore solution. The calcium content in the downstream solution will be monitored until the stage that no significant increase in calcium ions is observed. The specimens will then be analyzed for profiles chemical and mineralogical compositions which will be compared with those from the pH-stat and the flash column leaching tests. In this way, aged specimens with reasonably large sizes can be produced for testing mechanical properties as well as transport properties such as diffusivity and permeability.

2.3. Diffusion test

It is hard to model the real world conditions without information regarding actual diffusion coefficients of various ions. Long term immersion tests as well as natural diffusion cell test are implemented to reach this goal. Since the immersion test involves the effect of binding and adsorption, the results can be used for verification of the transport model incorporated in the thermodynamic model. The immersion test is done using paste and mortar specimens of diameter 46 mm coated with epoxy on all the surfaces except one and exposed to the groundwater in the real exposure field. The specimens will be analysed after 0.5, 1, 2 and 4 years for the profiles of chemical and mineralogical compositions in the specimens using LA-ICP-MS (laser ablation inductively coupled plasma mass spectrometry) and X-Ray.

Natural diffusion cell test will be used to determine the diffusion coefficients under both non-steady and steady state conditions. Cement paste and mortar specimens of diameter 50 mm cured over 6 months will be used in the test. Chloride solutions having the chloride concentration in the groundwater in the real exposure field will be used in one cell as upstream

and demineralised water in the other cell as downstream solution. The ionic concentrations in the downstream solution will be analyzed at certain intervals until reaching steady-state flow. The steady state diffusion coefficient can be obtained from the slope of the accumulative $c-t$ curve while the non-steady state diffusion coefficient can be obtained from the time-lag of the same $c-t$ curve. The results will be compared with those from the immersion test in order to establish the relationships between the laboratory diffusion coefficients and the profiles from the field exposure.

3. EXPECTED RESULTS

Knowledge concerning longevity of concrete structures such as ion diffusivity, ionic binding capacity, surface complexation, and mechanical behaviour of aged cementitious materials is expected to be improved through the outcomes of this ongoing project. Also test methods for accelerating aging process will be improved.

REFERENCES

1. Fagerlund, G., "Predicting the service life of concrete structures," proceedings of the Engineering Foundation Conference on Characterization and Performance Prediction of Cement and Concrete, united Engineering Trestees, Inc., New York, 1983.
2. Pommersheim, J., & Clifton, J., "Prediction of Concrete Service-Life," Materials and structures, Vol. 17, pp. 285-289.
3. Clifton, J., "Predicting the remaining service life of concrete," NISTIR-4712, U.S. Department of Commerce, national Institute of Standards and Technology, Gaithersburg, USA, 1991.
4. Tang, L., "Service Life Modeling in Durability of Self-Compacting Concrete," State of the art report of RILEM Technical committee 205-DSC, Edited by Greer De Schutter and Katrien Audenaert, RIREM Report 38, RILEM Publications S.A.R.L., 2007.
5. Maekawa, K., Ishida, T. and Kishi, T., "Multi-scale modelling of concrete performance", Integrated material and structural mechanics, J.Adv.Concr.Techn., Vol. 1, No. 2, 2003, pp. 91-126.
6. Kuhl, D., Banger, F. and Meschke, G., "Coupled chemo-mechanical deterioration of cementitious materials. Part I & II", Solid and Structures, Vol. 41, 2004, pp. 15-67.
7. Nguyen, V.H., Nedjar, B. and Torrenti, J.M., "Chemo-mechanical coupling coupling behaviour of leached concrete. Part II: Modelling." Nuclear Engineering and Design, Vol. 237, 2007, pp. 2090-2097.
8. Cronstrand, P., "Modelling the long-time stability of engineering barriers of SFR with respect to climate change", SKB report R-07-51, Swedish Nuclear Fuel Management Co, Stockholm.
9. Cement and Concrete Research 29. 1999. PP. 241-247.

Climatic Condition inside Nuclear Reactor Containments – A New PhD Project



Mikael Persson
M.Sc., Ph.D-Student.
Vattenfall Research & Development / Lund University, LTH
Älvkarleby Laboratory,
SE – 814 26 Älvkarleby
Mikael.Persson3@vattenfall.com

ABSTRACT

The climate conditions inside nuclear reactor containments depend on several parameters e.g. different moisture and heat sources; the containment design; material properties etc. Knowledge about the climatic condition is an important area to e.g. maintain a proper condition for mechanical and electrical equipment; minimize the corrosion risks of reinforcement and metallic components; prevent vapor condensations on thermal bridges; analysis of stress and strain conditions influenced by the drying shrinkage and temperature variations. This new PhD project will study how the concrete components affect and gets affected by the climatic conditions. This study will be done thru monitoring the temperature and relative humidity in the concrete, and in the surrounding air, during the plants operation.

Key words: Nuclear Power Plant, concrete, on-site measurements, RH & temperature.

1. INTRODUCTION

The climatic conditions inside the reactor containments on a Nuclear Power Plant (NPP) is of great significance and depends on e.g. what kinds of heat and moisture sources there are; the design of the reactor containment; material parameters and the ventilation system. The effect of the climate is of great importance for a number of reasons such as, maintaining an appropriate climate for mechanical and electrical devices; minimize corrosion risks on concrete reinforcement and metallic components; preventing vapour condensation on thermal bridges etc. The climatic conditions are also important when it comes to; analysing moisture- flow and fixations in the concrete; effects on the material parameters; the concrete shrinkage due to dehydration, and the stress and strain conditions due to that.

Today the climatic conditions inside the NPP are monitored and logged continuously e.g. is the air temperature, T, and relative humidity, RH, measured in different areas near important technical instruments. These measurement does not give a representative view of the whole containments due to their specific locations. The instruments used for this are seldom, or never, calibrated which leads to low accuracy of the data. This might not be a big problem if the T and RH trend in a certain area is of interest, but if the aim is to investigate the actual variations and what influence different components have on the overall climatic conditions this is not sufficient.

In the PhD project “Climatic Condition inside Nuclear Reactor Containments” a study will be done on what influence the concrete structures have on the overall climatic conditions and also

how the climatic conditions affects the concrete. For this, vast monitoring campaigns will be done on different containments, hopefully in both Sweden and Finland. The measurements will be done in areas that represent as much of the containment as possible. The biggest different between the ongoing measurements and the one's in this study is that besides measuring T and RH in the air the concrete it self will be studied. The measurements will be done in NPP of similar design and in different types; all measurements will be conducted during operation and during one operation year.

In Sweden and Finland there are (for the moment) three different types of NPP, Boiling Water Reactor (BWR), Pressurized Water Reactor (PWR) and Vodo-Vodyanoi Energeticheskoy Reactor (VVER), in operation. This project will only study the PWR and BWR reactors and it will focus on the structures inside the steel liner.

2. BACKGROUND

Previous work in this area have been done by Nilsson (2007) [1] and Nilsson, Johansson (2007, 2009) [2, 3]. In these studies the concrete on the outside of the steel liner have been in focus. The issues around the temperatures and climatic conditions, mostly the effect of it, have also been studied by Thorne (1961) [4] and Hora (2006) [5]. Hilsdorf (1967) [6] studied different ways to estimate the humidity levels in the concrete of a NPP. This study will follow the ideas from previous studies but with a focus on the actual conditions in the concrete and the volume inside the containment. With the result a model to predict past and future conditions will be establish.

The primary design differences between the (Nordic) BWR and PWR systems is that in a BWR the only key component that are located inside the concrete containment is the reactor vessel, contrary the PWR where almost all key components are placed within. Due to fewer components the total air volume of the containment is significantly lower for a BWR (c 12000 m³) [7] compared with a PWR (c 50000 m³). In spite of this big difference the relation between air volume and concrete is quite similar. A PWR consists of c 8000 m³ concrete inside of the steel liner and a BWR c 2000 m³, this leads to a relation of c 6-6.5 m³ air for 1m³ concrete. Another mayor difference is that the BWR consists of two volumes, Dry-Well and Wet-Well. The reactor vessel is placed in the Dry-Well and the Wet-Well holds water in a condensation basin. The water in Wet-Well has the purpose that, if the pressure inside the containment would raise the water in the basin will condensate and the pressure will decrease. The PWR only consists of one big volume and it dose not have a condensation basin.

The climates in the two types of containments have some differences. The Dry-Well, inside the BWR, is filled with Nitrogen and is expected to have a low humidity; measurements have despite this shown that the RH is around 40-50 %, the temperature is between 20-50 °C[3]. In Wet-Well the humidity should be quite high, due to the open water surface, and the temperature 20-40 °C. A PWR is filled with air and the temperature varies from approx. 20 °C in the lower levels and up to 45-50 °C in the highest [3]. The PWR dose not have any open water surfaces nether any large basins or external water sources, apart from the concrete and leaking from steam pipes.

3. OBJECTIVES

The main objective for this project is to develop a model that can quantify and predict future temperature and humidity conditions in any reactor containment. With the model it should also

be possible to predict consequences of e.g. a temperature increase in the containment due to an effect increase. Large monitoring campaigns will be done in different reactor containments to gather data to verify the model. Figure 1 illustrates a conceptual design of a PWR system with some expected conditions and moisture flows; figure 2 illustrates the same but for a BWR system.

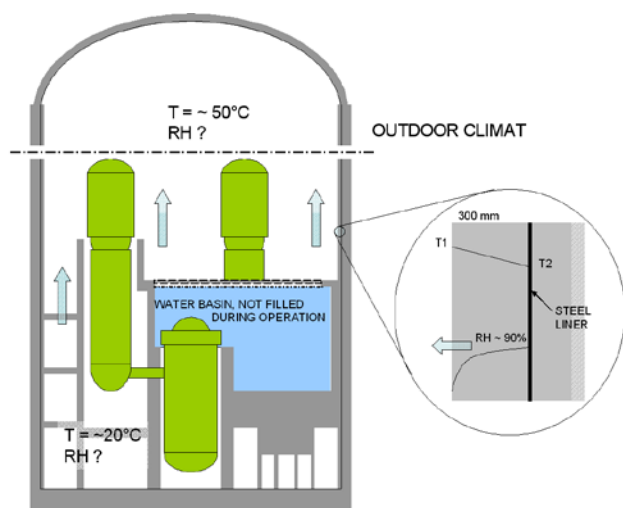


Figure 1 – Conceptual design of a PWR

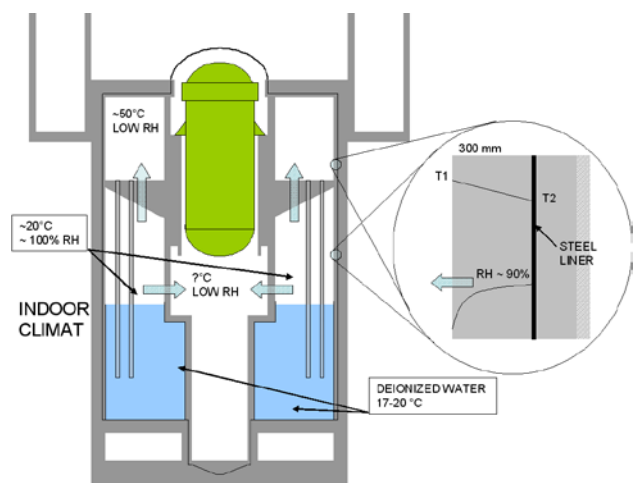


Figure 2 – Conceptual design of a BWR

4. PROJECT CONTENT

Several campaigns will be conducted and in each one a different NPP site will be monitored. Each campaign will go on for approximately one year, or one operation year. The measurements will be done on different heights and on each level the humidity and temperature will be monitored in the air and in the concrete on four depths. For these measurements RH&T probes from Vaisala will be used. All RH&T probes will be connected to a logger and data will be gathered ones every hour. The data from these measurements will verify the model and be the base to describe the variations; potential dehydration; moisture flow inside and through the concrete and to quantify what influence the concrete structures have on the over all climate conditions. Apart from the monitoring on the climatic conditions, for the model, crucial material parameters will be determined. The parameters are e.g. degree of hydration; diffusivity; moisture content; sorption and desorption -curves. In what extent these studies will be done

depends on the amount of concrete that is possible to use, this is due to the complexity to get concrete form the different facilities.

In the first campaign Ringhals in Sweden are planed to be studied. The goal is to do measurements on two of Ringhals NPP, R1 and R4. R1 is Ringhals only BWR, it was constructed in the beginning of the 1970th and it was put into operation in 1976. The second NPP in this campaign is R4 (sister reactor to R3) which is one of three PWR in Sweden and Finland, al located in Ringhals. It was constructed between 1974 and 1981 and put into operation in 1983. One of the main reasons why R4 was chosen is that the plants steam generators will be replaced during 2011. During this operation a 6*8 m³ concrete block, of the containment wall, will be removed and some of this concrete will be used to determine the material parameters which are of interest for the PhD project.

5. FUTURE STEPS and CONCLUDING REMARKS

Future steps in this project are to proceed with monitoring campaigns on other NPP sites in Sweden and Finland. Until the Licentiate, at least fore NPP:s will be studied and the data analysed. After licentiate, at least two more reactors should be monitored. Apart from the mathematical model that will be developed, the conditions and variations between the different plants will be identified and explained. The actual conditions will be compared with the as designed conditions and differences will be explained.

With this study it will be possible to describe the climatic conditions inside any reactor containment. No models of this kind are readely available today and it is of great significance for the maintenance, but also in case of new build. The project will also, with help of Nilsson's and Johansson's work [1, 2, 3], make it possible to describe the humidity and temperature variations through the entire containment wall – something that have not been possible before and is of great importance regarding e.g. relaxation of the tendons, due to dehydration and temperature variations in the concrete.

REFERENCES

1. Nilsson, L-O., "Drying of Reactor Containment Walls of Concrete During Past and Future Decades," Proceeding, The 19th International Conference on Structural Mechanics in Reactor Technology (SMiRT 19), Paper # DH01/3, Toronto, Canada, August 2007.
2. Johansson, P., Nilsson, L-O., "Climatic Conditions at the Surface of Concrete Containments – Examples for two BWR and PWR Reactors," Proceeding, The 19th International Conference on Structural Mechanics in Reactor Technology (SMiRT 19), Paper # DH01/2, Toronto, Canada, August 2007.
3. Nilsson, L-O., Johansson, P., "Förändringsprocesser I reaktorinneslutningar – Betongväggarnas klimatförhållanden och uttorkning," Elforsk rapport 09:100 (In Swedish), Elforsk, Stockholm, Sweden, September 2009.
4. Thorne, C.P., "Concrete Properties Relevant to Reactor Shield Behavior," *Journal of the American Concrete Institute*, Vol. 32, No. 57-66, 1961, pp. 1491-1507.
5. Hora, Z., & Patzák, B., "Analysis of Long-term Behavior of Nuclear Reactor Containment," *Nuclear Engineering and Design*, Vol. 237, 2007, pp. 253-259.
6. Hilsdorf, H.K., "A Method to Estimate the Water Content of Concrete Shields," *Nuclear Engineering and Design*, Vol. 6, 1967, pp. 251-263.
7. Picaut, J., et.al., "Nuclear Containments," Bulletin No. 13, Fédération Internationale du Béton (fib), Lausanne, Switzerland, June 2001, ISBN 2-88394-053-3, pp 24.

Nonlinear Analysis of Pre-stressed Concrete Nuclear Containments



Jan Cervenka
 Ing., Ph.D.
 Cervenka Consulting
 Prague
 Czech Republic
 jan.cervenka@cervenka.cz

ABSTRACT

Nuclear containments need to satisfy strong safety requirements that can be verified by modern numerical techniques, such as nonlinear analysis. Nonlinear analysis can provide useful information about the overall structural capacity and reliability. Cervenka Consulting in Prague, Czech Republic develops software tools and technologies for numerical simulation of concrete structures subjected to actions due to mechanical and physical effects. Nonlinear behaviour of concrete is modelled by theories of damage and plastic flow. Numerical simulation is applied to design and safety assessment of pre-stressed concrete containments in nuclear power plants.

Key words: Containment analysis and design, nonlinear analysis, finite element analysis, reinforced concrete modelling

1. INTRODUCTION

Numerical simulation of reinforced concrete structures must reflect all typical features exhibited by brittle cementitious materials, reinforcement and their interactions due to bond. The numerical model of reinforced concrete is usually complex, and is a result of various approximations. It is essential to employ a balanced approximation approach, in which the resulting response guarantees a good agreement with the real behaviour. This can be assured by a quality control system based on validation. Such validation should include comparison with experiments, blind bench mark tests, effects of numerical methods, namely criteria for iterative procedures and mesh sensitivity.

Validation as well as the main aspects of the concrete material model is discussed in more detail in Červenka & Pappanikolaou (2008) [1]. This paper presents several applications of ATENA to containment analysis and design.

2. NON-LINEAR ANALYSIS OF CONTAINMENT STRUCTURES

Model containment in the scale of 1:4 was tested in BARC laboratories in India, (Figure 1), in order to provide data for validation of analysis methods and software for design of containments in NPP. The numerical model of the test containment is shown in Figure 1 (right). The analysis was performed for a test under increasing internal air pressure up to failure. Figure 2 shows the deformed shape and cracks at maximum pressure. This figure also depicts the unique capabilities of the software for realistic visualization of material cracking. The load-displacement diagram of the test is shown in Figure 2. The ultimate pressure is determined mainly by yielding of pre-stressing cables and reinforcement near openings. The global safety factor obtained by the analysis was 3.2 times the design pressure of 0.14 MPa. The results of the

analysis will be compared with the results of test, to be performed during the year 2011 at BARC laboratories.



Figure 1 - Model containment tested in BARC (left) and its numerical model (right).

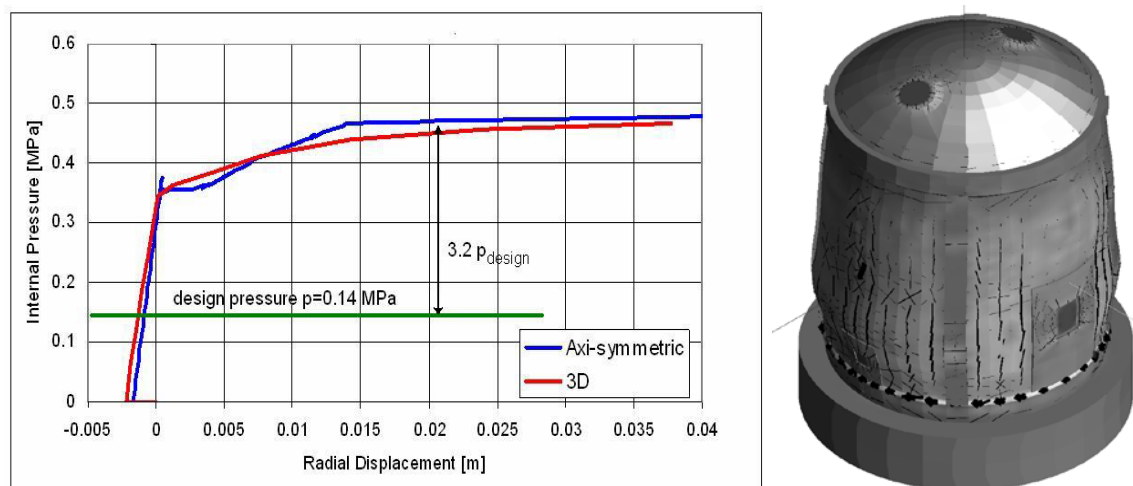


Figure 2 - Diagram of the pressure-radial displacement. Deformed shape at failure.

Efficient numerical model combines various finite element types. Walls and dome are modelled by special three-dimensional layered shell elements, which allow a significant reduction of the model size, while maintaining very good approximation of the stress state. The vertical ribs and the ring for anchoring of pre-stressing cables and the foundation slab are modelled by high order solid elements. Two types of models are used for reinforcement. Ordinary non-pre-stressed reinforcement is modelled by smeared reinforcement and for pre-stressing cables a discrete bar element is used. Altogether the numerical model consisted in this case of 17031 elements, which made it possible to perform a global containment analysis in reasonable time with sufficient accuracy.

In addition to global analysis some construction details need to be verified during containment design. Figure 3 shows an example of liner anchoring from a containment in northern Europe, which was used to investigate fastening function of the anchoring elements. In such analysis, two safety checks were performed. First nonlinear strains in the liner are verified to meet certain design requirements, and second goal is to calculate and verify the forces acting on the anchoring elements.

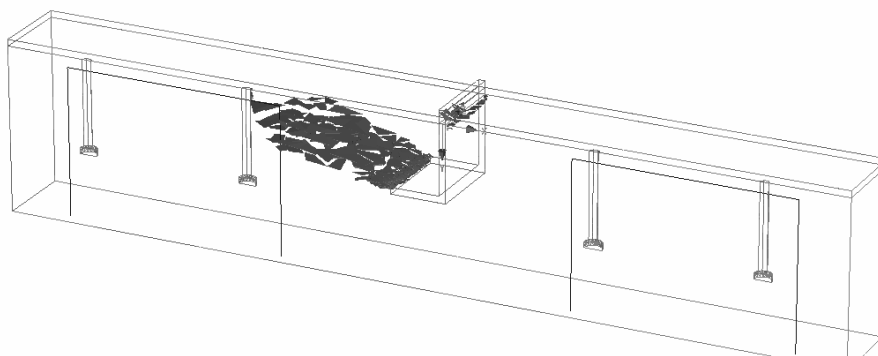


Figure 3 - Numerical model and cracks for liner anchoring analysis.

In case of NPP Crystal River 3 containment in the USA significant de-lamination cracks were observed after shut down and technological changes after 33 years in service (Figure 3). Similar damage occurred during construction in 1976, Moreadith at al. 1983 [2]. For a change of steam generator equipment in 2009 a part of containment wall was cut out and some cables were disengaged. After this a crack up to 40mm wide and parallel with containment surface occurred. The investigation effort was lead by Performance Improvement International, California. ATENA analysis was used to simulate crack propagation near the cable ducts. Cracks were caused by simultaneous effects of several actions: stress gradients due to temperature, low-cycle fatigue, low concrete quality and lack of transverse reinforcement. Damage due to cracks was estimated in an axially symmetrical model of cable ducts (Figure 5), and was consequently applied to global containment model illustrated in (Figure 6). In this case, the nonlinear analysis based on fracture mechanics of concrete proved to be a unique tool for the verification of causes of the de-lamination effect.



Figure 4 - Delamination crack in containment wall of NPP (photos www.tampabay.com).

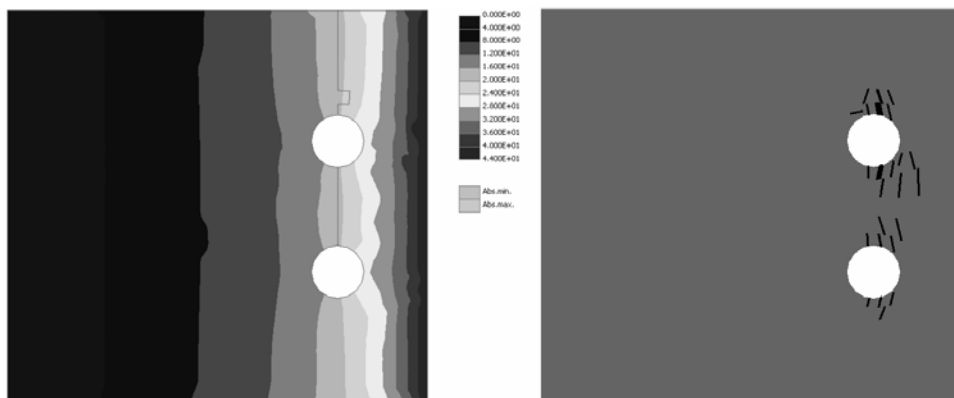


Figure 5 - Simulation of delamination cracks near cable ducts axially symmetrical analysis.

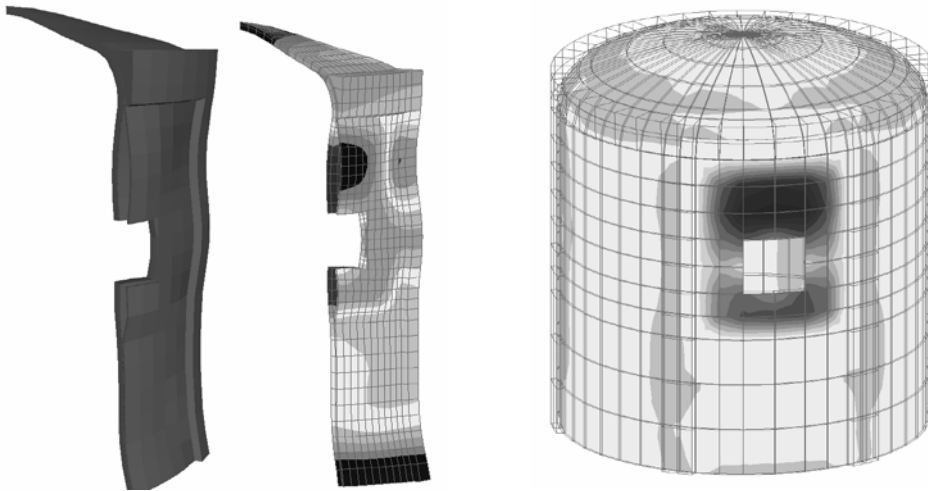


Figure 6 - Simulation of delamination cracks in containment

3 CONCLUSIONS

The article summarizes the application of the finite element software ATENA for the safety assessment of nuclear containment structures. In the modern design approach, it is becoming a standard procedure to verify the structural safety by a nonlinear simulation. This is especially necessary for structures requiring high safety margin such as nuclear containments.

The nonlinear simulation is a global assessment approach, which requires an application of global safety formats. Such formats are now becoming available in modern design standards such as for instance Eurocodes or the new model code from fib (fib – model code 2010) [3].

ATENA software supports these modern design approaches, and has been specifically developed for the analysis of reinforced concrete structures with strong emphasis on easy and robust modelling of reinforcement. The material models for concrete are designed to capture the main aspect of the brittle material behaviour, and are extensively tested by experiments and blind prediction competitions.

In the presented practical examples, ATENA also proved to be a useful tool for the analysis of pre-stressed containment structures.

The modelling approach was in part developed within the research project P105/10/1156, COMOCOS, Complex modelling of concrete structure, supported by the Czech Grant Agency.

REFERENCES

1. Cervenka, J., Papanikolaou, V. 2008, Three-dimensional combined fracture-plastic material model for concrete. Int. J. of Plasticity, Vol. 24, 12, 2008, ISSN 0749-6419, pp. 2192-2220
2. Moreadith, F., Pages, R.E., - Delaminated Pre-stressed Concrete Dome: Investigation and Repair, Journal of Structural Engineering, vol. 109, no. 5, 1983, pp. 1235-1249
3. fib – Model Code 2010, federation internationale du beton, 2010, bulletin 56, ISBN 978-2-88394-096-3

Session B7 – MAINTENANCE AND RENOVATION

Moisture Control in Concrete Bridges



Torsten Lunabba
M.Sc., Lic. Tech..
Destia Oy
Heidehofintie 2
FI - 01301 Vantaa
torsten.lunabba@destia.fi



Hemming Paroll
M. Sc., (Physics)
Westendintie 93 C
FI - 02160 Espoo
hemming.paroll@kolumbus.fi

ABSTRACT

Several methods have been used for moisture monitoring in concrete bridges; Sampling, measuring absolute humidity using gauges or optic fibres and measuring the relative humidity in concrete pores with resistive sensors. The capacitive sensors need stable conditions and are therefore not suited for outdoor conditions. Optic fibres provide a reliable method to determine absolute humidity at a certain time for the entire bridge. Resistive sensors provide an efficient method for continuous monitoring. The relative humidity in concrete pores is strongly temperature dependent. Therefore, monitoring the relative humidity in concrete requires full understanding of the moisture – temperature equilibrium behaviour.

Key words: Moisture, monitoring, temperature, humidity, concrete bridge.

1. INTRODUCTION

1.1 General

The changes of relative humidity in a concrete structure are reversely proportional to the relative humidity of the outdoor air. In other words, the relative humidity in the concrete pores of a bridge increases with increasing temperature. This occurs due the vaporisation of the water capillary bonded to the pores and the capillary passages between the pores. The equilibrium curve for two concrete classes, one having the water cement ratio 0.7 and the other 0.4, were presented 1974 by Professor Sven Pihlajavaara /1/, figure 1. On the vertical axle of figure 1 the absolute mass-percent humidity rate has been replaced by the water content - cement paste ratio because moisture transfer happens only in the cement paste.

When the temperature goes up, the relative humidity is determined from figure 1 by reading from the corresponding temperature curve horizontally to the right along the same moisture content line. The horizontal direction follows from the condition that there is no change in the water content in a short time. From the curves of figure 1, it can be seen that the temperature has more impact on the relative humidity than on the change of the water content.

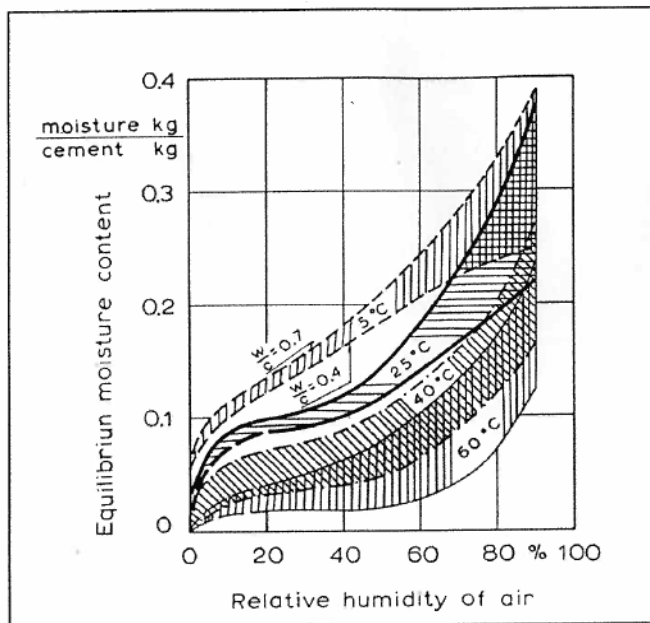


Figure 1 – Water content in cement paste – absolute humidity equilibrium curve. Sven Pihlajavaara /9/.

The relative humidity - temperature curves of the two concrete classes have been evaluated in figure 2 using the equilibrium curves of figure 1. The relative humidity of bridge concrete is assumed to be in equilibrium with the average relative humidity of the air that is 80 % RH at +5 °C. When the temperature rises to +35 °C or +45 °C, the relative humidity will rise to 100 % RH. The relative humidity rise in a concrete having a water cement ratio 0.4 is steeper than that having a water cement ratio 0.7.

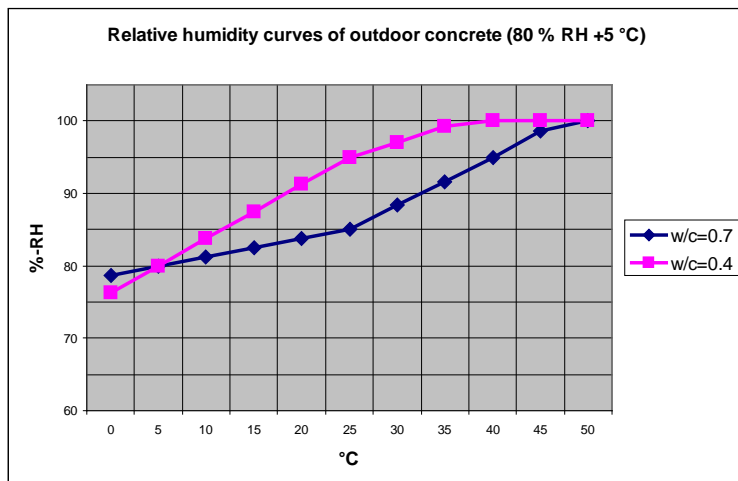


Figure 2 – Relative humidity – temperature curves evaluated from figure 1.

The curves of figure 1 and 2 require stable conditions, which can only be achieved during years after several watering and drying circles. In the initial stage the water content - relative humidity curve highly depends on whether the concrete is in an absorption (wetting) or a desorption (drying) stage, figure 3(a) and figure (3b). The lower line (blue) of figure 3(b) is starting at the left from a completely dry concrete. The line above (red) is starting at the right from a

completely wet concrete. When the two concretes have reached the balance with the outdoor air, that is some 80 % RH, there is a gap of almost 2 % between the two lines.

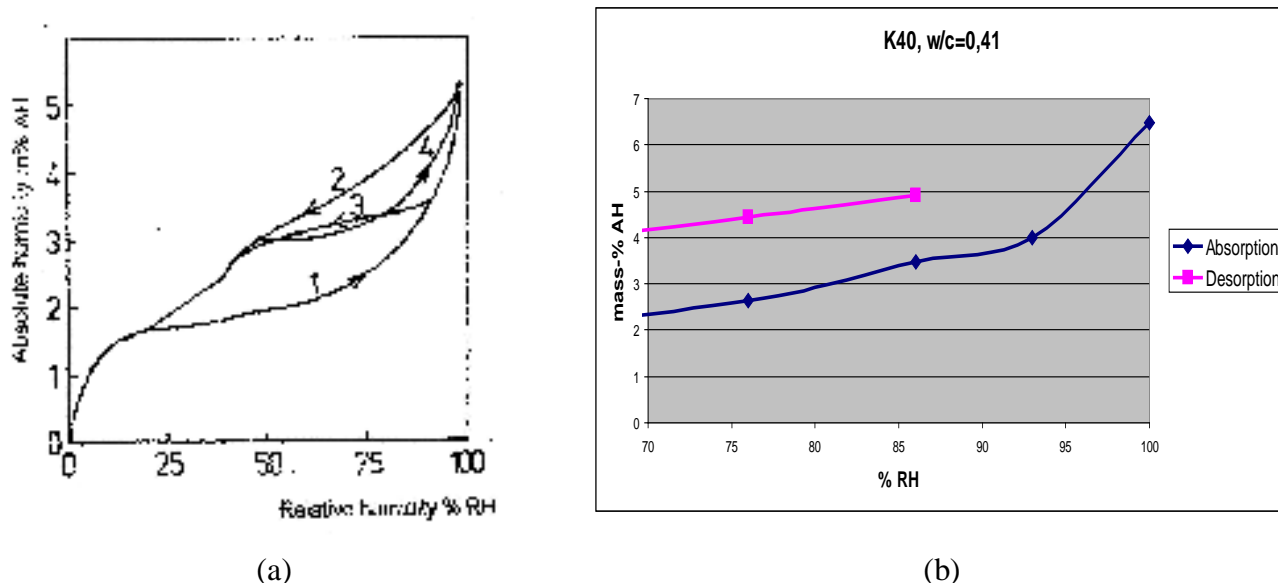


Figure 3 – Absolute humidity - Relative humidity equilibrium curves, figure (a) according to handbook /2/ and figure (b) according to Tampere University of Technology publication /6/.

2. MOISTURE MONITORING OF BRIDGES

2.1 New bridges

Moisture monitoring of new bridges reveals that the upper surface of the bridge deck is drying rapidly in good weather. However, this concerns only the top 10-20 mm layer. Obviously drying follows the red line of figure 3(b). The absolute humidity rate will remain high and the relative humidity will soon be back to 95-100 % RH after the waterproofing is laid, figure 4. There is risk of frost damages in the concrete under the water proofing.

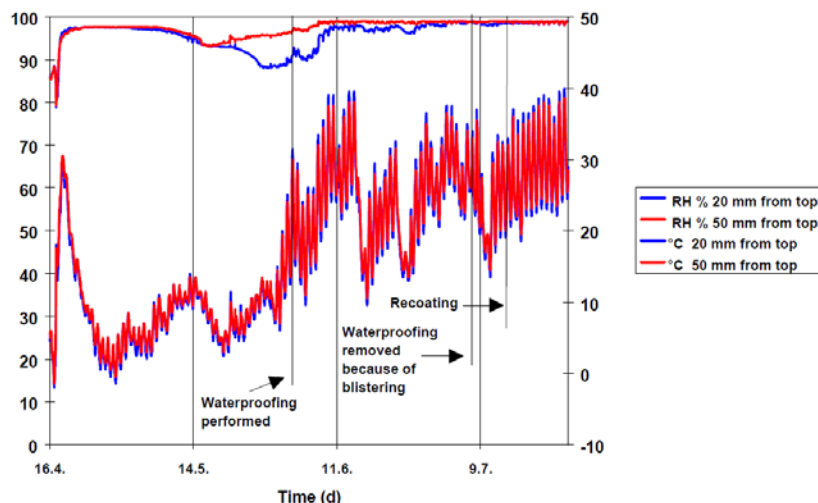


Figure 4 – Moisture content curves of Kasarminkatu bridge 1997. Temperature and RH rise caused blistering damage during moisture monitoring /4/.

2.2 Bridge repair

A renewal of bridge surface structures often necessitates a repair of the bridge deck top layer. A typical repair is comprised of a 30-50 mm layer of levelling concrete. By using low water – cement ratio concrete drying is guaranteed to a level as low as 3 mass-percent AH. However, this level is jeopardized due to capillary rise of water coming from the deck below, which has been wetted by water jet chiselling and rinsing.

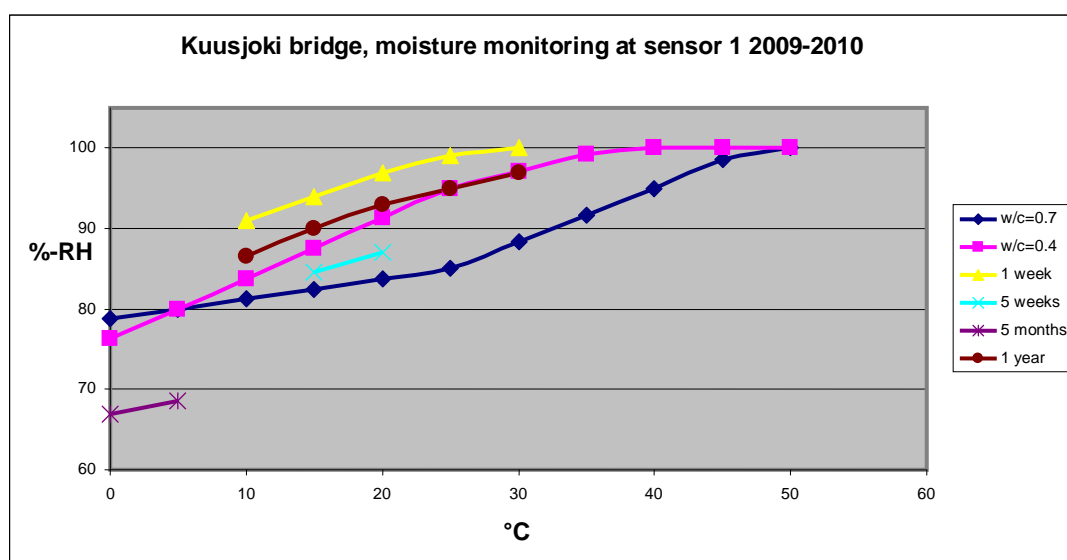


Figure 5 – Moisture content monitoring at Kuusjoki Bridge one week – one year after casting.

Moisture content monitoring by resistive sensors and optic fibres reveals there is an unintended fluctuation of the water content from one section to another [5]. The concrete mix is not always homogenous enough and particularly thin concrete layers are sensitive to excessive water from rain flow or from concrete below.

REFERENCES

1. Sven Pihlajavaara: Lecture on practical estimation of moisture content of drying concrete structures. Concrete seminar. Technical Research Centre of Finland. VTT. Helsinki. 1974b. 174 p. /10/.
2. Fukt-handbok. Lars Erik Nevander, Bengt Elmarsson. 3. upplagan, Svensk byggtjänst 1994.
3. Suhteellisen kosteuden ja lämpötilan mittaaminen uusilla betonisilloilla. Tutkimusraportti nro RTE4235/01. VTT 29.11.2001.
4. Measurement of relative humidity and temperature in new concrete bridges vs. laboratory samples. Hemming Paroll and Esa Nykänen. Nordic Concrete Research No. 21, 1998. p. 103-119.
5. SIMO/VTTV689706. TEKES 1819/31/06, SIMO/VTTV689706: Monitoring of Bridges. The Technical Research Centre of Finland (VTT) publication.
6. Ralf Lindberg, Jyrki Wahlman, Jommi Suonketo, Elina Paukku. Kosteusvirtatutkimus. Tampereen Teknillinen korkeakoulu, julkaisu 119, Talonrakennustekniikka, Rakennustekniikan osasto 2002.

Wireless Monitoring Sensor System for Tracking the Hydrothermal Behaviour and Deterioration of Building Structures



Mika Mäkitalo,
Special Researcher, Lic.Tech.
Aalto University School of
Engineering,
Department of Electronics.
mika.makitalo@aalto.fi



Fahim Al-Neshawy,
Senior Researcher, Lic.Tech.
Aalto University School of
Engineering,
Department of Civil and
Structural Engineering.
fahim.al-neshawy@aalto.fi



Tomi Laurila,
Project Manager,
Doctor in Tech.
Aalto University School of
Engineering,
Department of Electronics
ttlauril@cc.hut.fi,

ABSTRACT

The moisture is one of the main factors in deterioration of building materials. High moisture concentration will cause rapid physical, chemical and biological deterioration. The continuous monitoring of relative humidity, RH and temperature provides valuable information about the thermal and moisture behaviour of the buildings. The aim of this work is to develop a wireless moisture and temperature monitoring system for building structures and test the reliability of the sensors which are embedded inside the building materials. The study is focusing on the concrete building structures and consisting of laboratory work and field measurements.

Key words: Wireless, moisture, monitoring, concrete, sensor.

1. INTRODUCTION

Moisture is a major factor in physical chemical and biological deterioration processes of building materials. Physical deteriorations are typically caused by restrained moisture movements and freezing. Changes in the moisture and the temperature lead to the swelling and shrinking of the building materials. Chemical deteriorations will occur as a result of the reaction between the water and the cement based building materials. Biological deterioration is caused by a living organism which growth is determined by the levels of the RH and the temperature. Moisture will increase the heat flow through the building structures and thus increase the consumption of the energy. The continuous monitoring of the temperature and the relative humidity data provides a good piece of information about the performance of the building. Immediate actions can be done to prevent the expensive repair tasks if the system sends an alarm when the relative humidity exceeds a certain stress level [1].

2. MOISTURE MONITORING SYSTEM

The approach, which is taken in this research, is the placement of the sensors inside the building materials and the concept of automated and continuous moisture monitoring of the buildings. The required system needed to be different from the previously existing electronic hardware. The materials which are used in the devices need to be compatible with the building materials. This basically sets requirements for the protection of the device. The sensors must be designed for a long service time and they need to be well tested. The radio link needs to be suitable for transmitting and receiving through an appropriate distance of concrete. The energy source, which is needed for an active electronic device, needs to preserve and deliver energy for the sensor device for many years. The sensor device itself needs to be reliable for a long term usage. Picture of a final sensor (Railo-sensor) device is shown in Figure 1.

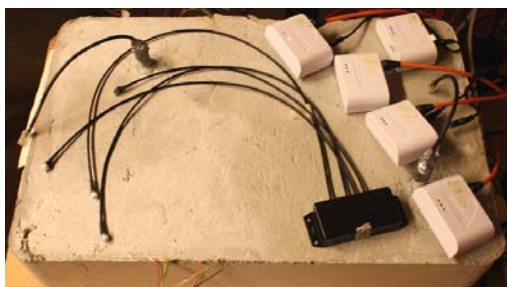


Figure 1. Picture of a Railo-sensor and the concrete slab which has one embedded unit.

2.1 Attenuation of the Radio Wave Inside the Concrete

Let's neglect the attenuation for the reflections from the concrete surface and the reflections for the surface angle. Electromagnetic wave simulators and measurements can be used to obtain accurate results. The setups and the results are shown in Figures 2-4. The selected BT-radios give 93 – 70 dBs for the radio link budget. The attenuation results are summarized in Table 1.

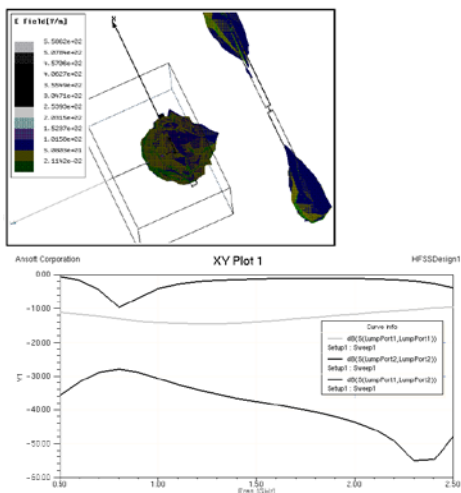


Figure 2. Simulation setup in HFSS.
Figure 4. Measurement setup

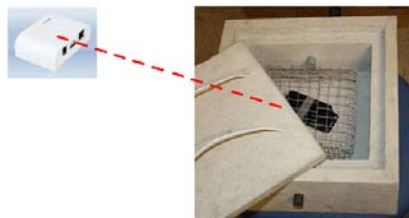


Figure 3. HFSS simulation results.

Table 1 – Attenuation of the 2,4 GHz radio wave in 2 cm of concrete.

Radio wave	Attenuation in 2cm of concrete [dB]	
	Simulated	Measured
almost dry	31*	20 – 30*
very wet	55*	na

* The results are from 2 cm of concrete. The system requirement is for 3 – 5 cm. The dipole antennas, which were used in the simulation, were properly matched for 900 MHz only (initial system specification).

2.2 Block Diagram of the Moisture Monitoring System

The moisture monitoring system is shown in Figure 5. The recharging device is shown in Figures 6 and 7. The device itself will instruct the user to locate the sensor units for finding an optimal charging position.

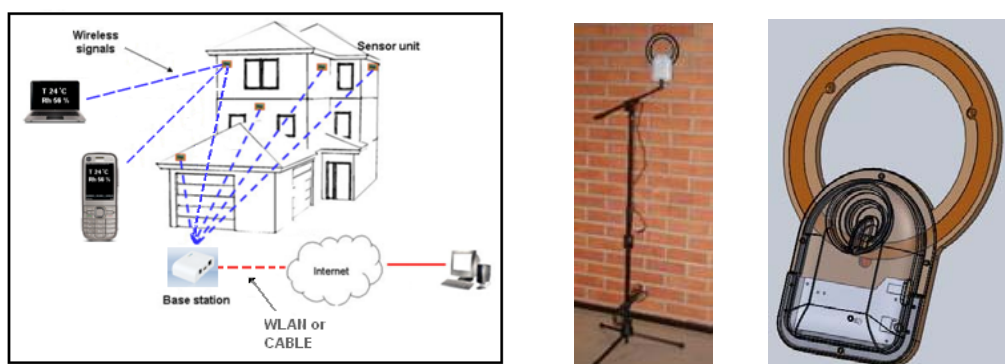


Figure 5. Block diagram of the moisture monitoring system.
Figures 6 and 7. Wireless recharging device.

3. PROPER PLACEMENT FOR THE HUMIDITY SENSORS

Some critical locations and short reasoning for the placements are listed in Table 2. At many locations several sensors are needed to map the moisture profiles and moisture differences as a function of location. Therefore 4 sensor elements were implemented for every wireless sensor device with 50–80 cm of extension cable. Locations inside the wall structures are shown in Figure 8.

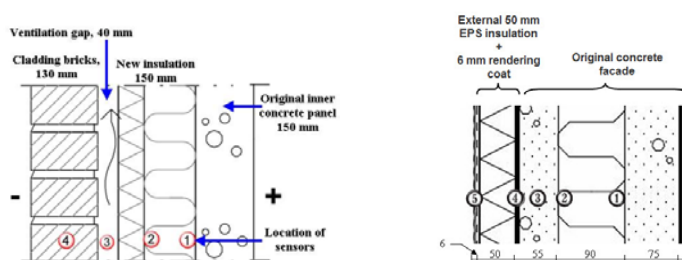


Figure 8. Examples of locations for the RH and temperature sensor elements which are installed inside the walls.

Table 2– Some critical locations are listed for the moisture sensors appropriate placement.

Monitoring Term	Location	Moisture sensors	Reasons
short	floor / concrete slab		Drying before covering the floor
long	floor / under the cover material	Remaining moisture which deteriorates the structures	
long	bathrooms	Drying after the water is used	
long	showers	Sufficient drying / leakage	
long	areas close to windows	Additional moisture / mould grow	
long	areas close to doors	Additional moisture / mould grow	
long	basements	Additional moisture / water pipes	
long	building foundations	Diffused water	
long	ventilation gaps in the structures	Convection / air flow	
long	building facades	Additional moisture below the panels / coatings	
long	roof insulations	Water leakages / ventilation pipes condensation water	

3.1 Constraints for the Placement of the Sensors

Because of the radio it is reasonable to place the device as close to the surface as possible. The maximum depth is limited by the attenuation of the radio wave (See Table 1). If there is a too thin layer of concrete which covers the sensor device, the concrete will crack. If the maximum size of aggregates is 16 mm, three centimetres of concrete will ensure that there is only a low probability that the concrete will crack. The final specification for the distance from the surface is 30 - 50 mm.

4. MEASUREMENTS WITH THE RHT SENSORS AND DISCUSSION

One sensor device together with a different type of moisture sensor from Vaisala Oy was casted inside a concrete slab of 62 cm x 40 cm x 11 cm. The rule of thumb would predict that the slab is dry (RH is lower than 85 %) in 3 – 4 months [2]. The cast was opened after 1,5 months. The drying process started after the frame was removed. The sensors were placed at different depths inside the cast and therefore some sensors indicated faster drying than the others. The measurement results are shown in Figure 9. The measurement results of Railo-devices are calibrated to the same maximum value than the high accuracy sensor from Vaisala Oy. The Railo-sensors showed more conservative drying trend but they are still well in line with the reference measurements.

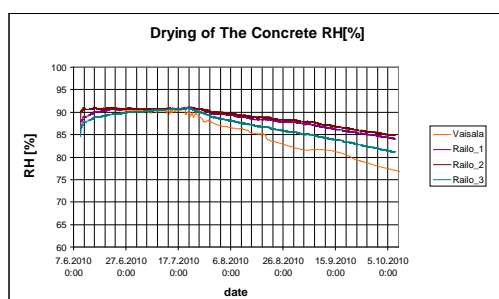


Figure 9. Meas. results of a drying concrete slab

The wireless radio link gives a benefit for an easy and fast assembly. In the wired solution the wiring work is very time-consuming and the major part of the total expenses comes from the

assembly work in any case. The wireless link is essential if the sensors are embedded inside the building structures. The placement of the sensors inside the building materials will give more precise results and the devices can be invisible for the user.

The concept of automated and continuous moisture monitoring of the buildings gives several benefits. Decisions on the repair actions can be done at the optimum time before the major problems occur. Estimations on the remaining service time of the building materials can be calculated based on the monitoring data. The record of the moisture values can be used as a proof of the good condition of the building structures and it gives a reason for a higher price of the building.

Also the hidden problems in the structures due to defecting building methods of the construction can be detected rapidly with the continuous moisture monitoring system through the Internet. Additionally, a leak in the water pipes can cause a sudden or a slow deterioration of building materials. Fast actions can be done because of the continuous monitoring and the savings can be substantial compared to rarely operated moisture measurements with handheld devices. Also, the long term monitoring is important, because typically the insurances do not cover the slow deterioration of building materials caused by the high moisture which is typically the key factor in deterioration of building structures.

5. CONCLUSION

The wireless moisture sensor system has passed a thorough testing and is being tested in the real use at the moment (in 2011). All the measurement results have been consistent.

REFERENCES

1. Al-Neshawy, F., "A Network System for Monitoring the Thermal and Moisture Performance of Repaired Concrete Facades" *Licentiate Thesis*, HUT, December 2007, pp. 1-23, pp .
2. <http://www.lmsrestoration.com/concrete2.htm>

Repair Possibilities of Concrete Facades Made Insufficient Frost Resistant Concrete



Jukka Lahdensivu
 Lic. Tech.
 Tampere University of technology
 Tekniikankatu 12, P.O. Box 600
 FI – 33101 Tampere
 jukka.lahdensivu@tut.fi

ABSTRACT

This paper is based on the *Repair strategies of concrete facades and balconies* -project. According to this research, 42.7 % of Finnish concrete facades made between 1960 and 1996 were seen visual frost damages. Again, 35.4 % of those were local, and 7.3 % were wide spread. The protective pore ratio of existing concrete facades very rarely fulfils the requirements of Finnish national building codes ($p_f \geq 0,20$). The protective pore ratio is less than 0,15 in about 70 % of concrete facades depending on the surface type of concrete facade. Moisture behaviour and environmental stress conditions have a strong impact on frost damage of concrete.

Key words: Concrete facade, condition assessment, deterioration, frost damage, service life.

1. INTRODUCTION

1.1 General

Since the 1960's a total of about 44 million square meters of concrete-panel facades have been built in Finland [1]. In fact, more than 60 % of the Finnish building stock has been built in the 1960's or later. Compared with the rest of Europe, the Finnish building stock is rather young.

Despite of the quite young age of the Finnish concrete building stock, several problems have been encountered in their maintenance and repair. The structures have deteriorated due to several different deterioration mechanisms whose progress depends on many structural, exposure and material factors. Thus, the service lives of structures vary widely. In some cases the structures have required remarkable and often unexpected, technically significant and costly repairs less than 10 years after their completion. For this reason many new methods have been developed in Finland for maintaining and repairing these concrete structures during the last 20 years. The methods include a condition investigation practice and its extensive utilization, rational repair methods and their selection, as well as first-rate repair products and appropriate instructions for managing repair projects. Concrete structures have been repaired extensively in Finland since the early 1990's. During the almost 20-year period, approximately 10 percent of the stock built in 1960 to 1980 has been repaired once [1, 2].

Because of the great amount of these existing concrete structures, it is very important to solve their incident repair need economically and in a technically durable way. This means that the

most suitable repair methods have to be used for each case and it is also important to be able to determine the optimal time of the repairs.

1.2 Structures of concrete facade panel

Prefabricated concrete facades have been the most common facade type in residential buildings in Finland since the late 1960's, at least in blocks of flats. A typical concrete element consists of an outer layer, thermal insulation and an inner layer. The outer and inner layers are connected together by trusses. The outer layer is typically between 40 and 85 mm thick, and the strength of concrete is typically near C20. The thermal insulation is usually mineral wool with a design thickness of 70 to 140 mm. Due to the compaction of thermal insulation; the actual thickness is usually between 40 and 100 mm. The thickness of the inner layer is normally from 150 to 160 mm (load bearing element) or 70 mm (non-load bearing elements).

1.3 Objective

This paper is based on the author's experiences from about 150 condition investigations of concrete structures, long-continued development of condition assessment systematic, and the *Repair strategies of concrete facades and balconies* -project. The general objective of this research was to study the factors that have actually had an impact on the service life, existence and progress of deterioration in concrete facades and balconies. The three sub goals of the research are:

1. To find out the factors that has actually had an impact on the existence and progress of different deterioration mechanisms in concrete facades and balconies.
2. To find out the relative importance of said factors.
3. To provide new reliable data on the service-lives of concrete facades and balconies for use in calculational durability design and LCC-analyses of concrete structures.

2. RESEARCH MATERIAL

The research material consist of the database of deterioration and material properties of existing Finnish concrete facade panels built up during 1961 to 1996, and weather observations since 1961 made by Finnish Meteorological Institute (FMI)

2.1 Database

Condition assessment systematic for concrete facades and balconies has been developed in Finland since the mid-1980's. A large body of data on implemented repair projects has been accumulated in the form of documents prepared in connection with condition assessments. About a thousand five hundred precast concrete apartment blocks have been subjected to a condition assessment, and painstakingly documented material on each one exists, including the buildings' structures and accurate reports on observed damage and need for repairs based on accurate field surveys and laboratory analyses.

The condition assessment data from 946 buildings has been gathered to a database. Those condition assessment reports have been collected from companies which have conducted such investigations as well as from property companies owned by cities.

2.2 Weather Data

Weather data consists of annual liquid precipitation i.e. rain and wet snow. Both of them can be capillary adsorbed to pore structure of concrete. Wind directions and wind speed during rain and in all times (including also snowfall and dry weather) during September to April was gathered, too. All weather data was gathered from Jyväskylä (inland), Vantaa (south costal area) and Turku (coast line) since 1961.

2.1 DETERIORATION OF INSUFFICIENT FROST RESISTANT CONCRETE FACADES

Basically all prefabricated concrete panels have been made in the same way, but there are a lot of differences in their surface finishing and manufacturing. Those have a strong influence, for instance, on the situation of reinforcement and the quality of concrete. In the database the most common surface finishing is brushed painted concrete, exposed aggregate concrete and painted plain concrete.

According to the database 42.7 % of Finnish concrete facades were seen visual frost damages during condition assessment. 35.4 % of the damages were local, and 7.3 % were wide spread. According to condition assessments made to existing concrete facades, the material properties related to frost resistant of concrete very rarely fulfils the requirements of Finnish national building codes. In frost resistant concrete the protective pore ratio should be 0.2 or higher. Approximately 70 % of existing concrete facades the protective pore ratio is less than 0.15. The frost resistant is very different depending on the surface type of concrete panel, see Fig. 1, and the manufacturing year of those panels. If the protective pore ratio is less than 0.10, concrete is not frost resistant in Finnish outdoor climate. The worst situation related to frost resistance is in concrete panels with surface type of exposed aggregate concrete, ceramic tile covered concrete and uncoated patterned concrete. The concrete facades made before 1980 has generally poorer material properties related to frost resistant than the newer concrete facades.

Moisture behaviour and environmental stress conditions have a strong impact on actual frost damage of concrete. For instance, the stress on concrete facade depends on the existence of proper waterproofing and prevailing wind direction during raining. Most of the cases the insufficient frost resistant has not lead far advanced or wide spread frost damages.

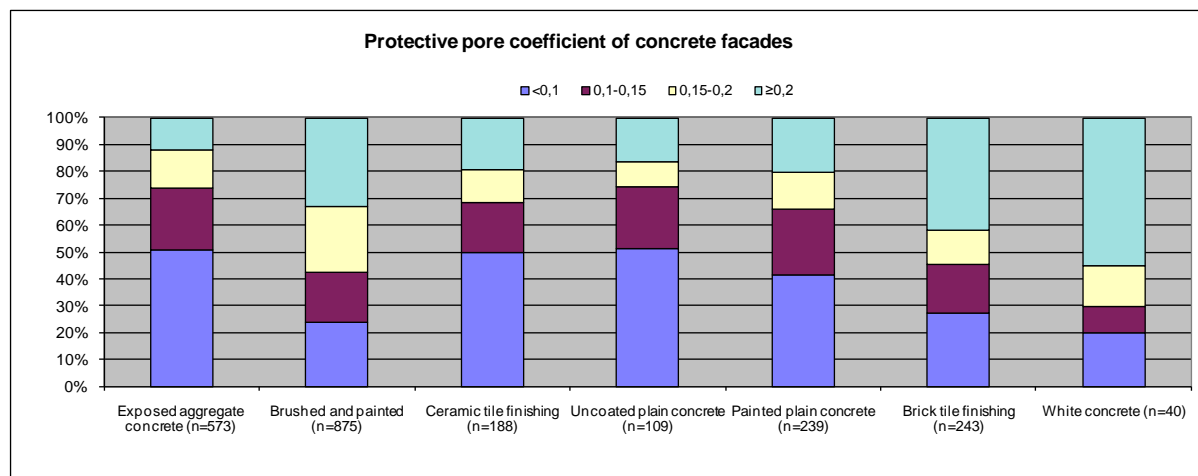


Figure 1 – The distribution of protective pore ratio in different surface finishing of concrete facades [3].

Despite of similar material properties of concrete in different facades, in several cases it has been noticed, that the frost damages occurs only on the facades faced from south-east to west. The explanation is prevailing wind directions during liquid precipitation.

3. REPAIR POSSIBILITIES

In Finland concrete facade renovation methods are divided into three categories (repair principles): protective repair methods, cladding and demolition of outer concrete layer and rebuilding. Protective repair methods are suitable mainly for structures where deterioration has just begun and the damage is not widespread. Possible protective repair methods suitable for concrete facades are divided into: painting over the old paint, protective painting after removal of old paint and thorough patch repair and protective painting.

If the existing structures are more severely damaged, protective repair methods are no longer effective. In that case, there are several repair methods for concrete facades that alter their appearance. Most of them use overcladdings or overlays. These repair methods are usually utilised in cases of widespread damage in the structure. Overcladdings stop or slow down the progress of the damage.

REFERENCES

1. Vainio, T., Lehtinen, E., Nuuttila, H. 2005. Building and renovation of facades. Tampere. VTT 26 p. + app. 13 (In Finnish)
2. Vainio, T. et al. 2002: Repair, maintenance and improvement work in Finland 2000-2010. Espoo 2002. VTT Research Notes 2154. 60 p. + app. 25 p. (In Finnish)
3. Lahdensivu, J, Varjonen, S, Köliö, A. 2010. Repair strategies of concrete facades and balconies. Tampere, Tampere University of Technology, Department of Structural Engineering, Research report 148. 79 p. (In Finnish)

Concrete Cylinders Confined with Basalt Fibre Reinforced Polymer



Eythor Thorhallsson
M.Sc
Associated Professor
Reykjavik University
Menntavegi 1
Reykjavik, Iceland
eythor@ru.is



Arngrimur Konradsson
M.Sc student
Reykjavik, University
Menntavegi 1
Reykjavik, Iceland
arngrimur05@ru.is



Stefan Kubens
Ph.D
Research Scientist.
Reykjavik University/
ICI Rheocenter
Menntavegi 1
Reykjavik, Iceland
Kubens.S@nmi.is

ABSTRACT

Concrete columns have an important function in many structures and can be vulnerable to exceptional loads. In older structures, columns often have a lack of transverse reinforcement, which is unable to provide sufficient confinement to the concrete core or to prevent buckling of the longitudinal reinforcement which causes premature strength degradation of the column. This paper presents a test program that was done on concrete cylinders confined with basalt fibre reinforced polymer (BFRP) and examination of its tensile strength. The test results show that the strength enhancement of the concrete cylinders consists of more ductile behaviour.

Key words: Concrete, confinement, basalt, BFRP and strengthening.

1 INTRODUCTION

The wrapping of FRP composite sheets around concrete columns is a promising method for structural strengthening and repair for their unique properties in terms of strength, lightness, chemical resistance and ease of application. This strengthening technique is of practical interest for their fast execution and low labour cost. The sheets provide a passive confinement to the concrete core and react against the lateral dilation of the column under compression, which delays the softening of the concrete and has shown to enhance both strength and ductility of the column [1]. Extensive work has been done in the experimental and analytical areas on concrete specimens of circular columns since the development of FRP wrapping started in the 1980s and later on, columns of square and rectangular cross sections [2-6]. The experimental work have mostly focused on the common FRP materials on the market which are carbon(CFRP), glass(GFRP) and aramid(AFRP) fibre. BFRP is a new material in civil engineering compared to carbon, glass and aramid and has shown to be a promising material for infrastructure strengthening. They are made from basalt rocks through melting process and contain no other additives in the producing process which makes advantages in cost. Basalt fibres show comparable mechanical properties to glass fibres at lower cost and exhibit good resistance to

chemical and high temperature exposure [5]. The ultimate strain of BFRP is higher compared to other common FRP materials and thus it is interesting to use this advantage in column strengthening to enhance the seismic performance. There is little research concerning the application of basalt fibre in civil engineering and its strengthening efficiency on concrete elements. This paper presents the tests that were performed on BFRP tensile coupon specimens and concrete cylinders confined with BFRP under concentric compression loading.

2 EXPERIMENTAL PROGRAM

2.1 Tensile Coupon Tests

Tensile coupon tests were made on five specimens to determine the actual material strength of the BFRP composite. The BFRP was formed from unidirectional woven basalt sheet and epoxy resin. The basalt sheet had a nominal thickness of 0.65 mm, which was used for the calculation of material properties. The dimensions of the tensile specimens were determined according to the ASTM standard recommendations [7].

A single layer of BFRP tensile specimen was prepared and tested of 25 mm width and 250 mm length. Each end had an additional layer on each side for more strength at the gripping zone. The preparation started with the usual wet layup process involving the impregnation of each basalt sheet with epoxy resin, followed by the application of an additional layer of sheet at each end. All the specimens were allowed to cure at room temperature for seven days before testing. All specimens were tested in a testing machine with a load capacity of 100 kN at a head displacement rate of 2 mm/min according to ASTM [7]. The longitudinal strains were measured simultaneously using two strain gages at opposite sides of the specimens with an active gage length of 6 mm. In the results, the strains are the average from the two strain gages. Two computers were used for data reading, one for the load reading and one for the strain reading.

2.2 Compression Tests on BFRP Confined Cylinders

Total of 12, 100mm x 200mm concrete cylinders, were casted with a concrete of 25 MPa compressive strength supplied by a local concrete manufacturer. To examine the confinement stiffness variation, the specimens were wrapped with one, two and three number of layers where one basalt sheet refers to one layer of BFRP jacket. Three cylinders were without jackets for examining the unconfined concrete strength. Three identical cylinder specimens were made for each number of BFRP layers.

After casting, the cylinders were let to cure in a humidity room for 14 days before they were prepared for wrapping. Before the wrapping procedure began, the concrete surface of the cylinders was wired brushed to remove loosely held powders and cleaned with compressed air and water and left to dry. The fabric sheets were cut with lengths of 0.46 m for one layer, 0.78 m for two layers and 1.09 m for three layers. The width was cut to 0.19 m, which provided 5 mm gap on each end of the cylinder to prevent axial load on the BFRP jacket. As the sheets were wrapped in a continuous way, these lengths allowed for an overlap of 150 mm. All cylinders were wrapped according to the wet layup process and cured at room temperature for seven days before testing. All specimens were axially loaded in a universal testing machine with a compressive capacity of 2500 kN under displacement control mode with a constant speed of

0.5 MPa/s. Axial load was recorded from an output signal from the test machine and the axial deformation was measured as the displacement of the loading base plate.

3 TEST RESULTS

3.1 Tensile coupon test specimens

All specimens showed a good linear response up to first failure at peak load. There the applied stress decreased when the fibre at the edge ruptured and then started to increase again until the whole section ruptured. Table 1 presents the test results from each specimen where F is the applied tensile force, σ is the tensile stress obtained from the tensile force and the cross section area, ϵ is the longitudinal strain measured by the strain gauges and E is the elastic modulus calculated according to ASTM [37].

Table 1 – Tensile coupon test results.

Specimen	F (kN)	σ (MPa)	ϵ (%)	E (GPa)
BU-1	11.99	780.58	2.53	31.059
BU-2	12.27	807.62	2.91	27.607
BU-3	11.44	732.57	2.84	31.489
BU-4	11.15	748.20	2.72	24.585
BU-5	11.66	732.71	2.56	29.613
Average	11.70	760.34	2.71	28.871

3.2 Cylinder specimens

Distinct hardening response was observed in all specimens after reaching the unconfined concrete strength where the BFRP jacket activates. The failure of the specimens can be divided into two modes, tensile rupture of the BFRP jacket and a combination of delamination at the overlap and tensile rupture of the BFRP jacket. Table 2 presents the average test results from each cylinder series where n is the number of layers, f_c is the unconfined concrete strength obtained from the plain cylinders, f_{cc} is the confined compressive strength, ϵ_{c1} is the axial strain corresponding to the unconfined concrete strength and ϵ_{cu} is the ultimate axial strain at failure. In figure 2 cylinders are shown before and after failure of the BFRP jacket.

Table 2 – Compression test results.

Specimen	n	f_c (Mpa)	f_{cc} (Mpa)	f_{cc}/f_c	ϵ_{c1} (%)	ϵ_{cu} (%)	$\epsilon_{cu}/\epsilon_{c1}$
SBU1	1	35.80	54.67	1.53	0.40	2.81	7.05
SBU2	2	35.80	79.34	2.22	0.40	4.01	10.09
SBU3	3	35.80	104.06	2.91	0.40	5.06	12.72

4 DISCUSSION

Where the fibres ruptured first at the edges on the tensile coupon specimens indicates that the orientation of the fibre to the applied tensile load was not perfectly parallel which however can be the case in structural strengthening. Therefore, the ultimate strength and strain were taken at the peak load which was considered to represent the material strength of the BFRP jacket. Figure 1 show very well the increase in compressive strength and axial strain obtained by adding

additional BFRP layer on the concrete cylinders. All cylinders show a good ductile behaviour where the maximum gain in axial strain is 12.7 times the unconfined peak strain and corresponding gain in compressive stress is 2.9 times the unconfined concrete strength. These results review the efficiency of BFRP as a strengthening material for concrete columns but as this paper only presents tests on small concrete specimens. further research needs to be done on reinforced columns of different cross sections.

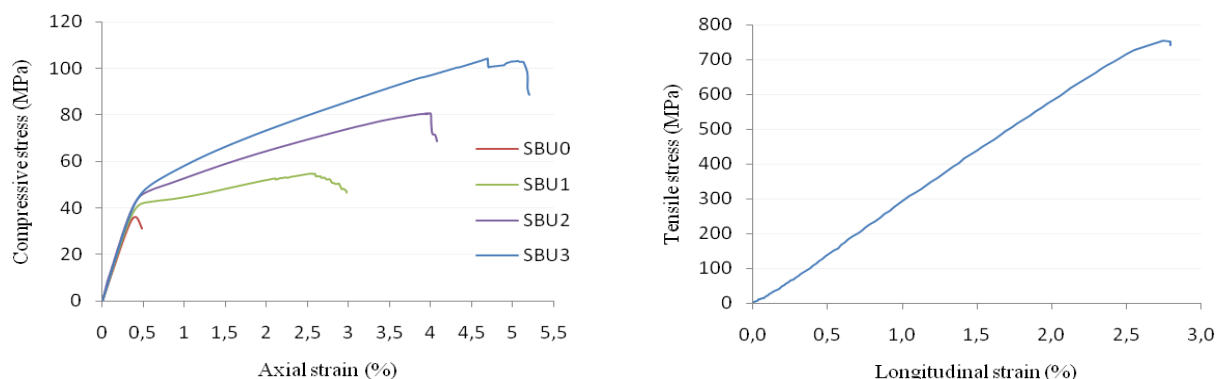


Figure 1 - Left: Average stress strain curves for cylinder specimens. Right: Average stress strain curve for BFRP.



Figure 2 - Test procedure on cylinders from being removed from humidity room to failure of bfrp jacket.

REFERENCES

- [1] A. Nanni and N. M. Bradford. "FRP jacketed concrete under uniaxial compression." *Construction and Building Materials*. vol. 9. pp. 115-124. 1995.
- [2] M. J. N. Priestley. *et al.*. *Seismic design and retrofit of bridges*. New York: John Wiley & Sons. Inc.. 1996.
- [3] H. Saadatmanesh. *et al.*. "Strength and Ductility of Concrete Columns Externally Reinforced With Fiber Composite Straps." *ACI Structural Journal*. vol. 91. pp. 434-447. 1994.
- [4] M. Demers and K. W. Neale. "Confinement of reinforced concrete columns with fibre-reinforced composite sheets-an experimental study." *Canadian Journal of Civil Engineering*.. vol. 26. pp. 226-241. 1999.
- [5] S. Matthys. *et al.*. "Axial Load Behavior of Large-Scale Columns Confined with Fiber-Reinforced Polymer Composites." *ACI Structural Journal*. vol. 102. p. 258. 2005.
- [6] F. Michael N and K. Homayoun. "Concrete Encased in Fiberglass-Reinforced Plastic." *ACI Structural Journal*. vol. 78. pp. 440-446. 1981.

- [7] ASTM. "Standard Test Method for Tensile Properties of Polymer Matrix Composite Materials." American Society for Testing and Materials. West Conshohocken, USA.2008.

The Calculated Repair Need of Finnish Concrete Facade and Balcony Structures



Arto Köliö
research assistant, B. Sc.
Tampere University of Technology
Korkeakoulunkatu 5, P.O. Box 600
FI - 33101 Tampere
arto.kolio@tut.fi



Jukka Lahdensivu
research manager, Lic.Tech.
Tampere University of Technology
Korkeakoulunkatu 5, P.O. Box 600
FI - 33101 Tampere
jukka.lahdensivu@tut.fi

ABSTRACT

Sustainable property management requires reliable information on the residual service life of buildings. An estimate for the repair need of prefabricated concrete facades and balconies has been calculated using a degradation model that is based on real data on existing facades. The model operates with input data that is first gathered with surveys. Of a sample of nearly 500 Finnish concrete buildings from five localities about two-thirds need repair measures. Mostly the need can be managed with light repair measures. Using predictive strategy in facade repair, the annual repair costs can be reduced remarkably.

Key words: condition assessment, property maintenance, service life, concrete facades and balconies, degradation.

1. INTRODUCTION

1.1 General

This paper discusses a study for a master's thesis where a new estimation was calculated for the repair need of existing concrete facades. The Finnish building stock consists of a total of 56 000 apartment houses that involves 44 million m² of concrete facade and 975 000 concrete balconies. Most of these apartment houses have been built in the 1960s and 1970s due to increasing demand of urban apartments. This estimate is the first one that relies on a database of real measured data. The study includes prefabricated concrete facades and balconies of residential multi-storey buildings in Finland from 1965 – 1995.

The repair need discussed here is induced by degradation of the structures and it does not include aesthetical, scheduled or other non-degradation related reasons to initiate facade repairs. In absence of reliable statistics on facade renovation, the effect of annual repair activity is not included in the calculation. The increment of repair need is assessed in a situation where the

facades degrade freely. This viewpoint gives us information on the annual volume of repairs that is required to maintain current “health” of the building stock and how the repairs should be distributed over time. It is arguable to believe that many facades are repaired needlessly with too heavy repair measures “just in case”. This study is meant to prove, that the annual costs of facade renovation can be reduced significantly with a predictive strategy to facade renovation.

1.2 Degradation of concrete facade structures

Concrete facades exposed to Finnish outdoor climate are deteriorated by several different degradation mechanisms, whose progress depend on many structural, exposure and material factors. Degradation may limit the service life of structures and, therefore, the possibility of retaining the present or original appearance of buildings and suburbs. It is important to know the basics of the degradation mechanisms of concrete to be able to successfully use suitable renovation measures. The most common degradation mechanisms causing the need to repair concrete facades, and concrete structures in general, are corrosion of reinforcement due to carbonation or chlorides as well as insufficient frost resistance of concrete which leads to, for instance, frost damage [1]. These very well known degradation mechanisms result in cracking or spalling of surrounding concrete, that reduces bearing capacity or bonding reliability of structures. Experience tells that defective performance of structural joints and connection details generally causes localized damage thereby accelerating local propagation of deterioration.

1.3 Repair

The repair of concrete facades is preceded by condition assessment of the facade. The goal of the assessments is to find out the current state, rate and extent of damaging and the tendency of damage propagation in the future. This information is used in planning of the facade repair work. [2]. Concrete facades and balconies can be repaired by methods of mainly three different magnitudes. Protective methods e.g. coatings are used for slowing down the advancing of degradation where patch repair is a traditional method widely used for repairing local damages caused by both weathering and corrosion. Properly made patch repairs together with protective coating can extend the service life of concrete structures remarkably [3]. If the damage is widespread the patch repair method is substituted by different cladding methods. Total renewal of the existing structure is arguable when cladding repair is not possible e.g. when majority of the facade are extensively deteriorated.

2. THE DEGRADATION MODEL

A comprehensive database of condition assessment data was collected during a research project on the factors contributing to the degradation of prefabricated concrete facades. Because of the tradition of using similar techniques in the fabrication of building elements these factors can be simplified and narrowed down to but a few major ones. [4]. The condition assessment database has enabled the development of a degradation model. The model takes into account frost weathering and carbonation in Finnish climate and evaluates the degradation tendency of different facades from the basis of real measured properties of the facade materials. Determining the correct repair measures is systematised with decision paths that lead, depending on material properties and the extent of damage, to a repair method proposal. The damage propagation was modelled by setting different propagation times for different ranges of damaging related material properties.

The model uses input data that consists of the surface type and age composition and the age and quantity of balconies of a building group. Acquiring the input data requires inventory surveys on the area of interest. The repair need is analyzed using this collected input data to produce distributions of damages and repair measures. These percentages are then converted to quantities and costs by multiplying them to the surveyed building group using the dimensions of an average type house and the number of buildings in that group. The calculation is shown in fig. 1.

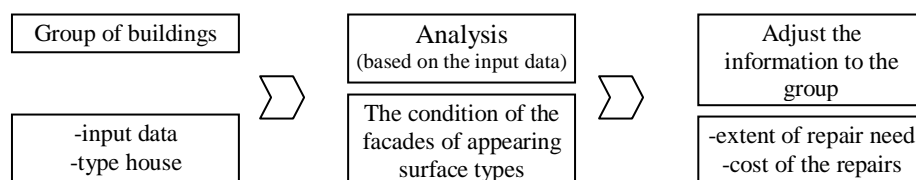


Figure 1 - The principle of calculation

3. REPAIR NEED OF FINNISH CONCRETE FACADES

3.1 Initial conditions

To acquire the input data for the degradation model a survey was conducted to gather a sample of 496 concrete buildings. The sample was distributed to the localities of Helsinki, Turku, Tampere, Jyväskylä and Oulu covering the majority of Finland. The sample inside these localities was also spread to cover the main areas of concrete multi-storey buildings and weighing larger areas over smaller ones. Most common types of facades throughout Finland were painted brushed, exposed aggregate and tile surfaced facades. The properties of a type house were also determined during the survey. The average height of residential buildings in the localities differs from the tallest 5.2 storey's in Turku to 4.6 storey's in Helsinki. The average facade area of one building was determined in Tampere 1230 m². This facade area was scaled to represent the other localities in respect to the average height of buildings.

For determining repair expenses, average cost estimates from the year 2009 were input to the model: facade repairs ranging from 40 €/m² to 195 €/m² and balconies 5000 - 9000 €/balcony depending on the repair method. The same repair costs were used in calculation in every locality regardless of the changes in local price levels. This will bring forth the differences caused by the technical repair need over the local price level.

3.2 Results

The study shows that at the moment, approximately 2/3 of Finnish concrete facades need repair measures, fig. 2. Still, majority of these facades can be repaired using light patch repairs or protective coatings. Only about 10 % of the facades need heavier cladding repairs.

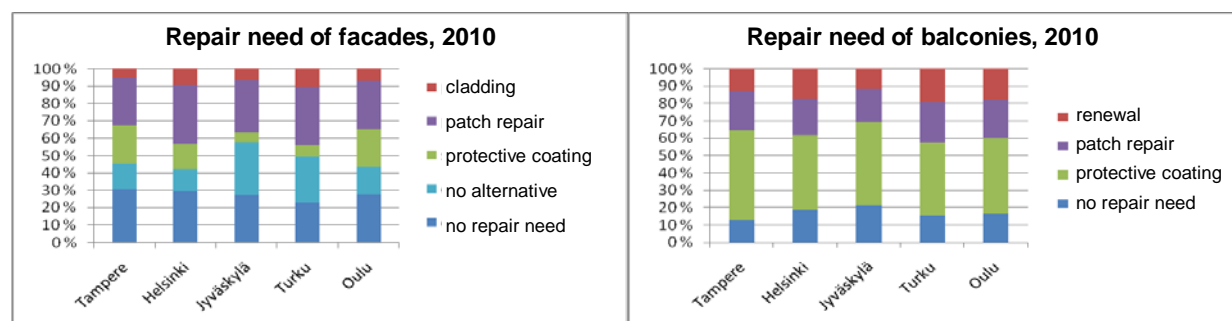


Figure 2 – Repair needs in concrete facades (left) and balconies (right)

When the facades are let to degrade and the repair need is calculated at a five years' interval the need of heavier repairs increases as seen in fig. 3. A total repair volume and cost forecast is formed when all of the results are summed together, fig. 4.

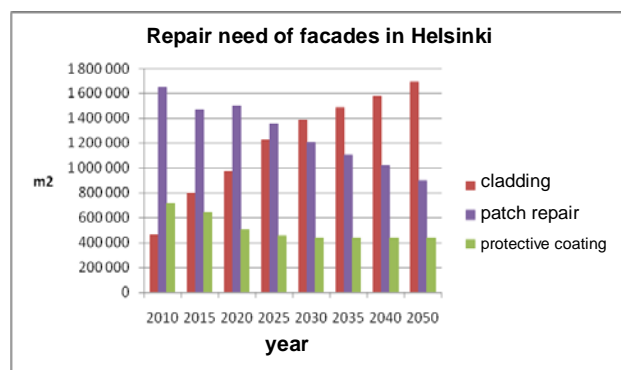


Figure 3 – The progression of repair needs of facades in Helsinki

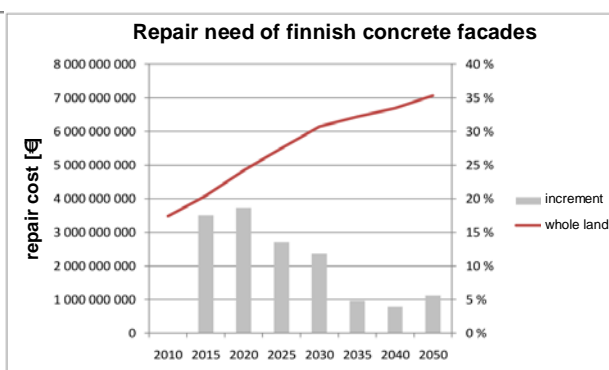


Figure 4 – The value of repair needs of 1965–1995 concrete facades in Finland

4. CONCLUSIONS

The degradation induced repair need of concrete facades is at the moment 3.5 billion € and continues to grow at an average 1.8 % annual increment. This increment, 63 million € is the minimum amount of repairs needed to maintain the current state of concrete facades. The annual value of repairs is remarkably small for it is calculated on the basis of predictive facade repair strategy where more facades are renovated in advance with lighter repair methods. The value is theoretical and there are occasions when the predictive strategy can not be explicitly followed due to other criteria. With this predictive strategy the annual repair cost of concrete facades can still be significantly reduced without compromising the service life of buildings. The reduction is simply the result of selecting the correctly sized repairs at the right time.

13 – 31 % of examined buildings had exposed aggregate or clinker or tile surfaced facades. This remarkably large number of facades can not be protected with protective coating and patch repairs are difficult when the patch has to blend to the existing facade. If new practical repair or coating methods could be developed for these facade types the application of these same principles would be possible also for this type of facades.

REFERENCES

1. Pentti, M., Mattila, J., Wahlman, J. 1998. *Repair of concrete facades and balconies, part I: structures, degradation and condition investigation*. Tampere, Tampere University of Technology, Structural Engineering. Publication 87. 157 p. (In Finnish)
2. Concrete Association of Finland. 2002. *Condition investigation manual for concrete facade panels*, Concrete Association of Finland, Helsinki. (In Finnish).
3. Mattila, J. 2003. *On the durability of cement-based patch repairs on Finnish concrete facades and balconies*, Tampere University of Technology, Structural Engineering. Publication 123, Tampere
4. Lahdensivu, J., Varjonen, S., Köliö, A. 2010, *Repair strategies of concrete facades and balconies*, Tampere University of Technology, Structural Engineering. Research report 148, Tampere (In Finnish)

Petroleum hydrocarbons in concrete and their effect on indoor air quality



Jaakko Sääntti
M.Sc.
Vahanen Oy
Linnoitustie 5
FI-02600 Espoo
jaakko.santti@vahanen.com



Jarno Komulainen
M.Sc.
Vahanen Oy
Linnoitustie 5
FI-02600 Espoo
jarno.komulainen@vahanen.com

ABSTRACT

Emitting petroleum hydrocarbons and PAHs from concrete can cause indoor air problems. Petroleum hydrocarbons and PAHs in concrete were analysed by GC-MS, indoor air was studied by VOC-sampling and emission from concrete by FLEC-sampling. According to our findings, already 100 mg/kg petroleum hydrocarbon content in concrete causes significant emissions from concrete to ambient indoor air.

Key words: concrete, hazardous material, petroleum hydrocarbons, polycyclic aromatic hydrocarbons (PAHs), polychlorinated biphenyls (PCBs), heavy metals, volatile organic compounds (VOCs), field and laboratory emission cell (FLEC)

1. INTRODUCTION

We have analyzed hazardous compounds like petroleum hydrocarbons, PAHs, PCBs and heavy metals from concrete samples collected during mapping of hazardous construction materials in buildings. The most common causes of these findings are a) oil leaks in the building (Figure 1) or b) the hazardous compounds have absorbed into concrete from adjacent materials that contain hazardous compounds. In some cases asbestos, water soluble chromium or PCBs have been added to special concretes. This research concentrates on absorbed petroleum hydrocarbons and PAHs in concrete and their effect on indoor air quality.



Figure 1 - Oil leak has happened in upper floor and oil has penetrated the concrete. This means that concrete has been polluted also in the areas where the original oil leak did not happen.

2. RESULTS

Concrete samples are drilled samples because structures are also studied when mapping hazardous compounds. Concrete samples were analysed, if the use-history of the building gave reason to suspect that concrete might contain petroleum hydrocarbons or other hazardous compounds. Analyzing is important when the intended use of the building is changed e.g. an old factory building is renovated to an office building. Analyzing is also necessary when determining the final placing to concrete waste from demolished buildings and structures.

According to our findings, with engine and waste oils, also PAHs and heavy metals are absorbed into concrete. Mastic asphalts contain petroleum hydrocarbons and old mastic asphalts can also contain PAH-containing creosote oils. Petroleum hydrocarbons of mastic asphalts are easily absorbed to adjacent porous materials, e.g. concrete. We have found that also PAH-containing creosote oils from mastic asphalts, bitumen coatings and wood transfer easily concrete. As a case example, table 1 shows how PAH-compounds are absorbed from creosote oil containing wooden floor (total PAHs 32 697 mg/kg) into underlying base floor concrete. According to Finnish regulations, the concrete in this case is not hazardous waste but it cannot be used as a fill. PCBs are present when e.g. old capacitors have leaked oil into concrete.

Table 1. PAH-content of the base floor concrete from the top to 90 mm

Distance from the concrete top (mm)	PAH (16) sum (mg/kg)
0-30	131
30-60	23
60-90	4.3

In indoor air studies we studied the effect of petroleum hydrocarbons and PAHs on the ambient indoor air quality. In the buildings the indoor air was studied by VOC-sampling and emission from concrete by FLEC-sampling. In one case we took concrete samples from old factory building, where the renovation to apartments was going on. Concrete samples were taken from concrete floors. Total petroleum hydrocarbon contents and VOC-emissions by FLEC were analyzed. Figure 2 shows clearly how total VOC-emission (TVOC) accelerates when petroleum hydrocarbon content increases.

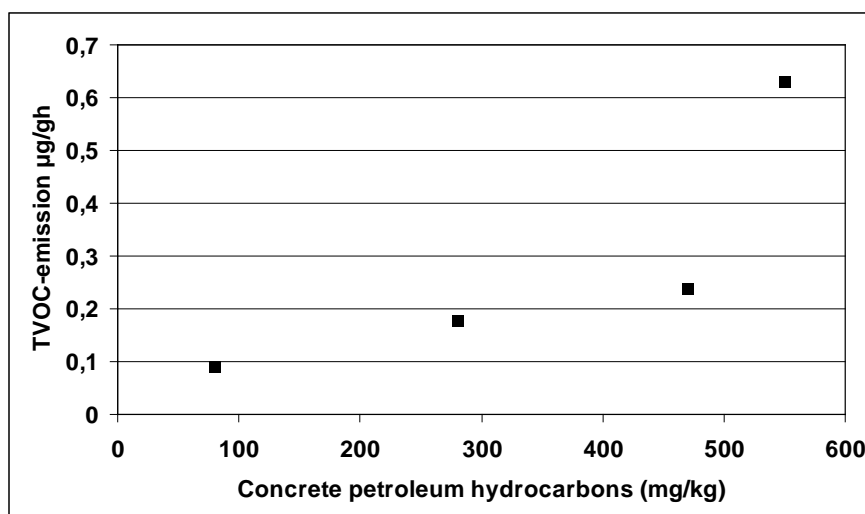


Figure 2 - Concrete petroleum hydrocarbon content vs. TVOC emission (µg/g/hour).

In other case we have shown that petroleum hydrocarbons have absorbed into concrete from overlying 15 mm thick mastic asphalt floor (Table 2).

Table 2. Petroleum hydrocarbon contents of mastic asphalts and underlying concrete

(mg/kg) / Sampling point	1	2	3
Mastic asphalt C ₅₋₁₀	-	-	17
Mastic asphalt C ₁₀₋₄₀	4 000	4 000	4 600
Underlying concrete C ₅₋₁₀	-	-	-
Underlying concrete C ₁₀₋₄₀	95	79	120

In this case we took also VOC- and FLEC-samples. VOC-samples were taken from indoor air and FLEC from the surface of mastic asphalt. Results are in table 3. FLEC1 and FLEC2 are from the same point. FLEC1 is from pristine surface of mastic asphalt and FLEC2 represent slightly scratched surface, therefore FLEC2 TVOC-result is almost two times higher. The FLEC-results show, that after installation the mastic asphalt layer surface hardens and encapsulates the hydrocarbons within the mastic asphalt. If the mastic asphalt surface is disturbed, the emission rate of petroleum hydrocarbons increases rapidly.

Table 3. VOC and FLEC sample results

Sample	VOC1 ($\mu\text{g}/\text{m}^3$)	VOC2 ($\mu\text{g}/\text{m}^3$)	FLEC1 ($\mu\text{g}/\text{m}^3 \text{ h}$)	FLEC2 ($\mu\text{g}/\text{m}^3 \text{ h}$)
TVOC	180	100	150	250

3. SUMMARY

Petroleum hydrocarbon contents in concrete varied from few tens of mg/kg to 10 000 mg/kg. According to VOC- and FLEC-sampling, already 100 mg/kg petroleum hydrocarbon content in concrete caused significant emissions from concrete to ambient indoor air and can cause indoor air problems. Careful encapsulation of concrete or special ventilation structures prevents indoor air problems.

Session B8 – SHRINKAGE AND CRACKING

Shrinkage cracking of thin concrete overlays



Jonas Carlswård
PhD, Research engineer
Betongindustri AB, Luleå Tekniska Universitet
Box 47 312 Stockholm
E-mail: jonas.carlsward@betongindustri.se

ABSTRACT

A research study has been conducted to develop recommendations on the execution of thin bonded concrete overlays. Full scale overlay tests were carried out, consisting of 50 mm concrete layers cast on hollow core slabs. Main test variables were the method of preparing the substrate prior to overlaying, type of reinforcement (none, steel fibres and mesh) and curing conditions. Results reveal that the bond between overlay and substrate is undoubtedly the most critical parameter. Another key parameter for a successful end result is sufficient curing, while reinforcement proved to be less significant.

Keywords: Shrinkage, Cracks, Steel fibres, Bond, Overlay, Curing.

1. INTRODUCTION

Concrete overlays on existing substrates are used at a frequent basis in the construction industry. One significant application area is the finishing layer on hollow core slabs and other prefabricated elements. Despite the fact that concrete is utilised on a regular basis for this application area there is no established practice regarding the design and execution. A consequence is that misapplied execution methods are common, resulting in a far too high degree of undesirable end results. Cracking, debonding and edge lifting are among the most frequent problems, all resulting from the differential shrinkage between the newly placed layer and the old sub-base material.

Development of relevant guidance on how to design and execute overlays in order to avoid the above mentioned problems can thus be seen as a high priority area. For this reason a research project is carried out in cooperation between Betongindustri AB, Strängbetong AB, Betongteknik i Nacka AB and Mariekälla Betong & Transport AB [1]. Funding for the project is provided by SBUF, the Development Fund of the Swedish Construction Industry. The study presented in this article represents one part of the project.

2. OVERLAY TESTS

A series of “full scale” overlay tests was conducted on hollow core slabs of the type HD/F 120/27 in one of Strängbetong AB:s prefabrication plants in Nykvarn. In total six slabs were

used, each divided into four separate areas, in which different substrate preparations were applied in order to obtain a variation in the bond quality, see Figure 1.

Preparations adopted were pre-moistening, primer and none (dry). Pre-moistening was conducted approximately 1 hour prior to overlaying, which resulted in a film of free water on the substrate. Priming was conducted in two ways, the day before (primer 1d) and just before overlaying (primer 1h). It should be pointed out that all substrates were thoroughly cleaned before preparation. The primer was of the type Maxit Floor 4716, which was mixed with water in accordance to the recommendations.

Slabs 1, 3, 4 and 6 were overlayed at the same time with a 50 mm layer of Self Compacting Concrete (SCC). Slabs 1 and 4 were un-reinforced while slabs 3 and 6 were reinforced with steel bar mesh $\phi 8s100$. Steel fibres, of the type Sika Fiber CHO 65/35 NB, were then mixed into the SCC at a dosage rate of approximately 30 kg/m^3 , before the last two slabs were overlayed (slabs 2 and 4).

Two of the areas on each slab were air-cured while the remaining parts were covered by plastic foil, see Figure 1. However, the covering was not done until the morning the day after casting, which means that the surfaces were uncovered for approximately 17 hours. The plastic foil was removed 6 days later.

Test series II

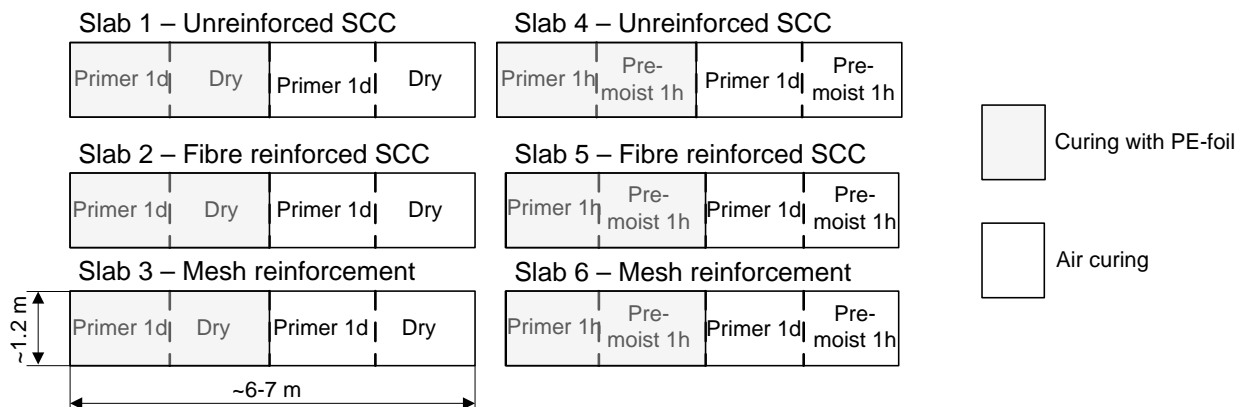


Figure 1 – Each hollow core slab was divided in four areas with different substrate preparation. Other parameters varied were the type of reinforcement and type of curing.

The mix design for the SCC is given in Table 1. The cement was of the type CEM II/A-LL 42.5R from Slite (Byggcement). The aggregates were of a natural occurring type from Riksten, south of Stockholm. Limestone filler, of the type Limus 40 from Nordkalk, was used to stabilise the SCC. The superplasticizer was Sikament 56 by Sika.

Table 1 – SCC mix composition.

Concrete grade	Cement kg/m^3	Sand 0/8 kg/m^3	Gravel 5/8 kg/m^3	Filler kg/m^3	Superplast kg/m^3	w/c
C35/45	445	1580	-	124	0.7%	0.47

3. RESULTS

The development of cracks was followed over a period of approximately 3 months from the time of overlaying. At the end of the period the crack widths were measured and the bond strength between overlay and substrates was determined by pull-out testing. Results from the bond strength measurements are given in Figure 2 (a) while crack widths are given in Figure 3 (a).

Regarding the effect of the substrate preparation on bond strength it is evident from the results in Figure 2 (a) that primer 1d was the best alternative irrespective of curing conditions. Dry substrate also gave reasonable bond strength in the areas that were cured under PE-foil while air curing resulted in zero bond strength for the same substrate condition. Curing thus seems to be extremely important if the overlay is cast on a dry substrate.

It can further be concluded from the results in Figure 2 (a) that late primer addition (primer 1h) and pre-moistening (premoist 1h) should be avoided considering that these preparation methods resulted in zero bond in most areas. The only exceptions were the primed areas (primer 1h) that were overlayed by fibre reinforced SCC. This implies that steel fibres may have a positive influence on the bond strength. The poor bond situation is illustrated by the photos shown in Figure 2 (b), where parts of the overlay on slab 4 are lifted off using an iron-bar lever.

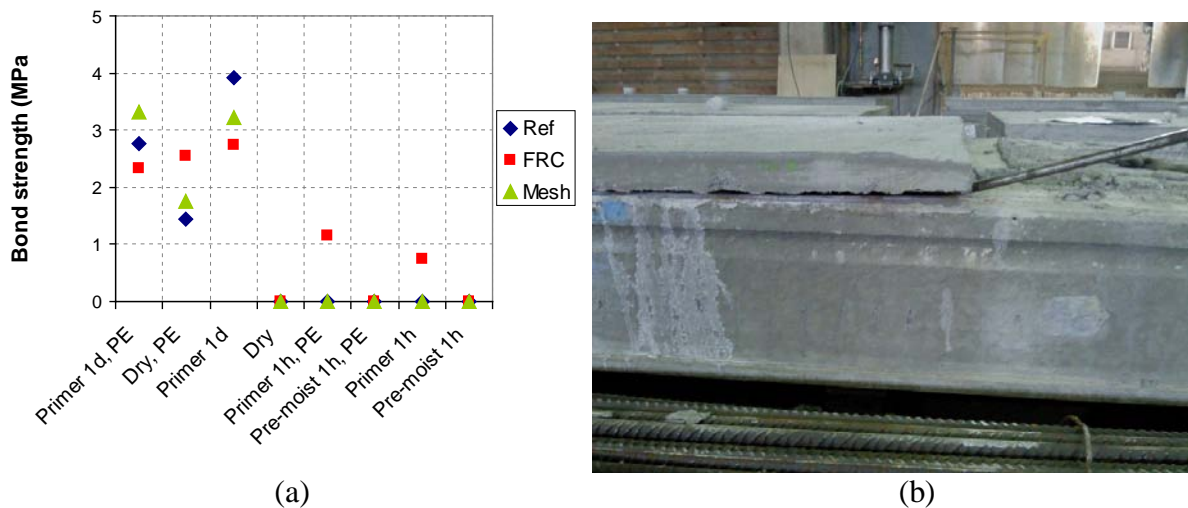


Figure 2 – (a) Measured pull-out bond strength. (b) Overlays on slabs 4, 5 and 6 could easily be lifted off by means an iron-bar lever.

It was expected that the poor bond of the areas with late priming and pre-moistening would give rise to large crack widths. However, this relation cannot be clearly discerned in the results given in Figure 3 (a), although the two largest cracks developed in low bond strength areas. A possible reason is that crack width growth was limited by the fact that most of the overlays on the slabs with late priming and pre-moistening debonded (see Figure 2 (b)). Regarding the effect of reinforcement the results imply that mesh may be favourable as none of the cracks in mesh reinforced areas exceeded 0.5 mm. However, it is not really possible to draw any clear conclusions except that reinforcement is clearly needed in case the bond strength is low (see crack in Figure 3 (b)).

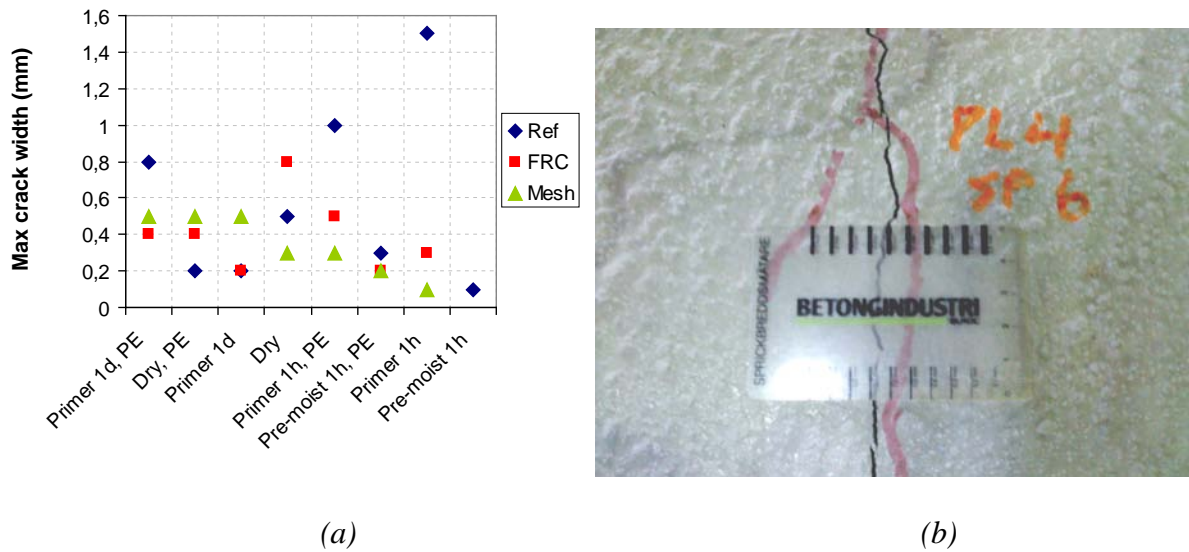


Figure 3 – (a) Maximum crack widths measured at the end of the test period. (b) Photo showing the largest crack on slab 4 (ref).

4. CONCLUSIONS

Results from the overlay test series described above revealed that the choice of preparation of the substrate prior to overlaying is an extremely important parameter. It was verified that late pre-moistening or priming is devastating for the bond strength development. Test results showed that a dry substrate may even be better than adding moisture or primer just prior to overlaying. However, the best preparation method, of the methods used in the investigation, proved to be when primer was applied a day in advance, in accordance to the recommendations.

Another parameter that was shown to influence the bond strength was the selection of curing method. Test results imply that curing the overlay under plastic foil increased the bond strength from zero to between 1.5 to 2.5 MPa in case of dry substrate. A similar difference was however not observed for the areas with other substrate preparations. This may indicate that curing is particularly important if the substrate is dry at the time of overlaying.

Regarding the effect of reinforcement on crack widths it can be concluded that reinforcement, mesh or steel fibres, most certainly contributes in case the bond strength between overlay and substrate is poor. However, in areas where the bond strength is high it is more difficult to conclude that reinforcement has a significant influence on crack widths.

REFERENCES

1. SBUF project nr 12001., "Steel fibre reinforced self compacting concrete overlays – crack limitation and bond strength," *SBUF*, www.sbuf.se.

Crack-Free Concrete – An Understanding of Creep



Peter Fjellström
M.Sc., Ph.D. Student
Luleå university of technology
Dept. of Structural Engineering
SE - 97187 Sweden
peter.fjellstrom@ltu.se



Henrik Bäckström
M.Sc., Ph.D. Student
Luleå university of Technology
Dept. of Structural Engineering
SE - 97187 Sweden
henrik.backstrom@ltu.se



Jan-Erik Jonasson
Professor.
Luleå university of technology
Dept. of Structural Engineering
SE – 97187 Sweden
jan-erik.jonasson@ltu.se

ABSTRACT

A durable structure of concrete is achieved when no cracking occurs during the young ages of the hardening process. Therefore, it's of importance to address shrinkage and creep correctly. Drying is the primary source of shrinkage, and the time development in shrinkage is an effect of the balance between drying and creep. Therefore, creep is to be measured on sealed and non-sealed specimens in order to investigate the nature of drying creep. Measurements will be performed for loading ages up to 1 year. These experimental data will be used to create accurate models, including both short and long term effects.

Key words: concrete, cracking, creep, shrinkage.

1. INTRODUCTION

1.1 General

Crack-free concrete is needed to achieve durable and functional structures, since cracks frequently lead to shortened lifetime unless costly repairs and maintenance are done. To counteract this destructive process, a Nordic research project, CFC (Crack-Free Concrete), has been started with several partners in Sweden and Norway.

To fulfil the task to achieve a crack-free concrete structure, one must analyse cracking during the young ages of the hardening process thoroughly. Therefore it is of importance to address and understand shrinkage correctly since its one of the main crack inducing factors. Standardized tests for shrinkage are not designed to be a proper base for theoretical analyses, and there is a general need to develop new test procedures.

Creep tests are planned to be performed on sealed and non-sealed specimens in order to investigate the nature of drying creep. These experimental data will be used to create models for drying creep, including both short and long term effects. In the end the project will contribute to a better understanding of the influential mechanisms and how to avoid crack related concerns,

i.e. by taking relevant measures to reduce the cracking risk. Research findings gained will be transformed and implemented for practical use.

1.2 Definition of shrinkage and creep

A concrete specimen will shortly after casting start to shrink due to chemical reactions, which after final setting is considered as the driving force of autogenous shrinkage. At sealed conditions the corresponding decrease in pore humidity is denoted self-desiccation or “internal drying”. If the specimen is not sealed and the environmental humidity is less than the humidity inside the concrete, shrinkage is increased due to external loss of water from the surfaces of the concrete body. This part of the shrinkage may be regarded as effects of “external drying”. Thus, in general terms, drying is the primary source of shrinkage.

Upon placing the specimen under constant load there is a quick deformation, see c in Figure 1 and [1] and [2]. When specimen is under constant load, deformation will increase over time; this process is known as creep. If the specimen is not sealed, the time development in deformation will be an effect of the balance between drying and creep. Since the amount of creep depends on load and drying conditions it is traditionally divided into basic and drying creep.

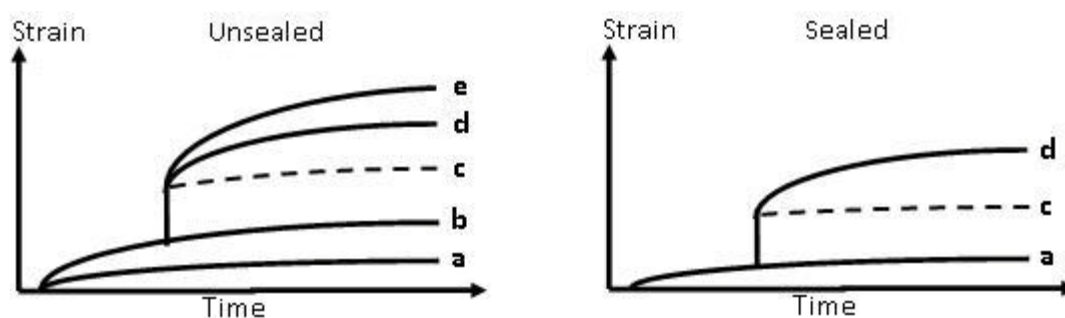


Figure 1 – At left a basic schematic over deformation in an unsealed concrete specimen depending on a) autogenous shrinkage, b) drying shrinkage, c) instantaneous (elastic) response to load, d) load induced basic creep and e) load and drying induced drying creep. The figure to the right corresponds to a sealed specimen.

The experimental measurement of the parameters in Figure 1 has in its simplest form been separated by using sealed specimens in loaded and unloaded conditions. Autogenous shrinkage is then assumed to be the same in both. A comparable unsealed specimen gives information about differences in deformation due to drying shrinkage and drying creep.

The elastic response upon loading is dependent on the strength and therefore the maturity level of the concrete specimen. Thus creep has to be measured on different maturity ages, for instance 1, 3 and 7 days [1]. Additionally there is many parameters affecting the maturity level, for instance in [3] it is shown how temperature is affecting the strength growth. In the LTU research group different creep and shrinkage models have been developed, [1], [3], [4], [5], [6] and [7], but still there is a need of analyses and models concerning drying shrinkage and drying creep.

Thus, it is important that the authors of this article will look into the behaviour of drying creep and create new, verify or modify existing models that include this phenomenon when predicting long and short term effects.

2. EXPERIMENTAL SETUP

For early age creep tests, i.e. loading at 1, 3 and 7 days old specimens, the measurements will be performed with hydraulic test rigs, see A in Figure 2. The mould is seen in B, diameter 80 mm and height 340 mm. In each of the rigs two specimens are placed, one for loaded and one for unloaded state. The unloaded specimen will give information about the total “free” shrinkage, i.e. the sum of autogenous and drying shrinkage. The loaded subject will give information about creep.

Two strain gauges of type Schaewitz LVDT010 MHR [1] (C in Figure 2) is placed symmetrically on opposite sides of the specimen. Upon strain, the primary core is moved in or out from the two secondary coils, and the differential voltage is measured; every μm in either direction corresponds to 20mV. The measurement equipment is made of invar since it shows little effect to temperature change, $2\mu/\text{°C}$. The relative humidity and temperature is continuously logged in each of the rigs so that movement compensation can be taken into account. Load is adjusted with a hydraulic pump.



Figure 2 –In A the hydraulic rigs used for early age creep measurement are seen and in B the moulds used for the specimen. In C the electromagnetically working gauge is seen together with its fastening equipment and calibration pin that ensures an accuracy of $1\mu\text{m}/\text{mV}$. D shows the mechanical rigs used for the creep tests on mature concrete (loading age 28 days or more).

Creep measurements on mature concrete (loading age 28 days or more) will be conducted using the mechanical rigs seen in Figure 2 (D). Three pairs of bowels (Figure 3) are placed symmetrically around the test specimen on 200 mm distance with strain stable glue. The glue merges into the near surface pores of the specimen and hardens within minutes. The gauge measurement device type is STAEGER and it measures changes in position with one μm accuracy. To ensure the precision of the measurement a reference bar is used before and after each measurement. When tests are conducted with sealed specimens the dowels are placed after the covering of the concrete body. The load is adjusted by using a hydraulic pump. Moisture and temperature will be continuously measured.



Figure 3 – The figure shows in A the tool used to give the right distance between the bowels in B. Before and after each measurement of a specimen the reference bar in C is used to ensure the accuracy of the STAEGER instrument in D.

3. FINAL COMMENTS

The concrete laboratory at LTU that have been used for more than 20 years to conduct tests of concrete regarding heat of hydration, strength development, shrinkage, thermal dilation and stress, is currently under upgrade. All gauges have been calibrated and old cables are replaced with new. The major change is the up to date computers together with National Instruments USB measurement devices. The functionality of the previously used control software [8] is transferred to Lab View with improvements in how measurement is performed and how data is retrieved. In addition, a climate room is under construction, which will be suitable for tests on mature concrete.

REFERENCES

1. Westman, G. 1999. Concrete Creep and Thermal Stresses: New Creep Models and Their Effects on Stress Development. Luleå University of Technology, Doctoral Thesis 199:20, 301 pp.
2. Neville, A.M. 1995. Properties of Concrete. 4th ed. Harlow: Longman Group.
3. Jonasson, J., Fjellström, P. & Bäckström, H. 2010a. Effects of Variable Hardening Temperature on Strength Growth. Bygg & Teknik, 102(7), 63-66. (In Swedish)
4. Emborg, M. 1989. Thermal Stresses in Concrete Structures at Early Ages. Luleå University of Technology, Doctoral Thesis 1989:73D, 285 pp.
5. Jonasson, J., Bäckström, H. & Fjellström, P. 2010b. Use of Linear Logarithmic Model for Estimation of Long Term Creep Based on Short Term Tests. Bygg & Teknik, 102(7), 37-40. (In Swedish)
6. Larson, M. 2003. Thermal crack estimation in early age concrete: Models and methods for practical application. Luleå University of Technology, Doctoral Thesis 2003:20, 190 pp.
7. Hedlund, H. 2000. Hardening Concrete: Measurements and Evaluation of Non-Elastic Deformation and Associated Restraint Stresses. Luleå University of Technology, Doctoral Thesis 2000:25, 394 pp.
8. Gustafsson, T. 1995. RegSim: A Software Tool for Real Time Control and Simulation. IEEE Conference on Control Applications - Proceedings: 168-173.

Autogenous deformation of concrete: Introductory tests with 7 new temperature controlled dilation rigs



Gunrid Kjellmark
M.Sc.
SINTEF
Building and Infrastructure
NO-7465
gunrid.kjellmark@sintef.no



Terje Kanstad
Professor
NTNU Department of Structural
Engineering
NO-7465 Trondheim
terje.kanstad@ntnu.no

ABSTRACT

During the last two years, seven temperature controlled dilation rigs have been developed at NTNU and SINTEF. This paper describes set-up and operational procedures, and presents results from test series where cement type was the main variable. For verification, the results were compared with corresponding results from SINTEF's standard shrinkage test method. Considering the results from the new rigs towards the SINTEF method, the agreement is very good. The new method, however, has some uncertain elements and is still under development, among other factors because an objective procedure to determine the specific time where the strain measurements shall start has to be decided.

Key words: Autogenous deformation, temperature control, dilation rigs

1. INTRODUCTION AND OBJECTIVE, [1]

Volume changes in concrete occur during the hardening process due to for instance temperature changes and self-desiccation. This often takes place under some form of restraint, which creates tensile stresses and possible cracking, and one consequence may be substantial repair costs. The visual impression of the structure may also be challenged, and cracks can compromise the durability of the structure.

Volume changes, the corresponding tensile stresses and cracking tendency may be strongly influenced by the concrete constituents and their volume proportions. The curing conditions are also very important. New types of cement and addition of other binder materials require better knowledge of their properties in concrete, with regard to autogenous deformation, thermal properties and mechanical properties.

To be able to investigate the deformation properties of new types of concrete and carry out the required experiments, a research group with relations to COIN has developed and built a new test-rig for measuring autogenous deformation at isothermal or realistic temperature conditions in concrete. The main objectives of the project is to map the autogenous deformation properties of various concretes, and to relate autogenous shrinkage to relative humidity in the hardening concrete. Furthermore, the influence of temperature and drying will be studied in particular.

The described activities are a part of the COIN-project: *Crack free concrete structures* and it is also coordinated with a Swedish project within the same topic, where Betongindustri, TU Luleå and Lund University are the most heavily involved partners.

2. DILATION RIGS – SET-UP AND OPERATIONAL PROCEDURES

The set-up, see Figure 1, consists of rectangular cuboid moulds which measure 100×100×580 mm inside. The moulds are made of 10 mm thick steel plates. The moulds are internally lined with a layer of adhesive plastic foil and two thin layers of plastic film. Talcum powder is applied between each layer to reduce friction. This makes it possible for the specimen to expand or shrink freely. The rig is located in a conditioned room which should hold 20 °C and 50 % relative humidity. Instruments for measuring temperature and relative humidity in the room are used to record the climatic conditions.

The length of the specimens is 500 mm, and the remaining parts of the mould are filled with pieces of extruded polystyrene on each short end. These pieces of polystyrene have a hole for LVDTs, which record deformation in the longitudinal direction on each short end of the specimens. The transmitters are connected to each other with an independent Invar steel bar, and they are connected to the specimen with Invar pins going through the polystyrene and into the specimen.

In addition, each mould is designed with two 6 mm copper pipes on three of the lateral surfaces. These are connected in series to a cooling/heating simulator (Julabo FP33). This is a temperature control system with a pump which provides that a fluid circulates through the rig. Temperature can be regulated from a computer or by manual programming. In the test series referred to in this paper, the simulator circulates water with a temperature of 19.5 °C to control the temperature development in the concrete. The temperature can, however, be altered and more realistic temperature histories can be described and applied to the concrete specimen.

Concrete is cast into the moulds and compacted by hand. Afterwards, the concrete surfaces is covered with plastic film, an aluminium foil and finally a 5 mm thick steel plate to protect the sealing. A thermo couple is placed centrally in each specimen, and once the hardening of the concrete is initiated, the piece of extruded polystyrene is liberated. This is done to ensure free movement of the specimens.

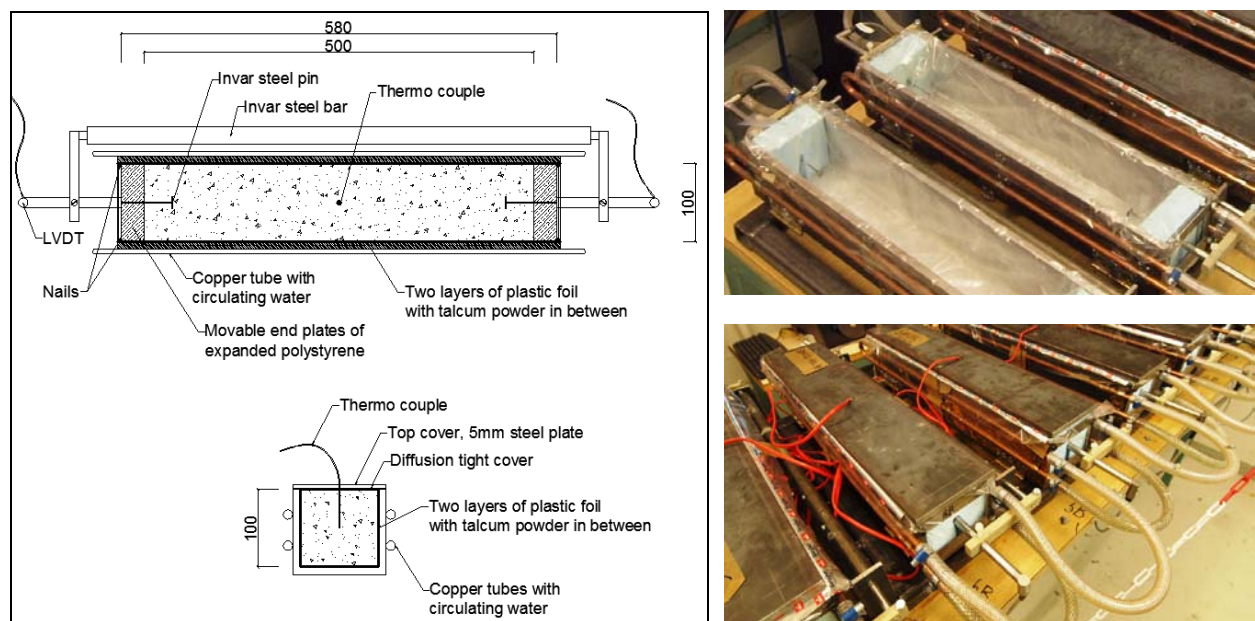


Figure 1: Dilation rig

3. DETERMINATION OF t_0 – START TIME FOR STRESS DEVELOPMENT, [2]

An objective method for determination of the time where the volume changes start to create stresses in restrained systems is important for evaluation of experimental results, and comparison of different concrete mixes. Previous experiments have shown that this parameter, often denoted t_0 , is difficult to detect through indirect methods such as early heat liberation, for instance $t_{Q=12kJ}$. Setting according to heat is experienced to be around 2-3 hours earlier than setting according to semi-adiabatic tests in e.g. a TSTM rig. An appropriate t_0 for stress calculations has shown to be the point in time where the TSTM has developed 1/10 of the maximum compressive stress during the heating period. Earlier experiments where t_0 was determined in a TSTM rig showed that t_0 increased from 13 hours to 15 hours when the fly ash content increased from 0 to 35 %. Silica fume has been shown to shorten t_0 .

4. RESULTS FROM INTRODUCTORY TEST SERIES, [3]

Three different mixtures were used; Mix 1 with Portland cement and 5,2 % silica by cement weight (Portland cement, class CEM I 52,5 N), Mix 2 with the same Portland cement only, and Mix 3 with the Portland cement and 50 % fly ash by cement weight. Three specimens (100×100×500 mm) were cast from each mixture; two in the new dilation rigs and one for SINTEF’s standard shrinkage test method. If the issues from chapter 3 are taken into consideration in this experiment, one can assume the following start time for the three mixtures:

Mix 1: $t_0 = 9$ hours

Mix 2: $t_0 = 11$ hours

Mix 3: $t_0 = 13$ hours

The deformation measurements in the dilation rigs were initiated 5-6 hours after casting. This is long before final set and therefore the “semi-plastic” phase would be part of the first hours of all curves if this is not compensated for. Figure 2 shows curves where t_0 is set to 9, 11 and 13 hours for Mix 1, 2 and 3, respectively. This probably gives a more correct picture of the autogenous deformation development. However, regardless of time zero, the results show that Mix 3 has the highest autogenous deformation the first 20 hours.

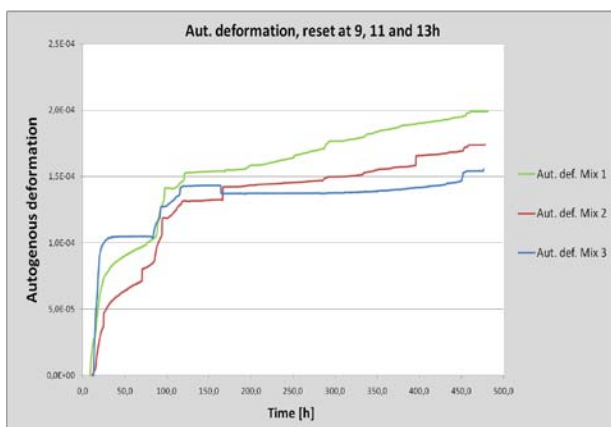


Figure 2: $t_0 = 9, 11$ and 13 hours

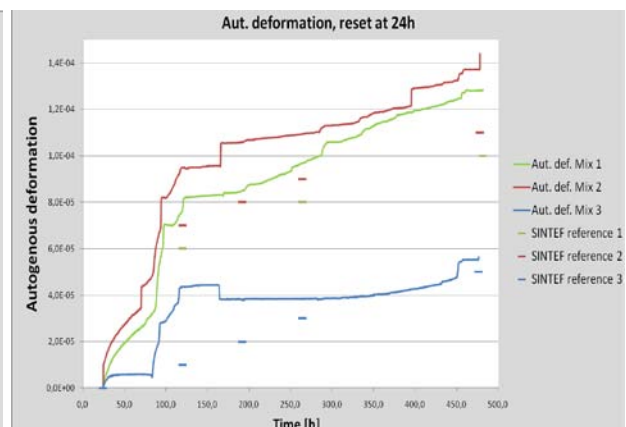


Figure 3: $t_0 = 24$ hours, incl. SINTEF results

The first measurements for the SINTEF reference prisms were performed after 24 hours. For comparison, the starting-point for the control prism curves is set to the 24h-value for the corresponding dilation rig curve. The results are shown in Figure 3.

When the strain development after 1 day is compared, it is seen that the fly-ash concrete has the lowest shrinkage. While mixture 1 has approximately $170 \cdot 10^{-6}$ shrinkage after 3 weeks, mixture 2 has $140 \cdot 10^{-6}$ while mixture 3 has only $60 \cdot 10^{-6}$. This means that the fly ash concrete might be considerably less vulnerable to shrinkage cracking than the two other mixtures.

Approximately 80 hours after casting, accelerated strain development (contraction) seemed to occur in all the specimens in the new test rig. Corresponding behaviour was not seen in the specimens for the SINTEF method. The explanation may be due to the uncontrolled variation in room temperature. The concrete is isothermal while the measuring equipment is somewhat affected by the room climate.

5. CONCLUSIONS

Considering the results from the new dilation rigs and the SINTEF standard method, the agreement is rather good. If one exclude the apparent increase of shrinkage at the point in time where the room temperature increases, the autogenous deformation measured with the two test methods gives a reasonably good correspondence; all final results are within limits of $\pm 25 \cdot 10^{-6}$ (micro strains).

As can be seen in Figure 2 and 3, the curves are not smooth, and include some jumps which are not related to material behaviour. This can be explained by external influence on the rig, i.e. temperature or mechanical disturbances. For later experiments actions are taken to reduce such effects.

ACKNOWLEDGEMENTS

The paper is based on the work performed in COIN - Concrete Innovation Centre (www.coinweb.no) - which is a Centre for Research based Innovation, initiated by the Research Council of Norway (RCN) in 2006. COIN has an annual budget of NOK 25 mill, and is financed by RCN (approx. 40 %), industrial partners (approx 45 % of which ¼ is cash) and by SINTEF and NTNU (in all approx 15 %). The Centre is directed by SINTEF, with NTNU as a research partners and with the present industrial partners: Aker Solutions, Norcem, Norwegian Public Roads Administration, Rescon Mapei, Skanska, Spenncon, Unicon, Veidekke and Weber Saint Gobain.

REFERENCES

1. Bjøntegård, Ø. (2009) *Volume changes and cracking tendency in concrete*. Technology report no. 2565, Norwegian Public Roads Administration, Road Directorate. 2009-09-07, ISSN 1504-5005
2. Bjøntegård, Ø., Kanstad, T., Sellevold, E.J. (2000), t_0 – *The startpoint of stress calculations*, in IPACS TASK 2 + 3 Memo meeting in Delft 20-21 March
3. Kjellmark, G. (2010) *Autogenous deformation and relative humidity – Concrete with Aalborg Portland cement and fly ash*. COIN Project report 24-2010. SINTEF Building and Infrastructure

Properties of shotcrete-shrinkage problems



Björn Lagerblad

Ph.D., Senior Researcher. Swedish cement and Concrete Research Institute, 10044 Stockholm, Sweden. bjorn.lagerblad@cbi.se

Guest Professor. Concrete structures, Royal Institute of Technology, Stockholm. Sweden

ABSTRACT:

Cracking of shotcrete in tunnels is a problem in Sweden. This is due to that shotcrete does not behave as a normal cast concrete. The main difference is due to the set accelerator and as a result the major cement reactions will take place in a stiff (but not hardened) material. The shotcrete is very sensitive to early shrinkage if not properly water cured. As the concrete cannot level the early shrinkage phenomena will give a basic different structure and mode of porosity, which in turn will increase shrinkage. Moreover, with alkali free set accelerator the shotcrete gets more and coarser porosity, which in turn will give significantly larger drying shrinkage than in cast concrete.

Key words: Shotcrete, shrinkage, set accelerators, curing

1 INTRODUCTION

In Sweden, especially in recent years, there has been problem with cracking of shotcrete in tunnels. This is especially the case where the shotcrete is covering drainage systems, where the bonding to the substrate is weak.

Commonly shotcrete has been regarded as a normal concrete as regard shrinkage and other properties but this is not the case. Normal cast concrete is liquid during the first period, while in shotcrete the early cement hydration reactions will take place in a stiff structure given by the set accelerator. Moreover, the set accelerator will interact with cement hydration.

1.1 Shrinkage

All concretes shrink but it is complex and due to several factors. The shrinkage is due to chemical reactions, development of the cement paste and to evaporation of water. Different causes will affect the concrete at different stages.

In the young fresh concrete shrinkage is mainly linked to cement hydration. The volume of water and cement is larger than that of the cement hydrates, which will create shrinkage forces as long as cement is hydrating. In the stiff young shotcrete the chemical shrinkage will result in an increased porosity. If the chemical shrinkage is not compensated for by water this will result in a dimensional shrinkage as the structure of the stiff but not hard shotcrete is not strong enough to withstand the tension.

In the properly hardened concrete one will mainly get drying shrinkage that is a result of evaporation of water from the capillary system. When the capillary pores are drying out they will contract and the concrete will shrink. Changes of the pore structure will affect the amount of shrinkage and one can not presume that shotcrete has the same porosity.

The consequences of shrinkage depend on several parameters. The shrinking forces may result in increased porosity, micro cracks, internal cracks or free shrinkage. In laboratory free shrinkage is measured. In most standard tests free shrinkage of hardened concrete is measured over time. As the shrinkage is not restrained larger cracks do not normally form but parts of the shrinkage may result in micro cracks. When the shrinkage results in internal cracks the free shrinkage will be less. Formation of cracks instead of free shrinkage is in most cases result of inner restraint caused by reinforcement, aggregates, fibres etc. Outer restraint gives large wide cracks as in the case of the drainage systems.

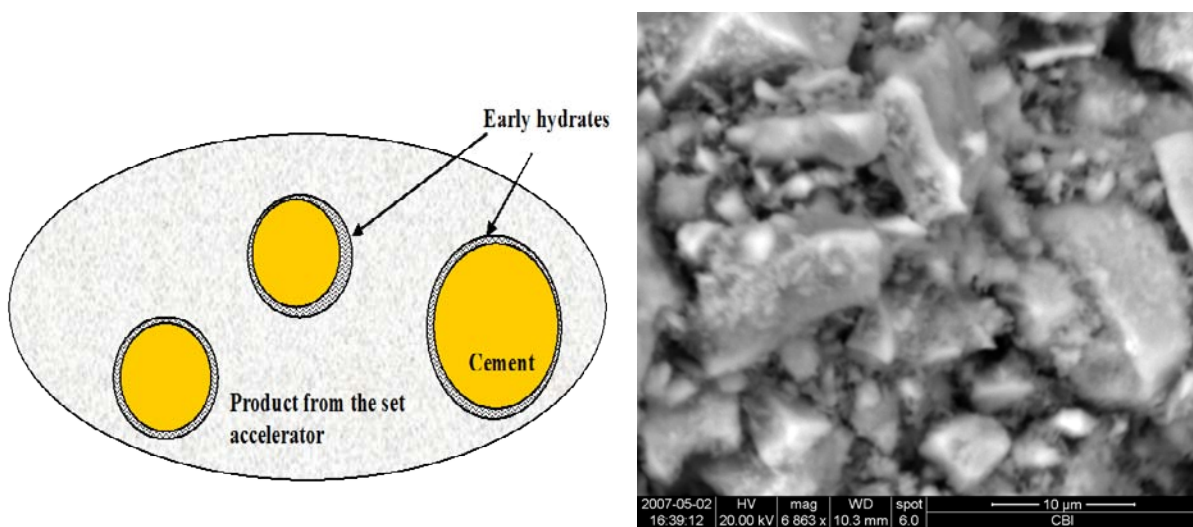


Figure 1. Sketch illustrating cement grains with an early shell of hydrates in a matrix of ettringite needles from the alkali free set accelerator. On the left side SEM photo taken one hour after mixing with alkali free set accelerator. It shows cement grains and a matrix of ettringite needles.

2 SET ACCELERATORS AND THEIR REACTIONS WITH PORTLAND CEMENT

The intension with the set accelerator is to make the concrete stiff momentary. The set accelerator will interact with the cement hydration during the dormant period but it will not start the cement acceleration period. Thus it must react with the pore fluids formed during the dormant period. In cement paste there are two major chemical systems, the silicate and aluminum systems. The set accelerator intervenes in this system and forms either calcium silicate hydrate or ettringite that are products of normal cement hydration. Presently here are two different types of set accelerators available, water glass (alkalisilicate) and one called alkali free accelerator where the first interacts with the silicate system and the later with the sulphate/aluminate system.

As the concrete is fluid, during the dormant period, the bulk of the cement is still unhydrated. The set accelerator will change the composition of the pore fluid but in general the hydration of the cement will occur independently of the set accelerator. This means that during the first period the early strength is wholly dependent on the structure of set accelerator products, Figure 1.

The later real strength will be due to cement hydrating in a structure given by the set accelerator. Thus the composite structure will not be the same as in an ordinary cast concrete.

3 EFFECT OF SET ACCELERATORS ON CEMENT HYDRATION

The effect of set accelerator was tested in an isothermal calorimeter. The cement used was Standard P Degerhamn from Cementa AB (CEM I-LH/LA/LA). The results [2] show some but not all of the alkali set accelerators delays, while water glass seems to accelerate the hydration of Portland cement. This can also be observed on the strength gain, Figure 2. These experiment shows that for some mortars it takes 24 hours until the strength increases from the strength of the stiff shotcrete to proper strength. With slow cement at a cold tunnel wall it can take several days until the shotcrete gets a proper strength.

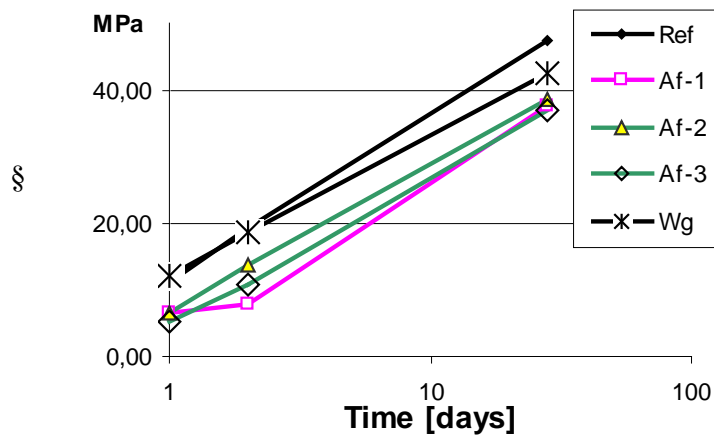


Figure 2. Compressive strength for 1, 2 and 28 days for sprayed cement paste. It is measured on prisms (40x40x160mm). Af = alkali free set accelerator, Wg = waterglass.

4 SHRINKAGE OF CEMENT PASTE

Experiments have shown [2] that the set accelerator do not give strength enough to stop chemical shrinkage.

Drying shrinkage was tested on mortar prisms. Accelerated mortar was sprayed into forms. Three different types of commercial alkali free set accelerators and one type of water glass were tested. Different dosages have been used. The paste consisted of cement mixed with 5 % silica fume and had a water/binder ratio of 0.38. Mixes with 5 % silica fume is practice in Sweden.

The moulds were dismantled after 20 hours and the prisms were kept in humid for 7 days. Thereafter they were put in a conditioning room at 65 % RH. The results show that the prisms during the first week when kept in humidity did swell around 0.3 ‰. When the prisms were put in the conditioning room (65 % RH). The results show that both the hardened pastes with set accelerators shrink more than the reference concrete. The samples with alkali free set accelerator shrank most, around 40 % more than the reference paste prisms. Moreover the prisms with alkali free set accelerator lost more water and lost it faster than the prisms with water glass and the reference. Results are presented in Figure 3. These results have been verified with more experiments where it also was found that shrinkage reducing agents did reduce the shrinkage [2].

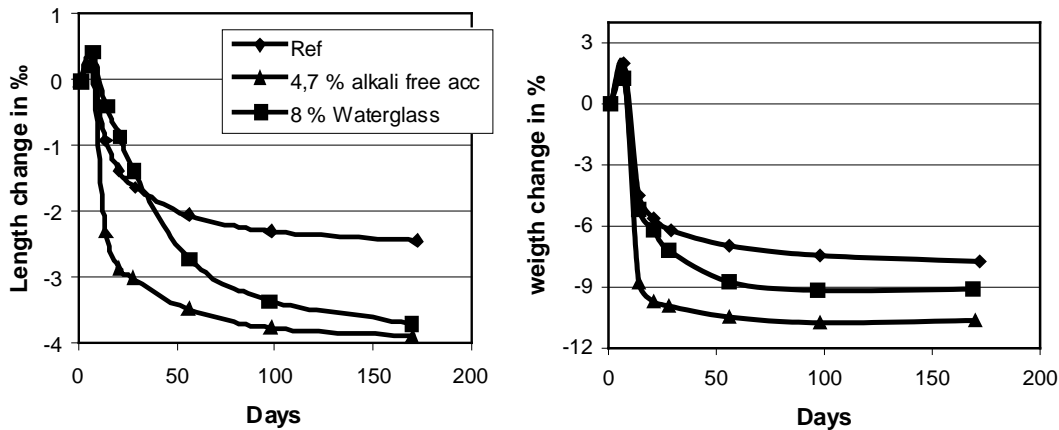


Figure 3. Results from experiments with cement paste and drying shrinkage and different types of set accelerators.

5 CONCLUSIONS

The results show that shotcrete cannot be treated as a normal concrete. Firstly the early cement reactions take place in a stiff structure. Thus the chemical shrinkage will in shotcrete result in an increased porosity while it in normal cast concrete will result in levelling of the surface. In an experiment described in Aziz [1, 2] panels with real shotcrete were measured from the shooting. In this experiment, the panels were covered with plastic to prevent drying. After 24 hours they were water cured. The panels showed during the first day an average shrinkage of around 0.7 ‰, which is in accordance with the results from the paste experiments on autogenous shrinkage. This shows that water must be added to the fresh shotcrete to avoid shrinkage.

The set accelerator and especially the alkali free type changes the structure of the cement paste. Mercury intrusion tests [2,3] shows that it becomes coarser. This results in faster loss of water and more intense drying shrinkage.

As a conclusion the problems with cracking of shotcrete is presumably due to bad curing and the fact that shotcrete is more sensitive to shrinkage than normal cast concrete.

References

1. Aziz, S. 2005, Experimentell undersökning av plastfiberarmerad sprutbetong. TRITA-BKN. Examensarbete 227, KTH, Betongbyggnad.
2. Lagerblad B., Fjällberg L. & Westerholm M. 2007. Sprutbetongs krympning-modifiering av betongsammansättning, SveBeFo Rapport 86, Stockholm.
3. Lagerblad, B., Fjällberg, L., Vogt, C., Shrinkage and durability of shotcrete. Proceedings of the third international conference on engineering developments in shotcrete, Queenstown, New Zealand, Mars 2010. In Shotcrete Elements of a System, Ed Bernard, S., CRC Press Taylor & Francis group. 2010.

The work has been financed by the BeFo, CBI and the Road authorities, which I want to thank.

Restrained Shrinkage Tests of Fibre Concrete for Shotcrete Applications in Hard Rock Tunnels



Lars Elof Bryne
Lic. Eng., Ph.D. Student
KTH Royal Institute of Technology
Division of Concrete Structures
SE-100 44 Stockholm, Sweden
lars-elof.bryne@byv.kth.se



Anders Ansell
Ph.D., Associate Professor
KTH Royal Institute of Technology
Division of Concrete Structures
SE-100 44 Stockholm, Sweden
anders.ansell@byv.kth.se

ABSTRACT

This study investigates shrinkage of accelerated shotcrete (sprayed concrete), especially in the case of shotcrete sprayed on drains, a part of a tunnel lining not continuously bonded to the rock. One of the goals is to find methods of avoiding shotcrete shrinkage cracks in such drain structures. If cracks yet develop the crack distribution is of great importance, i.e. fine cracks instead of one wide. By using both steel and glass fibres this may be achieved. The ongoing research focuses on the optimization of the glass fibre addition and the understanding of the interaction between shrinkage and creep of shotcrete.

Key words: Shotcrete, Steel fibres, Glass fibres, Testing, Restrained shrinkage.

1. INTRODUCTION

1.1 Background

Experiences from tunnelling projects have shown that a need for a better control of the shrinkage properties of shotcrete (sprayed concrete) is a matter of concern. Especially in the case of shotcrete sprayed on drains, a part of a tunnel lining not continuously bonded to the rock. Shrinkage is in this case only restrained by fixation of the shotcrete in areas several meters apart and the shotcrete between the fixed areas is subjected to tensile strains often exceeding its capacity. This project investigates accelerated shotcrete and the goal is to find methods of avoiding shrinkage cracks in such drain structures. If cracks yet develop it is important that the shotcrete contains fibres of a sufficient amount and of suitable types, making the material strain hardening. This means that its tensile strength increases after the formation of a crack, thus leading to the formation of several fine cracks instead of one wide. Normally steel fibre reinforced shotcrete is strain softening so only one crack develops. The crack width therefore often exceeds what is acceptable considering durability. Laboratory tests on restrained shrinkage are performed using cast concrete with rheology similar to that of shotcrete, i.e. sprayable concrete. The tests are performed as ring tests, i.e. concrete are cast in ring-shaped moulds with a stiff steel core preventing free shrinkage of the hardening concrete ring. This study is a part of

a more extensive project investigating the material properties of shotcrete. The outcome of this study will be used in the development of further tests, to be performed using more realistic geometries and sizes of test specimens.

1.2 Ring test

The ring test method is common in studies of how crack widths develop in fibre reinforced concrete and e.g. Malmberg and Skarendahl [1] has used the ring test to assess the efficiency of steel fibres. Shotcrete quality concrete was studied by Ansell and Holmgren [2] in a pilot study on the crack distribution in shotcrete reinforced by both steel and glass fibres. Beside steel fibres also different glass fibres, 6 and 12 mm long, were added up to the relatively high amount of 26 kg/m³. The goal of the present project is to optimize the amount of added glass fibres. The basic outlook of the test ring is illustrated in Figure 1. A concrete ring with outer radius R_o and an inner radius R_i is cast around an internal steel ring resulting in a cross section of the concrete ring that is 40×40 mm². After 7 days curing the concrete is exposed to drying through the face, top and the circumference.

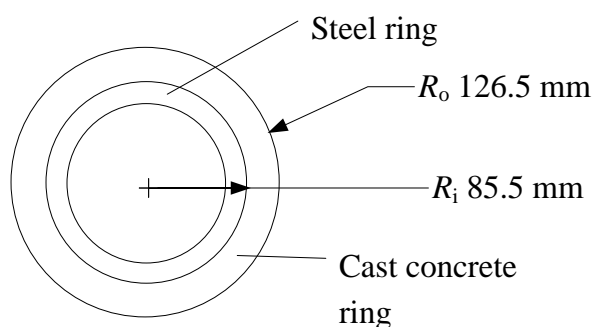


Figure 1 – A concrete ring with outer radius R_o and an inner radius R_i is simply cast around an internal steel ring.

Primary information revealed by the ring test is age of cracking and maximum or average crack width at a specified time and for a certain drying environment. Various mix compositions can be compared and the efficiency of different types of fibres regarding crack width limitation can be evaluated [3]. However, the ring test is not appropriate to predict cracking in actual service [4].

2. THE PROPERTIES OF CONCRETE

The specimen for the restrained shrinkage test series is cast with a shotcrete quality concrete with a wct of 0.45. Table 1 shows a general recipe and the main ingredients of the concrete, no accelerator was used in this case. The volume of each mix of concrete or batch was 20 litres. The steel fibre is Dramix 65/35 and the glass fibre is 6 mm long, manufactured by Saint-Gobain Vetrotex. The amount of aggregate has been changed due to the amount of steel and glass fibres of the various mixes. Cube specimens were also cast for compression testing after 28 days. All specimens were kept in a climate room with humidity (RH) of 100 % and 20°C. The specimens were demoulded after 24 hours and after totally 7 days the specimens were moved to a climate room with humidity (RH) of 50 % and 20°C. The specimens for the restrained shrinkage test then remained in the climate room (RH 50% and 20°C) for continuous observation of crack development of the rings. There were two ring specimens for each fibre mix.

Table 1 – General recipe and main ingredients for shotcrete of reference sample.

Material	Density (kg/m ³)	Mass per batch Concrete (kg)
Cement	3150	9.9
Silika 940U	2230	0.4
Filler	2800	3.2
Water	1000	4.4
Glenium	1100	0.04
Steel fibre Dramix 65/35	7800	See Table 2
Glass fibre (6 mm)	2600	See Table 2
Aggregate, 0-2 mm	2650	5.7
Aggregate, 0-8 mm	2650	22.7

The consistence of the fresh concrete was estimated by a slump test according to Swedish Standard [5]. The result of the slump test is shown in Table 2. The concrete cubes, with dimension 100×100×100 mm³, were measured and tested after 28 days. The density and compression strength are shown in Table 2, giving the mean values of three cubes.

Table 2 – Slump, and steel and glass fibre content for various concrete mixes. Density and compression strength of 28 days old concrete cubes, the standard deviation within brackets.

	Steel fibres (kg/m ³)	Glass fibres (kg/m ³)	Slump test (mm)	Density (kg/m ³)	Compressive strength (MPa)
1	0	0	230	2263 (15.3)	71.8 (1.4)
2	50	0	235	2293 (5.8)	72.9 (1.0)
3	50	5	220	2297 (11.5)	71.9 (0.6)
4	50	10	190	2283 (11.5)	74.2 (0.6)
5	50	15	155	2283 (5.8)	70.9 (1.1)
6	50	20	70	2267 (5.8)	70.0 (1.3)

According to Table 2, the slump tests show that the consistence varied a lot between the different mixes. Relative good workability seems to be achieved even for mixes up to test group 4, with a glass fibre content of 10 kg/m³. The compressive strength is somewhat higher than expected. The decreasing values for test group 5 and 6 are interesting, it could be a consequence of too high fibre content with poor distribution or cluster formation leading to lower wetting between concrete and fibre. However, the difference between the samples is relatively small.

3. RESULTS AND DISCUSSION

The two reference specimens, test group 1, cracked radially after 35–55 days. The crack width was 0.25 mm after 100 days for both specimens. One of the specimens in test group 2 showed a thin crack through the whole specimen after 50 days, the crack width after 100 days was 0.05 mm. The other specimen in the same group showed an initiation of a crack after 50 days, but no through crack after 100 days. This unexpected difference may be a consequence of the high compressive strength, or the fact that the specimen are allowed to dry from all sides, i.e. top, bottom and circumferential. Both specimens in test group 5 showed thin cracks in the upper surface, well distributed after approximately 85 days. The cracks are, however, not going into the concrete body. This is also not expected, because of the high amount of glass fibre, 15 kg/m³, but it can be a consequence of too much vibration at the time of casting. A part of the

cement paste has, through segregation, entered the top as a laitance scum, creating a whitish, weak and crazed surface layer. However, even if the initiation of cracks has started, the cracks are well distributed. All the other test groups have not shown any crack formation after 100 days, but the observation continuous.

The ring test results are similar to the results by Ansell and Holmgren [2]. The reference samples have both cracked, the crack width in this study has not developed as much as in [2], which were 0.4 mm. The time for crack initiation was longer in this study. The cracked specimen in group 2 show slightly lower crack width compared with [2]. The other specimen just showed crack initiation after 100 days, while all specimens were cracked after 65 days in [2]. The glass fibre reinforced samples show no general difference between the studies, besides the mix with 15 kg/m³, where thin surface cracks have developed in this study, see above.

These preliminary results indicate that the addition of steel fibres delays the crack development and limits the crack widths. The addition of glass fibres seems to eliminate micro cracking and thus also macro cracking during the curing process, to such an extent that creep eliminates shrinkage cracking. After 100 days a low amount of glass fibres, group 3 with 5 kg/m³ seems to give specimens with no visual cracks. However, it is at this point too early to decide if this is an optimal fibre content.

4. FUTURE WORK

The addition of glass fibres in a fairly high dosage increases the costs of the shotcrete substantially. Therefore, the ongoing research focuses on the optimization of the glass fibre addition and the understanding of the interaction between shrinkage and creep of shotcrete. Shrinkage tests will also be performed using more realistic geometries and sizes of test specimens. The idea is to model a drainage construction on a slab of granite. Shrinkage, creep and relaxation of fibre reinforced shotcrete will be studied in detail.

REFERENCES

1. Malmberg, B., & Skarendahl, Å., "Method of studying the cracking of fibre concrete under restrained shrinkage", CBI Report 2:78, Cement and Concrete Institute, Stockholm, Sweden, 1978.
2. Ansell, A., & Holmgren, J., "Sprutbetongs krympning – Fiberblandning för bättre sprickfördelning", SveBeFo Rapport 87, ISSN 1104-1773, Stockholm, Sweden, 2007. (In Swedish).
3. Carlswärd, J., "Shrinkage cracking of steel fibre reinforced self compacting concrete overlays – Test methods and theoretical modeling", Doctoral thesis, Dept. of civil and Environmental Engineering, Luleå University of Technology, Sweden, 2006.
4. Trisch, N., Darwin, D. & Browning, J.A., "Evaluating shrinkage and cracking behaviour of concrete using restrained ring and free shrinkage tests", SM Report No 77, Structural Engineering and Engineering Materials, The University of Kansas Center for Research Inc., Lawrence, Kansas, 2005.
5. Byggstandardiseringen, "Färsk betong – Konsistens – Sättningsmått", Svenska standard SS 13 71 21, Stockholm, 1984. (In Swedish).

Session B9 – STRUCTURAL BEHAVIOUR

A study of concrete shear keys in prefabricated bridges with dry deck joints



Robert Hällmark
M.Sc.
Ramböll/LTU
Kyrkogatan 2, Box 850
SE – 971 26 Luleå
martin.c.nilsson@ltu.se



Peter Collin
Professor/Bridge Manager
LTU/Ramböll
Kyrkogatan 2, Box 850
SE – 971 26 Luleå
peter.collin@ramboll.se



Martin Nilsson
Ph.D.
Luleå University of Technology
SE – 971 87 Luleå
martin.c.nilsson@ltu.se

ABSTRACT

In order to make prefabricated bridges even more competitive, a prefabricated concrete deck with dry joints has been developed. This type of bridge deck has been used on single span bridges in Sweden, and is now under development for multi span bridges. This paper describes how this prefabricated bridge deck system works. Results from laboratory tests of the shear keys in the dry joint are also presented, together with a summary about ongoing research in this area.

Key words: Bridge, prefabrication, element, dry joints, laboratory tests.

1. INTRODUCTION

There is always a need to rehabilitate, widen or rebuild bridges. To reduce the construction time and to minimize the impact on the traffic situation, prefabricated bridges can be used. Prefabricated steel girders are rather common but prefabricated concrete deck elements are still a rare exception. In order to make prefabricated bridges even more competitive, a prefabricated concrete deck with dry joints has previously been developed. This system has been used on a few single span bridges in Sweden and is now under development for multi span bridges. The aim of this R&D project is to enable the use of dry joint in multi span bridges, without the need of pre-tensioning. Particular attention has been paid to the ease of manufacturing.[1][2][3]

The concrete deck elements are match-cast and transfer forces, from one element to another, through shear keys. To transfer both lateral and vertical forces through the transverse joints, and to prevent vertical displacements between the deck elements at the joints, overlapping concrete keys are used. These keys are designed as a series of overlapping male-female connections along the joints, see Figure 1. In order to avoid miss match in the dry joint, the elements are match-cast.

The theoretical distance between the transversal reinforcement bars in the concrete deck elements and the shear studs on the steel girders is limited, and the tolerances can be demanding since the overlapping concrete keys require a longitudinal displacement of the elements at the assembling. The displacement has to be at least the depth of the



Figure 1 – Dry joint

overlapping concrete keys plus the tolerances, see Figure 2. [2]

If possible, it would be preferable to use shear keys with smaller depth. However, the shear keys must be able to transfer the forces given in the design codes [4]. By using a FE-model it can be shown that a maximum of about 40% of the traffic load acting on a single element is transferred through one of the joints. The rest of the load is transferred directly to the steel girders, or through the dry joint at the opposite side of the element. Therefore, the shear keys must be able to resist a load that is at least 40% of the design load given in the codes.

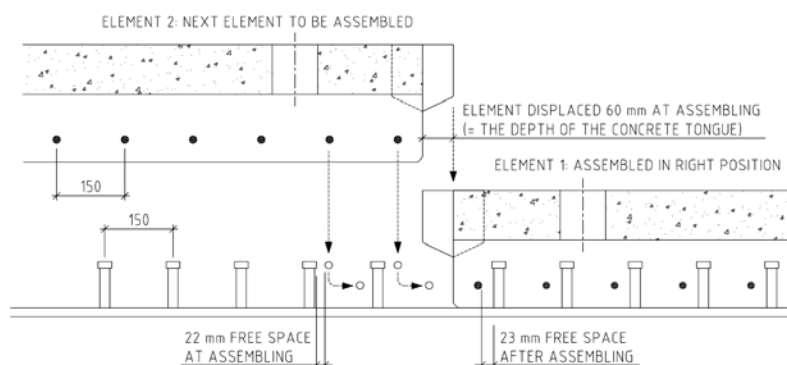


Figure 2 – Illustration of the limited tolerances. [2]

In order to find out how the shear keys transfer forces, and to be able to predict their strength, laboratory tests have been performed.

2. LABORATORY TESTS

The first tests series in the laboratory have been focused on a pure shear failure in the concrete shear key. Twelve static tests with three different layouts of the shear keys have been tested. The test set-up and the specimens are briefly described in the following sections.

2.1 Test set-up

The tests were focused on pure shear capacity of the concrete keys. This means that no positive or negative effects were simulated, such as prestressing from the steel girders, or any misfit between the elements. A schematic and simplified sketch of the test set up is shown in Figure 3.

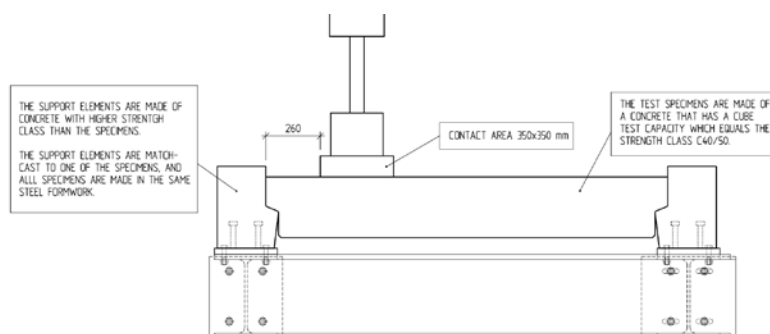


Figure 3 – Test set-up

2.2 Test specimens

The general geometry of the test specimens were 1,8 x 1,3 m, with a concrete shear key depth of 60 mm and a length of 540 mm, see Figure 4. The specimens were cast in a concrete with a cube test capacity that should equals the strength class C30/37. For each specimen, six concrete cube tests were performed, 3 compressive and 3 tensile.

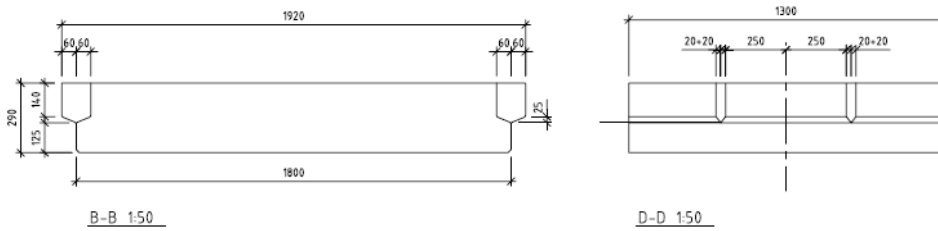


Figure 4 – General geometry of test specimens.

The first specimens were reinforced with exactly the same amount of reinforcement used in deck elements in previously constructed single span bridges. In these specimens the shear keys were the same in both ends. The second type of specimens had reduced shear key reinforcement, compared to the first specimens, in one of the shear keys. The second shear key was completely without reinforcement. With this design, 4 test results is gain for each type of shear key. Figure 5 shows the reinforcement drawing of the second type of specimens.

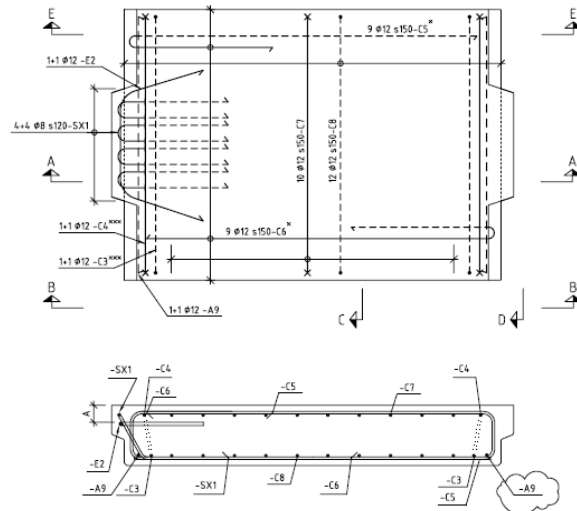


Figure 5 – Reinforcement drawing, specimen 2.

3. RESULTS

3.1 Shear key tests

Two different kinds of failures were observed when the reinforced shear keys of were tested. Firstly, five of eight specimens failed by cracks that activate the reinforcement, giving a ductile behaviour. The shear keys remained as one piece, but with some concrete crushing in the lower parts. Three specimen failed by cracks that were developed outside the reinforcement, resulting in a failure that separates the shear key from the rest of the specimen. This type of failure occurred under lower loads than the previously described failure. The load-time curves from the four tests with a specimen reinforced with the same amount of reinforcement previously used in single span bridges, is shown in Figure 6. The force presented in the diagram is the force that passes through the shear key during the test. The two different types of failures are illustrated by the photos in Figure 7. Table 1 summarises the results from all of the tests.

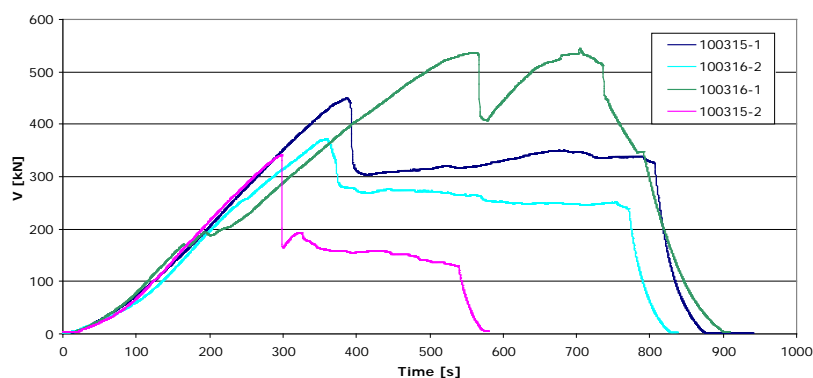


Figure 6 – Load-time curve for shear keys of Type 1.

Table 1 – Summary of test results.

Cast date	V_{max} [kN]		
	Ø12	Ø8	no
2010-03-15	449	-	-
2010-03-15	337	-	-
2010-03-16	532	-	-
2010-03-16	370	-	-
2010-03-18	-	285	-
2010-03-18	-	-	104
2010-04-07	-	222	-
2010-04-07	-	-	114
2010-04-08	-	363	-
2010-04-08	-	-	123
2010-04-12	-	376	-
2010-04-12	-	-	82



Figure 7 – Photos of two shear keys with different kind of failures.

3.2 Material tests

The mean values for each specimen is presented in Table 2 below.

Table 2 – Concrete parameters.

Cast date	Test date	Age [days]	δ [kg/m ³]	P_{cc} [kN]	f_{cc} [MPa]	P_{ct} [kN]	f_{ct} [MPa]
2010-03-15	2010-06-16	93	2334	1045	46,1	118	2,6
2010-03-16	2010-06-11	87	2345	1132	49,7	123	2,8
2010-03-18	2010-06-02	76	2372	1082	47,6	103	2,3
2010-04-07	2010-06-08	62	2330	967	42,6	94	2,1
2010-04-08	2010-06-11	64	2358	1009	44,5	115	2,6
2010-04-12	2010-05-31	49	2371	970	42,9	99	2,2

4. CONCLUSION AND FURTHER RESEARCH

The results from the tests differs quite a lot, still some interesting things can be noted. First, the tests show that unreinforced concrete can not transfer the design shear forces, caused by the vehicle models in Eurocode, from one element to another. This was an expected result, in line with the result from the calculations. However, in the reality we believe that the shear keys can transfer a higher load since the surrounding elements will deflect together with the loaded element which probably gives longitudinal compressive forces which would counteract the tensile stresses that occurs due to the shear forces.

Second, the load carrying capacity of the previously used shear keys seems to be larger than necessary, especially if we can avoid a failure that is developed by a crack growing through the

concrete covering. The shear keys with less amount of reinforcement ($\text{\O}8\text{mm}$) are still strong enough to carry the load. Therefore, we suggest some changes in the shear key reinforcement since we see some potential improvement. The layout of the reinforcement in the shear keys will be changed, and smaller rebars will be used in order to allow smaller bending radius. By doing this we will be able to strengthen the corners of the shear keys. The new shear key will be tested in new laboratory test in the spring 2011.

As a complement to the laboratory test, a ten year old bridge, built with these shear keys will be inspected and monitored, in order to prove that this kind of bridges behaves quite similar to composite bridges with in-situ cast bridge deck.

REFERENCES

1. Hällmark, R., Collin, P & Nilsson M., "Prefabricated composite bridges," Proceedings, IABSE Symposium, Bangkok, Thailand, Sept. 2009, Vol. 96, pp. 282-283.
2. Hällmark, R., Collin, P & Stoltz A., "Innovative Prefabricated Composite Bridges," Structural Engineering International, 2009, Vol. 19, no:1, pp. 69-78.
3. Collin et al., "International workshop on prefabricated composite bridges", March 4th 2009, Stockholm, ISBN: 1402-1536.
4. EN 1991-2, Eurocode 1 – Actions on structures - Part 2: Traffic Loads on Bridges. CEN, European Committee for Standardization: Brussels, 2005.

Short- and Long-Term Measurements of Resonance Frequencies on Prestressed Concrete Beams



Peter Lundqvist
M.Sc., PhD-student
Div. of Structural Engineering
Lund University
P.O. Box 118, SE-221 00, Lund
peter.lundqvist@kstr.lth.se



Nils Rydén
M.Sc., PhD
Div. of Engineering Geology
Lund University
P.O. Box 118, 221 00, Lund
nils.ryden@tg.lth.se

ABSTRACT

Currently, no method exists for determining the prestress forces in prestressed concrete structures. According to the theory of acoustoelasticity, the modulus of elasticity of concrete is stress dependent, which means that the resonance frequency of a concrete structure also is stress dependent. In this study, both short-term and long-term measurements of the resonance frequencies of four prestressed concrete beams were performed. The results show that the acoustoelastic effect in concrete is measurable and that the resonance frequencies increase with the applied compressive stress and that the prestress losses can be monitored through measurements of the resonance frequencies.

Key words: Concrete, Prestress Losses, Resonance Frequency, Acoustoelasticity.

1. INTRODUCTION

1.1 General

Currently, no method exists for determining the state of stress in a concrete structure, which for example, could be very useful for prestressed concrete structures where the safety and integrity of the structure depend on the induced compressive stresses. Due to creep and shrinkage of the concrete and the relaxation of the prestressing steel, the prestress forces decrease with time and there is thus a need for a non-destructive method to estimate the prestress losses. In this study, measurements of the resonance frequencies of four prestressed concrete beams have been conducted both during the post-tensioning process and continuously over a longer period of time. The purpose is to investigate the possibilities to estimate the state of stress in the concrete by simply measuring the resonance frequencies.

The beams were 3 meters long with a square cross section of 350 x 350 mm². The tendon, placed straight in the centre of the cross section, was of the type VSL consisting of 5 strands, each with a diameter of 15 mm. Three of the beams were prestressed and the fourth beam was used as a reference, the initial post-tensioning force was approximately 850 kN. The concrete quality was C35/45 with a water-cement ratio of 0.4.

1.2 Acoustoelasticity

The acoustoelasticity theory concerns the influence of stress on acoustic wave velocities in non-

linear elastic materials, normally the increase in wave velocity due to compressive stress [1]. The variation of the wave velocities is due to the change in modulus of elasticity in a material under stress. Since the resonance frequency depends on the modulus of elasticity the resonance frequency is also stress dependent. The acoustoelastic effect is very small and normally negligible. The relative change in modulus of elasticity is approximately 2 % for the stress levels used in this study.

2. MEASUREMENTS

The resonance frequencies of the beams were excited using an impact hammer and the vibrations were obtained by a piezoelectric accelerometer attached to the beams. Figure 1 shows the excitation points for the different modes of vibration. The signals were recorded by connecting both the impact hammer and the accelerometer to a data acquisition system. During all measurements the beams rested on two triangular steel supports, placed 672 mm from each end of the beams, see figure 1. This placement of the supports coincides with the nodal points of the fundamental flexural mode and is also close to the nodal points of the first higher longitudinal and torsional mode. The applied prestress force was measured using Glötzl anchor load cells placed under the anchor head at the passive end of the beams.

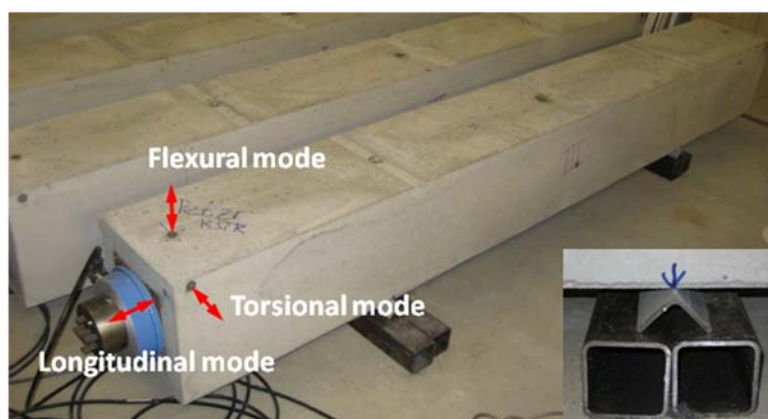


Figure 1. The excitation points for the different modes of vibration. The accelerometer was attached at the position at the other end of the beam. The small picture shows the outline of the supports.

2.1 Measurements during post-tensioning

The post-tensioning was performed in steps of approximately 100 kN, which corresponds to 1 MPa of concrete stress, up to 950 kN and reduced to zero load in similar steps. At each step the resonance frequencies for two modes of vibration, longitudinal and torsional, were measured. For beam 1, the resonance frequencies in the unstressed state for the first higher longitudinal and torsional mode were 1331.7 and 778.6 Hz. For each load step and mode of vibration the final value was the mean value of twenty resonance frequency measurements.

2.2 Long-term measurements

The resonance frequencies of the beams, including the unstressed reference beam, were measured continuously during a period of 11 months. During this time the beams were stored in a climate chamber with a constant climate of 20°C and about 60% RH. The resonance frequencies were measured for three modes of vibration; longitudinal, torsional and flexural. Similarly, the final values of the resonance frequencies were taken as the mean value of 20 measurements. For beam 1, the resonance frequency in the unstressed state for the fundamental flexural mode was 150.7 Hz. The loss of tendon force was recorded by the anchor load cells.

3. RESULTS AND DISCUSSION

3.1 Measurements during post-tensioning

The results from the measurements show that the acoustoelastic effect is measurable for concrete and that all of the studied resonance frequencies increased with the applied compressive stress. In figure 2, the result from the first higher torsional mode from one of the beams is presented.

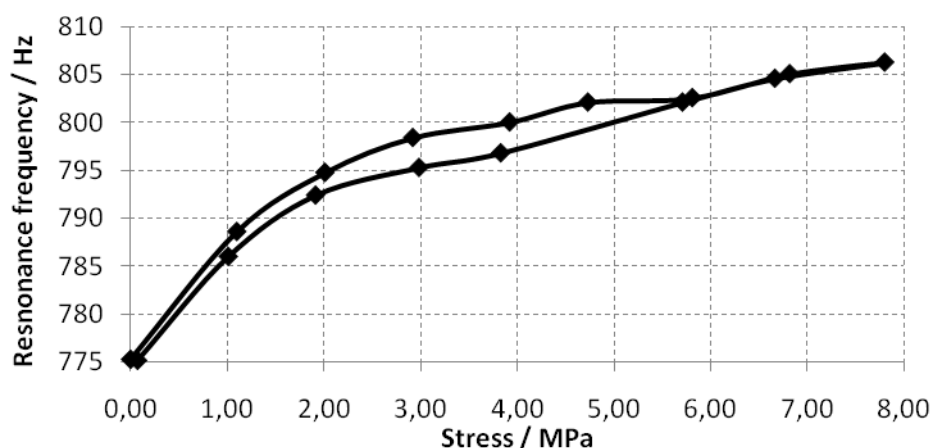


Figure 2. First higher torsional resonance frequency for beam 2.

The results from these measurements show that the resonance frequency for a simple prestressed concrete structure can be determined in a quick and simple way. Furthermore, the standard deviation between the 20 measurements performed for each load step and mode of vibration was low, ranging between 0.011 and 3.35 Hz, respectively. This shows that the method for measuring the resonance frequencies is both reliable and repeatable.

3.2 Long term-measurements

At a first view the results from the long-term measurements showed the opposite of what was expected, i.e. the resonance frequencies for all beams increased with time. Since the tendon forces decreased with time, the prestress losses were approximately 11% during the period, the resonance frequencies should also decrease. The fact that the resonance frequencies of the reference beam also increased indicated that the increase in resonance frequency and thus

modulus of elasticity was due to the cement reactions in the concrete and that this effect was greater than the acoustoelastic one and thus cancels it. However, by subtracting the results from the reference beam from the results for the other beams and hence eliminating all external and internal effects except for the acoustoelastic one, it was found that the resonance frequencies of the beams decreased over time, see figure 3. Further, the standard deviation for the 20 measurements were significantly lower than for the measurements performed during the post-tensioning, ranging between 0.002 and 0.05 Hz. The greater variation between the measurements during the post-tensioning may have been due to the influence of the hydraulic jack, which was attached to one of the ends of the beams during the entire procedure.

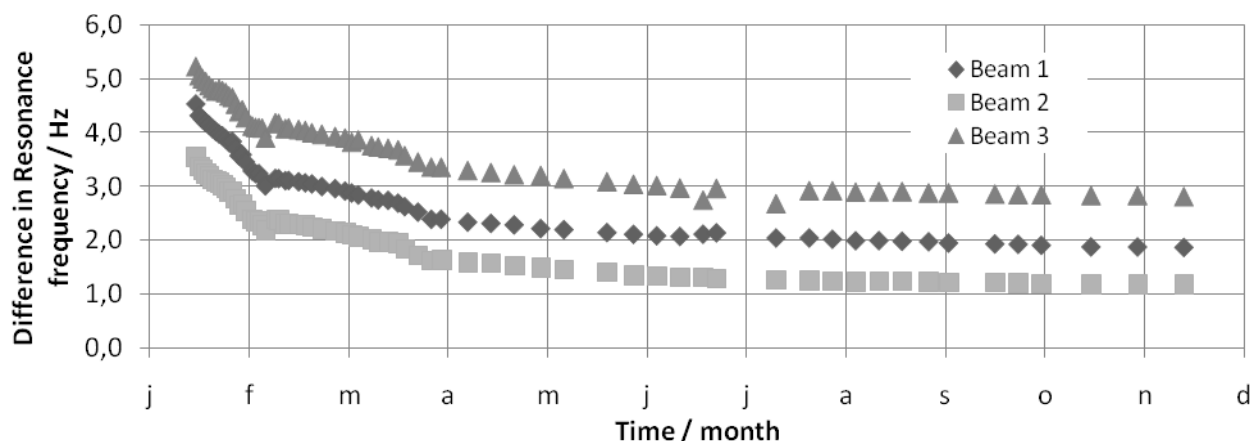


Figure 3. The difference between the resonance frequencies for the reference beam and the prestressed beams for the fundamental flexural mode of vibration.

The results shown in figure 3 indicate that by monitoring the development of the mechanical properties of the concrete, i.e. the cement reactions, and the ambient climate, i.e. temperature and relative humidity, the change in the state of stress in a simple concrete structure can be estimated by measuring the resonance frequency. Further, the increase in modulus of elasticity due to cement reactions will probably stabilize with time and thus only the acoustoelastic effect will be present.

4. CONCLUSIONS

- The measurements show that the acoustoelastic effect in concrete is measurable and that the resonance frequencies depend on the compressive stress.
- The resonance frequencies for a simple prestressed concrete structure can be determined in a quick, reliable and repeatable way.
- The results from the long-term measurements in this study indicate that the change in the state of stress in a simple concrete structure can be detected over a longer period of time by measuring the resonance frequencies of the structure and monitoring the development of the mechanical properties.

REFERENCES

1. Feldmann R., Shokouhi P., Wigggenhauser H., "Stress dependency of sonic velocity in concrete under uniaxial load", Transportation Research Board 87th Annual Meeting, Washington DC, 2008.

Highly Active Photocatalytic Innovative Concretes



Andrea Folli
M.Sc., Ph.D.
DTI - PostDoc Fellow
Gregersensvej 4
DK-2630 Taastrup (DK)
anfl@teknologisk.dk

ABSTRACT

The present study addresses the air pollution mitigation properties of TiO_2 – contained photocatalytic concrete by means of oxidation of nitrogen oxides (NO_x). From this starting point a novel research and development project (PhoEnICs) funded by the EU is outlined. The aim is to enhance the photocatalytic activity of such innovative concretes under visible light and in general under Northern Sky conditions to make this technology more attractive in Northern Countries where it is still restricted due to climatic conditions.

Keywords: TiO_2 , photocatalytic concrete, visible light, NO_x .

1. INTRODUCTION

Applications of TiO_2 photocatalysts to construction materials began towards the end of the 1980s. Redox reactions on the photocatalyst surface [1], promoted by sunlight (or in general, weak U.V. light), drive the oxidation of environmental pollutants. The photo-induced surface hydrophilicity [2] enhances this self-cleaning effect by mobilising dirt and stains through rainwater soaking between the adsorbed substance and the TiO_2 surface. Examples of TiO_2 – cementitious binders for enhanced aesthetic durability are included in many Southern European, North American and North African structures [3].

The pollution mitigation effect provided by TiO_2 in concretes is mainly achieved by oxidation of atmospheric nitrogen oxides (NO_x) to nitrates (NO_3^-). NO_x represents the total concentration of nitric oxide (NO) and nitrogen dioxide (NO_2) [4]. Amongst the most used technologies for NO_x remediation (combustions modifications, dry processes and wet processes), photocatalytic oxidation (PCO) has become a valid alternative since the catalyst can be supported on conventional structures and requires only light, atmospheric oxygen and water.

2. EXPERIMENTAL

2.1 TiO_2 sample

Table 1 shows the main physical chemical properties of the selected sample (Millenium Chemicals PC-105). For a full discussion of the characterisation work the reader should refer to another paper of the same author [5].

Table 1 – TiO₂ physical chemical characterisation data.

Sample	Crystalline Phase	Band Gap <i>eV</i>	<i>S</i> _{BET} <i>m</i> ² <i>g</i> ⁻¹	BJH Φ_{pore} \AA	Particle size		
					TEM <i>nm</i>	XRD <i>nm</i>	BET <i>nm</i>
PC-105	100% Anatase	3.34±0.02	78.9	79.6	18.4±5.0	16.6±2.0	19.5

2.2 Depollution, NO_x oxidation test

Mortar samples for the NO_x oxidation test have been prepared according to the procedure described in the European Standard ISO 679 [6]. Mortars were cast in 9 cm diameter x 1 cm thickness plastic Petri dishes. Two sets of twelve mortar discs each were produced, one set containing TiO₂ and one without photocatalyst as a control. Samples were cured for seven days at room temperature in sealed plastic bags and further seven days at room temperature and 60 % of relative humidity. NO_x oxidation experiments have been carried out in a continuous gas flow reactor equipped with a chemiluminescence analyser according to the Italian Standard UNI 11247 [7]. The system was kept at room temperature. U.V. light is provided by an OSRAM ULTRAVITALUX lamp having a main emission in the U.V.-A field distributed around a maximum intensity wavelength of about 365 nm. The lamp – sample distance was set to achieve on the upper sample surface an average irradiance of $20 \pm 1 \text{ W m}^{-2}$. A schematic diagram of the photocatalytic reactor equipped with the U.V. lamp is illustrated in Figure 1. Experiments were carried out at an inlet NO concentrations of 600 ppb in air with a ratio NO/NO₂ equal to 2 at three different flow rates: 3 l min^{-1} , 2 l min^{-1} and 1.5 l min^{-1} .

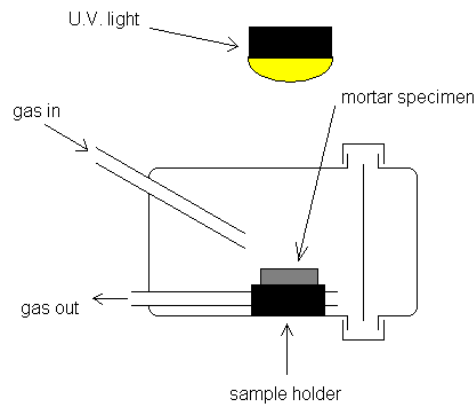


Figure 1 – Photocatalytic reactor for NO_x oxidation.

3. RESULTS AND DISCUSSION

Figures 2(a), 2(b) and 2(c) show the total nitrogen oxides concentration profiles obtained during the NO_x oxidation test at three different flow rates and under illumination. In each graph trends obtained with photocatalytic cement mortars are compared to trends exhibited by TiO₂-free white cement mortars. The flat character of profiles where TiO₂ is not present indicates very low impact on NO oxidation by the cement environment itself.

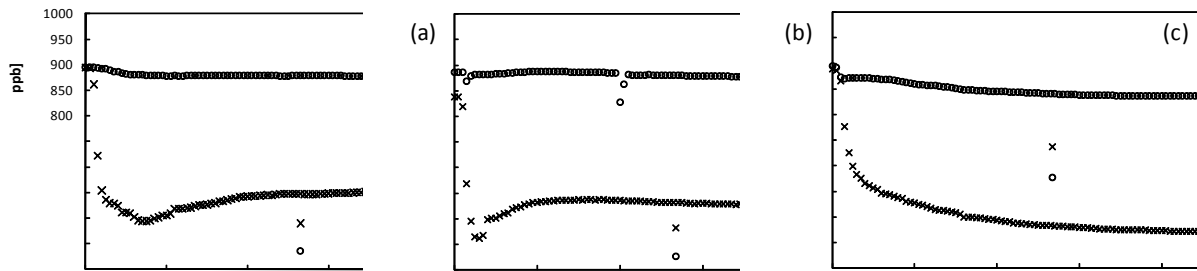


Figure 2 – NO_x (a), NO (b) and NO₂(c) concentration profiles.

The NO_x (NO + NO₂) pseudo steady conversion (after 90 min) versus flow rate is reported in Figure 3 (a). Results show that the lower the flow rate, i.e. the longer the average residence time in the reactor, the higher the final NO_x conversion. A decrease in the flow rate from 3.0 l/min to 1.5 l/min corresponds to an increase of about 10 % in the final conversion after 90 min. The NO_x conversion values here presented are highly dependent on the type of the reactor used, the initial NO_x concentration as well as irradiation conditions, however these experimental evidences are comparable with results obtained by other researchers [8].

The mechanism of NO_x oxidation on TiO₂ surfaces included in cementitious materials follows a pathway that is schematically illustrated in Figure 3 (b). NO₂ is oxidised to nitric acid, HNO₃ that is neutralised by Ca(OH)₂ to calcium nitrate, Ca(NO₃)₂. On the other hand, NO is promptly oxidised to unstable HONO that could either precipitate in the form of calcium nitrite, Ca(NO₂)₂ or continue the oxidative process to form NO₂ and therefore proceed to Ca(NO₃)₂.

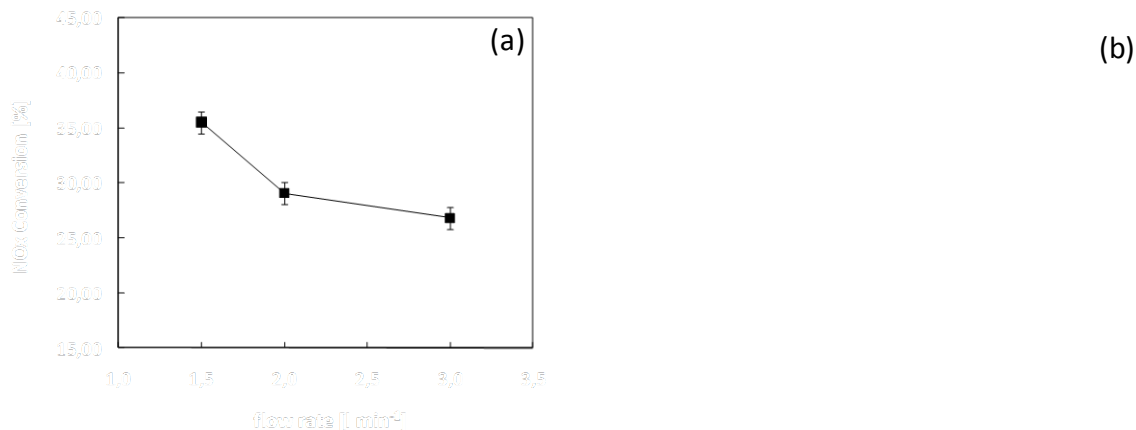


Figure 3 – NO_x conversion versus flow rate (a) and NO/NO₂ oxidation pathways (b).

4. PERSPECTIVES FOR APPLICATION OF PHOTOCATALYTIC CONCRETE IN NORTHERN COUNTRIES: THE *PhoEnICs* PROJECT

Laboratory tests here presented showed a significant NO_x abatement when TiO₂ – contained photocatalytic mortars are used compared to ordinary Portland cement mortars. NO_x drop has been observed being up to 35 % in the reactor design here adopted. Such a technology has also proved to provide major benefit in real outdoor conditions too. An assessment made by Zhu et al. [9] in 2004 showed that the implementation of ordinary TiO₂ in concrete over a total area of about 7000 m² of roadway in Milan (Italy) resulted in a 60 % drop in NO_x concentration in the air in 2002 compared to the relative value in 2001. Unfortunately, so far the application of TiO₂ – contained concrete technology is restricted to Northern European Countries due to their

geographical position within the least favourable belt according to the scheme of the world solar energy distribution (TiO_2 is mainly activated by UV light). At Danish Technological Institute a project denominated *PhoEnICs* (funded by the European Union under Marie Curie Actions FP7-PEOPLE-2010-RG n#268387) is ongoing in order to develop a *second* generation of photocatalytic concretes based on highly visible light sensitive TiO_2 systems obtained through innovative crystal and band structure engineering and/or metal ion coupling [10, 11]. The aim is to remove climate and seasonal considerations from the application of photocatalytic building materials and, through higher conversion efficiencies of the catalytic components, to reduce production costs, facilitating take up of the technology.

5. CONCLUSIONS

Laboratories and real world tests have shown that TiO_2 implemented in concrete is a valid technology to reduce the level of hazardous nitrogen oxides in the air, with % of reduction from 35 % to 60 %. However its application in Northern Countries is highly restricted to climatic and geographical conditions. The modification of TiO_2 through crystal engineering and ion metal implantation has shown good TiO_2 activity in the visible light spectrum. The application of these modified TiO_2 s to concrete will help the uptake of the technology in areas where the % of UV light in the solar radiation is much lower than areas within more favourable solar light belts.

REFERENCES

1. Fujishima, A. et al., "TiO₂ Photocatalysis: fundamentals and applications", Tokyo, BKC, 1999.
2. Wang, R. et al., "Light-induced amphiphilic surfaces", *Nature*, vol. 338, 1997, pp. 431-432.
3. Cassar, L. et al., "Photocatalysis of cementitious materials", in Int. RILEM Symposium on Photocat., Environ. and Constr. Mater., Florence ITALY, 2007, pp. 131-145.
4. Harrison, R. M., "Pollution: causes, effects and control", 2 ed, ed. R. M. Harrison, Cambridge, The Royal Society of Chemistry, Vol. 1, pp. 388, 1992.
5. Folli, A. et al., "Rhodamine B Discolouration on TiO₂ in the Cement Environment...", *J. Adv. Oxid. Technol.*, vol. 12, 2009, pp. 126-133.
6. ISO_679, "Cement - Test methods - Determination of strength", 2009.
7. UNI_11247, "Determination of the degradation of NOx...", Milan, 2009, pp. 1-11.
8. Strini, A. et al., "Low irradiance toluene degradation activity of a cementitious photocatalytic material...", *Appl. Cat. B.: Environ.*, 2011, in press.
9. Zhu, W. et al., "Application of nanotechnology in construction" *Mater. Struct.*, vol. 37, 2004, pp. 649-658.
10. Yang, H. G. et al., "Anatase TiO₂ single crystals with a large percentage of reactive facets", *Nature*, vol. 453, 2008, pp. 638-642.
11. Irie, H. et al., "Efficient visible light-sensitive photocatalysts: grafting Cu(II) ions onto TiO₂ and WO₃ photocatalysts", *Chem. Phys. Letters*, vol. 457, 2008, pp. 202-205.

Investigation of material parameters and structural performance of hybrid concrete beams



Linn Grepstad Nes
M.Sc., Ph.d. candidate
NTNU
Rich. Birkelandsvei 1A
N – 7491 Trondheim
linn.g.nes@ntnu.no



Jan Arve Øverli
Ph.d., Ass.Prof.
NTNU
Rich. Birkelandsvei 1A
N – 7491 Trondheim
jan.overli@ntnu.no

ABSTRACT

A hybrid concrete beam was composed by two layers of different types of concrete; the bottom layer consisted of fibre-reinforced lightweight concrete (FRLWC) and the top layer consisted of normal concrete. The top layer was cast one week later than the FRLWC. The investigation of material parameters and structural performance of this hybrid beam is based on both small scale testing and 4 point bending tests on larger beams designed for both shear and moment failure.

Key words: Hybrid concrete beam, fibre-reinforcement, small scale experiments, 4 point bending test

1. INTRODUCTION

The motivation for investigating the performance of such hybrid concrete beams is to design a structural element which utilises the most beneficial properties of different materials and combine them in one cross-section. The hybrid beams may represent one-way slab elements of which the bottom layer constitutes a precast formwork, resulting in a cost-effective product with respect to manufacturing, transport/assembling of the element and load capacity. Use of lightweight concrete minimizes the self-weight and the structural performance is taken care of by the conventional longitudinal tensile reinforcement and the 5cm top layer of normal concrete. A benefit of using fibre reinforcement is increased efficiency of manufacturing and the intention is that the requirement in Eurocode 2, concerning a minimum amount of secondary transverse reinforcement [1], can be fulfilled by using fibre reinforcement.

The investigation of material properties was based on preliminary small-scale testing covering the three point bending test [2], a uni-axial tension test [3,4] and a bi-surface shear test [5]. In order to study the structural performance a total of 16 beams were subjected to the four point bending test. Eight large beams were designed for shear failure containing different amounts of fibre reinforcement and another eight beams were designed for flexural failure with varying amount of fibre reinforcement and vertical reinforcement.

The work was carried out in cooperation with two graduate students, Tor Øystein Bjerve [6] and Hans Andreas Moe [7] and was a continuation of a similar project performed in spring 2010 [8].

2. EXPERIMENTS AND RESULTS

2.1 Small-scale experiments

The small-scale test program included three point bending tests, uni-axial tension tests and a bi-surface shear test.

The three point bending test was conducted according to the Norwegian Standard, NS-EN 14651 [2] on 6 small beams with 0.5% fibre content and 6 beams containing 1.0% fibres.

The uni-axial tension test was conducted on six specimens of FRLWC containing 0.5% steel fibres and the test method was a modification of both the RILEM Recommendation [3] and a method described by SINTEF [4]. The specimen size was 100x100x600 [mm] and a notch was located at the middle of the specimen. The notch had a width of 4mm and a depth of 10mm on each side of the specimen. The displacement was measured using transducers located on two opposite sides of the specimen over a distance of 100mm.

In order to obtain a reasonable value for the shear-stress capacity of the interface between concretes cast at different times, bi-surface shear tests were conducted on ten specimens [5]. The specimens were shaped as cubes with edges of length 150mm including a 5cm top-layer of normal concrete. The bottom layer of the cube was FRLWC containing either 0.5% or 1.0% steel fibres. Due to the sudden failure mechanism only the maximum load was recorded. The mean values of the shear-stress capacities were 2.8MPa and 2.0MPa for the specimens containing 0.5% and 1.0% fibres respectively.

The main results from the small-scale experiments are given in Table 1. In addition the mean cylinder compressive strength was measured to 17.2 MPa for the normal concrete.

Table 1 – Main results from small-scale experiments with LWC

Fibre content	Compressive strength f_c [MPa]	Tensile strength f_t [MPa]	E-modulus E [GPa]	Residual tensile strength $f_{ft,res2,5}$ [MPa]
0%	20.2	-	-	-
0.5%	20.4	1.4	17	1.3
1.0%	19.4	1.8*	12*	1.4

* Measured in another series of tension tests with similar concrete and fibre-reinforcement in March 2010

2.2 Four point bending test – shear failure design

Eight of the 16 beams were designed for shear failure focusing on studying the influence of different fibre content. Two beams had no fibre reinforcement at all, three beams contained 0.5% and the last three beams contained 1.0% fibres. The test setup is shown in Figure 1.

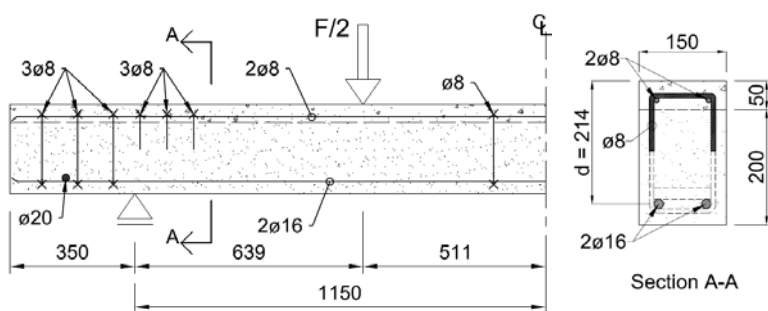


Figure 1 – Geometry and reinforcement for beams designed for shear failure (measures in mm)

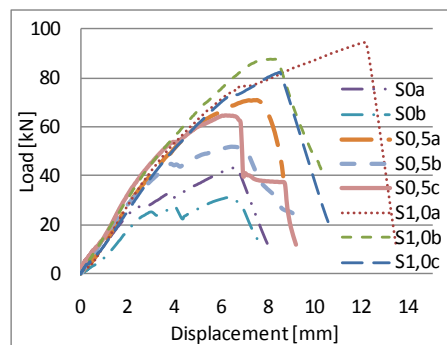


Figure 2 – Load-displacement diagrams, shear failure

The load-displacement diagrams for these beams are given in Figure 2. Despite the scatter, the results indicate that the maximum load increases with increasing fibre content.

2.3 Four point bending test – moment failure design

The remaining eight beams were originally designed for flexural failure and the tests focused on studying the influence of different fibre content (0.5% and 1.0%) and two different designs of reinforcement, see Figure 3 and Figure 5.

Reinforcement design 1

Four beams were designed with the placing of reinforcement shown in Figure 3. Two of the beams contained 0.5% steel fibres and two beams contained 1.0% fibres.

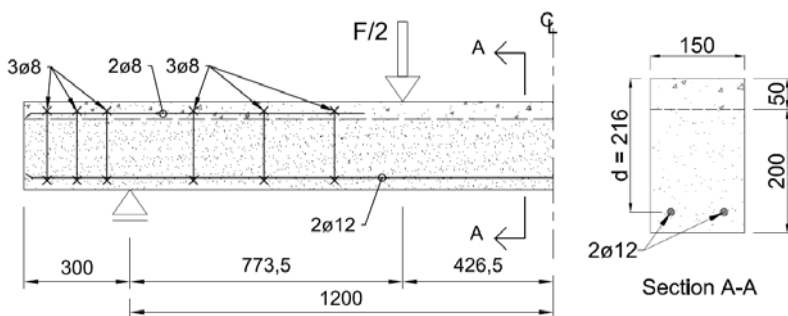


Figure 3 – Geometry and reinforcement for beams designed for flexural failure, design 1 (measures in mm)

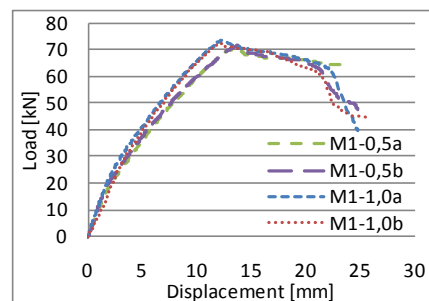


Figure 4 – Load-displacement diagrams, flexural failure 1

The load-displacement diagrams are given in Figure 4. The maximum load was approximately the same for all the beams and ranged from 70-73kN at a displacement of 12-13.6mm.

Reinforcement design 2

The remaining four beams were reinforced according to Figure 5. Two beams contained 0.5% steel fibres and two beams contained 1.0% fibres and the results are given in Figure 6.

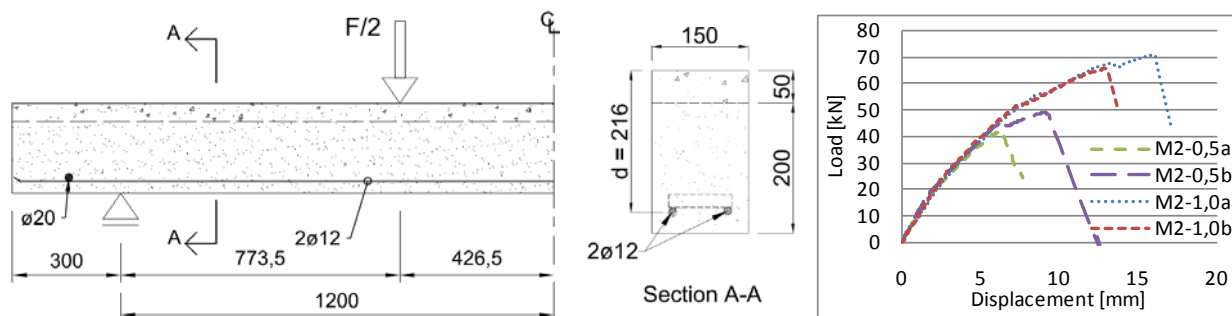


Figure 5 – Geometry and reinforcement for beams designed for flexural failure, design 2 (measures in mm)

Figure 6 – Load-displacement diagrams, flexural failure 2

All of these beams experienced shear failure although the preliminary design indicated flexural failure. Note that the maximum load for the beams containing 1.0% fibres is close to the failure load for the similar beams with reinforcement design 1.

3. CONCLUSION

The results indicate that the maximum load increases with increasing fibre content for the beams experiencing shear failure, while the moment capacity does not depend significantly on the fibre content. Shear-stresses at interface did not influence the structural performance of the beams.

The research presented in this paper is based on work performed in COIN - Concrete Innovation Centre - which is a Centre for Research based Innovation, initiated by the Research Council of Norway (RCN) in 2006 [9].

REFERENCES

1. NS-EN 1992-1-1:2004+NA:2008: Eurocode 2; “Design of concrete structures.”
2. NS-EN 14651:2005+A1: “Test method for metallic fibre concrete.”
3. Vandewalle, L. et al, RILEM TC 162-TDF: “Test and design methods for steel fibre reinforced concrete. Uni-axial tension test for steel fibre reinforced concrete“, *Materials and Structures*, Vol 34, Jan-Feb 2001, pp 3-6
4. Skjølvold, O.: KS 14-05-04-106 “Tensile test on concrete – Determination of Youngs modulus and tensile strength by uni-axial testing”, SINTEF Byggforsk 2007 (In Norwegian)
5. Momayez, A. et al, “Bi-Surface Shear Test for Evaluating Bond between Existing and New Concrete”, *ACI Materials Journal*, V. 101, No. 2, March-April 2004, pp. 99-106
6. Bjerve, T.Ø., “Hybride Betongkonstruksjoner”, Master’s Thesis NTNU, Trondheim, 2010. (In Norwegian)
7. Moe, H.A., “Hybrid Concrete Structures. Experimental testing and determination of shear capacity”, Master’s Thesis NTNU, Trondheim, 2010
8. Nes, L.G and Øverli, J.A.”Investigation of material parameters and structural performance of a concrete sandwich slab element”, submitted to fib Symposium Prague 2011
9. COIN. www.coinweb.no

Concrete Strategy for the Fehmarnbelt Fixed Link Project – Concrete Strategy for 120 years lifetime of the Concrete structures



Ulf Jönsson, M. Sc.
Concrete Expert
Femern A/S
Copenhagen, Denmark
E-mail: ujo@femern.dk



Christian Munch-Petersen,
M.Sc.
Senior consultant, Concrete
Expert
Emcon A/S
Copenhagen, Denmark
E-mail: cmp@emcon.dk

ABSTRACT

The Fehmarnbelt Fixed Link Project is one of the largest infrastructure projects in Europe. A 19 km broad crossing between Denmark and Germany served by ferries shall be connected with a bridge or a tunnel. The tunnel is the preferred solution, due to its lower risk profile. In any case a lot of high performance concrete shall be used. Construction is scheduled to start in 2014 and finalized in 2020. This paper presents some initial results of durability testing and discusses strategy for 120 years service life.

Key words: service life, exposure site, durability

1 CONCRETE STRATEGY

Femern A/S appointed therefore in March 2009 an Expert Group charged with the obligation of preparing Femern's requirements to concrete according to the agreed strategy and then to use these requirements for the tender documents for the Tunnel and/or the Bridge. The authors of this paper are in charge of the expert group. The strategy will be useful when general discussions occur during the formulation of the requirements and later in case of the Contractors request for deviations or in case of non-conformities.

Femern A/S will prepare the concrete requirements to Materials and Execution with the aim to ensure a service life of 120 years using well-known technology. The 120 years shall be obtained in a marine environment with frost action in the winter season.

Femern A/S will define a framework of requirements which will result in the desired the service life and which will ensure solutions within known technology.

For easier reference the requirements will be based on the framework of EN 206-1 and EN 13670-1 with sub standards for constituents and test standards. The amount of clarifications and amendments will of course be massive, as for example EN 206-1 is only securing a life time of 50 years.

Femern A/S wants an open competition between contractors, but it shall be ensured that the contractors do not compete on quality.

2 FIELD EXPOSURE SITE

The Expert Group contracted in 2010 the Laboratory at Danish Technological Institute as their house laboratory for among others the following tasks:

- Perform a comprehensive pretesting of different concrete mixes
- Arrange a Field exposure site in Rødbyhavn – close to the Fehmarnbelt.

with the aim to serve the following purposes:

- Collecting fresh, hardening and hardened concrete properties from various concrete compositions in order to have an input to the enquiry documents. For example the resistance against chloride ingress in concrete of age: 28 days, ½ year and 2 years old.
- Expose large test-panels from the Contractors pretesting in an environment identical to the environment for the coming Bridge or Tunnel.
- A field exposure site will make it possible to store the Contractors full scale trials in a secure and permanent way so that the development of the durability can be monitored. It will then be possible to conclude whether or not the actual used mix design follow the anticipated development from the pre-contract award trials.
- The Field Exposure Site will give an opportunity to collect data for future projects and serve as a platform for research activities for Universities and Institutes.

The Field Exposure Site will only give 3-4 years results before the construction of the Fehmarnbelt Fixed Link is started. The Expert group is therefore also collecting data from the construction of the two other major infrastructure projects (Storebælt fixed link – completed in 1998, and the Øresund fixed link – completed in 2000). The original data from these projects are supplemented with up to date durability inspections supported with a number of drilled out cores.

In this way the results from the pretesting can be calibrated to more than ten years of real life exposure of similar concrete in similar structures in a similar environment, and from these 10 years the results can be extrapolated to the required lifetime of 120 years.

3 RESULTS

Fifteen mix designs were developed with the aim to represent typical mix designs used for major civil engineering projects in southern Scandinavia plus some slag cement based mixes and SCC-variations. Target slump was set to 160 mm (except for SCC) and normal w/c-ratio to 0.40 (except mix H at 0.45 and mix I at 0.35). All mixes had a target air content of 4.5% except mix G and mix L, where the target air content was 2.0%. In mix O, the air content was generated by super absorbing polymers. Based on advice from the Expert Group and experiences from the construction of the Øresund Link as well as the Citytunnel in Malmö, Sweden it was chosen to perform the chloride migration testing with NT Build 492 and the frost resistance testing with SS 13 72 44-I (the Borås method).

Two wall slabs ($h \times w \times t = 2000 \times 1000 \times 200$ mm) from each mix design were cast in the laboratory. One slab was cored and analyzed, and one slab was transported to Rødbyhavn for field exposure. The initial results from the laboratory cured slabs are shown in Figure 1 and 2 below.

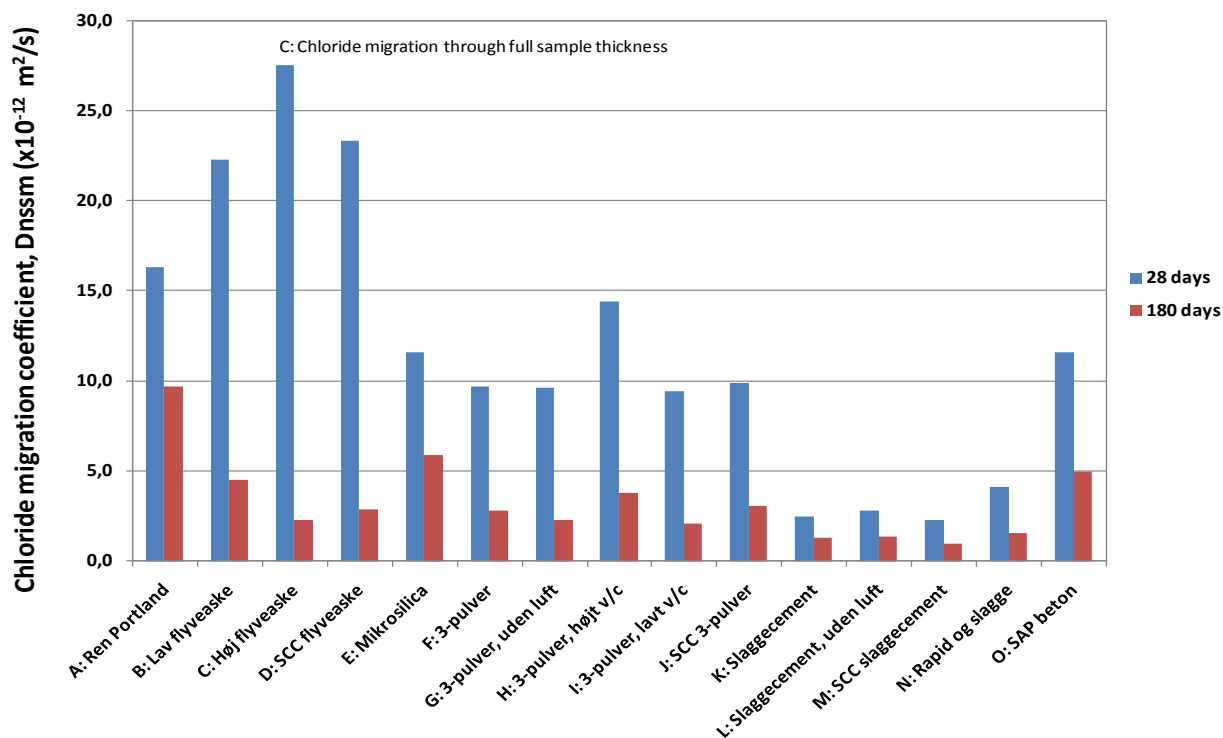


Fig. 1. Chloride migration coefficients after 28 and 180 days.

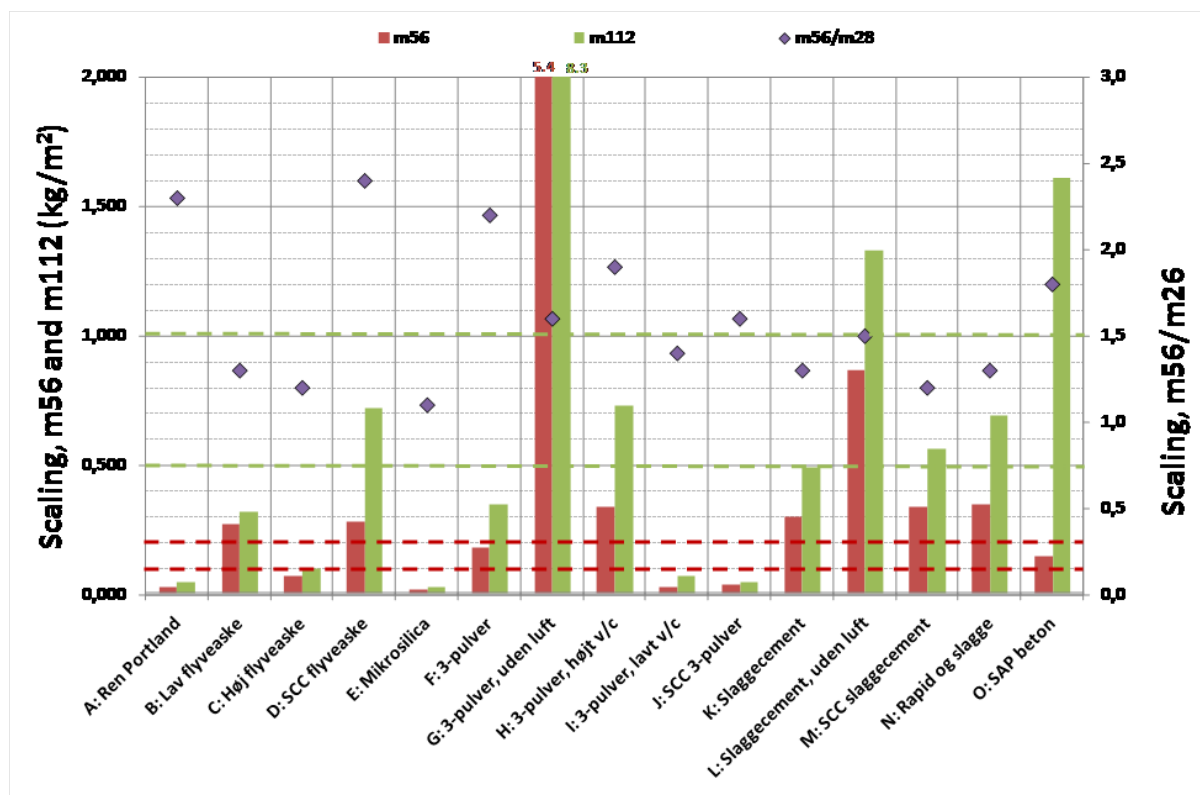


Fig. 2. Frost scaling after 56 and 112 cycles according to SS 13 72 44 A.

The data collected from the pre-testing indicates that:

- Frost-resistant concrete can be obtained with many different binder combinations
- Concretes with slag-cement do not have a sufficient frost-resistance, using the criteria from Øresund Link.
- Air-entrainment is necessary to obtain frost-resistance
- Concretes with flyash have a high chloride migration at 28 days – the more flyash the higher
- Concretes with flyash have a low chloride migration at 180 days – the more flyash the lower
- Concrete with high flyash content has a very low chloride migration at 180 days – almost as low as concrete with slag cement
- All binder combinations except the pure Portland cement mix has a Chloride Migration Coefficient of $3.5 \pm 2.5 \text{ m}^2/\text{s}$ after 180 days. Pure Portland Cement is higher.

4 CONCRETE REQUIREMENTS

Performance requirements can only be used in a contract if methods for calculating the lifetime based on test results are commonly agreed and scientifically accepted.

The Expert Group did not find the evidence for using the ultimate performance requirement: The concrete shall have a lifetime of 120 years!

An important part of this conclusion is the fact, that even if chloride migration can be evaluated with some certainty, the threshold value for chloride induced corrosion is not known or cannot be measured.

Another important lack in knowledge about durability is the influence of cracks.

Therefore the Expert Group is working with detailed requirements to subjects like:

- Constituents
- Mix Design
- Production facilities
- Casting
- Curing

In addition Quality assurance, Certification, Education, Traceability and similar topics are dealt with in the specification.

For special requirements – for example frost resistance – a performance based test method will be required for the pretesting.

Textile reinforced concrete sandwich panels



Katarina Malaga
M.Sc. PhD
CBI Betonginstitutet
katarina.malaga@cbi.se



Örjan Petersson
Civ. Ing. PhL
Strängbetong AB
orjan.petersson@strangbetong.se



Kristian Tammo
civ.ing. PhD
CBI Betonginstitutet
kristian.tammo@cbi.se



Thomas Blanksvard
Civ. Ing. PhD
Sto Scandinavia AB
t.blanksvard@stoeu.com



Mathias Flansbjer
Civ. Ing. PhD
SP Sveriges Tekniska
Forskningsinstitut
matias.flansbjer@sp.se

ABSTRACT

The main reason for the final thickness of the concrete facade element is the importance of the protection of the steel reinforcement. By changing the current steel reinforcement to non-corrosive textile fibre net the requirement for thick concrete cover could be strongly reduced. Use of textile reinforced concrete (TRC) makes it possible to produce much thinner and slimmer concrete facades in the future. This article presents selected results from the pilot production of new light weight sandwich element reinforced with AR glass fibre and carbon fibre net. This study is a part of a Formas-BIC project (2009-2011) ending in December 2011.

Keywords: concrete, sandwich element, textile reinforced concrete, AR glass net, carbon fibre

1. INTRODUCTION

During the recent years the development of fibrous materials applied for civil engineering applications has been receiving a great deal of attention by the textile, building material and construction sectors [1-3]. Textile reinforcement in form of oriented or randomly distributed fibrous structure has been widely used for last decades in concrete applications. Technical textiles are normally used for apparel applications, packaging, sport and medical equipment. Due to the flexibility of the textiles new application might be of great importance in the traditional construction sector. Technical textiles in combination with concrete can offer possibilities for modern shaping of the structures, reinforcement, rehabilitation and non load-bearing application such as in façade elements.

The requirements of the load capacity of concrete sandwich elements are often strongly over dimensioned. This is mainly due to the use of an inner concrete- or steel structure, which supports the vertical forces from snow loads and dead weights. The concrete facades shall often manage only to resist the horizontal wind load and local stresses from the anchorages and

connections of the facade into the load bearing structure behind. To secure the durability of the facade the concrete cover of the facade is often chosen to at least 30 mm. The deterioration of concrete is mainly due to steel corrosion. Normally, steel reinforcement corrodes with all deleterious types of effects when the structure is exposed to humid and salty environmental conditions. Thus, steel as a concrete reinforcement is limiting the service life of the concrete structures.

This concrete cover together with a typical placement of the reinforcement results often in concrete facade elements with a thickness of 80-120 mm. By changing the current steel reinforcement to non-corrosive textile fibres the demand on concrete cover due to durability is strongly reduced. A sandwich element with a thinner outer facade reduces not only the total weight but also the environmental impact from the manufacturing, handling and transportation process. Thinner outer layer in a sandwich element could also offer room, if needed, for a larger insulation layer. Since the dead weight of the facades is more or less directly proportional to the concrete thickness, using textile fibre reinforcement creates new possibilities to use these new types of concrete facades for repairs of older concrete buildings where light elements are to be preferred.

The goal of this project was to develop the technology for the production of different types of textile reinforced sandwich elements. In this project the main focus was on fibres in form of bars and net of carbon fibre and alkali resistant glass fibre. Alternative textiles have been also tested. The goal was to produce the concrete facade elements with as normal methods as possible and construction concrete concerning aggregate sizes, w/c and additives. The goal is to decrease the thicknesses of the outer layer of the facade elements to 20-40 mm.

2. RESULTS AND DISCUSSION

Before the production of the sandwich panels a FE modelling was performed. The modelled panels were of the following dimensions: length: 5400 mm; height: 2700 mm; thickness facade panel: 40 mm; thickness isolation: 200 mm; thickness inner-panel: 120 mm. The anchorage of the facade panel to the inner panel was done by the 12 SPA-B-5 and 3 SPA 2-8. The distance for the anchors was 1200x1200 mm, and in the corners 300 mm. The concrete strength class was assumed to be C30/37. The modelling was done by use of the continuum shell elements and the anchoring with beam elements. The sandwich panel was calculated for concrete's weight and wind load perpendicular to facade. The results demonstrated that it was fully possible to produce the sandwich panels with the textile reinforcement.

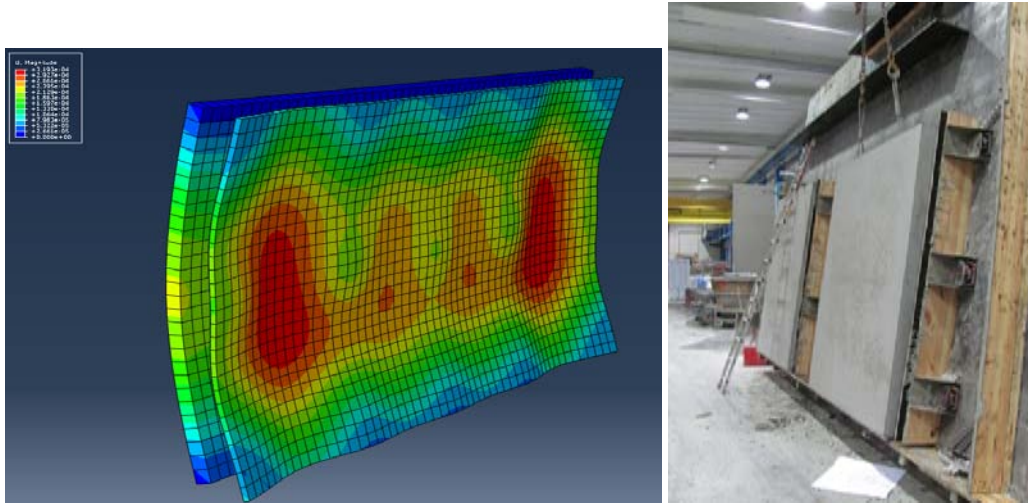


Figure 1 – FE model for the total deformation U for dimensioned wind $W = 1.57 \text{ kN/m}^2$ (left) and the produced sandwich panels.

Complementary load testing on concrete beams (800 x 100 x 40 mm) was performed for analysis of the different options of textile reinforcement for outer panel. Different types of reinforcement and their position were tested. In the pilot production of sandwich elements two textile reinforcement concepts were selected: 6 mm thick fibre glass rods arranged in a net pattern and carbon fibre net. The panels were of the following dimensions: length: 2000 mm; height: 2500 mm; thickness façade panel: 40 mm; thickness isolation: 150 mm; thickness inner-panel: 150 mm. The reinforcement was placed at the distance of ca 20 mm, in the middle of the façade panel. The casting of the glass fibre net reinforced sandwich was performed by a normal production procedure but the casting with the carbon fibre reinforcement required ‘casting in layers’: first the 20 mm bottom concrete layer was casted and after the placement of the reinforcement and arrangement of the specially designed textile anchoring the second layer was casted.

Figure 2 illustrates the production process of the panels.

The properties of the facade elements with the textile fibre reinforcement types will be further tested in full scale for a number of parameters:

1. Curvature and flexure due to an uneven moisture- and temperature distribution.
2. Risk of cracks.
3. Bond stresses between the textile fibre reinforcement and the concrete.
4. Sensitivities of transportation, lifting and installation of the facade elements.
5. The alkalinity resistance of the textile fibre material.
6. Different types of connections between the facade element and the load bearing element or structure.

The research project will be summarised in December 2011



Figure 2 – Preparation of the reinforcement (carbon fiber –left; glass fiber –right)

3. CONCLUSIONS

Preliminary results demonstrated full potential for production of the textile reinforced sandwich panels.

REFERENCES

1. RILEM Technical Committee 201-TRC, Textile Reinforced Concrete, State-of-the-Art Report. Edited by Brameshuber, W. RILEM Publications SARL, 2006
2. Hegger, J., Brameshuber, W and Will, N.” Textile Reinforced Concrete”. Proceedings of the 1st International RILEM Symposium. RILEM Publications SARL, 2010.
3. Peled, A.and Bentur, A. “Fabric structure and its reinforcing efficiency in textile reinforced cement composites”. Composites Part A: Applied Science and manufacturing, 34. Pp. 107-118, 2007.

Classification System for Formed Concrete Surfaces



Mari Bøhnsdalen Eide
M.Sc. Civil Engineering
SINTEF Building and
Infrastructure
NO-7465 Trondheim
E-mail:
Mari.B.Eide@sintef.no



Hedda Vikan
Ph.D
NPRA (The Norwegian
public Roads
Administration),
PB 8142 Dep,
NO-0033 Oslo
E-mail:
Hedda.Vikan@vegvesen.no



Kristin Kaspersen
Research Scientist
SINTEF ICT
NO-7465 Trondheim
E-mail:
Kristin.Kaspersen@sintef.no



Helene Schulerud
Senior Scientist
SINTEF ICT
NO-7465 Trondheim
E-mail:
Helene.Schulerud@sintef.no

ABSTRACT

Concrete Innovation Centre (COIN), is currently working with the development of a specification tool for concrete surfaces cast against smooth formwork. The tool covers greyscale and distribution of pores. Greyscale and pores shall be classified separately, which implies two separate systems for these parameters. Both classification systems will probably include four classes with demands. All classes will be illustrated with pictorial examples. Both systems shall include a project specific class for which demands can be made for a specific project. The systems shall also include a class without any demands.

Key words: Concrete surface, pores, greyscale, classification, image analysis

1. INTRODUCTION

To this date, no Norwegian tool for describing concrete surfaces with respect to the aesthetic expression exists. An architect must instead refer to existing projects or order a trial casting in order to describe what type of surface he or she wants. Subjective descriptions and misunderstandings can therefore often lead to time-consuming and expensive conflicts. Concrete Innovation Centre (COIN) is trying to develop a classification tool in order to describe smooth formed concrete surfaces objectively.

Development of methods for specification was started within the master thesis “Classification system for formed concrete surfaces” at The Norwegian University for Science and Technology (NTNU) in spring 2009 [1]. In this project greyscale, greyscale variation, pore size and the number of pores were considered as factors affecting the surface aesthetics. The thesis suggests an outline of a classification system for both pores and greyscale. A suitable method to measure these parameters is not established from the master thesis. The methods must be in place

before the classification criteria can be set. This paper will mainly cover the further work done within COIN to establish such methods.

2. THE CLASSIFICATION SYSTEM

2.1 Pore size and number

The classification system for pores will consist of pore classes and number of pores within a given size range. Pores are normally (in Norwegian standards) classified by the largest diameter. A long, narrow pore will, however, give a different visual expression than a circular pore. Classification by pore area will thus give a more realistic description of the surface. Pores that are smaller than 1 mm² will not be included by the classification tool. Pores with diameter larger than 15 mm, or areas larger than 177 mm², if a circular pore is assumed, are defined by Norwegian Standard (NS 4320) to be casting flaws [2]. Such flaws shall according to the standard be repaired and will thus not be included by the specification system. The pore groups are given in table 1. The classification system (including “Class 1-4”, project specific and class without demands) is not yet finalized as it is currently undergoing testing and proofing.

Table 1 - Classification of pores

Group	Pore diameter (mm)	Pore area (mm ²)
1	1-5	1 - 20
2	5-10	20 - 79
3	10-15	79 - 177

2.2 Greyscale and greyscale variations

Demands to greyscale are based on measurement of blackness. Tolerance limits of grey tone variation can be based on the black-white scale and expressed as \pm - values for the wanted value. One example of a symmetrical tolerance is 40 % \pm X %. The system will be based on differences in blackness and evaluate how discoloration appears. Limits of the classified groups (i.e. “Class 1-4”, project specific and class without demands) depends largely on the development of suitable measuring methods, and is not yet defined.

3. CHALLENGES CONCERNING DATA REGISTRATION AND METHODS DEVELOPED

3.1 General challenges

Manual registration and registration in the field can be both difficult and time-consuming. It is therefore preferable to have a more automatic system for data registration, and in this case a method based on photographic images is wanted. The method needs to ensure sufficient and reliable image quality. Challenges concerning the image quality are largely linked to lighting issues. Photographing surfaces for pore registration requires inclined lighting, preferably at an angle of 45°. Surfaces for greyscale analysis require diffuse and uniform lighting.

During the work with the classification system no suitable image processing programme has been encountered. Collaboration with SINTEF ICT, department of Optical Measurements and Data Analysis, was established to develop the photographic method and to create a programme for more automatic registration of data from images.

3.2 Method for photographing concrete surfaces

The methods for photographing concrete surfaces are under development and only the method for greyscale and greyscale variations have been tested in the field. In the setup two tripods are used, one for the camera and one for the flash. When photographing for pore registration the lighting should be inclined, and when photographing for grey scale analysis the lighting should be diffuse. It is therefore used a soft box around the flash. When the set-up is complete, four images are taken. First a picture of the test area, then a white paperboard is placed in front of the test area and a picture is taken. This image is used to adjust the final image for the flash distribution. Third, a picture of a large greyscale calibration tool inside the test area is taken for greyscale calibration. Finally, a picture of the test area alone is taken once again.

3.3 BetongGUI - a custom-made programme from SINTEF ICT

BetongGUI is an image analysis programme where pores, greyscale and greyscale variations can be analysed. An image in .jpg-format is loaded, the area to be analysed is marked and the programme then analyses every pixel with regards to greyscale. The pores are separated and are not included in the grey scale analysis, as they appear as dark due to shadows. A histogram for the greyscale in the image is produced, and the programme divides the test area into two areas showing the greyscale variation. Statistics for mean, maximum, minimum and standard deviation is part of the output. The pores are classified into three groups by their size, as shown in table 1. Screen shots for the different features are shown in figure 1, starting at upper left and going clock wise: main window, grey scale, pores and greyscale variations.

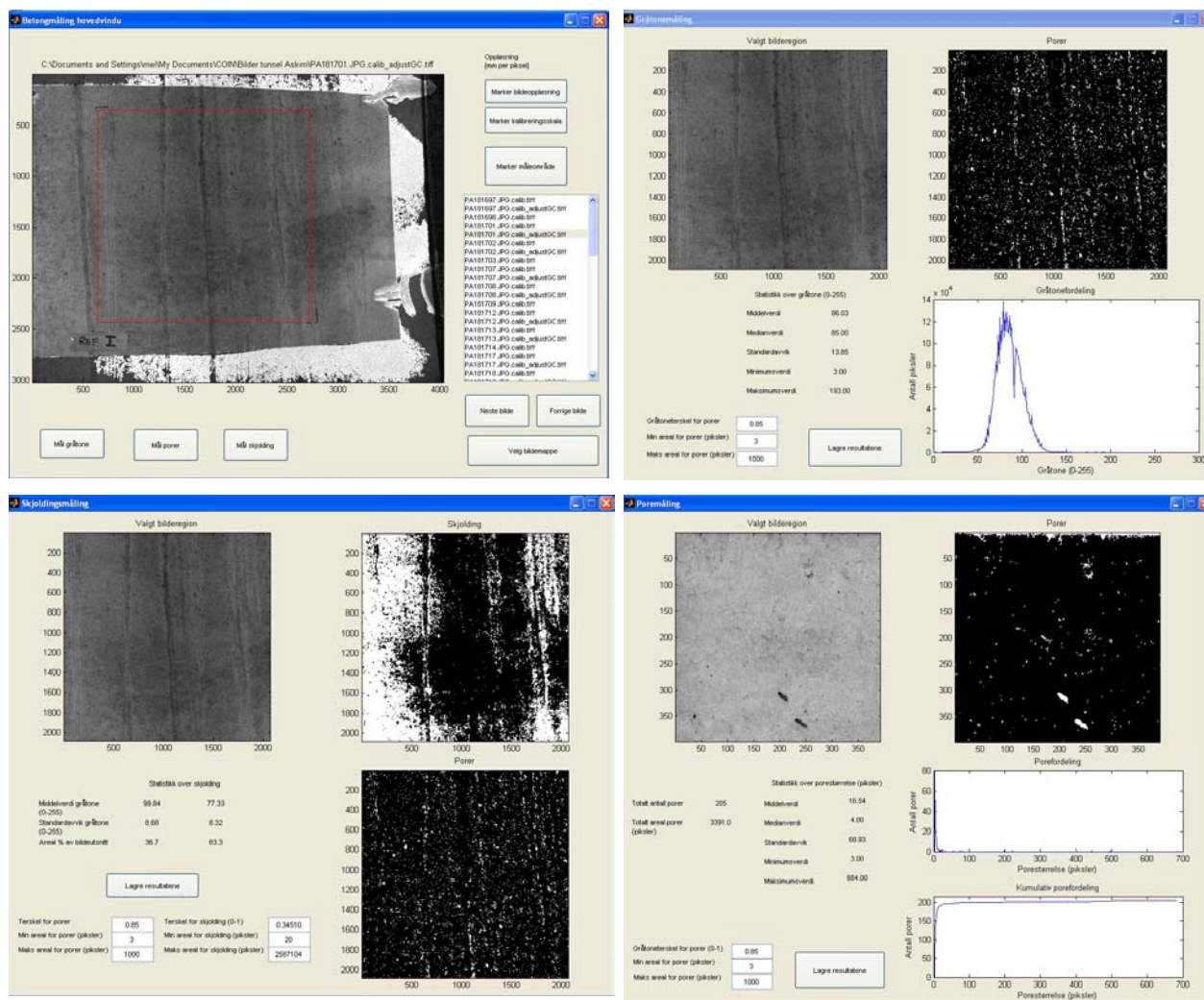


Figure 1 - Screen shots from BetongGUI

ACKNOWLEDGEMENT

The paper is based on the work performed in COIN - Concrete Innovation Centre (www.coinweb.no) - which is a Centre for Research based Innovation, initiated by the Research Council of Norway (RCN) in 2006. COIN has an annual budget of NOK 25 mill, and is financed by RCN (approx. 40 %), industrial partners (approx 45 % of which ¼ is cash) and by SINTEF and NTNU (in all approx 15 %). The Centre is directed by SINTEF, with NTNU as a research partners and with the present industrial partners: Aker Solutions, Norcem, Norwegian Public Roads Administration, Rescon Mapei, Skanska, Spenncon, Unicon, Veidekke and Weber Saint Gobain.

REFERENCES

1. Eide, Mari Bøhnsdalen and Hegseth, Ingrid "Classification system for formed concrete surfaces"
2. Norwegian Standard, NS 3420 - L:2008 "Beskrivelsestekster for bygg, anlegg og installasjoner - Del L: Betongarbeider"

Concrete Café – CONCRETE TEACHING

Renewing the teaching by using the students contributions



Per Goltermann
 Professor, DTU Byg, Department of Civil Engineering
 Technical University of Denmark
 Brovej, Bygning 118
 2800 Kgs. Lyngby, Denmark
 Direct: +45 4525 1684, Fax: +45 4588 3282
 pg@byg.dtu.dk

ABSTRACT

The teaching of concrete structures at DTU has been revised over the last years and the approach has been changed from a classic deductive to a more inductive approach, where teaching and understanding starts from observations of tests, videos, results etc. A large part of this material has been obtained from students CDIO-, bachelor- or master-projects as well as experimental courses, where e.g. the students own digital cameras record the testing and the resulting phenomena. This simple approach have lead to better projects work, better reports and presentations and also to a substantial amount of material for the basic courses in concrete structures. Students experimental data are also used in the courses, both improving the understanding and the students motivations.

Keywords: videos, students tests, teaching, inductive.

1. INTRODUCTION

1.1 General

DTU's Department of Civil Engineering (Byg) is responsible for the teaching of a large number of engineering students as e.g. BSc Building Technology, BEng Building Engineer, BEng, Arctic Engineering, BEng Architectural Engineering and MSc in Building Technologi, MSc in Architectural Engineering and MSc in Fire Safety.

These students will often have different goals, interests and knowledge levels, when they attend the courses in eg. Concrete Structures. This is a challenge for the teacher, who must motivate all these different types of students and at the same time explain things to these different students and this can create a problem.

The traditional, deductive teaching has worked very well for centuries and still works quite well for a number of teachers, even with just use of chalk and blackboard. However, the modern technology does have a number of new possibilities, which may be used to solve the problem and also enable a more inductive approach.

1.2 Where do we improve the teaching

DTU's building engineering educations aim at creating clear links between theories and the real behavior of real structures, or at least the behavior observed in experiments. DTU wish to teach the students to establish theoretical models on the basis of real observations and to design solutions, which will work in practice. This is considered to be an essential part of teaching the students to think as engineers.

The Department of Civil Engineering (Byg) and the study leaders have therefore ensured, that all bachelor students have more or less mandatory activities in the laboratories each semester. The BSc- and BEng-students are offered experimental work in each semester, supplemented by a CDIO-project for the BEng-students in each of the first four semester, in which they will produce and test one or several models.

These activities should ideally be combined testing in the auditorium during the traditional courses, but this is not always possible due to practical limitations and an alternative would be use of videos from testing. These videos could of course be produced by professionals, but would require quite large budgets, so we have instead decided to let the students produce the videos, as this is cheaper and seems to be better for the teaching and motivation.

2. AN EXAMPLE – TESTING OF A BEAM

It began when two students decided to use their own, little digital camera to take videos of their tests of load-carrying capacity of reinforced concrete beams. The student found it was an easy, simple and efficient way of making videos and that their own PC's had sufficient capacity for the editing with freely available software. This enabled also the students to extract pictures from the right 1/30 s of the video.



Figure 1 - Beam in the testing bench used by the BEng students during a CDIO-project.

2.1 Creating the video

Most students' record videos of their load-carrying tests to record the test and the failure mode, as they later may analyze the tests, extract pictures from the right moment of the test and also enhance the presentation of the projects, by showing a short video.



Figure 2 - Extracted photograph from the failure of the beam in Figure 1, indicating yielding of the reinforcement (large crack widths).

The planning, execution and analysis of the tests at Byg are carried out and reported in the traditional way and the videos are essentially just an additional documentation. The report contains all the information required to analyze and explain measurements and observations.

2.2 Using the videos

A number of lectures in the Concrete Structures courses are dedicated to the analysis of a certain failure mode (bending, shear, torsion or similar). These lectures may begin with a video, which clearly shows the failure. The theory can then be explained on the basis of the observations (see Figures 2 and 3), which seems to facilitate the understanding of the models and increase the students motivations.

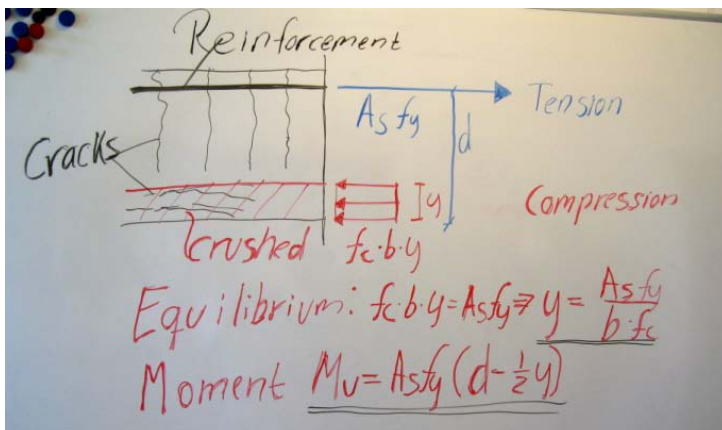


Figure 3 - Analysis of the failure mode in Figure 2 including estimation of the capacity.

The theory is often extended to a more general level after the initial, simple analysis and the limitations to the model are identified (e.g. the reinforcement ratios, required to obtain this kind of failure).

Experience so far shows, that a good test video and the test report can often be combined and used in a number of different lectures during a course (eg. bending failure, stress-strain curves for the reinforcement, test results for compressive test as an explanation of average, characteristic and design strength).

3. STUDENTS MOTIVATION AND IMPACT ON TEACHING

An essential part of the teaching is to motivate the students and to explain the theories and their basis to the students. This can be done in the traditional, empirical way (Traditional approach was used by a younger and an older coworker) or it can be done in the more inductive way including the videos (Inductive approach was used by the author) in combination with the theories.

The students rate the course and the teachers each semester in DTU's official course evaluations. They rate that the inductive approach helps them to understand the topics and helps the teacher to motivate them. This tendency seems to be equally significant for all types of BEng and BSc students

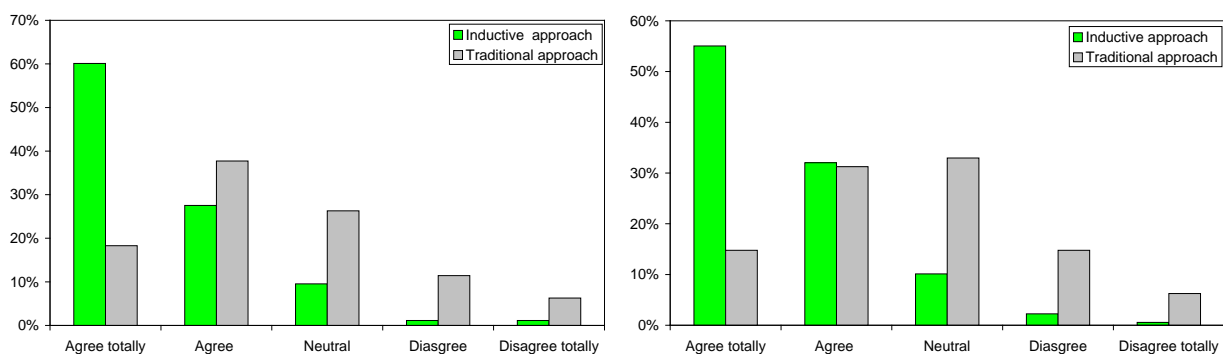


Figure 4 – Course evaluation statement and students response. Left: "I think the teacher is good at communicating the subject" and right: "I think the teacher motivates us to actively follow the class"

It is also the authors clear impression that the students actually prefer to see other students videos instead of more professional videos and that this clearly prove to them that their work and their results in projects and lab courses is valuable and useful.

4. CONCLUSIONS

It can be concluded that

- Using simple digital cameras for recording of tests is easy and provides the project students with significant new opportunities in projects and lab exercises.
- Using the students own videos and test results is a good, new possibility to improve the classic teaching – without any investment.
- Using the videos improve the teaching, understanding and motivation of the students.
- Using results from student projects, CDIO project and lab courses leads also to a renewal of classic courses, as it leads to a better cooperation between the different teachers and courses.

Examples of videos can be found at YouTube under ConStruct2800Lyngby or at www.concretestructures.byg.dtu.dk.

CLOSING SESSION

A study of the future for concrete bridge construction in Sweden



Johan Larsson
M.Sc., Ph.D. student
Luleå University of Technology (LTU)
971 87 Luleå, Sweden
Johan.Ojanen@ltu.se



Mats Emborg
Professor LTU / Head R&D Betongindustri AB
971 87 Luleå/Betongindustri AB, 100 74 Stockholm, Sweden
Mats.Emborg@Betongindustri.se
Mats.Emborg@ltu.se

ABSTRACT

The construction industry in Sweden has been considered to have a clear potential for a development to a higher degree of industrialization and efficiency. Despite the availability of new techniques for concrete bridge construction, the tradition of constructing in-situ with old methods is still the dominating construction method. To be able to describe, interpret and give an explanation to this phenomenon, this paper will investigate why new techniques are not commonly used. A comprehensive survey has been conducted and the results show that rules and norms, conservatism, and poor collaboration are some of the reasons for slow development.

Key words: Bridge construction, development, prefabrication, survey, future.

1. INTRODUCTION

The research project is studying how an industrialized process could benefit concrete bridge construction. The project starts by mapping the potential for prefabrication and industrialized methods and after, a development of new bridge parts and industrialized methods will be preformed. The pace of development for the construction industry is relatively slow compare to manufacturing industries [1] and reasons for that are under discussion during the last decade [2-3]. It is clear that the demand for lower production costs, faster construction time and better quality has increased over the last years. All kinds of partly or totally prefabricated bridge concepts are used frequently abroad, but in Sweden these kind of concepts are very rare. Prefabrication is a large part of industrialized construction, but you have to consider the whole process, from design to maintenance, to be able to get great benefits of an industrialized process. Prefabrication meant not only complete element that are mounted together at situ, but also left formwork that are designed to be a permanent structure and reinforcements that are prefabricated into cages or rebar carpets and mounted into the formwork [4, 5]. The question can be raised, what major forces are working against a development of the construction industry in general and especially the bridge building?"

A large survey with almost 70 respondents will form the foundation for this research. The respondents of the survey include contactors, suppliers, consultants and representatives from the Swedish Transport Administration, which in most cases are the client. Interviews and document studies will complement the survey to highlight the advantages and disadvantages of using more industrialized construction techniques. The interviews were semi-structured face to face-interviews, which according to [6] are defined as interviews with the aim to collect description from the informants' world, in order to be able to interpret the described phenomenon. The used documents are not produced to benefit the research, which makes them perfect as a rich and ready source of information, [7].

2. REASONS FOR LOW DEVELOPMENT SPEED

According to the survey, bridge construction industry is united in the fact that the efficiency has to increase in the future. Almost 80% of the total respondents are answering that they totally agree and 15% answer that they partly agree on the question; "Do you think that bridge construction need to be more efficient?" By creating an Ishikawa diagram (fishbone) of the reasons for low development speed, it is easy to systematically review factors from the survey that affect or contribute to hindering the development of the bridge construction.

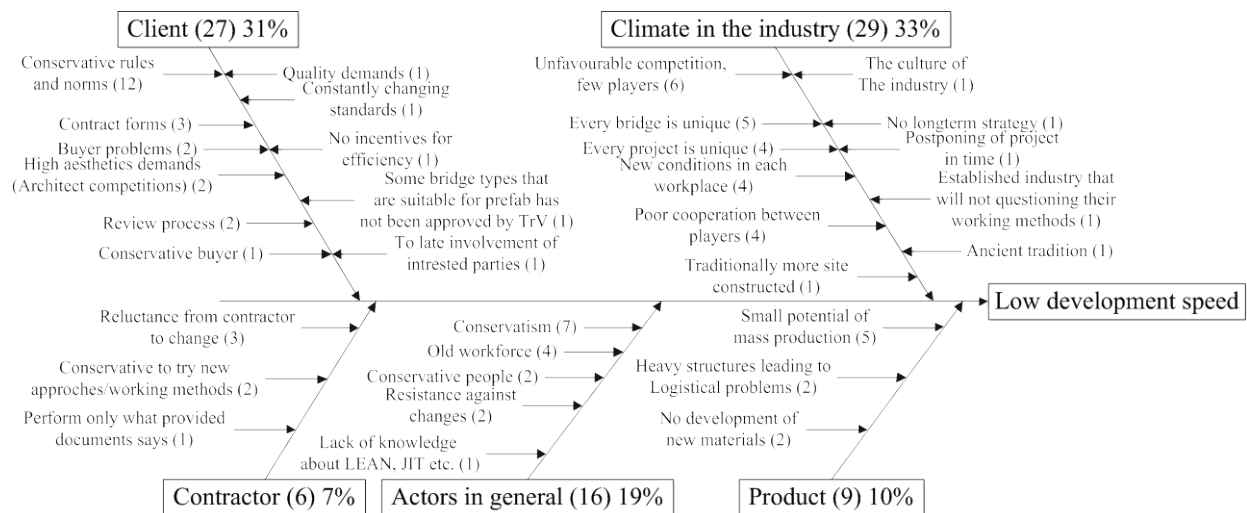


Figure 1 – Reasons for low development speed (The number in brackets behind each reason is the number of respondents)

The reasons are divided into five main categories, see Figure 1, and behind each reason and category are assigned the number of respondents. Behind each main category is also visible the percentage of the total number of respondents who are placed in this category. Some causes are difficult to put into a category, but since these causes have only one respondent each, the result is not dependent on where those are located. Some respondents have mentioned several reasons for this phenomenon which is why the total amount of answers is larger than the number of respondents.

The first category, *client*, could be divided into three groups, rules and norms, contract forms and the reviewing process. The rules are conservative and favour site-built bridges, prefabricated concepts are difficult to be approved. The most common contract forms do not allow contractors and other actors to be involved early in projects but when the design is already completed.

Thoughts that the industry is unique, each project is unique and that every workplace is different from the last are reflecting the *climate prevailing in the industry*. Because of this attitude, constructing the whole bridge in-situ is more common than using more industrialized concepts. According to [9], there is no research showing that the products and processes within the construction industry are more unique than in other industries. The largest factor within this category is that there are very few actors who can compete for major contracts, therefore the major contractors have no reason to change their methods and practices, because they are earning money anyway.

Contractors seem to be reluctant to change and in the previous section several reasons for that are stated. The contractors seem to be comfortable and only perform what provided documents require. One respondent summarized this category by the following remark:

“The major contractors are not interested; it is the same guys as before. The big contractors do not want prefabrication because then the competition is increasing; any contractor can build prefabrication, site casting+road+coating and so on can usually only the heavyweights do.”

Widespread conservatism among *actors in general* seems to be a major problem. According to [8], there are no research showing that people within this industry are more conservative than other, but people often use this as an excuse to defend the currently existing work methods and unsatisfactory conditions. [8] are pointing out four major hindrances for a faster development of construction industry in Sweden, the first is about that actors are trying to convince the public that it is not possible to work smarter. The other hindrances are according to [8]; customer focus, but still not .., improvement often results in increased administration and construction sector's structure prevents development.

The category *materials/product* is very intertwined with the claim that each product is unique and therefore it is almost impossible to build prefabricated bridges. This argument is not sustainable because we do not have to go far beyond our Swedish border to find countries where prefabricated bridges are the obvious choice. Over 80% of all built bridges in the Netherlands consist of prefabricated concrete. 53% of all respondents think that a combination of in-situ construction and prefabricated elements is the future for bridge construction. Noticeable is that consultants and contractors have a slightly more negative attitude against prefabricated elements than the clients. The superstructure or parts of it (bridge deck and edge beams) seems to be the parts that actors want prefabricated. Figure 2 highlight the most important factors of bridges construction and which concept that is most suitable for the situation.

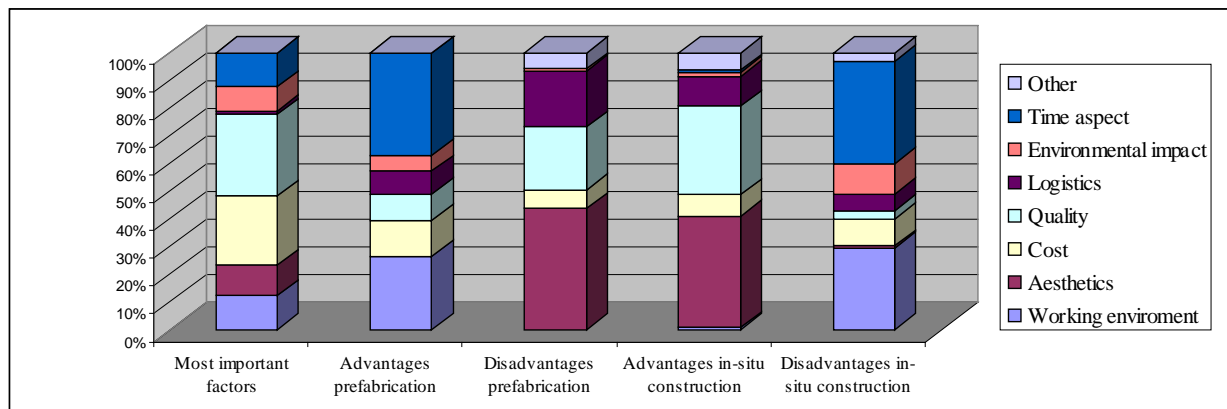


Figure 2 – Advantages and disadvantages of different construction methods

It is very important that bridges can be constructed with good quality as cheap as possible. Prefabricated bridges includes according to this survey, worse quality than in-situ constructed bridges, but to a cheaper price. A small study of inspection reports from the Swedish Transport Administration, [9], shows that there are no specific quality issues that can be linked to prefabricated bridges.

3. WHAT TO DO ABOUT THE PROBLEM

To address the problem of low efficiency growth, it is according to the survey the client organization which primarily has to change. Changes in rules and norms, and better contract forms with functional requirements need to become more common. More turnkey projects with functional requirements will lead to an earlier involvement of contractors and suppliers. According to [10], this lead to a faster development process and that the project team will be alerted to potential downstream problems in an earlier stage when these are easier and faster to fix. Meanwhile, the entire industry has to become more open and take better advantage of the knowledge and experience that already exists, to be able to develop improved products, whether it is built on site, prefabricated or a combination of the two different techniques.

4. DISCUSSION

Further investigations need to be done to verify this research and during autumn 2011, a workshop with people from the different actors will be performed to discuss the results from the survey. A journal paper containing more results from the survey and the workshop will hopefully be published during autumn 2011 this conference paper is a very brief summary of the result.

REFERENCES

1. Byfors, J., Jäderholm, B., Presentation FIA-day 2007, 2006 (In Swedish)
2. Bygghögskolekommisionen, "Skärpning gubbar! Om konkurrensen, kostnaderna, kvaliteten och kompetensen i byggsektorn," Stockholm, 2002, p. 442. (In Swedish)
3. Statskontoret, "Att mäta produktivitetsutveckling för anläggningsbranschen - en delrapport," Näringsdepartementet, Stockholm, 2009, p. 21. (In Swedish)
4. Rwamamara, R., Simonsson, P., Ojanen, J., "Advantages of industrialized methods used in small bridge construction," *International Group for Lean Construction*, IGLC, 18th annual conference on Lean Construction, Haifa, Israel, 2010, pp. 569-579.
5. Simonsson, P., Emborg, M., "Industrialized construction: benefits using SCC in cast in-situ construction," *Nordic Concrete Research no. 39*, 2009, pp. 33-52.
6. Kvale, S., Brinkmann, S., "Den kvalitativa forskningsintervjun," Studentlitteratur, Lund, 2009, p. 370. (In Swedish)
7. Merriam, S.B., "Fallstudien som forskningsmetod," Studentlitteratur, Lund, 2010, p. 228.
8. Josephson, P.-E., Saukkoriipi, L., "Slöseri i byggprojekt - Behov av förändrat synsätt," Sveriges Byggingdustrier, Göteborg FoU-väst, 2005, p. 56. (In Swedish)
9. <https://batman.vv.se/batman>, 2010.
10. Brown, S.L. and Eisenhardt, K.M., "Product development: past research, present findings, and future directions," *Academy of Management Review no. 2*, 1995, pp. 343-378.